Sensoral 98 International workshop on sensing quality of agricultural products

Véronique Bellon Maurel

ACTES DE COLLOQUE

Montpellier
24-27 février 1998
Cemagref France

volume 1

Sensoral 98

International workshop on Sensing Quality of Agricultural Products

Colloque international sur les capteurs de la qualité des produits agro-alimentaires

Edited by Véronique Bellon-Maurel

Cemagref EDITIONS

SENSORAL 98

International workshop on Sensing Quality of Agricultural Products

Colloque international sur "les capteurs de la qualité des produits agro-alimentaires"

Montpellier
24-27 février 1998

Volume 1

Edited by :
Véronique Bellon-Maurel

Colloque

SENSORAL 98

International workshop on Sensing Quality of Agricultural Products

Colloque international sur "les capteurs de la qualité des produits agro-alimentaires"

Montpellier, 24-27 février 1998

Edited by : Véronique BELLON-MAUREL

Actes du colloque **Sensoral 98 : International workshop on Sensing Quality of Agricultural Products.** 24-27 février 1998. **Volume 1**
Coordination de l'édition : Véronique BELLON-MAUREL. Secrétariat : Michèle EGEA. Mise en page : Sophie MORIN, Caroline REACH. Suivi de l'édition : Camille CEDRA
Impression et façonnage : Ateliers Cemagref-Dicova. Vente par correspondance : Publi-Trans, BP 22, 91167 Longjumeau Cedex 9, Tél. 01.69.10.85.85. Diffusion aux libraires : Tec et Doc Lavoisier, 14 rue de Provigny - 94236 Cachan Cedex.
ISBN 2-85362-499-4, dépôt légal 4ème trimestre 1998. Prix de vente : 195 F TTC

SENSORAL 98

International workshop on Sensing Quality of Agricultural Products

Colloque international sur "les capteurs de la qualité des produits agro-alimentaires"

Montpellier, France
24-27 février 1998

General abstract: *The Workshop SENSORAL 98 was aimed at sensor measurement of agricultural product quality. It dealt with 3 main objectives:*

1. Dissemination of the research results of two European projects:

- SHIVA « Integrated system for handling, inspection and packing of fruit and vegetables » funded by ESPRIT, to design and validate a new packing house concept with delicate handling systems and quality inspection of individual fruit (aspect, firmness, taste);

- « Objective plant quality measurement by image processing » supported by FAIR, to set up methods and technologies based on image analysis and artificial intelligence to control quality of pot plants such as Begonias, Hibiscus...

2. Scientific and technical presentations of sensors and fast measurement systems by international researchers;

3. Enhancement of industry/research exchanges through industrial presentations of joint research projects transferred to the industry. Round tables were organised on specific products [a) fruit, vegetables and flowers, b) animal products, c) wine and drinks, d) cereal products] allowing industrial managers to express their sensor needs.

For fruits and vegetables, the most important themes were: artificial vision, NIR spectrometry, aroma sensors and artificial intelligence simulating human classification. Animal product quality assessment through acoustic, NMR and electric impedance measurement was presented. Concerning process control, tracers (thermochromic liquid crystals, fluorescent particles, positron emitting particules) or emerging techniques such as Magnetic Resonance Imaging were mainly dealt with.

Over sixty papers have been presented in all and more than 140 participants attended SENSORAL 98. This book of proceedings offers the most relevant information of these four exciting days.

Résumé général : Le colloque SENSORAL 98 était axé sur les trois objectifs suivants :

1. Etre le support de dissémination des résultats de la recherche de 2 projets européens:

- SHIVA "Système intégré pour la manipulation, le contrôle et l'emballage des fruits et légumes" financé par un programme ESPRIT et dont l'objectif était de concevoir et valider un nouveau concept de station fruitière intégrant manipulation douce des fruits et inspection de la qualité globale (aspect, fermeté et goût) des produits ;

- "Mesure de la qualité des plantes en pot par analyse d'image" financé par un programme FAIR et qui tendait à mettre en place des procédures et techniques fondées sur l'analyse d'images et l'intelligence artificielle pour contrôler la qualité des plantes telles que bégonias, hibiscus...

2. Permettre aux chercheurs de la communauté internationale de présenter leurs avancées sur les systèmes capteurs et mesures rapides de produits agricoles ;

3. Favoriser les échanges industrie/recherche par une présentation industrielle de projets de recherche conjoints ayant abouti à des transferts et par des tables rondes organisées par filières pour faire "remonter" les besoins des IAA en capteurs.

Les filières concernées sont principalement les fruits, légumes et fleurs mais également la filière viande. Pour le contrôle des produits végétaux, les thèmes forts qui émergent de ce Colloque sont la vision artificielle, la spectrométrie proche infra-rouge, les capteurs d'arômes, les méthodes d'intelligence artificielle pour simuler la classification humaine. L'appréciation des produits carnés est présentée au travers de l'acoustique, la RMN et l'impédance électrique. Le contrôle des procédés est abordé en proposant des marqueurs (cristaux liquides thermochromes, molécules fluorescentes, particules à émission de positron), mais également des techniques en émergence telles que l'Imagerie à Résonance Magnétique.

Une soixantaine de présentations ont été faites sous forme orale ou poster. Plus de 140 participants ont assisté à SENSORAL 98.

Foreword

The original idea of SENSORAL 98 was to create an event where the results of two quality related European projects would be disseminated. These projects are SHIVA, a DGIII-funded project which stands for «Integrated System for Handling, Inspection and packing of Fruits and vegetables and a FAIR-funded project on the theme of «Objective plant quality measurement by image processing». This workshop also marks the starting point of ASTEQ, a FAIR concerted action involving 14 different organisations and companies, standing for «Artificial Sensing Techniques for the Evaluation of Quality».

This «junction» was an ideal opportunity to organise a meeting with more wide-ranging goals on the topic of **«Sensing Quality of Agricultural Products».**

Quality has now become a center stage topic. As you all know, the lack of adequate quality inspection, especially in the «mad cow» scandal, have increased the public awareness of a need for a stricter control of product quality in the food and agri-business.

In SENSORAL 98, we are going to concentrate on other aspects relating to quality such as organoleptic quality, on-line analysis of food composition and the monitoring of food processing. Even though these elements of quality control have a lower media profile, they are of prime importance to the people and organisations involved in the agri-business, and most of all, in the food processing industries.

By knowing the technological or organoleptic properties of the products or by accurately measuring the process variables, the food processor is able to apply a more precise process regulation, to guarantee more constant levels of quality and, consequently, to better meet the requirements imposed by its customers. Thus, in the long term, these aspects of quality are key elements for the company competitiveness and the success of its commercial strategy. By helping the food processors to better understand their products and processes, the researchers dealing with sensors transmute the information into profits for the industry and into satisfaction for the consumer. They really have to be very aware of the expectations of the industry and the consumers to continue to play this role.

Definitely, the aim of SENSORAL 98 was to help researchers and industrial companies to better work together in the area of food sensors and food quality. The high level of the presentations of this workshop and the large number of participants from both parties allows us to think that this objective was fulfilled.

Véronique Bellon-Maurel
Head of GIQUAL Research Unit
Chairwoman of SENSORAL 98

Sommaire général

Tomes 1 et 2
(Part 1 to 8)

General abstract T1 p.15

Part 1 - On-line measurements in food process

Positron emission particle tracking studies of high solid fraction solid-liquid food mixtures in tube flow T1 p.19
Etude de flux de mélanges alimentaires solide/liquide à haute teneur en solides par suivi de particules émettrices de positrons
P. FAIRHURST, J.P. PAIN, P. FRYER, D. PARKER

Hall effect sensors : a method to measure passage time distributions of solid particles in solid-liquid flow T1 p.33
Capteurs à effet hall : une méthode pour mesurer la distribution des temps de séjour de particules solides dans un flux solide-liquide
P. FAIRHURST, S. ELIOT, A. GOULLIEUX, J.P. PAIN

Determination of temperature maps using a method based on thermochromic liquid cristals T1 p.45
Détermination de cartes de distributions de températures par utilisation de cristaux liquides thermochromiques
J.P. GADONNA, A.B. JEMAI, C. MULLER, J.P. PAIN

Measurements play an essential role in Finnish food processing industry T1 p.59
Les mesures jouent un grand rôle dans l'industrie agro-alimentaire finlandaise
M. KANSAKOSKI

Determination of the residence time distribution in an experimental conditioner by fluorescence video imaging T1 p.67
Détermination de la distribution du temps de séjour par imagerie fluorescence
B. NOVALES, J. MABIT, Y. RIOU

Part 2 - Objective measurements of horticultural product quality

Pot plant quality prediction based on image analysis of half grown plants..... T1 p.81
Prédiction de la qualité des plantes en pots en partir de l'analyse d'images de plantes en cours de croissance
B.S. BENNEDSEN

Quality criteria used by human experts for pot plant begonia assessment T1 p.91
Critères de qualité utilisés par des experts humains pour le tri des bégonias en pot
P. FEUILLOLEY, S. GUILLAUME

Development of a virtual expert for colour classification of tobacco T1 p.105
leaves. Validation against human experts
Développement d'un expert virtuel pour la classification couleur de feuilles de tabac. Validation par comparaison avec des experts humains
M. GARCIA, P. BARREIRO, M. RUIZ-ALTISENT, R. ALONSO, L. JUDEZ

Objective plant quality measurement by image processing T1 p.117
Mesure objective de la qualité des plantes par analyse d'images
J. MEULEMAN, J. HOFSTEE, C. KAAM

A photogrammetric method to measure geometry of standing tree stems T1 p.133
Méthode photogrammétrique appliquée à la géométrie des arbres sur pied
R. THOMAS, M. FOURNIER-DJIMBI, M. LENOIR, C. GUIZARD

Vision system for sorting paphiopédilum using structural and statistical T1 p.141
pattern recognition
Système de vision pour le tri des orchidées en pot par des méthodes de reconnaissances de formes structurelles et statistiques
T. TIMMERMANS

Part 3 - Vision systems for food product quality

Principle and application of probabilistic neural networks in artificial vision T1 p.157
Principe et application des réseaux de neurones probabilistes en vision artificielle
D. Bertrand, Y. Chtioui, D. Demilly

Machine vision grading of agricultural products using pattern recognition T1 p.169
and neural networks
Agréage des produits agricoles par vision, reconnaissance de formes et réseau de neurones
A. Ghazanfari, J. Irudayaraj

Automatic potato sorting system using colour machine vision T1 p.185
Classification automatique des pommes de terre par système de vision couleur
C. Guizard, J.M. Gravoueille, M. Crochon

On-line quality evaluation and sorting for mushroom via neuro image processing T1 p.199
Evaluation de la qualité et tri en ligne de champignons par analyse d'images et réseaux de neurones
H. Hwang, C.H. Lee, S.C. Kim

Application of neural networks in quality control of "Jonagold" apples T1 p.211
Application de réseaux de neurones pour le contrôle de la qualité des pommes "Jonagold"
V. Leemans, F. Bieuvelet, M. Destain

Automatic inspection of olives using computer vision T1 p.221
Inspection automatisée des olives par vision artificielle
E. Molto, J. Blasco, V. Escuderos, M. Blasco, J. Garcia

Advanced information technologies for objective quality sensing of edible beans T1 p.231
Technologies de l'information pour la mesure objective de la qualité des haricots
S. Panigrahi

Part 4 - Textural measurements

Mealiness in apples. Comparison between human and instrumental procedures and results T1 p.245
Farinosité des pommes. Comparaison entre les mesures humaines et instrumentales
P. Barreiro, C. Ortiz, M. Ruiz-Altisent, I. Recasens, M.A. Asensio

Detection of mechanical stress and damage of fruit and vegetables T1 p.259
Détection des contraintes mécaniques et des meurtrissures sur fruits et légumes
B. Herold, B. Oberbarnscheidt, I. Truppel, M. Geyer

Woolliness assessment in peaches. Comparison between human and instrumental procedures and results T1 p.269
Farinosité des pêches. Comparaison entre les mesures humaines et instrumentales
C. Ortiz, P. Barreiro, M. Ruiz-Altisent, F. Riquelme

Measuring dynamic viscoelasticity of a microscopic organism T1 p.283
Mesure de la viscoélasticité dynamique d'un organisme microscopique
K. Shigeta, Y. Nagasaka, R. Otani, K. Taniwaki

Firmness quality measurement in fruits and vegetables T1 p.291
Revue des techniques de mesure de fermeté des fruits et légumes
I. Shmulevitch

Part 5 - Aroma sensors

Can an electronic nose replace sensorial analysis ? ..... T2 p. 329
Est-ce que le nez électronique peut remplacer l'analyse sensorielle ?
C. Di Natale, R. Paolesse, A. Macagnano, A. Mantini, E. Tarizzo, A. D'Amico

Flavour sensors arrays become virtual electronic olfactometers: ..... T2 p. 341
how to get reliable data from unstable sensors ?
Les capteurs d'odeurs deviennent virtuels : comment obtenir
des données fiables à partir de capteurs instables
P. Mielle, F. Marquis

Contribution of the gas sensors for the characterization of products ..... T2 p. 357
Contribution des capteurs d'odeurs à la caractérisation des produits
alimentaires
C. Nicolas, P. Carel, J. Hossenlopp, G. Trystram, D. Rutledge

Methodology for SnO2-gas sensor selection using stepwise multivariate ..... T2 p. 371
analysis
Une méthodologie pour sélectionner les capteurs gaz Sn02
en utilisant une analyse multivariée pas à pas
S. Roussel, P. Grenier, V. Bellon-Maurel

Utilization of the olfactory characteristics of fruit and vegetables ..... T2 p. 385
as a potential method for determining their ripeness and
readiness for harvest
La mesure de l'odeur des fruits et légumes :
une méthode potentielle pour déterminer leur maturité
et la date de la cueillette
Y. Sarig

Part 6 - Measurements in animal based products

Ultrasonic muscle sample classification ..... T2 p. 431
Classification d'échantillons de muscles par ultrasons
S. Abou El Karam, P. Berge, J. Culioli

Use of ultrasound reflexion for fresh hams classification ..... T2 p. 443
Utilisation de la réflexion des ultrasons pour classer la viande de jambon
M. Chanet

Application of electrical conductimetry to the control ..... T2 p. 453
of a meat emulsification process
Application de la conductrimétrie électrique
pour le suivi d'une opération d'émulsification de viande
C. Curt

NMR relaxometry as a rapid technique to evaluate ..... T2 p. 467
the consistency and the oxydizability of adipose tissues
La relaxométrie RMN, une technique rapide pour évaluer
la consistance et la tendance à l'oxydation des tissus adipeux
A. Davenel, P. Marchal, A. Riaublanc, G. Gandemer

Measurement of acoustic impedance to estimate the fish sol density ..... T2 p. 475
Mesure de l'inpédance acoustique pour l'estimation de la densité des soles
Y. Mevel, M. Mastail, R. Baron

Beef tenderness prediction by near-infrared reflectance spectroscopy ..... T2 p. 485
Prédiction de la tendreté du bœuf par spectométrie proche infrarouge
B. Park, Y.R. Chen

Part 7 - NIR spectrometry

Spectrometer techniques for process analysers ..... T2 p. 501
Techniques spectrométriques pour l'analyse de procédés
M. Kansakoski, P. Niemela, M. Aikio, J. Malinen, J. Tornberg

Influence of the optical configuration on model prediction ..... T2 p. 515
performance for non-destructive measurement of fruit
quality by means of NIR spectroscopy
Influence de la configuration optique sur la performance
du modèle de prédiction pour la mesure non destructive
de la qualité des fruits par spectroscopie NIR
M. Lammertyn, M. Nicolai, V. De Smesdt, J. De Baerdemaker

Spectral amplification in NIR spectroscopy and sorting ..... T2 p. 527
of whole apples
Amplification spectrale en spectrométrie laser NIR et tri des pommes
M. Meurens, E. Moons

Real-time NIR sensor to sort fruit and vegetables according ..... T2 p. 533
to their sugar content
Un système proche infrarouge temps-réel pour le tri en ligne des fruits
en fonction de leur taux de sucre
J.M. Roger, V. Bellon-Maurel, L. Dusserre-Bresson, P. Fayolle, G. Ranou

Part 8 - Classification and multisensor fusion

SHIVA (European project): a robotic system for fruit sorting ..... T2 p. 545
SHIVA (projet européen) : un système robotisé de tri des fruits
A. Bourely

A measurement method for ordered category scales ..... T2 p. 561
Une méthode de mesure pour les échelles de catégories ordonnées
M. Maurin

Real time quality evaluation of biscuit during baking using sensor fusion..... T2 p. 577
Fusion multi-sensorielle pour l'évaluation temps réel de la qualité des biscuits pendant la cuisson
N. Perrot,G. Trystram, E. Dugre, F. Guely

Adaptive simulation of human assessment of fruit quality..... T2 p. 589
Simulation adaptative de l'appréciation humaine de la qualité des fruits
M. Picus, K. Peleg

Use of sensor fusion to detect green picked and chilled tomatoes ..... T2 p. 609
Utilisation de la fusion de capteurs pour détecter des tomates cueillies vertes ou gelées
S. Schotte, J. De Baerdemaeker

A methodology for sensor fusion design: application to fruit quality assessment..... T2 p. 619
Une méthodologie pour la fusion de capteurs : application à l'appréciation de la qualité des fruits
V. Steinmetz, V. Bellon-Maurel, F. Sevila

Part 1

One line measurements in food process

Positron emission particle tracking studies of high solid fraction solid-liquid food mixtures in tube flow

Etude de flux de mélanges alimentaires solide/liquide à haute teneur en solides par suivi de particules émettrices de positrons

Peter Fairhurst, Jean-Pierre Pain

Département de Génie Chimique, Université de Technologie de Compiègne, 60206 COMPIEGNE Cedex FRANCE

Peter Fryer

School of Chemical Engineering, The University of Birmingham, Birmingahm, B15 2TT, U.K.

David Parker

School of Physics, The University of Birmingham, Birmingahm, B15 2TT, U.K.

Abstract: *Positron emission particle tracking has been used to track the motion of a single radioactively labelled tracer particle in high solid fraction solid-liquid food flow. Experiments were performed using 10 mm sodium alginate spheres flowing carboxymethylcellulose solutions. In certain conditions two flow regions were found to exist, a fast flowing central core and a slower moving annular region close to the tube wall. Fastest particles were found to travel at a maximum of 1.5 times the average fluid velocity.*

Keywords: *Positron, particle tracking, aseptic processing, HTST, solid-liquid flow, residence time.*

Résumé : Le suivi de particules émettrices de positrons a permis de déterminer le mouvement d'une particule-traceur marquée dans un flux liquide-solide à haute teneur en solides. Les expériences ont été menées en utilisant des solutions contenant des sphères d'alginate de sodium de 10mm de diamètre. Dans certaines conditions, deux régions coexistent dans le flux : un flux central rapide et une région annulaire près des parois du tube qui se déplace plus lentement. Les particules les plus rapides se déplacent 1,5 fois plus rapidement que la moyenne du fluide.

1. Introduction

The development of continuous sterilisation processes for food products containing particulate matter poses some fundamental problems. These include high pressure and temperature rheology of the heterogeneous food, prediction and measurement of heat transfer into the particles and passage time distribution (P.T.D.) for both solid and liquid phases.

High Temperature Short Time (HTST) processes require the food product to be heated up to about 140°C for few seconds, 10-30 s depending on the sterility specified. Small differences in the passage time of the product in the heating and holding sections can therefore cause large variations in product quality and sterility. As a result, detailed knowledge of solid-liquid flow dynamics is necessary for commercial development.

Different non-intrusive particle measuring systems already exist, none of these however are capable of following particle trajectories in opaque media. The visual technique of particle tracking velocimetry (PVT) has been used in a number of applications including that of the automobile and food industries [1]. The velocity profile is measured using small tracers and imaging the flow in two perpendicular planes and using a specialised image analysis approach to track the paths of the individual tracers to construct a vector plot of the area of interest. Such techniques can only be used in transparent liquids and at low solid concentrations. Liu [2], Lareo [3] and Fregert [4] for example, employed such a methods to follow tracers in solid-liquid food flows where the carrier fluid was transparent and the maximum solid concentration used was 10% . Magnetic Resonance Imaging (MRI) can be used to measure the liquid velocity field of opaque solid-liquid mixtures. McCarthy [5] studied the velocity profiles of 0.5% CMC solutions with particle loadings of 10, 20, and 30% w/w for 2.5 and 5 mm alginate beads in 26.2 mm i.d. transparent perspex pipe (flowrates 43 l/hr to 670 l/hr). Velocity profiles were modelled by a shear thinning power law fluid. As the flow rate increased the flow index n was found to decrease, indicating a flattening of the velocity profile in the centre of the pipe compared to that of a parabolic profile of a Newtonian fluid. Tracking individual particles is not possible however by this technique because of the time required to perform a scan is of the order of 10 s compared to the particle velocity (0.1 m/s) hence individual particle behaviour (velocity, migration across stream lines etc.) cannot be measured.

Other methods exist for measuring the residence or passage time of a tracer in pipe flow. Liu [6] wrapped some foil around a tracer particle and placed two copper detection coils around the pipe which were connected to an alternating bridge. When a tracer particle passed close to one of the coils the equilibrium of the bridge was disturbed and an output voltage measured. Alternatively, Segner [7] used Electromotive Force sensors (EMF) where a small magnet was embedded into a

turkey cube flowing in the holding tube. Two copper coils were wound around the pipe at the entrance and exit of holding section. These were connected to a small amplifier and connected to a potentiometer for detecting the electromotive force, such a method requires non-metallic tube walls. Fairhurst [8] used Hall effect sensors to measure passage times in an industrial pilot plant. A small magnet was placed in a particle made of sodium alginate and expanded polystyrene. Hall effect sensors were then placed at the entrance and exit of the measured section. The advantage of Hall effect compared to EMF sensors is that Hall effect sensors function through metallic walls. Toda [9] used a radioactive technique where γ- ray irradiated particles were used in straight pipes and bends. The particle velocity was determined by the trajectory length between two scintillation probes. These residence time measuring methods although operational in opaque media, can only measure the average velocity of a particle over a given section and not the radial position, velocity profile or the instantaneous velocity. Positron emission particle tracking (PEPT) a method that relies on detecting back-to-back pairs of γ-rays produced when positrons annihilate with electrons, is therefore the only present method capable of tracking particles in opaque media. It also has the advantage of being operational at high temperatures.

2. Positron emission particle tracking

Radionuclides which decay by β^+ decay with the emission of a positron (a positive electron) make useful tracers since this positron rapidly annihilates with an electron, producing a pair of 511 keV γ-rays which are emitted almost exactly back-to-back. Coincident detection of these two γ-rays in a pair of positron sensitive sensors defines a line passing close to the point of emission, collimation. This is the basis of the imaging technique of positron emission tomography (PET) often used in medicine. The concentration of the labelled phase can be reconstructed by standard tomographic techniques from the number of γ-ray pairs emerging along each line of sight.

Since the 511 keV γ-rays are very penetrating, PET also has considerable potential for engineering studies. The high cost of the detection equipment (£2 million for a state of the art medial system) has so far however, restricted its application. To date the only system dedicated to engineering applications is the Birmingham University positron camera [10]. Unlike most medical systems, this consists of a pair of multi-wire proportional chambers each with an active area 600× 300 mm^2 and capable of locating a detected γ-ray to within about 5 mm. The two detectors are placed either side of the system of study and operate in coincidence mode, an "event" only being recorded if the γ-rays are detected in both detectors with a resolving time of 12 ns. The principal weakness of the camera is that, due to it's poor efficiency, the data rate is limited to less than about 3000 coincidence events per second, so that acquiring sufficient to enable tomographic reconstruction of an extended tracer distribution my take many minutes. Use of the camera in this way has therefore concentrated on a range of steady state situations, and applications

have ranged from imaging lubricant distribution within an operating jet engine [11] to mapping the concentration of sand grains in a stirred slurry [12].

For the dynamic studies, the technique of positron emission particle tracking (PEPT) has been developed at Birmingham [13]. Here a single labelled tracer is used, whose position is determined by triangulation from a small number of detected γ-ray pairs. In practice many of the detected events are corrupt, for example because one of the detected γ-rays has been scattered, so that location requires acquisition of sufficient events that that the valid ones, whose reconstructed lines essentially meet at one point, can be distinguished from the corrupt ones, whose lines are broadcast in space, in order that the latter may be discarded. The actual number of events used depends on various factors, including the tracer speed, with the result that a slow moving tracer can be located to within 2 mm roughly 20 times per second, while a particle moving at 1 m/s can be located to within 5 mm 250 times per second.

The data then consists of a list of tracer co-ordinates (x_i, y_i, z_i) each with its associated time t_i. From the difference between successive locations, an estimate of the instantaneous vector velocity of the tracer can also be obtained. In practice a weight rolling average of 6 differences between locations i and i + 5 is currently used, and is generally accurate to within 10% [14].

Currently, tracer particles containing the positron emitting radionuclide ^{18}F (half-life 110 min) are produced by irradiating resin beads with a ^{3}He beam from a cyclotron. In this study resin beads 60 microns in diameter were embedded in tracer particles.

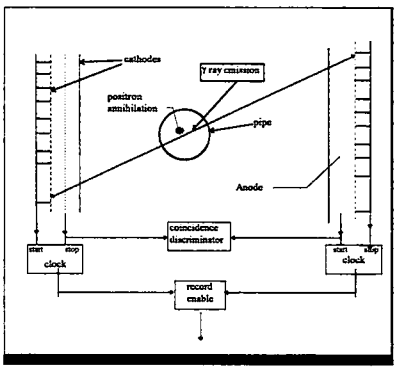

Figure 1: Principle of particle location in PEPT from detected pairs of back-to-back rays

3. Experimental procedure

Model food particles made from sodium alginate gelified in a calcium chloride solution were used throughout the experiments. These were fabricated on site and consisted of either 10 or 5 mm near spheres. For each batch made, the density, diameter, and eccentricity $\left(\frac{d_{\min imum}}{d_{\max imum}}\right)$ for a sample of 30 particles were measured before and after the experiments.

An analysis of the mechanical properties of the alginate near spheres was performed using a Analyser de Texture TAX:T2 (RHEO, 99 route de Versailles 91160, Champlan, France) and Texture Expert for Windows software. A number of sample particles was taken and compressed in different orientations between two flat plates. The elastic limit of the particles was found to be approximately 10% of the diameter of the sphere i.e. a compression of 1 mm for a 10 mm diameter particle. Beyond this point, the particles under went a plastic deformation and did not return to their original form. The equation listed below is the force-compression distance relation found for elastic deformation. The sedimentation velocities of the particles in the various carrier fluids used are displayed in table 1 and the eccentricity, density and mechanical properties of the particles in table 2.

	diameter mm	sedimentation velocity 0.5% CMC mm/s	sedimentation velocity 0.8% CMC mm/s
5 mm particles	5.0 ± 0.4	1.8 ± 0.1	0.40 ± 0.03
10 mm particles	10.2 ± 0.6 mm	4.3 ± 0.3	0.77 ± 0.08

Table 1: Sedimentation velocities of model food particles

Particle Diameter mm	Eccentricity	Density kg/m^3	force-compression relation force (g), x (mm)
5 ± 0.4	0.98 ± 0.02	1002 ± 4	$f = 15x^2+19x+5.2 \pm 7\%$
10.2 ± 0.6	0.97 ± 0.03	1002 ± 4	$f = 14x^2+31x+6 \pm 10\%$

Table 2: Mechanical properties of model food particles

The sodium alginate used for tracer fabrication was dyed with methyl blue, visual identification of the tracers particles was therefore possible. The tracer particles were made by drilling a hole in the alginate particle, placing the radioactive resin bead in the centre and then filling the hole with alginate solution. The particle was

then left in a concentrated calcium chloride solution for 5 minutes to gelify the fresh alginate solution. The tracer was then ready to be injected into the flow loop. Before placing the resin bead in the alginate particle the bead was sprayed painted to reduce leakage of ^{18}F from the bead into the alginate matrix and from the alginate into the carrier solution. The change in density of the tracer particle compared to that of an ordinary bead was negligible because the resin bead was only 60 microns in diameter and ρ_{resin} = 1100kg/m^3, taking a 5 mm bead as an example: ρ_{tracer} was 1.35 × 10^{-5} % heavier than an ordinary alginate particle.

Aqueous solutions of carboxymethylcellulose (CMC) 0.8 % w/w and 0.5 % w/w were used as carrier fluids in all experiments. The CMC (commercial name Blanose Cellulose Gum, type Blanose 7HF, distributor Hercules, Aqualon France, Z.I. 27460 ALIZAY) solutions were prepared by adding the CMC powder slowly to water under mechanical agitation (mechanical agitator Bertrand Groupe Dito, 58000 Nevers).

One minute of mixing per litre of solution was required to dissolve all the CMC powder, 60 litres therefore took one hour to prepare. Shear (during mechanical agitation) can possibly change the rheology of the liquid. Rheological measurements were therefore performed for solutions agitated for one minute per litre of liquid (table 3a), and for solutions agitated for two and a half minutes per litre of liquid (table 3b). No change in the rheological properties were found. During the mixing small air bubbles became entrapped in the solution, the liquid was therefore left for several hours to degas before use.

A HAAKE RV 100 co-axial viscometer was used to determine the rheological properties of the CMC solutions for steady shear conditions up to 400s^{-1}. A power law model was not found to fit the data over the shear range applied. An Ellis model fitted the data much better (eq. 1):

Rheological model for an Ellis fluid

$$\mu_a = \frac{\mu_0}{1 + \left(\tau / \tau_{1/2} \right)^{\alpha - 1}} \qquad (1)$$

The Ellis parameters were determined by a non-linear curve fitting (Curve Expert software), these values for are presented in table 3.

CMC concentration (w/w)	μ_0 Pas	$\tau_{(1/2)}$ Pa	α	R^2
0.5%	0.12	6.6	2.03	0.99
0.8%	0.62	7.4	2.03	0.99

Table 3a: Mixing time per litre 1 min/litre of solution

CMC concentration (w/w)	μ_0 Pas	$\tau_{(1/2)}$ Pa	α	R^2
0.5%	0.12	6.8	2.07	0.99
0.8%	0.62	7.5	2.04	0.99

Table 3b: Mixing time per litre 2.5 min/litre of solution

Fresh solutions of CMC were prepared for each experimental run. The rheological properties of the CMC solutions were tested before and after the experiments, no significant variations were detected.

A gravity driven flow loop was designed and built. A schematic diagram of the flow loop used is shown below figure 2.

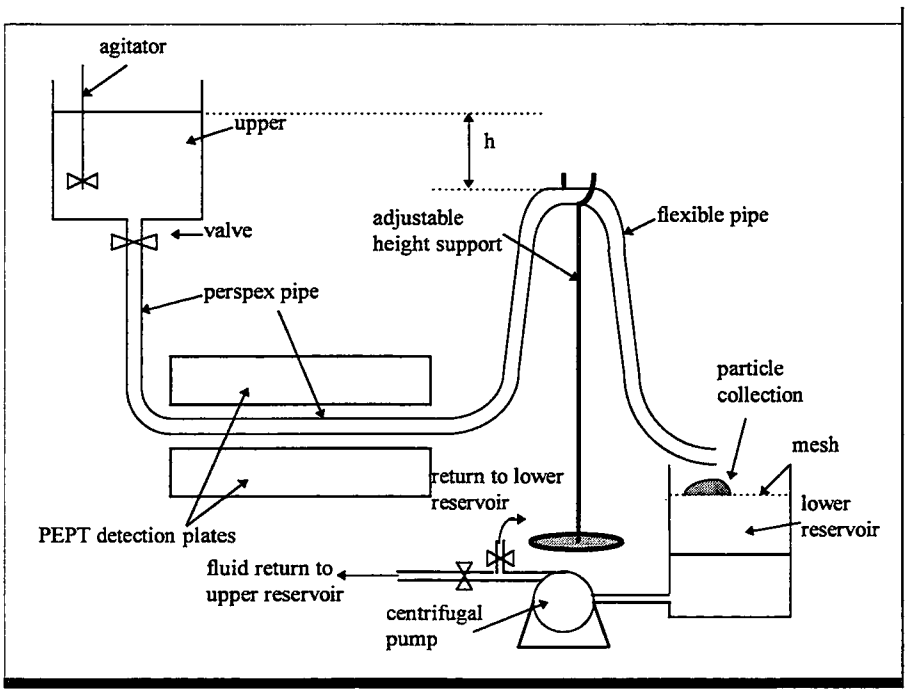

Figure 2: Schematic diagram of experimental apparatus

The solid particles were kept in suspension in the upper reservoir by a mechanical agitator. The solid-liquid mixture then flowed from the reservoir through two sections of transparent perspex pipe (i.d. 45 mm). One of these (horizontal or vertical) depending on the geometry desired to be studied was placed between the PEPT detection plates. Joined to the perspex pipe was a length of flexible tubing.

This flexible pipe was supported by an adjustable height stand, the height of which controlled the fluid drop distance (h) from the upper reservoir and hence the flow rate.

The larger the drop the higher the flowrate. The solid-liquid mixture then flowed over a mesh, into the bottom reservoir. The solid particles were collected manually from the mesh placed in a bucket and returned to the upper reservoir. The CMC carrier fluid was pumped back into the upper reservoir using a centrifugal pump. The fluid return flowrate was controlled by adjusting the bottom reservoir return using a valve. A large volume (120 litres) upper reservoir was used to reduce the changes in solid concentration. Solid particles gathered from the mesh were added regularly through out the length of each experimental run. Each bucket load contained approximately 2 kg of solid, this therefore caused a step increase in the upper reservoir solid concentration of 1.7% i.e. from 19% to 21 % if a global concentration of approximately 20 % was being used. The solid delivery concentration was measured by taking 2 litre samples of the solid-liquid mixture flowing out of the flexible pipe. The solid particles were then washed, left to dry and weighed. The volumetric delivery concentration was then calculated, volumetric delivery concentrations used were 21% ± 2%, 30% ± 2% and 39.5% ± 2%. In order to reduce variations in the flowrate, the upper reservoir used had a large cross-sectional surface area 0.27 m^2. The flowrate was calculated by measuring the time for the solid-liquid mixture to fill a 2 litre beaker. The beaker was placed at the outlet of the flexible piping and the flowrate was measured several times during each experimental run in general the flowrates were found to vary by ± 4% e.g. ± 15 l/hr for 400l/hr. The flowrates used ranged from 150 l/hr to 700 l/hr. This corresponds to a tube Reynolds number of 3 to 63 based on the average theoretical viscosity for an Ellis fluid in single phase flow at the same flowrate [15]. The radioactive tracers were injected just above the upper reservoir outlet. A new tracer was injected when the previous one had passed through the PEPT detection plates. The tracers were collected at the flexible tube outlet and reinjected. The location of the perspex pipe between the plates was measured before and after experimental runs by sticking a tracer on the tube wall of the perspex pipe at different radial and longitudinal locations. The pipe never moved during an experimental run. For each flowrate used a minimum of 50 particle passages through the detection plates were measured in order to obtain a representative sample of particle behaviour.

4. Results

The trajectories and velocities of the tracer particles were successfully measured using PEPT. The absence of entry effects was proven by comparing data for the first half of the horizontal pipe section in the camera's field of view with the second half, each section therefore being 250 mm long. Figure 3 below shows the instantaneous velocity range for 50 particles passages (experimental conditions v_{mean}=34 ± 2 mm/s, delivery concentration 21% v/v, 10 mm particles, 0.8% CMC carrier fluid). Figure 3a shows this velocity distribution for the first half of the

horizontal section and fig 3b the second half. The results are displayed in terms of cylinderical polar co-ordinate velocity vectors, the z axis along the tube axis.

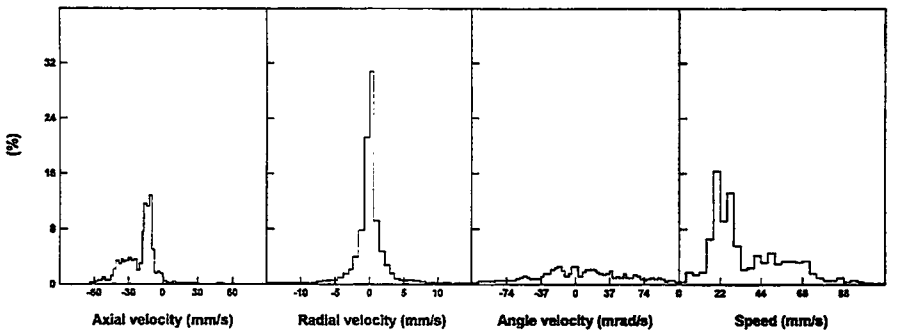

Figure 3a: Velocity range of first half of horizontal section

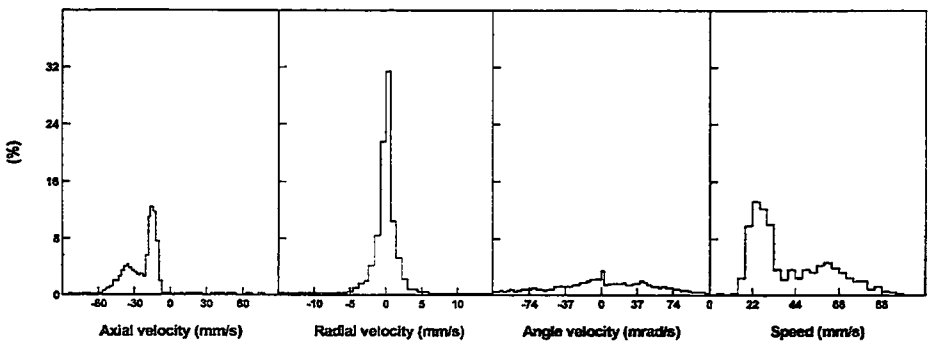

Figure 3b: Velocity range for second half of horizontal section

As can be seen in these two plots the velocity distributions are very similar. The radial velocities are minimal, angular velocities are approximately evenly spread from +74 mrads/s to-74 mrad/s and the instantaneous speeds and axial velocities of the particles form a bimodal distribution. For the particle axial velocities there is a first peak at about -14 mm/s slower than the average mixture velocity (36 mm/s) and a second one, smaller but more spread out at about -34 mm/s i.e. about equal to the average solid-liquid mixture velocity. The axial velocities are quoted as negative simply because of the orienatation of the camara with respect to the direction of flow. The first peak corresponds to visually observed slow moving particles close to the tube wall, the second wider peak corresponds to the range of faster particle velocities of particles observed to flow near the centre of the pipe. The speed distribution although bimodal has its peaks located at higher values than those of the axial velocity distribution at 25 mm/s and 60 mm/s apparently indicating that although most particles appear to remain in one of the two flow regions visually observed, there is considerable particle movement within each region (generally angularly and not radially).

The theoretical centre line velocity for a single phase Ellis fluid is

$$v_{centre\ line}(r=0) = \frac{\tau_w R}{\mu_0}\left\langle \frac{1}{2} + \left(\frac{\tau_w}{\tau_{1/2}}\right)^{\alpha-1} \frac{1}{(\alpha+1)} \right\rangle$$

which for 0.8 % CMC and v_{mean} =34 mm/s gives a $v_{centreline}$ = 65 mm/s or 1.92 v_{mean}. Comparing this value to the maximum axial velocities measured, roughly 60 mm/s or 1.76 v_{mean}, it would appear as that the velocity profile has been considerably flattened due the presence of solid particles confirming [5]

In figures 4a and 4b below, the speeds of a slow moving particle (4a) and the speeds of a fast moving particle (4b) are plotted against time, for the same experimental conditions as figure 3. The speed of the slow particle varies from about 15-25 mm/s whereas for the fast particle the speed varies from 45- 55mm/s. The speeds do not appear constant through the measured section, this possibly being because of random particle movement within each flow region.

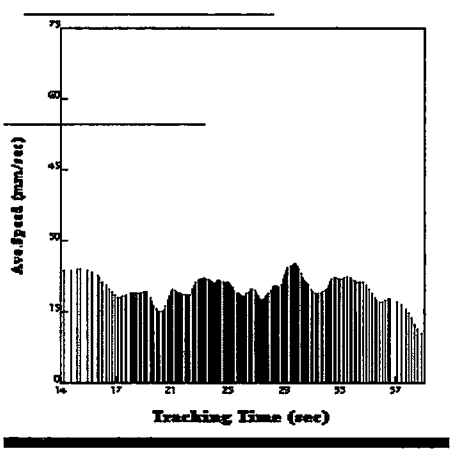

Figure 4a: Slow moving particle

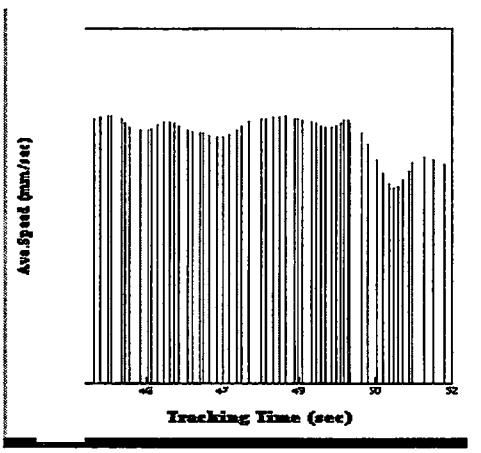

Figure 4b: Fast moving particle

Figures 5a and 5b display the angular, radial and axial position of the two particles through the measured 600 mm section. The slow moving particle(fig 5a) has a radial position of between 15 and 20 mm. As the pipe's internal radius is 22 mm and the particle's radius is about 5 mm the largest theoretical particle radial position (in terms of particle centre) would be 17 mm. This range therefore clearly shows a particle occupying a radial position close to the tube wall. The azimuthal position is constant at about 180° indicating that the particle remained close to the bottom of the pipe. The faster moving particle on the other hand occupies a radial position between 4-10 mm from the central axis of the pipe, it's azimuthal position is also

less constant varying form about - 100° to 160° indicating substantial movement within the fast flowing central core region.

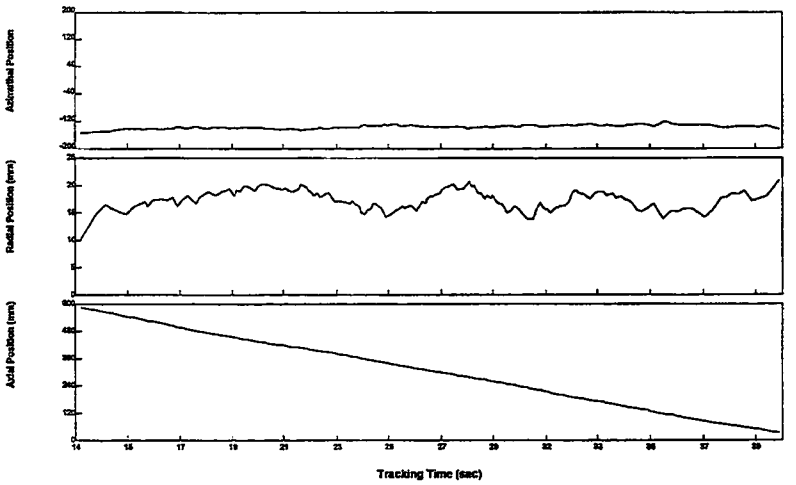

Figure 5a : Trajectory of a slow moving particle

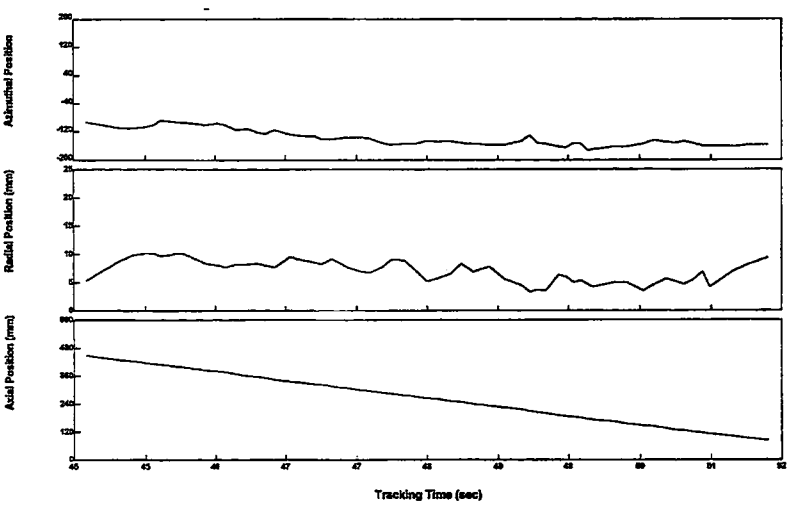

Figure 5b: Trajectory of a slow moving particle

Conclusion

Positron Emission Particle Tracking is an effective means of elucidating particle dynamics of solid-liquid food flows where high solid concentrations and opaque non-Newtonian carrier fluids are often present. Furthermore, PEPT has sufficient accuracy to determine velocity fields and particle migration across stream lines within a pipe. The results displayed here show the potential of the PEPT and furthermore that under certain experimental conditions two distinct flow regions can exist in the pipe, a central fast flowing core and a slower moving annular region close to the tube wall. Particles in the central region flow approximately twice as fast as particles close to the tube wall and between 1 and 1.6 times faster than the average axial fluid velocity. The commercial standard is to assume that fastest particles travel at twice the average axial fluid velocity. As a result in the experimental conditions investigated this assumption is conservative leading to over processing and hence a reduction of the solid-liquid food product. Further analysis of the results is however necessary to calculate velocity profiles, quantify angular and radial motion of the solid particles, and to investigate the effect of experimental parameters, viscosity, flowrate, solid concentration etc. on particle motion.

Nomenclature

$d_{maximum}$	largest diameter of alginate particle
$d_{minimum}$	smallest diameter for alginate particle
n	flow index for power law fluid
v_{mean}	mean axial velocity of the solid-liquid mixture
$v_{centre\ line}$	theoretical centre line velocity for single phase carrier fluid flow
α	ellis fluid parameter
μ_a	apparent viscosity
μ_0	ellis fluid parameter
$\tau_{1/2}$	ellis fluid parameter
τ_w	wall shear stress

Acknowledgements

The authors would like to thank Hélène Guichard for her financial support.

References

[1] *S. Sastry & K. Zitoun Proceedings of ICEF 7 Brighton U.K., Sheffield Academic Press. 1997.*

[2] *S. Liu, P.J. Fryer & J.-P. Pain. The flow and velocity distributions of particles in liquids: application to food processing, In Entropie, Vol. 28, N°170, pp. 50-58, 1992.*

[3] *C. Lareo, C.A. Branch and P.J. Fryer. Particle velocity profiles for solid liquid flows. Multiple particles Powder Technology. Vol 93, pp.35-45 1997.*

[4] *J. Freget. Solid- liquid flow in a horizontal pipe, Proceedings International Synopsium: Advances in Aseptic Processing & Packaging Technologies. Sept. 11-12 1995.*

[5] *K.L Mc Carthy, W.L. Kerr, R.J Kauten & J.H Walton. Velocity Profiles of fluid particulate mixtures using M.R.I. In Journal of Food Process Engineering, Vol. 20, pp. 165-177, 1997.*

[6] *S. Liu, J.-P. Pain, J. Proctor, A.A.P. de Alwis & P.J. Fryer. An experimental study or particle flow velocities in solid-liquid food mixtures. In Chem. Eng. Comm., Vol. 124, pp. 97-114, 1993.*

[7] *W.P. Segner, T.J. Ragusa, C.L. Marcus & E.A. Soutter. Biological evaluation of a heat transfer simulation for sterilising low-acid large particle foods for aseptic packaging. In Journal of Food Processing and Preservation, Vol. 13, pp. 257, 1989.*

[8] *P. Fairhurst, S. Eliot, A. Goullieux, J-P. Pain, Hall Effect Sensors: A method to measure passage time distributions of solid particles in solid-liquid flow, Proceedings Sensoral 98, 24-26 February 1998, Montpellier, France.*

[9] *M. Toda, T. Ishikawa, S Saito & S. Maeda. On the particle velocities in solid-liquid two-phase flow through straight pipes and bends. In Journal of Chemical Engineering of Japan, Vol. 6, pp.140, 1973.*

[10] *D.J. Parker, A.E. Dijkstra, T.W. Martin & J.P.K. Seville. Positron emission particle tracking studies of spherical particle motion in rotating drums Chem Eng Sci Vol 52, N°13, pp. 2011-2022, 1997.*

[11] *P.A.E. Stewart, J.D. Rogers, R.T. Skelton, P.L. Slater, M.J. Allen, R. Parker, P. Davis, P. Fowles, M.R. Hawkesworth, M.A. O'Dwyer, J. Walker & R. Stephenson. Positron emission tomography- a new technique for observing fluid behaviour in engineering systems. Non-destructive testing Proc.4th European Conf., London, pp. 2718-2726. Pergamon, Oxford. 1987.*

[12] *S.L. McKee, D.J. Parker & R.A. Williams Visualisation of size-dependant particle segregation in slurry mixtures using positron emission tomography. Frontiers in Industrial Process Tomography, pp.249-259. Engineering Foundation, New York 1995.*

[13] *D.J Parker, C.J. Broadbent, P. Fowles, M. R.Hawkesworth & P.A. McNeil Positron Particle Tracking- A technique for studying flow within engineering equipment. Nucl. Instrum. Meth. A Vol.236, pp.592-607, 1993.*

[14] *D.J. Parker, M. R. Hawkesworth, C.J. Broadbent, P. Fowles, T.D. Fryer & P.A. McNeil. Industrial positron-based imaging: principles and applications A technique for studying flow within engineering equipment. Nucl. Instrum. Meth. A. Vol.348, pp.583-592, 1994.*

[15] *P. Fairhurst & J-P. Pain. Passage Time Distributions for High Solid Fraction Solid-Liquid Food Mixtures in Horizontal Flow: mono-size particle distributions. J.Food Eng (submitted).*

Hall effect sensors: a method to measure passage time distributions of solid particles in solid-liquid flow

Capteurs à effet Hall : une méthode pour mesurer la distribution des temps de séjour de particules solides dans un flux solide-liquide

Peter Fairhurst, Sandrine Eliot, Jean-Pierre Pain

Département de Génie Chimique, Université de Technologie de Compiègne B.P. 649, 60206 Compiègne Cedex, France

Adeline Goullieux

Département de Génie Biologique, Institut Universitaire de Technologie 80025 Amiens Cedex, France

Abstract: *A method of measuring passage time distribution using Hall Effect Sensors is described in the following paper. Initially several practical problems were encountered, including the successful injection of tracers into the ohmic system and sensitivity calibration of the sensors. After these had been solved, Hall effect sensors were successfully used to measure particle passage times for 12 mm potato cubes, in 7% thermtex carrier fluid, in the heating column and holding sections of a 10kW ohmic heating plant. At a flowrate of 200 l/h, passage times in the column were found to be more spread out than in the holding tubes possibly indicating dead zones within the electrode geometry.*

Keywords: *Sensors, hall effect, Residence time, HTST, aseptic process, solid-liquid flow.*

Résumé : Une méthode pour mesurer la distribution, les temps de séjour basé sur les capteur à effet Hall est décrite dans ce papier. Originalement, de nombreux problèmes pratiques ont été rencontrés, incluant le problème de l'injection de traceur dans le système ohmique et la sensibilité des capteurs. Après la résolution de ces problèmes, les capteurs à effet Hall ont été utilisés avec succès pour mesurer les temps de séjour de particules pour des cubes de pommes de terre de 12 mm dans un fluide porteur à 7% dans une colonne de chauffage et dans les sections supports d'une usine de chauffage ohmique de 10kW. Lorsque le débit est de 200l par heure, les chercheurs ont trouvé des temps de séjour plus distribués dans la colonne que dans le tube support, ce qui indique probablement des zones mortes dans la géométrie de l'électrode.

1. Introduction

The development of continuous sterilisation processes for food products containing particulate matter poses some fundamental problems. These include high pressure and temperature rheology of the heterogeneous food, prediction and measurement of heat transfer into the particles and passage time distribution (P.T.D.) for both solid and liquid phases.

High Temperature Short Time (HTST) processes require the food product to be heated up to about 140°C for few seconds, 10-30 s depending on the sterility specified. Small differences in the passage time of the product in the heating and holding sections can therefore cause large variations in product quality and sterility. As a result, detailed knowledge of solid-liquid flow dynamics is necessary for commercial development.

Ohmic heating is a continuous HTST process, in which solid-liquid food mixtures are simultaneously heated by passing an electric current through them [1]. This passage of current generates heat due to the electrical resistance of the food [2]. The major advantage of this process is that heat is generated directly in the food product, and hence fast heating rates are possible. The resistive power generation rate depends on the voltage gradient and the electrical conductivity of the product [3]:

$$q = k(\text{grad}V)^2$$

As a result, the longer the food stays in an electrical field, or in the ohmic column, the greater the amount of heat generated [4].

Different non-intrusive particle measuring systems already exist, none of these however are practically applicable to measuring passage times in industrial installations where opaque carrier fluids and metallic pipes often exist. Furthermore, access problems and constraints on what type of tracers are allowed to be passed through the installation can pose further problems.

Various optical methods have been used to determine the velocity profile or passage time distribution of solid particles flowing in solid-liquid flow. Toda [5] for example, visually measured transition velocities for food particles in solid-liquid flow. Ohashi [6] used a photographic method to study the local velocities of very small particles (diameters 0,321 to 1,84 mm). Later, they developed two laser beam methods for measuring local particle concentration and velocity [7]. They found that the laser beam methods yielded more accurate results than the photographic methods, however, the optical equipment needed was costly.

Dutta & Sastry [8] &[9] used play back video taping to study the velocity distribution of particle suspensions in simulated holding tube flow. Such a technique is capable of monitoring bulk interactions in the holding tube, but requires much time and labour to analyse the results from frame to frame. Recently other visual methods have been developed for measuring the velocity and radial position of a particle in a solid-liquid pipe flow. The visual technique of particle tracking velocimetry (PVT) for example, has been used in a number of applications including that of the automobile and food industries. The velocity profile is measured using small tracers and imaging the flow in two perpendicular planes and using a specialised image analysis approach to track the paths of the individual tracers to construct a vector plot of the area of interest. Yang [10] used photo-electric sensors to produce an optical grid. When a particle passed through the grid it blocked off certain beams allowing the residence time and radial position to be recorded. Liu [11] and Lareo [12] used mirrors at 45° to the pipe to follow tracers in solid-liquid food flows, to prevent distortion a glycerol box (glycerol having a similar refractive index as the perspex pipe used) was placed around the pipe. Freget [13] also used a similar method. Visual methods are generally simple but have limited applications as low solid concentrations (about 10% max), transparent carrier fluids and pipe walls are necessary.

Radioactive techniques exist, Toda [14] used γ- ray irradiated particles in straight pipes and bends. The particle velocity was determined by the trajectory length between two scintillation probes. Fairhurst [15] used Positron Emission Particle Tracking (PEPT) to measure particle trajectories and velocities of model food particles in solid-liquid horizontal and vertical tube flow. PEPT relies on detecting back-to-back pairs of γ-rays produced when positrons annihilate with electrons. This method therefore, has the advantage of being able to track particles in metallic pipes in opaque media. The field of view of the camera is 500×500×250 mm^3 and therefore is not suited to measuring entry and exit times for large pieces of equipment, for example, long holding tubes. Radioactive techniques can also pose safety problems in industrial installations. Furthermore, PEPT is a very expensive technique.

Magnetic Resonance Imaging (MRI) can be used to measure the liquid velocity field of opaque solid-liquid mixtures. Mc Carthy [16] studied the velocity profiles of 0.5% CMC solutions with particle loadings of 10, 20, and 30% w/w for 2.5 and 5 mm alginate beads in 26.2 mm i.d. transparent perspex pipe (flowrates 2 to 18.6 cm^3/s). Tracking individual particles is not possible however by this technique. The time required to perform a scan is of the order of 10 s comparing this to the particle velocity (0.1 m/s), clearly individual particle behaviour (velocity, migration across stream lines etc.) cannot be measured. Furthermore, MRI cannot easily be applied to industrial installations, very strong magnetic fields are used (order of 1 Tesla) meaning that the machine has to be operated in a specially designed insulated room.

Different types of sensors have been developed to detect either the presence of metal foil wrapped around, or a magnet embedded in, a tracer particle. Liu [17] wrapped some foil around a tracer particle and placed two copper detection coils around the pipe which were connected to an alternating bridge. When a tracer particle passed close to one of the coils the equilibrium of the bridge was disturbed and an output voltage measured. Alternatively Segner [18] used Electromotive Force sensors (EMF) where a small magnet was embedded into a turkey cube flowing in a holding tube. Two copper coils were wound around the pipe at the entrance and exit of holding section. These coils were connected to a small potentiometer which detected the electromotive force. Both of these methods require non-metallic tube walls and are therefore not practical in most industrial installations. Hall effect sensors also detect the presence of a tracer particle in which a small magnet has been embedded. These sensors however, do not require non-metallic tube walls and are therefore ideal for measuring particle velocities in industrial installations.

2. Material and methods

2.1 Hall effect sensors

Hall effect sensors use the Hall principle. This is where a suitable material usually a semi-conductor supplied with a constant current produces an output voltage e_0 when a transverse magnetic field is applied (Figure 1).

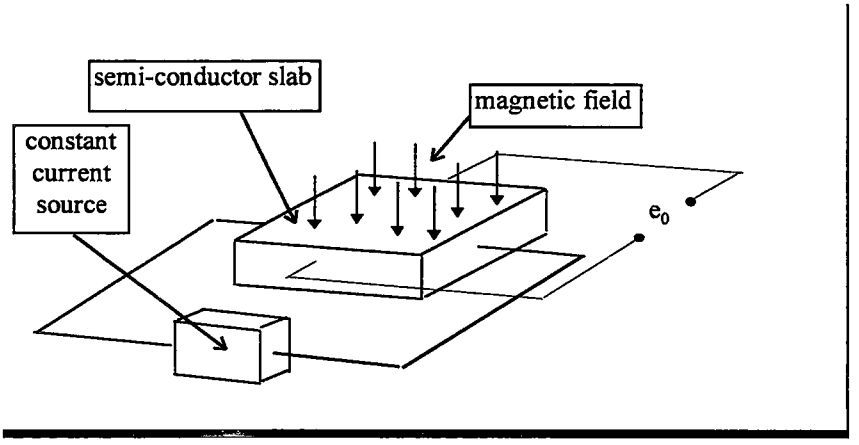

Figure 1: Hall Effect

Sensors are therefore made out of a semi-conductor material supplied with a constant current and placed around the pipe. As a result, when a tracer containing a permanent magnet passes close to a sensor, an output voltage e_0 is produced.

This hall element output voltage triggers a standard TTL circuit. The circuits used were SS94A analogue position sensors (Micro Switch, Honeywell, U.K.).

Tracers were fabricated using a quarter of a Recoma 20 magnet (Ugimag Distribution, St.Pierre d'Allevard, France), some expanded polystyrene to compensate for the density of the magnet (×7 denser than gelified sodium alginate) and some sodium alginate solution.

The magnet was dipped into a 2% (w/w) sodium alginate solution (alginate gel MP/8, Société Française des Colloïdes, Vernon, France), then into 2 % (w/w) calcium chloride solution and finally into a beaker containing ground up expanded polystyrene, before repeating the process. By this method, layer by layer of a sodium alginate and polystyrene mix coated the magnet. This process was continued until the desired particle diameter was achieved.

As the desired density of the tracers was about 2% denser than water, any slight difference in density could produce an enormous difference in the sedimentation velocity of the tracer (see below). As a result, about 100 tracers needed to be fabricated, to obtain 5 or 6 tracers with the same $v_{sedimentation}$ as that of the food product to be tested.

For example, $$v_{sedimentation} = \frac{2r^2}{9\mu}\rho_f(s-1) \quad \text{(Stokes' Flow)}$$

$$\Rightarrow v_{sedimentation}(s=1.015) = 1.5\times v_{sedimentation}(s=1.01)$$

i.e. a 50% increase in the sedimentation velocity

The error of the Hall effect sensors was determined by measuring the particle to sensor detection distance for different tracers at different radii and velocities. The maximum difference was found to be 5 mm. This relates to an error of about 1% in the passage times measured in the holding section.

2.2 Ohmic heating pilot

Passage time distribution were measured for a 10 kW ohmic system (APV Baker, Crawley, UK) located at a Technical Centre for the Preservation of Food Products (Centre Technique de Conservation des Produits Agricoles, CTCPA, Amiens, France). A schematic representation of the installation is presented in Figure 2.

The column consists of three electrode housings, each containing a cantilever electrode. The electrode housings are connected with spacer tubes constituting two heating sections. At the exit of the ohmic column, the product then entered in the holding section of the installation, through a bend and three tubes thermally isolated. Three lengths of holding tube are possible to adjust the time of thermal

treatment in function of the level of sterility required. In this experiment, the product was collected at the exit of the cooling section and was then directly returned to the pump.

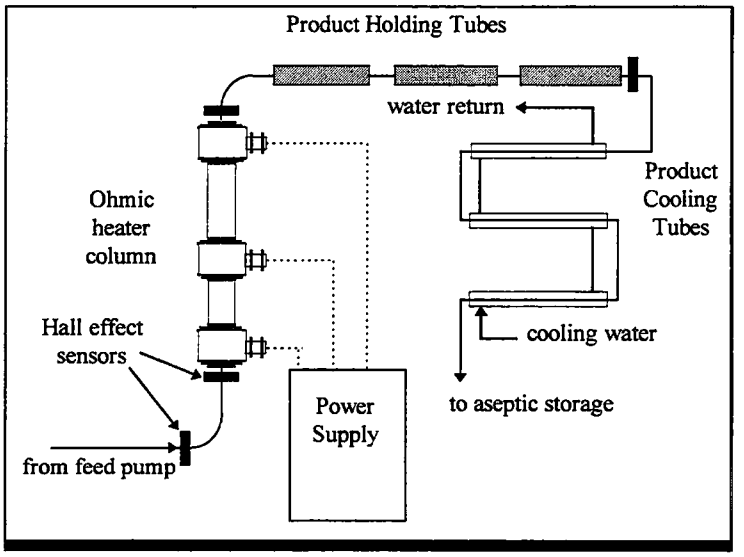

Figure 2: Schematic description of the ohmic heating installation

The description of experimental conditions used in this experiment and the process specifications are presented in Table 1.

To determine the passage time (PT) of particles in the ohmic system, four Hall effect sensors were placed on different parts of the pilot (see Figure 2) : at the beginning of the last bend before the column, at the entrance of the column (exit of the bend), at the exit of the column (entrance of the bend of the holding section), and finally at the exit of the holding tube. A minimum of 50 passage times were measured in the bend, column and holding tube. Minimum, maximum, mean passage times and standard deviations were calculated. Histograms of the distribution of passage times were plotted.

Parameters	Specifications
Bend	right-angle 30 cm (axial length)
Column	3 electrode housings 2 heating tubes
Holding	
Constitution	bend : 30 cm (axial length) tube : 120 cm
Internal diameter	48 mm
Carrier fluid	Thermtex
concentration	70g/kg
volumetric flow rate reading	200 l/h
Particles	potatoes cubes
dimension	12 x 12 mm
concentration	15kg/100kg
Temperature	20-30 °C

Table 1: Experimental conditions and process specifications

2.3 Solid-liquid food studied

The carrier fluid employed was a 7% (w/w) food grade starch solution (Thermtex, National Starch & Chemical S.A., Villefranche sur Saône, France). This solution was preheated to 100°C in a tank and then mixed with potato cubes (12 x 12 mm) delivered by Vico (Vic sur Aisne, France). The concentration of particles in the mixture was 15% (w/w) and a total weight of 130 kg of the mixture was prepared for the experiment. The temperature of the mixture during experiments varied between 20 and 30°C. The weighted flow rate was several times estimated during the experiment and varied between 223 and 230 kg/h.

3. Results and discussion

3.1 Passage Time Distribution

Minimum (PTmin), maximum (PTmax), mean Passage Times (PTmean) and standard deviations (SD) for 15% diced potatoes in 7% starch carrier fluid are reported in Table 2.

Passage Time	PTmin	PTmax	PTmean	SD
Column	85	194.4	116.6	25.2
Holding	32.7	50.1	40.7	4.1

Table 2: Passage Times of particles in the heating and holding sections of an ohmic heater

Passage times of particles in the ohmic column varied in the range 85 to 194.4 s, with an average passage time of 116.6 s. The distribution of passage times in the column is presented in Figure 3. The standard deviation of this distribution is relatively high (22% of the mean passage time), and the results show that, in the experimental conditions studied, the ratio PTmax/PTmin was around 2.3. As a result the passage time of the slowest moving particle can be more than two times that of the fastest moving particle. This information is of great importance since, in HTST processes, a small variation in passage times may result in a great variation in the heating of the particle, inducing overprocessing of parts of the product.

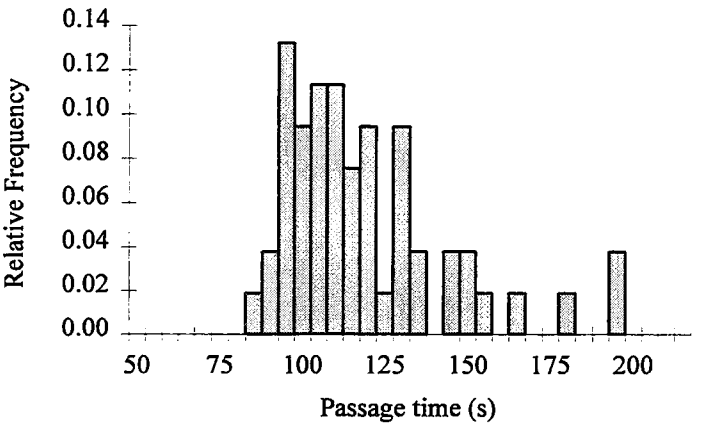

Figure 3: Passage time distribution of tracers in a heater column

Passage times of particles in the holding section varied in a 32.7-50.1 s range, with a mean passage time of 40.7 s. The distribution of passage times (Figure 4) is narrower as compared to Figure 3, and the standard deviation is 10% of the mean passage time of particles. The ratio PTmax/PTmin is only 1.5 in this case, showing that the variation between the fastest moving particle and the slowest moving particle is more reduced in this section of the pilot. This results in a better homogeneity of the lethality accumulated in particles during holding.

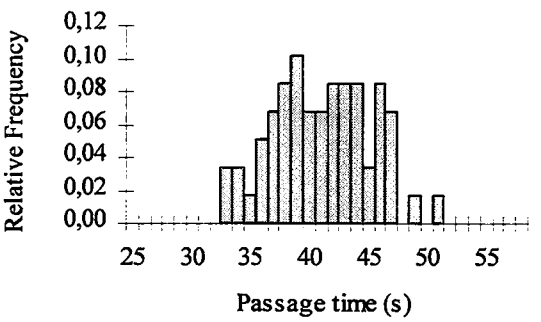

Figure 4: Passage time distribution of tracers in a holding section

The difference in the two passage time distributions is to be expected, the more complex geometry of the heating column producing a wider range of passage times. The slowest particles in the heating column would appear to indicate dead zones within the column, these particles travelled well over two times slower than the fastest particles.

Theoretical sterilising values reached during holding were predicted for both configurations (fastest and slowest moving particle) at 135 and 140°C. They are presented in Table 3. In the experimental conditions studied, these results demonstrate that the level of sterility reached by the slowest moving particle could be more than 3 times those reached by the fastest moving particle. But in the same way, the slow particle will suffer a more important cooking effect, resulting in a heterogeneous quality of the final product.

	Passage Time (s)	**$F_{135°C}$**	**$F_{140°C}$**
Slowest moving particle	50.1	20	65
Fastest moving particle	32.7	13	42

Table 3: Prediction of the level of sterility reached by the fastest and the slowest moving particles in the holding section

The velocities of particles may also be compared to the theoretical average fluid velocity in the tube of the holding section, this being calculated from the tube geometry and the flow rate (Table 4). The mean normalised particle velocity is 1.3 i.e. the particles on average flow quicker than the fluid. Such a result is probably because of particles tending to migrate to the centre of the pipe. If a parabolic type velocity profile exists, the mixture velocity will be greater near the centre of the pipe and hence particles travelling in this region will have velocities greater than the solid-liquid mixture average. Indeed approximately only the slowest 10% flow slower than the mean velocity. The maximum normalised velocity is 1.8 and is fairly close to the Newtonian fluid where the maximum velocity is twice that of the average fluid velocity, this assumption is often used for aseptic processes.

Flow rate (l/h)	200
Mean flow velocity (m/s)	0.031
Mean particle velocity (m/s)	0.040
Maximum particle velocity (m/s)	0.055
Mean normalised[1] particle velocity	1.3
Maximum normalised[1] particle velocity	1.8
10% slowest moving particles	46.3-50.1 s
10% fastest moving particles	32.7-35.1 s

Table 4. Comparison of particle and fluid velocities in the holding tube

[1] *normalised velocity = particle velocity / average solid-liquid velocity*

Conclusion

Hall effect sensors are a simple and practical method for measuring passage times of particles in solid/liquid flow. The main difficulty of this technique lies in the fabrication of tracers suitable for the product. The tracers have to behave exactly as other particles in the mixture. As this flow is governed by many parameters such as shape, dimension, concentration and weight of particles, tracers must have the same dimensions, density and the same surface properties as the other particles.

There exists however a problem between the sensitivity of sensors and the power or tracers. If the magnetic field created by tracers is too strong, the tracers do not pass through the feed pump, the magnet being attracted to iron sections or magnetic fields within the pump. If the magnetic field is too weak, the tracers will not be detected by the sensors. Appropriate tracer fabrication is hence critical in obtaining an accurate passage time distribution.

This method seems to be particularly appropriate to the measure of passage time distributions of particles in food aseptic processing systems, the sensors being easy to handle and install. Hall effect sensors can be used with heterogeneous, highly viscous, opaque carrier fluids, in laminar or turbulent flows, and in high temperature and pressure conditions. They also work whatever the type, shape, dimension, concentration and distribution of particles.

Heterogeneous solid-liquid flows are complex, in the study performed, passage times were found to vary greatly within the ohmic heating column (PTmax/PTmin>2), possibly indicating dead zones around the electrodes. Traditionally fastest particles are assumed to travel twice as fast as the average mixture velocity. In this study fastest particles in holding tube flow were found to travel 1.8 the mixture velocity indicating that this is a safe assumption, ensuring a sterile product.

Nomenclature

q	resistive power generation rate
gradV	voltage gradient
k	electrical conductivity
e_o	output voltage across a semi-conductor slice due to the Hall effect
r	radius of tracer particle
s	density ratio of solid to carrier fluid density
$v_{sedimentation}$	sedimentation velocity of tracer particle
ρ_f	carrier fluid density
μ	carrier fluid viscosity

Acknowledgements

The authors would like to thank the Conseil Régional de Picardie for their financial support and François Zuber and Frédéric Da Silva from CTCPA for their technical assistance.

References

[1] T.C.S. Yang, J.S. Cohen, R.A. Kluter, P. Tempest, C. Manvell, S.J. Blackmore, & S. Adams. Microbiological and sensory evaluation of six ohmically heated stew type foods. In *Journal of Food Quality*, Vol. 20, pp. 303-313, 1997.

[2] P.J. Skudder. Ohmic heating in food processing. In *Asean Food Journal*, Vol. 4, N°4, pp. 10-11, 1989.

[3] K. Halden, A.A.P. de Alwis & P.J. Fryer. Changes in the electrical conductivity of foods during ohmic heating. In *International Journal of Food Science and Technology*, Vol. 25, pp. 9-25, 1990.

[4] P. Zoltai & P. Swearingen. Product development considerations for ohmic processing. In *Food Technology*, Vol. 50, pp. 263-266, May 1996.

[5] M. Toda, J. Yonehara, T. Kimura, & S. Maedea. Transition velocities in horizontal solid-liquid two-phase flow. In *International Chemical Engineering,* Vol. 19, N°1, pp. 145, 1979.

[6] H. Ohashi, T. Sugawa, K. Kikuchi & T. Henmi. Mass transfer between particles and liquid in solid-liquid two phase up-flow in a vertical tube. In *Journal of Chemical Engineering of Japan,* Vol. 12, pp. 190, 1979.

[7] H. Ohashi, T. Sugawa, K. Kikuchi & M. Ise. Average particle velocity in solid-liquid two-phase flow through vertical and horizontal tubes. In *Journal of Chemical Engineering of Japan,* Vol. 13, pp. 343, 1980.

[8] B. Dutta & S. Sastry. Velocity Distributions of Food particle suspensions in holding tube flow: Experimental and Modelling Studies on Average Particle Velocities. In *Journal of Food Science*, Vol. 55, N°5, pp. 1448-1453, 1990.

[9] B. Dutta & S. Sastry. Velocity Distributions of Food particle suspensions in holding tube flow - Distribution characteristics and Fastest particle velocities. In *Journal of Food Science*, Vol. 55, N°6, pp. 1703-1710, 1990.

[10] B.B. Yang & K.R. Swartzel. Photo-sensor methodology for determining residence time distributions of particles in continuous flow thermal processing systems. In *Journal of Food Science*, Vol. 56, pp. 1076-81, 1086, 1991.

[11] S. Liu, P.J. Fryer & J.-P. Pain. The flow and velocity distributions of particles in liquids: application to food processing. In *Entropie*, Vol. 28, N°170, pp. 50-58, 1992.

[12] C. Lareo, R.M. Nedderman & P.J. Fryer. Particle velocity profiles for solid liquid flows in vertical pipes. Part II. Multiple particles. In *Powder Technology,* Vol. 93, pp. 35-45, 1997.

[13] J. Freget. Solid-liquid flow in a horizontal pipe. PhD Thesis, Lund University, Sweden, 1995.

[14] M. Toda, T. Ishikawa, S. Saito & S. Maeda. On the particle velocities in solid-liquid two-phase flow through straight pipes and bends. In *Journal of Chemical Engineering of Japan,* Vol. 6, pp. 140, 1973.

[15] P. Fairhurst, P. Fryer, J-P. Pain & D. Parker. Positron Particle Tracking Studies of High Solid Fraction Solid-Liquid Flow in Tube Flow. In *Proceedings Sensoral 98,* Montpellier, France, 24-27 February 1998.

[16] K.L. Mc Carthy, W.L. Kerr, R.J. Kauten & J.H Walton. Velocity Profiles of fluid particulate mixtures using M.R.I. In *Journal of Food Process Engineering,* Vol. 20, pp. 165-177, 1997.

[17] S. Liu, J.-P. Pain, J. Proctor, A.A.P. de Alwis & P.J. Fryer. An experimental study or particle flow velocities in solid-liquid food mixtures. In *Chem. Eng. Comm.*, Vol. 124, pp. 97-114, 1993.

[18] W.P. Segner, T.J. Ragusa, C.L. Marcus & E.A. Soutter. Biological evaluation of a heat transfer simulation for sterilising low-acid large particle foods for aseptic packaging. In *Journal of Food Processing and Preservation,* Vol. 13, pp. 257, 1989.

Determination of temperature maps using a method based on thermochromic liquid cristals (TLC)

Détermination de cartes de distributions de températures par utilisation de cristaux liquides thermochromiques

J.P. Gadonna, A.B. Jemai, C. Muller, J.P. Pain

Université de Technologie de Compiègne
Génie Chimique, Division Technologies Agro-Industrielles
Centre de Recherches de Royallieu, 60200 COMPIEGNE, France
e-mail: gadonna@utc.fr

Abstract: *Thermal treatments have been of interest to the food processing industry. Their successful implementation requires a thorough knowledge of temperature histories at every point of the treated product.*

An original non-intrusive technique has been developed to visualize and to measure temperature distributions inside a cavity (container, tube, plate...) containing either a newtonian or a non-newtonian fluid. The method consists of using Thermochromic Liquid Crystals (TLC's) as a non-intrusive temperature sensor. TLC's, type TCC1075 from Merck Clevenot, are mixed in a parallelepipedic tank with a fluid at a concentration of 0.01 % by weight. Thermochromic reaction of the liquid crystals is then observed through a white colored wide light beam generated by a complete light source system (a source equipment and a set of cylindrical lenses). Liquid crystals microcapsules reflect the incident light in a temperature range between 35 and 50°C with a color variation from red to blue as the temperature to be measured rises due to heating.

To digitalize and to treat the images, an acquisition system has then been developed and applied to obtain temperature maps. An RGB (Red, Green, Blue) video sequence is recorded using a high performance video camera, and then digitized. The images are recorded regularly beginning with the color change phenomenon. A computer program written in MATLAB® environment, converts the images from the RGB space to the HSI one (Hue, Saturation, Intensity). In the present study, we are interested only in the hue value which conveniently characterizes the color tint. A correlation linking the hue values to temperatures has been previously defined. The thermal map of a particular image can thus be established by assigning every given temperature to a hue value.

In the future, the use of this method will potentially be of interest in the fields of fluid mechanics and heat transfer, not only in small scale laboratory works but also directly in pilot scale.

Résumé : Les traitements thermiques sont très intéressants dans les procédés agro-industriels. Leur succès exige une connaissance approfondie de la cartographie des

températures du produit traité. Une technique originale non invasive a été développée pour visualiser et pour mesurer les distributions de température à l'intérieur d'une cavité (un container, tube, assiette) contenant soit un fluide newtonien soit un fluide non-newtonien. La méthode consiste à utiliser des cristaux liquides thermochromiques (TLC) comme capteur de température. Les TLC de type TCC1075 de Merck Clevenot sont mélangés dans un tank parallélépipédique avec un fluide à une concentration de 0.01%. La réaction thermochromique des cristaux liquides est alors observée à partir d'un rayon de lumière blanche généré par une source (une source et un jeu de lentilles cylindriques). Les micro-capsules contenant des cristaux liquides réfléchissent la lumière incidente à une température entre 35 et 50°C avec une variation de couleur du rouge au bleu lorsque la température à mesurer augmente pendant le chauffage.

1. Introduction

The measurement or the determination of temperature are generally achieved using three main methods: the use of thermocouples, the use of phase-change materials, and the use of Thermo-chromic Liquid Crystals (TLC).

Recent advances in the development of TLC's, have led to the resurgence of the interest in their utilization. TLC's are particularly preferred because they don't disturb the fluid flow.

Parsley (1991) and Moffat (1990) have summarized the properties of liquid crystals and presented the different applications in which they are used. Two types of TLC's are distinguished according to their chemical composition:

Cholesteric	cholesterol and other sterol-related chemicals
Chiral nematic	non-cholesterol based chemicals

A combination of these two types represents an existing third category of product.

The cholesteric and chiral nematic are generally used in heat transfer studies because they can accurately reflect color changes in a large temperature range (-30°C to 100°C).

Pure liquid crystals (LC's) are extremely difficult to manipulate because they are fragile and easily degradable. In practice, they are present under two forms:

- micro-encapsulated liquid crystals in a gel,
- non-encapsulated material trapped in a black tainted plastic sheet.

The micro-encapsulated LC's reflect about 50% of the incident light in a given temperature range. With increasing temperature, the color of the product generally passes from colorless to red, then via colors of the spectrum up to the bleu/violet to finally become colorless again. The temperature at which color change begins (red) can be any value between -30°C to +70°C. The color range (temperature difference between red and bleu colors) can be adjusted according to the user needs from 0.5 to 20°C. The liquid mixture characteristics are thus defined by the starting temperature corresponding to the red and by the color range.

These types of liquid crystals have been used in electronics as well as in aerospace research or in flow visualization and heat transfer. Surface temperature distribution maps or heat transfer coefficients have thus been elaborated (Cooper et al. 1975, Akino et al. 1989, Stoforos et al. 1990, Moffat 1990). In all cases, in order to obtain the best color reflection effect, liquid crystals must be applied on a black tainted or

dark background. And to insure a sufficiently contrasted effect, the background should be larger than the tested surface.

Liquid crystals have also been used to visualize velocity and temperature fields in liquids (Kuriyama et al. 1981, Dabiri et al. 1991, Akino et al. 1991, Braun et al. 1994, Dzodzo et al. 1994). The technique simply consists in mixing a very small quantity of liquid crystals with the fluid (water, glycerol, glycol, etc.). The micro-capsules then serve as a thermal or hydrodynamic tracers. In such studies, highly dilute mixtures are recommended; for instance, a concentration of liquid crystals in water of 0.01 % by weight largely suffices. A larger concentration of liquid crystals renders the mixture milky which causes light to disperse and color visualization difficult.

The visualization of color changes in a fluid section is possible only when illuminating this section by a fine wide white light beam. In literature, the intensity of this light source varies from one author to the other. Hence, Kuriyama et al. (1981) used a 300W Xenon lamp, while Braun et al. (1994) and Dzodzo et al. (1994) utilised a 1000W arch Xenon lamp. Akino (1991), on the otherhand, simply used a halogen lamp.

In order to generate a white light nap, these authors adopted several techniques. Kuriyama et al. and Dabiri et al. (1991) defocalized a light beam through two cylindrical lenses. This defocalized beam passes through a narrow opening dimensioned to the size of the light nap. Dzodzo et al. (1994) and Braun et al. (1994) first tried to condense the emitted light by the Xenon lamp, then to defocalize similarly to the previous authors, the light beam to generate a nap using an aligned set of cylindrical lenses.

In addition to liquid crystals and to the illumination system, a system of visualization and image treatment should be at hand in order to obtain temperature maps. In the field of TLC's, experimental setups differ from one author to the other. In 1975, for instance, Cooper et al. used several types of calibrated liquid crystals, corresponding each to a temperature range. These crystals were applied over a cylindrical surface which is then photographed. The human eye is then used to detect color changes. Colors detection using this subjective method is equally utilized later on by Kuriyama et al. (1981) and Dzodzo et al. (1994). In 1981, Kuriyama et al. qualitatively visualized color changes of liquid crystals by positioning a photo camera at 45° with respect to the light nap and by triggering a round of snap shots. More recently, Dzodzo et al. (1994) perpendicularly photographed a fluid flow using a long lap exposure time (30s.) and a low shutter opening.

In 1989, Akino et al. ameliorated the technique by eliminating the human visual perception. Using a camera equipped with band-pass filter and with an image digitalization system (256 gray levels), they spot the pixels which have the highest light intensity. For each filter, prior calibration tests had permitted to assign a

temperature to this maximum light intensity. By superposing different iso-intensity pixels they had thus been able to obtain isothermal curves.

Recent development of image treatment software came to supplement subjective analysis methods by completely eliminating human visual perception. The technique consists, in general, on acquiring a sequence of images using a video camera (color or black and white) either an NTSC composite type (video camera) or a CCD (Charged Coupled Device) or else a CID type (Charge Injected Device). The camera is generally placed perpendicular to the light nap. The images are recorded on a video tape (preferably super VHS or Hi8 type) and can be re-visualized on a hi-fi video player. These images are digitized using an appropriate system of image processing (both soft and hardware). In the majority of works (Akino et al. (1991), Dabiri et al. (1991), Dzodzo et al. (1994), Braun et al. (1994), Peterson et al. (1995), Lee et al. (1997)) , color images are obtained in the standard colorimetric space RGB (Red, Blue, Green). But this space is not the best suited to characterize colors. Consequently, authors develop or use systems to transform images from the RGB space to the HSI one (Hue, Saturation, Intensity). Only the H component is then used for the characterization of colors.

In a manner similar to that of Akino et al. (1989), calibration tests using thermocouples, are necessary to assign a given temperature to an H value. In the case of a polychromatic image, the technique consists, first, on sweeping the $[H]$ matrix, from which obtaining iso-value contours, and then via the correlation T=f(H), tracing isothermal curves.

The object of this work is to conduct experiments to obtain temperature maps inside a plastic container filled with a fluid at rest. The visualization of natural convection and conduction inside the container has thus been obtained for three types of fluids.

2. Material and methods

2.1 Fluid types

Three different types of fluids have been used throughout this study: a solution of distilled water and two viscous solutions containing carbopol® at 0.1 and 0.2%. The distilled water solution served as a Newtonian fluid and those containing carbopol® as non Newtonian ones. Carbopol® solutions have been chosen for their viscosity and transparency. They are obtained by mixing carbopol® resins EZ2 (BF Goodrich) in distilled water. A solution of NAOH at 10% was then used in order to neutralize and to increase the viscosity of the carbopol® solution. Micro encapsulated thermochromic liquid crystals (type TTC1075 by Mereck Clevenot) have then been mixed at 0.01% by weight in the three different fluids. The liquid crystals react in the temperature range of 35 to 50°C.

2.2 *Visualization of a fluid section*

A schematic of the experimental setup is represented by figure 1. Three rectangular beakers (E), made of plastic transparent material, each filled with 50ml of the three fluids, are positioned one at a time, on a temperature regulated heating plate (P) (up to 50°).

Different test sections can be visualized using an illumination system composed of a complete light source with appropriate cylindrical lenses. The light source (S) comprises a 75W Ozone-free Xenon lamp (USHIO), a universal ORIEL setup composed of a lamp receptacle, a reflector, a light condenser and a power supply for a 50 to 200W arching lamp.

In order to vertically generate a fine wide white light nap, two plano-cylindrical lenses having dimensions of 25x12 mm (f/12.7 mm) and 60x50 mm (f/150 mm), are used between the light source and the test beaker.

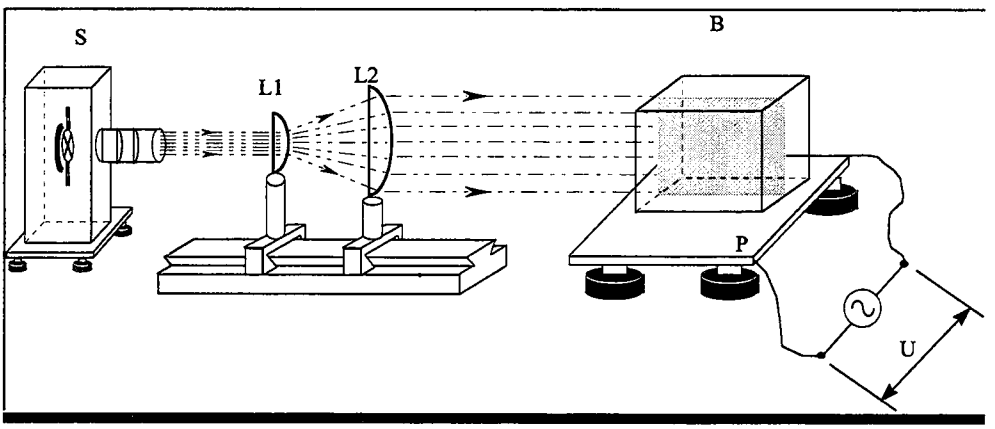

Figure 1: Illumination system

2.3 *Images acquisition and digitizing*

The technique of thermal cartography requires recording the observation on a video support and an adequate image treatment. Figure 2 shows the system used.

RGB video images are continuously recorded on a Hi8 tape using a VCR (Sony EV-S800B) and a video camera (CCD Sony) connected to a color monitor. The visualization of liquid crystals color changes is best obtained by positioning the camera at a 45° angle with respect to the white light nap.

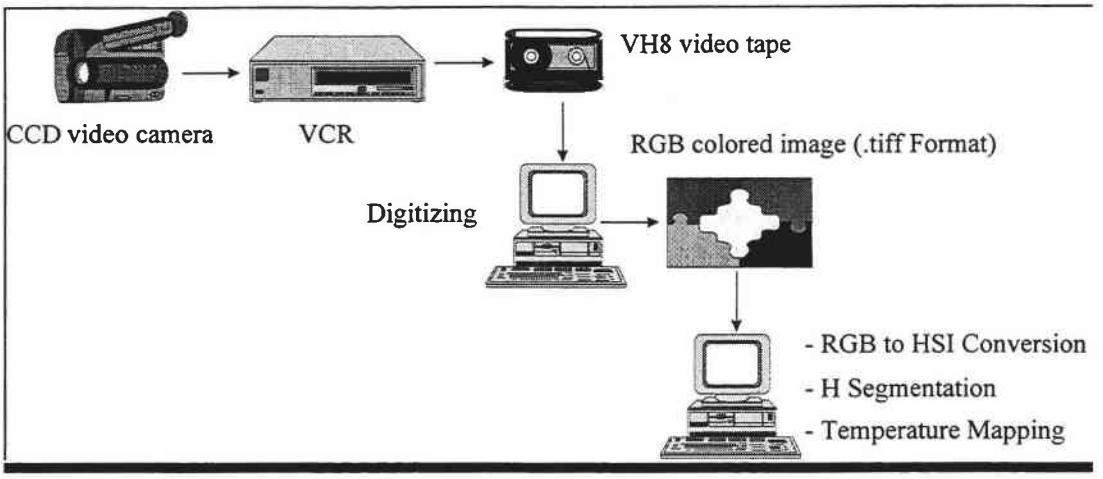

Figure 2: Acquisition and image treatment system

Once video recording is obtained, the needed images are digitized and treated using a computer. The digitization is performed via an adequate card and a software (video machine by FAST).

Appropriate images are taken at the rate of one image every 10 seconds beginning from the moment when color change starts. All images are recorded under the format ".TIF" with 256 color levels (8 bits) then treated using a computer program written under the MATLAB© environment.

2.4 Image processing

In order to obtain temperature maps, a computer program requiring the tool box "Image Processing" of MATLAB©, was written. The program algorithm is given by figure 3.

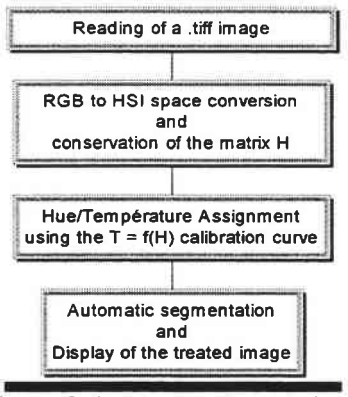

Figure 3: Image treatment algorithm

2.5 Color analysis

The International Commission of Lighting (ICL) has created color space standard known as the RGB. In this space, an image is represented by 3 color matrices : R (Red), G (Green), and B (Blue). Any given color X in an image is in fact a combination of these three primary colors ; hence, it can be written as X = r(R) + g(G) + b(B).

In reality, the RGB space does not characterize best colors. Other coordinate systems such as the XYZ, LUV, LAB, HSI, etc., have thus been devised.

In the present study, the HSI system is perfectly convenient for the characterization of the colors at hand. The hue value, representing the color taint, is the only parameter of interest.

When using the MATLAB functions, all matrix values are indexed (i.e. between 0 and 1). Consequently, contrary to the literature, the hue values used here are 0<H<1.

2.6 Hue/Temperature calibration curve

In order to trace temperature maps, it is necessary to indicate, before hand, the correlation between hue values and temperature for each type of TLC. The calibration step is performed by progressively elevating the temperature of the water-TLC mixture. A thermocouple submerged inside the beaker is used to obtain actual temperature values of the liquid. Images in areas surrouding the thermocouple, are recorded using the acquisition system. Average hue values as well as temperature readings are thus obtained. The operations are reproduced several times in order to estimate experimental errors occasioned by this technique. The results of this calibration scheme including errors are given by figure 4.

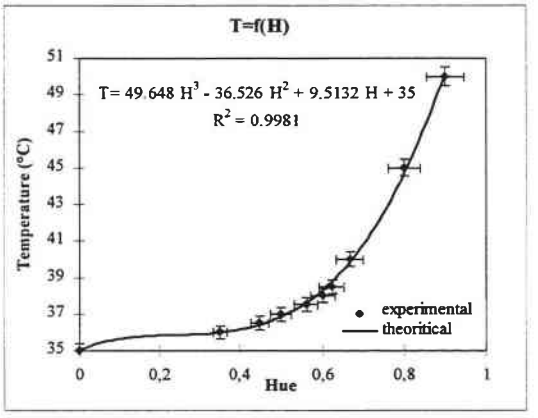

Figure 4: Calibration curve for the TCC1075 liquid crystals

2.7 Experimental procedure

It consists of exerting a temperature gradient on the fluid so as to observe the heat transfer phenomenon taking place as a result. To do this, a metal plate is heated up electrically to a set temperature of 50°C ; the beaker containing the liquid mixture initially at 20°C, is then placed on top of it. A temperature gradient is consequently instantaneously created from bottom to top. Color change phenomena taking place inside the beaker, are then recorded.

3. Results and discussion

The evolution of heat transfer as a function of time inside the rectangular container is given in Figure 5. The first four images show the evolution for the water solution after time periods of 2, 2.5, 3 and 5 minutes. The following four images characterize heat transfer evolution for the first carbopol® solution (0.1%) at 2, 3, 5 and 8 minutes. The last four images correspond to the second carbopol® solution (0.2%) at 2, 3, 5 and 10 minutes.

These images clearly show that the more viscous a solution is, the more slowly thermal equilibrium becomes. In the case of Newtonian fluid (water solution), a natural convection movement is obtained as a result of heating. While for a non Newtonian fluid, only thermal conduction is present.

In the case of a Newtonian fluid, irregularly shaped isotherms known as "Bénard" cells reflect the presence of complex heat transfer mode. In addition to an overall bottom to up heat transfer, heat packets having a rotational movement are distinguished. Thermal equilibrium is attained when the rotation of these packets has stopped.

In contrast, in the case of a non Newtonian fluid, the image analysis clearly reveals that heat transfer is for the most part obtained by conduction. For instance, in the case of 0.1% carbopol®, the images show that heating takes place mainly by successive horizontal layers. Nevertheless, as heating proceeds, the thermal front seems to curve from one snapshot to the other. This phenomenon maybe explained by the fact that in addition to bottom-to-top conduction a second heating effect is taking place. In fact, as heating proceeds, heat coming out of the container walls causes the fluid to heat up laterally and so regions closer to the walls heat faster than those in the center of the container. This is not the case for the 0.2% carbopol® where the images show that heating due to the walls is not significant compared to that coming from the plate. This shows that in addition to fluid type, viscosity affects the heating mode.

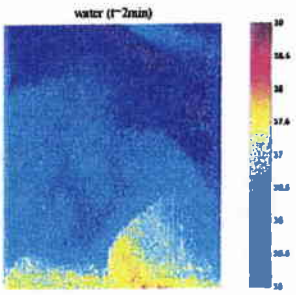
water (t=2min)

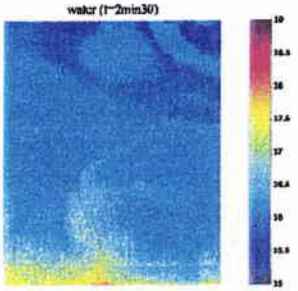
water (t=2min30')

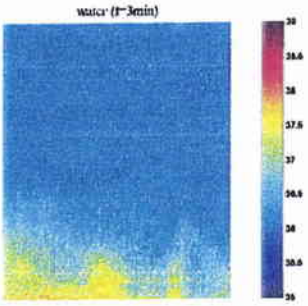
water (t=3min)

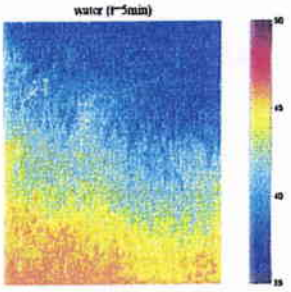
water (t=5min)

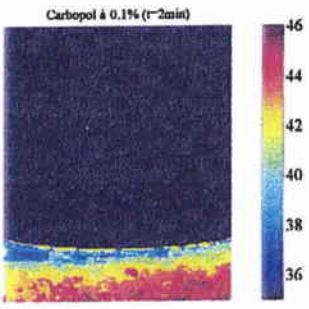
Carbopol à 0.1% (t=2min)
46
44
42
40
38
36

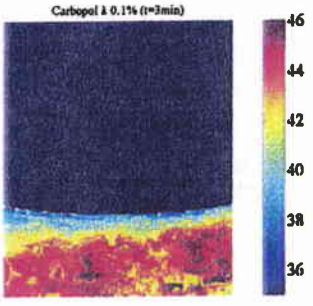
Carbopol à 0.1% (t=3min)
46
44
42
40
38
36

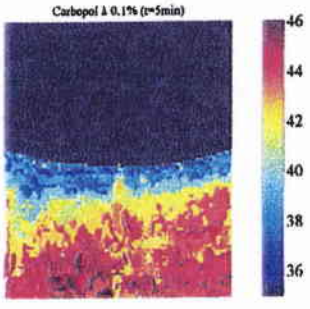
Carbopol à 0.1% (t=5min)
46
44
42
40
38
36

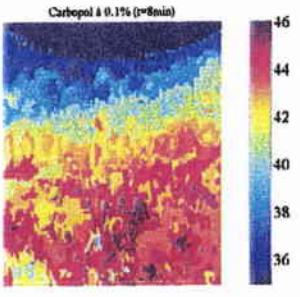
Carbopol à 0.1% (t=8min)
46
44
42
40
38
36

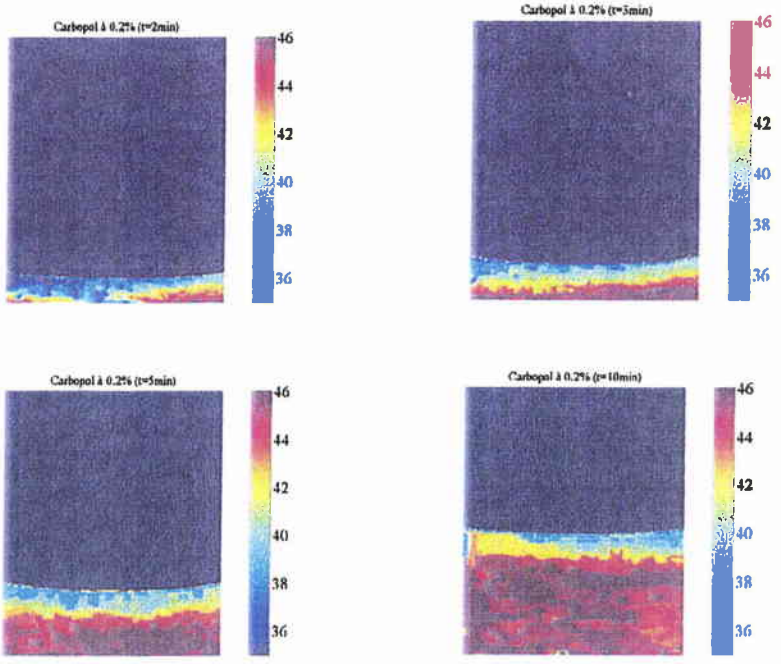

Figure 5: Temperature maps In the fluids

Conclusion

The work conducted in this study has allowed to validate an original method of thermal mapping in a stationary fluid. The experimental procedure uses thermochromic liquid crystals (TLC's) in a mixture (water, carbopol® at 0.1% and 0.2%), a visualization system, and an appropriate image processing computer program. The application of the method is illustrated in the study of natural convection and conduction inside a closed rectangular cavity. The results stemming from this study show that it is possible to characterize a heat transfer without the need to use an intrusive sensor such as thermocouples or others. Indeed, solutions containing thermochromic liquid crystals allow to adequately study heat transfer phenomena. Rigorous experimental procedures coupled with an adequate images analysis system can be extremely useful in conducting such a study. In future, this technique would be potentially useful in heat transfer studies and temperature sensors development for measurement conditions in which intrusive sensors such as thermocouples are not appropriate.

References

[1] AKINO, N., T. KUNUGI, et al. Improved liquid-crystal thermometry excluding human color sensation. *Journal of Heat Transfer* ,111: 558-565, 1989.

[2] AKINO, N., T. KUNUGI, et al. Thermo-chromatic characteristics of liquid-crystal suspensions. *2nd Symposium on Experimental and Numerical Flow Visualisation*, ASME Winter Annual Meeting, Atlanta (Georgia,USA), 1991.

[3] BEJAN, A. *Convection Heat Transfer*, John Wiley & Sons, New York, 1984.

[4] BRAUN, M. J., F. K. CHOY, et al. A non intrusive computer automated method for temperature and velocity evaluation based on thermochromic liquid crystals. *Imaging in Transport Processes*, 1994.

[5] COOPER, T. E., R. J. FIELD, et al. Liquid crystal thermography and its application to the study of convective heat transfer. *Journal of Heat Transfer* , **97**: 442-450, 1975.

[6] DABIRI, D. and M. GHARIB. Digital particle image thermometry : the method and implementation. *Experiments in Fluids* , **11**: 77-86, 1991.

[7] DZODZO, M. Visualisation of laminar natural convection in romb-shaped enclosures by means of liquid crystals. *Imaging in Transport Processes*. 1994.

[8] DZODZO, M., M. J. BRAUN, et al. (1994). A non intrusive computer automated investigation of natural convection using thermochromic liquid crystals and comparison with numerical simulation. *Proceeding of the 10th international heat transfer conference*, Brighton (UK), 1994.

[9] KURIYAMA, M., M. OHTA, et al. Heat transfer and temperature distributions in a agitated tank equipped with helical ribbon empeller. *Journal of Chemical Engineering of Japan* **14**(4): 323-330, 1981.

[10] LEE, K. C. and M. YIANNESKIS. Measurement of temperature and mixing time in stirred vessels with liquid crystal thermography. *Récent Progrès en Génie des Procédés*. 1997.

[11] MOFFAT, R. J. Experimental heat transfer. *Proceeding of the 9th international heat transfer conference*, Jerusalem, 1990.

[12] PARSLEY, M. The use thermochromic liquid crystal in research applications, thermal mapping and non-destructive testing. *Proceeding 7th IEEE semi thermal symposium*. 1991.

[13] PETERSON, D., S. H. HU, et al. The measurement of droplet temperature using thermochromic liquid crystals. *30th National Heat Transfer Conference*. 1995.

[14] STOFOROS, N. G. and R. L. MERSON .Estimating heat transfer coefficients in liquide/particulate canned foods using only liquid temperature data. *Journal of Food Science*, **55**(2): 478-483, 1990.

Measurements play an essential role in finnish food processing industry

Les mesures jouent un grand rôle dans l'industrie agro-alimentaire finlandaise

Markku Känsäkoski

VTT Electronics, P.O. Box 1100, FIN-90571 OULU, Finland
Tel +358 8 551 2290, Fax +358 8 551 2320
e-mail: markku.kansakoski@vtt.fi

Abstract: *The measurement needs in Finnish food processing industry have been studied. An inquiry sheet was sent to over 200 companies, of which 78 answered the survey. The answers covered a wide range of manufacturing branches, e.g., bakery, dairy and meat industry. Food processing companies in Finland are typically small-scale manufacturers, featuring a versatile product mix and relatively rapid changing of products in the production lines. Quality control is essential in food industry, and efficient quality assurance is becoming increasingly important. The most important objectives in food production are hygiene, uniform quality of raw materials and final products, along with product safety, which is considered very important by almost all food processing companies. The development of new measurement techniques was found to be the most important factor in improving the quality of products and the efficiency of food processing.*

Keywords: *Food, processing, industry, measurement, quality.*

Résumé : Les besoins en mesures des industries agro-alimentaires finnoises ont été étudiés. Un questionnaire a été envoyé à 200 industries et 78 réponses ont été reçues. Les réponses couvrent une grande gamme de branches : panification, industries de la viande ou des produits laitiers.

Les IAA finnoises sont typiquement de petite taille, proposant une gamme de produits et changeant rapidement de produits sur leurs lignes. Le contrôle de qualité est essentiel et l'assurance qualité a pris beaucoup d'importance.

Les objectifs les plus importants sont l'hygiène, la constance de la qualité des matières premières et du produit final, la sécurité alimentaire qui est considérée comme essentielle par presque toutes les industries. Le développement de nouvelles méthodes de mesures a été mentionné comme le facteur primordial pour améliorer la qualité des produits et la compétitivité des IAA.

1. Introduction

When Finland joined the European Union in 1995 many experts were afraid of the common European market possibly proving harmful to the national food industry sector because of more stringent competition. However, Finnish companies have survived well in this new situation. Finns have been, and still are, highly quality-oriented consumers, who know how to appreciate a high quality of foods. Consumers are more and more aware of competing products, and so manufacturers must be prepared for a strong competition. High quality, safety, large assortment and a competitive pricing of products are becoming more and more important. Consequently, manufacturers are now calling for improved processes, better process control and advanced logistics.

The process control commonly used today is very often manual or semiautomatic and it is highly dependent on the experience of the operator. The operator controls not only the physical properties objectively, but also sensorial properties subjectively, i.e. taste, smell, appearance and structure. The development of analytical measurements and their combination with physical measurements is of vital importance when increasing productivity, improving quality and producing safer products.

The need for adequate process control and a better knowledge of the raw materials and the process itself are the main reasons for developing new tools for controlling the process and for measuring the quality of the raw material and that of the final product. Fast, simple, accurate and preferably on-line measurements and analysis of production chains will improve the quality of processes and products. In the 1980's the automation level in food processing industry (like in all processing industries) started to rise rapidly. The most important contributing factor was the development of the microprocessor, which made it possible to create more complex control algorithms and systems. Thus it was possible to replace batch processes with automated production methods. Although the methods, devices and systems for process control and measurements are more advanced now, they can only be applied to food processes, if the operating principles of the instruments and the properties of food processes are understood well enough. The latest measurement methods, devices and applications give more information of the food, processes and their interplay. Table 1 summarises some requirements for on-line instruments in food processes. [1]

❑ reliable
❑ free from contamination
❑ hygienic sensing head
❑ no foreign part hazard
❑ cleaning tolerant
❑ maintenance free
❑ total cost is affordable
❑ repeatable measurements
❑ robust
❑ no interference to process
❑ no need for highly skilled operator
❑ no need for calibration or simple calibration procedure

Table 1: The requirements for on-line instruments

Food processing in Finland is typically small-scale manufacturing, where the product mix is wide and different products change rapidly in the production lines. Consumers are also expecting a wide range of competitively-priced food products of consistently high quality. Quality control is essential in the food industry, and efficient quality assurance is becoming increasingly important. Skjöldebrand [2] also expects new techniques to appear, e.g., biosensors, crispiness sensors, on-line water activity measurement, etc.

2. The process of this review

The measurement needs in Finnish food processing industry have been studied. A group of companies, all with more than 50 employees, were selected for this review. An inquiry form was sent to over 200 companies, of which 78 answered with a good percentage 35%. The answers covered a wide range of food manufacturing branches, e.g., bakery, dairy and meat industry. The answers were still supplemented with interviews. Representatives from six most active manufacturing branches (bakery, dairy, meat, feed, convenience food and sugar industry) answering to this review were selected and interviewed. Two bakeries were selected, because bakeries were most active in this survey. The inquiry form was rather long, comprising nine pages. However, obviously the subject was interesting enough, as a good number of answers was received. The inquiry form contained questions concerning background information, production objectives, expectations for R&D work and a broad variety of different aspects of measurements for present and future needs. All the answers were handled confidentially and only a summary of these answers is presented here.

3. Summary of the results

The answers covered almost all food manufacturing branches, bakeries being most active in responding, see Figure 1 [3]. Larger groups (branches) will be handled in more detail later. The group «Others», one of the largest, covers a large number of replies from various smaller fields. In general, only one or two answers were received from a single branch. It is not possible to make any general assumptions based on only a one or two opinions.

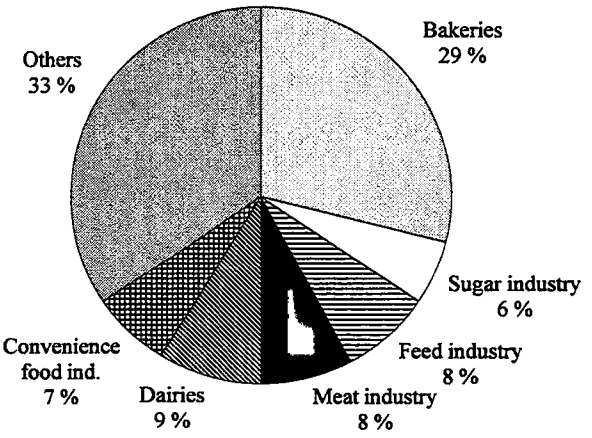

Figure 1: The distribution of answers into different food manufacturing branches

Food processing in Finland is typically small-scale manufacturing, which is also reflected in the answers. The turnover was typically less than 100 million FIM. Also the number of people involved in R&D is rather low in these companies, typically 1 to 5 persons. The same number of employees is also typically working in the field of process automation, measurement and analysis. It is also remarkable that almost 20% of the companies in this review did not have any employees assigned to process automation or measurement.

The most important objectives in food production are: uniform quality of raw materials and final products, hygiene and product safety, which almost every company finds very important as regards their production, see Figure 2 [3, 4].

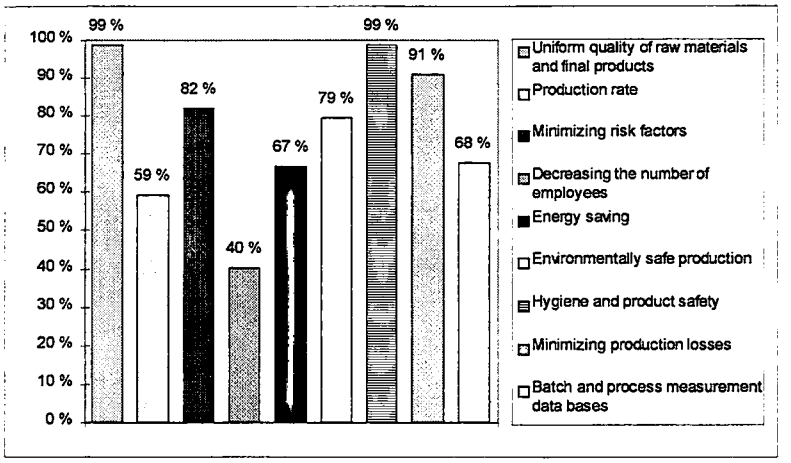

Figure 2: Main objectives in food production in Finland

Measurements play a key role in quality assurance. Over one third of the Finnish companies replying this review consider measurements very important to their production. The rest of the companies find measurements at least significant. Measurements are highly regarded especially in the dairy and sugar industry. Over 50% of the companies were working on projects to develop process measurements and automation.

The most important features to be measured for raw materials, intermediate and final products are: moisture, temperature, protein, pH, ash, fat, sensory properties, pressure, foreign bodies, micro-organisms, reservoir level, mass and volume flow, see Table 2 [3].

Property measured in processes	*A*[a] */%*	*B*[a] */%*	*C*[a] */%*	*D*[a] */%*	*E*[a] */%*	*F*[a] */%*	*G*[a] */%*
Temperature	83	**77**	**100**	**100**	71	**100**	**100**
Sensory properties	62	62	75	71	57	67	40
Foreign bodies	59	54	75	71	14	67	60
Reservoir level	58	31	75	29	71	67	**100**
Time	56	62	63	86	14	**100**	40
Moisture	53	58	25	57	57	50	60
Mass flow	50	23	63	14	71	67	**100**
Pressure	50	23	88	57	**86**	67	80
pH	49	38	**100**	71	43	50	**100**
Volume flow	41	15	75	29	**86**	83	80

[a] A = All; B = Bakeries; C = Dairy Industry; D =Meat Industry; E = Feed Industry; F = Convenience Food Industry; G = Sugar Industry

Property measured in laboratory	A[a] /%	B[a] /%	C[a] /%	D[a] /%	E[a] /%	F[a] /%	G[a] /%
Moisture	59	42	50	57	43	83	60
Micro-organisms	55	46	**100**	**86**	14	**100**	80
Sensory properties	55	31	75	71	14	**100**	80
pH	55	**50**[b]	63	71	29	**100**	80
Protein	46	27	75	71	43	83	40
Ash	45	35	38	57	86	83	**100**
Fat	42	15	75	71	71	**100**	0
Carbohydrates	40	23	38	43	43	83	**100**
Pathogens	35	15	75	**86**	29	**100**	40
Colour	35	12	13	29	29	33	**100**

Table 2: Typical properties measured in processes and laboratory

In improving the quality of products and the efficiency of production, the development of new measurement techniques is regarded as the most important factor. The most attractive techniques include cultivation, near infrared, colour measurement, colour machine vision, machine vision, electronic nose, microscopic rapid methods and optical moisture measurement techniques, see Table 3 [3].

Measurement technique	A[a] /%	B[a] /%	C[a] /%	D[a] /%	E[a] /%	F[a] /%	G[a] /%
Cultivation	19	23	25	57	14	67	20
Near Infrared (NIR)	19	8	0	29	14	33	80
Colour Measurement	18	8	13	29	0	67	20
Colour Machine Vision	18	12	13	43	0	83	40
Machine Vision	17	8	13	43	0	50	20
Electronic Nose	17	8	13	29	14	33	60
Microscopic Rapid Methods	17	15	0	43	14	50	40
Optical Moisture Measurement	13	8	13	14	14	17	40
Texture Measurement	12	12	0	14	14	50	0
Fourier Transform Infra-Red Spectroscopy (FTIR)	10	4	0	0	14	17	80

Table 3: Ten most interesting measurement technologies

The interviews confirmed that the questions in the rather complex and long inquiry form had been understood, thus the results achieved in this review can be regarded as reliable. Some aspects were more present in the interviews than in the answers received. Most of the people interviewed were not satisfied with the level of

[a] A = All; B = Bakeries; C = Dairy Industry; D = Meat Industry; E = Feed Industry F = Convenience Food Industry; G =Sugar Industry

instrumentation for detecting foreign bodies. These instruments were considered difficult to use and dedicated to only one type of foreign body, e.g., metal. Furthermore, and the instruments were thought to be unreliable and rather expensive. The on-line measurement of particle size was also considered a big problem. There are several different laboratory-scale particle size measuring instruments (also very expensive) available, but there is a distinct lack of equipment for on-line particle size measurement and control. In Finland food processing is typically small-scale manufacturing where the product mix is wide and different products change rapidly in the production lines. Therefore, the demand for automation flexibility is high. Unfortunately, the availability of such systems is limited, while most of the control systems are designed for higher volumes and smaller mix.

Conclusion

This review project has made it possible to identify a number of important factors in food processing industry that are calling for further research and development. The development of new on-line measurement equipment is considered to be of great importance. For optimum quality assurance the manufacturer requires cost-effective methods for rapid assessment, preferably on-line, of chemical and physical properties and microbial status of raw materials, process streams and end products.

Finnish companies are very interested in co-operating with national research institutes and universities to find some added value for their R&D-work. Unfortunately, only larger Finnish export companies find international, especially European, R&D co-operation interesting. The idea of participating in pan-European R&D work is still very young in Finland, though the chance of joining common EU programmes has been there for several years now. Some effort is still needed to encourage the SME companies to join EU projects and to propose new ones.

Acknowledgements

Technology Development Centre Finland is greatly acknowledged for financing this project. A great deal of work in this project was done by Jaana Suutarinen VTT Bio- and Food Technology and Eero Hietala VTT Electronics, to whom I wish to render special thanks. I'd also like to thank all the people in Finnish food industry for spending their valuable time answering the inquiry and many other questions during this project.

References

[1] Erika Kress-Rogers (ed.), *Instrumentation and Sensors for the Food Industry*, Butterworth-Heinemann Ltd, Oxford, 1993, p. 780.

[2] Christina Skjöldebrand, On-line sensors - tools for increased productivity and greater efficiency, *The European Food & Drink Review*, Autumn 1996, pp. 71-75.

[3] Markku Känsäkoski, Jaana Suutarinen, Eero Hietala, Elintarviketeollisuuden mittaukset, *Teknologiakatsaus 51*, TEKES, 53 p., 1997.

[4] Markku Känsäkoski, Prosessimittausten kehittämisellä tehokkuutta elintarviketuotantoon, *Tekniikan näköalat,* vol. 3, 1997, pp. 12-13.

Determination of the residence time distribution in an experimental conditioner by a fluorescence video imaging

Détermination de la distribution du temps de séjour par imagerie fluorescence

B. Novales

INRA Nantes
LTAN BP 71627
44316 Nantes Cedex 03
e-mail : novales@nantes.inra.fr

J. Mabit

TECALIMAN BP 71627,
44316 Nantes Cedex 03

Y. Riou

TECALIMAN BP 71627,
44316 Nantes Cedex 03

Abstract: *In the present work, a fluorescent marker (fluorescein) was used for the determination of the RTD in an experimental conditioner. For the RTD determination, 50 g of marked particles were injected in the conditioner. A sample was collected at the outlet of the conditioner each 10 seconds from 30 to 230 seconds after the injection. The fluorescent particles were detected with a video imaging system The results showed that it was possible to predict the percentage of marked particles in the samples with a correlation coefficient of 0.987 and the residence time distribution was expressed as the predicted percentages of marked particles at the outlet of the conditioner as a function of time after injection.*

Keywords : *Residence time, video imaging, fluorescence.*

Résumé : Un marqueur fluorescent (fluorescéïne) est utilisé pour déterminer la distribution des temps de séjour (DTS) dans un conditionneur expérimental. Pour cela, 50 g de particules marquées sont introduites dans le conditionneur. Un échantillon est prélevé à la sortie du conditionneur toutes les 10 secondes de 30 à 230 s après l'injection. Les particules fluorescentes sont détectées par un système d'analyse d'images. Il est possible de prédire le pourcentage de particules marquées dans l'échantillon avec un coefficient de corrélation de 0,987. La DTS est exprimée par le pourcentage de particules marquées à la sortie du conditionneur en fonction du temps après injection.

1. Introduction

In the animal food industry, the destruction of pathogen agents, such as salmonella, involves a hydrothermic treatment [1]. The most commonly used processes to realize this treatment are realized on conditioners with a continuous flow rate. These processes are efficient if the treatment is applied the same time for all the particles. The efficiency is then depending on two parameters : time and temperature. The time parameter is the most difficult to control due to the residence time distribution (RTD) phenomenon.

A theoretical approach of the behavior of a conditioner uses the concept of a perfect reactor with two kinds of flow : plug flow and continuous stirred flow. The total time spent by a particles in the conditioner corresponds to the residence time. The plug flow is characterized by an unique residence time for all the molecules. In a continuous stirred flow, any residence time can be observed and the composition is uniform in every point. The combination of these two kinds of flow allows the description of more complex reactors [2]. In a real reactor, the particles can stay on the reactional volume during variable times depending on the hydrodynamic profile and the geometry of the reactor. This phenomenon leads to a distribution of the residence times [3]. In a process of destruction of pathogen agents, it is very important to have a perfect control of the time parameter because particles having the shortest residence time could quit the conditioner without being decontaminated. The determination of the residence time distribution can be done by applying an input signal with a tracer injected in the flow or by marking the particles [4]. The tracer may be radioactive, a dye or any molecule having the same hydrodynamic properties than the particles. It may not react during the hydrothermic treatment and not modify the particle flow. The choice of the tracer depends on many parameters including the scale of the experiment (some tracers are not allowed at an industrial scale but can be used for laboratories experiments), its stability to steam, its extractability...

Different kinds of injections of the tracer can be used to determine the residence time distribution. The two main methods are called step and pulse injection. In a step injection (Step Heavyside function), at a time t=0, the tracer is continuously feed into the reactor. In a pulse injection (Pulse Dirac function), a small amount of tracer is instantaneously injected at a time t=0. The concentration of the tracer in the particle flow leaving the conditioner is analyzed as a function of time.

From the residence time distribution, it is possible to compute various parameters such as the mean residence time and the variance of the distribution. The mean residence time can be calculated according to the following formula :

$$\bar{t} = \frac{\int_0^\infty tC(t)dt}{\int_0^\infty C(t)dt}$$

with C(t) the concentration of tracer at a time t.

This parameter can be used to identify a malfunction in the reactor, to predict the model and the kind of flow in the reactor. The variance σ^2 which is indicative of the spreading around the mean residence time is often used to characterize the RTD. This parameter can be obtained according to :

$$\sigma^2 = \frac{\int_0^\infty t^2C(t)dt}{\int_0^\infty C(t)dt}$$

In the present work, the use of a fluorescent marker was investigated for the determination of the residence time distribution in an experimental conditioner. The fluorescence corresponds to the emission of light by a molecule at a given wavelength after excitation of this molecule by a specific radiation at a lower wavelength [5]. In the present study, the fluorescent particles injected in the conditioner were detected by a video imaging system [6].

2. Material and methods

2.1 Feed description

The feed used for the determination of the residence time distribution was a maize ground with a FORPLEX grinder through a grid of 3 mm. The feed obtained had a mean diameter of 593 µm, a volumic mass of 617 g/l and a moisture rate of 13 %.

2.2 Tracer

The fluorescein tracer was prepared by embedding maize with a fluorescein solution at a concentration of 5g/l. The maize used for the fluorescence tracer had the same particle size distribution than the feed. Ten liters of solution were used to mark 18 kg of maize. After one hour of mixing and 48 h of wetting, the tracer is washed on a büchner filter and dried on an incubator in order to obtain the original moisture. The volumic mass of the tracer was 592 g/l. The fluorescein tends to agglomerate the particles of maize leading to a mean diameter of the tracer of 771 µm. The moisture rate of the marked particles was 16.4 %.

2.3 *Conditioner description*

The conditioner used during this study was an experimental conditioner built in the laboratory [7]. The shaft speed ranged from 1 to 3000 rpm. The internal diameter of the conditioner was 100 mm. The total volume of the reactor was 3756 cm^3 and the accessible volume was 2720 cm^3. A steam injection could be realized inside the conditioner for a hydrothermic treatment. A modification of the tracer inlet allowed the injection of 50 g of tracer in less than one second.

For the RTD experiments, a pulse injection was used. The feeding rate was 40.4 kg/h. The shaft speed was set at 42 rmp. These settings allowed a spending time of 107 seconds. This spending time was calculated according to the volume filled by the feed for a filling ratio of the conditioner estimated at 66 %. All of the experiments were completed without steam injection.

2.4 *Residence time distribution*

It was necessary to calibrate the video imaging system before realizing the RTD determination. For this purpose, a calibration set of samples was prepared by adding the fluorescein tracer in the feed samples with a proportion of marked particles ranging from 0 to 25 %. A calibration equation was calculated from these samples, which was used for the RTD determination. For the RTD determination, 50 g of marked particles were injected in the conditioner. The fluorescent particles were detected with the video imaging system and the RTD was expressed as the percentage of marked particles at the outlet of the conditioner as a function of time after injection.

A sample was collected at the outlet of the conditioner each 10 seconds from 30 to 230 seconds after the injection. The residence time distribution was normalized by dividing each value by an equivalent concentration (7.188 marked particles/g). The equivalent concentration was obtained by considering that the tracer is uniformly spread in the reactional volume. The RTD was also corrected by dividing each value by the recovery rate.

2.5 *Image acquisition system*

The prototype used for the image acquisition was developed by Novales et al. [8]. The image acquisition system included a 200W mercury vapor lamp, a cooled-CCD camera with the PMIS image processing software (Photometrics, USA), and two filters in order to observed specifically the fluorescein fluorescence. In the present work, the fluorescein fluorescence was obtained by placing an excitation filter at 486 nm behind the lamp and an emission filter at 510 nm behind the camera. The camera, with a Nikon 55 mm photographic lens, was placed about 12 cm above the sample cell. Each image corresponded to a rectangular surface of the sample measuring 30 x 30 mm. The images were digitized with a resolution of 512 x 512

pixels. Intensity values were coded on 14 bits resolution (with 0 corresponding to black and 16383 to white). Ten images were recorded for each sample.

2.6 Image processing

Erosion, a basic operation of mathematical morphology [9], was used in order to estimate the proportion of marked particles in the images. This method which is usually applied to binary images can be easily implemented for gray level images [10]. The operation is applied to the image through a structuring element of a given size and shape. A very usual structuring element is a square of size 3x3 with a reference pixel at the center of the square. The structuring element is successively moved over all the image. The erosion consists in searching the minimum value of all the pixels covered by the structuring element. The minimum value is then attributed to the reference pixel. For white objects on a black background (like fluorescent particles in a non-fluorescent feed sample), when the structuring element is not totally enclosed in an object, the minimum value is the background value and the object size decreases. It is possible to apply successively the erosion until all the objects in the image have disappeared.

For each image, 100 erosions steps were performed. At each erosion step, the volume of the image (sum of all the gray level) was measured in the resulting image. The volume is characteristic of the decrease in the gray level values at each erosion step. By gathering the remaining volume at each erosion step with the volume of the original gray level image, 101 values were obtained. For each image it was possible to obtained « erosion curves » that were considered for each image as a continuous signal and treated by statistical analyses.

2.7 Statistical analysis of the erosion curves

The erosion curves were treated by Principal Component Analysis (PCA) [11]. From the original variables, PCA calculates synthetic variables called « principal components » which are uncorrelated and describe the main variations observed among the samples. The percentage of the total variance of a principal component indicates the amount of variation of the original data table it describes. Similarity maps can be drawn by plotting the scores of two principal components.

The proportion of fluorescein marked particles in the calibration set was predicted by Principal Component Regression (PCR). PCR is simply a multiple regression for which the original variables have been replaced by their principal components [12]. The principal components were introduced in order of their predicting ability. A calibration equation was obtained that was used for predicting the percentages of marked particles in the samples collected at the outlet of the conditioner. The RTD was expressed as the percentage of marked particles in the samples as a function of time.

All the image processing and mathematical softwares were developed in C language in the laboratory.

3. Results and discussion

An example of images obtained with the video imaging system is shown figure 1. As the background constituted by the feed was absolutely not fluorescent, the marked particles appeared white on a black background. Obviously, the number of fluorescent particles was more important with the increase of the percentage of marked particles. Even at very low concentration (0.2 % of marked particles) it was possible to detect the fluorescent particles in the feed.

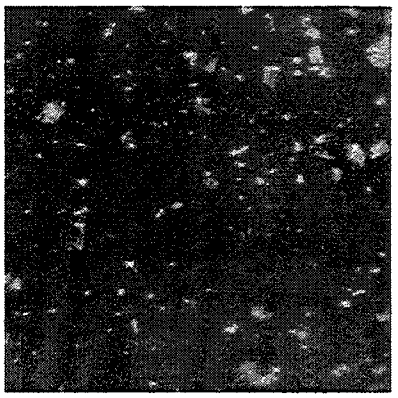

Image of feed with 5 % of fluorescent particules

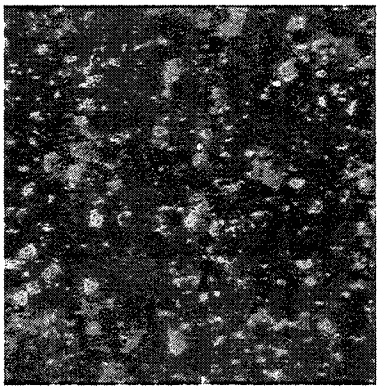

Image of feed with 25 % of fluorescent particles

Figure 1: Images of fluorescent particles in feed samples

The erosion curves corresponding to the images in figure 1 are given figure 2. The initial volume of the original image was more important when the number of fluorescent particles increased. The curves exhibited a decrease at each erosion step reaching the minimum value observed in the images. Principal Component Analysis was applied to the erosion curves corresponding to the images recorded for the calibration set of samples.

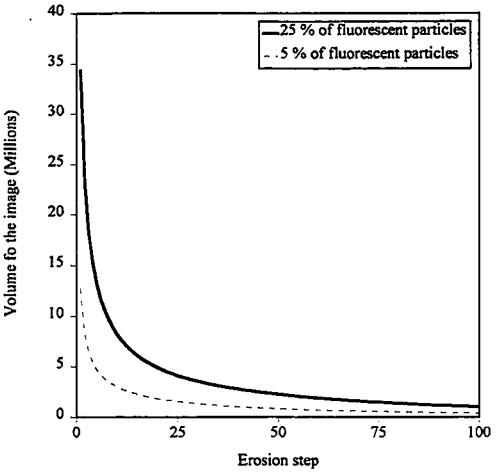

Figure 2: Erosion curves

Figure 3 shows the similarity map of the first two principal components that take into account 99.69 and 0.26 % of the total variance, respectively. On this figure, the number corresponds to the percentage of markers in the feed samples. Principal component 1 classified the samples according to the percentage of fluorescein marked particles. The samples with the lowest percentages of marked particles were observed in the left part of the map while the highest percentages were observed in the right part.

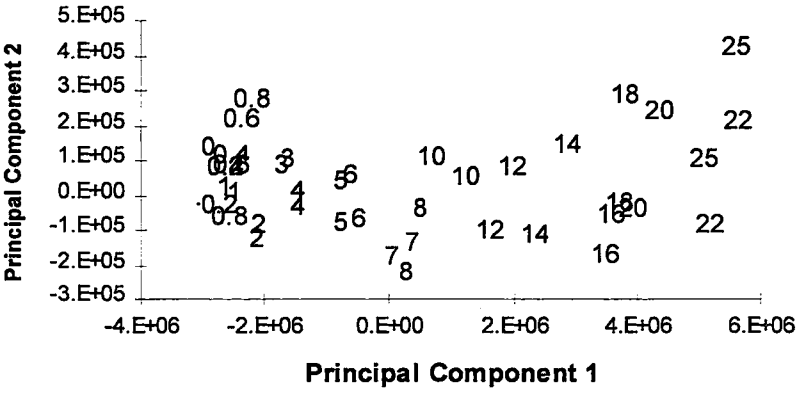

Figure 3: Principal component analysis of the erosion curves

The percentages of marked particles were predicted by Principal Component Regression with the principal components as predicting variables and the percentages of marked particles as predicted variables. Table I shows the results of the PCR according to the number of images used for characterizing a sample (number of erosion curves averaged) and the number of principal components introduced in the prediction model.

For example, if a sample was characterized by only one image and if only one principal component was used, a correlation coefficient of 0.944 was obtained with a standard error of prediction of 1.87. The correlation coefficient increased with the number of principal components introduced in the model and with the number of images used to calculate the average erosion curves. The model with 2 components and 10 images (each erosion curve was the result of the averaging of 10 images) was selected for the determination of the residence time distribution. The two components selected in the model were the first two and the correlation coefficient obtained was 0.987 with a standard error of prediction of 0.95. With 10 images, the third principal component introduced increased the correlation coefficient. But this component was the nineth which taken into account less than 0.01 % of the total variance. A component with a low eigen value can introduce noise in the prediction model and should not be retained.

Number of components	1 image	2 images	3 images	5 images	10 images
1	0.944 1.872	0.956 1.678	0.963 1.549	0.972 1.358	0.976 1.286
2	0.948 1.808	0.962 1.580	0.968 1.438	0.981 1.119	**0.987** **0.955**
3	0.952 1.755	0.966 1.478	0.972 1.375	0.984 1.054	0.992 0.785
4	0.953 1.724	0.968 1.445	0.972 1.364	0.986 0.993	0.993 0.748

Table 1: Results of the principal component regression

The first number corresponds to the correlation coefficient and the second to the standard error of prediction.

The percentages of marked particles in the samples collected at the outlet of the conditioner were predicted from the equation obtained on the calibration set. The predicted percentages expressed as a function of time gives the RTD shown figure 4. The mean residence time calculated from the distribution was 98.4 seconds with a variance of 642. The recovery rate was 149 %.

The recovery rate **RR** is calculated according to the following formula :

$$RR = \frac{100 * Tc * Mp}{Ti * Me}$$

with **Tc** Mass of tracer observed at the outlet,
Mp Mass of product treated during the RTD determination,
Ti Tracer introduced,
Me Mass of samples collected during the RTD determination.

The recovery rate indicates the percentage of tracer introduced in the reactor that have been observed at the outlet during the RTD determination. It is useful to be sure that all of the tracer has left the reactor at the end of the RTD determination. The recovery rate higher than 100 % can be explained by the fact that the erosions were applied on the surface of the images whereas the percentages of marked particles in the feed were calculated in weight. Moreover, when a particle is very fluorescent, this particle can « illuminate » the particles in its neighboring leading to an overestimation of the number of fluorescent particles. The mean residence time calculated from the experimental RTD was lower than the time expected (107 seconds). However, the calculated mean residence time was the same with other methods such as Red Cogilor staining. As the feeding rate was kept constant during the 2 experiments, this may indicate that the accessible volume in the reactor was lower than expected.

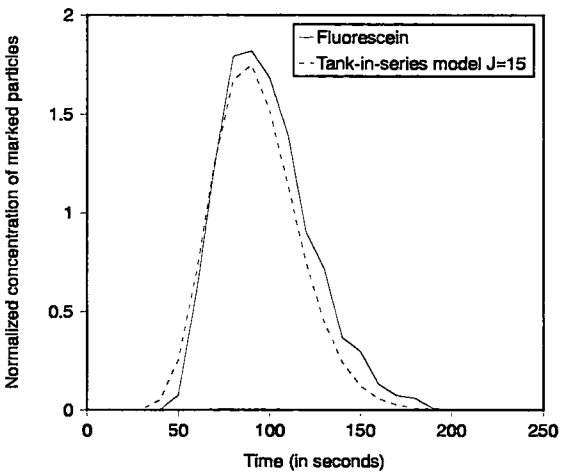

Figure 4: Residence time distribution

It is possible to modelize the reactor from the residence time distribution. Different kinds of models can be used depending on whether the flow is close to plug or

mixed flow. The two main models are the dispersion model and the tanks-in-series model. The dispersion model uses a plug reactor with an axial dispersion characterized by a dispersion coefficient. The tanks-in-series model considers that the conditioner is equivalent to J perfectly stirred tanks in series and the RTD with respect to this model is given by :

$$E(t) = \left(\frac{J}{t}\right)^{J} \frac{t^{J-1}}{(J-1)!} \exp\left(\frac{-Jt}{t}\right)$$

where J is the number of equal tanks-in-series. The main interest of this model is that it is possible to express the RTD by only one parameter which is the number of tanks. The number J of tanks in the model can be obtained by the following formula :

$$J = \frac{t^2}{\sigma^2}$$

A J value of 1 corresponds to a perfectly stirred reactor. When J tends to the infinite, the RTD is near to a symmetric gaussian and the reactor can be assimilated to a plug flow reactor with no axial dispersion.

In the present work, the tanks-in-series model was used to model the experimental residence time distribution. A J value of 15 was obtained from the mean residence time and the variance of the distribution. The application of the tanks-in-series model showed a very good fit between the experimental curve and the calculated curve with a J value of 15 (figure 2 : dotted line).

Conclusion

In the present work, a fluorescent marker was used for the determination of the residence time distribution in an experimental conditioner. This method was found to be relevant for the RTD determination and gave similar results with reference methods such as Red Cogilor coloration. Even if the use of fluorescein is not allowed at an industrial scale, the very high sensibility of this fluorescent tracer makes it possible to detect fluorescent particles even at very low concentration. It is often very important to be able to detect the beginning of the RTD, especially in the case of the destruction of pathogen agents, to ensure that all the particles have been treated during a sufficiently long time. For laboratories experiments, such marker seems to be very interesting for the RTD determination.

References

[1] M. Israelsen, E. E. Jacobsen and I. Dorthe Hansen. High product temperature key to salmonella control. In *Feedstuffs,* Vol. 66, N° 9 pp 31- 1994.

[2] J. J. Bibenet and M. Loncin. Bases du génie des procédés alimentaires, Masson, Paris, 1995 pp 193-204.

[3] J. Villermaux. *Techniques de l'ingénieur,* Vol. J84, 11-19, 1996.

[4] J. M. Bouvier. Preconditioning In the extrusion cooking process, In *International Milling Flour and Feed*, pp 34-37, December 1995.

[5] J. R. Lakowicz. *Principles of fluorescence spectroscopy*, Plenum Press, New York, 1983.

[6] L. Munck and A. De Francisco. *Fluorescence analysis in food*, L. Munck Ed, Longman Scientific and Technical, 1989.

[7] P. Papineau and A. Sire. Un mini conditionneur expérimental pour les pulvérulents. In *Cahier des Techniques INRA,* N° 32, Décember 1993.

[8] B. Novales, D. Bertrand, M. F. Devaux, P. Robert and A. Sire. Multispectral fluorescence imaging for the identification of food products. In *J. Sci. Food Agric.,* Vol. 71, N° 3, 376-382, 1996.

[9] J. Serra, *Image Analysis and Mathematical Morphology*, Academic Press, London, 1982.

[10] M.F. Devaux, P. Robert, J. P. Melcion and F. Le Deschault de Monredon, Particle size analysis of bulk powders using mathematical morphology. *Powder Technology, 90* (1997) 141.

[11] I. T. Jolliffe, *Principal components analysis*, Springer-Verlag, New York, 1986.

[12] P. Robert, M. F. Devaux and D. Bertrand. Beyond prediction : extracting relevant information from near infrared spectra. In *J. Near Infrared Spectrosc.*, Vol. 4, pp 75-84, 1996.

Part 2

Objective measurements of horticultural product quality

Pot plant quality prediction based on image analysis of half grown plants

Prédiction de la qualité des plantes en pots à partir de l'analyse d'images de plantes en cours de croissance

B.S. Bennedsen

Agricultural Engineering
Royal Veterinary and Agricultural University
Agrovej 10- DK 2630 Taastrup, Denmark
e-mail: bsb@.kvl.dk

Abstract: *This paper reports work on establishing the basis for an automatic sorting system for half-grown pot plants. pot roses and Hibiscus are used as examples. The system uses a computer vision system to inspect half-grown pot plants and extract selected features. Information on feature values are used as input to a decision system for classifying the plants according to the future development of the plants. A fully implemented system will give a producer the possibility to sort and group plants according to their specific needs and speed of growth, and thus to optimize the production. Encouraging results were obtained with pot roses, while more work are needed to establish useful results with Hibiscus.*

Keywords: *Automatic sorting, image processing, pot plant, plant quality, pot rose, hibiscus.*

Résumé : Cet article rapporte les travaux sur l'établissement d'une base pour trier de manière automatique des plantes en pots à demi-poussées. Les pots de rose et d'hibiscus sont utilisés comme exemples. L'appareil utilise un système de vision pour inspecter les plantes semi-poussées et pour sélectionner les paramètres d'intérêt. L'information sur les paramètres d'intérêt est utilisée comme entrée d'un système de décision pour classer les plantes en fonction de leur développement attendu. Un système complètement développé permettra aux producteurs de trier et de regrouper les plantes en fonction de leur besoin spécifique, de leur vitesse de croissance et ainsi d'optimiser la production. Des résultats encourageants ont été obtenus avec des roses en pot mais du travail supplémentaire est nécessaire pour établir des résultats utilisables avec l'hibiscus.

1. Introduction

Modern greenhouse production of pot plants is highly automated, and in many respects, the production principles are close to that of industry. However, there is one aspect of the production which differs from industry, namely the fact, that even though the products are highly uniform, no two pot plants are exactly alike, and evaluation of quality is, to a high degree, subjective. This means, that human expert are needed to sort the pot plants according to quality.

In 1994, an EU-AIR project was established with the purpose of developing methods for automating this part of pot plant production. The work focussed on two aspects: Labour saving and increased objectivity by developments of automatic sorting of the final product; the marketable plants, and increased productivity by sorting pot plants at the half-grown stage. Preliminary results are reported by Moth-Poulsen et. al. [3], and Bennedsen et. al. [4].

2. Materials and experimental setup

2.1 Plant material

The plant species, chosen for this project were pot roses (*Rosa hybrida*) and Hibiscus (*Hibiscus rosa-sinensis*). Previous researches, among others Dijkstra (1994) [1], have show, that it is possible to construct digital image processing systems which will extract features from images of plants, and classify the plants according to quality, based on the value of a combination of those features. This requires previous knowledge about, which features determine the quality, and how. The challenge of this project was, that these plants are not currently sorted at the half-grown stage, and producers and other experts deny knowledge of features, which are important to the development, and of course of the possible value of such features. The choice of plant species was made in order to try to extend the capabilities of automatic plant sorting systems beyond the point of repeating the skills of trained graders.

Pot roses and Hibiscuses are produced from cuttings. The normal way is to plant four cuttings in each pot for roses and three for Hibiscus. After rooting, the plants are allowed to develop for some time, before they are pruned. pot roses are pruned two times, normally by using a sort of hedge cutter. Hibiscuses are pruned only once during their development, and this is done manually, in order to influence the shape of the plant. Pruning induces the formation of side shoots. Approximately one week after the last pruning the plants are rearranged for larger spacing, and this would also be the time for sorting.

The plants used in these experiments were all supplied by Research Centre Aarslev. The plants were part of a growth experiment, during which the plants were exposed to two different levels of artificial light, combined with two different plant spacings. Plants which are the result of such a growth experiment tend to form a less homogeneous group than plants produced under commercial conditions. However, these plants were produced during the summer season, which generally gives a better quality of the pot plants, due to more light and higher temperature. The treatments of the plants from half-grown to a marketable stage were included as parameters.

After the photographic session at the half-grown stage, the plants developed into full grown plants. At this stage, they were evaluated by expert, according to their marketable quality. The number of plants used in the experiments reported here is 235 pot roses, and 166 Hibiscus. The initial number of Hibiscuses were 298. Of these only 198 were also photographed from the side. This number was further reduced, as some of the plants were removed for shelf life testing at Research Centre Aarslev. Hence, the final number of plants, for which all data were available was 166.

2.2 Image acquisition

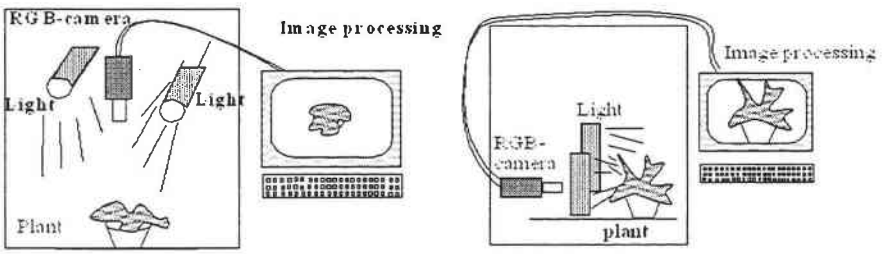

Figure 1: Image acquisition scenes

Images were taken in RGB (16,6 mill colours) using a Matrox Comet frame grabber, combined with a SONY DXC-930P 3-CCD camera. Image acquisition was done, using a special designed box, fig. 1. This contained object lighting, which consisted of two Osram Dulux L, 24W, 317 mm, light sources, with a colour temperature of 5400 K, which is very close to daylight (5600 K). Images could be taken both from top view and from side view, as shown in fig. 1. A small turntable was mounted in the bottom of the box. This would ensure, that all the plants were positioned at exactly the same place, both for top and side view, while allowing plants to be photographed from 3 sides by rotating it through 120 degrees. Images were taken against a uniform, blue background.

3. Feature extraction and data processing

3.1 Segmentation

The images were segmented, using an unsupervised segmentation routine, the k-mean segmentation (Keller 1989) [2]. The routine uses the RGB values, and segments the image into clusters of pixels, where the distance in colour between the centre of each cluster is maximum.

Images of pot roses were segmented into three classes: background, old leaves and younger leaves (fig 2). For Hibiscus the images were only segmented into background and object (plant). The younger leaves are not as easy to distinguish from the older leaves as for Roses. Further, the leaves of the Hibiscus are more glossy and sometimes light reflections influence the segmentation routine.

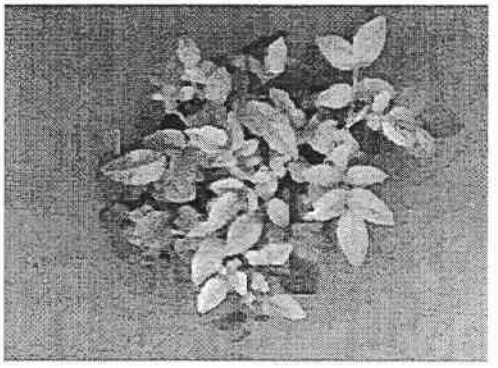

Figure 2 Left: Gray shade image of half-grown pot rose

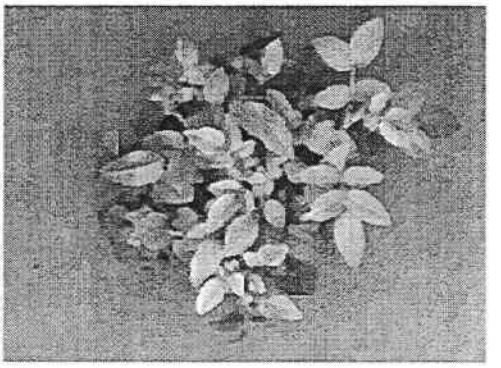

Figure 2 Right: K-mean segmentation of the same image,using RGB colour band

3.2 Features

As mentioned earlier, there were no prior knowledge about which features one should measure on the half-grown stage, in order to predict the final quality of the plant.

At the marketable stage, the plant should be circular or quadratic. Hence, it seemed natural to base the evaluation, and hence the features, on the possibility for an equal, radial development in all directions. As there are four cuttings in each pot, it was decided to reduce this to checking for equal development in four directions, represented by four segments as shown on figure 3.

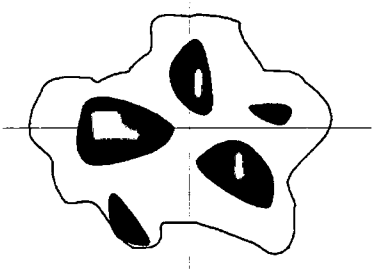

Figure 3: Schematic drawing of half-grow pot rose image, segmented into old and younger leaves, and divided into four segments for feature extraction

For pot roses, the features extracted from a combination of the four segments and the total area were:

- total leaf area,
- Euclidian centres of gravity deviation of the total leaf area from pot centres,
- compactness of the total leave area,

- young leaf area,
- Euclidian centres of gravity deviation of the young leaf area from pot centres,
- compactness of the young leaf area,

- standard deviation of the four squares total leaf area ,
- standard deviation of the four squares young leaf area.

For Hibiscus rosa-sinensis no distinction was made between younger and older leaves, on the other hand, additional information could be extracted from the side view images. This resulted in the following features:

Top view:

- leaf area,
- Euclidian centre of gravity deviation of the leaf area from the pot centre,
- compactness of the top view leaf area,
- standard deviation of the four squares leaf area, normalized with area.

Side view:

- leaf areas, one for each view angle,
- Euclidian centre of gravity deviation of the leaf area from the pot centre. One value for each view angle.

3.3 Decision system

The decision system is based on neural networks, and forms the core of the sorting equipment. It uses features from half-grown plants as input parameters, and it is trained and tested using the expert evaluation of the quality of the plants at the full grown stage.

Marketable roses are graded into three classes by the experts: 1. quality, 2. quality and a non saleable product, referred to as category 3. Each plant was graded by three experts; one graded all the plants, the other experts graded each about half the batch of plants. Combining the verdicts of the experts caused some problems. In only 72 (30.6%) out of 235 cases, all three graders agreed upon the quality. In 8 (3.4%) cases they totally disagreed. In the following decision system these plants were excluded from the data set.

The qualities of marketable Hibiscuses does have some more concrete parameters than the pot roses. Graders estimate the plant quality on the basis of branches, where only branches with three or more flower buds are considered as relevant. Branches, which are 60-80% the heights of the longest branches are regarded as half branches. Smaller branches are not counted. The total number of branches then describes the quality of the plant. Due to this more quantitative approach to quality evaluation, only one expert evaluation the of the Hibiscus plant quality was used. The result of the evaluation was presented as marks for quality, Top view marks ranged from 1 to 4, 1 being best. Side view marks from 1 to 5. Total quality was also presented on a scale from 1 to 5, corresponding to 5 quality classes.

The actual data processing was done using the SAS statistic programme package. For pot roses, linear and quadratic discriminant analyses were used. As these experiments did not show any significant difference between linear and quadratic discrimination, only the linear discrimination was used for Hibiscus.

4. Results

Since the plants were part of a growth experiment, they were exposed to different growth conditions, regarding light and distance. These treatments were included as features. The idea is, that given an equal growth conditions, the end quality should be predictable using the decision system. Including the growth parameters as linear input to the model normalizes the experiment.

4.1 Pot roses

For pot roses, the first approach to establishing a correlation between measured features and end quality was done using the 3 quality classes employed in the final evaluation. As shown in table 1, the result was not convincing.

	Training set			Test set		
class \ classified as	**1**	**2**	**3**	**1**	**2**	**3**
1	**65**	19	16	**0**	0	100
2	32	**40**	28	66	**24**	10
3	12	18	**71**	8	23	**69**

Table 1: Pot roses, linear discrimination, all three quality classes

Improved results can however be obtained by adding two of the classes. Joining class 1 and 2 against class 3 gives a result of 75 % and 69% for the test set, while 69% and 72%, is obtained when joining class 2 and 3 against class 1. Tables 2 and 3.

	Training set		Test set	
class \ classified as	**1+ 2**	**3**	**1+ 2**	**3**
1+ 2	**74**	26	**75**	25
3	18	**82**	31	**69**

Table 2: Pot roses, linear discrimination, quality class 1 and 2 against 3

	Training set		Test set	
class \ classified as	**1**	**2+3**	**1**	**2+3**
1	**71**	29	**69**	31
2+3	34	**66**	28	**72**

Table 3: Pot roses, linear discrimination, quality class 1 against 2 and 3

Joining classes at the half-grown stage does make sense: By sorting into class 1+2 and 3, the producer can discard class 3 plants at this stage, thus saving resources. Alternatively, using class 1 and 2+3 offers the possibility to subject class 2 and 3 plants with adjusted growing conditions, and possible increase the end quality.

4.2 Hibiscus

As a first approach, top and side view data were classified against marketable stage marks for top view and side view respectively. As expected, this did not provide useful results.

Then all the features were combined in an attempt to classify the plants according to their overall quality. Using all five classes yields the results listed in table 4 lists the result

	Training set					Test set				
class \ classified as	**1**	**2**	**3**	**4**	**5**	**1**	**2**	**3**	**4**	**5**
1	**100**	0	0	0	0	**0**	0	0	0	100
2	0	**100**	0	0	0	0	**0**	0	0	100
3	4	0	**44**	26	26	25	0	**33**	8	25
4	5	0	19	**48**	27	15	10	10	**40**	38
5	3	0	13	30	**53**	6	0	12	43	**33**

Table 4: Hibiscus, linear discrimination, all features used. 5 quality classes. Training and test set consisted of 117 and 49 plants respectively

As with the pot roses, and as expected, the result is not acceptable. Consequently, it was attempted to merge the classes. The result of joining classes 1+2 and 3+4+5 is listed in table 5.

	Training set		Test set	
class \ classified as	**1+2**	**3+4+5**	**1+2**	**3+4+5**
1+2	**100**	0	**0**	100
3+4+5	10	**90**	23	**77**

Table 5: Hibiscus, linear discrimination, all features used. 2 quality classes, 1+2 and 3+4+5
Training and test set consisted of 117 and 49 plants respectively.

Trying to merge classes 1+2+3 and 4+5 yield basically the same results. The major problem is, that there is less than 3 plants in some of the classes, and even no plants in class 2.

Conclusion and future work

Based on the results of the rose experiment, it can be concluded, that a correlation between objectively measured features of pot plant at half-grown stages and the end quality at marketable stages does exist. The classes in this experiment had to be gathered into only two classes, where recognitions of around 70% are reached. For Hibiscus, the correlation is not so pronounced. The main reason for this is the low number of available plants, the higher number of classes, and, probably, the fact, that the relation between young leaves and older is not considered for Hibiscus.

The results obtained on pot roses seemed so encouraging, that it was decided to test the system under commercial scale. During the winter of 1997/98, images of a batch of 1000 half grown pot plants were acquired from a commercial producer. The idea was, that the plants should be returned to normal production, after which the final quality would be recorded by the time the plants were sold. The large scale of production would ensure, that all the plants were subjected to a uniform treatment. Further, the producer would evaluate the quality of the final product according to his needs, and hence only one evaluation would be given, and it would be consistent with the target output of the decision system. Unfortunately, the results were lost by the producer, and since the production from half grown to marketable plant takes some time, it was not possible to repeat the experiment in time for the results to be included in this paper.

References

[1] Dijkstra, J. 1994. ✐Application of Digital Image Processing for Pot Plant Grading. Thesis Wageningen, 1994. P. 1-195.

[2] Keeler, J.M., Chen, S., Crownover, R.M., 1989. Texture Description and Segmentation Through Fractal Geometry. *Computer Vision, Graphics, and Image Processing 45, p. 150-166.*

[3] Moth-Poulsen, H. and B. S. Bennedsen, 1996: ✐Objective quality measurement of pot rose and hibiscus by image processing✍.*AgEng 96. Paper no. 96F-077.*

[4] Bennedsen, Bent S. and Moth-Poulsen, H. Measuring Quality Potentials of Half-grown Pot-Plants. *Paper presented at the 3. International Symposium on Sensors in Horticulture, Israel, August 1997.*

Quality criteria used by human experts for pot plant Begonia assessment

Critères de qualité utilisés par des experts humains pour le tri des bégonias en pot

P. Feuilloley, S. Guillaume

CEMAGREF. Sensors and Information Engineering for Food Quality Assessment Division (GIQUAL Division.). 361, rue JF Breton. BP 5095.
34033 Montpellier Cedex 1 France.
Sensoral 98, Feb. 1998, Montpellier, France

This research is done in an international EC funded co-operation with Danish, French and Dutch partners *(contract AIR3-CT94-1072)*.*

Abstract: *The aim of this work is the assessment of Begonias pot plants quality using artificial vision and image processing calibrated on human appreciation from an international experts panel. Another aim is to build an expert system (neural network) that simulates the behaviour of these experts and able to sort plants using digital images. Experts gave 1 mark per pot plant. Experiments were carried on 434 Begonia pot plants from which one top image was grabbed. These images were processed by our Dutch and Danish colleagues, in order to extract features. Using statistical analysis, relevant parameters were selected and were used as data inputs for a neural network. The neural network was calibrated using 217 plants. Tests were done using the 217 remaining plants. Results show that quality criteria mainly used by experts are rather rough and deal more with size parameters than with quality criteria. Neural network systems simulate the experts behaviour with a correct accuracy.*

Keywords: *Begonia, quality, criteria, human experts, neural network.*

Résumé : Le but de ce travail est d'apprécier la qualité des bégonias en pot en utilisant la vision artificielle étalonnée à partir d'une appréciation humaine issue d'un panel d'experts internationaux. Notre objectif est de construire un système expert à base de réseaux de neurones qui simule le comportement de ces experts et qui est capable de trier des plantes en utilisant des images numériques. Les experts donnent une note par plante en pot. Les expériences sont menées sur 434 pots de bégonias à partir desquels une image est prise par le haut. Ces images sont analysées par les collègues danois et hollandais de manière à extraire les paramètres. Par analyse statistique, les paramètres pertinents sont sélectionnés et utilisés comme des entrées d'un réseau de neurones. Le réseau de neurones est calibré en utilisant 217 plantes. Des tests sont effectués en utilisant les 217 plantes restantes. Des résultats montrent que les critères de qualité principalement utilisés par les experts sont relativement rustiques et correspondent à plus de 16 paramètres. Les réseaux de neurones simulent le comportement de l'expert avec une bonne fiabilité.

1. Goals

The aim of this decision system is to reconstitute expert opinion concerning Begonia pot plant quality using artificial vision, image analysis and data processing. This decision system should be able to grade pot plant of Begonias with an accordance very near to the expert's one.

By «decision system» we mean mainly a software that uses artificial intelligence (neural networks) or statistical analysis to do the above purpose.

But, this decision system should include the hardware (TV camera, image grabber, illumination system, computers, ...) and the software needed to process the data (image analysis and statistical software) whose influence on the response of the decision system itself is slight but not quantifiable.

2. The decision system

We may consider that the decision system we used is made of 2 parts:

- a statistical analysis of data in order to reduce their number
- a neural network processing and/or a discriminant analysis that simulate the behaviour of experts for Begonia grading.

2.1. Statistical analysis: principal component analysis (PCA)

PCA is a basic method for data analysis and constructs linear combinations of the original data set with maximum variance. It can be used to reduce the number of variables represented by the physical measurements, to a smaller number of components regarded as useful, with a loss of information as lower as practicable. For instance, a set of 220 samples defined with 28 criteria, is reduced to a 7 criteria definition and with 90% of the initial variance.

2.2. Neural network

2.2.1. The neural network

The network type in use was a learning network based on error back propagation. A neural network is organised into multilayer interconnected neurones. Typically, there are 2 layers connected with the outside: the input layer where data are input, and the output layer which is the network response. Intermediate layers are called hidden layers.

The learning stage consists in modifying connection strengths due to input and output stimulus. If output data are given by experts, the learning is supervised, and stimulus are recorded in a learning file.

The test stage allows the network behaviour observation after the learning stage. Input stimulus are only shown to the network, and network responses are compared to expert marks. Stimulus are then recorded in a test file.

2.2.2. Implementation

We used the NeuralWorks (NeuralWare, Inc.) software. This network could use up to 10 000 neurones.

Network inputs were principal components of the above PCA from where we kept 90% of inertia, and the output was the average expert marks of each pot. The neural network was set up as follows:

neurones number per layer
- neurones number of the input layer = principal components number
- neurones number of the hidden layer = neurones number of the output layer = 3 or 4 according to the simulated expert.

- learning rule: back propagation of error
- transfer function: sigmoid function:

$$T = 1 / (1 + e^{(I_x g)})$$

with I: input value and g: gain (in this application g was fixed and g = 3).

In addition, the «default schedule» dialogue box was selected and activated in order to set up automatically the «learning coefficients».

3 Application and results

3.1. Application

The Begonia experiment took place in Alsmeer and in Arsleev during June 1997.

For each plant, we got 1 mark from each one of the 10 experts.

For each plant and for each top view, we also got features extracted using vision. Images were processed by our Dutch and Danish colleagues. These data were translated into a reduce centred pattern. During notation, experts looked to the plants from a top view.

For the neural network, learning phases was achieved on 217 plants and test phases on the 217 remaining plants. Therefore, we used the cross validation method on the same experiment.

For various reasons (time, experts results very closed, and global results more or less significant), we processed he results concerning only 3 experts of the 10, i.e. one expert per country.

3.2. Statistical and neuronal analysis results

3.2.1. Data overview

Before giving statistical results, it would be interesting to have a look on the available data.

Table 1 summarises the variables that have been used for the computations.

Number	Name
0	Plant height, cm
1	Number of flowers
2	Object area, mm2
3	Flower area, mm2
4	Object perimeter, mm
5	Object convex perimeter, mm
6	Flower convex perimeter, mm
7	Object convex area, mm2
8	Flower convex area, mm2
9	Max. width object, mm
10	Perp. width object, mm
11	Angle
12	Max. width flower, mm
13	Perp. width flower, mm
14	object-pot Offset, mm
15	flower-pot Offset, mm
16	object-flower Offset, mm
17	object Filling grade
18	convex hull Filling grade
19	object Eq diameter
20	object X dispersion
21	object Y dispersion
22	total object x*y dispersion
23	flower Eq diameter
24	flower X dispersion
25	flower Y dispersion
26	flower total x*y dispersion
27	Object compactness
28	flower Compactness
32	Expert mark
33	Plant number

Table 1: Variables list

In this table, variables 0 and 1 have been calculated manually and variables 2 to 16 have been calculated by the image analysis system. Variables 17 to 28 have been re-calculated by CEMAGREF and added to the list already provided by the co-ordinator.

Another interesting set of data is the expert's marks distribution, i.e. the frequency of grading per mark and per expert. This is shown in table 2.

Recoded classes	1	2	3	4	5
Classes	A	B	C	D	E
F1[1]	60	126	138	100	8
F2	72	127	139	74	20
F3	91	123	131	54	33
NL1[2]	41	103	97	82	109
NL2	123	154	150	3	2
NL3	223	190	16	0	3
DK1[3]	198	120	75	39	0
DK2	46	320	55	11	0
DK3	28	174	208	22	0
DK4	161	122	95	54	0

Table 2: Expert's mark distribution

In this table, for instance, the F1 expert gave mark A: sixty times, mark B: 126 times, etc. We notice that Danish experts do not gave mark D, and almost as well as the NL2 and NL3 experts.

A last an interesting general and useful information is the correlation between variables. This is shown in table 3.

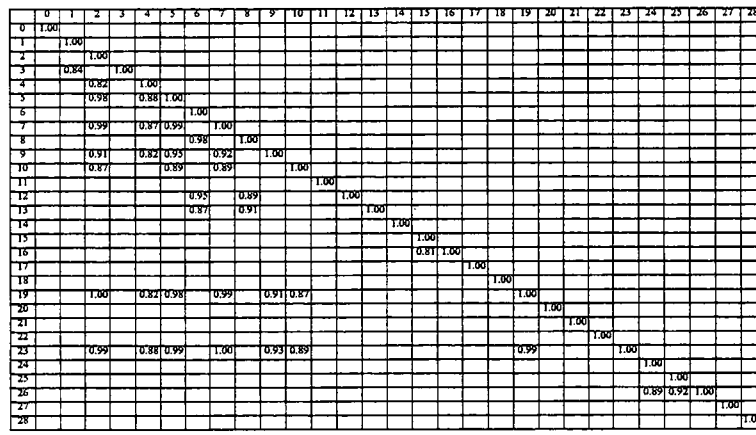

Table 3: Correlation between variables (level > 80%)

[1] F1 = French expert N°1,

[2] NL1 = Dutch expert N°1,

[3] DK1 = Danish expert N°1, etc...

In this table are noticed correlations whose level is upper than 80%. This table will be very efficient to sort variables and to keep only those that are strongly correlated between themselves.

3.2.2 PCA analysis

Computation shows, in table 4, that 15 components explain the variance of the 28 variables and that 7 are needed to get 90% of inertia.

	1	2	3	4	5	6	7	8	9	10	11	12	13	14	15
Value	10.75	5.86	2.86	1.94	1.66	1.33	0.99	0.90	0.83	0.57	0.53	0.26	0.21	0.14	0.05
Inertia	0.37	0.20	0.10	0.07	0.06	0.05	0.03	0.03	0.03	0.02	0.02	0.01	0.01	0.00	0.00
Cumulated inertia	0.37	0.57	0.67	0.74	0.80	0.84	0.88	0.91	0.93	0.95	0.97	0.98	0.99	0.99	1.00

Table 4

Eigen vectors examination allows to select active variables, i.e. those the absolute coefficient value of which is upper than 0.2. Therefore, the selected variables for the first principal component are: 2, 4, 5, 6, 7, 8, 9, 10, 12, 13, 18, 19, 23. This is summarised in table 5.

	1	2	3	4	5	6	7
0	0.0867	-0.1544	0.1296	0.025	0.0788	-0.092	-0.1734
1	0.1702	-0.1655	-0.0586	0.1529	-0.396	0.003	0.0468
2	0.2636	0.1679	-0.1527	0.0849	-0.0087	-0.0095	0.0034
3	0.1829	-0.2345	-0.0288	0.1633	-0.3606	0.0153	-0.0808
4	0.2513	0.1763	0.1099	-0.03	-0.0137	-0.0819	-0.0505
5	0.2644	0.1886	-0.0532	0.0798	-0.0389	-0.0522	-0.0028
6	0.2768	-0.1447	0.0008	-0.1218	0.0302	0.0165	0.0113
7	0.2688	0.1767	-0.0793	0.0762	-0.011	-0.0298	-0.0046
8	0.2752	-0.1443	-0.0231	-0.0732	-0.0034	0.0203	0.0002
9	0.2453	0.1875	-0.0091	0.0461	-0.1371	-0.1969	0.0199
10	0.2448	0.1597	0.031	0.2261	0.0608	0.2613	0.0198
11	0.0038	-0.0165	0.0329	-0.0974	-0.1797	0.0291	0.9149
12	0.2658	-0.1058	0.0295	-0.1601	0.0487	-0.0112	0.0152
13	0.2401	-0.1827	-0.0275	-0.0692	0.0186	0.0775	-0.012
14	0.0032	0.0789	0.0246	-0.4079	-0.3407	0.3205	-0.2513
15	-0.0511	0.234	-0.0197	-0.3868	-0.3123	0.3121	-0.0834
16	-0.0699	0.2828	-0.0354	-0.2277	-0.1597	0.1787	0.0835
17	-0.0375	-0.0492	-0.5014	0.0596	0.018	0.1475	0.0503
18	-0.1686	-0.0626	-0.0123	0.3422	-0.4489	-0.0111	-0.1302
19	0.2617	0.1738	-0.1534	0.0825	-0.0134	-0.0072	0.0023
20	0.0207	-0.0418	-0.3357	0.0748	0.2913	0.4587	-0.0405
21	-0.0409	-0.0189	-0.3365	-0.3122	-0.144	-0.5659	-0.0454
22	-0.0227	-0.0417	-0.4999	-0.2238	0.0616	-0.1963	-0.0665
23	0.2671	0.1821	-0.0797	0.0738	-0.0161	-0.0278	-0.0059
24	-0.149	0.2693	-0.0899	0.2426	-0.0905	-0.0291	-0.0353
25	-0.1345	0.3159	-0.0272	0.1262	-0.0459	-0.0967	-0.0045
26	-0.1483	0.3169	-0.0608	0.1962	-0.0748	-0.0773	-0.0247
27	-0.1082	-0.0916	-0.3887	0.1532	0.0145	0.1457	0.109
28	-0.0255	-0.3534	-0.0839	0.1583	-0.2824	0.0693	-0.0427

Table 5: Coefficient values of the 7 first eigen vectors

The above correlation matrix allows to eliminate some of these variables. For instance, variable N°2 (object area) has high correlation coefficients with variables N°4 (0.82), 5 (0.98), 7 (0.99), 9 (0.93), 10 (0.89), 19(1.00), 23 (0.99), and consequently we could keep only one variable of this set. Variable N°6 is strongly correlated with variables N°8 (0.98), 12 (0.96) et 13 (0.87).

Thus, we could keep for this axis, variables N°2, 6 and 18.

The angle square cosine between variable and factor allows to verify the choice efficiency of variables. These values are respectively 0.77, 0.84 et 0.36 for variables N°2, 6 et 18 (i.e. 29°, 24° and 53° of angle). For factor N°2, variable N°26 is correlated with variables N°24 and 25. An examination on the square cosine allows to eliminate variable N°24 ($\cos^2 = 0.4$), and rather to keep variable N°25 ($\cos^2 = 0.6$).

Accordingly, we get the following table:

Variables	Axis	Cos^2
0	6	0.05
2	1	0.75
3	2	0.32
6	1	0.86
11	7	0.90
14	4	0.4
16	2	0.46
17	3	0.7
18	5	0.4
20	3	0.3
21	3	0.3
22	3	0.3
26	2	0.6
27	3	0.4
28	5	0.1

Table 6

3.2.3 Stepwise discriminant analysis

Variables explaining the inertia are not compulsory discriminant. For this reason, a stepwise discriminant analysis has been done using a 68 examples file (20 of grade A, 20 of grade B, 20 of grade C and 8 of grade D). We used 2 methods:

- Using the Wilks λ method we got the following table :

Variable n°	Det (Intra) / Det (Inter)
2	0.29143
15	0.20516
0	0.15297
19	0.12124
26	0.09934
25	0.07882
12	0.06350
9	0.05718
21	0.05218
10	0.04531
23	0.04078
6	0.03739
18	0.03429
3	0.03029
20	0.02726
7	0.02506
11	0.02285
27	0.02135
4	0.01963
24	0.01788

Table 7

- Using a Student Fisher test on the averages, variables N°2 , 0, and 15 are selected by the test. Thus, the variable N°16 has been replaced by the variable N°15 in the further calculation.

3.3 Results per expert (statistical and neuronal analysis)

Per expert, a learning and a testing files have been established. Each file is made of with the same number of examples.

3.3.1 Danish expert N°4 (DK4)

- Using the stepwise discriminant analysis we obtained the following results, (classification errors):

	Learning					Test				
Number of examples	80	61	47	27	Total	81	61	48	27	Total
Grade	1	2	3	4		1	2	3	4	
Variables in use										
2	26	43	27	6	102	23	47	34	13	119
2, 0	32	34	22	7	95	26	42	28	15	113
2, 16	23	39	30	6	98	25	45	36	12	120
2, 0, 16	27	31	22	7	87	26	42	28	15	113
2, 0, 16, 17	31	30	21	9	91	29	43	26	16	116
All	28	38	20	7	93	30	41	30	19	122

Table 8

Results are not significant, and could be explained by the low rate of linear relationship between inputs and outputs.

- Using the neural network we got the following test results, using variables N°0, 2, 6, 14, 15, and 18:

	Predicted				
Real	Grade 1	Grade 2	Grade 3	Grade 4	Total
Grade 1	72	5	4	0	81
Grade 2	26	12	17	6	61
Grade 3	11	6	28	3	48
Grade 4	0	1	20	6	27

Table 9

The above results are not very significant. The network architecture is not involved: indeed, tests conducted using various neurone numbers in the hidden layer (from 4 to 20!) do not change the performance significantly. Nevertheless, the best results were got with 6 input neurones (variables N°0, 2, 6, 14, 15, and 18), 4 hidden neurones and 4 output neurones The performance of this configuration is 56% of success (Table 9).

3.3.2 Dutch expert N°2 (NL2)

In this case, we used a neural network set with 3 hidden neurones, 3 output neurones and 7 input neurones (variables N°0, 2, 6, 12, 13, 15, and 16). We got the following test results:

	Predicted		
Real	Grade 1	Grade 2	Grade 3
Grade 1	48	10	4
Grade 2	17	51	9
Grade 3	6	9	60

Table 10

The above table shows 74% of success (correct classification).

3.3.3 French expert N°1 (F1)

The selected variables using the discriminant analysis are N°0, 2, 16 and 28. Learning and testing samples are: 30 examples for grade 1, 63 for grade 2, 69 for grade 3 and 50 for grade 4. Grade 5 has not been take into account. Thus, the network has the following configuration: 4 input neurones, 4 hidden neurones and 4 output neurones.

The test results are summarised below:

	Grade 1	Grade 2	Grade 3	Grade 4	
Grade 1	5	24	1	0	30
Grade 2	4	49	9	1	63
Grade 3	2	33	14	20	69
Grade 4	0	10	12	28	50

Table 11

The performance of the model is 45% of correct classification. A test with the 28 variables has given a 47% of correct grading.

3.4 Sensitivity of the neural network

Another mean to test the efficiency of the neural network model, is to make a 5% variation on the input and to examine the response on the output using the «Explain» and «Input contribution» network commands.

Variable	0	2	6	12	13	15	16
Grade 1	-27.1	84.4	-1.1	-0.8	5.5	-23.1	-25.0
Grade 2	-41.1	47.1	-29.3	-18.9	-12.4	5.1	32.1
Grade 3	55.1	-105.7	24.7	16.4	6.2	14.7	-6.8
Total (Absolute values)	123.3	237.2	55.1	36.1	24.1	42.9	63.9

Table 12: Model response to a 5% Input contribution (DK4 expert)

The above table shows again that variables N°0 and 2 are very sensitive to a slight variation and therefore are the key variable of the model. Variables N°6 and 16 are also sensitive.

Conclusion

One of the objectives of this work, among the others, was to detect the main features used spontaneously by experts in order to take their decision. This aspect was not considered in our first report. It was also an objective of the contract. A tentative conclusion of this quality criteria extraction is given below:

	Experts		
Decision System	DK4	NL2	F1
DA[4]	0, 2	0, 2	
NN[5]	0, 2, 6, 14, 15, 18	0, 2, 6, 12, 13, 15, 16	0, 2, 16, 28

The above table summarises the variables correlated most often with expert judgement and to the decision system:

- variables 0 and 2 are selected in every case,
- variables 6 and 15 are selected twice,
- the rest of variables are used once.

We may then conclude that the quality criteria used by experts are as follows in the decreasing order:

A) 0 and 2, i.e. plant height and object area,
B) 6 and 15, i.e., flower convex perimeter and flower-pot offset,
C) the rest are: number of flowers and convex hull filling grade, object convex perimeter, object convex area, perp width flower and object-pot offset.

A) are rough criteria which are associated with the global size of the pot plant. It would seen to the experts the bigger is the plant, the bigger is the quality. This is

[4] DA: Discriminant analysis,

[5] NN: Neural network.

understandable for a non professional person, but it would seen a little short-sighted for an expert.

B) and C) are criteria which requires more the quality, as flower parameters and symmetries are taken into account.

The decision systems, especially the neural network ones, established for this work performs as well as the experts' methods of assessment. This was to be expected. But, pot plants selected were from the A1 and A2 grades (best quality) and not representative of the whole. The experts were requested to create 4 new sub-grades: A and B for A1, and C and D for A2. This is a very difficult task and why the performance and consistency in grading of experts are rather low. The pot plant should have been chosen among an ungrading batch production in order to have a quality larger range.

References

BENET B., *Rapport de DEA 1990.* Détermination des paramètres caractéristiques des cyclamens.

BENET B., 1990. *Utilisation des réseaux de neurones pour la notation automatique de ces plantes,* ISIM USTL.

B. BENNEDSEN, P. FEUILLOLEY, A. GRAND D'ESNON, juin 1991. Appréciation de la qualité des plantes en pots : Utilisation de la vision artificielle en couleur - *CEMAGREF, BTMEA N°58.*

BRONS A., *Thèse de doctorat (PhD Thesis) 1992.* Contribution des techniques connexionnistes à l'évaluation qualitatives des produits agro-alimentaires par leur aspects visuels, ENGREF.

DIJKSTRA J., 1994. *Application of digital image processing for pot plant grading.* PhD thesis, University of Wageningen.

Panel Producteur 1992. *CNIH-ONIFLHOR-BVA-SOFRES.*

SHALKOFF R.J,. 1992. *Pattern recognition: statistical, structural, and neural appoaches.* John Wiley & Sons Inc.

V. STEINMETZ, P. FEUILLOLEY September 1996. Quality assessment of Begonias with machine vision. *Ag. Eng Paper N° 96F-024, Agr. Eng.* Conference, Madrid.

FENELON J.P, 1981. *Qu'est ce que l'analyse de données ?* LEFONEN ; 5 Rue Michal, 75013 Paris.

Development of a virtual expert for colour classification of tobacco leaves. Validation against human experts

Développement d'un expert virtuel pour la classification couleur de feuilles de tabac. Validation par comparaison avec des experts humains

M. García, P. Barreiro, M. Ruiz-Altisent

Rural Engineering Dept. E.T.S.I.A.
Alonso R.; Júdez L., Agricultural Economy Dept. E.T.S.I.A.
Avda. Complutense s/n 28.040 Madrid. Spain

Abstract: *Instrumental color assessment is already a well-established procedure. However, in the case of biological products, the lack of homogeniity in color distribution leads to low efficiency in the establishment of a color base and a sampling procedure in comparison to human ability. The current research is the validation of a color assessment procedure against a set of four human experts belonging to a commercial company. It shows that statistical clustering procedures enable to generate a homogeneous color data base (6% intra-class variation) out of a set of products with low homogenity within some product-based color classes (20% intra-class variation). In the case of tobacco leaves, the new color data base shows to be stable through 3 consecutive seasons. The use of the color classification histograms of the humans versus the virtual expert enables to extract features on the amplitude of the color classes used by human and instrumental procedures. On this basis, further optimization in the generation of a new color base has been achieved. The final percentage of well classified leaves obtained for the virtual expert (73.6%) shows to be within the human experts' range (66%-84%, when comparing each expert to the average human expert).*

Résumé : L'appréciation de la couleur par un système instrumental est une procédure bien établie actuellement. Cependant, dans le cas de produits biologiques, du fait d'un manque d'homogénéité dans la distribution des couleurs, l'établissement des bases de couleur est peu efficace, de même que les procédures d'échantillonnage comparées aux possibilités humaines. La recherche actuelle concerne la validation d'une procédure de mesure des couleurs par rapport à un ensemble de 4 experts humains qui appartiennent à une société commerciale. Cette recherche montre que les procédures de clustering permettent de générer une base de couleur homogène (variation intra-classe : 6%) à partir d'un ensemble de produits avec une faible homogénéité dans chaque groupe de couleur (20% de variation intra-classe). Dans le cas de feuilles de tabac, cette nouvelle base de couleur est stable pendant 3 saisons consécutives. L'utilisation d'histogrammes de classification établis par des humains par rapport à l'expert virtuel permet de mettre en évidence l'amplitude des classes de couleur utilisée par les humains ou les procédures instrumentées. Sur cette base, l'optimisation de la génération d'une base de couleur a été réalisée. Le pourcentage final de feuilles bien classées obtenu avec l'expert virtuel (74%) appartient à la fourchette des experts humains (66 à 84% lorsque l'on compare chaque expert à l'appréciation humaine moyenne).

1. Introduction

An objective laboratory procedure to assess color in tobacco leaves was proposed by Garcia et al. (1996). This study used leaves from cv «Virginia» provided by CETARSA (a large tobacco production company) along the 1993 and 1994 seasons. The color of the leaves ranked from «Pale Lemon» to «Oxidized Brown». Using the human expert classification uncertainty level was considerable, due to the high intra-leaves color variation which leads to overlapping color ranges between classes. A redefinition of the standard color classes is proposed by means of statistical management of data (clustering) on the basis of the color coordinates (X,Y,Z) assessed with a Monolight spectrophotometer. The ascription of a leaf to a color class is done by evaluating 12 color observations per leaf. The decision criteria used to assign global color class to leaves showed a high correspondence with the classification made by a CETARSA expert.

In order to check the feasibility of the color assessment procedure a validation test of several human experts versus the instrumental expert was needed. The considerations used by Brons et al. in 1993 on human experts for assessing the beauty of cyclamen have also been taken into account in this research.

2. Objectives

- To verify «in situ» the established classification method by its comparison against several CETARSA experts;

- To improve, if necessary, the decision system employed, looking for a higher correspondence between the classifications made by human experts with the «virtual expert» (automatic).

3. Materials and methods

3.1 Materials

Tests were carried out in 1996 in Talayuela (Cáceres), at the premises of CETARSA. 240 tobacco leaves cv. «Virginia» pertaining to 12 commercial color categories covering the range from «Pale Lemon» to «Oxidized Brown» were used. Leaves were randomly distributed in 4 sets of 60 leaves, identifying each leaf with a number from 1 to 240. Measurements were performed according to this random disposition.

3.2 Methods

4 CETARSA experts made a leaf by leaf classification in consecutive leaf number order and without contact between them, assigning a color class from pale lemon to oxidized brown to each leaf. At the same place, samples were analyzed by using a Monolight spectrophotometer calibrated at the beginning with a laser and a white reference, and each 2 hours according to the 7.5YR sheet from the Munsell table. 12 observations per leaf were taken using a plastic grid (see Figure 1) containing 6 squared cells. The visible spectrum (400 a 700 nm) was measured in all cases.

Tristimulus coordinates X, Y, Z for F7 iluminant the same (used by CETARSA experts) were calculated from the obtained spectra by integration according to Calvo C., **1996.** The overall methodology is showed in Figure 2.

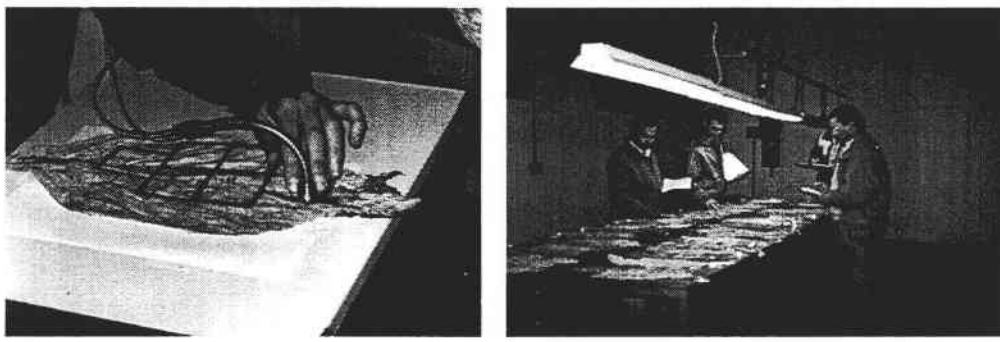

Figure 1: Sampling procedure followed for the instrumental assessment of color (left image) and color assessment by CETARSA experts

3.3 Data analysis

Data analysis were analyzed with Statistica for Windows 4.1.

3.3.1 Generation of an Average Human Expert

The Classification scores corresponding to «average» human expert were calculated as the aritmethic mean of the 4 human experts classifications per leaf.

Correlations and % of well classified individuals between each human expert and the average human expert were attained. The percentage of well classified individuals was calculated as the proportion of individuals classified in the same class by 2 different experts, considering correct a classification also when scored in the inmediately upper or lower class.

3.3.2 Generation of the virtual expert

2/3 of the Monolight color observations (1911 observations) were used to generate 12 color classes through cluster analysis. Clusters were supported on the tristimulus coordinates X, Y, Z pertaining to the spots measured on each leaf. Each cluster was assimilated to a commercial color class, starting in cluster 1= Pale Lemon up to 12= Oxidized Brown, and then compared with the previous clusters created in 1994 and 1995. From this stage, clusters were employed as a new color base as their internal variability (6%) was much lower than in the original color classes according to CETARSA (20% aprox.).

A Bayes classifier was used with the new color base considering each class to follow a normal distribution. This method enabled to establish the ascription probability of a color observation (12 per leaf) to each one of the clusters previously generated. The final color class assigned to each observation is: the class with maximum probability if this is higher than 60 % or the mean of the 2 classes with maximum probability, if the maximum is lower than 60 % (these last individuals are named frontier individuals between 2 classes).(SAS 1988). All observations (2880) were reclassified on the basis of the new color base (1911 observations) as a verification of the Bayes classification procedure. Four different «virtual experts» were created to assign a final color class to each leaf, utilizing the following criteria: mean (AM), mode (MO), geometric mean (GM) and harmonic mean (HM) of the 12 observations per leaf.

3.3.3 Comparison between the human an the virtual experts

The Correlation matrix between the classes assigned by human and virtual experts as well as the % of well classified individuals were calculated.

4. Results and discussion

4.1 Generation of an average human expert

Correlations between each one of the four human experts with the named «Average Human Expert» range between 0.89 and 0.93, which indicates a high concordance among them (See Table 1). It is outstanding that correlations among human experts are always lower than correlations of each one of them with the average expert. This fact justify the use of Average Human Expert as valuation parameter of the virtual expert (objective color classifier). Also the percentages of well clasified observations are higher when comparing each expert with the Average Human Expert than with the other 3 experts.

A study was made of the accumulation or trend of errors made by experts throughout each set. When an error appears, it takes to the expert a certain number of leaves to classify correctly again (the cases when it takes more than 6-7 leaves have been marked). It is also shown that errors appear more frequently in intermediate color classes (See Figures 4).

In Figure 5, the histogram corresponding to the classes assigned to the total of 240 leaves by the average human expert is shown. The most frequent values correspond to lemon classes.

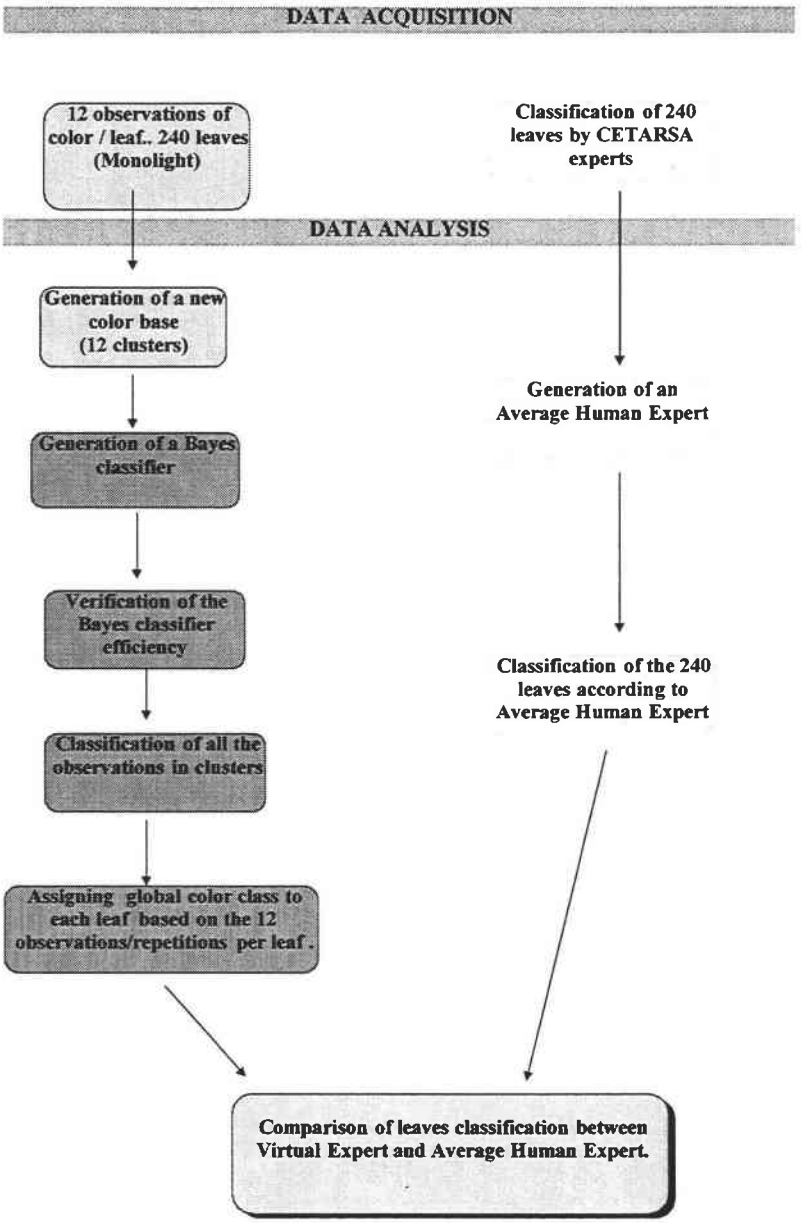

Figure 2: Summary on the overall methodology

	Exp 1	Exp 2	Exp 3	Exp 4
Exp 1	1.00	.76	.70	.77
Exp 2	.76	1.00	.83	.81
Exp 3	.70	.83	1.00	.78
Exp 4	.77	.81	.78	1.00
Avg Exp	.90	.93	.89	.92

% well clas	Exp 1	Exp 2	Exp 3	Exp 4
Exp 1	100	60.34	45.49	55.36
Exp 2	60.34	100	60.08	58.4
Exp 3	45.49	60.08	100	55.36
Exp 4	55.36	58.4	69.03	100
Avg Exp	66.09	76.05	79.91	84

Table 1: Correlations and % of well classified individuals between variables EXP1 (Human expert 1), EXP2 (Human expert 2), EXP3 (Human expert 3), EXP4 (Human expert 4), Average (Average human Expert) corresponding to observations of all the sets

4.2 Generation of a virtual expert (objective color classifier)

The color base created (clusters) is very similar to the one obtained in the 1995 season (see Table 2); therefore the color base can be consider stable through seasons..

Clusters	Ymean 1995	Ymean 1996	CV 95	CV 96
1=Pale Lemon	43.87	43.46	2.87	8.31
2=Soft Lemon	39.54	36.44	3.14	5.59
3=Moderate Lemon	33.38	32.13	4.79	3.72
4=High Lemon	28.9	28.43	3.98	3.28
5=Deep Lemon	26.02	25.49	2.96	3.39
6=Pale Orange	23.1	22.9	3.68	3.08
7=Soft Orange	20.65	20.7	2.91	3.13
8=Moderate Orange	17.14	18.32	6.65	3.77
9=High Orange	14.13	15.76	5.31	5.07
10=Deep Orange	11.47	13.17	6.97	6.31
11=Light Brown	7.49	10	20.69	9.21
12=Oxidized brown	-	6.63	-	19.94

Table 2: Average values and CV of tristimulus coordinate Y for the clusters created in 1995 and 1996

The Bayes classification procedure for color observations (see Table 3), shows similar success levels than in previous seasons, overcoming 90 % in the 3 seasons, with errors lower than 4 % in all cases.

From the 4 different virtual experts used for global color leaf evaluation: mean (AM), Mode (MO), geometric mean (GM) and harmonic mean (HM) from 12 observations per leaf, the virtual experts aritmethic mean (AM) and mode (MO) show a

correlation of 0.99 (see Table 4), which indicates that all of them tend to assign as the global value per leaf the most frequent color.

Classes	% Well classif.	% frontier points	% Bad classified
Total 94	93.3	2.6	4.09
Total 95	94.8	4.6	0.57
Total 96	90.16	7.43	2.41

Table 3: Percentage of well classified observations (12 per leaf), frontier points (in-between two classes) and bad classified observations with respect to the class assigned in the cluster analysis when utilizing Bayes method

r	AM	MO	HM	GM
AM	1.00	.99	.99	1.00
MO	.99	1.00	.98	.99
HM	.99	.98	1.00	1.00
GM	1.00	.99	1.00	1.00
Averg. H.E.	.81	.81	.81	.81

% well clas	Averg. H. Exp.
AM	53.13
MO	51.04
HM	56.48
GM	58.15

Table 4: Correlations between variables AM (average virtual expert), MO (mode virtual expert), HM (harmonic mean virtual expert), GM (geometric mean virtual expert), Average (average human expert) corresponding to observations of all the sets

4.3 Comparison of average human expert with the virtual expert

In Table 4 is indicated that correlation levels of Average Human Expert with virtual experts are in all cases 0.81, lower value than those obtained by CETARSA experts with respect to Average Human Expert ranging from 0.89 to 0.92. This fact is understable when comparing Average Virtual Expert (AM) histograms with the Average Human Expert ones (see Figure 5). The first expert tends to assign global color class taking into account the most frequent color on the leaf, while the Average Human Expert tends to penalize the presence of lemon colors. Thus, he assigns most frequently lemon colors classes. This fact determines that the virtual expert show less well classified individuals with respect to the Average Human Expert (between 58 and %) than each four of the human experts (between 66 and 84 %, see Table 4).

When trying to optimize the virtual expert, it was concluded that the reason why the human experts tended to have a wider number of leaves classified in the lemon classes was the use of a wider amplitude within those classes when compared to the more homogeneous cluster categorization (see Figure 6). Therefore it was decided to generate new color classes according to the quantils made by the

average human expert (% of individuals within each class). To do so the callibration set (1911 observations) were sorted in ascending order according to the Y coordinate and categorized according to the human quantils. This procedure leads as expected to wider amplitudes in the lemon classes (see Figure 6). The global color classification per leaf in this new virtual expert is assigned as the quantil corresponding to the average Y of all 12 color observations per leaf. The optimizarion of the virtual expert leads to 73.64% of well classified leaves, value which is within the range of well classified individuals shown by human experts (between 66% and 84%).

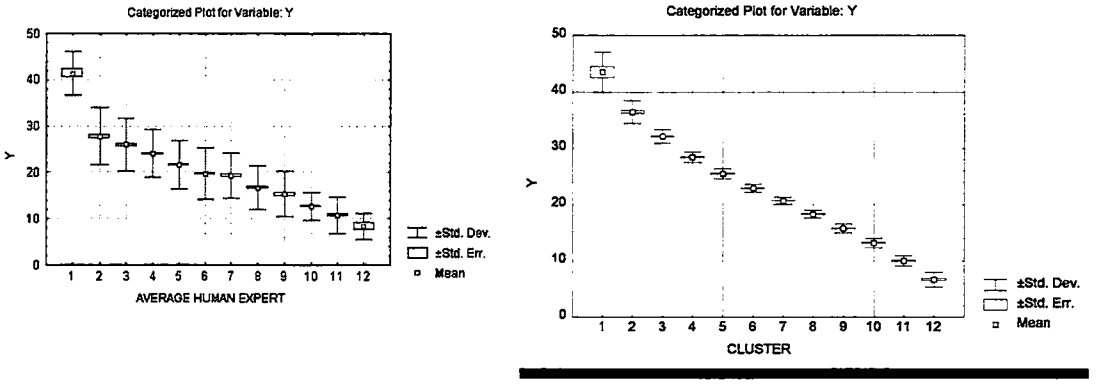

Figure 3: Plot of averages and standard deviations for Y coordinate in each class established by CETARSA and created by cluster analysis by using variables X, Y and Z. (see means and CV in Table 2)

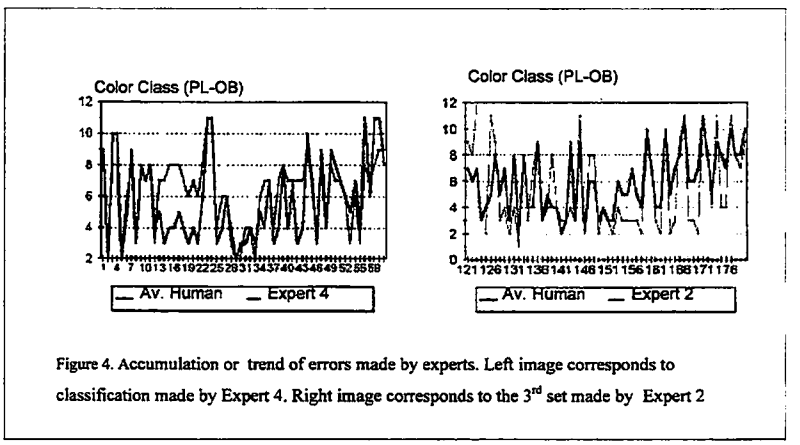

Figure 4. Accumulation or trend of errors made by experts. Left image corresponds to classification made by Expert 4. Right image corresponds to the 3rd set made by Expert 2

Figure 4: Accumulation or trend of errors made by experts. Left image corresponds to classification made by Expert 4. Right image correspond to the 3rd set made by Expert 2

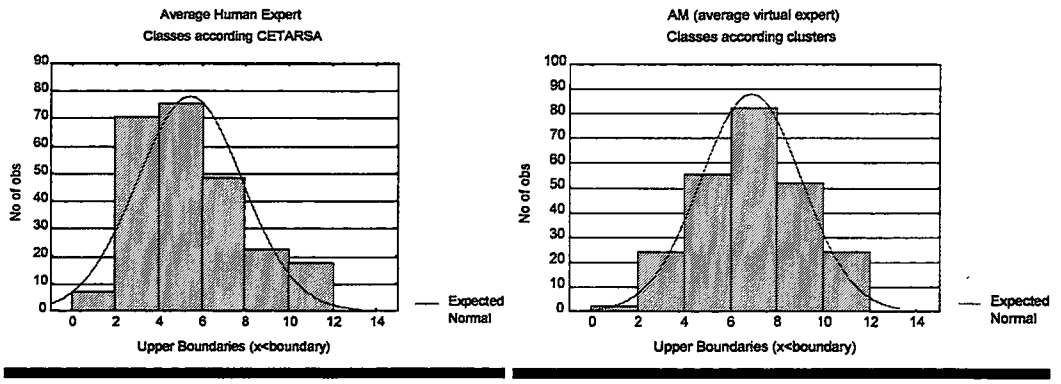

Figure 5: Frequency of CETARSA colour classes (average of 4 experts) and Average Virtual Expert (AM) classes

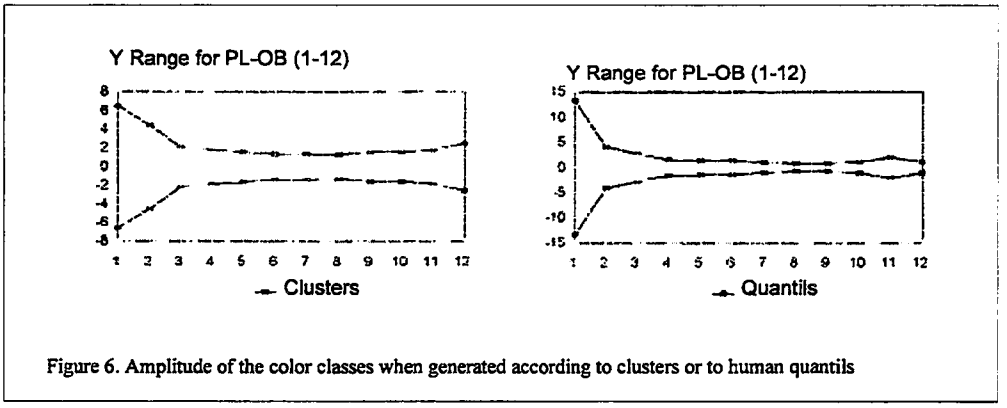

Figure 6. Amplitude of the color classes when generated according to clusters or to human quantils

Figure 6: Amplitude of the colour when generated according to clusters or to human quantils

Conclusion

- An Average Human Expert has been established for comparison purposes with the objective color classifier.

- The stability of the color base created in 12 clusters showing an intrinsical variability of 6 % approximately has been proved for three consecutive years.

- Therefore, it is possible to fabricate specific color charts for tobacco leaves according to the new color base. It would be based in the spectrums corresponding to the medium value of the triestimuli coordinate Y of each cluster.

- The Virtual Experts Mode and Average show a high correspondence index with the Average Human Expert (0.81).

- The Average Virtual Expert (AM) tends to assign as the global color to a leaf, the most frequent one, while the Average Human Expert tends to classify more frequently the leaves into lemon classes.

- A final optimization of the color classes into human quantil classes allows to obtain a higher performance for the virtual expert (similar histograms) with a percentage of well classified leaves of 73.64%. This value is within the human range of well classified leaves (that ranges between 66% and 84%).

References

Brons A., G. rabatel, F. Ros, F. Sevila, C. Thouzet. 1993. Plant grading by vision using neural networks and statistics. *Computers and Electronics in Agriculture, Vol.9, nº 1.(August) :25-39.*

Calvo, J. 1996. *Handbook of Food Analysis, Volume I, Ch.5 :* Optical properties. DE. Nollet. Marcel Dekker.

García Pardo E.; Barreiro P.; Ruiz-Altisent M.; Alonso R. 1996. Objective optical classifier for tobacco leaves. *International Conference on Agricultural Engineering.* Madrid. Paper 96F-034.

Júdez L. 1989. *Técnicas de análisis de datos multidimensionales.* Ed. Ministerio de Agricultura, Pesca y Alimentación.

SAS Institute Inc. 1988. *SAS/STAT* User´s Guide, Release 6.03.* Ed. Cany, NC: SAS Institute Inc. 1028.

Objective plant quality measurement by image processing

Mesure objective de la qualité des plantes par analyse d'images

J. Meuleman

Department of Agricultural, Environmental and Systems Technology, Wageningen Agricultural University, Bomenweg 4, NL-6703 HD Wageningen, The Netherlands
Institute of Agricultural and Environmental Engineering (IMAG_DLO), Mansholtlaan 10-12, P.O.Box 43, NL-6700AA Wageningen, The Netherlands
e-mail: jan.meuleman@user.AenF.WAU.NL

J.W. Hofstee

Department of Agricultural, Environmental and Systems Technology, Wageningen Agricultural University, Bomenweg 4, NL-6703 HD Wageningen,
The Netherlands

C.V. Kaam

Department of Agricultural, Environmental and Systems Technology, Wageningen Agricultural University, Bomenweg 4, NL-6703 HD Wageningen,
The Netherlands

Abstract: *Three year of research are spent at the development of objective quality measurement at pot plants. The research project was possible due to the financial support by the EC, on the base of contract AIR3-CT94-1072. The research is done in an international co-operation with Danish , French and Dutch partners from October 1, 1994 until October 1, 1997.*

As a result of ongoing reset before 1994 at the Wageningen Agricultural University (WAU) and the Cemagref, reported by Brons(1992) and Dijkstra(1994), it could be expected that the introduction of plant grading will have benefits for horticultural practise. Both, the WAU and the Cemagref, investigated ability to apply neural networks in combination with image processing. Nevertheless, to built successful applications still a lot of fundamental work had to be done. In stead of solving these bottlenecks separately an international co-operation is formed. The main objective of this international research group was the further development of image processing techniques and decision systems as neural networks, making this combination of techniques suitable for grading off plants. At that time human grading of plants was experienced as a highly subjective process.

The project concentrated on quality assessment of half grown plants, related to the expected growth and development, and (as most important) marketable plants related to ornamental value. The research was split up in following main parts:

- development of feature measurement methods;
- defining the GSTO (Grading System Target Output);
- development of decision systems;
- testing of the system.
- logistic aspects with respect to the introduction of grading
- technical and economical feasibility of grading

The project has dealt with a great variety of pot plants: half grown plants(DK & NL), marketable flowering plants(DK, F,NL) and marketable green plants(NL), including Begonia, Rosa, Hibiscus and Ficus.

During the project (horticultural) research stations developed the GSTO.
The Cemagref and the Universities of Wageningen and Copenhagen developed both the feature measurement, based on image processing and the decision systems to calibrate the output of computer neural decision systems to the human experts' judgement of plant quality. In the half grown stage the computer models have been calibrated to the expected development of plants, as given by horticultural experts. In the marketable stage the computer models have been calibrated to the ornamental value (human appreciation) of the plants.

The main results of the total project will be presented. Attention will be paid to future applications of the developments, especially regarding growth and development of plants in a protected environment: Since plant quality now can be measured in an objective way, both at the half grown and at the marketable stage, future research can be concentrated on 'how to produce a well defined quality of a plant in the most efficient way'.

Keywords: *Image processing, quality assessment, neural networks, grading.*

Résumé : Lors d'un contrat AIR3-CT94-1072, a été développé une méthode objective de mesure de la qualité des plantes en pot. La recherche est menée en collaboration internationale incluant des Danois, des Français et des Hollandais du 1er Oct. 94 au 1er Oct. 97. Le principal objectif de ce groupe de recherche international est le développement de techniques basées sur l'analyse d'images et les systèmes de décision à réseau de neurones afin de faire l'agréage des plantes en pot.

Actuellement, l'agréage est fait par des humains, ce qui rend le procédé très subjectif. Le projet s'est concentré sur l'évaluation de la qualité en fonction de la croissance, du développement attendu et de l'aptitude à la commercialisation des plantes relative à leur valeur ornementale. Ce projet a mis en jeu un grand nombre de variétés de plantes en pots : des plantes à demi-poussées, des plantes à fleurs commercialisables et des plantes vertes commercialisables incluant bégonia, rose, hibiscus et ficus.

Pendant le projet, des stations de recherche horticole ont développé les classes d'agréage. Le Cemagref et les Universités de Wageningen et de Copenhagen ont développé à la fois la mesure des paramètres basés sur l'analyse d'image et le système de décision permettant de calibrer la sortie d'un réseau de neurones en fonction du jugement d'un expert sur la qualité des plantes. Pour le stade "à demi-poussée", le modèle a été calibré par rapport au développement attendu d'une plante indiqué par des experts horticoles. Pour le stade commercialisable, le modèle a été calibré par rapport à la valeur ornementale appréciée par un expert. Les principaux résultats du projet sont présentés. Une attention particulière est donnée aux applications futures de ce projet, plus particulièrement au niveau de la croissance et du développement des plantes en environnement protégé. Puisque la qualité des plantes peut maintenant être mesurée de manière objective à la fois au stade en semi-hauteur et au stade commercialisable, les futures voies de recherche doivent être concentrées sur le problème suivant : comment produire une plante de qualité bien définie de la manière la plus efficace possible ?

1. Introduction

In a three years research contract, based on contract AIR3-CT94-1072, financed by the EC, the objective quality measurement of pot plants has been developed. Danish , French and Dutch partners were involved in the project from October 1, 1994 until October 1, 1997.

As a result of earlier research at Wageningen Agricultural University (WAU) and the Cemagref, reported by Brons(1992) and Dijkstra(1994), it could be expected that the introduction of plant grading will have benefits for horticultural practise. Both, the WAU and the Cemagref, investigated the ability to apply neural networks in combination with image processing. To built successful applications a lot of fundamental work had to be done. The main objective of the international research group was to develop the image processing together with decision systems as neural networks for the application of plant grading. At that time human grading of plants was experienced as a highly subjective process.

The project concentrated on quality assessment of half grown plants, related to the expected growth and development, and (as most important) marketable plants related to ornamental value.

2. Material, methods, experiments

The research has been split up in the following main parts:

a) development of feature measurement methods;
b) defining the GSTO (Grading System Target Output);
c) development of decision systems;
d) testing of the system;
e) logistic aspects with respect to the introduction of grading;
f) technical and economical feasibility of grading.

The partnership consisted of two universities(WAU1 and KVL2), one research institute(CEMAGREF3) and two horticultural research stations(PBGA4 and SP5).

---

1 WAU: Wageningen Agricultural University, Department of Agricultural, Environmental and Systems Technology (NL).
2 RVAU: Royal Veterinary & Agricultural University, Department of Agricultural Sciences (DK).
3 CEMAGREF-Montpellier:Division Génie instrumental pour la qualité agro-alimentaire(F).
4 PBGA: Research Station for Floriculture and Glasshouse Vegetables, department «Aalsmeer»(NL).
5 SP:Danish iInstitute of Agricultural Science, Department of Ornamentals, Aarslev(DK).

To generalise the results of the project, representatives of green and flowering pot plants were chosen: Ficus benjamina exotica, Hibiscus rosa-sinensis, Rosa hybrida and different types of Begonia's.

2.1 The development of feature measurement methods

The developed set of features, applicable for side-view or top view images, can be divided in primary features, derived features and features with a new object as result. For primary features, for example the number of object pixels, the original image is required. Derived features, for example compactness, can be calculated from the set of primary features. An example of a features with a new object as result is the histogram of polar co-ordinates: The polar co-ordinates (r,■) of each object pixel are determined and for each angle between 0 and 360° (in steps). The number of pixels per angle can be counted with the centre of the top of the pot as the origin. Table 1 gives an overview of the groups of developed features6.
Also a procedure to test the consistency of the measured features in an experiment is developed. The consistency of a feature is defined by: equation 1. To exclude the effect of absolute values depending on difference in size of each plant, the test compares the measured values per plant with the mean of the measured values per plant. In general a consistency of 94% or better is considered as acceptable.

$$consistency = \left(1 - \frac{\sqrt{\sum_{i=1}^{m}\sum_{j=1}^{n}\left(\frac{x_{ij}}{\bar{x}_i} - \bar{x}\right)^2}}{\frac{n.m - m}{\bar{x}}}\right).100\% \qquad (1)$$

- m = the number of plants in the consistency test;
- n = the number of repetitions for feature measurement per plant;
- x = the measured value of a feature of plant i and repetition j.

2.2 Defining the GSTO (grading system target output)

To define the target output of the grading process, the horticultural research stations have set up growing experiments for green and flowering pot plants. In the half grown stage images are collected and experts are asked to grade the plants in distinguishable groups with respect to the expected growth and development. In some cases (Ficus benjamina) also plant features are measured by hand in a destructive way, for example to measure the total leaf area, number of leaves, branching, length of internodia, etc. Comparing hand measured features and

6 Contact the author for more datailed descriptions of the features:e-mail:jan.meuleman@user.AenF.WAU.NL.

The total leaf area, measured by hand could be linearly related to (4.17 times) the number of object pixels, counted by machine vision, explaining 96% of the variance. However, in most cases no satisfactory relationships between hand measured and machine vision measured features could be found by means of MLR(multiple linear regression). So it was concluded that translating machine vision measured features into hand measured features to explain the quality of the plant is a wrong approach. Instead of it, the approach has been followed that machine vision looks differently to plants than a human does, measuring other features which sometimes are hard to deal with for a human. The length of the convex hull and the location of the optical centre of the plant are for example very difficult features to handle for human, but not for machine vision. With the decision systems a map between quality assessment of plants by experts and the set of features, measured by machine vision had to be made.

Besides the quality assessment by an expert panel in the half grown stage, the same plants are also measured by machine vision and evaluated on quality by the panel with respect to ornamental value at the marketable stage.

The consistency of the experts is also tested in some experiments. Experts are given the same group of plants to grade a second time. A good expert is able to place 80 until 85% of the plants both times in the same grade. Some experts are even better.

To relate the machine vision measured features to the quality assessment of the expert panels, decision systems have been developed.

2.3 The development of the decision systems

For grading Ficus benjamina plants in the marketable stage as well as half grown, the same decision system software could be used. The software, partly developed during the project, consists of a Neural Network(NN), programmed in the C/C++ language. NN are particularly suitable for grading tasks because of their capability to sensibly interpolate between learnt cases and sensibly extrapolate to a certain extend beyond learnt cases and NN have the added advantage, compared to linear regression, of handling non-linearity's and discontinuities on an easy way. Fully connected networks with one hidden layer are used, with a unipolar sigmoid activation function in the hidden layer an a threshold neuron added to both the input and the hidden layer. Because in general there is no ranking order among the grades, distinguished by the experts, for each grade a separate output neuron is used. Batch training is applied instead of pattern training because the gradient vector can be estimated more accurately (experts are also making mistakes, having a consistency far below 100%).To avoid learning the mistakes of the experts, the learning process of the network is stopped after reaching maximum performance (percentage of objects which are identically classified by NN and expert) on the test

set, while learning on the training set. The number of neurons in the hidden layer is always optimised to get better inter- and extrapolation properties.

For the half grown Rosa hybrida and Hibiscus rosa-sinensis plants, linear and quadratic discriminant analysis, implemented in the SAS statistical program package were used to classify the plants. Features, measured at the half grown stage were used as input, together with information on the treatment of the plants from half grown to marketable stage. At the marketable stage the plants are graded by experts and the result of this grading is used as the parameter, according to which the half grown plants were classified.

The decision system, used to grade the Begonia at the marketable stage, consists of two parts: Statistical analysis of data by means of PCA (Principle component analysis) in order to reduce the number of variables, followed by a MLR and a NN processing (NeuralWorks from NeuralWare Inc.) that simulates the grading behaviour of experts.

2.4 Testing of feature measurement and decision systems

The task testing in the project is divided into two parts. Part 1 is the testing of the decision systems developed by the different partners. Part 2 is testing of the objectivity of plant quality. The main objective is to answer the question whether the conception quality (human appreciation) is objective in itself or that human appreciation is a subjective concept, but can be only measured in an objective way. An experiment in which plants are judged by experts from different countries (DK, F, NL) has been carried out All plants have also been measured by machine vision. Partners are supplied with the machine vision measured features and the expert judgements to test their developed decision systems. In total 864 flowering Begonia barcos plants have been purchased. These plants are divided over two places: 432 at the PBGA and 432 at the SP. On both places the plants are measured by identical machine vision systems, consisting of a PC, a Sony DXC-930P camera and a Matrox Comet framegrabber. At the PBGA the plants are judged by Dutch and French experts and at the SP by the Danish experts.

2.5 Logistic aspects with respect to the introduction of grading and technical and economical feasibility

The effects of the introduction of grading in horticultural practise are investigated by means of a case study. Using the simulation and visualisation package ARENA, a virtual production system for a Ficus benjamina is built with a yearly production of 500.000 plants on a virtual nursery of 32.000 gross m^2 (28.000 m^2 growing area).The plants are brought to the market at 3 different heights: 90 cm, 120 cm and 150 cm, growing respectively in 17, 21 and 24 cm pots.

The main disadvantages of the introduction of grading in practise are besides the investment in the grading system also the capacity of the intern transport system has to be increased with a factor 3. The main advantages are increase of the quality (due to better control of growth and development), better use of the growing area and an improved production planning.
The total system is virtually created by a project group, consisting of members from WAU, PBGA, and a grower. The technical feasibility is judged by suppliers of horticultural equipment. The logistic aspects of the system are judged in terms of required capacities of machines, robots and transport tools. To complete the economical aspects of the introduction of grading, not only the simulation is done but also growing experiments to investigate the effects of grading on growth and development.

3. Results

3.1 The feature measurement

The quality of the feature measurement is tested in both the Ficus benjamina and the Begonia barcos experiments by calculating the consistency of the values of the features. The features, suitable to evaluate with equation 1, show a high consistency, as can be seen in table 2.

3.2 The grading system target output (GSTO)

Table 3 gives an overview of the relative distribution of plants over grades and the consistency of the different experts in the Begonia barcos experiment. The experts show an unexpected low consistency, compared to the results in similar experiments of earlier research work (Dijkstra, 1994). For this experiment experts with knowledge both from the producers quality appreciation as well as consumers quality appreciation are invited. Perhaps the Begonia barcos is a difficult plant for quality judgement, but it is clear that some experts showed a much higher consistency than others. Experts have been asked to grade the plants in four classes: high quality 1, low quality 1, high quality 2, low quality 2 and a class to reject. Experts were asked to apply their national opinion about quality appreciation.

3.3 The decision systems

The developed decision systems worked in general very well. Although 79 features are measured for Ficus benjamina, in the marketable stage a very simple NN was able to imitate a grower. With only three features as inputs:

1. number of object pixels;
2. vertical position of the optical centre and
3. length of the convex hull

a performance around 80% could be found. Only three hidden neurons were required. Table 4 shows typical results of the NN, showing also that, when using three features as input, it is enough to use three neurons in the hidden layer. Furthermore it is clear that, when using combined machine vision and NN decision systems, other features have to be used than nowadays a human eye is attuned to. A good plant quality can be expressed in terms of features, determined by machine vision.

Imitating different experts/growers shows that for some experts more input features are required than for others. Table 5 illustrates this effect. Using no features, the NN places all plants in experts largest class.

In case of expert 2 the performance is hard to improve by adding input features, while imitating expert 5 the performance can be improved with 12% by adding two input features.

For each expert a ranking order is made for the 79 features, based on the performances that could maximally be reached by using each feature separately as the only input for the NN. For none of the six growers involved, the ranking orders were the same. The most important features in the raking order of all six experts are:

1. the vertical position of the optical centre of the plant;

2. the width of the plant in the 2nd layer7 from the side view image with the largest width;

3. plant density (plant pixels/total number of pixels) in the convex hull in the 2nd layer from the side view image with the largest width;

4. width of the plant in the 2nd layer in the image perpendicular to the side view image with the largest width;

5. area covered by the plant;

6. density in the convex hull.

For all six experts in the experiment the ranking order of the features has been correlated. Table 6 shows for example that the ranking order for grower 2 correlates relatively low with each of the other experts.

7 Some features are calculated per layer. Layer 2 starts at 20% and ends at 40% of the total height of the plant.

3.4 Testing the decision systems

The data from the Begonia barcos experiment are processed in Denmark, France and in the Netherlands.

Denmark found that the performance of the decision system decreases rapidly when distinguishing five classes, as defined in paragraph 3b. The number of classes have been reduced to three, merging the subclasses of quality 1 and the subclasses of quality 2. Table 9 gives an overview of the results, using linear discrimination. By combining classes performances between 58 and 75% could be reached.

In the Netherlands classes are not merged. For each individual expert an optimal combination of 3 variables is selected, resulting in the performances as given in table 7. Also the ranking order of the 29 measured features is calculated. For all available experts the same six single input variables are in the list of single variables, giving the best performances if the NN is trained with one feature. This was more than we expected. It means that experts from different countries are unconsciously taking into account the same plant features, given in table 8. From these features also the average ranking number is calculated per country. The lower the rank, the more important the feature is. We can learn from table 8 that there are some differences between the importance of the features between the experts from the different countries. The experts agree generally about the important features, but do not appreciate all features in the same way.

The French analysed one expert per country: Danish expert 4, Dutch expert 2 and French expert 1. After reducing the number of variables by means of PCA, the NN was applied on the individual experts. The results are given in table 10. In this analysis class 5 (plants to reject) is not used.

The Danish expert could be imitated with a performance of 54%, the Dutch expert with 74% and the French expert with 45%. A test with all 28 features, without PCA, could bring the correct classifications from 45% to 47%.

3.5 Logistic aspects with respect to the introduction of grading and technical and economical feasibility

A new tool for further research is developed: a complete virtual plant factory. The simulation package reads the file with orders from last year and starts planting rooted seedlings on the planting machine. All important data, as capacity, required labour, etc. can be linked to the action «planting». The pots with the rooted cuttings leave the planting machine for transport to a grading machine to divide the plants in two grades. After grading a robot groups the pots, making rows. After the total processing the plants are placed in the compartment of the greenhouse. Than the

growing process starts. After a pre-determined period the plants are brought to the grading machine and graded again in two new grades. All transport of the plants is visualised, so the total process can be verified. If a resource, for example a buffer, has not been given enough capacity, it can be seen that the process works inefficient. In the simulation data from practise are used, for example capacities of robots, required labour, etc.

Besides simulation also growing experiments have been carried out. these growing experiments have shown that grading can result in a better control of growth and development. It is found that the required cultivation period can be reduced with about 30%: an increase of the throughput of 45%, using the same growing area and realising at least the same quality. One comment has to be placed: to realise the increased throughput it is required to adjust environmental control to the need of the plants. In practise it means that a greenhouse has to be divided in more compartments with independent environmental control. This is expensive. However: an increase of the throughput with one percent is globally equal to an increase of production value per m^2 of one Dutch guilder. With respect to the economical feasibility, also some remarks have to be made: The increased throughput justifies very high investments, under the assumption of unchanging prices, but even slowly decreasing prices over several years justify an investment in a grading system. Under the assumption of unchanging end prices it is possible to do an investment in the total system of one million Dutch guilders.

Table 1: List of developed features

A	(Groups of) **primary features**
1	Number of object pixels [-]
2	Number of background pixels [-]
3	Number of background pixels enclosed by object pixels [-]
4	Position of optical centre (centre of gravity) of the object in X and Y direction [mm]
5	Optical centre offset [mm]
6	Object height [mm]
7	Object width [mm]
8	Number of object pixels in four quadrants [-]
9	Number of old and young leaf pixels in four quadrants [-]
10	Length of the convex hull [mm]
11	Length of the perimeter [mm]
12	Standard deviation in X and Y-direction [-]
13	Normalised difference left and right
B	(Groups of) **derived features**
1	Compactness [-]
2	Compactness of young leafs [-]
3	Dispersion X and Y [-]
4	Total dispersion [-]
5	Percentile heights [mm]
C	(Groups of) **features with an object as result**
1	Histogram of polar co-ordinates [-]
2	Width per image line [mm]
3	Object pixels per line [-]
4	Object runs per image line [-]

Feature (Values after normalisation)	Sum of squares	df	Error variance	St. dev.	Consistency in %
Object area leaves [mm^2]	17.73	48	0.37	0.61	99.4
Flower area [mm^2]	24.54	48	0.51	0.72	99.3
Object perimeter [mm]	136.82	48	2.85	1.69	98.3
Object convex perimeter [mm]	12.76	48	0.27	0.52	99.5
Flower convex perimeter [mm]	4.09	48	0.09	0.29	99.7
Object convex area [mm^2]	35.64	48	0.74	0.86	99.1
Flower convex area [mm^2]	17.25	48	0.36	0.60	99.4
Maximum width object [mm]	70.25	48	1.46	1.21	98.8
Perpendicular width object [mm]	431.54	48	8.99	3.00	97.0
Maximum width flowers [mm]	18.90	48	0.39	0.63	99.4
Perpendicular width flowers [mm]	626.89	48	13.06	3.61	96.4

Table 2: Overview of consistency of feature measurement

Expert	Largest <----------class (in %)----------> smallest class					consistency (%)
French 1	31.9	29.4	23.1	13.7	1.9	47
French 2	32.2	29.4	17.1	16.7	4.6	38
French 3	30.3	28.5	21.1	12.5	7.6	57
Dutch 1	25.5	23.8	22.2	19.0	9.5	–
Dutch 2	35.6	34.7	28.5	0.7	0.5	75
Dutch 3	51.6	44.0	3.7	0.7	0.0	71
Danish 1	45.8	27.8	17.4	9.0	0.0	70
Danish 2	74.1	12.7	10.6	2.5	0.0	68
Danish 3	48.1	40.3	6.5	5.1	0.0	70
Danish 4	37.3	28.2	22.0	12.5	0.0	65

Table 3: Relative distribution of plants over classes and consistency of grading

number of neurons in hidden layer	performance on train set	performance on test set
0	31.1%	31.8%
1	60.3%	60.8%
2	74.8%	75.7%
3	79.5%	82.4%
4	78.8%	82.4%
5	81.5%	81.8%
6	82.1%	80.4%
7	80.8%	82.4%

Table 4: Performances reached when grading Ficus benjamina at the marketable stage, showing also the effect of the number of neurons in the hidden layer

Expert/ grower	Largest class (0 features)	Best reached performances using		
		1 feature	2 features	3 features
1	35%	82%	86%	89%
2	68%	72%	74%	75%
3	30%	70%	79%	80%
4	59%	73%	80%	85%
5	31%	67%	71%	79%
6	50%	62%	68%	71%

Table 5: Best performances reached, using combinations of 0 until 3 input features for 6 grower-experts

Expert-grower	1	2	3	4	5	6
1	1	0.67	0.97	0.80	0.95	0.87
2	0.67	1	0.67	0.60	0.66	0.65
3	0.97	0.67	1	0.79	0.97	0.86
4	0.80	0.60	0.79	1	0.75	0.92
5	0.95	0.66	0.97	0.75	1	0.83
6	0.87	0.65	0.86	0.92	0.83	1

Table 6: Correlation between ranking orders of features for 6 grower-experts

Expert	Performance	Expert	Performance	Expert	Performance
Danish 1	66 %	Dutch 1	51 %	French 1	57 %
Danish 2	80 %	Dutch 2	74 %	French 2	58 %
Danish 3	68 %	Dutch 3	82 %	French 3	60 %
Danish 4	61 %				

Table 7: Performances attained with the best combination of 3 input features (Dutch analysis)

Feature	Average rank of French experts	Average rank of Dutch experts	Average rank of Danish experts	Average rank of all experts
Plant area	1.7	1.8	1.6	1.7
Convex perimeter	3.8	3.3	4.0	3.8
Area within convex hull	3.0	3.7	3.0	3.2
Maximum width of plant	5.5	4.7	6.3	5.6
Width perpendicular maximum width	6.8	5.7	5.3	5,9
Equivalent diameter of plant8	1.5	2.2	1.4	1.7

Table 8: Ranking orders of the important features

DANISH EXPERTS						
classified as->	Training set			Test set		
class	1	2	3	1	2	3
1	72	19	9	73	15	11
2	23	53	23	19	38	44
3	49	25	26	0	31	69
Performance	58%			68%		
	Training set			Test set		
Number of used plants per set	class 1	class 2	class 3	class 1	class 2	class 3
	173	47	71	99	16	26

8 The equivalent diameter of the plant = $\sqrt{4.area / \pi}$

DUTCH EXPERTS						
classified as->	Training set			Test set		
class	1	2	3	1	2	3
1	85	9	6	86	8	6
2	15	63	23	23	31	46
3	14	29	58	17	14	56
Performance	75%			72%		
	Training set			Test set		
Number of used	class 1	class 2	class 3	class 1	class 2	class 3
plants per set	178	40	73	87	13	41
FRENCH EXPERTS						
classified as->	Training set			Test set		
class	1	2	3	1	2	3
1	82	14	3	82	13	4
2	6	69	25	11	54	35
3	18	24	58	6	39	56
Performance	74%			68%		
	Training set			Test set		
Number of used	class 1	class 2	class 3	class 1	class 2	class 3
plants per set	131	127	33	69	54	18

Table 9: Danish result of testing procedure

Danish	Predicted								
Real	Grade 1		Grade 2		Grade 3		Grade 4		Total
Grade 1		89%	5	6%	4	5%	0	0%	81
Grade 2		43%	12	20%	17	28%	6	10%	61
Grade 3	11	72	6	13%	28	58%	3	6%	48
Grade 4	0	26	1	4%	20	74%	6	22%	27
Dutch	Predicted								
Real	Grade 1		Grade 2		Grade 3				Total
Grade 1	48	77%	10	16%	4	6%			62
Grade 2	17	22%	51	66%	9	12%			77
Grade 3	6	8%	9	12%	60	80%			75
French	Predicted								
Real	Grade 1		Grade 2		Grade 3		Grade 4		Total
Grade 1	5	17%	24	80%	1	3%	0	0%	30
Grade 2	4	6%	49	78%	9	14%	1	2%	63
Grade 3	2	3%	33	48%	14	20%	20	29%	69
Grade 4	0	0%	10	20%	12	24%	28	56%	50

Table 10: French results of testing procedure

Conclusion

Since plant quality now can be measured in an objective way, both at the half grown and at the marketable stage, future research can be concentrated on 'how to produce a well defined quality of a plant in the most efficient way'. Next challenge is to control growth and development in the right direction towards the desired end

quality. This can be done by modelling growth and development. Not only plant features have to be brought in such a system, but also temperature and light. In this project it is proven that learning from data can result in very efficient systems. Why not modelling growth and development of plant types with decision systems as neural networks, even if we do not understand all physical aspects of plant growing systems.

Plant grading seems to be the first step on the way to utilising a part of the difference between the potential production and the realised production.

Acknowledgement

We would like to express our thanks to the EC for financing this project. Also Erik Persoon from nursery Zwethlande for supplying us with data from their plant factory. However, last but not least also all partners for their contributions to this project.

References

Brons, A. (1992). *Contribution des techniques connexionistes à l'évaluation qualitative de produits agro-alimentaires par leurs aspects visuels.* PhD thesis. De l'ecole nationale du genie rural, des eaux et des forets, Paris, France.

Dijkstra, J. (1994). *Application of digital image processing for pot plant grading.* PhD thesis Agricultural University, Wageningen, the Netherlands.

A photogrammetric method to measure geometry of standing tree stems

Méthode photogrammétrique appliquée à la géométrie des arbres sur pied

R. Thomas

CEMAGREF GIQUAL, BP 5095, 34033 Montpellier Cedex 1, France

CIRAD Forêt, BP 5035, 34032 Montpellier Cedex 1, France

M. Fournier-Djimbi

CIRAD Forêt, BP 5035, 34032 Montpellier Cedex 1, France

M. Lenoir

ITMI APTOR, BP 177, 38244 Meylan Cedex, France

C. Guizard

CEMAGREF GIQUAL, BP 5095, 34033 Montpellier Cedex 1, France

Abstract: Adjustment and description of a photogrammetric process allowing to measure trunk morphology of trees. This instrument computes clues of taper, tilts, slope, diameters and volume that are the base of biomechanical studies.

Résumé : L'article décrit la mise au point d'une méthode photogrammétrique pour apprécier la morphologie du tronc des arbres. Cet instrument calcule des diamètres, des volumes et des indices de décroissance, d'inclinaison et de courbure, qui sont à la base d'un grand nombre d'études biomécaniques.

1. Introduction

An accurate measurement of the stem geometry in the standing tree is of great interest for both wood quality appraisal and biomechanical studies. On the one hand, foresters sell standing trees and the estimate of heights, diameters, taper, sweeps... is necessary to value the commercial volumes [1]. On the other hand, a good knowledge of the structure geometry and especially of lean (which is impossible to measure on fallen trees!) is necessary to analyse i) the mechanical behaviour of tree stems against external forces as winds, gravity ... [2] , [3] , [4] and ii) the relationships between external morphology and the formation of reaction wood [5]. However, forest trees are tall structures that grow in a wild environment, and thus morphometric measurements on the field are difficult [6]. Our work aims at developing photogrammetric techniques (taking of photographs and image analysis) adapted to commercial trunks (8 to 10 meters of height).

For clarification of the photogrammetric system, about fifty Scots Pines (*Pinus sylvestris*) from Lozère (uplands, South of France) were photographed. This operation taken place in the research project between the CEMAGREF, ITMI, and the AFOCEL. The system principle is to use the external trunk morphology to study wood quality.

2. Materials & methods

2.1 Photographic sub-system

The first work was conception of the photographic sub-system. The latter must deliver a sharp trunk image with a homogeneous lighting on the first 8 meters high. The distance between the trunk and the focal plane, the focal axis slope are necessary for the processing of the images. For each tree, two perpendicular images are used to rebuilt tridimensional features of the trunk. To fit with these needing, a special photographic device was developed. It includes an horizontal plate [
Figure *1*], a common camera (Reflex , Nikon FM2) positioned vertically with a lens of 20mm or 35mm, a ultrasonic/infrared telemeter to give the exact distance trunk/focal plane and a slopemeter. The film is also a common one (100 asa). A distance of about 7 meters from the object for the 35mm lens, and 10 meters for the 20mm one, is necessary for a global capture of the trunk.

Figure 1: Photogrammetric Sensor

An homogeneous lighting is necessary to facilitate the outline of the trunk. In the natural site, daylight is variable and to mask shadows, a single flash isn't satisfactory. It's necessary to have a powerful light positioned near the trunk. Also, the cable use on the ground slows down the operation. For this reason, a master flash placed on the camera activates a photocell fixed on the mast which controls two slave flashes [
Figure 2]. This mast is displaced from the focal axis so that it doesn't perturbates the trunk image acquisition. A good trunk illumination from the base to the height of 10m is obtained by using two flashes fixed on a mast at two different heights : 5,5m and 2m. It located at 4,5m from the trunk base (horizontal distance). As done in [7], each tree is photographed in two perpendicular planes (stereovision). A vertical standard ruler of 2 meters high put on the tree bottom uses as reference on pictures.

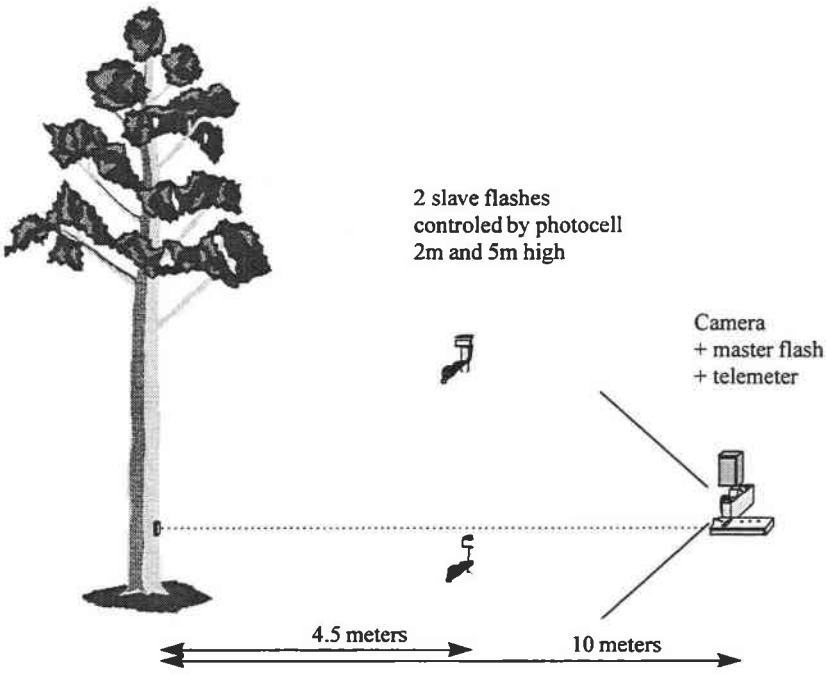

Figure 2: Lighting System

2.2 Analysis images sub system

For the analysis, a special software (QAP, "Qualité des Arbres sur Pied") was developed (Figure 1) with ITMI. This software accepts images of trunk outline photographs. The pictures are digitised from the negative film and saved as images .TIFF. The outline is extracted with common graphic software.

The distance between the focal plane (film) and the trunk, and the focal of the lens are necessary to compute the conversion meter/pixel. The height of the trunk cut is necessary too compute the outline image.

After the extraction of contour, the skeleton (mean line) is calculated.
From the contour, skeleton points and the conversion, several parameters are computed :

2.2.1 *The base bend*

- on the skeleton line, the software researches for the straight line passing through the biggest number of points (median method). This straight line is different of the one resulting from the first degree polynomial interpolation of the skeleton;

- Computation of variation between this lines.
The gaps and gap squares brings to the fore the base bend.

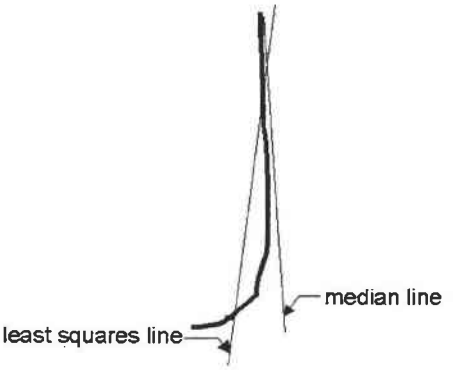

2.2.2 *The bend*

- extraction of contour;

- research for the skeleton;

- 1st ,2nd ,3rd and 4th degree polynomial interpolation line of the skeleton;

- computation of holding currently gaps from the skeleton to this polynomial interpolation lines.

Polynomial coefficients are good indicators of bend, and type of bend.

- a 2nd degree polynomial interpolation of the skeleton is enough to describe a single bend;

- if 3rd degree polynomial interpolation described better the trunk, its bend is double one;

- a 4th degree polynomial interpolation describes trees with multiple bend

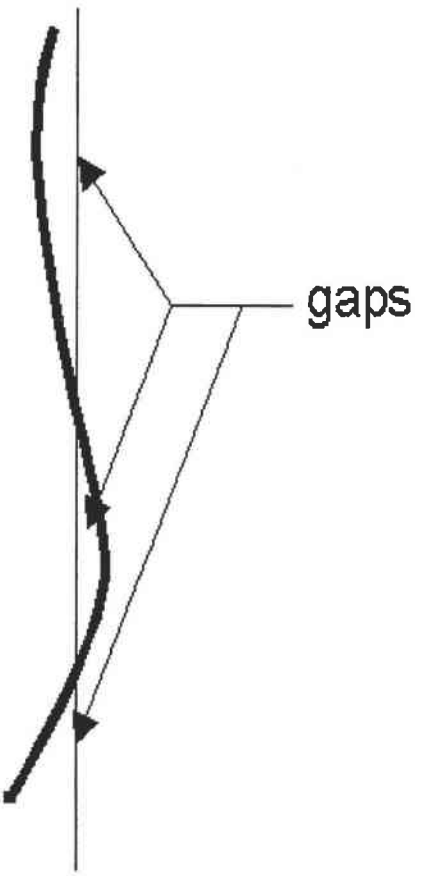

2.2.3 *The diameters*

Computation of 1,30 meters (base) and 8 meters (height) diameters on the 4th interpolated polynomial curve of trunk contour

2.2.4 *The tilt*

- contour extraction;
- research for the skeleton;
interpolation of the skeleton.

2.2.5 *The estimated volume below 8 meters*

- computation of diameter for each height (line by line) up to 8 meters high on the 4th interpolated polynomial curve of trunk contour;

-volume estimation.

2.2.6 *The taper*

- contour extraction;
- computation of the 1st and 2nd degree polynomial interpolation of the contour points.

The polynomial coefficients show in mean way the diameter variation.

The software compiles all this results in a .TXT file, and gives coordinates (XZ or YZ) of outline points in an other file.

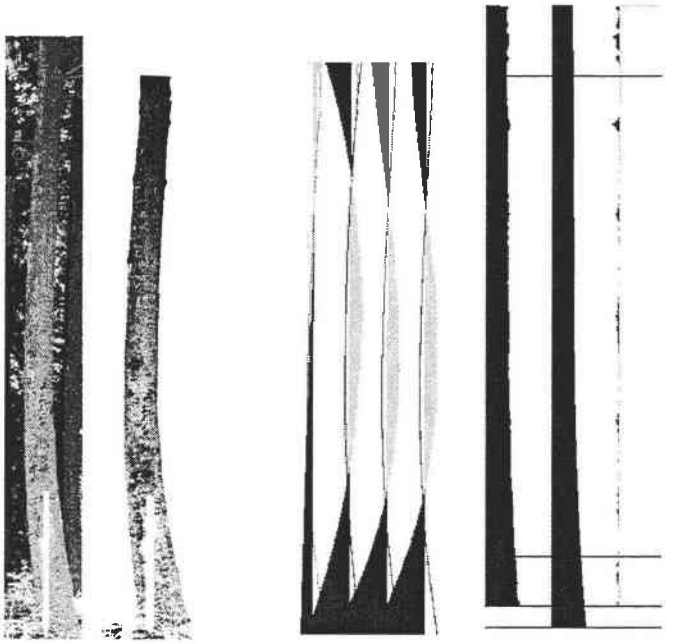

Figure 3: Numerical processing is performed to obtain the following geometrical parameters : diameters at different heights (volume and taper), sweeps and leans (on different spans)

3. Results

The method is validated (Figure 4) by comparison of the computed geometry with direct measurements on the standing stems (to measure the leans, we climb on the tree with special ladders and use a digital inclinometer fixed on a 1 meter long bar) and on the felled trunks (volumes, diameters, lengths, sweeps).

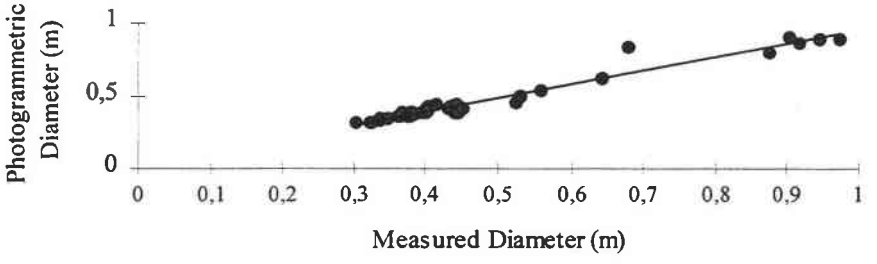

Figure 4: Example of results : comparison of measured and computed diameters

4. Future prospects

Further works will concern the relationships between this external geometry and the internal quality of wood : yield and quality of sawing, formation of compression wood (estimated from Longitudinal Strains Measurements in the standing trees, and from macro-anatomical studies on disks) ...

References

[1] CTBA. 1991. Classement des bois ronds resineux. Ed. CTBA Paris, France.

[2] Esser M.H.M., 1946. Tree trunks and branches as optimum mechanical supports of the crown. *Bull. Math. Biophys.* 8.

[3] Gardiner B.A., Quine C.P., 1994. *Wind damage to forest.* Biomimetics **2 (2)** 139-148.

[4] Wessolly L., 1994. *Two methods to measure the strength and stability.* 1st Plant Biomechanics Conference. Proceedings. Ed. Elsevier. Paris. France.

[5] Fournier M., Baillères H., Chanson B., 1994. *Tree biomechanics* : Growth, Cumulative prestresses and reorientations. Biomimetics **2 (3)** 229-252.

[6] Radi M. *Analyse morphologique de l'arbre en vue de sa modélisation mécanique.* Thesis Doctorat in Wood Sciences. University of Bordeaux 1, France.

[7] Shelbourne C.J.A., Namkoong G., 1966. *Photogrammetric technique for measuring bole straigthness.* Southern conference on forest tree improvement, 8, Savannah.

Vision system for sorting paphiopedilum using structural and statistical pattern recognition

Système de vision pour le tri des orchidées en pots par des méthodes de reconnaissances de formes structurelles et statistiques

Toine Timmermans

Agrotechnological Research Institute (ATO-DLO)
P.O.box 17, 6700 AA Wageningen, the Netherlands
e-mail: a.j.m.timmermans@ato.dlo.nl

Abstract: *A multi-functional system for sorting pot-orchid plants has been developed and is now operational for six months in a Dutch greenhouse. The vision system grades half grown plants on volume and width. Plants that show a bud are recognised and placed on separate containers. The recognition process of small buds is supported by manual placing of a stick and an information label. Plants that are returned to the greenhouse are aligned in the same position to minimise the empty space at the containers. Plants with flowers are sorted on development stage and height of the flower and are transported to the packaging belts.*

The vision system uses two colour cameras, a lightning box, image processing hardware and specially developed software. The upper image and four side view images are segmented using statistical discriminant analysis, after training with example plants. The sticks, stems and buds are recognised with a structural pattern recognition technique, based on the Hough transform and a model description of the objects. Flowers are recognised using the unique colour of a part of the flower. This part is used as a seed to identify the whole flower.

Keywords: *Image processing, computer vision, colour segmentation, discriminant analysis, hough transform, pot plant grading, paphiopedilum.*

Résumé : Un système multi-multifonctions pour trier les orchidées en pot a été développé et est opérationnel depuis plus de 6 mois dans une serre hollandaise. Le système de vision trie des plantes à moitié développées en fonction de leur volume et de leur épaisseur. Les plantes avec un bouton sont reconnues et placées dans un container différent. Le processus de reconnaissance des petits boutons est réalisé en plaçant manuellement une étiquette d'information. Les plantes qui sont renvoyées dans la serre sont alignées dans la même position pour minimiser la place vide dans les containers. Les plantes fleuries sont triées en fonction du développement et de la hauteur de la fleur et sont transportées vers les tapis d'emballage. Le système de vision utilise 2 caméras couleur, une chambre d'éclairage, une électronique d'acquisition et un logiciel spécialement développé. L'image vue de haut et les images de 4 vues de coté sont segmentées en utilisant l'analyse discriminante, après entraînement sur des exemples. Les étiquettes, tiges et boutons sont reconnus par le système de reconnaissance des formes basé sur la transformée de Hough et une description modèle des objets. Les fleurs sont reconnues en utilisant la couleur d'une partie de la fleur. Cette partie est utilisée comme un noyau pour identifier la fleur entière.

1. Introduction

The sorting of pot plants on for example size, height, shape, quantity of flowers and product quality was originally a task that had to be performed by humans. Besides the high labour costs another disadvantage of human grading is the subjectivity of the judgement. The human eye is very good in recognising different patterns but has limited capabilities to perform objective estimates of for example size. Computer vision techniques have proven to be successful for objective measurement of pot plants [1,2,3,4,5]. Since about five years automatic sorting systems, mainly based on computer vision technology, have been introduced in greenhouses to replace the human graders. At this moment about 25 automatic sorting systems are realised in Dutch greenhouses for sorting plants and several growers have the intention to implement such a system in the near future.

The performance of the sorting systems improves continuously, because of evolution in computer hardware technology, but mainly because of the development of more sophisticated software tools. For example the first operational system of ATO-DLO only used one image to measure the flower percentage, flower colour and diameter of Saint Paulia [6]. In one of the more recently installed systems two colour cameras take seven images of each plant to measure not only the basic plant features, like size, height and flowering percentage, but also recognise variety and the bad quality plants [7].

2. Paphiopedilum

A Paphiopedilum is a variety of pot-orchid that has a growing period up to three years before flowering. Many varieties exist with a different number of flowers that appear in diverse colours. Because there is a large difference in the length of the period before flowering, it is a labour intensive product. Sorting of half-grown plants is necessary three to four times a year. When a plant develops a flower or a large bud it is ready to be sold. Typically the plants are grown on aluminium containers.

The grouping of plants in the growth process with the same size and development stage will improve the uniformity of the plants at the containers and reduce the amount of labour involved in sorting and handling of the plants. Also the amount of free space at the containers can be minimised. The leaves of the plants basically are oriented in a more or less straight line. If the plants are aligned in the same position they can be put close together. Full grown paphiopedila are sorted on the height of the flower and the development stage of the flower.

The goal of the research project was to develop a multi-functional vision system that can be used in all growing stages of the plants. Half-grown plants will be sorted on volume and width. Orchid plants that produce a bud will be separated in different

groups based on the length of the stem and the size of the bud. And finally the plants with mature flowers are sorted on the height of the flower and the development stage of the flower. In all sorting processes the plants will be aligned in the same direction and can therefor be put at close distance on the containers without damaging of the leaves. In co-operation with several horticultural mechanisation companies a complete transportation system for handling of the plants is installed. Plants are taken from the containers with a handling robot, put in transportation holders, are transported through the vision unit and divided onto six different conveyer belts. Three belts are used to return the plants to the containers, three other belts are used to supply the packaging lines. It should be possible with the vision system to easily switch from one sorting task to the other. Also sorting criteria should be easy to adjust and be stored for different species. Depending on the application the capacity of the system should be between 2000 and 3000 plants per hour.

3. Description of the vision system

3.1 System requirements

In principle all sorting operations have to operate automatically. There is however a limitation to visibility and the accuracy of recognition of the small buds in the plants. A small bud is covered by leaves and can in some cases hardly be seen or differentiated from a fresh leave with the human eye. In the feasibility stage of this project it appeared to be impossible to construct a camera and lightning set-up with a guaranteed visibility of the hidden buds given the system specifications for capacity and budget. As a solution to this problem the sorting procedure is supported with human action. In the first step that a bud appears in the plant a green stick is planted in the flowerpot. In the second step that small and larger buds have to be separated a coloured label with product information is placed in the pot. Both objects have to be recognised by the vision system. Since each plant is always checked before passing the vision system, because dead leaves have to be removed, this procedure is acceptable and hardly affects normal operation. Because each full grown plant gets a supporting stick and an information label before packaging, these object don't have to be removed from the plants at a later time.

3.2 Equipment

A colour vision system is developed to analyse the pot-orchids. The vision system operates as a stand alone system that gets a signal to start a new measurement via serial communication from a PLC (Programmable Logical Computer). For each plant the destination belt is send to the PLC, directly after the measurement cycle is finished. A 3-CCD colour camera is used to take 4 side images of each plant at different views. The plant is rotated in front of the camera while moving forward on

a conveyer belt, using 2 parallel strings that run at different speeds. A second 1-CCD colour camera grabs a single top view image of each plant. The top view image is only used to determine the main direction of the plant. Using two parallel strings, that are operated by a PLC, the plants are aligned at an angle of 45 degrees with the transportation direction. This way plants can be positioned at close distances without damaging the leaves. In a closed cubic shaped box of about 2 meters wide two lightning units with high frequency tube lightning are attached to the ceiling. The images are being processed with a 200 MHz PC with Pentium processor. A Matrox Meteor PCI-bus framegrabber is used to digitise the images with a spatial resolution of 768*576 pixels in RGB format (red, green and blue). All software is written in Watcom-C and operates at the MsDos platform.

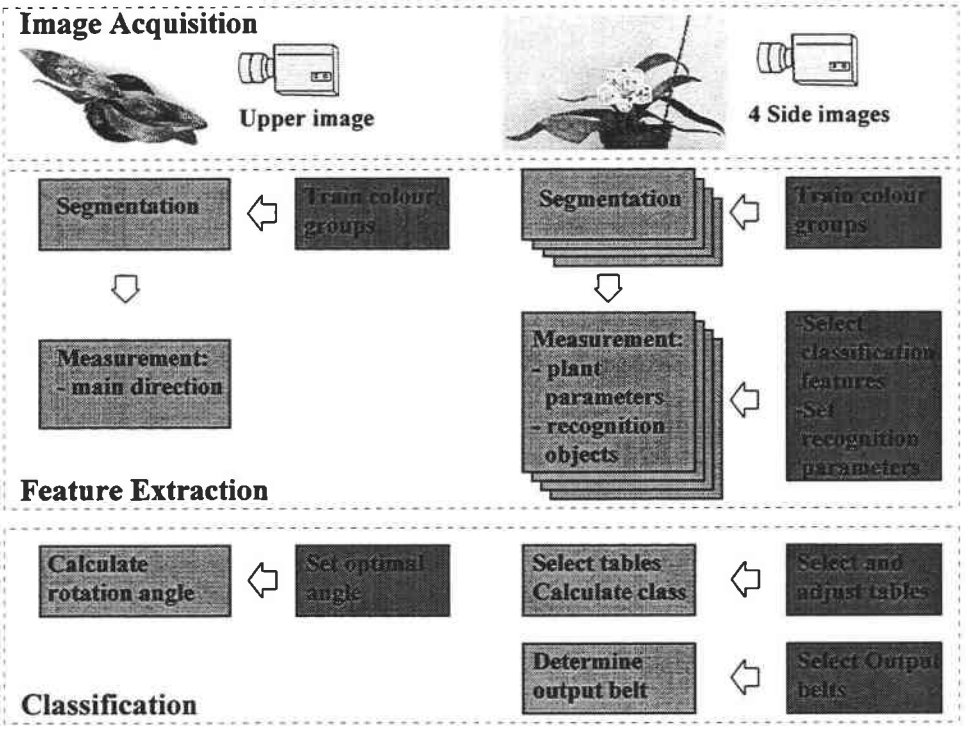

Figure 1: Schedule of the measurement procedure

3.3 Measurement procedure

In figure 1 the schematic overview of the software is displayed. In the top view image only the main direction is calculated and a the rotation angle is send to the PLC. All four side images are processed independently and information is combined after feature extraction. The segmentation of the colour images is based

on a statistical pattern recognition technique. With representative example plants the colour segmentation is trained, clicking object pixels with the computer mouse and indicating to what colour group a pixel belongs. A colour segmentation function is calculated in the 3-dimensional colour space with a classification tool. From the image a runcode description of all objects is derived to represent data in a more efficient manner. From this runcode description the relevant features are calculated. The measurement features can be divided in two groups. First the group of objects that have to be recognised and therefor have a Boolean value (true or false): stick, bud, information label and flower. The other group contains the features that are used to classify the plant: volume, width, flower size, bud size, stem length and flower height. The class and destination belt of the plant are read from a classification and output table.

4. Image segmentation

A Paphiopedilum is one of the most difficult type of plants to be analysed with an image analysis system, because there is a large natural variety in colour and appearance of the plants. For example a pixel with a yellow colour can either be part of a leave, a flower or a label. Small buds are hardly visible and flowers can have an overall light green colour. Segmentation of objects based on the RGB level of a pixel only is not possible. A two step segmentation procedure is developed to analyse the side view images. In a first step all pixels are classified as an object group. In the second step of segmentation information about the neighbourhood and position of the pixels is added. For the upper image a one step classification of the pixels is sufficient.

A colour segmentation function is calculated in the 3-dimensional colour space using discriminant analysis [6,7]. Statistical discriminant analysis construct separating surfaces in the multidimensional variable space, such that different groups are separated. Discriminant axes are calculated so that the projections of the data points of the classes on the axes are separated maximally. Two different versions of this technique are used: linear discriminant analysis (LDA) and quadratic discriminant analysis (QDA). With LDA linear separating surfaces are calculated, with QDA the surfaces are curved [8]. Five different groups are identified: background, leave, flower, leave/flower and flower/label. For the first three groups only pixels with a unique colour are trained. Colour values that can either belong to a leave or a flower (yellow leave, green flower, etc.) are trained is the group leave/flower. Colour values that can be part of the information label or a flower (white, red, etc.) are trained as flower/label pixels. To improve performance of the clustering algorithm for each object group multiple object classes are defined. In total 21 different object classes are used, as shown in table 1.

Colour group	Colour classes
background	light blue, dark blue, shadow, pot
leave	dark, bright, stick, dark stem, brown stem, green stem
flower	pink, yellow
leave or flower	yellow, dark flower, light flower, dark brown , light brown
flower or label	red, pink, yellow, blue

Table 1: Definition of colour groups and colour classes for image segmentation

Building the training set for colour segmentation of this type of plant is a elaborate task. All different colours have to be shown to the system and be trained manually. Especially the differentiation between pixels that could be part of the flower or a leave was difficult. If in the segmentation process large flower areas are identified on the leaves, a non existing flower would be recognised. Also some orchid varieties have a shiny surface that could disturb the segmentation process. Finally, after retraining several times, acceptable results were obtained for the image segmentation. This is however the first application area for pot plant sorting where classification results were this low. In table 2 the percentage errors in assigning the correct class and group are displayed. These data are based on a training set of 200 pixels and a test set of 400 pixels.

Technique	Error in class assignment (%)	Error in group assignment (%)
LDA	50.1	24.6
QDA	32.5	15.1

Table 2: Error in colour segmentation with LDA and QDA for 400 data points

Finally the QDA classification technique is applied, because it gives the best classification results. Information about the region of the pixels and its neighbourhood is necessary to improve recognition results. This is especially important for the recognition of the flowers in the image.

5. Object recognition

5.1 Stick recognition

A stick always has a dark green colour, but it has a shiny surface and the light reflection can be influenced by shadow or differences in lightning. It is not possible to have a robust recognition of the stick on colour information only. The classification results of colour clustering with the procedure of trained segmentation were unacceptable. With QDA 25% of the pixels of a stick are misclassified in the test set and 12% of the leave pixels are classified as a stick. As a solution a structural pattern recognition technique is used to recognise the presence of a stick.

A stick can be seen as a part of the object with on both sides a straight contour and a specific width. A popular technique to identify the existence of line structures is the Hough transform. The Hough technique is useful for curve detection if little is known about the location of a boundary, but its shape can be described as a parametric curve. Its main advantages are that it is relatively unaffected by gaps in curves and by noise [9]. The equation for a line is $y = mx + c$. All possible combinations of a potential edge-point are transformed from the image space to the *m-c* space. In the *m-c* space a maximum appears for the pixels in image space that lie on a straight line.

Implementation of the Hough-technique for line detection is rather straightforward. In a 2-dimensional accumulator array the combinations for the *m* and *c*-value are stored. Limits are set for the minimum and maximum values for *m* and *c*. In this case a maximum slope of 45 degrees is set and the intercept with the basis should be in the image area. A dynamic range of 128 different values in the accumulator array for both parameters is sufficient to detect all potential stick parts. In fact two different accumulator arrays are defined, one for the edges on the left side of the object and one for edges on the right side. Potential sticks in the image are evaluated using the maximums in both arrays, using the information of the minimum and maximum width of a stick. Figure 2 shows an example of an image with a mature Paphiopedilum and a stick with an overlay of the Hough space. The highest maximum, corresponding with the stick, and the second for the flower stem are visible in *m-c* space.

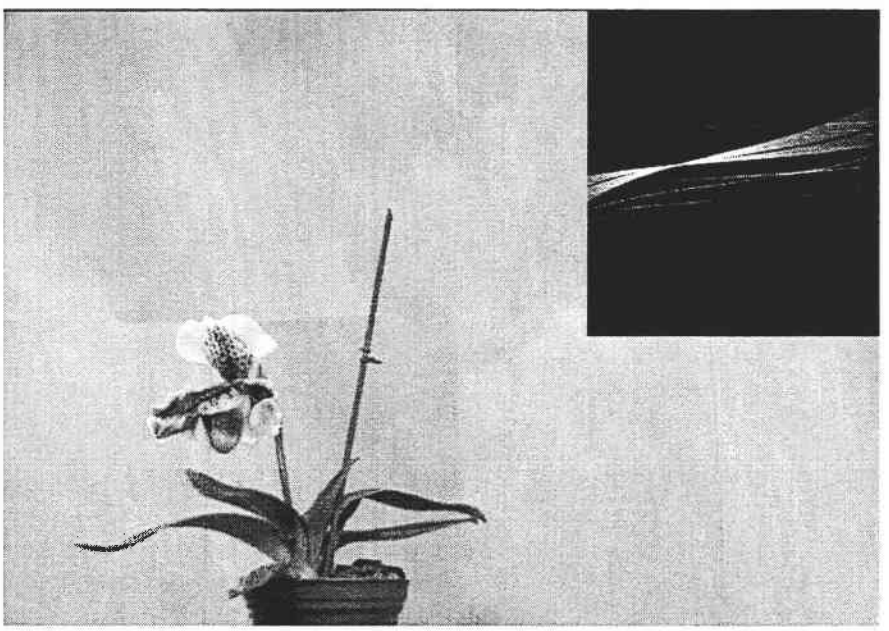

Figure 2: Example of a full grown orchid with overlay of Hough space

A more precise model is necessary to evaluate all potential sticks in the images. Since the outer ends of the leaves can appear as a shape with the same width and straightness as a stick, more information of the stick is included in a reference model to improve robustness of the recognition. As a first step the line description is used to detect the image pixels that are part of the stick. The position information is matched with the runcode description of the object. All strokes in the object that match the position of the line and the width of the object are selected as potential object parts.

The following model information is checked:

- since a stick is put in the pot, the lowest part of the stick should be in the region of the image where the flower pot is detected;

- a stick has an unbroken connection from the top to the pot level, this means that in the runcode at every vertical position an object stroke must exist;

- at the upper point of the stick there should be no connection of a blob in a specific size range, since this could indicate that a bud is connected and the potential stick is in fact a stem;

- the outer end of the stick is not sharp, the direction of the edges on both sides of the stick are calculated and the difference in slopes should be below an adjustable value.

All potential maximums in the accumulator array are evaluated. All maximums that correspond with a minimum length of 3 cm are investigated. After evaluation of a potential stick object, using the matched runcode stroke, the points on the line are removed from the *m-c* space.

5.2 Bud recognition

A bud normally has a light to dark green colour and can appear in different sizes. Buds that are hidden between the leaves cannot be detected and are recognised by means of the supporting stick and label. Buds that are in a stage that have to be recognised are connected with a stem. The stem has a brown or green colour. As with the recognition of the stick, detection on its colour is not possible. Since a stem is more or less visible as an object with straight contours, each stem will show as a maximum in the Hough-space. A method comparable with the detection of the sticks is used to recognise the stem and bud. The information about the appearance of a stem with bud cannot be modelled as strictly as a stick, since stems can be bent, have different widths, buds have a different shape and size, etc. Therefor a more global model with limits to the specific features is applied to recognise a bud.

The following model information is checked:

- a potential stem part does not satisfy the specifications of a stick;

- since a stem grows from the centre of the plant, the lowest part of the stick should be in the region of the image where the pot is detected;

- a stem has an unbroken connection from the top to the pot level, this means that in the runcode a connection with the base level must exist;

- at the upper point of the stem there should be a connection with a blob in a specific size range, with a certain shape.

As a result of this method all stems with a bud that are visible as a separated object in the image with a length of 4 cm or more are detected. When a stem is found the size and shape of the bud are calculated.

5.3 Flower and label recognition

Flowers cannot be detected using only the colour of the flower-pixels, since flower regions can have the same colour as parts of a leave. In most cases however each flower will have a part that has a unique colour (white edge, red sepal, etc.). The flower recognition is performed in three steps. First all blobs with a unique flower colour are detected. These pixels belong to the flower or flower/label class. This is possible because a label is never present in the region where flowers are expected. These blobs are used as a seed to grow with all regions that have a possible flower colour (leave/flower class). In a final step the blobs are analysed based on size, shape, colour and position. The flower size and height are used to classify the plant.

Labels are recognised in the region of the image where the labels can be expected. With blob analysis for pixels that are classified in the flower/label class all labels are detected. If a blob with a adjustable size is detected it is concluded that a label is present.

6. Measuring plant parameters and classification

6.1 Calculation of the main direction

The main direction of a plant is calculated to determine the optimal position to rearrange the plants on the containers. Two different techniques were implemented to calculate the main direction: (a) moment mathematics to calculate the optical axis and (b) the recognition of two extreme outer leave points. With the first method an

average main axis through the optical centre is calculated using all plant pixels. With the second method the directions from the two outer points to the optical centre are calculated. To assure that not two leaves at the same side of the pot are identified as outer points, a minimum angle of 90 degrees must exist between the lines from the outer points to the centre. As main direction the average direction is used. The results for both methods are good for normal plants, but with plants that don't have a structure with two main leave parts the results with method two are better. The method with detection of the outer points is finally selected.

6.2 Measurement of plant features

Depending on the sorting task, different plant features are used for classification. For sorting of half-grown plants the volume and width are used. The volume is the average plant area of the 4 side views. The maximum width in one of the 4 images is defined as the width of the plant. For sorting of plants with a bud the size of the bud and the height of the upper bud level are used for classification. Mature plants are sorted on the size of the flower and the height of the highest flower level.

In principle the plant parameters are measured objective and reproducible. The average area of the plant has a deviation of maximum 4%, because of different positions during rotation. This is acceptable, because the plants are only graded in three classes, and with sorting of plants always an area of doubt exists. The size of the buds and flower are the features that cannot be determined accurately. The variation in position of the bud and flower in front of the camera makes the difference.

6.3 Plant classification

Basically there are three sorting tasks, with different allocation of the transportation belts. For sorting of half-grown plants three belts are used to return plants to the container in three different size classes. For sorting of plants with difference in development stage one belt is used for plants without a bud, a second for small stems and a third for the larger buds. For sorting of flowering plants the plants are classified at six different heights.

In all classifications task the sorting criteria are adjusted in a two-dimensional table. In the table thresholds for separation of classes can be set. Always a combination of two features is used, for example flower height and flower size.

7. Results

7.1 Overall performance

The sorting system is implemented in a period of 6 months and is fully operational since 6 months. Classification and recognition results are not only based on research in a laboratory environment, but also gathered in operational circumstances. The implemented system saves 4% of space on the containers and only this advantages makes the investment worthwhile. Another advantage are the estimated 30% lower labour costs. This is mainly due to the fact that because of the objective sorting the half-grown plants only have to be sorted 2 times a year, instead of 3 to 4 times.

7.2 Object recognition

The recognition results for detection of sticks are good. A 100% accuracy for recognition of the sticks is achieved. A false detection rate of about 0.1% occurs in one variety with long straight leaves. The results of the recognition of buds are acceptable. All stems with a bud that are visible as a separated object in the image with a length of 4 cm or more are detected. All smaller buds are supported by a stick that is recognised in all cases. A problem is the detection of a bud in a plant with a high density of leaves close to the stem. If in none of the 4 images the bud and stem are free from the leave, the stem is not detected. If a bud is partly opened, it will be recognised by the colour of the flower. However an error in detection is not fatal, because the detection of the bud is assured with the presence of a stick and a label. This means that even if a large stem is not detected, it will never be placed at a container for plants with no bud. When the containers are sorted again a few weeks later a bud is more opened and the chance of being recognised is much higher.

The accuracy for recognition of labels is 100%. When a label is present in a pot it is in all cases detected in one of the four side views. Since a label has a size of about 25 cm^2 no false objects are identified as labels. The accuracy for recognition of flowers is 100% for most varieties. There is however a problem with flowers that have an overall light green colour. These flowers have no part that has a unique colour and therefor have no part that can be used as the seed that will grow with the light green part. Because in the near future the variety with this type of flower will be eliminated by breeding and reproduction techniques, this problem will be solved. Except for green flowers all clearly visible flowers are detected and are transported to the packaging belts. That means that no mature flowers are returned to the containers, which is definitely unacceptable, because when the containers are sorted again a few weeks later the flower has probably finished blooming.

Conclusion

A sorting system for Paphiopedilum has been developed and is operational for six months in a Dutch greenhouse. This type of pot plant has a large variety in colour and appearance and is one of the more difficult plants to be sorted with a vision system. With two colour CCD cameras of each plant in total four side view images and one top view image are taken. The system performs objective measurement of size, orientation and height. Also specific recognition tasks for stems, buds and flowers had to be implemented. In general vision systems perform better as humans in objective assessment of geometric and density parameters, but humans are still superior to computers in specific recognition tasks. To improve the recognition performance for small and hidden buds, manually a stick and information label are placed.

Both statistical and structural pattern recognition techniques are implemented to solve the classification and recognition tasks. Quadratic discriminant analysis is used as pattern recognition technique for the image segmentation. The typical shape of a stick and a stem are recognised using the Hough transform and a model based recognition with a formal description of both objects. Flowers are recognised using the unique colour of a part of the flower. The unique coloured part is used as a seed to identify the whole flower. Based on the typical shape of the plants, with two opposite leaves structures, the optimal position of the plants on the container is determined. The plants are oriented in this position to minimise the empty space on the containers.

The recognition results are good for flowers, sticks, buds and labels. Only problems occur with the detection of light green flowers. This problem can be solved with development of a specific structured recognition technique, but will not be implemented because the problem will be eliminated with new reproduction techniques. The estimation of flower and bud size is influenced by the orientation of the object towards the camera, and this can in some cases result in a misclassification of larger buds that are just ready to be sold. Altogether the sorting system saves 4% of space on the containers and a reduction of the labour costs with 30% is achieved for the sorting process.

References

[1] A. Brons, G. Rabatel and F. Sévila, 1991. Neural network techniques to simulate human judgement on quality of potplants, *On machine vision systems for the agricultural and bio-industries*, pp. 153-161.

[2] J. Dijkstra, 1994. *Application of digital image processing for pot plant grading*, PhD thesis, University of Wageningen.

[3] V. Steinmetz and P. Feuilloley, 1996. Quality assessment of begonias with machine vision, *AgEng Madrid 96*, Paper 96F-024.

[4] H. Moth-Poulsen and B.S. Bennedsen, 1996. Objective quality measurement of pot rose and hibiscus by image processing, *AgEng Madrid 96*, Paper 96F-077.

[5] T. Rath, 1995. Artificial neural networks for plant classification with image processing, *AI in Agriculture*, 2:197-202.

[6] A.J.M. Timmermans and A.A. Hulzebosch, 1996. Computer vision system for on-line sorting of pot plants using an artificial neural network classifier, *Computers and Electronics in Agriculture*, 15, pp. 41-55.

[7] A.J.M. Timmermans, T.J.A. Borm and M.B.J. Meinders, 1996. Color vision system for on-line sorting of begonia based on learning techniques, *SPIE conference on Optics in Agriculture, Forestry and Biological Processing II*, Volume 2907, pp. 100-108.

[8] H. Voet and J. van der Hemel, 1988. *Multivariate classification methods and their evaluation in applications*, PhD thesis, University of Groningen.

[9] D.H. Ballard and C.M. Brown, 1982. *Computer vision*, Prentice-Hall Inc, Englewood Cliffs, NJ.

Part 3

Vision systems for food product quality

Principle and application of probabilistic neural networks in artificial vision

Principe et application des réseaux de neurones probabilistes en vision artificielle

D. Bertrand **Y. Chtioui** **B. Novales**
Institut National de la Recherche Agronomique, LTAN
BP 71627, F-443126, Nantes Cedex 03, France
e-mail: bertrand@nantes.inra.fr

D. Demilly
Station Nationale d'Essais
de Semences, GEVES,
Rue Georges Morel, 49071,
Beaucouzé Cedex, France

Abstract: *In the domain of artificial vision, many applications are based on the discrimination of qualitative groups from features that are extracted from numeric images. In such situation, either discriminant analysis or multilayer perceptron network (MLPN) are very often used. Probabilistic neural networks (PNN), can be a relevant alternative to MLPN. They offer the advantage to cope with non-linearity and they are based on relevant statistical rules. PNN follows the Bayesian approach, in which the attribution of an unknown observation into a qualitative group depends on the conditional density probabilities associated to each group. They give a heuristic making it possible to estimate these density probabilities from the data of a training set. An example of application is shown, that deals with the discrimination of seed species from their numeric images. In this experiment, 2400 seeds of 4 species were studied. The collection was divided into a training and a validation set of respectively 1600 and 800 seeds. 73 features were extracted from the images. Stepwise discriminant analysis allowed the selection of 4 variables among the 73 available ones. MLPN and PNN were compared. MLPN incorrectly classified 44 and 28 seeds of the training and test sets respectively. PNN gave 17 and 19 misclassifications on the same data sets.*
Keywords: *Probabilistic neural networks, artificial vision, seed, artificial intelligence, bayesian statistics.*

Résumé : Dans le domaine de la vision artificielle, de nombreuses applications sont fondées sur la discrimination de groupes qualitatifs à partir de paramètres extraits d'images numériques. Les analyses discriminantes ou les réseaux de neurone multi-couche sont très souvent utilisés pour cela. Des réseaux de neurones probabilistes peuvent être une alternative intéressante aux réseaux de neurones multi-couche. Ils ont comme avantage de répondre au problème de non-linéarité et ils sont fondés sur des règles statistiques. Les réseaux de neurones probabilistes suivent une approche Bayesienne dans laquelle l'attribution d'une observation inconnue à un groupe qualitatif dépend de la densité conditionnelle associée à chaque groupe. Une heuristique peut être développée pour estimer cette probabilité à partir d'un lot d'entraînement. Un exemple d'application est donné. Il est lié à la discrimination d'espèces de graines à partir d'images numériques. Dans cet exemple, 2400 graines de 4 espèces sont étudiées. La collection est divisée en un lot d'entraînement et un lot de validation faisant respectivement 1600 et 800 graines. 73 paramètres sont extraits des images. Une analyse discriminante pas à pas permet la sélection de 4 variables sur les 73 disponibles. Les réseaux de neurones multi-couche et probabilistes sont comparés. Le réseau multi-couche classe de manière incorrecte 44 et 28 graines des lots d'entraînement et de validation. Le réseau probabiliste donne 17 et 19 mauvaises classifications sur les mêmes lots des données.

1. Introduction

In many applications, artificial vision is used for the prediction of the category membership of a set of samples from the information that can be extracted from their digitised images. This is the case for example for the grading of agricultural products such as fruit and vegetables, flowers or meat products: the samples are classified in quality classes from the processing of the acquired images. Such applications generally involve two main steps.

The first one consists in extracting a feature vector from the studied images. This vector x includes information such as shape, colour and texture features and is supposed to be representative of one studied sample. The feature vectors of the whole sample collection, including many observations, are gathered in a matrix X dimensioned n x p, where n is the number of observations and p the number of measured features. The goal of the second step of the application is to find a procedure able to predict the category membership of a given observation from its feature vector. The applied learning procedure may be either unsupervised or supervised. Supervised learning, an aspect of which is presented here, refers to a suite of techniques in which a priori knowledge (or assumptions) about the category membership of a set of samples is used to develop a classification rule. The purpose of the rule is to predict the category membership for new samples (Sharaf et al., 1986). The classification rule is developed on a training set of samples with known classifications. The model can then be tested on a validation set, which also includes samples with known classifications, but which were not used for developing the classification rule. Linear discriminant analysis (LDA) (Tomassone et al, 1988) is one of the best known supervised learning approach. However, LDA has several limitations. In particular, it makes the assumption that the decision frontiers of the available populations are hyper planes. This assumption is not usually met, for example when the studied population has a non-convex distribution.

Numerous methods have been proposed in order to cope with such problems. Neural networks are based on parallel distributed processing (McClelland and Rumelhart, 1986). The most common neural network architecture is the multilayer perceptron system, using the well-known back-propagation algorithm as a learning rule (Widrow and Lehr, 1990). The method has proven to be useful in the domain of artificial vision. Multilayer perceptron networks (MLPN) however present some drawbacks. The learning phase of MLPN can be very long. When the system has been developed, it is uneasy to update it by adding new observations in the training set. Moreover, as the knowledge of such a system is distributed in the weights associated with the inputs of each neurone, it is almost impossible to understand the behaviour of the system. From examining a trained MLPN, it would be very difficult to identify the variables that play the most important role in the classification. The probabilistic neural networks (PNN) (Specht, 1990) do not

present these drawbacks. They are based on the Bayesian rule, which gives them a clear statistical foundation. The involved heuristic is simple and makes it possible to adapt MLPN to new problems and situations. The purpose of the present communication is to give the principle of PNN and to show how this neural system can be used in the domain of artificial vision. The illustrative examples are about the discrimination of the seed species from their digitised images.

2. Principle of probabilistic neural network

2.1 Bayesian rule

PNN can be seen as a heuristic making it possible to apply the Bayesian rule. We will begin presenting PNN in an intuitive fashion. A clear and more complete presentation of PNN can be found in the book of Masters (1995).

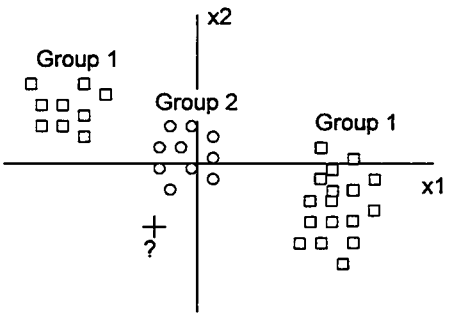

Figure 1: Example of biplot of two representative variables

Let us suppose we have observations belonging to one among two quality classes. Each observation (or pattern), is described by a vector x which is the result of the measurement of several variables. In the example presented below, x will be a vector of characteristics extracted from the digitised images of seeds (such as the length, the width, the texture features, etc). The quality classes of the observations will be the seed species. An imaginary example is shown on figure 1, in the case of two predictive variables.

Squares represent the points of group 1 and circles represent those of group 2. An unknown observation, represented by + is to be classified in one of the two groups. The situation presented on figure 1 can not be satisfactorily handled with LDA which assesses a single centroid for each group. As the group 1 is split into two sets, it will be impossible to find a single representative pattern for the group 1. Neural networks, which follow a non-linear approach, are able to cope with non-

linearity. The Bayesian method is illustrated on figure 2, with an imaginary example about seed discrimination. Let us suppose that a single variable (say the length of the seed) is used for the classification of each seed in one among 3 species. The species 1 has two typical morphologies and can have two typical lengths corresponding to very large or very small kernels. If we have many samples on the learning set, it is very easy to establish the histograms of the lengths of the seeds for each species. For each class of length, an observed probability can be assessed. For classifying an unknown seed, it is possible to measure its length and to estimate, from the histograms, the probabilities of the seed to belong to the different species. In the example, 3 probabilities, p_1, p_2 and p_3 can be estimated.

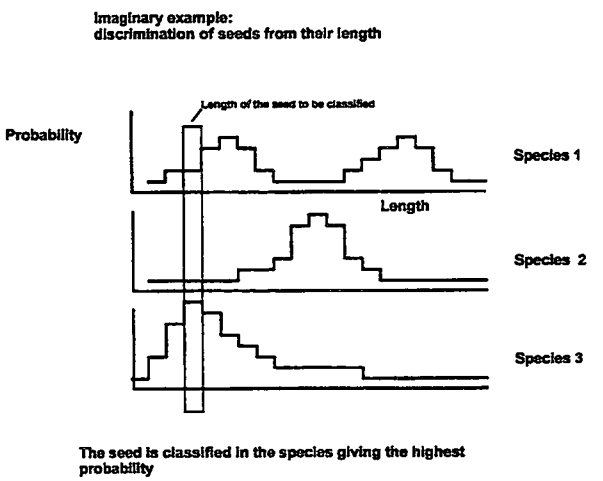

Figure 2: Illustration of the Bayesian approach on an imaginary example

The more relevant rule of decision consists in supposing that the seed belong to the species corresponding to the highest probability (species 3 in the example). In fact, this rule is only the best if we suppose that the 3 species are equiprobable in the studied natural population of seeds. As, in general, the natural proportions of the quality groups are not known, this assumption will be taken. The proposed rule of decision is, in principle, very simple. However, its practical application is slightly more difficult. The more critical point is that the histograms associated to each group are to be assessed from the observations of the learning set. For example, it is clear that if the class intervals are narrowed, the histogram could be very badly shaped, with some classes of length even not represented. If we use the proposed rule of decision, we will be, of course, unable to classify a seed the length of which lies into a class of null probabilities. The problem is accentuated if we use more than one variable for classifying the samples. For example, if the seeds are classified by using two variables (the length and the width), the histogram is two-dimensional and the risk to have a pair of values not observed in the learning set is important.

2.2 *Architecture of Probabilistic Neural Network*

PNN gives a practical way to smooth the histograms in order to avoid this problem. The principle is illustrated on figure 3, for a one-dimension problem. The method first requires the definition of a potential function or weight function W(d). In principle, many functions can be used. They must only respect some conditions. They must have their largest values at d = 0 and rapidly decrease as the absolute value of d increases. In practice, the Gaussian function is almost always used. The (unnormalised) Gaussian function is given by:

$$W(d) = e^{-d^2}$$

d is some distance measurement between an observation x_i of the learning set, and x, a point in the considered vector space. In the one-dimension case, d can simply be the absolute value of the difference x - x_i divided by a smoothing factor σ

$$d(x, x_i) = \frac{|\, x - x_i \,|}{\sigma}$$

The role of the smoothing factor will be later explained.
The smoothed histogram (more exactly the probability density function) of a given group k is proportional to the sum of the weight functions corresponding to the n_k observations belonging to this group:

$$f(x/k) = \frac{1}{n_k} \sum_{i=1}^{n} \delta_k(i) W[d(x, x_i)]$$

$\delta_k(i)$ takes the value 1 if x_i belongs to the group k, and 0 otherwise.
This method is applied for assessing the probability density function of each group.

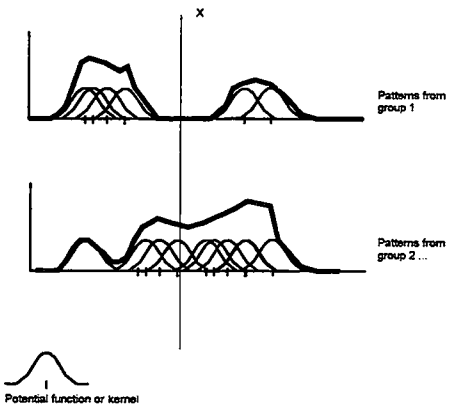

Figure 3: Estimation of probability density by using a weight function

It is clear that, providing that the weight function is correctly chosen, the method gives a way to estimate the probability functions from the data of the learning set. It must be noticed that the shape of the weight function plays an important role. If it is very «narrow», the assessed density functions will be very irregular. On the contrary, if the weight function is very «large», the density function will be very smooth. The value of the smoothing factor σ regulates the extent of the functions.

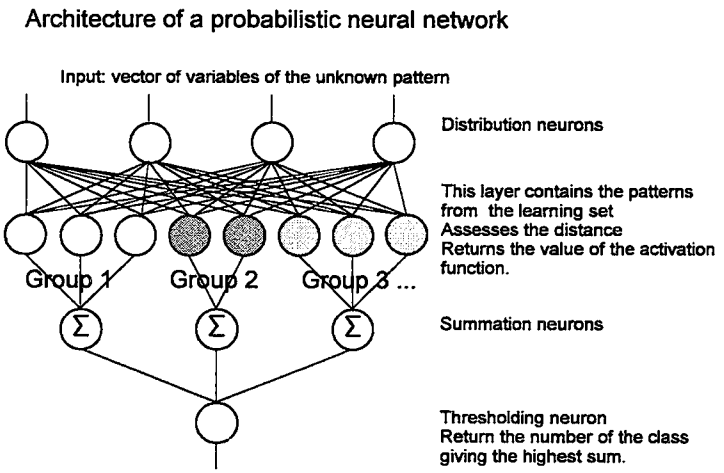

Figure 4: Architecture of probabilistic neural network

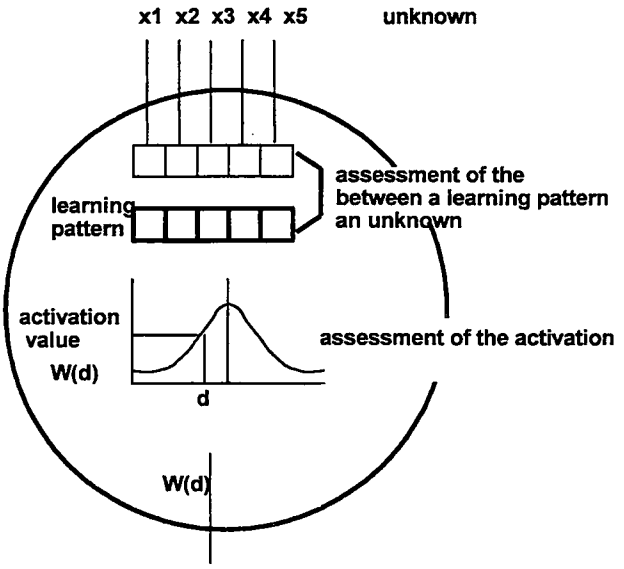

Figure 5: Organisation of an activation neurone

The problem is then to optimise the value of σ in order to obtain the best classification results. This can be obtained from the application of PNN. A typical PNN architecture is shown on figure 4. The system includes 4 layers, which are of heterogeneous nature. As in MLPN, the first one is a distribution layer. Each of the input corresponds to an element of the feature vector x. The second layer is able to assess the weight functions, which is, using the vocabulary of MLPN, the activation function. The number of neurones in the second layer is equal to the number of observations in the learning set. Each activation neurone indeed corresponds to a given observation of the learning set. It is necessary to give some details on the inside organisation of the activation neurones (figure 5). Each activation neurone contains the feature vector x_i of an observation of the learning set (learning pattern). The inputs of the neurone are the values of the elements of a feature vector x of some other observation. The neurone assesses the value of the distance $d(x, x_i)$ and then $W[d(x, x_i)]$. The third layer is devoted to the summation of the outputs of the preceding layer. There are as many summation neurones as quality groups to be identified. The connection between the activation and summation layers is particular. An activation neurone corresponding to an observation of a given group is only connected to the summation neurone of this group. The outputs of the summation neurones are therefore the functions f(x/k) defined previously. The last layer includes a single neurone. This unit compares the results of the summations, and returns the number of the group giving the highest value.

2.3 Learning step

When, as usual, the feature vector is multi-dimensional, the distances can be assessed from:

$$d_i^2(x,x_j) = \sum_{k=1}^{p} \left(\frac{x_k - x_{jk}}{\sigma_{ik}} \right)^2$$

where $d_i(x,x_j)$ is the distance of an unknown observation x to a learning pattern x_j belonging to quality group i, p is the number of variables.

When knowing $d_i(x,x_j)$, it is possible to assess the corresponding weight $W[d(x,x_i)]$. It is then easy to assess the probability densities f(x/k) for each qualitative group k according to the formula given previously. The problem is to find the values of the smoothing factors σ_{ki} which give the best classification results. It is possible to develop 3 models of increasing complexity. The simplest one consists in having a single smoothing factor for all the variables and all the quality groups. The second one assesses a smoothing factor for each variable (p smoothing factors). The more complex one includes a different smoothing factor for each quality group and each variable (p x g smoothing factors, with g the number of quality groups).

The optimisation of the smoothing factors is achieved by using an iterative approach, very similar to that used in MLPN for the assessment of the weights. At first, the smoothing factors are set at an initial random value. An iteration includes several steps:

- Random Selection of a pattern of the training set.
- Presentation of the selected pattern as an input of the PNN.
- Calculation of an error that estimates the accuracy of the current model.
- Slight Modification of the vector σ in order to reduce the error.
- Continuing the process until some stopping criterion is met.

The activation neurones that correspond to the currently selected input pattern are temporally removed from the activation layer.

It is easy to develop an efficient error criterion from the outputs of the summation neurones. It can be assessed from:

$$e(x) = [1 - f(x/k)]^2 + \sum_{j \# k} [f(x/j]^2$$

For x actually belonging to group k.

This criterion simply means that the best results consist in having a value of the density probability function f(x/k) equal to 1 for the output corresponding to the expected class and 0 for the other outputs.
As the error criterion e(x) is of a continuous nature, many optimisation techniques can be employed for optimising the vector σ . In our work, we have used an iterative optimisation method, the well known conjugate gradient algorithm (Specht, 1990;. Schioler et al., 1992).

3. Examples of applications

Before their commercialisation, seed batches must be controlled in order to assess their quality and to guarantee that they are not contaminated with foreign material and adventitious seeds. The examination of the batches is currently performed by human visual assessment. It was therefore interesting to investigate the potentialities of artificial vision as an alternative to the human expertise. The presented example has been published elsewhere in more details (Chtioui, 1997; Chtioui et al., 1996, 1997). The relative interest of MLPN and PNN architectures was compared.

3.1 Material and methods

Samples of four species were provided by a French national seed station (Station Nationale d'Essais de Semences, Beaucouzé, France). The studied species were two adventitious seeds (namely wild oats and rumex and two cultivated seeds (red fescue and perennial rye grass). The objective of the experiment was to attempt discriminating seeds from their digitised images.

The seeds were placed in the field of a CCD colour camera in random orientation and in non-touching position. The numeric images were formed of 512 x 768 pixels and represented a spatial resolution of 6 x 9 cm. In this way, the images of 600 seeds were acquired for each of the four species. Applying a median filter reduced the noise of the images. An algorithm of binarisation was used for extracting the images of the seeds from the background.

In order to characterise individual seeds, 73 features were measured on each seed. These features included 25 size and shape parameters, and 48 texture features (16 x 3 colour channels).

3.2 Mathematical processing and classification by neural networks

The results of the measurements were randomly gathered into two matrices: a matrix of sire 1600 x 73 for the training set and one of 800 x 73 for the test set. As some variables may have no predictive ability, it was necessary to select a subset

of relevant variables before using the neural networks. This selection was performed by stepwise discriminant analysis (SDA) (Romeder 1973). SDA is able to order the variables according to their discriminant abilities.

The 4 selected variables were the inputs of the tested neural networks, MLPN and PNN. The MLPN had four inputs, one hidden layer with four units and four outputs. Each output corresponded to one of the four qualitative groups representing the seed species. The activation function was the sigmoid. The PNN models were implemented with standard Gaussian function as activation function.

3.3 Results

SDA made it possible to select 4 variables from the 73 measured ones. The selected variables were two shape features (elongation and length) and two texture features (blue channel skewness and long run emphasis of the blue channel). Elongation is the ratio of the width to the length of the seed. Blue channel skewness characterises the degree of asymmetry of the grey level histogram of the blue channel. The long run emphasis of the blue channel is an indication on the homogeneity of the texture. It gives a high value for a homogeneous texture.

MLPN and PNN were applied with these variables as inputs. On the training set both methods gave satisfactory results, with 97.6 and 98.9 percent of correct classifications. The more important results, which were the result of classification on the verification set are shown on table 1. On this table, the row indicates the actual nature of the seed, and the column the species predicted by the networks. For example, in the case of MLPN, 15 seeds of rye grass (among 200) were misidentified as red fescue. The wild oat and rumex species were well identified. However, PNN performed better than MLPN. MLPN incorrectly classified 28 seeds, whereas PNN gave only 19 misclassifications.

	Predicted species							
	Multilayer perceptron network				Probabilistic neurones			
Actual species	Red Fescue	Rye Grass	Wild Oat	Rumex	Red Fescue	Rye Grass	Wild Oat	Rumex
Red Fescue	188	12			195	5		
RyeGrass	15	185			14	186		
Wild Oat	1		199				200	
Rumex				200				200

Table 1: Comparison of the classification results obtained with multilayer perceptron and with probabilistic neurones networks (verification set)

Conclusion

In our studies, and in many other situations not presented here, PNN performed as well or slightly better than MLPN. PNN seems to present several advantages in comparison with MLPN. MLPN requires that the user a priori defines the network topology. In particular, it is necessary to choose the number of neurones in the hidden layer of MLPN. This choice is rather arbitrary, and may lead to many experiments for determining the optimal number. The most interesting aspect of PNN is that the applied statistical rules are easy to understand, and bridge the gap between the distributed processing approach followed in the domain of artificial intelligence and the more traditional statistical approach. However, a drawback of PNN comes from the fact that there are as many activation neurones as observations in the training set. We have attempted to reduce this drawback by using a few numbers of weighted activation neurones (Chtioui et al., 1996).

References

Chtioui Y. (1997). *Reconnaissance automatique des semences par vision artificielle basée sur des approches statistiques et connexionnistes.* Thèse de Doctorat, IRESTE, Université de Nantes, 25 Septembre.

Chtioui Y., Bertrand D., Barba D. (1996). *Reduction of the size of the learning data in a probabilistic neural network by hierarchical clustering.* Application to the discrimination of seeds by artificial vision. Chemometrics and Intelligent laboratory Systems, 35: 175-186.

Chtioui Y., Bertrand D., Devaux M.F., Barba D. (1997). *Comparison of multilayer perceptron and probabilistic neural networks in artificial vision.* Application to the discrimination of seeds. Journal of Chemometrics, 11:111-129.

McClelland J.L., Rumelhart D.E. (1986). *Parallel distributed processing,* The MIT Press, San Diego, USA.

Masters T. (1995). *Advanced Algorithms for Neural Networks,* Wiley and Sons, New York.

Romeder J.M. (1973). *Méthodes et programmes d'Analyse* discriminante. Dunod, Paris.

Schioler H., Hartzmann U. (1992). *Mapping neural networks derived from the parzen window estimator.* Neural networks, 5(6): 903-909.

Sharaf M.A, Illman D.L., Kowalski B.R (1986). *Chemometrics*, John Wiley & Sons, New York, 228-239.

Specht D. (1990). *Probabilistic neural networks*. Neural Networks, 3: 109-118.

Tomassone R., Danzart M., Daudin J.J., Masson J.P. (1988). *Discrimination et classement*, Masson, Paris.

Widrow B., Lehr M. (1990). *30 years of adaptive neural networks: Perceptron, Madaline, and Backpropagation*. Proceedings of the IEE, 78(9), 1415-1442.

Machine vision grading of agricultural products using pattern recognition and neural networks

Agréage des produits agricoles par vision, reconnaissance de formes et réseau de neurones

Ahmad Ghazanfari

Dept. Agriculture Machiner
Shahid Bahonar University
Kerman, Iran

Joseph Irudayaraj

227 Agric. Engineering Building
The Pennsylvania State University
University Park, PA 16802, U.S.A

Abstract: *Grading pistachio nuts using machine vision in conjunction with pattern recognition techniques, including neural networks, offers many advantages over the conventional optical or mechanical sorting devices. When neural networks are used as pattern classifiers, the sorting device can be equipped with a training option through which the machine can be trained for recognizing new grades or for different products. The main objective of this research is to compare the different classification schemes for classifying pistachio nuts into four classes of "Grade One" (G1), "Grade Two" (G2), "Grade Three" (G3), and "Unsplit" (UN). Methods used for classification are string matching technique, fourier descriptor method, gray level histogram method, multi-layer neural network, and multi-structure neural network. The discrimination power of the individual set of features for separating the four classes was investigated using Gaussian classifiers. Features considered are gray levels, morphological features and fourier descriptors. Different feature selection methods including forward selection, backward elimination, Fisher criterion, and graphical analysis were applied. The selected features were used as input to different classifiers such as Gaussian, Decision trees, Multi-layer neural networks (MLNN), and Multi-structure neural networks (MSNN). The MSNN classifiers were the most suitable method for this multi-category classification problem. These classifiers learned their input-output mapping faster and were more robust compared to the MLNN classifiers.*

Keywords: *Neural networks, pattern recognition, pistachio nuts, classification.*

Résumé : L'agréage de noix de pistache utilisant des systèmes de vision combinés à de la reconnaissance de formes incluant les réseaux de neurones présente de nombreux avantages par rapport aux procédés optiques ou mécaniques conventionnels. Lorsque les systèmes à réseaux de neurone sont utilisés comme des classifieurs, l'appareil de tri peut être équipé d'une option d'apprentissage qui permet à la machine d'être entraînée à reconnaître de nouvelles qualités ou différents produits. Le principal objectif de cette recherche est de comparer les différents schémas de classification pour classer les noix de pistache dans 4 classes : classe 1 (G1), classe 2 (G2), classe 3 (G3) et fermées (UN). Les méthodes utilisées pour la classification sont basées sur du "string maching" et descripteurs de Fourier, la méthode des histogrammes de niveau de gris, les réseaux de neurones multi-couche et les réseaux de neurones pluri-structure. Le pouvoir de discrimination des ensembles de paramètres individuels pour identifier les 4 classes est

analysé à partir des classifieurs Gaussiens. Les paramètres considérés sont les niveaux de gris, les paramètres morphologiques et les descripteurs de Fourier. Différentes méthodes de sélection des paramètres incluant la sélection pas à pas, l'élimination pas à pas, les critères de Fisher et l'analyse graphique sont appliquées. Les paramètres sélectionnés sont utilisés comme entrées dans différents classifieurs, tel que classifieur Gaussien, arbre de décision, réseau de neurones multi-couche et réseau de neurone multi-structure. Le réseau de neurones multi-structure est le plus facilement applicable pour ces problèmes de classification multi-catégorie. Ces classifieurs apprennent leur cartographie entrée/sortie plus rapidement et sont plus robustes comparés aux classifieurs réseau de neurones multi-couche.

1. Introduction

Inspection and grading of pistachio nuts by machine vision is an attractive alternative to conventional methods because it offers the potential for high speed, non-destructive classification of the nuts using a single machine. The continual improvement of price/performance of digital computers has made it practical to automate visual inspection in many areas. Much of the on-going research in food and agricultural processing is focused on the application of machine vision to quality control. Examples include maturity detection of peanuts, sorting of dried prunes, and potato inspection. These industries are extremely competitive, hence efficiency and quality are primary means to increase market share and profit. Automation is not a luxury in these industries, but an essential requirement.

Currently, on-farm separation of split from unsplit pistachio nuts is accomplished by flotation methods. The United States Department of Agriculture (USDA) standards for pistachio nuts designate size grades of "Extra Large", "Large", "Medium", and "Small" for these nuts. Grading pistachio nuts using machine vision in conjunction with pattern recognition techniques, including neural networks, offers many advantages over the conventional optical or mechanical sorting devices. Multiple sensors can be used to gather the necessary information from the nuts and send suitable signals to a computer where they can be decoded for multi-category classification. Image processing algorithms can be used to extract higher-level information from the input signals for improved classification performance. The classification parameters can be easily modified to take into account annual variations in the product. When neural networks are used as pattern classifiers, the sorting device can be equipped with a training option through which the machine can be trained for recognizing new grades or for different products.

An extensive literature search and direct communication with industrial sources have indicated that no pattern recognition machine or neural network-based system has been used for sorting or grading of the pistachio nuts. Bench-mark studies are thus needed to develop an efficient and a practical machine vision-based method for grading pistachio nuts. Research must be conducted to determine suitable image features and proper classification methods for accurate grading of pistachio nuts.

The main objective of this research was to study the feasibility of classifying pistachio nuts into four classes of "Grade One" (G1), "Grade Two" (G2), "Grade Three" (G3), and "Unsplit" (UN) using a machine vision system. Specific goals were:

-to investigate the feasibility of classifying pistachio nuts into their appropriate classes using the selected features by (a) Designing or selecting appropriate

statistical pattern classifiers and (b) Designing suitable multi-layer neural network based classifiers;

- to compare the performance of the applied classifiers and determine an efficient classification technique.

2. Background

Machine vision is a technology that has arisen from a union between camera and computer. A video camera acts as an eye to a machine vision system [1]. Analog signals generated by the camera are digitized into a sequence of numbers and stored as an image in the computer. Image processing algorithms are used to extract a pattern from the image to represent the object. The pattern is classified by a classification algorithm, which in turn may generate a signal to activate an actuator to direct the object into its proper route.

An image is stored in a computer memory as an array of numbers that may contain over 300,000 elements. Therefore, image processing and/or image analysis algorithms are applied to the gray scale images to extract some quantitative information known as "features". The features are used as inputs to a classification algorithm to determine the class of the object. A complete survey of shape algorithms for analysis is given by Pavlidis [2,3]. He distinguished two main categories of image extracted features, namely, external and internal features.

External image features are those type of features which encode the boundary information (Pavlidis 1978). Examples of external image features are morphological features, Fourier descriptors, boundary chain code, and boundary sequences. The internal image features are obtained by analysis of the pixels within the boundary of an image. The location of a pixel and its gray level may play an important role. There are many different types of features that may be considered for different applications. Moments, textural features, and gray-level histograms are examples of internal image features.

2.1 Feature Selection

The performance of a classification system depends chiefly on selecting an appropriate set of features which best describe their associate classes. Mathematical feature selection techniques are classified into two major categories : (1) feature selection in the measurement space, and (2) feature selection in the transformed space. The methods in the first category are referred to as "feature selection" and the methods in the latter category are known as "feature extraction" methods. Feature extraction methods include Interclass/Intraclass, forward selection, and backward elimination methods.

2.2 Classifiers

Classifiers are algorithms implemented on digital computers for purposes of classification. Classification algorithms are developed and applied in two stages. In the first stage, called the training stage, the required classification parameters are estimated from a set of patterns called the "training set". During the second stage, called the test stage, the algorithm uses the parameters to determine the class of a new set of patterns called the "test set". Once a classifier gives an acceptable accuracy for the test data, it can then be used for the real world applications. Examples of classifiers are the Bayesian classifier, Discriminant function classifier, Nearest neighbor classifier, Minimum distance classifier, and Decision tree classifier.

2.3 Neural network classifiers

Artificial neural networks are synthetic networks inspired by the biological nervous system found in living organisms. Due to the limited knowledge available about the nervous system, the correspondence between these systems and artificial neural networks is still rather weak. Neural networks learn to perform a specific task. Learning in a neural network is accomplished by a systematic procedure for altering the connection weights in order to reduce the network errors. Learning is performed in either supervised or unsupervised mode. In supervised learning the desired response for an input is provided to a "teacher". The teacher implements a reward-and-punishment scheme to adapt the network weights. In unsupervised learning, the desired response is not known and the network must discover possible existing patterns, regularities, separating properties among its inputs.

2.4 Multi-layer neural networks

Multi-layer neural networks are created by cascading neurons in layers. Continuous activation functions such as sigmoids are used in the neurons. Here, the input vector feeds into each of the neurons in the first layer. The outputs of the first layer feed the second layer neurons and so on. Often the neurons are fully interconnected between the layers and flow of information is from the inputs toward the outputs (feedforward). It has been demonstrated that two-layer feedforward networks are capable of forming a close approximation to any nonlinear decision boundary [4]. However, many problems are solved more efficiently using 3-layer networks [5,6].

2.5 Back-propagation training for MLNN

Error back-propagation is the most common training algorithm for MLNN. In this training procedure the network weights are randomly initialized with small values,

usually between 0.0 and 1.0. Then the input patterns and their desired outputs are sequentially submitted to the network. If the output of the network for a pattern is not equal to the desired output, the connection weights are adjusted to reduce the network error. The weights are adjusted from output layer through the hidden layers toward the inputs.

2.6 Application of MLNN classifiers

Neural network classifiers are being considered and applied for quality inspection of different agricultural products. Elizondo et al. [7] presented two neural network models for predicting the flowering and physiological maturity of soybeans. Delta learning rule and back propagation algorithm were used to train a three-layer network. The models performed well in predicting the phonology of soybean crop. Other examples include the neural network model for determining the maturity level of green tomatoes [8] and that for determining the maturity level of green tomatoes at harvest [9].

Park and Chen [10] applied different neural network models to develop an accurate, reliable, and economical sensor for on-line inspection of cadavers and detecting the infected carcasses at poultry processing units. They used spectral reflectance data obtained by a diode array spectrophotometer as the discrimination features. They compared feedforward back-propagation, self-organization map with back-propagation and counter-propagation methods with classical discrimination methods such as multiple linear regression, closest cluster mean, k-nearest neighbor, and principle component analysis with Mahalanobis distance. Feedforward back-propagation network was also superior to these classical classifiers.

Dowell [11] used a feedforward neural network for classification of damaged and undamaged peanut kernels. The spectral reflectance from 400 nm to 700 nm in 10 nm intervals were used as the recognition features. Sayeed et al. [12] used feedforward neural network to develop a methodology to evaluate quality of a snack product through nondestructive analysis. Inputs to the network included visual texture and morphological characteristics. Stepwise linear regression was used to reduce the number of features. The neural network was shown to predict the sensory attributes of the snack with a reasonable degree of accuracy.

3. Methods and materials

A sample of pistachio nuts was manually sorted into four classes of "Grade One", "Grade Two", "Grade Three", and "unsplit nuts". The images of the nuts were captured using a Macintosh-based machine vision system. Classification features including morphological features, Fourier descriptors, and gray-level histograms were extracted from the images using image processing software. The potential of

the features for classification and capabilities of various classification schemes in recognizing the four classes were investigated.

The extracted image features, after being put in proper file formats, were used as the inputs to Gaussian classifiers to investigate their potential in recognizing the different classes of nuts. The Gaussian classification of the features was performed using the DISCRIM procedure of SAS [13] software which was installed on the VAX/VMS computer. Then, based on the primary classification results, various feature selection methods were applied to the features in order to select an optimum subset of features for this classification problem. The selected features were then used as inputs to different classification schemes such as Gaussian, decision trees and two types of multi-layer neural networks. Details on the Gaussian and decision tree and MLNN classifier are available [14,15]. The MSNN is presented below.

3.1 The MSNN classifier

A MSNN classifier consists of *C* parallel discriminators corresponding to the *C* classes followed by a maximum selector (Fig. 1). Each discriminator (Fig. 2) is a multi-layer feed-forward neural network with multiple inputs but only one output.

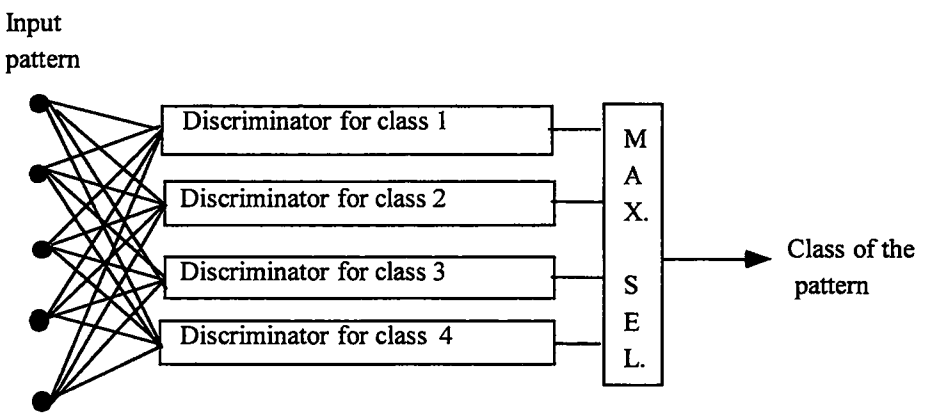

Figure 1: Typical MSNN for four-class classification

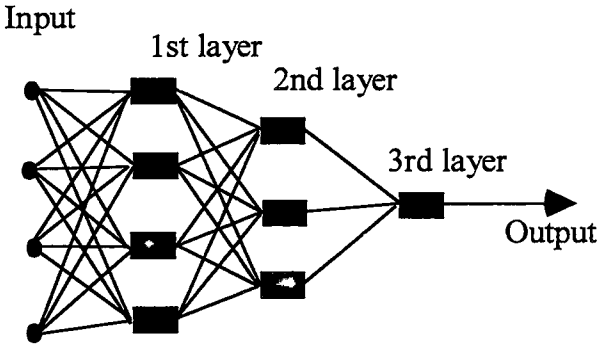

Figure 2: Typical discriminator of a MSNN

The internal structure of a discriminator depends on the complexity of the input patterns. In this research multi-structure neural network (MSNN) classifiers were applied to recognize the four classes of pistachio nuts. An MSNN class discriminator is individually selected and trained. The procedure for selecting a network topology, a proper learning rate, and training the MSNN discriminators are the same for MLNN. However, to maintain a smaller network for the discriminators, the number of neurons in the hidden layers of a discriminator are increased only if the addition of a neuron causes a significant increase in its classification performance. The discriminators are trained to respond "high" (+1) to the patterns belonging to their own class, and to respond "low" (-1) to the patterns belonging to other classes.

In this method of training which is referred to as "bias training", the training set consists of more patterns of the class of that discriminator and less patterns of other classes. With bias training, the discriminators more rapidly learn their input patterns and their ability in detecting the patterns of their own class increases and subsequently decreasing the probability of error of the discriminators.

In this study the training set consisted of 120 patterns from the discriminator's class, and 120 patterns (40/class) from other classes arranged in an alternate form. After training all of the discriminators using a particular set of features, the weights of the trained discriminators were saved in separate files. For testing the MSNN, a UNIX shell script was used to send the test patterns to the trained discriminators and reroute their outputs to the maximum selector.

3.2 Computational complexity calculations

3.2.1 Computational complexity for Gaussian classifier

In calculating computational complexity for Gaussian classifiers, it was assumed that the covariance and its determinant, and the mean for each class, were determined

using the training set and were stored in the computer memory. The Gaussian classifier is given as:

$$p(\mathbf{X}|\omega_i) = k_i \exp[-\frac{1}{2}(\mathbf{X}-\mu_i)^t \Sigma_i^{-1}(\mathbf{X}-\mu_i)] \quad (1)$$

where

$$k_i = \frac{1}{(2\pi)^{1/n}|\Sigma_i|^{1/2}} \quad (2)$$

In Eq. (1) the parameter k_i is constant for each class and, for computational complexity measurements, it was assumed to be stored in computer memory. The bracketed term in Eq. (1) consists of following: a constant number, 0.5, an N-dimensional row vector ($(\mathbf{X}-\mu_i)^t$), an N×N square matrix (Σ_i^{-1}), and a 1×N column vector ($(\mathbf{X}-\mu_i)$). Multiplication of these terms require $(N^2 + N + 1)$ multiplication operations. Here N is the number of features in the input pattern $\mathbf{X}$. The number of multiplications for calculating e^X is calculated using the series approximation (Kreyszig 1988):

$$e^x = 1 + x + \frac{x^2}{2!} + \ldots\ldots\ldots \frac{x^n}{n!} \quad (3)$$

Since the denominators are constant they can be stored in computer memory and the Eq. (3) reduces to :

$$e^x = 1 + \frac{x}{p_1} + \frac{x \cdot x}{p_2} + \frac{x^2 \cdot x}{p_3} \ldots\ldots\ldots + \frac{x^{n-1} \cdot x}{p_n} \quad (4)$$

where (5)

$$p_i = i!, \quad i = 1,2,\ldots.n$$

The above approximation requires (2*n*-1) multiplications. In calculating the time complexity, the first 10 terms (six digits accuracy) of the series were used, so that approximating e^X required 19 multiplications. With this analysis the computational complexity, TC_g, for Gaussian classifier (Eq. 1) is given by

$$TC_g = C(N^2 + N + 21) \quad (6)$$

where C is the number of classes. As an example, when a three-feature (N=3) pattern is used for a three-category (C=3) classification, a Gaussian classifier requires 99 multiplication operations for classifying this pattern.

3.2.2 Computational Complexity for MLNN and MSNN

For a MLNN shown in Fig. 2, the computational complexity, TC_m for a three-layer neural network can be defined as:

$$TC_m = N_{m1} + N_{m2} + N_{m3} + N_{mn} \quad (7)$$

where N_{m1}, N_{m2}, N_{m3} are the number of multiplication operations in the first, second and third layers, respectively, and N_{mn} is the number of multiplications taken place within the set of neurons. Since the neurons use the activation function (sigmoid)), each neuron requires two multiplications and one e^X approximation (19 multiplications). Considering a bias input to each neuron in addition to the other inputs, so Eq. (7) may be refined as:

$$TC_m = [(N+1)(L1)] + [(L1+1)(L2)] + [(L2+1)(L3)] + [N_n(21)] \quad (8)$$

where $L1$, $L2$, and $L3$ are the number of neurons in the first, second, and third layers of the network, respectively, and N_n is the total number of neurons in the network. As an example, the MLNN shown in Fig. 2 has three input features (N=3), three neurons in the first layer ($L1$=3), five neurons in the second layer ($L2$=5), and three neurons in the output layer ($L3$=3). Substituting in Eq. (8), this network requires 281 multiplications for classifying one pattern. An identical procedure can be used for calculating the computational complexity of individual discriminators in a MSNN classifier. The summation of computational complexity of the discriminators was taken as the complexity of that MSNN classifier.

4. Results and Discussion

4.1 Comparison of Classifiers' Performances

The average classification performance and the time complexity of the classifiers using selected features are summarized in Table 1. It can be seen that the classifiers' performances were very close to each other and they ranged from 81.1% to 95%. The MSNN classifiers had the highest performances and were closely followed by the MLNN classifiers. In terms of computational complexity, the decision tree classifiers required the minimum, and the MSNN the maximum, computational time.

Features	GL-56 & A		FD's & A	
Classifiers	Performance	Complexity	Performance	Complexity
Gaussian				
Tree				
MLNN				
MSNN		X 320		X 385

Computational complexity is in terms of the number of multiplications

Table 1: Comparison of performance and computational complexity of the classifiers using GL-56 & A and 7FD's &*

4.2 Performance of Gaussian classifiers

These classifiers are based on the assumption that the individual features in a class are normally distributed. Thus when observations are concentrated near the mean, they are better classified by Gaussian classifiers. However, when the spread in data increases, or when the classes' distributions deviate from normality, the classification performance of these classifiers degrades.

In the experiments with classification of pistachio nuts, it was noticed that G2, with its tight distribution, was better estimated by the Gaussian than by any other classifiers. This classifier did not, however, have high performance in recognizing G1 and G3, because their distributions deviated highly from normal. To explain this in more depth, consider here a sample of split pistachio nuts. The sample naturally contains various amount of small, medium, large, and extra large nuts. The whole sample can be approximated by a normal distribution function. The portion of a hypothetical normal distribution of the split pistachio nuts that contains G1, G2 and G3 is presented in Fig. 3. The small and the large nuts lie on the extreme side of this distribution and clearly they do not have normal distributions. Therefore a Gaussian will not be a suitable classifier choice for classification of G1 and G3. On the other hand the medium nuts which are selected from the middle region of the distribution have a distribution which can be described fairly well by a normal distribution so they can be accurately classified by the Gaussian classifier.

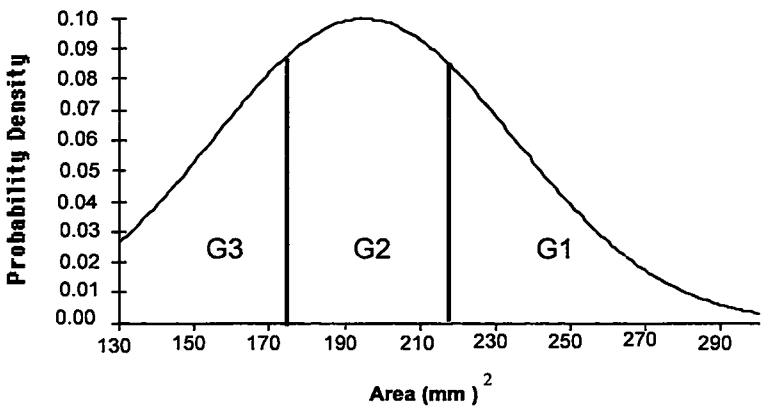

Figure 3: The location of G1, G2 and G3 classes on a hypothetical normal distribution curve

4.3 Performance of decision tree classifiers

When using a decision tree classifier, one needs to have some prior knowledge about the relationship between the features and the classes. For example, the FD's can separate split pistachios from unsplit, or that the G2 class generally lies over a certain range of areas. With this type of knowledge one can construct a decision tree classifier. The decision tree classifiers are easy to implement and usually require small processing time. However they have two main drawbacks. First, they form abrupt decision boundaries between classes whereas in reality, the boundaries are "fuzzy". Second, the probability of error increases as more nodes get involved in making decisions. The effect of the abrupt decision boundaries was noticed when the tree based classification results using GL-56 & A were compared with the output of MLNN using the same set of data. In general, the decision tree classifiers are the most suitable for problems where the processing time is more important than obtaining high accuracies and when a affirmative thresholds can be defined between the classes.

4.4 Performance of the MLNN classifiers

In general, the performances of MLNN classifiers were higher than the other classifiers, using the same inputs. The high performance of the MLNN classifiers stemmed from their high power in approximating the *a posterior* density functions. For example the MLNN classifiers approximated the distributions of G1 and G3 with higher accuracy than the Gaussian or tree classifiers. As mentioned earlier, these two classes had skewed distributions.

In theory, the MLNN's should attain 100% classification accuracy when a sufficient number of neurons are used in their hidden layer. These networks, in this research never gave 100% accuracy, except for the UN class. In fact their accuracy decreased when the number of neurons exceeded an optimum. Results of these experiments showed that when the classes described by the features are 100% separable, e.g., UN, then using a sufficient number of hidden layers and a proper training procedure will result in 100% classification. But when the classes, as described by the features, have some overlap, then the MLNN will not yield 100% classification and the final accuracy is governed by the data rather than the network. In this research, since the classes based on the considered features, e.g., area, had some overlap, the classification results using the MLNN gave some percentage of misclassification.

The MLNN, using GL-56 & A, estimated the boundaries separating the area of three classes of split nuts with high accuracy. However, for the decision tree classifier threshold values (i.e. the area thresholds) had to be estimated and supplied to the classifier. Several trial and error methods were used to estimate

these thresholds. However, boundaries estimated by the MLNN were superior to what was obtained by our best estimate.

The MLNN classifiers demonstrated their high classification power when they were used to classify the nuts using 7FD's & A. In other classifiers the 7FD's were used for distinguishing the split nuts from the unsplit and the area for separating G1, G2, and G3. The MLNN could go even further, and found useful information contained in the FD's for more accurate separation of G1, G2, and G3 classes. The high classification performance was an indication of the power of MLNN in mapping their inputs and outputs.

4.5 Performance of MSNN classifiers

The performances of the MSNN classifiers in this research were almost identical to those obtained by the MLNN classifiers. This was because a threshold of 0.0 was considered for interpreting the output of the networks. For example, if a MLNN classifier's outputs for a particular pattern were -0.65, -0.36, 0.01, and 0.06, the pattern would be assigned to the class associated the neuron that had the output of 0.06. This is would not be the case if, for example, a threshold value of 0.5 had been set for accepting the outputs. In this case the pattern would be considered as "Unclassified". When a threshold of +0.6 was considered for interpretation of the neural network classifiers, the performance of the MLNN using GL-56 & A was reduced. Classification accuracies for G1, G2, G3, and UN are 89.2, 48.8, 76.0, and 100 respectively, while MSNN retained the same performance as those given in the Table 1.

The discriminators in the MSNN classifiers generally had a high output (over 0.90) for the patterns of their respective classes. Whereas the neurons in output layer of the MLNN classifiers had an output between 0.0^{+} to 0.9^{+} for the patterns of their respective class, with a higher concentration around 0.35. The high output of the MSNN discriminators in turn make them more reliable in making decisions.

The MSNN classifiers required significantly lower training cycles than MLNN classifiers. This was because of the bias training of the MSNN discriminators. Bias training makes the discriminators more reliable for detecting their corresponding patterns and reduces the training burden.

In general, the MSNN classifiers are more suitable for multi-class classification problems because each class has its own discriminator. Since MSNN are designed to be implemented in parallel, the processing time does not increase with the number of classes. Another advantage of MSNN is that the small network topology of its discriminators makes them more suitable for both software and hardware implementation. The use of small topologies for discriminators increases their generalization power and subsequently makes them less sensitive to variation in input patterns.

Summary

The main classification schemes used in this research were Gaussian, decision tree, MLNN, and MSNN. The input to these classifiers were morphological features, Fourier descriptors and the gray level histograms of the nuts. From the morphological features, area had the highest discrimination power for separating G1, G2, and G3 from each other. The FD's had high discrimination power to separate the split nuts from the unsplit nuts.

The preliminary classifications and feature selections results indicated that 7FD's & A and also GL-56 & A were the most suitable features for classification of the four considered classes. In general, the MSNN classifiers had the highest performance and they were closely followed by the MLNN. Gaussian classifier had the lowest performance in recognizing the four classes of pistachio nuts. In terms of computational complexity, the MSNN required longer processing time than other classifiers.

References

[1] Batchelor, B.C., D.A. Hill and D.C. Hodgson. 1985. *Automated Visual Inspection.* London, UK: IFS (Publications) Ltd.

[2] Pavlidis, T. 1978. A review of algorithm for shape analysis. *Computer Graphics and Image Processing* 7(2):243-258.

[3] Pavlidis, T. 1980. Algorithm for shape analysis of contours and waveforms. *IEEE Transactions on Pattern Analysis and Machine Intelligence* 2(4):301-312.

[4] Makhoul J., A. El-Jaroudi and R. Schwartz. 1989. Formation of disconnected decision regions with a single hidden layer. In *Proceedings of the International Joint Conference on Neural Networks*, Washington D.C., a publication of the IEEE: San Diago, CA, Vol. 1, 455-460.

[5] Chester, D.L. 1990. Why two hidden layers are better than one. In *Proceedings of the International Joint Conference on Neural Networks*, Washington D.C., a publication of the IEEE: San Diago, CA, Vol. 1, 265-268.

[6] Lippmann, R.P. 1987. An introduction to computing with neural nets. *IEEE, Acoustics, Speech and Signal Processing Magazine*, 4(2):4-22.

[7] Elizondo, D. A., R.W. McClendon and G. Hoogenboom. 1992. *Neural network models for predicting crop phenology.* ASAE Paper No. 92-3596. St. Joseph, MI:ASAE.

[8] Thai, C.N., J.N. Pease and E.W. Tollner. 1991. Determination of green tomato maturity from X-ray computed tomopraphy images. *Proceedings of the 1991 Symposium on Automated Agriculture for 21th century*, A Special publication of the ASAE, 134-143, St. Joseph, MI: ASAE.

[9] Murase, H., Y. Nishiura, N. Honami and N. Kondo, 1992. *Neural network model for tomato fruit cracking*. ASAE Paper No. 92-3593. St. Joseph MI:ASAE.

[10] Park, B. and Y.R. Chen. 1994. Intensified multi-spectral imaging system for poultry carcass inspection. In *Food Processing Automation* III, *Proceedings of the FAAC III Conference*, Orlando, Florida, 9-12 Feb. 1994. A Special Publication of the ASAE, 97-106. St. Joseph, MI: ASAE.

[11] Dowell, F.E. 1993. *Neural network classification of undamaged and damaged peanuts kernels using spectral data*. ASAE Paper No. 93-3050. St. Joseph, MI:ASAE.

[12] Sayeed, M.S., Whittaker A.D. and Kehtarnavaz N.D. 1995. Snack quality evaluation method based on image feature extraction and neural network prediction. *Transactions of the ASAE* 38(4):1239-1245.

[13] SAS. 1991. *Users Guide:Statistics*, Cary, NC: SAS Institute Inc.

[14] Ghazanfari, A. , J. Irudayaraj and A. Kusalik. 1996. Grading pistachio nuts using a neural network approach. *Transactions of the ASAE*. 39(6):2319-2324.

[15] Ghazanfari, A., J. Irudayaraj, A. Kusalik, M. Romaniuk. 1997. Machine vision grading of pistachio nuts using Fourier descriptors. *J. agric. Engng Res. 68 :247-252.*

[16] Kreyszig, E. 1988. *Advanced Engineering Mathematics*, 6th ed. New York, NY: John Wiley and Sons.

Automatic potato sorting system using colour machine vision

Classification automatique des pommes de terre par système de vision couleur

Christophe Guizard

CEMAGREF, GIQUAL
361, rue J.F. Breton
B.P. 5095
34033 Montpellier Cedex 1
Tél : 04 67 04 63 00
Fax : 04 67 04 63 06
e-mail : christophe.guizard@cemagref.fr

Jean-Michel Gravoueille

ITPT -ITCF Service
qualité agro-industrielle,
Halle Technologique
91720 BOIGNEVILLE
Tél : 01 64 99 22 89
Fax : 01 64 99 22 45

Michel Crochon

CEMAGREF, GIQUAL
361, rue J.F. Breton
B.P. 5095
34033 Montpellier Cdx 1
Tél : 04 67 04 63 00
Fax : 04 67 04 63 06

Abstract: *Potato appearance quality assessment, a highly subjective exercise, is today an important factor for the food market. Work undertaken by Cemagref in cooperation with ITPT has lead to the validation of an experimental classification method based on the potatoes appearance. This method based on two colour component analyses which performs a classification function related to tuber brightness and blemishes. The software developed in this project has allowed us to validate the method against human expertise, with a 80% success rate.*

Keywords: *Potato, quality, vision, machine vision, image analysis, classification, identification.*

Résumé : Fortement subjective, la notion de qualité de présentation des pommes de terre est aujourd'hui un point important pour leur commercialisation. Les travaux du Cemagref menés en collaboration avec l'ITPT ont permis de valider une méthodologie expérimentale de classification de la qualité d'aspect des pommes de terre. Cette méthode basée sur l'analyse de deux composantes colorimétriques permet de réaliser une classification fonction de la clarté et des altérations superficielles du tubercule. Le logiciel développé a permis de valider la méthode sur des échantillons préalablement classés par des experts de l'ITPT, avec un taux de réussite proche de 80%.

1. Introduction

In France the potato is a product representing about 15% of the fruit and vegetable supermarket profit margin. Consumers demand undamaged products. Today quality evaluation of potato appearance must be carried out for both commercial and hygiene reasons. This classification or **agreement** is undertaken on samples through a subjective manual operation. Cemagref and ITPT have co-ordinated their efforts to develop an objective method using Machine Vision [1] to sort potatoes based on colour and defects. This study has focused on the brightness of the flesh and on the computation of blemish areas [2]. No particular research had be done on shape analysis [3] [4].

This automatic **agreement** method permits the classification of potatoes using an indication of brightness while appreciating the percentage of alteration through colour machine vision.

2. Materials and method

This study has focused on several varieties of potatoes provided by ITPT i.e. Ostara, Record, Agria, Nicola, Monalisa, Mondial, Early Nicola. They are used to create an important image database including healthy tubers with different brightness and tubers suffering from different diseases.

Concurrently CTIFL has developed a color reference pattern data base representing the basic tints of the different potato varieties (figure 1).

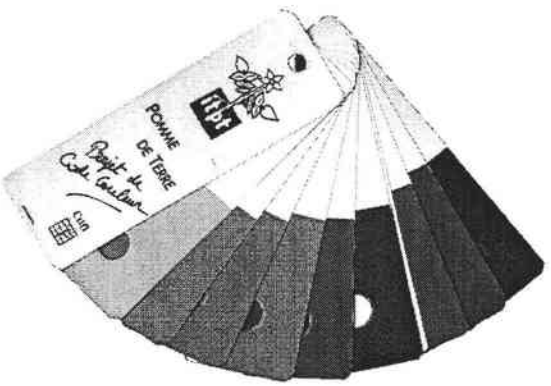

Figure 1: CTIFL colour chart

The machine vision system used (Figure 2) consists of:

1. a CCD colour camera, Sony XC77 (Mono sensor with stripe filter),
2. a fluorescent high frequency lighting system (Philips E98 tube),
3. a RGB frame grabber : IMAGRAPH Precision from IMASCAN,
4. image processing software : OPTIMAS 6.0.,
5. an Avenir Zoom lens 12,5-75mm F1.8,
6. a Gateway 166Mhz computer.

The project has been devided into 5 steps:

1. lighting system design,
2. building of image data base,
3. brightness classification,
4. determination of defect levels,
5. experimental validation of the classification model compared to expert classification.

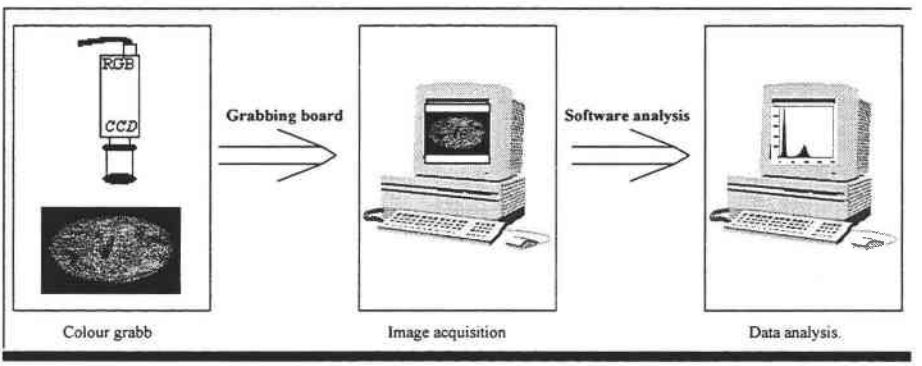

Figure 2: The basic principles of the system

2.1 Lighting system design

This study has been conducted to create a specific lighting system that can generate a uniform level of lighting around the potato surface. To illuminate the external volume of the tuber as effectively as possible, we have used a strong indirect lighting system based on a diffusing bell (figure 3) and four high frequency fluorescent tubes placed just under the level of the potato.

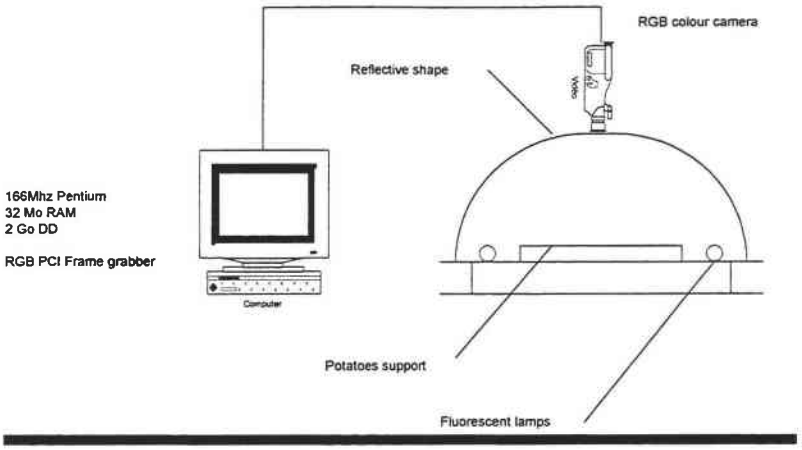

Figure 3: Grabbing system

2.2 Image data base

Each potato image has been grabbed and digitalized separately on one side, with a resolution of 712 x 548 pixels on 24 bits. Each of the color components (Red, Green and Blue) has been stored separately on 8 bits level. The data bank contains approximately 300 files, related to 7 varieties.

3. Experimal results

3.1 Brightness classification

The first study has focused on potato colour characterization. A Minolta spectrophotometer has been employed to measure the La*b* value of 10 potatoes by variety, on three different healthy locations of the skin. Experimentation has shown that the Luminance value (L) correlates well to the human assessment of brightness.

This observation has led us to work directly on the green component of the image. The green plane is comparable to the Luminance plane. Each grabbed image contains three zones, the background, the healthy surface and the defective surface.

The background is easily discriminated by using a background support different from the color of the potato. For example, in our experiment we use a dark blue background.

The healthy part has used to appreciate the brightness index. The identification of the altered part of the tuber is more difficult if the blemished area is significant. Indeed, in this case, the healthy part of the skin can not be clearly seen.

Working on the smoothed histograms (figure 4) has shown that «the most frequent grey level» (the most common surface tints) and «the brightness level of grey» (the brightness tints) are strongly linked to the human assessment of brightness.

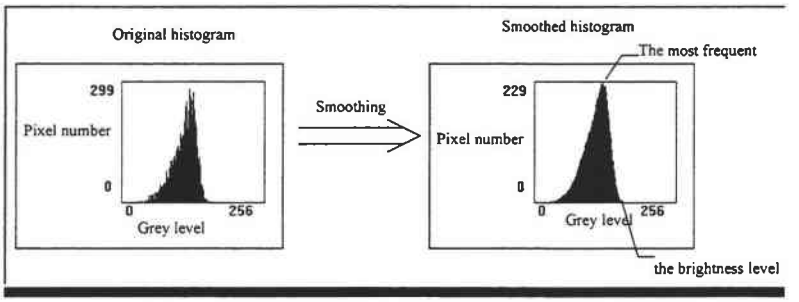

Figure 4: Histogram of grey level

A more accurate analysis of these two components (figure 5) showed that it can be possible to use only one of them. We have chosen «the brightness level of grey» because it offers the advantage of being practically independent from the degree of alteration. The only exception of this rule occurs with «Silver scurf» on dark flesh. It will have to be processed in a different way.

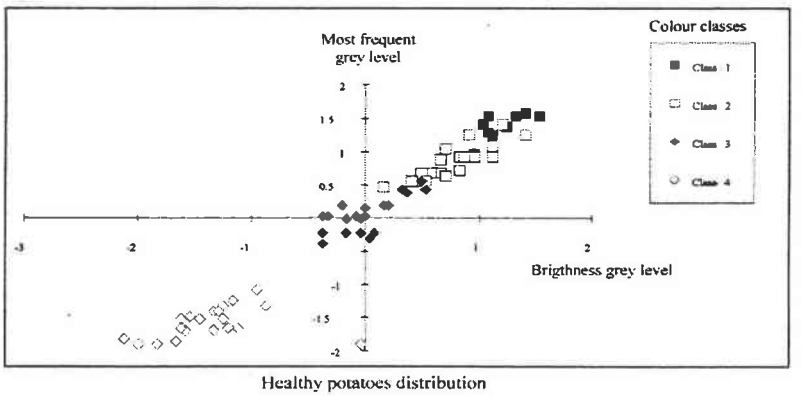

Figure 5: Component analysis «most frequent grey level» and «brightness grey level»

These first results show that:

1. the green colour or the luminance is heavily discriminent;
2. the blemish surface does not affect the results obtained by analyzing «the sharpest level of grey».

To obtain 6 classes of brightness in accordance with ITPT's demand. It is necessary to combine the red component and the green component classification, as can be seen in figure 6.

Each of 6 colour references defined by ITPT corresponds to a class of brightness assessed by human: the colour code n°3 corresponds to the class of brightness n°3.

To determine the limits of each class the average of «the brightness levels of grey» in the luminance plane is caculated for each coloured surface belonging to this class. For example in the figure 6: the colour code n°1 is equal to 152.

A similar computation is made to determine the frontiers of class 3 and 4, but this time in the Red plane.

Then, to determine the class limit between two classes, we evaluate the distance separating the grey levels average of these two classes. For example, the frontier between the class 1 and 2 is $\frac{(126+152)}{2} = 139$.
These limits allow the definition the membership of each class.

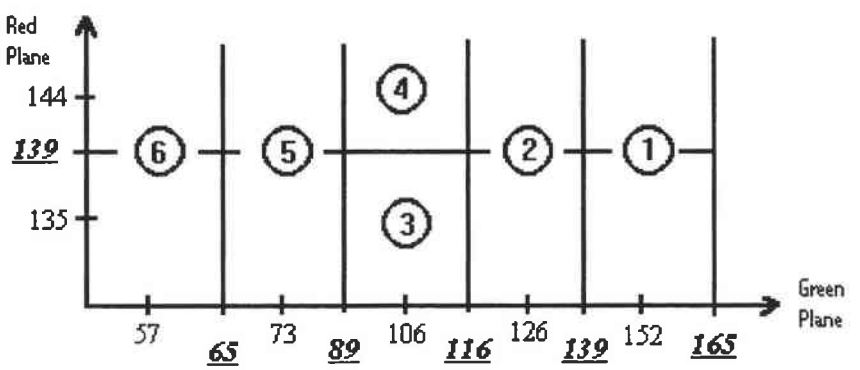

Figure 6: Green and red planes classes repartition

For example, if the average of «the brightness grey level» of potato A2 is 135.5. The potato is assigned to the class n°2 because the resulting value $\in[116;139]$

Green plane				Red plane			
Variety	min	max	sensitivity	Variety	min	max	sensitivity[1]
ostara	78	88	10	ostara	111	127	16
record	78	87	9	record	112	125	13
agria	104	114	10	agria	151	155	4
nicola	107	122	15	nicola	153	170	17
monalisa	121	138	17	monalisa	168	182	14
mondial	122	139	17	mondial	169	179	10
n_primeur	134	149	15	n_primeur	179	194	15

Table 1: Example of results given by the grey level analysis calculated by variety

3.2 Blemish classification

The visual analysis of damaged potato is more difficult than the previous classification. It consists essentially of calculating the percentage of the blemish surface. Human beings are very sensitive to spatial distribution : small defects distributed evenly on the tuber surface do not provoke the same sensation than when they are aggregated. We have observed that data given by experts relating to blemish areas are, in some cases, overestimate these defects and strict comparison with the system output is difficult.

To evaluate blemishes ITPT uses a 5 category classification (table 2). The frontier between classes is particularly difficult to appreciate by human beings. It is the principal value of the machine vision system.

Blemish categories with area percentage of defect				
Category A	Category B	Category C	Category D	Category E
No defect	< 5%	5%à 25%	25%à 75%	> 75%

Table 2: ITPT blemishes classification

To be able to identify blemishes on the potato surface it is necessary to automatically segment the image. The observation of different histograms of CTIFL colour chart, shows that each 6 brightness class have the appearance of gauss curves.

[1] Sensitivity = threshold variability with no resulting incidence

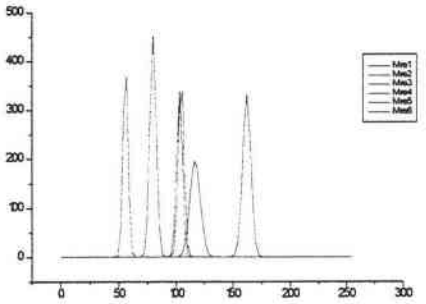

Figure 7: Luminance histogram (8 bits) for CTIFL reference patterns

These gauss curves can be modelised by:

$$G = y0 + \frac{A}{w * \sqrt{\frac{\pi}{2}}} * \frac{1}{e^{\left[\frac{-2*(X-Xc)^2}{w^2}\right]}}$$

A, Gauss area
y0, interior limit value of Gauss curve
w, half height width of the Gaussian curve
Xc, center of the gaussian curve

CTIFL colour chart represents an ideal case. For real cases the Gauss curve factors have been computed for each variety on a healthy and representative surface of the tuber, to do this 10 samples have been used.

For example, the following parameters were obtained for the Nicola variety:

A=8277,7 y0=0 w=26,4 Xc=96,1

Experimental results shown that pixels related to the ideal color are found within an interval centered on the peak of the gauss curve. Values outside of this interval are assimilated to blemishes.

This last experimentation allows the identification of blemishes through a simple image processing label of surfaces using a brightness index computed beforehand. The case of the «silver scurf» on darker potatoes is a unique case that is processed separately.

Blemish discrimination is calculated automatically by the threshold:

Threshold = average of gray brightness level - size of « ideal » gauss curve

A learning process is necessary to determine the «Gray brightness level values» of each class. This operation is conducted with tubers free of blemishes and representative of the class.

The percentage of blemish area is calculated by simple image segmentation applying the threshold formula above:

%Blemish = (blemish area) / (tuber area)

Final organigram of the process is shown below:

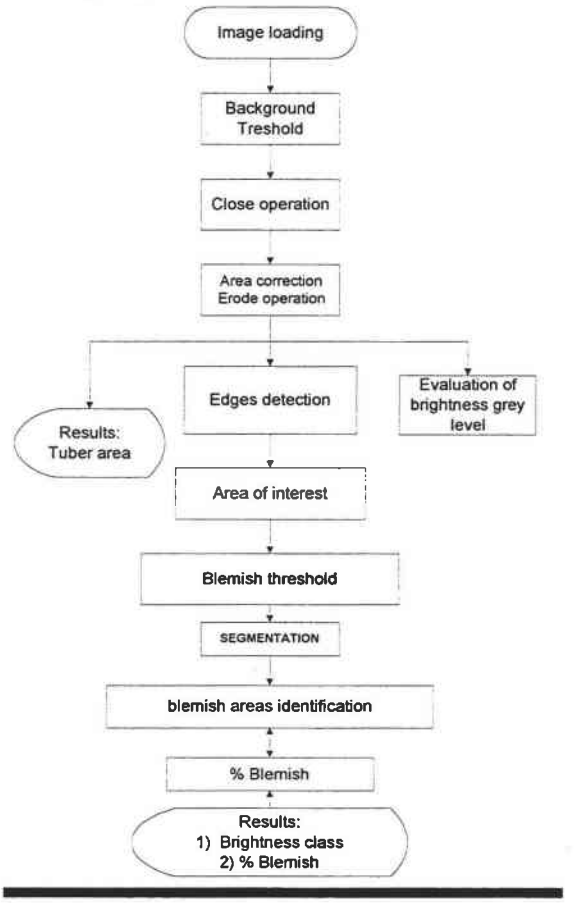

Figure 8 : Program organigram

3.3 Data validation

A software (figure 9) is developed with this method to help us to validate results during an experimental campaign undertaken by ITPT.

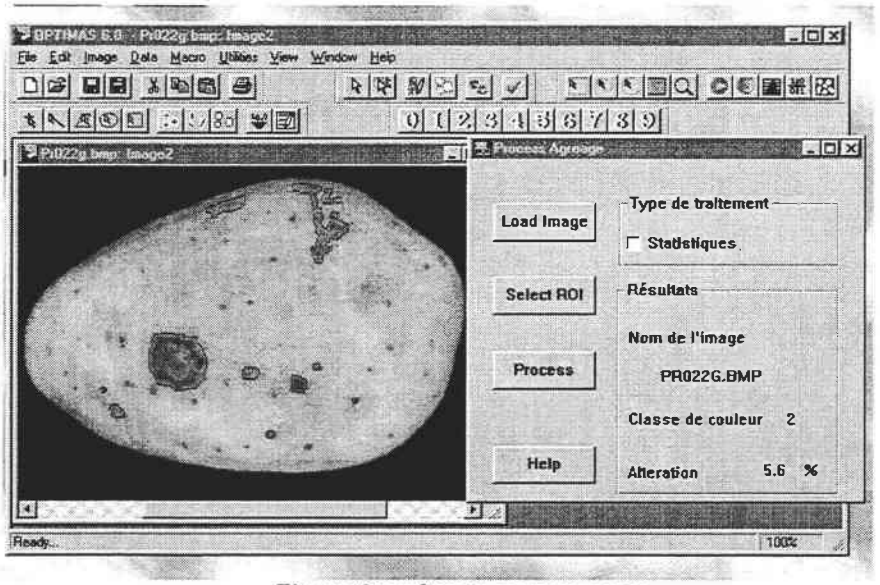

Figure 9: software screen copy

The system has been tested in real conditions on fifty potatoes identified beforehand by two ITPT experts. It has been previously calibrated directly on reference samples of potatoes.

Images have stored on hard disk and then processed automatically by the software. Values extracted as well as results of classification are given in table 4.

Experimental measurements Color		**Experimental measurements Defects**	
Brightness class error	% Potato	Blemishes % gap	% Potato
0	36	<2.5	26
0.25	22	2.5 à 5	22
0.50	18	5 à 10	22
0.75	6	10 à 20	15
1	18	20 à 30	11
>1	0	>30	4

Tableau 3: Software classification in comparison with expert's (see table 4)

Table 3 summarizes the errors **between** the expert and the automatic classification. Results show that 76% of potatoes present an absolute error inferior to 0.5 class between the value predicted by the system and the class provided by experts. During the validation of the system, no potato is classified outside its true class.

Concerning blemishes the results are also very satisfactory : 70% of tubers have been classified with an error rate inferior or equal to 10% in comparison to the expert classification. The system does not take into account all the small defect sizes , this point can be parametered using software.

It's worthwhile to compare the automatic classification and the difference between the two expert (figure 10).

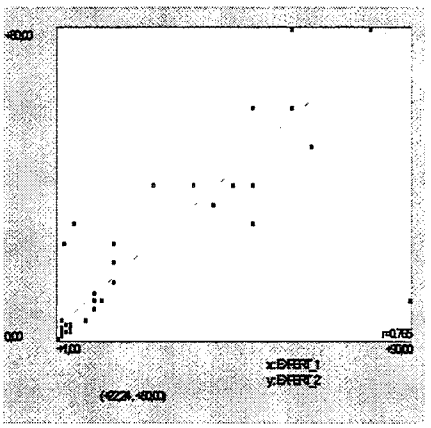

Figure 10: Expert correlation

On 47 tested samples, correlation coefficients as high as 0.863 for brightness and 0.79 for blemish areas were obtained. The last coefficient is also close to the correlation between the two experts, 0.765 as shown in figure 10.

Conclusion

The system has given results close to human assessment which means that around 80% of potatoes are classified correctly according to colour and 70% for blemishes. These results can be considered as satisfactory, and they do not take into account the subjectivity of human assessment. Differences can be observed when defects are small and numerous. In these cases, the defect areas are overestimated by operators. This phenomenon is due to reasons linked to human behaviour characteristics .

It seems possible to improve results by looking more closely at the non-linearity of human perception, it's one of the new research objectives of our laboratory.

Classification data analysis

	Automatic Classification		Expert classification		
Potato	Software Class	Blemish	Expert Class	Exp1 - Blemish	Exp2 - Blemish
PR001	1,00	3.8	1,00	2,00	5,00
PR002	1,00	3.0	2,00	2,00	3,00
PR003	2,00	1.5	3,00	3,00	4,00
PR004	3,00	0.3	4,00	2,00	2,00
PR005	5,00	0.0	5,00	10,00	10,00
PR006	1,00	1.1	2,00	3,00	2,00
PR007	1,00	16.8	2,00	15,00	15,00
PR008	2,00	23.6	2,50	25,00	40,00
PR009	2,00	26.2	2,00	35,00	40,00
PR010	2,00	27.2	2,00	15,00	20,00
PR011	2,00	33.7	2,50	45,00	40,00
PR012	1,00	18.5	1,75	8,00	5,00
PR013	2,00	36.6	2,50	25,00	40,00
PR014	2,00	10.1	2,25	10,00	12,00
PR015	2,00	24.2	2,00	15,00	25,00
PR016	1,00	5.3	2,00	4,00	2,00
PR017	1,00	5.1	2,00	4,00	3,00
PR018	1,00	10.0	2,00	4,00	2,00
PR019	1,00	2.0	2,00	2,00	1,00
PR020	1,00	26.1	2,00	10,00	8,00
PR021	1,00	30.1	2,00	10,00	10,00
PR022	1,00	12.6	2,00	10,00	8,00
PR023	1,00	9.0	2,00	10,00	10,00
PR024	1,00	15.0	1,50	12,00	10,00
PR025	1,00	13.2	1,50	10,00	8,00
PR026	1,00	0.9	1,75	1,00	0,00
PR027	1,00	3.3	1,25	4,00	3,00
PR028	1,00	14.3	2,00	2,50	25,00
PR029	4,00	10.2	3,25	15,00	20,00
PR030	3,00	26.9	3,50	65,00	50,00
PR031	1,00	7.6	0,98	15,00	15,00
PR032	2,00	24.6	2,75	50,00	60,00
PR033	2,00	49.8	2,00	80,00	80,00
PR036	2,00	10.0	2,75	40,00	35,00
PR038	2,00	32.8	2,25	50,00	40,00
PR039	3,00	13.6	4,75	5,00	30,00
PR040	2,00	36.2	2,75	90,00	10,00
PR041	1,00	11.3	2,00	15,00	15,00
PR042	1,00	36.5	1,75	60,00	60,00
PR043	1,00	7.0	1,25	12,00	10,00
PR044	2,00	7.2	2,75	15,00	15,00
PR045	2,00	23.1	2,50	25,00	40,00
PR046	4,00	23.7	3,50	50,00	30,00
PR047	3,00	33.0	3,00	60,00	80,00
PR048	1,00	1.7	2,00	4,00	4,00
PR049	1,00	4.5	1,75	8,00	5,00
PR050	2,00	15.3	2,50	2,50	25,00

Table 4: Experimental results of computer classification versus human expertise for brightness and blesmishes

References

[1] Guizard C., Marty-Mahé P., 1996- Vision Industrielle: un capteur pour la qualité, *Cahiers Agricultures; 5: p. 43-51.*

[2] Tao, Y.; Morrow, C. T.; Heinemann, P. H.; Sommer, J. H., 1990- Automated machine vision inspection of potatoes, *American Society of Agricultural Engineers. (No. 90-3531) : 23 pp.*

[3] Jelinek, O.; Plasek, J.; Maskova, H., 1990- Technical possibilities for automatic sorting of healthy and damaged potato tubers, *Zemedelska Technika. 36 (7): p. 433-441.*

[4] De Koning C.T.J., Speelman L., de Vries C.P., 1994- *Size grading of potatoes: development of new characteristic parameter, JAER 57, p. 119-128.*

On-line quality evaluation and sorting for mushroom via neuro image processing

Evaluation de la qualité et tri en ligne de champignons par analyse d'images et réseaux de neurones

H. Hwang **C.H. Lee** **S.C. Kim**

Assoc. Professor Research Associate Research Assistant
Dept. of Bio-Mechatronic Engineering
Sung Kyun Kwan University, KyungKi-Do, Suwon, Korea 440-746
e-mail: hhwang@yurim.skku.ac.kr

Abstract: *In Korea, quality evaluation of dried oak mushrooms are done first by classifying them into more than 10 different categories based on the state of opening of the cap and the surface pattern and color of the cap and gill. And mushrooms of each category are further classified into 3 or 4 groups based on its shape and size, resulting into total 30 to 40 different grades. Quality evaluation and sorting based on the external visual features are usually done manually. Since visual features of mushroom affecting quality grades are distributed over the entire surface of the mushroom, both front(cap) and back(stem and gill) surfaces should be inspected thoroughly. In fact, it is almost impossible for human to inspect every mushroom, especially when they are fed continuously via conveyor.*

In this paper, considering real time on-line system implementation, neuro-net based image processing algorithms for the quality grading of a mushroom has been developed. The neuro image processing utilized the raw gray value image of fed mushrooms captured by the camera without any complex image processing such as feature extraction and enhancement to identify the feeding state and to grade the quality of a mushroom. Developed algorithm was implemented to the prototype on-line grading and sorting system. The prototype was developed to simplify the system requirement and the overall mechanism. The system was composed of automatic devices for mushroom feeding and handling, a set of computer vision system with lighting chamber, one chip microprocessor based controller, and pneumatic actuators.

The proposed grading scheme was tested using the prototype. Network training for the feeding state recognition and grading was done using static images. 200 samples(20 grade levels and 10 per each grade) were used for training. 300 samples(20 grade levels and 15 per each grade) were used for verification of the trained network. By changing orientation of each sample, 600 data sets were made for the test and the trained network showed around 91% grading accuracy. Though image processing itself required approximately less than 0.3 second depending on a mushroom, because of the actuating device and control response, average 0.6 to 0.7 second was required for grading and sorting of a mushroom resulting into the processing capability of 5,000/hr to 6,000/hr.

Keywords: *Automatic sorting and grading system, dried oak mushroom, computer vision, neural net, gray image processing.*

Résumé : En Corée, la qualité des champignons secs de bois de chêne est évaluée en classant les champignons en plus de 10 classes en fonction de l'ouverture du chapeau et de l'état et de la couleur du chapeau et des lamelles. Dans chaque catégorie, les champignons sont classés en 3 ou 4 groupes (en fonction de la forme et de la taille), ce qui fait 30 à 40 groupes en tout. L'évaluation de la qualité et le tri en fonction des paramètres externes sont généralement faits manuellement. Comme les paramètres visuels des champignons qui régissent les classes sont distribués sur toute la surface du champignon, à la fois le dessus (chapeau) et le dessous (lamelle et pied) doivent être analysés avec soin. En fait, il est impossible pour un humain d'inspecter chaque champignon, surtout quand ils sont amenés continuellement par un convoyeur.

Dans cet article, des algorithmes basés sur l'analyse d'image à base de réseaux de neurones sont développés. Le traitement d'image neuronal utilise les niveaux de gris bruts des champignons, après acquisition par une caméra, sans traitement complexe tel que l'extraction de paramètres et l'amélioration des contrastes. L'algorithme a été implanté sur un prototype de tri, développé pour simplifier les spécifications du système et le mécanisme complet. Le système est composé d'une alimentation automatique, d'un système de vision avec chambre de mesure d'un contrôleur à micro processeur et d'actionneurs pneumatiques.

Le protocole d'agréage a été testé sur le prototype. L'entraînement du réseau pour reconnaître l'état physiologique et pour trier a été fait sur images statiques -200 exemples (20 niveaux de qualité et 10 échantillons par niveau) sont utilisés pour l'entraînement ; 300 échantillons (20 niveaux et 15 échantillons par niveau) sont utilisés pour la validation. En changeant l'orientation de chaque échantillon, 600 données sont enregistrées pour le test et un bon classement de 91 % est atteint. L'analyse d'images demandant 0,3 secondes, du fait des actionneurs, un cycle de 0,6 à 0,7 secondes par champignon est nécessaire, soit une capacité de 5 000 à 6 000 pièces/h.

1. Introduction

Most bio-production processes involve labor intensive and tedious simple repetitive tasks. In fact, automating simple repetitive task handling bio-products often requires real time computer image(gray or color) processing, AI information processing, and sophisticated handling maneuver because of their various and irregular shape characteristics. Since amongst of various agricultural processes, the process of quality inspection and control has been one of the most labor intensive and time consuming operations, R&D for quality grading and sorting automation of bio-products have been very active throughout the world.

Generally, human expert is the best in grading an individual object in a sense of precision, adaptability, and robustness. Human grading, however, usually suffers from the speed and the lack of consistency because of the fatigue, illusion, and time-varying emotional state, which are popular symptoms of the mental state caused by the long-lasting continuous work. As a result, the overall productivity gets usually lower as the amount of objects to be graded increases.

Considering the inherent quality factors of bio-products, grading and sorting system should be developed in a manner of being capable of human like robust and efficient visual data processing while keeping in real time speed. As a substitute of human vision, computer vision technology has shown great potential in the evaluation of different quality attributes of agricultural and food products. Currently computer image processing has been incorporated with the emerging AI technologies such as expert system, neural network, genetic algorithm, fuzzy logic, etc. and resulted into the improvement of the information processing capability. Since quality of bio-products can not be precisely defined in an objective manner because of the inherent fuzziness and irregularity and it is usually determined synthetically from various features, this kind of approach is very effective in quality control of bio-products.

In Korea, dried oak mushrooms distributed in the market are classified into many different categories based on its external visual quality. They are classified into more than 10 different categories based on the state of opening of the cap and the surface pattern and color of the cap and gill. And mushrooms of each category are further classified into 3 or 4 groups based on its shape and size, resulting into total 30 to 40 different grades. However, only size sorting is done partially by a series of conveyor and vibrating feed plate having different sizes of punched round holes. Since visual quality features of a dried mushroom are distributed over both sides of the gill and the cap surface, precise grading used to be done manually one by one via shape and texture. In fact, it is almost impossible for human to inspect every mushroom, especially when they are fed continuously via conveyor.

In this paper, considering real time on-line system implementation and the hardware, neuro-net based image processing algorithms for quality grading are presented. The neuro-net based mushroom identification and grading utilized the raw gray value image of fed mushrooms directly captured by the camera without any complex image processing such as feature extraction and enhancement. The proposed algorithms were implemented to the prototype automatic grading and sorting system, which has been developed in our laboratory. Results of grading and sorting performance of the proposed system are also presented.

2. Materials and method

2.1 Neuro grading

Quality grading of bio-products via extracting visual features often requires too much computing and time-consuming operation. Real-time and on-line image processing constraint used to be a bottleneck to the successful system implementation of quality evaluation algorithms. And visual features extracted from certain image processing may sometimes lose some important information due to the enhancement and the simplification processes resulting into inaccurate results. If a pattern can be recognized without extracting quantitative features, the real time and robust system implementation can be easily achieved. The neural network based image processing was devised to realize the quality grading of a mushroom without employing the complex feature extraction.

Since visual quality features of a dried mushroom are distributed over both sides of the gill and the cap surface, nce visual quality features of a dried mushroom are distributed over both sides of the gill and the cap surface, both side images should be captured and inspected. To automate the grading process first, the side recognition should be done from the image captured by the camera. In this paper, the well known BP network was utilized to identify the feeding state of a mushroom, whether the mushroom is fed as the front side(cap) up or back side(stem and gill) up. Also BP network was used for quality grading of a mushroom.

For the front and backside recognition, two types of network inputs were previously tested. First, the segmented binary image obtained from the combined type automatic thresholding was tested for network inputs. And gray valued raw camera image was tested directly as an input to the network. Since the segmented binary image by the combined type thresholding may lose important details of the gray valued image or distort some information, the recognition performance of the network with the binarized image input was worse than the network with the raw gray valued image[2].

Once the fed mushroom was identified from the optic sensor, the image was captured. Using the captured raw gray level image, location of the mushroom was identified and the network input region was assigned from the measuring

window(170x180) by scanning gray level difference between the background and the mushroom pixels. The network input region was determined from the Min/Max pixel coordinate obtained after scanning. The network input region was converted to the rectangular input grids being composed of 64(8x8) grids. Though the size of rectangular input grid varies according to the size of the fed mushroom, the total number of grids is kept same. Value of each grid was computed by averaging the gray values of pixels that belong to each grid and was normalized between 0 and 1. Using these converted input values the feeding states of mushrooms were identified as either front side up or not via network processing. The converted network input values were kept for further processing.

Then, mushroom was reversed and the image was captured again. Exactly same process was repeated for the reversed mushroom. The converted network input values of the reversed mushroom were also kept after identifying the feeding state. Two sets of the converted network inputs, 128 normalized grid values with normalized 8 size factors(x, y, |x-y|, x+y) computed from two measuring windows were used for the network input for quality grading. verted network inputs, 128 normalized grid values with normalized 8 size factors(x, y, |x-y|, x+y) computed from two measuring windows were used for the network input for quality grading. The size difference of two images (before and after reversing) caused by the distance difference from the camera was compensated at the initial system set identifying the feeding state. Two sets of the converted network input performance is sensitive to the illumination condition. The brightness level of the camera input gray level image varies very sensitively to the lighting condition, the average brightness of the input window was measured. And then according to the predefined values at the initial stage of training, gray values of input image were compensated. The compensation process provides nearly the external lighting invariant consistent input image to the trained network. Fig. 1 shows the grading scheme and the network structure.

Network training for the feeding state recognition and grading was done using static images. etwork training for the feeding state recognition and grading was done using static images. 200 samples (20 grade levels and 10 per each grade) were used for training 300 sample mushrooms (20 grade levels and 15 per each grade) were used for verification of the trained netword. By changing orientation of each sample, 600 ample data sets were made and used for the test.

2.2 Implementation

The previously mentioned neuro image processing algorithm was implemented to the prototype automatic grading and sorting system. The prototype was designed and built first, to meet the requirements of the developed algorithm and then to improve the grading performance and sorting capacity while simplifying the system requirement. As mentioned previously, the proposed grading algorithm utilized both side images of a mushroom. Since simultaneous acquisition of both side images of

the incoming mushroom required two cameras and was quite difficult from the viewpoint of the system implementation, the scheme of the sequential image acquisition of the mushroom was adopted. Either side image of a fed mushroom was acquired sequentially via automatic side reversing device. One set of vision system was used and the field of the view of the camera was adjusted enough to cover the both side images of mushrooms before and after reversing. And then both side images were utilized for quality grading of a mushroom.

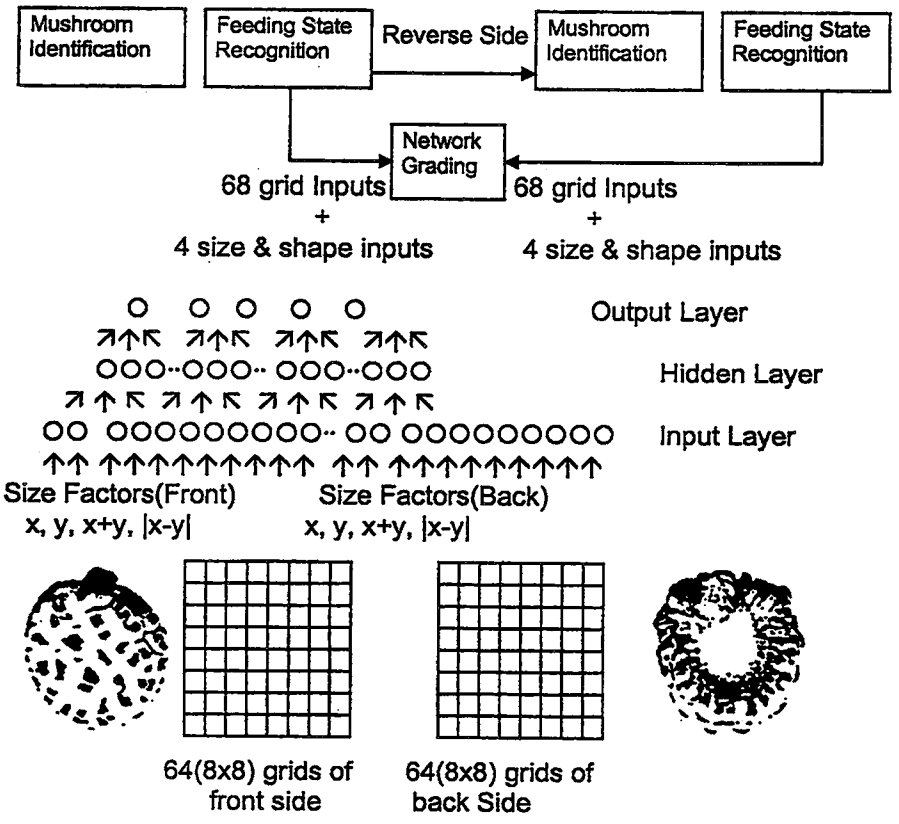

Figure 1: Grading scheme and network structure composed of 136 input

Once the fed mushroom was checked from the optic sensor, the image was capture0d. Using the raw gray level image captured from the camera, the location of the fed mushroom was identified and the network input range was assigned from the predetermined measuring window(170x180) by scanning the gray level difference. Fig. 2 shows the schematic diagram of the process that generates the network input from the mushroom fed on a conveyor. Then recognition of feeding status(either front or back side up) was done first via trained network and the network grid input data and size data were kept with side labeling.

Major modifications were made from defects of the previously developed 1st prototype[3,4]. The developed prototype was composed of vibrating hopper and feeder for storage and feeding, variable speed conveyors, one set of computer vision system, automatic side reversing device, and multi-stage sorting device. Two vibrating feeders were installed to control the amount of mushrooms being fed and to feed one by one in a row while avoiding overlapping each other. The pendulum type narrow thin plate with the proximity switch was installed over the vibrating feeder to control the feeding amount of mushroom from the storage/feeding hopper. When the amount of mushrooms in a feeder was too much to be aligned in a row, the pendulum switch was turned on. Then, the vibrating storage/feeding hopper was turned off and stopped feeding to the next vibrating feeder until the signal backed up. By adjusting the height of the tip of the pendulum plate, the amount of

Figure 2: Schematic diagram of the process generating network input from the mushroom fed on a conveyor

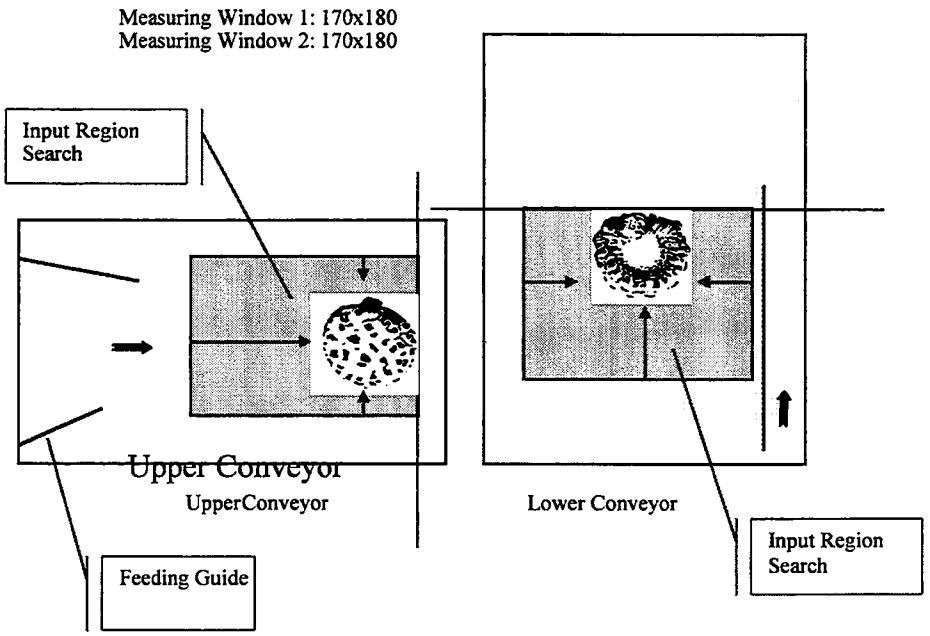

mushrooms to be fed was controlled. The «U» shape cross-sectioned plate was specially designed and mounted on the vibrating feeder to make mushrooms feed in a row. Utilizing the speed variation of feedings between the vibrating feeder and the conveyor, mushrooms were isolated each other and fed at a certain distance apart.

A «V» shaped plate driven by DC motor was devised and installed between the two feeding conveyors to automatically reverses the side of continuously fed

mushrooms. This reversing device allowed capturing each side image sequentially. Fig.3 shows the functional sequence of the automatic grading and sorting process.

An illumination chamber was designed and 4 high frequency(20,000Hz) inverter fluorescent lighting was installed in the chamber to reduce the shade. Oculus B/W frame grabber(TC-MX, CORECO Inc.) was used to digitize and store the incoming video signal with an accuracy of eight bits at a rate of 30 frames per second. In a case of processing dynamic image, the captured image is usually blurred. Though blurring effect could be compensated through filtering by convolution theorem, high-speed electronic shutter was adopted to reduce the blurring effect and to save the processing time. Generally, high-speed shutter requires more intense illumination. For the developed prototype, considering response time of actuating parts, the shutter speed of 1/500 second was good enough. The area variance from the blurring effect was testified using the sample square primitive(side length: 5cm) with various conveyor speeds. Measurement errors of the sample square under 1/500 second shutter speed at the speed of 150mm/sec conveyor speeds was less than 2.5%.

Five sorting stations were built and each sorting station was composed of a set of air nozzles mounted over two-channel bucket along the conveyor. The crevice type pneumatic cylinder was used to move the inside guide plate of the two-channel bucket. The position and blowing angle of the air nozzle at each sorting stage was adjusted based on the size of mushrooms to be sorted. Each sorting station was designed to handle 4 grading categories. The optic sensor was mounted at each sorting station to check the mushroom passing. Bad mushroom was sorted to the bucket located at the end of the conveyor.

An automatic multi-station-sorting algorithm was developed to handle mushrooms being fed randomly and continuously on the conveyor. The controller for sorting mechanism was built using one chip microprocessor(Chips F8086, Chips Tech Inc.), I/O board, and driver for solenoid valves. Fig.4 shows the block diagram of the function of the controller.

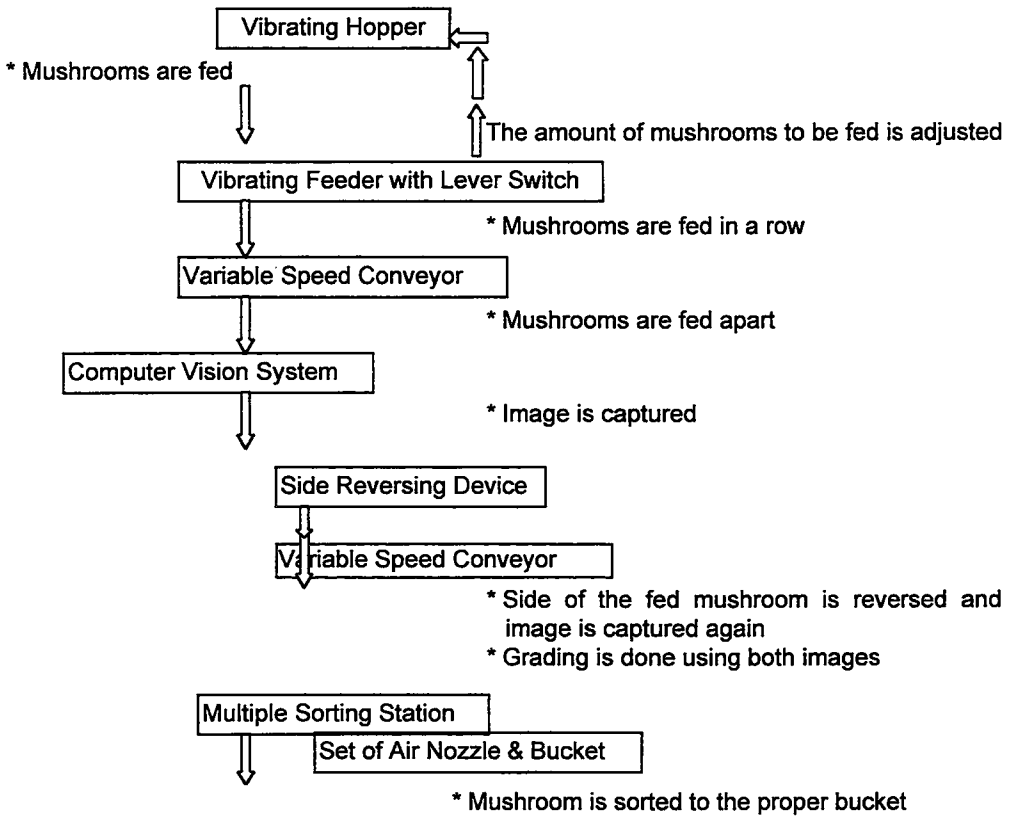

Figure 3: Functional sequence of automatic grading and sorting process

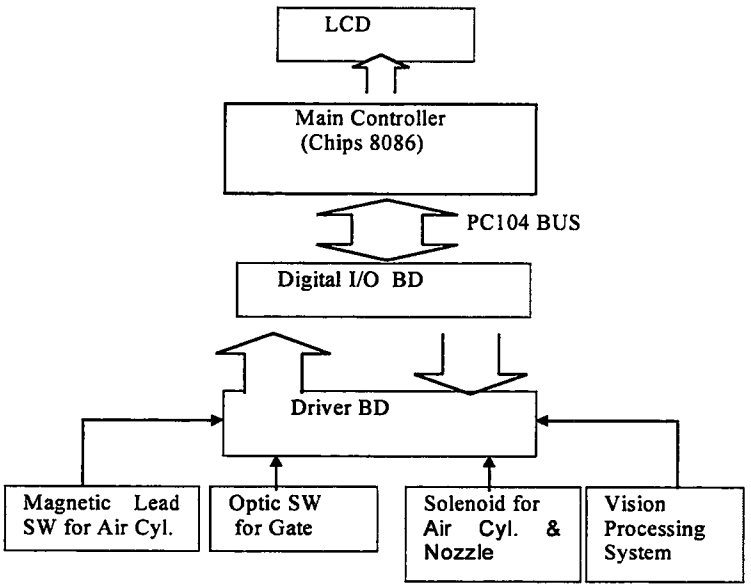

Figure 4: Block diagram of the function of the controller

3. Results

Network training for the Front and Back side recognition was done using static images of 200 samples(20 grades and 10 per each grade). Results of feeding state recognition for training samples showed near 100% accuracy. 300 sample mushrooms(20 grades and 15 per each grade) were used for verification of the trained network. By changing orientation of each sample, 600 sample data sets were made and used for the test. And the trained network showed around 91% grading accuracy for the static images.

Grading performance of the network, which was trained by 200 static samples, was then tested for moving mushrooms. And it showed around 94% accuracy of grading. And 10 untrained samples per each grade(20 grades), total 200 samples were arbitrarily selected and tested. Grading accuracy was around 88% with the conveyor speed of 150.6mm/sec. As a result, it could be seen that the blurring effect of the camera captured moving image under the 1/500sec shutter speed was negligible in grading performance.

Considering the actuator including the reversing device and control response, average 0.6 to 0.7 second was required for grading and sorting of one mushroom resulting into 5000/hr to 6,000/hr processing capability. Fig. 5 shows the developed prototype, which the proposed neuro image processing algorithm was implemented to.

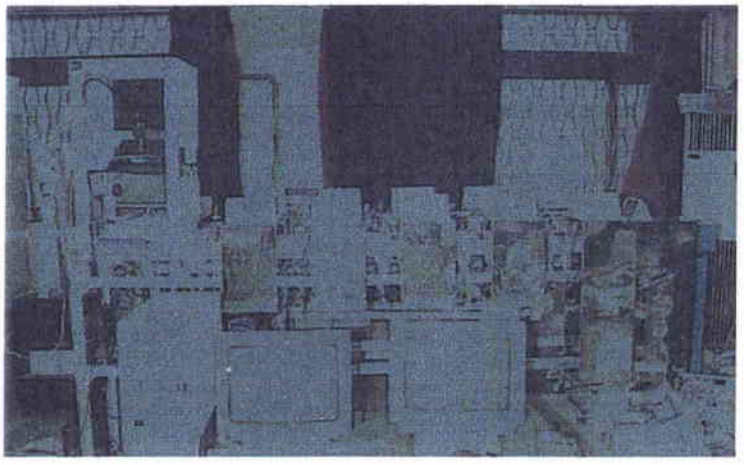

Figure 5: Developed real time on-line automatic grading and sorting system

Conclusion

According to the previous research, grading scheme based on the rule set up with some experimental heuristic utilizing quantitative features showed the inherent deficiency of the robustness and the problem of real time implementation. Since all oak mushrooms have their own unique shapes and unfortunatly some of those have fuzzy and abnormal features, recognition rules could not handle all shape patterns correctly though they were enforced by the heuristic. Neuro image processing for the mushroom grading was developed to satisfy the real time on-line processing and to overcome the robustness problem.

The gray valued raw camera images of both sides of mushrooms were directly input to the network without extracting any visual features. The neural net based gray valued raw image processing showed successful results for our grading task in its processing speed, grading accuracy, and the robustness. The prototype was developed to implement the proposed neuro-grading algorithm appropriately.

The system was composed of one set of computer vision system and automatic handling devices such as feeding in a line, side reversing, and simultaneous sorting. A series of a set composed of two pneumatic air nozzle and two two-channel buckets were designed and built to reduce the activation and reset time of the sorting mechanism.

sorting. A series of a set composed of two pneumatic air nozzle and two two-channel buckets were designed and built to reduce the activation and reset time of the sorting mechanism.

The proposed implementation scheme for automatic grading of dried oak mushrooms fed on the conveyor belt revealed successful results of more than 88% grading accuracy, the sorting capability of around 5,000 to 6,000 mushrooms/hr per each line i.e. average 0.6-0.7sec/mushroom. The major constraint of the processing speed was due to sequential acquisition of the image followed by the reversing mechanism. To improve the system performance, more efficient mechanism for the acquisition of both side images of mushrooms fed on the conveyor should be developed.

Acknowledgement

This research was funded by the MAF-SGRP(Ministry of Agriculture and Forestry-Special Grants Research Program) in Korea.

References

Hwang. Development of Automatic Grading and Sorting System of SHIITAKE Based on Neuro-processing of Visual Image, *In Proc. of 4th New Horizon of Technology for Agricultural Machinery Engineering*, pp.1-25,Oct. 1994.

Hwang, C. H. Lee. Automatic Recognition of the Front/Back Sides and Stalk States for Mushrooms(Lentinus Edodes L.). *In Journal of the Korean Society for Agricultural Machinery*, Vol.19, No.2, pp.125-135, 1994.

C. H. Lee, H. Hwang. Development of Robust Feature Recognition and Extraction Algorithm for Dried Oak Mushrooms. *In Journal of the Korean Society for Agricultural Machinery*, Vol.21, No.3, pp.325-335, 1996.

H. Hwang, C.H. Lee. Development of a Prototype Automatic Sorting System for Dried Oak Mushrooms *In Journal of the Korean Society for Agricultural Machinery*, Vol.21, No.4, pp.414-421, 1996.

Application of neural networks in quality control of 'Jonagold' apples

Application des réseaux de neurones pour le contrôle de la qualité des pommes "Jonagold"

V. Leemans **F. Bieuvelet** **M.F. Destain**

Faculté universitaire des Sciences agronomiques de Gembloux
Passage des déportés, 2 - B 5030 Gembloux Belgium
e-mail: leemans.v@fsagx.ac.be

Abstract: *This paper studies the possibilities to grade the 'Jonagold', a bicolour apple, using neural networks and Fisher's linear discriminant analysis. In a first step the pixels are sorted into three areas, the blush colour area, the intermediate colour area and the ground colour area; the accuracy reached 95% with the neural networks. In the second step the fruit are graded into four categories on their ground colour basis; the accuracy reached 68% whatever the method used. It is also shown that there is no need to separate the ground colour and the intermediate colour to compute the ground colour classification parameters.*

Keywords: *Computer vision, colour vision, coulour sorting, apple.*

Résumé : Cet article étudie les possibilités d'apprécier les pommes Jonagold, bicolores, en utilisant un réseau de neurones et une analyse discriminante linéaire de Fisher. Dans un premier temps, les pixels sont triés en trois classes : la couleur du blush, la couleur du fond et une couleur intermédiaire. Puis les fruits sont triés en quatre catégories en fonction de la couleur du fond. Une précision de 68 % est atteinte.

Il n'est pas nécessaire de séparer la couleur du fond de la couleur intermédiaire pour faire un bon tri.

1. Introduction

The apple colour has a major influence on quality grading. Most of the studies devoted to colour sorting of apples by machine vision concerns monochrome fruits, like 'Golden Delicious'. To sort these apples, Heinemann et al. [1] converted the R, G, B values issued from a colour camera to the HSI (hue, saturation, intensity). They used the only hue information to grade the fruits in two categories. Leemans et al. [2] sorted the fruits into four categories and showed that better classification results were obtained when taking into account 3 colourimetric parameters instead of 1, whatever the chosen colour space. Furthermore, they indicated the interest of using a single sorting parameter, the canonical variate, which expresses the independence between the 3 colourimetric values. Classification of apples presenting several external colours ('San Fuji' apples) was studied by Nakano [3] who used a method based on neural networks. The precision of the classification varied according to the categories : the grade judgement ratios for 'superior', 'poor colour' and 'injured' categories were very high, but the ratios for 'excellent' and 'good' categories were much lower.

This study addresses the colour classification of 'Jonagold' apples. In the European and Belgian standards, two criteria may be distinguished to classify these apples according to the colour. The first one is related to the percentage of blush area. The second one sorts the fruits into four classes on the basis of their ground colour (classes noted ++, +, ' ' *i.e.* normal and r), from the greenest to the ripenest. The present work focuses on this latter problem. In a first stage, the frequency distribution of the fruit colour was studied. After that, ground colour sorting was operated in three steps:

1. sorting the pixels of the images in one area "ground colour", "blush colour" or other;
2. computation of the mean ground colour;
3. discrimination in sub-classes "++" to "r" on the ground colour basis.

Two different methods were considered for the classification of the pixels and for classification of the fruits into classes "++" to "r" : neural networks and Fisher's linear discrimininant analysis.

2. Material and method

Measurements were performed with colour machine vision. Images were taken under diffuse illumination provided by two fluorescent tubes (36W each, Philips model 33, colour temperature 4100K), positioned in the lower part of an horizontal reflector cylinder (1.25 m long, diameter 0.5 m). The interior surface of the cylinder was painted flat white. A window at the top of the cylindrical chamber was made so

that a 3-CCD camera (XC-003P - Sony) can acquire an image of the upper part of the fruit. The camera was placed at about 400 mm from the top of the fruit and was fitted with a 16 mm lens. A dark conveyor belt was chosen to provide a high contrast between the fruit and the background. The camera acquired colour images with three sensors R, G, B (red, green, blue) whose spectral response curves peak in the red, green and blue regions of the spectrum. The images were converted by a frame grabber (Imascan Chroma - Imagraph) with the maximum colour resolution (3*8bits) and a spatial resolution about 1.9 pix/mm. The images were reframed to eliminate unnecessary background area. A 5*5 median filtration was applied in order to remove small spots (lenticels,...). The fruit boundaries were eroded to avoid the darker parts of the fruit image (10 pixels were removed all around the boundary). The remaining "patches" (stem, ...) were eliminated by an operator. Fig. 1 presents the original image and the pre-treated one. The basic pre-treatments were made using ImagePro software (Media Cybernetics), while other algorithms were developed in C++ (Visual C++ - Microsoft Corporation). The neural networks were developed with MatLab (The Math Works, Inc.). The statistical treatment were made using SAS (SAS Institute Inc.) and Minitab (Minitab, inc.).

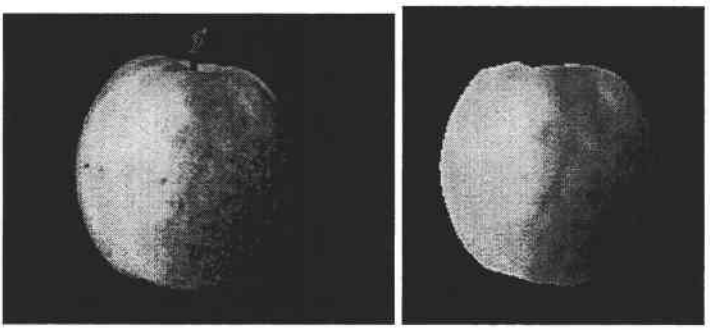

Figure 1: Original fruit image (left) and the same after the pre-treatment

A set of 400 fruits belonging to the class A3 was studied. This class was chosen as it ensured good representation of the ground colour (at least 25% of the surface is in blush colour; in practice we noted a ratio of 46% for the blush colour and 44% for the ground colour). These fruits were sorted by professional controllers of the "Belgische Fruit Veiling" (St. Truiden, Belgium) into four ground classes (A3++, A3+, A3 and A3r) and presented no external defects. Four images of the cheeks of each fruit were acquired (in a whole 1600 images were considered).

3. The frequency distribution of the fruits colour

The first step consisted to define on each image the ground colour area (g.c.) and the blush colour area (b.c.). The remaining area was called the intermediate colour area (i.c.). This operation was made by an operator using the software, an example of result is presented in Fig. 2. On this basis, the R G and B frequency distribution

was computed, for each area, on a basis of 50 fruits per class (800 images ≈ 11 10^6 pixels). The result is shown in Fig. 3 where the frequency distribution was projected on the planes defined by the axis R-G and R-B. On the upper diagrams (Fig. 3a), a dark area indicates an important frequency, which means that the colour was often observed. On the lower diagrams (Fig. 3b), the grey level indicates into which area a colour belongs : the blush colours are in black; the intermediate colours are in light grey; the ground colour are in medium grey.

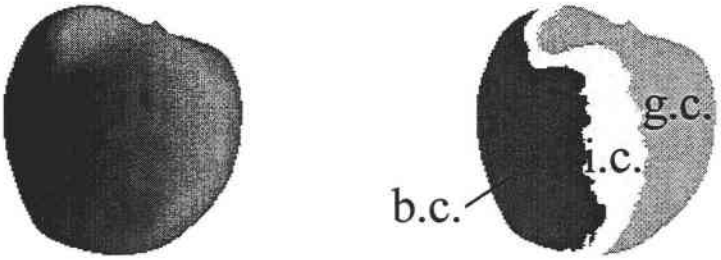

Figure 2: The three areas on a fruit : blush colour area (b.c.); intermediate colour (i.c.); ground colour (g.c.). Left : pre-treated image. Right : image after segmentation

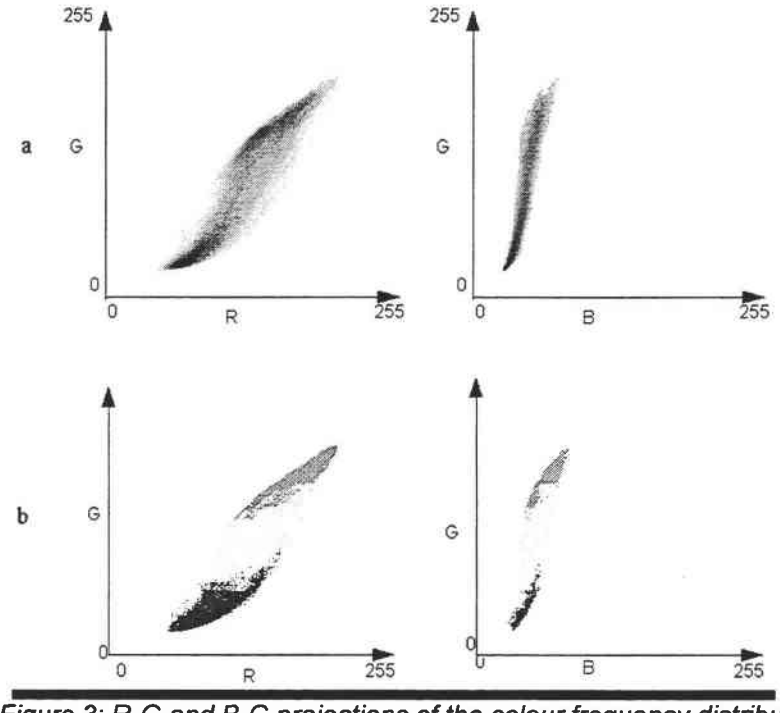

Figure 3: R-G and B-G projections of the colour frequency distribution

The frequency distribution showed a complex shape:

- It was bimodal, presenting two local maxima, one around the R, G, B co-ordinate (59, 28, 28) representing the blush colour and the other one around (137, 146, 52) corresponding to the ground colour;

- The central area i.c. was in a "pass" between the two maxima (Fig. 3a) : it has a lower frequency than the blush and ground colours. On an other way, the i.c. area filled a larger surface which represents a wider range of colours (Fig. 3b).

- The distribution was not symmetrical.

The areas b.c., i.c. and g.c. represented respectively 46%, 10%, 44% of the total numbers of the pixels belonging to the images. On the other hand, amongst the 16 millions available colours (a colour is coded on 8 bits in each R, G B channel), 264 182 represented the apples. The colours were grouped into classes (the class interval was 8 units for each parameter R, G and B) and the grouped frequency distribution was used to compute the decision functions : it included 1116 classes.

4. The classification methods

4.1 Pixels classification

The problem consists in finding the decision function able to sort the pixels into one of the three areas : b.c., g.c. or i.c. This was performed by Fisher's linear discriminant analysis (LDA) and neural networks classifiers (NN). The first method assumes that theoretical populations are gaussian, with the same covariance matrix, and equal prior probabilities. The frequency distribution shown above (Fig. 3) indicated that these hypothesis were not satisfied. Nevertheless, LDA was retained because linear decision functions seemed acceptable to sort the pixels as it came from Fig. 3b. A neural network with a single layer of neurones was also used. As the LDA, it provides a linear decision function, but without assumptions about the theoretical populations.

The neural network structure was quite simple, as shown in Fig. 4. It included a single layer with 3 inputs, one for each colour channel, and two outputs, one for each discriminant function. The transfer function was of sigmoïdal type. The R, G, B data used to compute the frequency distribution were introduced during the supervised learning, and the output of the neurones were compared with the target value. This latter is a binary value for each neurone : 0 for one class and 1 for the other. The different possible combinations for the two outputs are:

0 0 for b.c.;
0 1 for i.c.;
1 1 for g.c..

The backpropagation with momentum and adaptive learning rate was used during the learning phase. The amount of data restricted the use of more powerful learning methods. The learning parameters were:

- starting learning rate : 10^{-10};
- learning rate increase : 1.05;
- learning rate decrease : 0.7;
- momentum : 0.9.

The learning rate was chosen very small, but it is multiplied by the sum square error computed on around 11 million terms. The output of the i^{th} neurone was given by :

(1) $$z_i = f\left(\mathbf{w}_i * \mathbf{x} + b_i\right)$$

with: z_i the output value of the i^{th} neurone;

f the transfer function of type $1/\left(1+\exp(-x)\right)$;

$\mathbf{w}_i$ the weight vector joined to the i^{th} neurone;
b_i the bias joined to the i^{th} neurone;
$\mathbf{x}$ the column vector (R, G, B) of the studied pixel.

After the training, the linear combination $\mathbf{w}_i * \mathbf{x} + b_i$ of the R, G, B parameters (equation 1) gave the decision function.

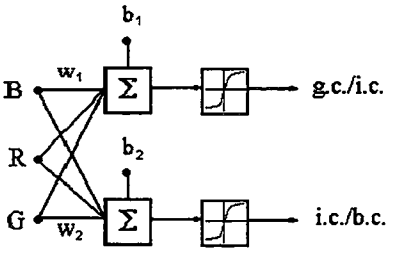

Figure 4: Neural network structure used for pixels classification

The linear discriminant analysis used the mean value of each channel (R, G, B) computed on each class (b.c., i.c., g.c.), and the pooled covariance matrix to compute a similar decision function.

4.2 Fruit classification on the ground colour basis

When the decision functions separating the three colour areas were known, the pixels characterizing the ground colour were automatically identified and treated to grade the fruits into four classes noted ++, +, ' ' (normal) and r. In a first time, the discrimination was based on the mean of the three variables R, G and B computed on the g.c.+i.c. area. This required the use of only one decision function for the pixel classification amongst the two computed above. The results obtained with the neural networks and those obtained with Fisher's linear discriminant analysis were compared. These tests were performed with two learning/validation ratio (50/50 and 80/20) in order to test the influence of the learning sample size. In a second time, the classification, using the statistical linear discrimination, was based on the means computed only on the g.c. area (this required the use of the two decision functions previously computed). The fruits into the learning or validation sets were randomly selected.

The neural network used in this case was similar to the one used for the pixel classification. The structure is presented in Fig. 5. The linear discriminant analysis used the mean value of each channel (R, G, B) computed on each class (++, +, ' ', r), and the pooled covariance matrix.

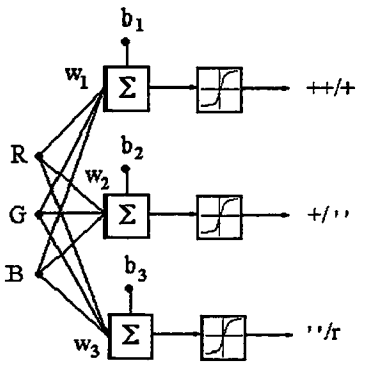

Figure 5: Neural network structure used for fruit classification

5. Results

5.1 Pixels classification

Table 1 gives the percentage of correctly classified pixels on the learning data by using NN and LDA. The results were quite similar, with a slight advantage for the neural network. This latter sorted better the pixels belonging to the b.c. and gc

areas but clearly worst for the i.c. area pixels. During the training, the parameter adjustment took into account the error on the whole data. As the i.c. area is lesser represented than the other one, an error on the pixels of this class had a lesser influence on the whole error, or a bigger error on the pixels of this class had a comparable influence on the whole error. The neural network took thus into account the prior probabilities. This was not the case for the linear discriminant analysis.

Area	Neural network	Linear discriminant analysis
b.c.	95	85
i.c.	76	97
gc	99	90
Total	95	88

Table 1 : Pixels classification rate (%) with the neural networks and the linear discriminant analysis

5.2 Fruit classification on the ground colour basis

When using a learning/validation ratio of 50/50 the global classification performances were almost the same for the learning data either with linear discriminant analysis or with neural networks (79% of the fruits correctly classified with NN, 71 with LDA). However, the linear discriminant analysis was more robust since it presented better values with the validation data (56% and 64% of the fruits correctly classified respectively with NN and LDA).

Table 2 presents the results for a learning/validation ratio of 80/20. In this case, the learning classification rate and the validation classification rate were quite similar whatever the method used. The global results were the same with 68 percent of the fruits correctly graded. However, the error was better shared with the neural networks.

Ground colour class.	Neural	network	Linear	discriminant
	Learning	Validation	analysis Learning	Validation
++	95	80	100	95
+	60	70	53	65
' '	53	50	46	45
r	74	70	80	65
Total	71	68	70	68

Table 2: Fruit classification rate (%) with the neural networks and the linear discriminant analysis; learning /validation ratio=80/20; the colour parameters are computed on the g.c. + i.c. area

Table 3 presents the classification rate obtained with the linear discriminant analysis, a learning/validation ratio of 80/20 and the mean R G B parameters computed only on the gc area. The results obtained on the validation data (65% fruits correctly sorted) were lesser accurate than those obtained previously (68%, Table 2). This shown that there was no interest to consider separately the ground colour and the intermediate colour.

Ground colour class.	Learning	Validation
++	97	95
+	67	45
' '	56	30
r	83	90
Total	76	65

Table 3 : Fruit classification rate (%) with the linear discriminant analysis; the learning /validation ratio=80/20; the colour parameters are computed only on the g.c. area

Conclusion

'Jonagold' apples present a complex colour frequency distribution. The neural networks and Fisher's linear discrimant analysis were compared to sort pixels into three areas on the fruits (blush colour, intermediate colour, ground colour). The neural networks gave more accurate results than discriminant analysis (7% enhancement). This was due to the complex situation which was far from the statistical discriminant analysis assumptions. Grading of the fruits into 4 categories (++, +, ' ',r) based on the ground colour was achieved with the same methods. Both of them gave the same precision (68% of the fruit were correctly classified). However, the neural networks require more data to reach the results of the linear discriminant analysis. It was also shown that there is no interest to separate the ground colour and the intermediate colour to compute the ground colour classification parameters.

References

[1] Heinemann P.H., Varghese Z.A., Morrow C.T., Sommer III H.J., Crassweller R.M., [1995], "Machine vision inspection of Golden Delicious apples". *Applied Engineering in Agriculture, ASAE 11 (6), 901-906.*

[2] Leemans V., Magein H., Destain M.-F., "The quality of 'Golden delicious' apples by colour computer vision. *Preprints from the "Mathematical and control applications in agriculture and horticulture", IFAC workshop.* 28 septembre - 2 octobre 1997, Hannovre, 175-179.

[3] Nakano Kazuhiro, [1997], "Application of neural networks to the color grading of apples", *Computers and Electronics in Agriculture, 18, 105-116.*

Automatic inspection of olives using comuter vision

Inspection automatisée des olives par vision artificielle

E. Moltó **J. Blasco** **V. Escuderos**

Instituto Valenciano de Investigaciones Agrarias
Cra. Moncada-Náquera, km 5
E-46113 Moncada (Valencia) Spain
e-mail: emolto@ivia.es

J. García **R. Díaz** **M. Blasco**

AINIA - Instituto Tecnológico Agroalimentario
Apdo. Correos 103
E-46980 PATERNA (Valencia) Spain

Abstract: *The European Project «New Image Processing for Characterisation of Olives and Other Fruit» is aimed at solving two major problems in the agrofood sector: produce sorting and adequate quality control. At present, it is possible to find both manual and semi-automatic commercial systems, but these systems are expensive and slow. Moreover, their accuracy is incompatible with existing market demands. With the objective of improving the existing technology, several disciplines developed in other industrial sectors such as robotics, artificial vision and automated systems are being used in this project. The main result of this work will be to develop a system that will be applicable directly or indirectly to a wide range of agricultural products, but it focuses on two specific products in line with the interest of the SMEs participating in the project: olives and potatoes.*

Encouraging results have been obtained during the preliminary work, which has been devoted to develop a sorting system for olives after fermentation. One of the major problems solved is related to the fact that the produce is wet. Different segmentation procedures to discriminate the olives after fermentation from the background and to detect skin blemishes have been tested. Further work will consist in improving these algorithms to achieve real-time requirements and treating moving images.

Keywords: *Olives, produce sorting, machine vision, real-time.*

Résumé : Le projet européen "New Image processing for characterisation of olives and other fruit" a pour objectif de répondre à 2 problèmes majeurs du secteur agro-industriel : le tri des produits et le contrôle de qualité adequat. Actuellement, il est possible de trouver des systèmes commerciaux semi-automatisés ou manuels pour le tri. Les systèmes commerciaux sont chers et peu rapides. De plus, leur fiabilité est incompatible avec la demande du marché. Dans l'objectif d'améliorer ces technologies existantes, plusieurs disciplines développées dans d'autres secteurs industriels tel que la robotique, la vision artificielle et les systèmes automatisés sont utilisées dans ce projet. Le résultat principal de ce travail est de développer un système applicable directement ou indirectement à une

large gamme de produits agricoles. Cependant, dans un premier temps, on se focalise sur 2 produits dont l'intérêt est grand pour les PMEs qui participent au projet : olives et pommes de terre. Des résultats encourageants ont été obtenus durant les travaux préliminaires qui ont eu pour objectif de développer un système de tri pour les olives après fermentation. Un des problèmes majeurs résolus est lié au fait que les produits sont humides. Différentes procédures de segmentation pour séparer du fond de l'image les olives après fermentation du fond et pour détecter les défauts sur la peau ont été testées. Les travaux futurs consistent à améliorer ces algorithmes pour réaliser un travail en temps réel et traiter des images en mouvement.

1. Introduction

Currently, several manufacturers have developed manual and semi-automatic commercial systems for quality control and sorting that can be adapted to processed olives. However, the relative low added value of the produce and the speed required for the process, make these systems to be expensive and slow for the Spanish agro-food enterprises. Moreover, their accuracy is incompatible with existing market demands.

The major problem that arises when classifying these products is related with the important variability of defects to be analysed, which introduces a great level of complexity in the vision system. Consequently, image analysis has to be fast enough to amortise the equipment, by maintaining a very high productivity. A survey showed that final users only can afford these systems if the cost is lower than 70 kECU. For this reason, several commercial multipurpose systems have not succeeded.

Olives for consumption at table are classified after harvesting, in order to select specific ripen stages that are suitable for being fermented without loosing their particular properties. The major added value is obtained by processing green fruits. These are picked before they ripen, when they reach a green-yellow colour, and always before they start changing to brown. Then, they are treated in lye and immersed in brine, where lactic fermentation takes place. After fermentation, they are sorted by size and category, for further processing (stuffing) or immediate packing. With the existing machinery and methodology, these processes are expensive, slow and do not allow individual inspection of fruit. Moreover, manual sorting damages the olives and causes pitting. An important added value that can be obtained through automatic classification consists in improving the homogeneity of the colour of fruits that are contained in each can.

2. Materials and methods

2.1 Category characterisation

Olive variety employed along the present work is called Manzanilla (*Olea europea pomiformis)*, which has an average weight of 200 to 280 fruits per kg. After being harvested, ripe fruits are separated from the green ones because ripe fruits produce a low quality, soft product after fermentation, that can not be marketed. Once olives are fermented, they are classified into four categories, depending on their size, colour and the number and extension of their skin defects.

First category presents a skin surface without stains and an homogeneous colour. Second category shows a few skin defects, such as small stains and dark green

spots. Third category has the same kind of defects, but are widespread. Fourth category shows very heterogeneous colours and a large number of stains.

A preliminary study has been conducted in order to objectively characterise the differences in colour between olive categories. For this purpose, 100 olives from each category were individually weighted, with an error of less than ± 0.5 g, and size (diameter and height)of each olive was measured using a slide calliper, with an error of less than ± 0.02 mm.

Colour of each olive was determined with a colorimeter, using a circular plastic box with black background (8 cm diameter), optical glasses and a rubber fastener. Olives were cut longitudinally to the stone and placed in the box. Several colour co-ordinates were calculated (L* a* b*, Lch, HSI, etc.), under different illuminants (D50, D60, D75, A, C, TL84, FCW) and two standard CIE observers (10° and 8°). The surface measured was 5026 mm2. Analysis of the variance (ANOVA) was employed to study colour differences.

In parallel, different images of olives were digitised using different colour co-ordinates (RGB, (R-Y)Y(B-Y) and Yuv). Then, a study of colour differences between the sound skin of the four classes was carried out. In this case, a human operator selected different windows containing pixels of sound skin of olives from the 4 categories, then ANOVA was applied to these data. A similar study was conducted on the blemishes and the background, in order to determine which colour co-ordinates increased the contrast between the skin of the olives and the blemishes, and between the olive surface and the background.

2.2 The sorting machine

A prototype of a machine for fast speed classification of olives has been built. Olives move through the system in small orifices on a specially designed roller band. The basic architecture of the prototype is shown in figure 1. It consists of:

- A mechanical system that individualises the fruit,
- a roller conveyor that transport the olives,
- one machine vision system that analyses the quality of fruit, installed on a PC,
- an ejection system capable of separating fruit in classes,
- a PC that controls the whole line, by regulating the speed of the roller conveyor commanding the ejectors and providing an interface to the user,
- a computer network that connects both PCs through TCP/IP.

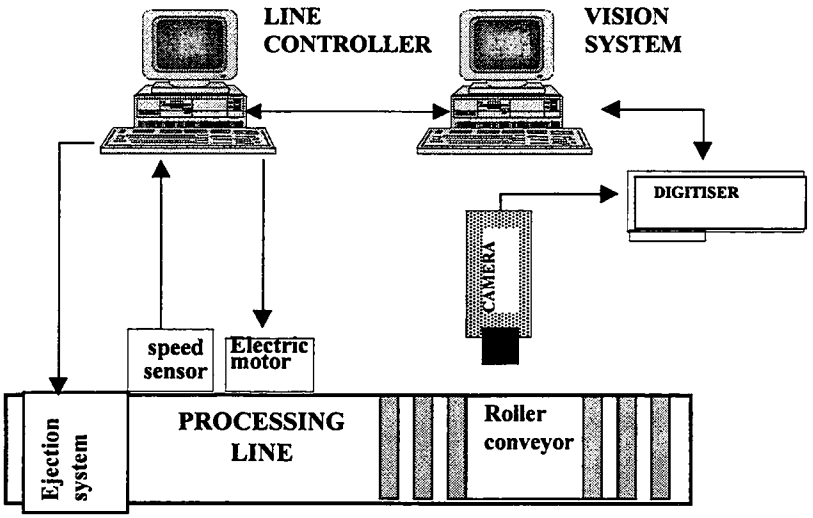

Figure 1: Scheme of the prototype

2.3 The vision system

One of the major constraints of the vision system is its targeted final price, which has to be lower than 6.000 ECU in order to allow a competitive price for the machine . Currently, it is based on a PC containing one conventional frame grabber board connected to a 3 CCD colour camera. The software basically consists in three modules: *Off-line training*, *Simulation* and *Inspection.*

The *Off-line training* module is used to generate the segmentation model that will be used by the vision system to inspect the surface of the olives. It consist in two steps: during the first one, a human operator manually selects, using small windows, the different regions of interest of an image: the background, the sound skin and the blemishes. During this phase, the operator tries to show to the system the colour variability of each of these regions or classes in several pre-stored images. The second step consists in generating a model, based on Bayesian Discriminant Analysis, in order to assign the RGB colour components of each pixel to one of the three pre-defined classes during image segmentation.

The *Simulation module* has been developed to observe the results of segmentation after training with the previous module. It consist in applying all the algorithms for artificial vision inspection in pre-stored images, measuring the processing time, storing the data obtained or passing them to the controller using TCP/IP as in the on-line operation of the machine. If results are not satisfactory, a new model must be generated.

Finally, the *Inspection module* is used for on-line operation. The machine vision system is able to discriminate background, olives and blemishes in the image. After applying morphological filters, it can separate olives that are touching and provides data of each fruit to the line controller.

The vision system normally works with three views of each olive, in order to explore an important percentage (close to 85 %) of its surface. Table 1 summarises other specifications of the vision system.

Views per olive	Image field	Resolution	Processing speed
3	108 olives (384x288 mm)	0.5 mm/pixel	160 ms per image

Table 1: Vision system specifications

3. Results

3.1 Category characterisation

Tests carried out for finding significant differences between the average values of classes by means of ANOVA were similar for all the illuminants and observers. Table 2 shows the average and standard error of each parameter and class. Significant differences (α=0.05) for L* b* c and h were found between all categories. However, co-ordinate a* gave different results depending on the illuminant.

Category	L*	a*	b*	h	c*
1st	50.31±1.81	5.24±0.73	29.68±2.28	1.40±0.03	30.15±2.27
2nd	47.82±2.13	5.22±0.63	26.02±2.85	1.37±0.03	26.55±2.80
3rd	44.26±2.66	5.48±0.60	21.05±3.38	1.31±0.06	21.78±3.22
4th	43.22±2.72	5.82±0.81	17.45±3.49	1.24±0.09	18.45±3.26

Table 2: Values of co-ordinates L, a, b, h and c for different categories of olives

In the second study, the following co-ordinates demonstrated to have the best discrimination capabilities:

- for differentiating categories based on the colour of the sound skin: R,
- for detecting the stains: B-Y,
- for separating the olive from the background: Y.

Thus, the features that have to be determined for each olive are based on:

- the average of the R component of the total surface,
- average of the R component after a grey-level self-adjustment,
- the total area of the object in the Y space,
- the total area of defects obtained through thresholding in the B-Y space.

3.2 The machine vision system

Encouraging results have been obtained during the preliminary work, which has been devoted to develop a sorting system for olives after fermentation. One of the major problems solved is related to the fact that the produce is wet. Different segmentation procedures to discriminate the olives after fermentation from the background and to detect different skin blemishes have been tested. Further work will consist in improving these algorithms to achieve real-time requirements and treating moving images.

The current system is able to separate the background, the olive sound skins and the stains. The major problems encountered are related with the lack of illumination of the boundaries of the olives that are confused with some stains, due to the similarity between their RGB co-ordinates.

Current average processing time is 593 ms per image. Table 3 shows time consumed by the different image analysis procedures on the current system. These times were measured in images having 768x576 pixels, corresponding to 108 olives.

OPERATION	*PROCESS*	*TIME*
ACQUISITION	IMAGE ACQUISITION	60 ms
IMAGE ANALYSIS	SEGMENTATION	200 ms
	OLIVE SEPARATION	33 ms
	FEATURE CALCULATION	300 ms
TOTAL PER IMAGE		**593 ms**

Table 3. Average processing time of the vision system
Hardware: Pentium 200 MHz, Matrox Meteor. Image with 108 olives

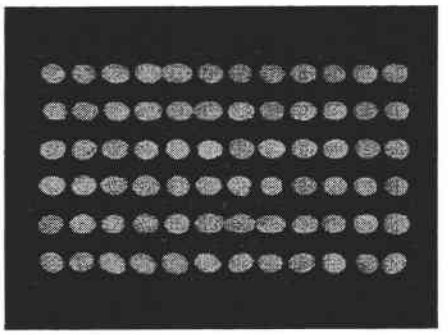

Original image

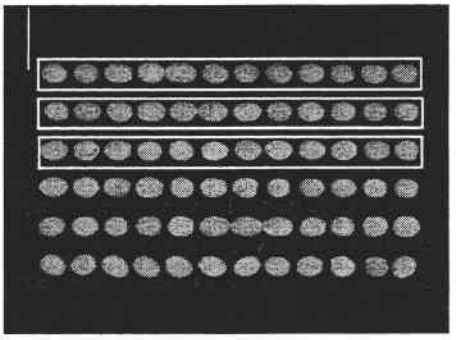

Detection of rows

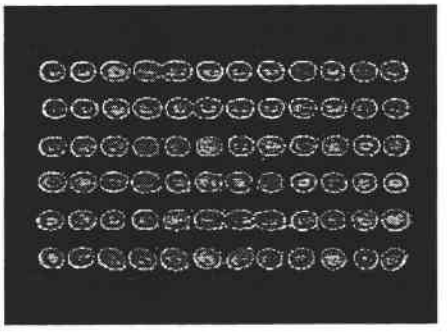

segmented image

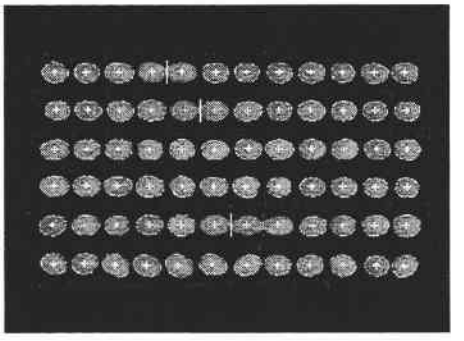

Olive singulation

Conclusion

Preliminary developments of a low cost machine vision system for green olive sorting after fermentation has been presented. It is based on a colorimetric study using different colour co-ordinates and illuminants. Currently, the machine vision system can be easily trained by an operator, who trains the algorithms by presenting examples of background, sound skin and blemishes to a Bayesian classifier. Processing time consumed by the vision system is over the requirements (593 ms instead of 160), although it will be easily decreased by dividing the image in 108 small windows, corresponding to individual olives. More effort will be put in improving the decision algorithms in order to distinguish between different kind of blemishes.

Acknowledgements

This work is partially funded by the European Commission (FAIR programme), through the Project «New Image Processing for Characterisation of Olives and Other Fruit» (NIPCO).

References

Bains, N. and David, F. (1990). *Machine vision inspection of fluorescent lamps.* Proceedings SPIE-The International Society for Optical Engineering,8-9 November. Boston.

Davenel, A., Guizard, CH., Labarre, T. and Sevila, F. J. (1988). *Automatic detection of surface defects on fruit by using a vision system.* Agric.Engng Res. 41:1-9.

Delwiche, M.J., Tang, S. and Thompson, J.F. (1993). *A high speed sorting for dried prunes.* Transactions of the ASAE, 36(1):195-200.

Department of Agriculture, Food Safety & Quality Service (1977). *United States Standards for Grades of Green Olives.* United States of America, UNITED-STATES-STANDARD: 727-735.

Heinemann P.H., Varghese Z.A., Morrow C.T., Sommer III H.J., Crassweller R.M. (1995) *Machine vision inspection of «Golden Delicious» apples*, Appl. Eng. Agricul 11: 901-906.
Heinemann, P.H., Hughes, R., Morrow, C.T., Sommer, H.J., Beelman, R.B. and Wuest, P.J. (1994). *Grading of mushrooms using a machine vision system.* Transactions of the ASAE, 37(5): 1671-1677.

Karaoulanis, G.D. and Bamnidou, A. (1995). *Colour changes in different processing conditions of green olives.* Grasas y aceites, 46(3): 153-159.

Paulsen, M.R. and McCleure, W.F. (1986), Illumination for computer vision systems. *Transactions of the ASAE, Vol. 29(5).* September-October: 1398-1404.

Sanchez, A.H., Rejano, L., Duran, M.C., de Castro, A., Montaño, A., Garcia. (1990). *Elaboracion de aceitunas verdes con tratamiento alcalino a temperatura controlada.* Grasas y aceites, 41(3): 218-223.

Advanced information technologies for objective quality sensing of edible beans

Technologies de l'information pour la mesure objective de la qualité des haricots

Suranjan Panigrahi

Assistant Professor,
Department of Agricultural & Biosystems Engineering

Curt Doetkott

Statistical Consultant,
Information Technology Service

Ronald Marsh

Graduate Assistant,
Department of Agricultural & Biosystems Engineering North Dakota State University

Fargo, ND USA 58105
e-mail: panigrah@plains.nodak.edu

Abstract: *Objective sensing of quality attributes (color, surface cracks, broken beans, foreign materials) of edible beans is very critical for both fresh and canned food markets. This paper provides an overview of a bean quality sensing system that integrates different advanced information technology including computer imaging technology and internet technology. The development of computer imaging system and associated color classification algorithms for color classification of red beans are presented. Different color classification models were evaluated. They used histogram-based color difference measures in r, g, and b color coordinates and two derived features in Hue, Saturation and Intensity color coordinates. The development of color classification algorithms and the associated statistical analyses for evaluating their performances are described. The classification accuracies of the developed algorithms for classifying any red bean sample into one of the three possible color groups (light, medium and dark) are presented. The highest accuracy obtained for color classification of red beans was 100%.*

Keywords: *Color computer vision, food products, beans, pattern recognition, color.*

Résumé : L'appréciation objective des attributs de qualité des haricots (couleur, craquelures de surface, haricots cassés, corps étrangers) est cruciale pour les marchés du frais ou des conserves. Cet article offre une revue des systèmes d'appréciation de la qualité des haricots intégrant différentes technologies avancées telles que la vision artificielle et Internet. Nous présentons des systèmes de vision artificielle et des algorithmes de classification couleur associés. Plusieurs modèles de classification couleur sont évalués. Ils intègrent des différences de couleur d'histogrammes en R, V, B et deux caractéristiques dérivées dans le référentiel Teinte, Intensité, Saturation. Le développement d'algorithmes de classification en fonction de la couleur et les analyses statistiques pour les évaluer sont présentés. La précision de la classification obtenue par ces algorithmes pour classer un échantillon de haricots rouges dans un des 3 groupes possibles (clair, moyen, foncé) est présenté. La meilleure précision obtenue est 100 %.

1. Introduction

Edible beans are important leguminous crops that have many different food applications. With the increased awareness of health and nutrition, their use in different food products has increased over the years. A few of their important food applications are for fresh and canned food. Though it often sounds trivial, different quality parameters of the beans are used to select their appropriateness to be used as fresh or canned food products. Quality attributes such as color, surface cracks, diseased beans, and foreign materials(i.e; such as stones, soil clods, and broken beans) play a very critical role in their marketability in the domestic as well as in international markets.

At present, the bean processors evaluate bean qualities by taking a small sample and making a decision on the bean quality. There are many problems associated with this present evaluation process. Human beings are often subjective and therefore, the quality evaluation process lacks in consistency and is prone to error. Again, the lack of a consistent quality evaluation process poses difficult challenges in domestic as well as international marketing of the beans. Sometimes, this issue causes unexpected economic losses for the sellers. On the contrary, the lack of a consistent and accurate quality sensing system might cause the buyers to pay higher prices for low quality beans.

Therefore, there is a need for developing quality sensing system for objective evaluation of edible beans. To fulfill this need, a research project was developed at North Dakota State University, Fargo, ND for developing and integrating different advanced sensing and computer-based information systems technologies for quality evaluation of beans.

2. Objectives

The objectives of this paper are to: 1) present an overview of the proposed quality sensing system, and 2) develop and evaluate a computer imaging system for color evaluation of edible beans.

Objective 2 focuses on the color evaluation and classification of only red kidney beans, a type of widely used edible bean. Generally, good quality red beans have a dark red color and the low quality red beans have light red color. Many times, the dark and light colored red beans are mixed in different proportions to create another undesirable color group «mixed».Thus, in the second objective, our goal was to develop and evaluate different image processing techniques for color evaluation and classification of three different color groups (dark, light and medium) of red beans.

3. Overview of the bean quality sensing system

A schematic representing an overview of the bean quality sensing system is presented in figure 1. The bean quality sensing system consists of three modules: 1) color evaluation module, 2) defect detection module, and 3) information delivery module. The color evaluation module consists of a color computer imaging system to evaluate different quality attributes (e.g.; color group of bean sample, uniformity of color in a given bean sample) related to the color of beans. This module requires 500 grams of bean per sample.

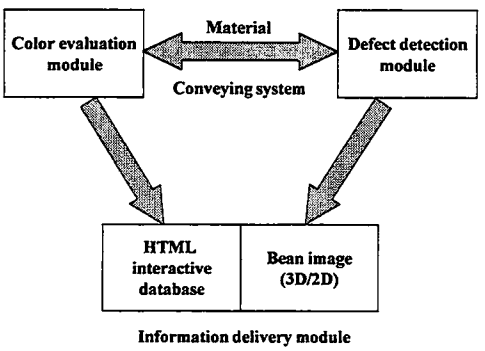

Figure 1: Overview of bean sensing system

The color evaluation module is interfaced with the defect detection module through a specially designed material conveying system. The beans are separated into three, single row streams by the conveying system and are conveyed at a rate of 26-28 beans per second per row. A high speed progressive scan camera captures the images of the beans (in three rows) in a single image (512 x 480 pixels) by another PC-based computer imaging system. The images of the beans are captured when the beans are still in the air after they leave the conveying system and before they touch the ground. The associated computer imaging system analyzes the images of the acquired beans for different defects such as presence of foreign materials, broken beans, surface cracks, etc.

The quality information of bean sample, as evaluated by the two modules, along with its color image are then passed into the «information delivery module». This module is an internet-based information management subsystem based on HTML and VRML. This module stores the quality information along with the bean image in a worldwide web site. This module also has the capability to develop and display

photo-realistic 3-D images to be displayed on the internet. The module creates a database using different quality attributes of the beans and the corresponding image. The user can interactively search through the database and visualize different bean samples and corresponding bean qualities. This module is designed so that the bean sellers and buyers can interactively communicate and evaluate bean products for exporting/importing process. The sellers can objectively evaluate bean samples using color evaluation and defect detection modules and post the quality related information in the information delivery module. The buyers, from any part of the world, can use this information to make a buying decision.

4. Development and evaluation of imaging system for color evaluation of beans

4.1 Color computer vision and its application

Color computer vision or imaging technology has the potential to fulfill the requirements of accurate and objective color evaluation of agricultural and food products. Several researchers have investigated the applications of color imaging technology for color evaluation and classification of different agricultural and food products. Panigrahi et al.[2] developed a color imaging system for evaluation and subsequent classification of french fries using image processing and neural network techniques. Panigrahi [1] has also investigated the applicability of color imaging technology for automatic evaluation and classification of corn. Shearer and Payne [3] reported the sorting of bell peppers based on color using a computer imaging system. Unklesbay et al. [5] developed image analysis techniques for internal color evaluation of beef rib-eye steaks. The development of a generalized computer vision system and the use of L*, a*, b* color coordinates for color evaluation of food products has been investigated by Ling and Ruzhitsky [6]. However, no work has been done to investigate the applicability of color imaging technology for color evaluation of beans. Though many computer imaging related investigations have been made for color evaluation and classification of different agricultural and food products, the inherent color variability, and the use of different color-based features to define product specific acceptance or rejection parameters often creates the situation, where the color imaging system developed for corn might not work with the same accuracy and efficiency for evaluating beans. Thus, it often becomes necessary to develop computer imaging system independently for specific agricultural/food products.

4.2 Development of the color imaging system

A PC-based color imaging system was developed in the Biosensing and Imaging laboratory of North Dakota State University, Fargo, ND. The imaging system consisted of a PC (Pentium-166 MHZ) with an image processing board (Image 640 series board with image CLD from Matrox) capable of digitizing color images with a

resolution of 8 bits per pixel. The imaging system used a CCD high resolution color camera (Panasonic) with a tele-zoom lens. The zoom lens has the magnification capability of 14x. A specially built lighting chamber was used for providing uniform and diffuse illumination to the beans samples because of the importance of diffuse illumination in color accuracy [4]. The inside of the cylindrical lighting chamber (66 cm diameter with 50.8 cm length) was painted flat white and there was a square hole (15 cm x 15 cm) on the top-middle region of the chamber for the camera to look at the bean samples. Two tungsten halogen lamps (with 12V and 12 watts) were provided inside the chamber to act as the two light sources for providing illumination. Provisions were made for adjusting the configuration of the light sources to adjust the direction of lighting. A special object tray (10 cm x 12 cm x 3 cm) was built to hold the bean samples and was coated with flat black paint. The object tray was kept on the object platform located in the middle of the chamber at a distance of 10 cm from the bottom surface of the chamber. The camera was located at a distance of 13 inches from the top surface of the bean sample. The imaging system was calibrated for color using the procedure mentioned in Panigrahi [1]. A total of 150 color images of bean samples (50 from each color group i.e. dark, mixed and light) were acquired.

4.3 Color evaluation and classification techniques

The acquired color images were captured in R, G, B color coordinates. Preliminary investigation were conducted in determining suitable features based on R, G, and B color coordinates and were found less promising. Thus, RGB color images of bean samples were converted to HSI (Hue, Saturation and Intensity) color coordinates. Subsequently, they were also converted to r,g,b (normalized RGB) color coordinates. To discriminate any bean sample into one of the possible three color groups, two different approaches were used. Figure 2 shows the flow chart of the color classification technique.

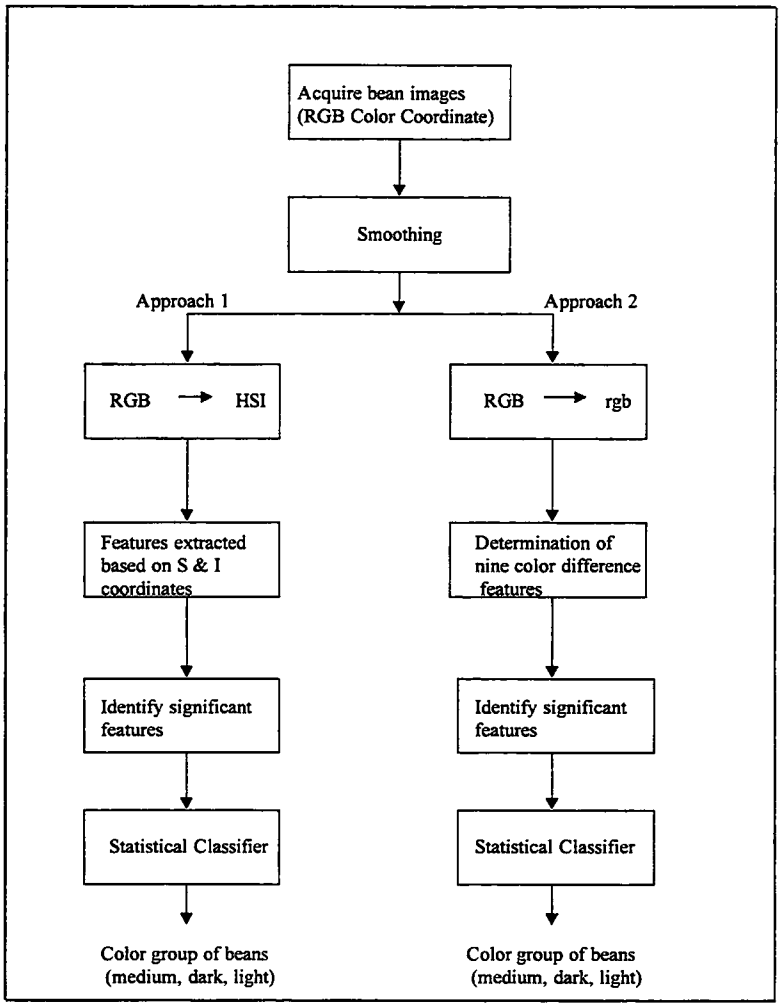

Figure 2: Flowchart for color classification of red beans

4.3.1 Approach 1

Color features based on saturation and intensity (HSI color coordinate) histograms were calculated using the following equations:

$$C1 = \text{Sqrt}\,(S_m * I_m) \quad (1)$$

$$C2 = (S_m * I_m)/(S_m + I_m) \quad (2)$$

where S_m and I_m represent the mean values of the Saturation and Intensity histograms respectively.

These two features were determined for all 150 color images of beans. A stepwise discriminat analysis was used to identify features significant at the 95% confidence interval [7]. A linear discriminant classifier was then developed for classifying unknown bean samples into one of the three possible color groups.

4.3.2 Approach 2

In this approach, rgb images were used. Three standard images (one from each of three color groups) were identified and their information were stored in rgb color coordinates. The color differences of the any bean sample from these three standard (reference) images were determined based on their histogram differences in rgb color coordinate. These color differences were determined using the following equations:

r sub k = (1/256) { sub { i=0 } sup 255 { SQRT (r sub u(i) - r sub sk (i)) } sup 2} (3)

g sub k = (1/256) { sub { i=0 } sup 255 { SQRT (g sub u(i) - g sub sk (i)) } sup 2} (4)

b sub k = (1/256) { sub { i=0 } sup 255 { SQRT (b sub u(i) - b sub sk (i)) } sup 2} (5)

Where, k= dark, mixed and light colors respectively,

r_u, g_u, and b_u = normalized red, green and blue histogram of any bean image

r_{sk}, g_{sk}, and b_{sk} = normalized red, green and blue histogram of standard bean image for any, k.

Consequently, for each bean image, nine color difference features (*rd, rm, rl, gd, gm, gl, bd,bm, and bg*) were determined and stored. A stepwise discriminant analysis was again used to identify features significant at the 95% confidence level. These features were then used to build a linear discriminant classifier for classifying unknown bean samples into one of three possible color groups. Internal (resubstitution) and external (leave-one-out cross validation) error rate estimation were used to asses the accuracy of this classifier [8].

4.4 Bootstrap analysis of features for color classification

Bootstraping is another technique that may be used in external error rate estimation. In this study, the developed color classification models were further evaluated by bootstrap analysis.

Let the available sample, F^, be representative of some multidimensional distribution, F. A single bootstrap sample is selected from F^, by randomly drawing, n, observations with replacement. The simplest approach to bootstraping the estimate of prediction error in discriminant analysis is as follows [11].

1 generate B bootstrap samples, 50-100 seem to be sufficient for this type of problem [9];
2 estimate the model for each bootstrap sample (i.e., use the bootstrap sample as the training set for building the model);
3 apply the fitted model to the original sample, F^ (i.e., use the original sample as the validation set). This yields B estimates of the prediction error;
4 average the B error rate estimates to get the overall prediction error estimate.

Efron [10] carried out simulations to compare the performance of cross-validation and bootstraping in error rate predictions. He determined that cross-validation estimates of the error rate tend to be unbiased but highly variable. The simple bootstrap method described above tends to have lower variability but is biased. Efron and Tibshirani [11] describe a simple bias correction method that can be used to improve the quality of the bootstrap error rate estimates.

Let err(x,F^) denote the error rate when we use the original sample as both the training and validation sets. Let err(x*,F^*) denote the error rate obtained when we use a bootstrap sample as both the training and validation sets. In addition, let err(x*,F^) be the error rate associated with using the bootstrap sample as the training set and the original sample as the validation set. We can define the bias or optimism of the simple bootstrap as the difference between err(x*, F^) and err(x*, F^*) averaged over the B bootstrap samples. The refined bootstrap estimator is then simply the optimism added to err(x, F^).

5. Results and discussion

5.1 Evaluation of linear discriminant color classifier

The color features C1 and C2 were both determined to be significant features at the 95% confidence level. Based on these two feature models, the accuracy of classifying a bean image into the correct color group was found to be 100% using leave-one-out cross-validation. Separate tests were also conducted to identify the color classification capability of each individual feature. Again using leave-one-out cross validation, the feature C1 provided a color classification accuracy of 100% for all three color groups. Using color feature C2, all the medium and light colored bean images were correctly classified in their respective classes showing an 100% classification accuracy. However, one of the dark colored bean images was misclassified into the mixed color group, thereby showing 98% accuracy for classifying dark bean images.

Stepwise discriminant analysis showed that eight of nine histogram-based color-difference features *(rl, rm , gl, gm, bl, bd, bg*) were significant at 95% confidence level. This eight feature linear discriminant classifier yielded an accuracy of 100% using leave-one-out cross validation when applied to the 150 bean images.

5.2 Bootstrap analysis of different classification models

Tables 1 through 3 show the different errors (as estimated by bootstrap analysis) associated with several color classification models. The refined estimators (error) for nine different color classification models, each based on a single histogram-based color difference measure (i.e; *rl,gl, bl* etc.) are shown in table 1. The model based on *bm* shows the lowest errors rate of 8% compared to the highest estimated error rate (56.7%) provided by the model based on *rl.* On the other hand, the highest estimated error provided by three histogram-based color difference measures is 7 % (Table 2). The lowest estimated error was less than 1% (0.7%) and was provided by 3 histogram-based color difference measures from the standard mixed color bean sample (rm, gm, bm). From both these tables it was found that histogram-based color difference measures (rm, gm, bm) provides low error rates compared to other features.

Color Classification Model	err (X,F^)	err (X*,F^*)	err (X*,F^)	Bias / Optimism	Refined Estimator
bl	0.280	0.263	0.291	0.028	0.308
bm	0.053	0.038	0.066	0.028	0.081
bd	0.193	0.130	0.156	0.026	0.219
gl	0.153	0.123	0.154	0.031	0.184
gm	0.240	0.226	0.263	0.037	0.277
gd	0.373	0.383	0.447	0.064	0.437
rl	0.293	0.086	0.360	0.274	0.567
rm	0.080	0.053	0.085	0.032	0.112
rd	0.093	0.086	0.124	0.038	0.131

Table 1: Bootstrap error analysis of different color classification models based on r, g, b histogram differences

Color Classification Model	err (X,F^)	err (X*,F^*)	err(X*,F^)	Bias / Optimism	Refined Estimator
bl gl rl	0.040	0.040	0.048	0.008	0.048
bd gd rd	0.046	0.047	0.072	0.025	0.071
bm gm rm	0.006	0.008	0.009	0.001	0.007

Table 2: Bootstrap error analysis of 3 features-based color classification models

The bootstrap error analysis based on C1 and C2 showed very promising results (table 3). The highest error estimated was only 1.3%. The color classification models based on feature C1 and C2 showed less than 1% error (0.2%). Though the color classification model based on rm, gm and bm also showed similar error (0.7%), the hardware implementation of the color classification model based on C1 or C2 will be more efficient because of the less computational complexities involved in calculating C1 or C2 compared to rm, bm and gm.

Color Classification Model	err (X,F^)	err (X*, F^*)	err (X*, F^)	Bias / Optimism	Refined Estimator
C1	0.0	0.0	0.0002	0.0002	0.0002
C2	0.0067	0.0014	0.008	0.006	0.013

Table 3: Bootstrap error analysis of two color classification models based on S & I

Conclusion

A study was conducted in developing a color computer imaging system for color evaluation and classification of red beans. Two color features C1 and C2 based on saturation and intensity histogram showed 100% color classification accuracy for all three color groups of beans. The second approach used the histogram-based color differences (from three standard images in three color groups) in rgb color coordinates and resulted in a total of nine color features (*rl ,rg ,rd ,gl, gm, gd, bl, bd, bg*). Eight of them (except feature, *gd*) were found to be significant based on the statistical analyses and the developed classifier using these eight features could also provide a 100% color classification accuracy for all three bean color groups.

Based on bootstrap analysis for external error rate estimation, it was also confirmed that color classification model based on C1 and C2 could provide high accuracies with the estimated error of less than 1%. The color classification model based on three histogram-based color difference measures (rm,gm,bm) also showed low estimated error (bootstrap analysis) of less than 1%. From hardware implementation view points, the color classification model based on C1 or C2 would be preferred because of the associated low level of computational complexities. Future work will involve integrating this algorithm for real-time color classification of bean images.

References

[1] Panigrahi, S. Color. *Computer vision for characterization of corn germplasm.* Unpublished Ph. D. Thesis. Iowa State University, Ames, IA.1992.

[2] Panigrahi, S. And D. Wiesenborn. Computer-based neuro-vision system for color classification of french fries. SPIE Vol. 2345. pp.204-209. 1994.

[3] Shearer, S.A. and F.A. Payne. *Color and defect sorting of bell peppers using machine vision.* In Transactions of the ASAE, 33(6):2045-2050. 1993.

[4] Jain, A. *Fundamental of digital image processing.* Prentice Hall. London. 1989.

[5] Unklesbay, K., N. Unklesbay and J. Keller. Determination of internal color beef rib-eye steaks using digital image analysis. *In Food Microstructure. Vol. 5: 247-258. 1994.*

[6] Ling, P, and V. N. Ruzhitsky. *Color sensing of food materials using machine vision.* Proceedings of the Food Processing Automation III. Orlando, Fl. ASAE. St Joseph. MI. 1994.

[7] SAS Institute, Inc. SAS/STAT. SAS Institute, Raleigh, NC. 1990.

[8] Huberty, C. *Applied discriminant analysis.* John Wiley & Sons. New York, NY. 1994.

[9] Efron, B and R. Tibshirani. *Improvements on cross validation: The .632+ bootstrap method.* In J. of the American Statistical Asscn. 92:548-560. 1997.

[10] Efron, B. *Estimating the error rate of a prediction rule: some improvements on cross validation.* In *J.* of the American Statistical Asscn. 78:316-331. 1983.

[11] Efron, B and R. Tibshrani. *An introduction to the bootstrap.* Chapman & Hall Inc. New York. N.Y. 1993.

Part 4

Textural measurements

Mealiness in apples. Comparison between human and instrumental procedures and results

Farinosité des pommes : comparaison entre les mesures humaines et instrumentales

P. Barreiro **C. Ortiz** **M. Ruiz-Altisent**

Rural Engineering Dept. E.T.S.I.A Madrid. Spain
e-mail: labpropfis@iru.etsia.upm.es

I. Recasens **M.A. Asensio**

Postharvest Dept. CeRTA. Centro UdL-IRTA. Lerida, Spain

Abstract: *Mealiness has been described as a sensory texture attribute. Two years of collaborative work between instrumental and sensory research groups allowed to propose a destructive instrumental procedure for mealiness assessment: Confined Compression. Instrumental mealiness has been defined as a multidimensional parameter gathering the loss of crispness, hardness and juiciness. Within this work an integration criterion for crispness, hardness and juiciness, measured by means of Confined compression, is proposed following human priorities in mealiness perception . The mealiness scale proposed (based on Golden and Top-Red samples) shows a high correlation when compared to the sensory descriptor («harinosidad» ; r=0.87 and 0.82 for Golden and Top-Red respectively in a sample by sample comparison). It allows to extract features on the storage effect and therefore build some recommendations for professional purposes: only small size Golden apples should be stored 6 months. For Top-Red apples only the earliest date of harvest can be submitted to a 6 months storage period without controlled atmosphere.*

Résumé : La farinosité a été décrite comme un attribut de texture. Après 2 ans de travail en collaboration entre des groupes d'évaluation sensorielle et des groupes travaillant en génie instrumental, un appareil destructif pour apprécier la farinosité des pommes est proposé : c'est la compression confinée. La farinosité a été définie comme un paramètre multi-dimensionnel regroupant la perte de croquant, de fermeté et de jutosité. Dans ce travail, un critère intégrant le croquant, la fermeté et la jutosité mesuré au moyen de compression confinée est proposé pour répondre aux perceptions humaines de farinosité. L'échelle de farinosité proposée basée sur des échantillons de goldens ou de top-red marque une forte corrélation lorsqu'elle est comparée à un descripteur sensoriel (R=0.97 et 0.82 pour les échantillons golden ou top-red respectivement). Cette étude permet d'extraire les paramètres reliés à l'effet du stockage et ainsi de donner quelques recommandations aux professionnels. Seules les goldens de petites tailles devraient être stockées 6 mois. Pour les pommes top-red, seules les dates précoces de récolte peuvent être soumises à un stockage de 6 mois, hors atmosphère contrôlée.

1. Introduction

Mealiness is a negative attribute of sensory texture that combines the sensation of a dis-aggregated tissue with the sensation of lack of juiciness. Since January 1996, a wide EC Project entitled: «Mealiness in fruits. Consumers perception and means for detection» is being carried out. Within it, three sensory panels have been trained at: the Institute of Food Research (IFR, United Kingdom), the Institute of Agro-chemistry and Food Technology (IATA, Spain) and the Institut voor Agrotechnologisch Onderzoek (ATO-DLO, Netherlands) to assess mealiness in apples. In all three cases, mealiness has been described as a multidimensional sensory descriptor capable of gathering the loss of consistency and of juiciness (Individual Annual and 18 months Reports). Also a Repertory Grid has been carried out on 4 countries (Belgium, Denmark, Spain and UK) and 5 languages (Danish, English, French, Flemish a Spanish) on 120 consumers per country. The result can be summarised by saying that the consumers perceive mealiness in apples as the loss of crispness, of hardness and of juiciness (18th month Report).

Also within the EC Project several instrumental procedures have been tested for mealiness assessment. In this sense the Physical Properties Laboratory (ETSIA-UPM) has focused its aims on performing instrumental tests for assessing some textural descriptors as crispness, hardness and juiciness. To do so the results obtained by Paoletti in 1993 have been taken into account. This study showed that Magness-Taylor firmness (measured as maximum penetration force) had a 0.91 correlation coefficient with the sensory «durezza» (hardness) ; failure stress during compression showed a 0.92 correlation coefficient with the sensory «fratturabilita» (crispness) ; instrumental juiciness (juice area of the spot obtained during compression) showed a 0.74 correlation coefficient with the sensory assessment of «succosita» (juiciness).

The results obtained by UPM in the instrumental assessment of crispness, hardness and juiciness have shown to correlate well with the sensory measurements (Barreiro et al, 1997) in apples, but also have succeeded when trying to generate several texture degradation levels on peaches from which mealiness appears to be the last stage (1st Year Report). Also, it has been confirmed that mealiness does not appear for all fruits at the same time (1st Year Report) and therefore it is essential to assess mealiness on individual fruits.

2. Objectives

- To define a instrumental mealiness scale reproducing human perception of mealiness;
- To extract features on the storage effects by means of the instrumental mealiness scale.

3. Materials and methods

Apples cv *Golden and Top-Red* have been studied for mealiness assessment. Apples were grown in Lérida, the main area of pome fruit production in Spain by UdL-IRTA according to the following factorial experimental design :

- harvesting date: three different dates of harvest corresponding to early, common and late harvesting dates;

- size of the fruit: two different sizes: < 75mm and > 75mm;

- storage temperature: three different temperatures have been tested under non-controlled atmosphere: -0.5, +0.5 and 2 °C respectively;

- storage period: three different modalities have been tested for this factor: at harvest, 3 month storage and 6 month storage period.

Apples were stored in commercial chambers. The apples were sent along the 96/97 season during the harvesting period (September 96) and after 3 and 6 months of storage (December 96/ January 97 and April 97 respectively). Considering a sample size of 10 fruits, the total amount of fruits that have been tested per variety has been: n° samples = 3 dates * 2 sizes (at harvest) + 3 dates * 2 sizes * 3 temperatures * 2 periods (under cold storage) = 42 samples =====> 420 apples per variety.

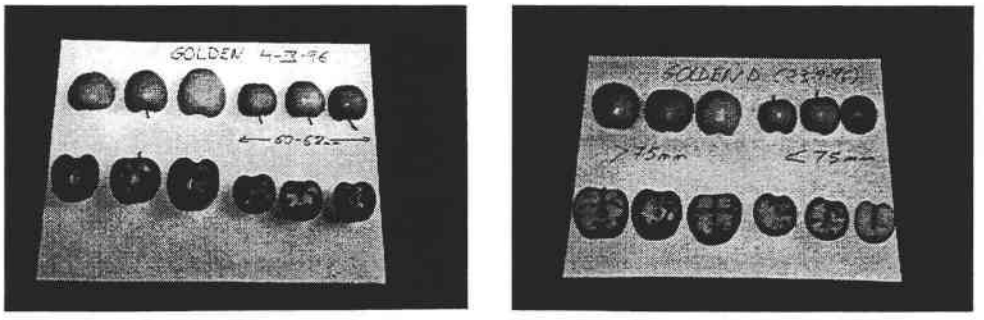

Figure 1: Results of the Iodine test for starch content assessment of Golden apples at early and late harvesting date

The tests carried out on these samples can be summarised as follows:

- weighting of samples,
- mechanical tests:

- Magness-Taylor penetration test: Carried out with a Texture Analyser XT2 on whole fruits. Magness-Taylor flesh penetration test (without skin) was performed

with a 8mm diameter rod. A maximum penetration of 8mm was applied at 20 mm/min speed rate. The maximum penetration force was registered and will be used as Magness-Taylor firmness (MT, N).

- Confined compression test: It was carried out with the same Texture machine on cylindrical probes of 1.7 cm height and 1.7 cm diameter. Probes were confined in a disc of 1.7 cm height, with a hole of the same diameter as the probe (see Figure 2). A maximum deformation of 2.5 mm was applied at 20 mm/min speed rate. The rod used in this test had a 15.3 mm diameter in order to avoid rod/disc contacts during compression. Deformation was immediately removed at the same speed rate; one repetition was made per fruit. The following parameters were registered through these tests:

- maximum Force (N, CF1) corresponding to a 0.5N threshold if failure occurs or to force at 2.5mm;
- deformation at CF1 (mm);
- force at 2.5mm deformation (N, CF2);
- force/deformation ratio within the elastic behaviour (N/mm, CFD1), this magnitude will be used as instrumental hardness.

Juice area (mm2, JUICE) of the spot accumulated in a filter paper placed underneath the probe during the test, and this magnitude will be used as compression juiciness (Paoletti, 1993).

- Compression rupture test: It was carried out with the same Texture machine on fruits probes of similar sizes as the previous test; one repetition was made per fruit. In this case a flat plate is used (diameter 3.2 cm). A non confined probe (1.7 cm diameter and 1.7 cm height) was compressed at a 20mm/min speed rate until rupture point was achieved, registering the maximum force (resistance) at that point.

- Shear rupture test: To perform this test a special device developed in 1992 by Jaren and Ruiz-Altisent was used. It is formed by a metacrilate cubic box (8cm wide), with a prismatic hole in the centre (3x8x0,7 cm). Inside this hole a longer prism of 3x9x0.7 cm can be placed, and slid. Both the rectangular part and the cube have a transversal cylindrical hole where a fruit probe is placed in order to be cut by the rectangular element when pushed by the Texture machine. Two cylindrical nylon pieces joint together by a rubber band compress the probe to maintain it in a fixed position during the test (see Figure 2).

This test was carried out on probes of 1.4 cm diameter and 2.0 cm height. In this test an increasing deformation was applied at a 20mm/min speed rate until probe rupture was achieved; one repetition was carried out per fruit. The maximum force (resistance) at the shear rupture point was registered, which will be used as shear crispness (N), (Paoletti, 1993).

Chemical tests:

- soluble solids content (SS), measured by a digital refractometer PR-101 ATAGO,
- titratable or total acidity using NaOH 0.1 N and phenolphthalein indicator, calculating meq/l.

Also a sensory profile of duplo samples has been carried out by the Institute of Agro-chemistry and Food Technology (18th months Report) for samples stored 3 and 6 months.

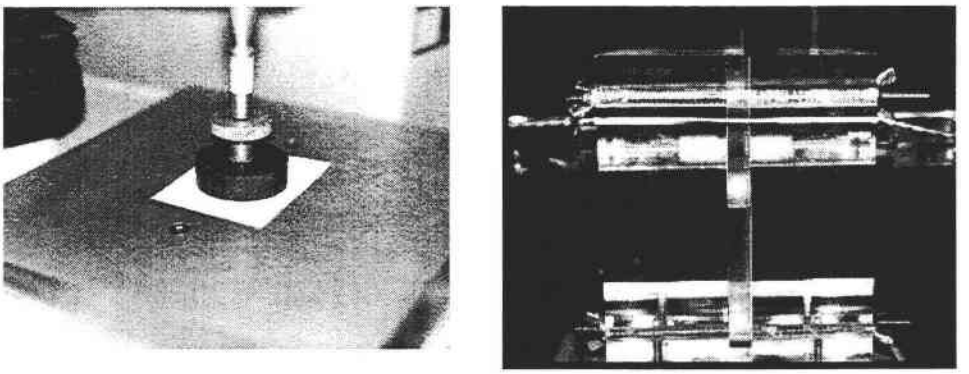

Figure 2: Confined compression (left image) and shear rupture (right image) tests on fruit probes

4. Results

4.1 Mechanical and chemical characterisation of samples

The results for *Golden* apples are shown in Table 1:

- the most important effect for Acidity, Magness-Taylor firmness and Soluble Solid content is storage time (F=1218.8 ; 163.4 ; 91.3 respetively);

- the date of harvest is the 2nd most important factor (F~25). The interaction storage time/harvest date deeply affects Acidity (F=60.7) & Soluble Solids Content (F=58.1) and less to Magness-Taylor Firmness (F=5.3);

- fruit size is the 3rd factor. For Acidity size (F=30.9) is more important than the harvest date (F=16.1);

- the effect of storage temperature (-0.5°C, +0.5°C & +2°C) is not significant for Magness-Taylor Firmness and Acidity. It shows a minor effect on Soluble Solids Content (F=4.3);

- as for the non-standard test for texture assessment, the ranking of effect of factors is similar to the standard tests : 1) storage time, 2) date of harvest, 3) size and 4) temperature. However, Not always Crispness (SF) & Harness (CFD1) evolve in the same way. Date of harvest affects more to Crispness (SF, F=81) than to Hardness (CFD1, ns);

- juiciness (JUICE) is not affected by the date of harvest or the size of the fruit, it is affected by the interaction date of harvest/storage time (F=9.7);

- storage temperature affects Crispness (SF, F=5.5) and Hardness (CDF1, F =5.3), unlike Magness-Taylor Firmness.

The results for *Top-Red* apples in comparison with *Golden* apples are shown in Table 2:

- only for Soluble Solids Content, fruit size (F=315.5) is more important than storage time (F=75.0);

- the effect of storage temperature (-0.5°C, +0.5°C &+2°C) is significant for Magness-Taylor Firmness (F=12.2);

- juiciness (JUICE) is not affected by the storage temperature (-0.5°C, +0.5°C &+2°C), but the same interaction as for Golden is found for date of harvest/time of storage (F=11.4);

- storage temperature affects Hardness (CFD1, F=17.6) slightly more than to Magness-Taylor Firmness (F=12.2).

Golden	Time 1	Temp 2	Harv 3	Size 4	12	13	23	14	24	34	123	124	134	234	all
Weight	29.0	ns	47.3	3634	ns	3.8	3.3	26.2	ns	47.4	9.0	ns	ns	2.5	6.8
MT	163.4	ns	33.5	17.6	3.2	5.3	3.4	ns	ns	7.4	2.3	ns	3.6	ns	ns
SS	91.3	4.3	20.3	13.0	ns	58.1	6.1	ns	ns	4.6	2.0	2.2	3.9	18.4	6.0
Acidity	1218.8	ns	16.1	30.9	ns	60.7	ns	26.8	ns	ns	ns	ns	6.0	4.2	ns
CFD1	861.7	5.2	ns	24.2	5.5	8.1	ns	ns	ns	ns	ns	ns	ns	ns	ns
CF2	352.2	9.4	74.3	50.4	6.7	28.4	5.6	ns	ns	ns	3.1	ns	4.7	1.3	1.4
JUICE	148.9	6.7	ns	ns	ns	9.7	2.5	ns	ns	3	6.3	ns	3.2	ns	3.1
RF	1360.6	5.5	81.0	ns	3.7	5.3	ns	ns	ns	17.3	ns	2.4	7.8	ns	ns
SF	4011.9	5.3	81.5	16.1	2.6	5.3	ns	20.7	ns	13.4	ns	ns	10.4	ns	2.0

Table 1: Analysis of Variance (F values) of Golden 96 for the mechanical and chemical parameters

Top-Red	Time 1	Temp 2	Harv 3	Size 4	12	13	23	14	24	34	123	124	134	234	all
Weight	118.8	ns	135.8	3461.0	2.8	4.3	4.3	25.5	ns	45.5	3.0	ns	ns	4.1	5.2
MT	631.5	12.2	106.1	56.1	3.7	8.9	4.6	ns	ns	5.1	3.3	ns	6.5	ns	ns
SS	75.0	ns	20.0	315.5	2.7	22.7	ns	6.9	5.7	9.3	ns	ns	7.1	6.0	3.3
Acidity	742.0	ns	ns	ns	4.9	50.3	6.3	43.2	12.7	ns	ns	8.3	4.6	11.3	10.0
CFD1	297.8	5.0	69.7	30.5	9.0	29.9	3.7	ns	ns	ns	5.0	ns	ns	ns	ns
CF2	891.2	5.9	12.6	23.5	6.3	6.8	ns	3.8	ns	ns	ns	ns	ns	ns	ns
JUICE	505.5	ns	30.0	52.5	ns	11.4	ns	ns	ns	ns	ns	ns	4.4	ns	ns
RF	436.7	17.6	168.2	78.5	8.9	14.7	5.4	ns	ns	12.7	2.9	ns	6.6	ns	ns
SF	671.1	12.5	169.1	34.1	5.4	20.2	3.7	ns	ns	7.8	ns	ns	ns	3.0	2.0

Table 2: Analysis of Variance (F values) of Top-Red 96 for the mechanical and chemical parameters

4.2 Studying the sensory perception of mealiness

The feature that sensory mealiness («harinosidad») is a combination of loss of crispness, of hardness and of juiciness has also been corroborated by the sensory panel at the Institute of Agro-chemistry and Food Technology (2nd Year Report) on the sensory profile performed on duplo samples (3 & 6 months) of this study:

- TopRed : mealiness is a lack of crispness (r=-0.90), of denseness (r=-0.87), of hardness (r=-0.84) and of juiciness (r=-0.76) combined with an increase of granularity (r=0.76). It is associated with a loss of acidity (r=-0.68);

- Golden : mealiness is a lack of crispness (r=-0.91), of hardness (r=-0.92), of denseness (r=-0.80) and of juiciness (r=-0.83), combined with an increase of granularity (r=0.84). It is associated with a loss of acidity (r=-0.82) and of the intensity of flavour (r=-0.74).

The above mentioned results indicate that sensory «Harinosidad» (Mealiness) is mainly related to a decrease in sensory crispness and hardness and to a second extent related to juiciness decrease. This priority was also chosen in order to build up a mealiness scale.

4.3 Generation of an instrumental mealiness scale

A general overview of the three instrumental parameters (Shear resistance, Force-deformation ratio and juice area) that can be matched to sensory crispness, hardness and juiciness respectively indicates that crispness is the first texture attribute to be lost. In the case of Golden apples (See Figure 2) there is a very quick transition between very crispy fruits (SF>=60N) and lower stages of crispness. This fact is also confirmed by previous ANOVA analysis as samples

belonging to different harvest dates show at harvest a significant difference in the instrumental crispness (F= 81.5) while there is no significant difference for the instrumental hardness.

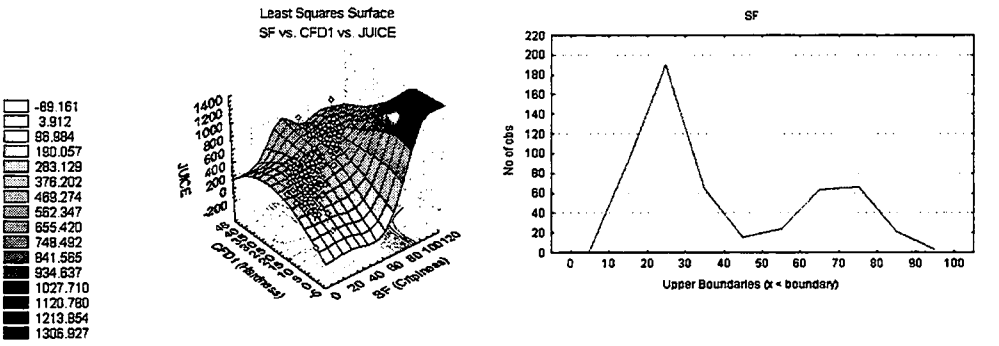

Figure 3: General Overview of Instrumental Crispness, Hardness and Juiciness for Golden apples (left image) indicating a very quick transition between very crispy fruits and lower stages of crispness before hardness and juiciness decrease. This quick transition also leads to a bimodal histogram of SF (right image)

The fact that the texture parameters do not evolve at the same time indicates that instrumental crispness, hardness and juiciness should not be gathered all together at a time when trying to describe the texture degradation towards mealiness but sequentially within several intervals. Therefore the following stage consisted of segment instrumental crispness, hardness and juiciness into several categories. The histograms of those variables were used to discretize the instrumental texture parameters (see Figure 4). A common discretization for both varieties was searched in order to build general mealiness scale.

The final categorisation for the instrumental texture parameters is summarised in Table 1. In it, a compression resistance boundary equivalent to the shear resistance one is given to allow further mealiness assessment through a single instrumental test : Confined Compression.

Once the categorisation of the texture parameters had been carried out, it was the time for achieving a combined criterion for crispness, hardness and juiciness. For this purposes it was decided to reproduce the human priorities within a classification tree shown in Figure 5. Juiciness is only considered when the texture attributes go down to hard nor crispy fruits, that is, it is considered not to be important for very crispy or very hard fruits. A nine degrees mealiness scale (see Figure 6) has been built based on the classification tree shown in Figure 5.

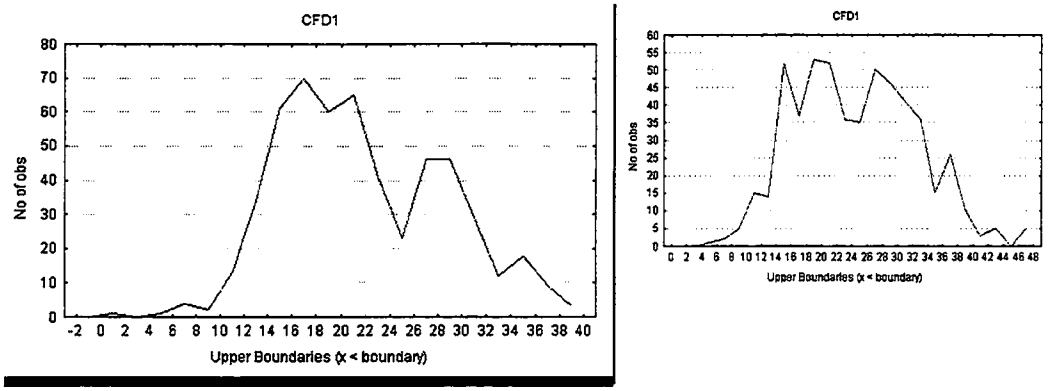

Figure 4: Use of histograms to categorise instrumental hardness in Golden (image to the left) and Top-Red (image to the right)

Texture attribute	Classes	Magnitude categorisation
Crispness	Very crispy	Shear Resistance (SF)>=60N or
	Not very crispy	Compression Resistance (CF2)>=70N
		Shear Resistance (SF)<60N or
		Compression Resistance (CF2)<70N
Hardness	Very Hard	Force-Deformation Ratio (CFD 1)>=34N/mm
	Hard	24N/mm<=Force-Deformation Ratio (CFD 1)<34N/mm
	Soft	14N/mm<=Force-Deformation Ratio (CFD 1)<24N/mm
	Very Soft	Force-Deformation Ratio (CFD 1)<14N/mm
Juiciness	Very juicy	Juice area >= 500mm2
	Juicy	400mm2<=Juice area<500mm2
	Low juicy	300mm2<=Juice area<300mm2
	Non juicy	Juice area < 300mm2

Table 1: Categorisation of texture parameters to generate a mealiness scale

4.4 Comparison between human and instrumental mealiness scales

A comparison between Sensory («Harinosidad») and instrumental (MEALLEV) mealiness scales has been performed for *Golden* and *Top-Red* apples. It is based on average sample by sample (n=12) comparison as there is no possibility of making a fruit by fruit (n=120) comparison. The minimum amount of fruit needed to perform a sensory profile is one quarter of fruit per assessor and at least 12 assessors should be included in a panel.

There is a significant correlation between the instrumental and sensory mealiness scales for both Golden and Top-Red apples (r=0.87 and r=0.82 respectively, see Figure 7). The lack of use of texture references in the sensory profiles leads to a low sensory mealiness index for *Golden* apples that already had lost their crispiness (not so low instrumental mealiness index). This is not the case of *Top-*

Red apples were at least one of the samples remained very crispy (very low instrumental and sensory mealiness index) after 3 months of storage. It is also significant that no average instrumental or sensory sample could reach the top of the mealiness scale which does not indicate that none of the fruits became mealy as it will be shown in the next paragraph.

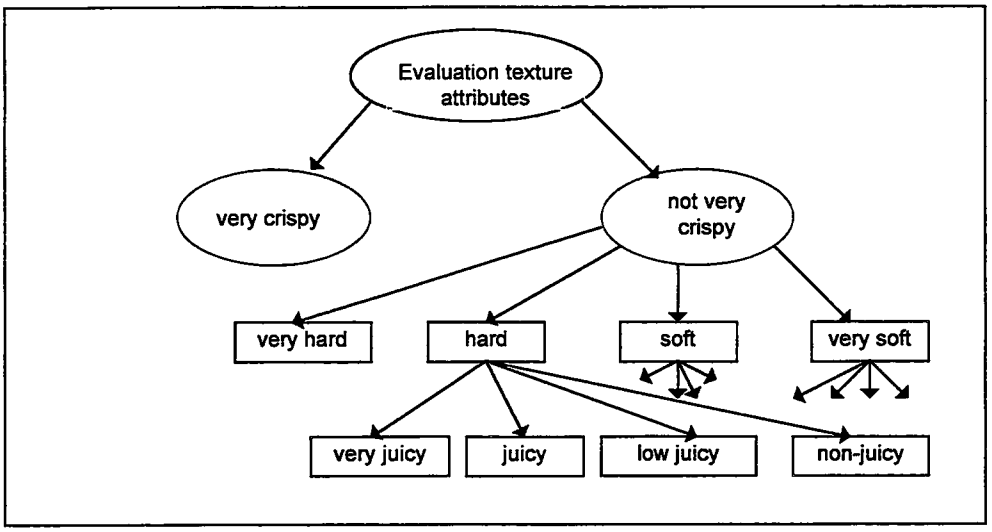

Figure 5: Classification tree for instrumental mealiness assessment. Juiciness is only considered when consistency goes down to hard

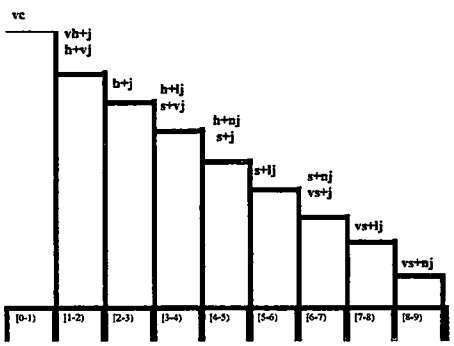

Figure 6: Final mealiness scale combining discrete classes of instrumental crispness, hardness and juiciness. The decrease in height of the column refers to decreasing quality in texture

4.5 Use of the instrumental mealiness scale to extract features on storage effects

The instrumental mealiness scale has been used to extract features on mealiness onset as a function of harvest date and fruit post-harvest treatments combining with different storage temperatures and periods. The results of a Anova analysis are shown for *Golden* apples in Figure 8. In it only the experimental factors that showed a significant effect (Fruit size and storage period : F=739.37 and 34.91 respectively) are displayed ; therefore 30 is the number of items averaged at harvest (storage 0) and 90 fruits are averaged for 3 moth and 6 month samples. Figure 8 indicates within brackets the number of fruits for each average which lay in the 3 highest instrumental mealiness classes. This value helps to quantify the effect of treatments : for large size apples (size=1) 60 fruits out of 90 became very mealy after a 6 months period while only 30 fruits out of 90 became very mealy for small size *Golden* apples. The critical storage period appears to be between 3 and 6 months as there is a sudden increase in the number of very mealy fruits between both periods.

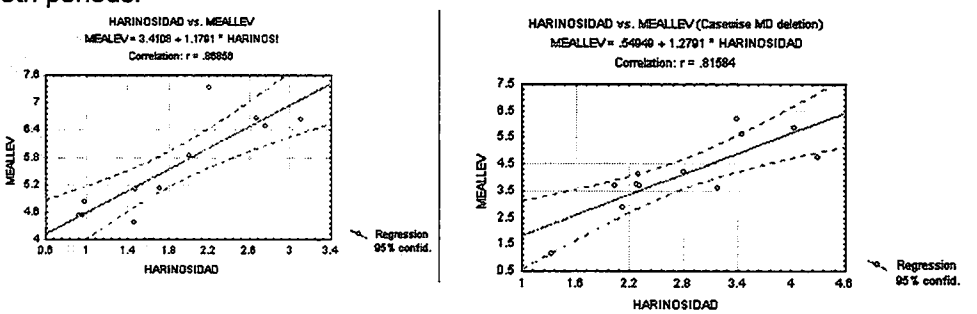

Figure 7: Comparison between sensory («Harinosidad») and instrumental (MEALLEV) mealiness scales for Golden (left image) and Top-Red (right image) apples

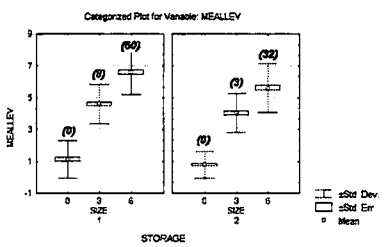

Figure 8: Extraction of features on mealiness onset for Golden apples. Size 1 & 2 refer to big and small sizes respectively. Storage 0, 3 and 6 refer to the number of months under cold storage. At harvest (storage 0) 30 items are averaged while in 3 months and 6 months samples 90 items are averaged. Numbers within brackets refer to the number of fruits within the three highest levels on instrumental mealiness

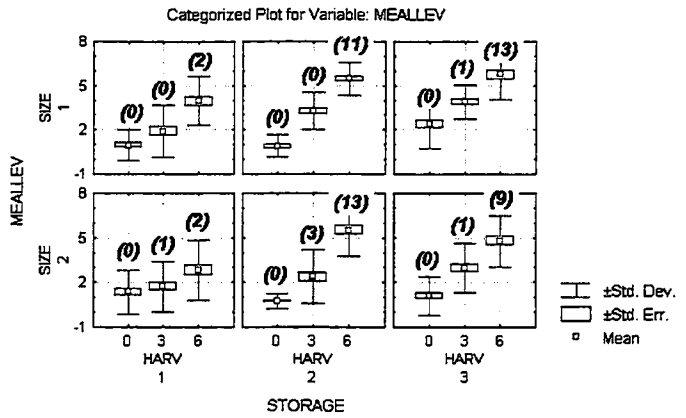

Figure 9: Extraction of features on mealiness onset for Top-Red apples. Size 1 & 2 refer to big and small sizes respectively. Harvest 1,2 & 3 refer to early commercial and late harvesting dates. Storage 0, 3 and 6 refer to the number of months under cold storage. At harvest (storage 0) 10 items are averaged while in the rest of samples 20 items are averaged. Numbers within brackets refer to the number of fruits within the three highest levels on instrumental mealiness

Figure 9 shows the results of the ANOVA analysis for Top-Red apples. In this case three experimental factors show a significant effect : storage period, harvest date and fruit size (F=269.69 ; 42.87 & 34.91) respectively. As before only the significant factors are displayed, therefore samples at harvest (storage 0) average 10 fruits, while the rest of samples average 30 items. When looking at the number of fruits within the three highest mealiness classes there is no clear effect of the size of the fruit. Nearly none of the Top-Red samples after 3 months of storage showed very mealy fruits. After 6 months of storage show, commercial and late harvest dates there are around 10 very mealy fruits out of 30, while early picked Top-Red apples only show 2 very mealy fruits out of 30.

Conclusion

The use of selected non-standard texture tests allows to assess crispness, hardness and juiciness by instrumental means.

The categorisation of the individual texture attributes followed by an integration criterion that reproduces human sensing of mealiness can be used to generate an instrumental mealiness scale

The instrumental mealiness scale shows a high correlation with the sensory mealiness (r=0.87 and r=0.82 for *Golden* and *Top-Red* apples respectively).

The instrumental mealiness scale allows to build recommendation for picking and storaging conditions : there is no high risk of mealiness after a 3 months of storage period. Only small size Golden apples or early picked Top-Red apples should be stored for a 6 months period without controlled atmosphere.

Acknowledgements

To the European Project FAIR CT 95-0302 : Mealiness in fruits.

References

Barreiro P.; M. Ruiz-Altisent; C. Ortiz; V. De Smedt; S.Schotte; Z. Bhanji; I. Wakeling. 1997. *Comparison between sensorial and instrumental measurements for mealiness assessment in apples. A collaborative test.* Submitted to the Journal of Texture Studies

Jarén C.; Ruiz-Altisent M. 1992. *Clasificación de la madurez de los frutos mediante impactos no destructivos. Actas de la 24 CIMA* pp:545-552 Zaragoza 1-4 Abril.

Paoletti, F.; Moneta, E.; Sinesio F. *1993. Mechanical properties and sensory evaluation of selected apple cultivars* Lebensm.-Wis. u. - Technology 26 :264-270

Various authors. 1996, 97 & 98. *Mealiness in fruits, consumer perception and means for detection ; Individual Annual Report, 18 months & 2nd Year Report.* EC Project FAIR CT960302

Detection of mechanical stress and damage of fruit and vegetables

Détection des contraintes mécaniques et des meurtrissures sur fruits et légumes

Herold Bernd Oberbarnscheidt Bernd Truppel Ingo Geyer Martin

Institute of Agricultural Engineering Bornim
Max-Eyth-Allee 100, D-14469 Potsdam / Germany
e-mail: atb@atb.uni-potsdam.de

Abstract: *Detection of mechanical stress in handling technique is necessary to improve the handling technique. Artificial fruits are used to detect the mechanical stress and potential damage sources in practical handling. The produce damage risk can be estimated based on significant relations between data of artifial fruits and stress response of real products. Specific effect of different pressing surfaces on produce can be detected by means of tactile thin-film sensor. This sensor allows to determine the contact pressure distribution as well as beginning rupture failure of cell tissue on the produce surface e.g. on apple fruits.*

Detection of mechanical bruises on produce is required to evaluate the damaging effect of handling and to complete the fruit quality sorting. External produce damage can be determined by using computerized image analysis.

Keywords : *Mechanical stress, damage, fruit handling, sensing techniques.*

Résumé : La détection des chocs mécaniques lors du convoyage est nécessaire pour améliorer ce dernier. Des fruits artificiels sont utilisés pour détecter les chocs mécaniques et les sources de meurtrissures potentielles. Le risque d'abîmer le fruit peut être estimé sur des relations significatives entre la réponse du fruit artificiel et celle du produit réel. L'effet spécifique de différentes surfaces de compression sur le produit peut être déterminé au moyen d'un film tactile. Ce capteur permet de déterminer la distribution de la pression de contact ainsi que le début de la rupture des cellules du tissu physiologique du fruit (pomme par exemple). La détection de meurtrissures sur le produit est nécessaire pour évaluer l'effet de la manipulation et pour accomplir un tri à la qualité. Les meurtrissures peuvent être identifiées en utilisant un système d'analyse d'images.

1. Mechanical stress during handling processes

Mechanized harvest and postharvest handling cause a considerable mechanical stress on perishable fruits and vegetables. In many cases the use of non-gentle handling technique results in produce damage and high quality losses.

Previous engineering research has been directed to developing objective methods for detection of damage sources by use of artificial fruits. Artificial fruits are designed as instrumented spheres and used to mimick real fruit and to acquire information on mechanical loads applied to fruit during handling. Since several years two types of instrumented spheres have been available that are able to record mechanical load data together with time from an internal clock. Both spheres were developed for basically the same purpose.

The PMS-60 system presented here was developed at ATB and consists of a Pressure Measuring Sphere, an interface device for data transfer from and to a personal computer, and the software to operate the system and process the recorded data (Figure 1).

Optionally a remote control unit is available which allows to record time markers on the PC by pressing a special hardware key for wireless operation up to 100m distance. The pressure measuring sphere's diameter is 62 mm, and its mass is 180 g. The sphere consists of a rubber ball filled with silicon oil, whose hydraulic pressure level changes in response to external mechanical load. An electronic data acquisition unit is embedded inside the sphere. It is able to detect pressure caused by both static and dynamic mechanical load events, if they exceed a preset threshold. The measured data are stored, together with time from an internal clock. Size, mass and elastic compliance of the PMS are similar to that of onions and potatoes, although the sphere's average density (ρ = 1.4 g/cm^3) is higher than that of these commodities. It should also be noted that the spherical shape causes the PMS to roll more easily.

Figure 1: PMS-60 measuring system

The measuring sphere was calibrated in relation to the compressive force between parallel plates under static load conditions. Under these conditions the measuring range is 0 to 100 N, and the measuring error is approximately 5%. Under dynamic load conditions (dropping the sphere at random orientation onto horizontal surface) the measured pressure values depends strongly on the direction of load application. Therefore the measuring error is higher, and 10 to 15 measuring runs are required to obtain representative average results. Presuming the existence of mechanical similarity between PMS-60 and bulb onions and potato tubers, the PMS-60 load data could be used to describe approximately their impact behaviour.

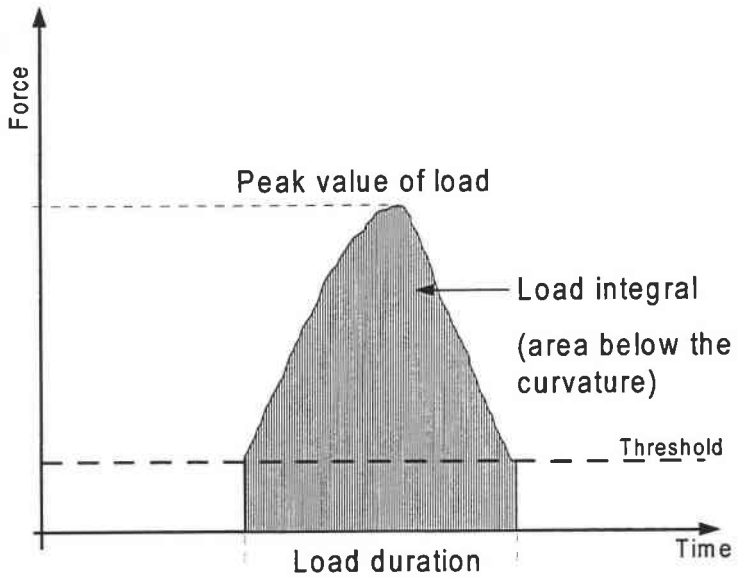

Figure 2: Definition of parameters of a mechanical load event based on data of PMS-60

From measured data of each mechanical load event three parameters could be derived:

(1) duration of the load event,
(2) peak force (i.e. the maximum value of the load event), and
(3) load integral (i.e. the area under the force-time curve for the load event).

An example of an load event and definition of load parameters is shown in Figure 2.

The number of recorded mechanical loads or impacts, the peak force and the load integral of each load event were used to evaluate the measured handling process.

For data acquisition under laboratory drop tests as well as under practical conditions the sampling rate was set at 3 kHz (sufficient to acquire both static loads and short impacts), and the preset sampling threshold was 20 N (load values below 20 N were assumed to be without damaging effect, and so only load values exceeding 20 N were recorded).

The main alternative to the PMS-60 is the impact recording sphere IS100. The IS100 shell consists of bee's wax or plastic and is relatively rigid. The sphere was originally developed to detect causes of apple bruises and is not very robust. Inside the sphere accelerations are measured with a triaxial acceleration sensor. The

IS100 is calibrated under dynamic load conditions using drops from different heights onto horizontal surface. Its measuring range is 0 to 500 g's (g's expresses the earth's acceleration, g = 9.81 ms^{-2}) corresponding to drop heights onto steel plate from 0 to 25 cm, and the measuring error is nearly 5%. The IS100 measures impact acceleration, but it cannot detect static load events.

An analysis of stress data acquired by means of PMS-60 allows to define the causes (locations) and the influence parameters of mechanical stress during mechanized handling and to derive measures for stress reduction (reduction of drop height, use of cushioning material, change in design of produce flow). Comparing the mechanical load data of different technologies to perform the same operation, e.g. the sizing, it is possible to evaluate their stress effect and to select the most gentle technology.

Based on the relation between the stress data acquired by means of artificial fruit under well-defined stress conditions and the data of stress response of real produce under equivalent conditions (increased respiration rate, additional storage losses) the allowed threshold of mechanical stress can be defined, for instance of bulb onions and carrots [2].

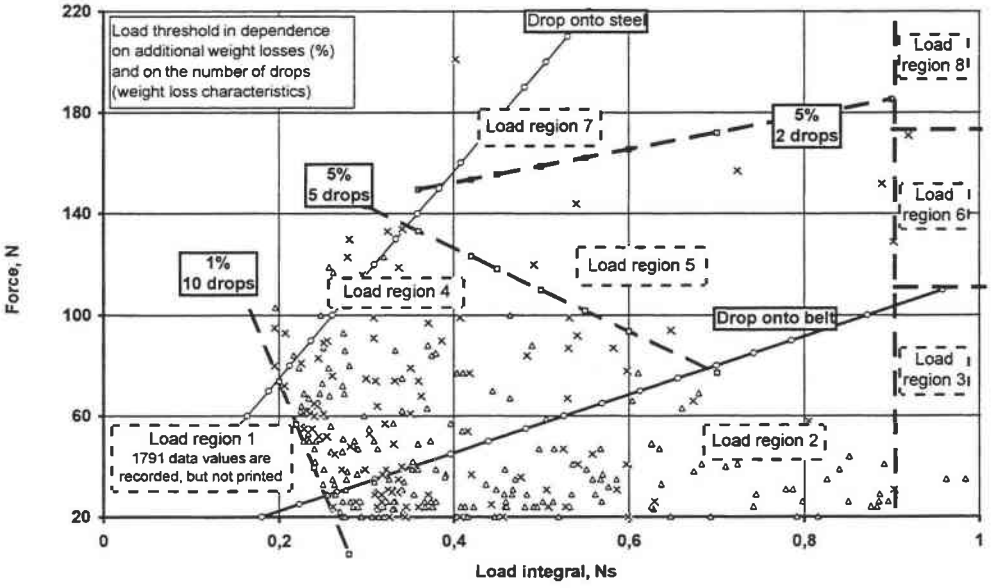

Figure 3: Classification of mechanical load regions for bulb onions in dependence on number of mechanical loads, peak load and load integral measured by means of PMS-60

In Figure 3 the data from 21 measuring runs of PMS-60 through onion harvester (Δ) and the following transition onto truck (x) are entered. Each load event is

represented by a point in the diagram. The given load regions have been derived from results of drop tests with bulb onions. They reflect the percentages of additional onion storage losses in dependence on the mechanical stress parameters (number, peak value and integral value of mechanical loads). The load regions 1, 2 and 3 represent insignificant impacts and compressions. But impacts of increasing damaging potential are placed in load regions 4, 5 and 7, and compressions of increasing level in load regions 6 and 8, respectively.

2. Contact pressure distribution and rupture failure on superficial fruit tissue under compressive load

A tactile thin-film sensor was used to determine the dimensions of contact surface and the change of contact pressure distribution during compression of fruit by using different-shaped pressing tools. This tactile sensor, consisting of a pressure sensing grid deposited onto thin flexible film, can be placed between fruit and pressing surface. The PC controlled system scans the sensing grid and provides results as sequence of two-dimensional pressure profiles [3].

Compression tests were carried out on apple fruits cv. 'Elstar' and 'Boskoop' at room temperature under gradually increasing load (speed 30 mm / min) by means of a universal testing machine (Figure 4).

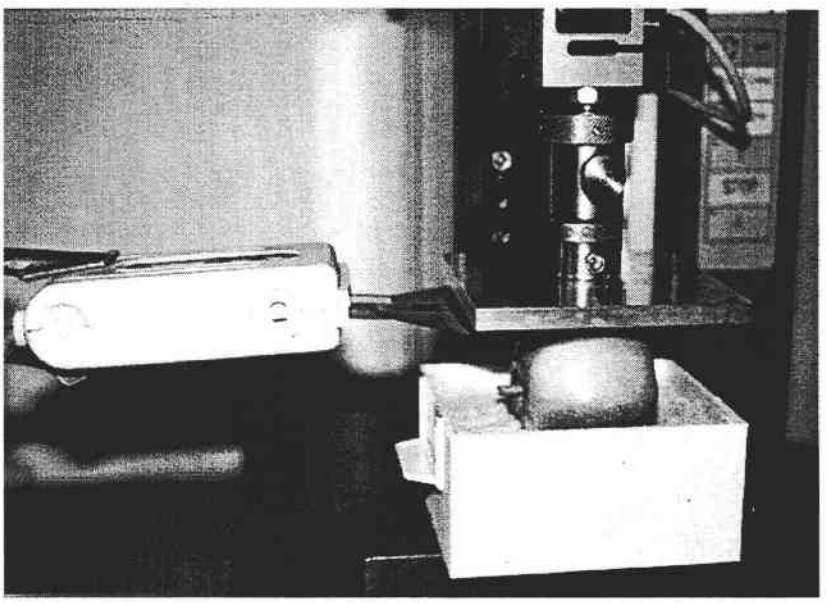

Figure 4: Arrangement for compression test on apple
(thin-film tactile sensor is placed between plate and upper fruit part)

Each fruit was taken with horizontal stem-calyx axis and embedded in moist sand, and pressed from above by different surfaces: steel rod (∅ 10 mm), steel rod coated with rubber profile (∅ 18 mm), steel rod coated with soft profile of hollow rubber (∅ 24 mm), and flat steel plate.

Pressure distribution on the apple surface was detected by using a sensor Type I-Scan 75, Tekscan, Inc., with measuring range of 50 psi (≈ 0.35 MPa)[3]. This sensor consists of a conductive gridwork of 44 rows and 44 columns in distance of 0.075-in (1.9 mm).

Using Tekscan software, changing pressure information was displayed in real time on a PC screen. The sampling rate was 10 frames per second.

During the test the sensor Type I-Scan 75 was placed between pressing surface and upper part of fruit. Comparison of results of tactile sensor with those of force sensor (load cell) shows that differences exist mainly in lower load range. Here the tactile sensor seems to be more sensitive, but the sensors are rather similarly in the medium and upper load range. Considering that the error of load cell is 0.1% the measuring error of tactile sensor is estimated to be about 6%.

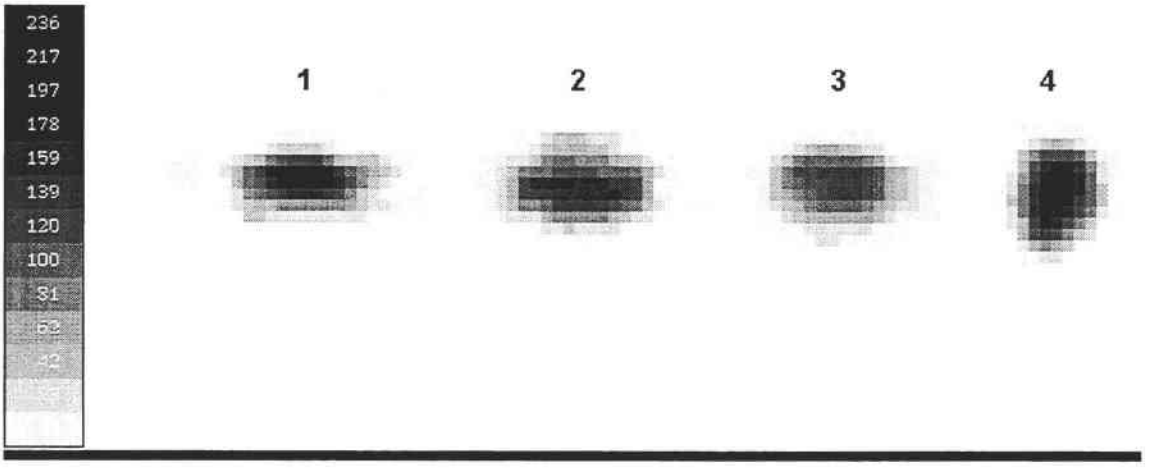

Figure 5: Pressure distributions for compression of apple fruits under different surfaces (1 to 4) at force level of 80 N

Figure 5 shows the 2D plots of pressure distribution caused by the four above mentioned pressing tools at a force level of about 80 N on 'Elstar' apples. Below the 80 N level no significant tissue failure was observed. As expected the „print« of 10 mm steel rod (1) has a longish shape and highest peak value of pressure. The „prints« of steel rods with coating of rubber (2) and of hollow rubber (3) exhibit larger contact areas with significant lower pressure levels. The steel plate (4) causes a relatively small and nearly circular contact area with in average high

pressure level. Its pressure gradient over the contact area is smaller than in the case of steel rod [4].

An analysis of fruit tissue failure was carried out based on the histogram of contact area proportions at different pressure load levels measured by tactile sensor. The distribution of contact area over the load levels changes with increasing compression. If rupture failure of fruit cell tissue occurs, then proportions of contact area move from higher to lower load levels. The level of highest load level covered before failure corresponds to the fruit firmness and depends on apple variety and other factors. For the varieties 'Boskoop' and 'Elstar' the critical pressure levels were determined. Data were selected from nine examples of 'Boskoop' failure and from twelve of 'Elstar' failure during compression under flat plate. The critical pressure level is defined as the lowest of high load levels, in that the proportion of contact area is decreased due to failure. The critical pressure level for 'Boskoop' was found to be 170 to 190 sensor units, and for 'Elstar' 150 to 170 sensor units, respectively [4].

At present the sampling rate of this sensor is restricted to a maximum of 100 frames per second. Therefore impact conditions could not be studied. It is estimated that the use of this sensor could promote the development of advanced three-dimensional theoretical models to describe the damage behaviour of fruit, and the more gentle design of handling and packaging technology.

3. Image analysis for bruise detection

CCD camera and computerized image analysis are used not only to determine size, shape and colour of fruits but also to detect bruises on apple fruit.

A special project was directed to apply the stripe projection technique for visualization of deformed but not discoloured parts on fruit surface. The triangulation principle was used to transform the original three-dimensional information into two-dimensional data, which are taken by video camera (Figure 6).

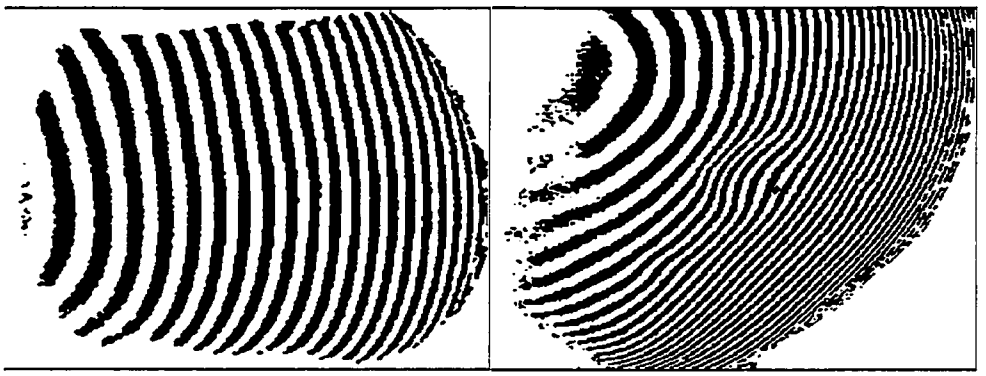

Figure 6. Binary stripe projection images of non-deformed (left) and bruised (right) apple surface

The detectivity for deformations depends on projection angle and on distance between projected stripes. The detectivity can be increased by a great projection angle, but in this case a greater number of pictures is required in order to cover the entire fruit surface. If the pixel resolution and pixel congruence of camera, frame grabber, and memory card are not sufficiently, then undesired Moiré-patterns can occur, and the spatial resolution is reduced. The distance between the stripes detected by camera have been analysed and classified related to typical parameters for non-deformed, and deformed fruit surface, and calyx and stem areas as well. Preliminary results (projection of parallel stripes with distance of 1 mm on apples surface under an angle of 35 to 45 degrees) show that deformed parts with depth of about 2 mm can be detected. An adaptation of classification parameters to apple variety seems to be necessary [5].

Another project is dealt with application of diffuse illumination onto apples and RGB camera to measure the colour data of fruit surface. The RGB colour data are transformed into CIELAB colour space in order to evaluate them adapted to human perception characteristics. By using of experiences in the colour television technology special transformation equations have been developed and tested on apple fruits. In comparison with calibrated colourmeter (MINOLTA type CR-300) high correlations were found for the parameters L* (R^2 = 0.95) and a* (R^2 = 0.91), while the parameter b* showed less correlation (R^2 = 0.68). The camera data of parameter b* could be improved by using nonlinear camera transfer function instead of usual linear transfer function. Additionally the detectivity for defects on fruit surface depends on type of illumination source. Illumination by a fluorescent lamp (narrow band spectrum) was found to be more efficient than by an incandescent halogen lamp (broad band spectrum). Further work is necessary to define the thresholds for defect detection.

References

[1] B. Herold, I. Truppel, G. Siering, M. Geyer. *A Pressure Measuring Sphere for monitoring handling of fruit and vegetables.* In Computers and Electronics in Agriculture. 15 (1996), p. 73-88.

[2] B. Herold, B. Oberbarnscheidt, M. Geyer. *Mechanical load and its effect on bulb onions due to harvest and post-harvest handling.* Proceedings AGENG´96, Madrid. September 23-26, 1996, Paper 96F-037.

[3] Sensor Presentation Software, User´s Manual. Tekscan, Inc., 307 W. First Street, South Boston/MA 02210, USA, 1993.

[4] B. Herold, G. Siering, M. Geyer. *Grid-based Surface Pressing Sensing during Load and Damage of Intact Fruit.* Proceedings of the Technical Program for the Fifth Symposium on Fruit, Nut and Vegetable Production Engineering. Session 14 No. 3, Davis, California, USA, September 3-10,1997.

[5] K. Hother, B. Herold, U. Schmidt. Qualitaetserkennung am Apfel mit Hilfe der Streifenprojektion.
In Bornimer Agrartechnische Berichte, Potsdam-Bornim 1997, No. 14, S. 120-134.

Woolliness assessment in peaches. Comparison between human and instrumental procedures and results

Farinosité des pêches. Comparaison entre les mesures humaines et instrumentales

C. Ortiz **P. Barreiro** **M. Ruiz-Altisent**

Rural Engineering Dept. E.T.S.I.A Madrid. Spain

F. Riquelme

Institute of Soil Science and Biology Applied to Segura Area. CSIC. Murcia. Spain

Abstract: Woolliness, a negative attribute of sensory texture, is characterised by the lack of juiciness without variation of the tissue water content an incapacity of ripening although there is external ripe appearance. In this study, peaches cv Springcrest (early and soft flesh peaches) and Miraflores (late and hard flesh peaches) corresponding to three different maturity stages at harvest, stored 0, 1, 2, 3 and 4 weeks at 1 and 5ºC have been tested by instrumental and sensory means. A Instrumental classification of woolliness has been compared to the sensory assessment. For Springcrest peaches the sensory results match with those found for the instrumental procedure. In this case , Woolliness appears after 2 weeks of storage at 5ºC, changing abruptly from crispy to woolly. Miraflores peaches did not develop woolliness during storage. After comparing with sensory results, it is shown that a common instrumental scale may be appropriate to classify for woolliness all peach varieties.

Résumé : La farinosité, attribut négatif de la texture, est caractérisée par le manque de jutosité, sans variation de la teneur en eau du tissu et une incapacité à mûrir alors que l'apparence externe est mûre. Dans cette étude, des pêches Springcrest (précoces et à chair molle) et Miraflores (tardives et à chair ferme) correspondant à 3 stades de maturité à la récolte et stockées, 0, 1, 2, 3 et 4 semaines à 1° et 5°C ont été testées sensoriellement et par des appareils. Les classifications faites à partir de l'analyse sensorielle et instrumentale ont été comparées. Pour les Springcrest, l'analyse sensorielle correspond aux résultats trouvés par la procédure instrumentale. Dans ce cas la farinosité apparaît après 2 semaines de stockage à 5°C, avec un changement abrupt de croquant à farineux. Les Miraflores n'ont pas montré de farinosité. Après comparaison des résultats sensoriels, il a été montré qu'une échelle instrumentale commune pouvait être appropriée pour classer toutes les variétés de pêches en fonction de la farinosité.

1. Introduction

The results shown in this paper are involved in the European project FAIR CT 0302 'Mealiness in fruits: consumers perception and means for detection'.

Mealiness is a negative attribute of sensory texture, characterised by the lack of juiciness without variation of the tissue water content (Harker and Hallet, 1992). Peach mealy textures are also known as «woolliness» and «leatheriness». Besides the lack of juiciness and flavour, that characterises mealy fruits, in peaches it is associated with internal browning near the stone and incapacity of ripening although there is external ripe appearance (Kailasapathy and Melton, 1992). It is considered as a physiological disorder that appears in stone fruits combined with an unbalanced pectolitic enzyme activity during storage. Mealiness is characterised by a dissolution of the middle lamella, a separation of cells, some irregular thickening of the primary wall and a plasmolysis of the cells located in the mesocarp parenchyma (Luza et al, 1992). In woolly textures, the lack of juiciness is caused by gel structures that retain the water molecules. These gel structures are characterised by a high molecular weight combined with many ramifications which cause the woolly sensation (Kailasapathy and Melton, 1992). In peaches mealiness is associated with fruits under cold storage combined with low maturity stage at harvest (Snowdon, 1990).

Consumers and retailers from California consider mealy peaches a problem that should be specifically addressed (Bruhn, 1994). Also a survey on Madrid consumers retailers showed how mealiness was considered a negative attribute, which reduced sales and price, (Lopez et al, 1995).When studying sensory appreciation of mealiness in apples, lack of crispness, hardness and juiciness have been pointed out to be the major causes for the mealiness sensation (Institute of Agrochemistry and Food Research Eighteen Months Report, 1997).

Up to date there is a first proposal for defining woolliness in *Springcrest* peaches (Ortiz et al, 1997) although it has to be compared to a trained sensory panel as a reference.

2. Objective

To develop an instrumental method to quantify mealiness by comparison to trained sensory assessors.

3. Materials & methods

Two varieties of peaches, early soft flesh peaches (Cv. *Springcrest*) and late hard flesh peaches (Cv. *Miraflores*), have been used for the study. Peaches were grown

in Murcia and split in samples within a factorial experimental design. These activities which have been performed at the production area were carried out by the Institute of Soil Science and Biology (CEBAS, CSIC, Murcia).

The experimental design can be summarised as:

maturity stage: three different stages at harvest were selected by experts, in a batch of fruits harvested on the same date in the same orchard, and according mainly to visual références

- 1st maturity stage (reflectance at 680 nm 34,6%),
- 2nd maturity stage (reflectance at 680 nm 41,4%),
- 3rd maturity stage (reflectance at 680 nm 43,5%),

- storage temperature: two different storage temperatures were tested under non-controlled atmosphere :+1° and +5°C;

- storage period: five different modalities were tested for this factor: at harvest, and weekly for a month period : 0, 1, 2, 3 and 4 weeks.

This design was searched in order to achieve as wide mealiness/woolliness range as possible. A total amount of 27 samples were sent to the Institute of Agro-chemistry and Food Research (IATA, Valencia) for sensory assessmet (by a expert sensory panel) and to the Physical Properties Laboratory (LPF, UPM, Madrid) for instrumental assessment.

The total amount of fruits used at LPF for the experiment was 270 (10 fruits per sample).

The fruits were stored in the CEBAS in Murcia and sent the night before the measurements were carried out. Isolated boxes with ice bags were used for transportation.

In this paper the results from the LPF are shown. Further analysis needs to be developed comparing LPF and IATA results.

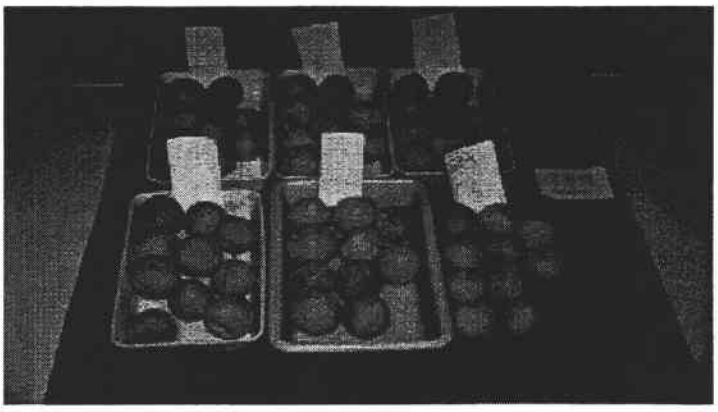

Figure 1: Peaches used for the instrumental and sensorial assessment

The tests carried out on these samples can be summarised as follows:

- weighting of samples,
- mechanical tests:

- Magness-Taylor penetration test: Carried out with a Texture Analyser XT2 on whole fruits. Magness-Taylor flesh penetration test was performed with a 8mm diameter rod. A maximum penetration of 8mm was applied at 20 mm/min speed rate. The maximum penetration force was registered and will be used as Magness-Taylor firmness (N).

- Confined compression test: It was carried out with the same Texture machine on cylindrical probes of 1.4 cm height and 1.4 cm diameter (see Figure 2). Probes were confined in a disc of 1.4 cm height, with a hole of the same diameter as the probe. A maximum deformation of 2.0 mm was applied at 20 mm/min speed rate (0.017 m/m.s). The rod used in this test had a 12.5 mm diameter in order to avoid rod/disc contacts during compression. Deformation was immediately removed at the same speed rate; one repetition was made per fruit. The following parameters were registered through these tests:

- force/deformation ratio within the elastic behaviour (N/mm),

- juice area (mm^2) of the spot accumulated in a filter paper placed underneath the probe during the test, and this magnitude will be used as compression juiciness (Paoletti, 1993),

- shear rupture test : To perform this test a special device developed in 1992 by Jaren and Ruiz-Altisent was used (see Figure 3). It is formed by a metacrilate cubic box (8cm wide), with a hole in the centre of a rectangular piece (3x8x0,7 cm). In

that hole a piece of 3x9x0.7 cm can be placed. Both the rectangular piece and the cube have a transversal cylindrical hole where a fruit probe is placed in order to be cut by the rectangular piece when pushed by the Texture machine. Two cylindrical plastic pieces joint together by a rubber band compress the probe to maintain it in a fixed position during the test.

This test was carried out on probes of 1.4 cm diameter and 2.0 cm height. In this test an increasing deformation was applied at a 20mm/min speed rate until probe rupture was achieved; one repetition was carried out per fruit. The maximum force at the shear rupture point was registered, which will be used as shear crispness (N), (Paoletti, 1993).

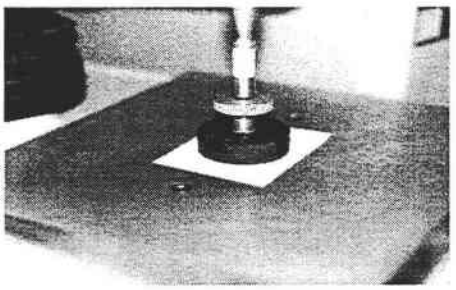

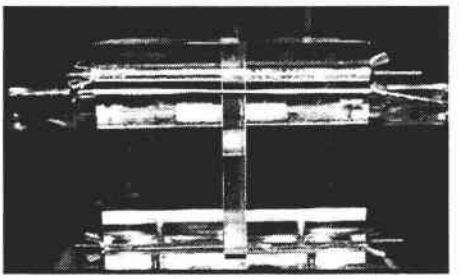

Figures 2 and 3: Confined compression and shear rupture tests

Chemical tests:

- solid soluble content, measured by a digital refractometer PR-101 ATAGO,
- titratable or total acidity using NaOH valoration 0,1 N, carried out by a titration system, Titrator TR 85 and automatic burete T80 (Schott Gerate equipment) attached to a pHmeter, calculating meq/l.

The samples were assessed for texture disorders at LPF by an expert who tasted each peach and classified it into woolly or not woolly. Further information on texture and flavour was also registered

4. Results

4.1 Characterisation of the samples

When comparing Magness-Taylor force (N) for the two varieties, *Springcrest* peaches show a wider variation range (mean values from 43.0 N to 29.2 N) than *Miraflores* (mean values from 40.3N to 31.6 N), see Figure 4. For both varieties there is a gradual decrease of this parameter for increasing maturity stage from 1 to 3.

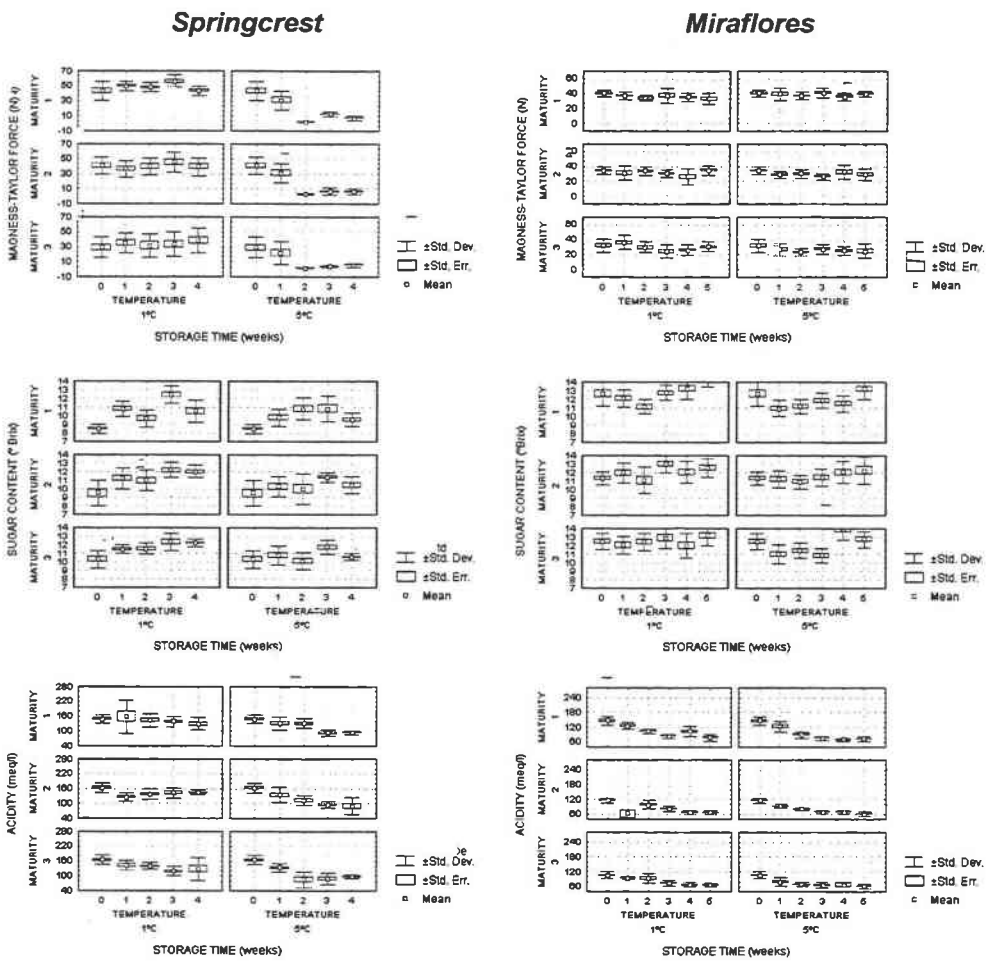

Figure 4: Magness-Taylor Force, sugar content and acidity evolution during cold storage at 1°C and 5°C

Sugar content at harvest for *Springcrest* peaches is lower than for *Miraflores*. In *Miraflores* there is not a clear increase in sugar content when increasing maturity stage, the third maturity stage has less sugar values than the second maturity stage (12.6, 11.3 and 12.5 °Brix, maturity stages from 1 to 3 respectively). In spite of *Springcrest* where there is a gradual increase there is a gradual increase in sugar content (8.5, 9.5 and 10.3 °Brix, as increasing maturity stage from 1 to 3).

Acidity follows a different pattern when comparing both varieties. Although, for the first maturity stage at harvest both varieties have similar acidity values, for *Miraflores* acidity decreases when increasing maturity stage (from 145.2 to 106.2 meq/l) and in *Sprincrest* it tends to increase (148.7, 162.7 and 164.2 meq/l, for the 1, 2 and 3 maturity stages).

4.2 Sensory assessment of woolliness

Table 1 shows the main result of this sensory assessment for Springcrest. In this case the UPM assessor did not doubt whenever classifying a woolly peach, that is, woolliness can be easily recognised. The identification of woolly peaches made by the sensory assessor indicates the onset of woolliness after 2 weeks of storage under 5°C.

This feature has also been pointed by the sensory panel at IATA (2nd Year Report of the EC Project FAIR CT960302, 1998), as it shows a very high increase of woolliness in peaches stored at 5°C in spite of those stored at 1°C, which do not show an increase in sensory wolliness. Also sensory denseness, hardness and crispness evaluated by IATA panel, show a deep decrease after 2 weeks of storage at 5°C. Again peaches stored at 1°C maintain their values during storage.

For *Miraflores* peaches, the UPM assessor has large difficulties to recognise woolliness as not all the attributes conforming a mealy fruit (lack of crispness, hardness and juiciness) appear at the same time. This textural disorder does not start at a certain storage time and at a specific storage temperature. *Miraflores* peaches have an intermediate woolliness stage, where fruits are soft but still juicy and not woolly. Again this features matches with the sensory woolliness evaluated by the IATA expert sensory panel. For *Miraflores* peaches woolliness does not appear to increase neither at 1°C nor at 5°C. In the same way crispness, hardness and denseness maintain their values during storage, though they have lower values in the beginning than *Springcrest* peaches.

Storage period	Maturity at harvest	Sensory mealy peaches	
		1°C	5°C
0 weeks	Lowest	0	0
	Medium	0	0
	Highest	0	0
1 week	Lowest	0	0
	Medium	0	0
	Highest	0	0
2 weeks	Lowest	0	4
	Medium	0	1
	Highest	0	3
3 weeks	Lowest	0	10
	Medium	1	8
	Highest	0	6
4 weeks	Lowest	0	9
	Medium	0	10
	Highest	0	10

Table 1: UPM sensory assessor woolliness classification for Springcrest peaches

4.3 Instrumental procedures

Up to date there is already a proposal for woolliness assessment by instrumental means (Ortiz et al, 1997). To do so, In this study a combination of instrumental cripness and juiciness assessed by shear rupture test and confined compresion test respectively is used. According to the procedure establish there, *Springcrest* and *Miraflores* have been classified into four woolliness categories : *crispy, non crispy-high juiciness, non crispy-medium juiciness and non crispy-low juiciness.* A clustering procedure based on the shear rupture force (N) and the confined compression force deformation ratio (N/mm) has been used to categorise fruits into crispy and non-crispy, and then categorised into different degrees of juiciness within the «non crispy cluster», based on the confined compression juiciness (mm^2). In

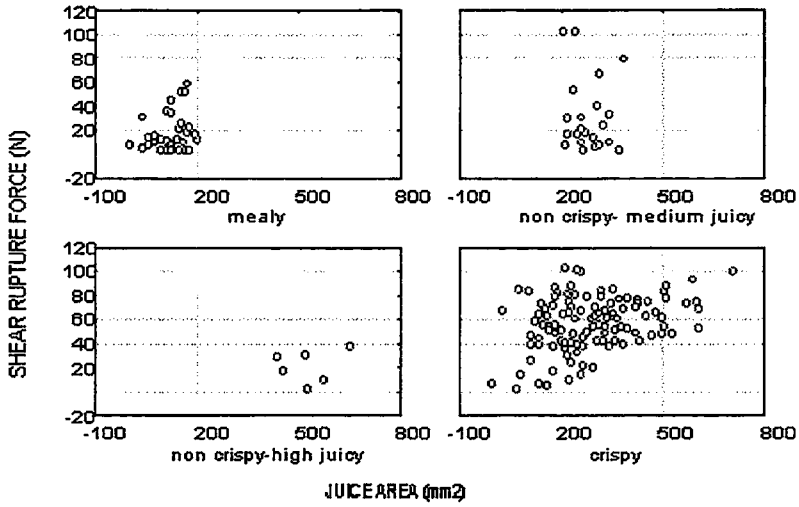

Figure 5: Instrumental segregation of woolly peaches by clustering procedure in Springcrest peaches

Figure 5. Shows that *Springcrest* peaches are mainly classified in the crispy and the mealy (woolly) . There are no many intermediate fruits. However, *Miraflores* peaches are distributed gradually in the four woolliness categories, see Figure 6. Also, it is shown how *Miraflores* peaches have a lower shear rupture force and less variation range of compression juiciness.

Tables 2 and 3 show woolliness onset related to the experimental factors. Crispy and woolly fruits correspond to those shown in Figure 5 and 6. labelled as crispy and mealy clusters. Intermediate clusters in Figure 5 & 6 are not shown in Tables 2 & 3. However, as each sample (each row of tables) is formed by 10 fruits the number of fruits within the intermediate clusters correspond to those missing until 10. For *Springcrest* peaches, fruits labelled as «woolly» appear mainly for 5ºC of storage temperature. The starting point for mealiness onset is 2 weeks. At that point nearly a 50% of the fruits show woolly characteristics for 5ºC storage confirming that this disorder does not appear at the same time for all the fruits.

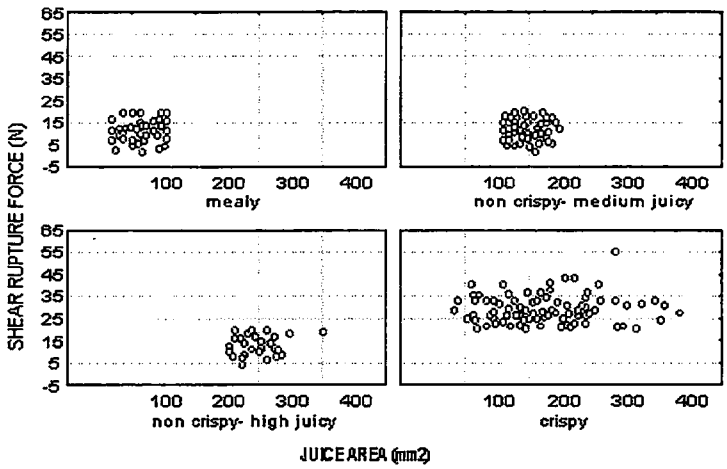

Figure 6: Instrumental segregation of woolly peaches by clustering procedure in Miraflores peaches.

		1°C		5°C	
Storage period	**Maturity stage at harvest**	**Crispy**	**Woolly non crispy, low juicy**	**Crispy**	**Woolly non crispy, low juicy**
0 weeks	*Lowest*	10	0	10	0
	Medium	6	0	6	0
	Highest	2	1	2	1
1 weeks	*Lowest*	10	0	8	1
	Medium	10	0	4	0
	Highest	2	1	0	0
2 weeks	*Lowest*	10	0	5	4
	Medium	9	0	0	4
	Highest	6	0	0	5
3 weeks	*Lowest*	10	0	0	8
	Medium	7	1	0	7
	Highest	5	0	0	1
4 weeks	*Lowest*	10	0	0	7
	Medium	6	0	0	8
	Highest	6	0	3	3

Table 2: Springcrest instrumental classification of woolly peaches

However, in *Miraflores*, fruits classified as woolly by the instrumental procedure do not correspond to the sensory classification (no wooly peaches were identified). Also instrumental classification does not start to detect woolliness at a certain time and at a certain temperature storage as it was in *Springcrest* (see Table 3).

4.4 Comparison between sensory and instrumental results: Conclusions

Springcrest (early and soft flesh peaches) classified as woolly by instrumental means correspond to those defined as woolly by the UPM sensory assessor. *Woolliness appears after 2 weeks of storage at 5ºC, peaches change abruptly from crispy to woolly.* This feature has also been pointed by the sensory panel at IATA (2nd Year Report of the EC Project FAIR CT960302, 1998) where the evaluation of woolliness made by an expert sensory panel shows that peaches stored at 5ºC have a strong increase in sensory woolliness and a strong decrease in sensory denseness, hardness and crispness, after two weeks of storage. These sensory results correspond to those find out with the instrumental procedure.

		1ºC		5ºC	
Storage period	**Maturity stage at harvest**	**Crispy**	**Woolly non crispy, low juicy**	**Crispy**	**Woolly non crispy, low juicy**
0 weeks	*Lowest*	10	0	10	0
	Medium	7	1	8	0
	Highest	7	0	7	0
1 weeks	*Lowest*	9	0	8	0
	Medium	7	0	4	0
	Highest	8	0	7	0
2 weeks	*Lowest*	6	0	4	0
	Medium	4	1	5	0
	Highest	6	0	6	0
3 weeks	*Lowest*	6	1	7	1
	Medium	6	1	9	1
	Highest	4	3	4	2
4 weeks	*Lowest*	3	6	3	0
	Medium	5	0	3	0
	Highest	5	1	7	0

Table 3: Miraflores instrumental classification of woolly peaches

On the other hand, along the storage time, Miraflores (late and hard flesh peaches) have not been classified as woolly by the UPM assessor. They *maintain an intermediate degradation stage* (between crispy and woolly), they had lower shear rupture force and less wide compression juiciness range. Sensory woolliness, hardness, crispness and denseness assessed by the IATA panel maintain their levels during storage (2nd Year Report of the EC Project FAIR CT960302, 1998). They are in a middle stage between crispy and woolly, remain soft but still juicy and do not become woolly during the storage conditions studied. These results do not correspond to those find out with the instrumental procedure. Comparing with *Springcrest*, data it is shown how *Miraflores* peaches start storage with lower crispness (shear rupture force (N)) and have less variation range of juiciness (compression juiciness (mm^2)). *Miraflores* peaches, stored at 5ºC during 4 weeks, are not really woolly when comparing with *Springcrest* peaches. According to this it can be conclude that the *clustering analysis enlarge the woolliness scale and classify as crispy and woolly peaches which are in an intermediate degradation stage.*

These results indicate different degradation patterns in both types of varieties. After comparing with sensory results, it is shown that a common instrumental scale may be appropriate to classify for woolliness all peach varieties.

Acknowledgements

To the EC Project FAIR CT960302 : Mealiness in fruits, consumer perception and means for detection within which this study has been carried out, under which financial aid has been carried this study and to the ALI 94-1082 Project : «Sensing colour stability and mixtures of powder paprika using optical reflectance and image analysis».

References

Various authors. 1996. *Mealiness in fruits, consumer perception and means for detection; Individual Annual Report, 18 months & 2nd Year Report.* EC Project FAIR CT960302.

Barreiro P.; M. Ruiz-Altisent; C. Ortiz; V. De Smedt; S.Schotte; Z. Bhanji; I. Wakeling. 1997. *Comparison between sensorial and instrumental measurements for mealiness assessment in apples. A collaborative test.* Submitted to the Journal of Texture Studies.

Bruhn, C.M.; 1995. *Consumer and retailer satisfaction with the quality and size of California peach.* Journal of Food Quality 18(3) :241-256.

Kailasapathy, K; Melton, L.D. 1992. *Woolliness in stone fruits.* ASEAN Food Journal 7(1) :13-16 .

Lopez, J,L.; Valero, M.M.; Ruiz-Altisent, M. *Mealiness in apples and peaches: a survey on Madrid consumers*. Under correction.

Luza, J.G.; Van Gorsel, R.; Polito, V.S.; Kader, A.A. 1992. *Chilling injury in peaches a cytochemical and ultrastructural cell wall study* . HortScience 117(1) :114-118.

Paoletti, F.; Moneta, E.; Sinesio F. 1993. *Mechanical properties and sensory evaluation of selected apple cultivars* Lebensm.-Wis. u. - Technology 26 :264-270.

Snowdon, A.L. 1990. *Postharvest diseases and disorders of fruits and vegetables.* Wolfe Scientific ltd. Barcelona ISBN 07234 093.

Measuring dynamic viscoelasticity of a microscopic organism

Mesure de la viscoélasticité dynamique d'un organisme microscopique

K. Shigeta R. Otani Y. Nagasaka K. Taniwaki

Dept. of Farm Mechanization
National Agriculture Research Centre
Tsukuba 305, Japan
e-mail: kazuto@affrc.go.jp

Abstract: *A dynamic viscoelasticity measuring system for small-sized bio-materials like small organs or cells has been developed. A mathematical model that describes the experimental system was implemented and the solution in the steady state was given. The control program of an atomic force microscope (AFM) was modified to apply sine waves to a material through the piezoelectric device of AFM. The test material is vibrated up-and-down, bending a cantilever which has been in contact with the upper part of the material. The tip of this micro-cantilever was also modified in order to make flat contact with the material. The linearity of deformation of the vibrating device and the spring constant of the micro-cantilever were measured in order to perform quantitative analysis.*

Dry yeast was used as test sample to investigate the properties of the measuring device. The results showed that it was possible to detect internal losses caused by the viscoelasticity of the yeast.

Keywords: *Dynamic viscoelasticity, AFM, bio-material, micro-cantilever.*

Résumé : Un système de mesure de la viscoélasticité dynamique pour des bio-matériaux de petites tailles tels que les petits organes ou les cellules a été développé. Un modèle mathématique décrivant le système expérimental est mis en œuvre et une solution est donnée en statique. Le programme de gestion d'un microscope à force atomique a été modifié pour appliquer des ondes sinusoïdales à un matériau au travers d'un piezo électrique. Le matériau à tester est mis en vibration (de haut en bas), ce qui fait ployer un cantilever mis en contact avec la surface supérieure. L'aiguille de ce micro-cantilever est également modifiée pour créer un contact plat avec le matériau. On mesure la linéarité de la déformation du système en vibration et la constante du ressort du micro-cantilever pour quantifier le phénomène. Des levures déshydratées sont utilisées comme matériau test pour étudier les propriétés de ce système. Les résultats révèlent qu'il est possible de détecter les pertes internes d'énergie causées par la viscoélasticité de la levure.

1. Introduction

This paper describes a dynamic viscoelasticity measuring system for micro bio-materials like small organs or cells. Measurements were taken to understand the relationship between the displacement of a piezoelectric device on the one hand and applied electric voltage and spring constant of a micro-cantilever on the other.

In order to develop a micro machine using microscopic organisms like proteins or cellulose, it is necessary to measure the mechanical characteristics and electrical properties of these organisms. With regard to the mechanical characteristics of organisms, it is more important to measure dynamic viscoelasticity than static stress and distortion since the viscoelasticity has an effect on the transfer characteristics of kinetic energy and the absorption of applied forces. Although there are several studies about the viscoelastic characteristics of a materialbos surface[1], or metal bars[2], studies about the dynamic viscoelasticity of micro bio-materials are rare.

In conventional measuring apparatus, the displacement of the stress sensor used in the apparatus and the size of the microscopic organism, such as a plant cell, make little difference. Since the displacement of the stress sensor itself is disregarded, it is difficult to use a conventional measuring apparatus for microscopic organisms. Moreover there are no known methods for measuring the dynamic viscoelasticity of a microscopic bodies.

In order to measure the dynamic viscoelasticity of a material, the frequency response of a distortion should be detected with very little stress in a sinusoidal wave applied to the test material. The piezoelectric device of the AFM has a minute vibrating mechanism which allows it to measure the deflection of a micro cantilever which is in contact with the object, by laser and photo detector. In this study, AFM was modified to take dynamic viscoelasticity measurements of a microscopic organism.

2. Dynamic viscoelasticity measuring system

Fig. 1 shows the schematic diagram of the dynamic viscoelasticity measuring system in this study. Since the AFM standard was not fit for measurement, it was modified. The potential amplitude of the AFM piezoelectric device was about 100 nm, too low to adequately deform the test sample. Therefore by modifying the internal hardware of the AFM, the maximum amplitude was increased to about 2 micrometers. Since a feedback loop makes the output from the photodetector constant in normal AFM use, it is impossible to detect the deformation of a test object. Therefore, the control program was modified to follow this deformation precisely by the micro-cantilever. Usually the AFM tip, which is sharpened to get

higher resolution, will damage test samples. Fig. 2 shows the tip processed to give flat contact to the test object by fixed ion beam method (FIB). By such modifications of the original AFM, sufficient vibration amplitude was able to be applied to the object. The micro cantilever which has made flat contact with the top of the object is able to bend to measure the stress which is added to the object.

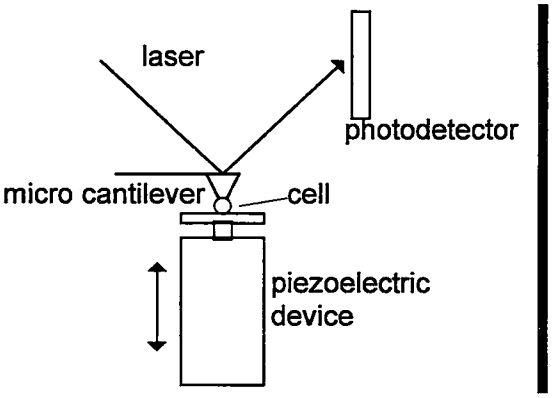

Figure 1: Schematic diagram of dynamic viscoelasticity measuring system

Test sample, such as a plant cell, is set on a stage which is connected to the upper part of the piezoelectric device. As a sine wave is input on the piezoelectric device of the AFM, test object is vibrated up-and-down, bending a cantilever which has been in contact with the upper part of the object. The force added to the sample can be determined from the deflection of the cantilever.

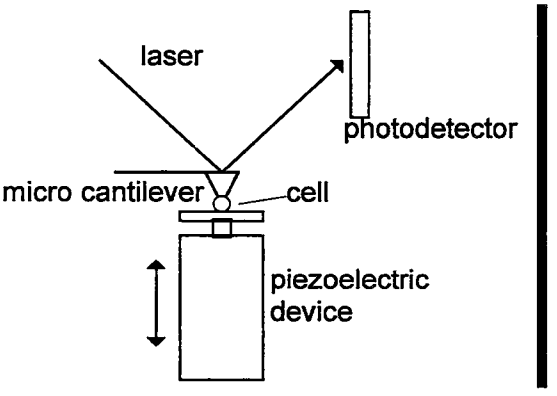

Figure 2: AFM tip processed to make flat contact with the test sample

3. A theoretical analysis of the experimental system

Fig. 3 shows the vibration model of the experimental system. In order to simplify the vibration model of the test system, the following assumption was applied: The mass of the micro-cantilever is concentrated at the tip, the mass of the sample was ignored beçause it was very small compared with the mass of the micro-cantilever, and the sample is a set of the Voigt model. The third assumption was applied because many kind of bio-materials have a characteristic to recover its shape when the applied force removed. By these assumptions, the motion equation of the micro-cantilever is described as follows:

$$m\frac{d^2x}{dt^2}+c_1\frac{dx}{dt}+(k+k_1)x=c\frac{dx_1}{dt}+k_1x_1$$

$$=A\cos(\omega t-\alpha)\ -----\ (1)$$

$$where\ \ A=a\sqrt{(c_1\omega)^2+k_2{}^2},\ \ \tan\alpha=\frac{c_1\omega}{k_1}$$

Where k is the spring constant of the micro-cantilever, m is the mass of the micro-cantilever, c1 is the coefficient of viscosity of the sample, k1 is the spring constant of the sample and "a" is the amplitude of the forced vibration actuated by the piezoelectric device.

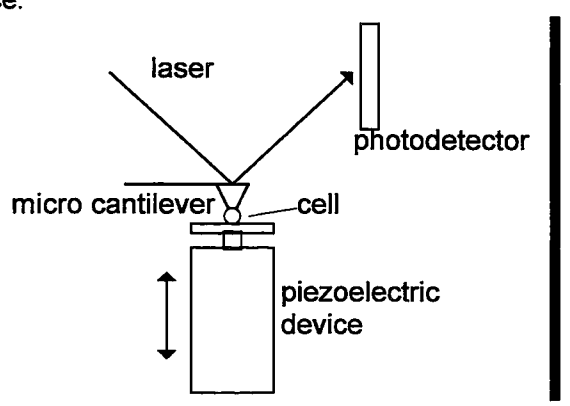

Figure 3: The mathematical model of the experimental system

The solution of the motion equation (1) in the steady state is as follows:

$$x=x_0\cos(\omega t-\delta)\quad -----(2)$$

$$where\ x_0 = a\sqrt{\frac{k_1^{\,2} + c_1^{\,2}\omega^{\,2}}{(k+k_1)^2 + c_1^{\,2}\omega^{\,2} - 2m(k+k_1)\omega^{\,2} + m^2\omega^{\,4}}}$$

$$\tan\delta = \frac{c_1\omega + \dfrac{c_1\omega\,(k+k_1-m\omega^{\,2})}{k_1}}{k+k_1 - \dfrac{c_1^{\,2}\omega^{\,2}}{k_1} - m\omega^{\,2}}$$

By means of measuring x0 and δ, the viscoelastic characteristics can be grasped.

4. Strain linearity of the vibrating device and the spring constant of the micro cantilever

In order to measure the dynamic viscoelasticity of a micro bio-material quantitatively, it is necessary to calibrate the sensitivities of sensors and the linearity of vibrating devices. In this study, a micro-laser interferometer was used to measure the linearity of the piezoelectric device. Fig. 4 shows a schematic diagram of the piezoelectric device deformation measuring system. The beam emitted by the laser diodes is split into two parts, i.e., the reference and measurement beams. After being reflected back by a mirror onto a moving object, the measurement beam interferes with the reference beam. Fig. 5 shows that the deformation of the piezoelectric device was almost linear.

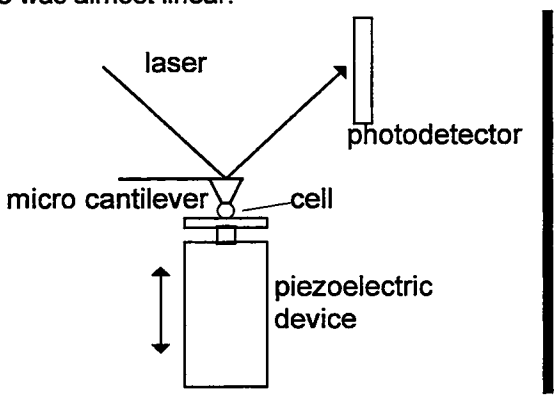

Figure 4: Laser interferometer to measure the deformation of a piezoelectric device

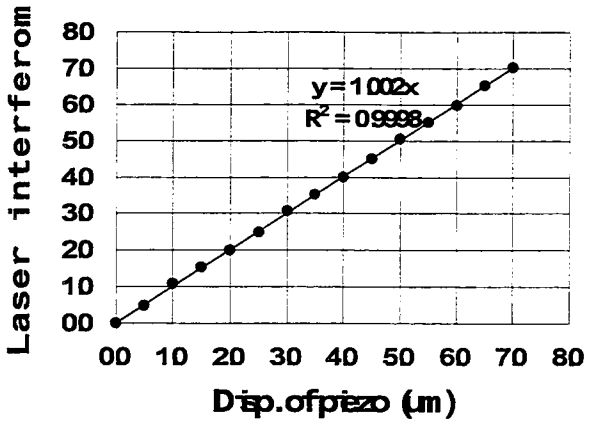

Figure 5: The linearity of piezoelectric device deformation

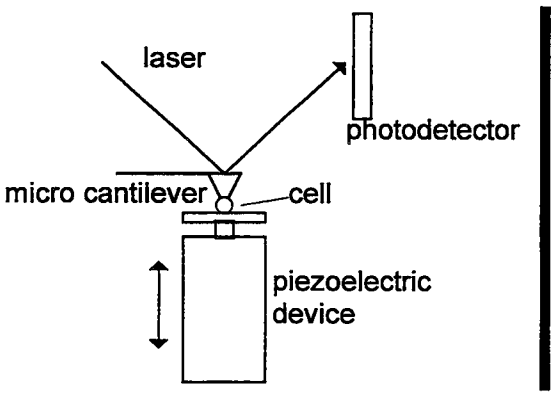

Figure 6: A precision micro balance and a piezoelectric device used for measuring the spring constant of the micro cantilever

The stress applied to test objects is detected by means of converting the bend of the micro cantilever into force. Fig. 6 shows a schematic diagram of the spring constant measuring system.

At the point where the micro cantilever make a little contact with the top of the table of micro balance, the piezo started to deform by 0.5-micrometer steps. Fig. 7 shows the spring constant measurement result used a micro-cantilever which nominal value was 0.2 N/m. Here we can see that the spring constant of the micro cantilever used for the dynamic viscoelasticity measuring system was 0.17 N/m.

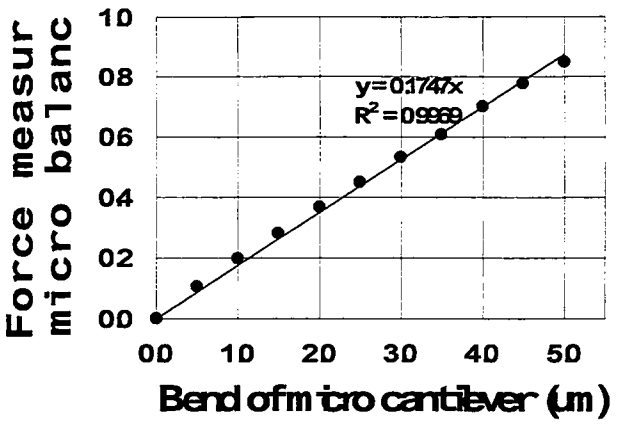

Figure 7: Spring constant of the micro-cantilever

5. Dynamic viscoelasticity measurements

Dry bread yeast of about 3 micrometers in diameter was used as the bio-material sample. Silicon wafers were also measured for comparison. In order to measure one grain of yeast, it is necessary to locate the yeast just under the tip of the micro cantilever. A rough image of the yeast was measured by contact with the AFM in advance, then the top of the image was moved immediately under the tip of the micro cantilever. The piezoelectric device was vibrated in a frequency range from 10Hz to 100Hz and the frequency response of the micro cantilever was measured. It was possible to detect a phase lag of about 55 degrees in the frequency range of 20Hz to 100Hz, which is a time delayed response caused by the inside loss of one grain of yeast (Fig. 8). This method is expected to come into use for many kinds of microscopic organisms. However, in order to apply it to irregularly shaped materials, it is necessary to consider the influence of shape, which can affect the deformation of test objects.

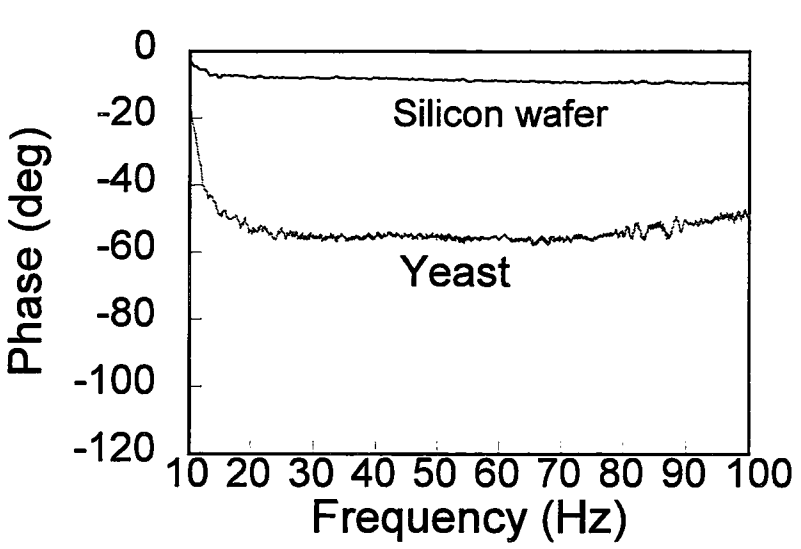

Figure 8: Phase shift of the deformation of dry yeast and silicon wafers detected by the dynamic viscoelasticity measurement system

Conclusion

In order to measure the dynamic viscoelasticity of small-sized bio-materials like small organs or cells, AFM was modified to develop a suitable measurement system. A test specimen is vibrated up-and-down, bending a cantilever which has been in contact with the upper part of the specimen. The linearity of the piezoelectric device deformation was verified and the spring constant of the micro cantilever was measured in order to perform quantitative analysis. Dry yeast was used as a test specimen to investigate the properties of the measuring device. The results showed that it was possible to detect internal losses caused by the viscoelasticity of the dry yeast.

References

T. Kajiyama, 1995. Analyses of Aggregation Structure and Viscoelastic Characteristics of a Polymeric Surface (in Japanese). *J. Adhesion, Vol. 31, No. 9, pp 363-368.*

A. Umeda, et al, 1995. Measurement of the Dynamic Mechanical Properties of Microstructures by Impact, Proc. *Int. Sym. on Microsystems, pp 169-172.*

A review firmness quality measurements in fruits and vegetables

Revue des techniques de mesure de fermeté des fruits et légumes

Itzhak Shmulevich

Faculty of Agricultural Engineering
Technion-Israel Institute of Technology, Haifa, 32000, Israel
e-mail: agshmilo@tx.technion.ac.il

Abstract: *High-quality standards and the need of shelf-life determination for the modern market have heightened the need for on-line evaluation of internal properties for each individual fruit and vegetable. The rapid development of fast and low-cost microprocessors, signal analysis methods and special sensors has opened new possibilities for non-destructive dynamic testing of agricultural products. Important findings in these areas will be summarized and discussed in this work. Research reported on firmness measurement by force, impact, sonic, ultrasonic excitation and other technology such as NMR and Fluorescent Measurement will be presented. More specifically, quality detection by fruit response to acoustic impulse will be given for apples, melons, avocados, mangos, and tomatoes. An example of a state-of-the-art, non-destructive texture evaluation method for classification and quality control of fruits and vegetables will be given.*

Keywords: *Non-destructive, firmness, acoustic, fruit, vegetables.*

Résumé : Les standards de qualité et les besoins de déterminer la durée de vie des produits ont accentué le besoin d'une évaluation en ligne des propriétés internes de chaque fruit et légume. Le développement de microprocesseurs rapides et peu coûteux, de méthodes d'analyse du signal et de capteurs spécifiques ont ouvert de nouvelles possibilités au test dynamique non-destructif de produits agricoles. Les découvertes importantes sont rapportées et discutées dans cet article : mesures par force, impact, excitation sonique ou ultrasonique ainsi que d'autres technologies telles que la RMN ou la fluorescence. La mesure de qualité par la réponse d'un fruit à une impulsion acoustique est décrite pour les pommes, melons, avocats, mangues et tomates. Un exemple de méthode non destructive pour contrôler la qualité des fruits et légumes est donné.

1. Introduction

High-value fresh agricultural products, particularly for export, must be carefully handled and sorted, in order to meet quality standards and customer demand. Many methods are available for quality detection and sorting according to internal and external fruit properties and defects. According to Mohsenin [1], texture, together with appearance and flavor, are three sets of qualities which govern the acceptability of fruit and vegetables by the consumer. In recent years, the demand for higher quality fruits and vegetables has led researchers to develop new technology in order to improve the quality of products in the market. A major contribution to this goal has come from application of developments in the High-Tech areas such as electronics, computers, sensors, materials etc. Researchers are using the technology available to quantitatively define texture, appearance and flavor. Texture can be defined by subjective terms such as: hardness, softness, brittleness, ripeness, toughness, chewiness, smoothness, crispness, oiliness, springiness or firmness. It can also be defined objectively using physical terminology from continuum mechanics such as: elasticity, plasticity, viscoelasticity, or viscosity. This may be the reason that researchers define textural quality in different ways; one may refer to the textural quality "firmness", another may use the terminology "modulus of elasticity" while yet another may grade firmness indirectly by measuring chemical bonds. Absence of one quantitative definition for textural quality has resulted in different understanding of how to define texture and what is so-called «firmness». Because of the different firmness definitions, it is difficult nowadays to change standards of quality used and to switch from destructive methods to non-destructive methods. One of the well known examples is the hopeless attempt of replacing the destructive Magness-Taylor (MT) pressure tester by one of the non-destructive techniques. It is obvious that these two types of techniques measure different physical properties and therefore, can not present firmness using the same unit scale. As a result of this situation, numerous researchers have correlated the performance of their measuring technology with Magness-Taylor measurements, while others have concentrated on the advantages of newer, non-destructive technology. Using non-destructive techniques, one can inspect the same fruit throughout its ripening process to determine the fruits' optimum post-harvest treatment.

In recent years, several reviews have been published by Chen and Sun [2], Sarig [3], and Pitts et al. [4] on subjects directly and indirectly related to firmness measurement. The need for quality detection by firmness technology has encouraged the scientific community to conduct conferences and workshops on non-destructive measurement. Important developments over the past five years have been published in the proceedings of conferences held in Spokane, USA [5], Orlando, USA [6], Tiberias, Israel [7] and others.

Major efforts have been directed towards dynamic quality detection by determining fruits' response to: force; impact force; forced vibrations; mechanical or sonic impulse; and ultrasonic testing techniques; or by measuring the fruits' internal composition. A summary of the findings applying to these methods will be presented. The objective of this paper is to review the non-destructive techniques available to measure the textural quality known as firmness. The review will cover several promising techniques for adapting firmness measurement to on-line sorting of fruit and vegetables.

2. Quality detection by fruit response to force

Several portable devices have been developed, by researchers such as Bellon et al. [8] and Fekete [9], to detect the force and deformation of fruit (about 0.3-0.9 mm). The researchers claim non-destructive operation as a result of using sensitive sensors. High correlation to destructive tests have been reported. Another device, commonly used nowadays for quality detection in tomatoes, is based on pressing a spring-loaded half-sphere indentor, 5 mm in diameter and 2.5 mm in height, into fruit. This device is similar to the method used to define stiffness of plastics and rubber (Shore standard). Mizrach et al. [10] developed a «mechanical thumb» to measure the force deformation of a peel using a spring-loaded pin (3 mm in diameter). The device was constructed on a flexible beam instrumented by strain-gages to measure the beam's deflection. Good results were obtained in sorting tomatoes and Shamouti oranges. Hung and Prussia [11] presented a non-destructive Laser-puff detector to measure firmness of various foods. The excitation of the food was performed by a short puff of pressurized air which can be regulated to a certain degree according to the firmness scale of each product. The deflected surface of the fruit is measured by a laser displacement sensor. The Laser-puff values correlated well (R^2=0.78) with destructive measurements in peaches.

3. Quality detection by impact force

Among the first investigations on impact is the work of Finney et al. [12], who recorded force versus displacement of a pendulum impacting a fruit. No practical conclusions were drawn, however. DeBaerdemaeker et al. [13] suggested determination of firmness according to impact force on apples that were dropped onto a force transducer. The frequency response of the impact was obtained via FFT. Several signal measurements were examined, among them: amplitude of the response at a predetermined frequency, e.g. F250 at 250 Hz, and frequency at which a response is 20 dB lower than at 0 Hz, w(-20). Results were compared to those of MT and standard compression tests. Similar experiments were conducted on blueberries by Rohrbach et al. [14]. The results were compared to impact model results that were developed by Franke and Rohrbach [15]. An impact firmness index, C2 = F_p/T_p^2, was calculated according to the time domain impact response, where F_p is the maximum force and T_p is the time from the beginning of impact until

its maximum. Results indicated that this firmness index is not appropriate for blueberries, although it was later proven to be more appropriate for some other fruit varieties. Delwiche [16] and Delwiche et al. [17] found good correlation between two impact indices and results from MT and standard compression tests. The first impact index was defined as C1 = Fp/Tp and the second was C2, as defined above. Correlation coefficients between the impact parameters and fruit characteristics are presented in Table 1.

reference	Delwiche et al. (1987)				De Baerdemaeker et al. (1982)		Rohrbach et al. (1982)
fruit	peach				apple		blueberry
	C_1	C_2	F275	F295	F250	$\omega(-20)$	C_2
E	0.82	0.85	0.86	0.87	0.68	0.75	0.52
M.T.	0.76	0.75	0.82	0.81	0.77	0.85	------

Table 1: Correlation coefficients between impact force parameters and some fruit characteristics

Nahir et al. [18] found good correlation between firmness of tomatoes predicted according to their impact response and the results of compression tests. Lichtensteiger et al. [19, 20] conducted experiments on tomatoes and concluded that it is possible to sort tomatoes since they show different impact responses at different stages of maturity.

A prototype of a sorting unit, based on the impact firmness index C2, was developed and tested by Delwiche et al. [21]. The fruit, which discharged from a conveyor-belt, hit a piezoelectric force transducer. An on-line computer analyzed the measured impact force and sorted the fruit into three groups - hard, firm, and soft - using a pneumatic device. Delwiche and Sarig [22] developed another impact firmness sensing device, which releases a small mass to impact the fruit. The acceleration of the small mass is used as a measure of the impact force. The signal, picked-up by an accelerometer, is analyzed in the same manner as the impact force response of the drop impact. The impact indices are normalized according to the height, h, from which the mass is dropped. Results for apples, peaches and pears are shown in Table 2 where the impact firmness indices are compared to results from standard compression and MT tests.

reference	Delwiche and Sarig (1991)						Delwiche et al.(1989)		
fruit	apple		peach		pear		peach		pear
	C_2	C_2/h	C_2	C_2/h	C_2	C_2/h	C_1	C_2	C_2
E	0.52	0.53	0.80	0.80	0.68	0.67	0.90	0.90	0.81
M.T.	0.49	0.49	0.87	0.87	0.80	0.81	0.86	0.84	0.78

Table 2: Correlation coefficients between impact force parameters and fruit characteristics

As mentioned by various authors, local variations in texture around the surface of fruit limit the accuracy of firmness prediction by impact testing. This is an inherent disadvantage of the method since the impact force is naturally a measure of local properties of the impact zone, rather than overall properties of the intact fruit. Hertz assumed that the impact pressure for a curved body with a flat surface was distributed as a semi-ellipsoid, erected on a flat contact surface. For the case of dropping a sphere onto a rigid plane, the resulting impact pressure distribution is a hemisphere on the contact area. Based upon the Hertz assumption, it may be possible to relate deformations within the sphere to impact forces for elastic and viscoelastic materials. Luan and Rohrbach [23] and Luan [24] undertook research directed towards developing experimental evidence on the validity of the Hertz assumption by investigating the real pattern of impact pressure distribution during viscoelastic impact. Since the shape of the impact area differs according to the local shape of the fruit, information on local impact pressure distribution may reduce the effect of local variability on impact firmness measurements. Thai [25] presented preliminary tests of a Soft Transducer/Tactile Sensor (STTS). The sensor is a 1 mm thick, resilient foam that changes its electrical resistance when mechanically deformed. Upon impact, the STTS senses changes in volume as opposed to changes in force, as in piezoelectric transducers. The time derivative of the measured signal is used to calculate an apparent coefficient of restitution. This value was found to be independent of drop height and mass of the fruit. The findings can be further explored for various fruits and compared to destructive tests. Schaare and McGlone [26] reported on a SoftSort firmness sensing assembly that is based on measuring the dwell time, which is the half-height width of the force/time peak measured during an impact. The method was used to detect Kiwi fruit firmness by four sensor units made of piezo film sensor under an aluminum and rubber pad. The sensor units were concave in shape. Good sorting efficiency was reported for Kiwi fruit as compared to hand grading.

The advantages of the impact method are its simplicity and speed. The disadvantages are mainly that the method detects local phenomena only and with some technologies, it does not account for the fruits' mass which can, however, be overcome by presorting for size.

4. Quality detection by fruit response to forced vibrations

A vibration test is referred to as an experiment where a fruit is excited by a commercial vibrator on its one side, while the response is measured by an accelerometer or a microphone attached to its opposite side. Usually, the response in time is transformed to give frequency response in order to detect the resonant frequencies of the fruit. The resonant frequencies depend on the mechanical properties of the fruit and therefore can be used to characterize fruit firmness. One of the first studies on non-destructive evaluation of fruit quality factors and their dependence on mechanical properties was done by Finney [27], who reported on a correlation between the extent of fruit ripeness in apples, pears and peaches and the Young's modulus of the fruits. The Young's modulus was calculated according to the resonant frequency of a fruit specimen, which was vibrated at frequencies ranging from 20 - 3000 Hz. The results showed a change in the modulus of elasticity within a range of 3% per day during the last two weeks of ripening. Similar results were reported for bananas by Finney et al. [28]. Finney and Norris [29] found a sound correlation between the modulus of elasticity of whole fruit and fruit specimens, and their resonant frequencies. Abbott et al. [30, 31] vibrated intact fruits, which were hung by their stems, and suggested a firmness index, FI = m $(f_{n=2})^2$; calculated according to the second resonant frequency of the vibrated fruit, $f_{n=2}$, and its mass, m. Finney [32, 33] showed a high correlation between this firmness index, calculated from the response of intact fruit, and the firmness from a standard Magness Taylor (MT) compression test. Utilizing a similar approach, Stephenson et al. [34] and Peleg and Hinga [35] reported good results in separating green from red tomatoes according to the difference in their frequency response. Peleg et al. [36] reported good classification results of avocado based on the same measuring system but using four quantities of modal firmness indexes, which were calculated directly by measuring the input and output vibration signals. A new statistical calibration method was developed by Peleg [37-39] to determine the parameters of a chosen calibration model in the complex domain. This method significantly increases the correlation beyond the value obtained by conventional regression. The method can be used to compare between non-destructive and destructive measurement. Abbott and Massie [40] proposed a non-destructive dynamic force/deformation measurement for kiwi fruit firmness using a force transducer and accelerometer on the head of an electrodynamic vibrator. Both transducers measured the input and output signals from the same side of the fruit. Technically, this arrangement is more convenient for on-line adaptation. From the dynamic force deformation frequency response, they calculated the ratio of the output to input at each frequency, to obtain the frequency response. Using the firmness index term, low correlation (R=0.6) was achieved between dynamic force versus deformation variables and the MT. Improvements on the correlation were achieved (R=0.8) by taking into account the two frequency ranges, using a multiple regression technique.

Cooke and Rand [41] developed a mathematical model for investigating the dynamic response of fruit. The model was based on the classical theory of free vibrations of an elastic body. The mathematical model was used to calculate the free vibration modes of a spherical fruit composed of three layers, each having different elastic properties. The free vibrations of the sphere were divided into three basic classes: (1) spherical, breathing mode of vibrations, S_{0j}, for which the volume of the sphere changes while its shape remains unchanged, (2) torsional vibrations, T_{ij}, for which the volume and shape of the sphere remain unchanged while different parts of the sphere move relative to one another, and (3) mixed modes vibrations, S_{ij} (i >1), for which both the volume and the shape of the sphere change. In addition, a correction of the firmness index, $FI = m^{2/3} (f_{n=2})^2$, was derived from this theoretical study and found to be independent of the fruit mass.

Yong and Bilanski [42] measured the frequency response at the top and side of a fruit and derived the modal shapes of vibrations. The first resonance was found to be similar to a single degree of freedom system (SDOF), where most of the fruit may be considered as a solid mass. Only a thin layer, at the point where the fruit rests upon the vibrator, may be considered as a spring and dashpot. The second resonance was found to be a mixed mode of vibrations - S_{20} - which is called the oblate prolate mode. The higher resonances were assumed to be of the same type but of a higher order - S_{30}, S_{40} etc. These conclusions were experimentally confirmed by Van Woensel et al. [43, 44].

Rosenfeld et al. [45, 46] developed a Boundary Element simulation which extends the model of the elastic sphere of Cooke and Rand [41]. The simulation provided the acoustic response of a viscoelastic fruit, of arbitrary shape, that was excited at its bottom. The numerical simulation yielded the shapes of the first and second vibration modes which were experimentally detected in previous work. The simulation also showed the dependence of the resonant frequencies on the viscoelastic properties of the fruit, as well as on its mass. The results corroborate the fact that it is possible to sort fruit for firmness when the mass and the resonant frequency of the fruit are known. Chen and De Baerdemaeker [47, 48] and Chen et al. [49] analyzed the modal shapes of fruits using a finite element model. Kimmel et al. [50] used a lumped parameter model, based on a multidegree-of-freedom system (MDFS), and verified the modal shapes of fruits.

A comparison between three experimental studies on a red delicious apple is given in Table 3. The results show a marked difference in the value of the first resonant frequency. The second and third resonances have similar values, although the fruit differs in mass.

Reference	f_1 (Hz)	f_2 (Hz)	f_3 (Hz)	f_4 (Hz)	m (gr)
Finney (1970)	350	950	1500	1800	200
Abbott et al. (1968a)	80	900	1600	------	157
Yong et al. (1979)	110	900	1400	------	------

Table 3: Resonant frequencies of an apple (red delicious) obtained by different vibration systems

An explanation of the large variation in frequency for the first resonance lies in the difference of the excitation methods used by each of the investigator. The high value found by Finney is due to the large contact area between the fruit and the vibrator; whereas Abbott excited the fruit using a pin that was inserted into the flesh of the apple resulting in a small excited area. This leads to the conclusion that when vibrating a fruit, the first resonant frequency is not an appropriate measure for fruit properties since it depends on the area of excitation. This area differs according to the local shape of the fruit and the vibrating device. Additional work in this area was performed by Affeldt and Abbott [51].

Pitts et. al, [52] found that the Peleg Firmness Tester (PFT) was sensitive to apple size and location of the sensor, but not to varieties of apples. Van Woensel et al. [53] used a spectral analysis method to follow the ripening of apples during their storage. A wide band random vibrator of the range 0 - 1,600 Hz was used to excite the fruit. The results showed a clear change in the firmness index during the entire season. In a following research, Van Woensel et al. [43] found a good correlation between indices calculated from vibration tests and fruit texture and its acceptability to the consumer.

From the studies presented, it can be concluded that the forced vibrations technique is feasible as a method for detecting maturity and degree of ripeness of fruit. Nevertheless, these findings have not yet led to the construction of an on-line quality sorter, mainly because of problems associated with coupling the measuring device to each individual fruit.

5. Quality detection by a mechanical or sonic impulse

Several researchers have studied fruit response through mechanical or sonic impulse excitation. Garrett and Furry [54] used a modified audio speaker to induce a force impulse through an apple. The propagation velocities of sound waves were measured to calculate the mechanical properties such as Young's modulus, tissue density and Poisson's ratio of the apple. Clark [55] used a similar method and found high correlation between the decay time of sound waves crossing watermelons and their firmness. It was found that sound decay time increased with watermelon

ripeness. This work was further developed by Robinson [56] who designed equipment appropriate for ripeness detection in watermelons, based on acoustic decay time.

An alternative method for evaluating textural quality via frequency response was suggested by Yamamoto et al. [57, 58]. The fruit was placed on a rigid surface and hit by a pendulum. The acoustic emission was sensed by a microphone and the signal was analyzed using an FFT algorithm to extract the fruit's resonant frequencies. The researchers showed a significant correlation between the acoustic parameters of apples and their apparent Young's modulus, ultimate strength and firmness. The correlation for watermelons was poor. Abbott et al. [30] indicated similar resonant frequencies for the same modes of vibration, which were excited by forced vibrations. Table 4 compares the results for an apple from the work of Yamamoto et al. [57, 58] and Abbott et al. [30].

Reference	f_1 (Hz)	f_2 (Hz)	f_3 (Hz)	f_4 (Hz)	m (gr)
Yamamoto et al. (1980)	------	800	1190	1550	------
Abbott et al. (1968a)	80	650	1100	1460	155.7

Table 4: Resonant frequencies obtained from mechanical impulse and vibration test on apples (golden delicious)

The first mode from Abbott's vibration test does not appear in Yamamoto's study, since it is a forced vibration mode, as previously explained. To prove this hypothesis Van Woensel et al. [44] used the following two experimental set-ups to measure the resonant frequencies and damping ratios: (1) forced vibrations by the standard vibrating method, and (2) free vibrations by a small pendulum which hit the fruit that was hung by its stem. They found that the first resonance measured by the forced vibrations setup was not detected by the free vibrations setup, which measured natural frequencies only. The frequencies and damping ratios of the higher modes of vibration, measured by the two experimental setups, were very close to each other. These results confirmed the findings of Yong and Bilanski [42], that the first resonance is of a SDOF type, and the higher resonances are of the mixed modes.

Armstrong et al. [59, 60] caused vibrations by striking the apple with a ball of wax. Young's modulus, calculated from the acoustic response, highly correlated with that measured in compression tests of specimens taken from the same fruit. Poor correlation was found with the results of a standard MT test. Good repeatability results were obtained from impulses applied at the equator of the apple, while those applied at the stem or blossom ends and detected at the equator did not show good results. Chen, P. et. al. [61] reported good correlation of the first two resonant frequencies between acoustic sensing and human auditory sensing. In the

experiments, several apple varieties were struck mechanically while fruit response was detected by a microphone. Significant differences were not found among sound signals obtained at different locations tested around the fruit. Chen, H. et al. [62] tested apples and concluded that the acoustic impulse response method appears to be more efficient and accurate than random vibration methods, and the instrument, more practical to use. Sugiyama et al. [63] developed a portable firmness tester for melons. The device was based on detecting the response of a melon, by two microphones, resulting from mechanical impulse excitation. Correlation of about R=0.943 was reported between the transmission velocity measured by the microphones and the apparent elasticity of the melons, measured destructively. Farabee and Stone et al. [64] developed a nondestructive firmness tester to measure the maturity of watermelon using sonic impulse. The probe is a closed end, plexiglass cylinder approximately 5 cm in diameter and 15 cm long. A thin, disk shaped ceramic piezoelectric element, bonded to a similar sized thin brass disk, was mounted at the end of the cylinder in contact with the melon. A solenoid, inside the cylinder, was used to deliver a mechanical impulse to the flat face of the piezo ceramic. The impulse is transferred through the ceramic to the watermelon. The resulting vibration of the melon, due to the impulse, drives the piezo element. The signal from the element was amplified and filtered through a fourth order low-pass active filter before digitization by the data acquisition unit. This equipment was used by Armstrong et al. [65] in recent research to detect internal damage of watermelons and by Stone et al. [66] to detect watermelon maturity in the field.

Thus, several techniques are available for fruit quality evaluation through mechanical and acoustic excitation. The most promising quality factor seems to be the resonant firmness index, calculated through impulse excitation. Analysis of the response to a mechanical impulse is a feasible method to obtain the firmness index, and can be adapted more easily to sorting machines. However, as stated by Pitts et. al. [4], judging the effectiveness of a new sensor system for fruits can be a very difficult task; besides the variation capability in the sensor system and the sensor's correlation to firmness, there is variation in firmness around the fruit as fruit size changes.

These investigations of the response of fruit to a mechanical or sonic impulse indicate that this method is reliable and easy to apply. However, the excitation method and measuring techniques must be further developed and adapted to actual conditions in a sorting process.

6. Determining fruit properties by ultrasonic techniques

Ultrasonic diagnostic testing is a well-established, non-destructive technique used in medical and industrial applications. In industry, these techniques are used to detect internal defects such as air pockets and cracks in welding and casting, whereas in medicine they are used to determine normal and abnormal tissues, as well as internal structure of organs in the human body. The frequency of ultrasonic waves is a very important factor in fruit penetration, since the attenuation of high frequency waves in fruit tissue is very high. Sarker and Wolfe [67] found high attenuation coefficients of ultrasonic waves at the frequency range of 0.5 - 1 MHz in tissues of potatoes, cantaloupes and apples, due to the porous nature of these tissues. They pointed out that at lower frequencies (100 - 500 kHz), a transducer of higher energy output might be useful in fruit penetration. They also proposed a method for ultrasonic measurement of the smoothness of citrus fruit peel and detected skin cracks in tomatoes by analyzing the reflected signals. Arad et al. [68] carried out various tests, including transmission of light, specific gravity, radiography and ultrasound, for predicting failure in melons. Results showed that the ultrasonic technique was the most promising when compared to the other methods. It was pointed out that the detection capacity of the technique could be significantly improved if more appropriate equipment was available.

Spectral analysis of ultrasonic acoustic waves was investigated by Upchurch et al. [69, 70], for the purpose of detecting damage in apple tissue. It was observed that undamaged tissues contained a larger percentage of air space than that of damaged tissues. However, due to the high acoustic impedance and attenuation coefficient of apple tissue, this change in tissue construction could not be consistently detected by using the ultrasonic technique.

A comprehensive review of techniques for detecting hollow heart in potatoes was presented by Watts and Russell [71]. The authors pointed out the advantages of the ultrasonic testing for detection of internal defects in potatoes which included its freedom from radiation hazards and the possible ease of automation. They also indicated several challenges to be overcome before ultrasonic methods can be used commercially. These included development of a proper transducer, and selection of the optimum frequency to obtain reproducible results with maximum resolution.

Mizrach et al. [72] investigated problems in determination of fresh fruit and vegetable properties by ultrasonic excitation. Specimens of the selected fruit were tested using a high power, low frequency ultrasonic instrument. Two 50 kHz transducers were used to determine the sound velocity and attenuation coefficient by the through–transmission method. Reflection properties of the tissue were measured using a single 500 kHz transducer operating in the pulse–echo mode.

The results demonstrated the feasibility of low frequency ultrasonic testing of agricultural products. Mizrach et al. [73, 74] studied acoustic, mechanical and quality parameters of melons and avocado using a 50 kHz transducer. the attenuation signal correlated well with firmness in 'Ettinger' avocados. Low correlation was found for Galia melons.

The literature survey indicates that ultrasonic techniques can be used to detect some local properties and specific defects in selected products. Yet, the commercially available, low frequency ultrasonic transducers are suited for laboratory use only, because of their large dimensions, rigid construction, and poor coupling features. The success of firmness measurement is limited to certain fruits.

7. Indirect firmness measurement

As stated by Pitts et al. [4], physiological changes that take place during softening of fruit or vegetables could affect the state of the water in the fruit or the relative proportion of water found in intercellular spaces. This would indicate the potential for correlation between firmness and the magnetic resonance signal. Stroshine et al. [75] used low resolution NMR to detect firmness of fruit and vegetables. This method measured the response of photons to the external magnetic field. This technology is suitable for detecting internal properties and defects as was demonstrated by Cho and Chung [76]. Although they correlated the measurements of NMR to sugar content, it showed the potential of the method to detect firmness in fruit, which exhibits changes in sugar content during the ripening process. Abbott et al. [77] and Beaudry et al. [78] showed the potential of measurement by fluorescence to detect fruit firmness. DeEll et al. [79] concluded that there is reasonable correlation (R=0.79) between measurement of fluorescent parameters and firmness in McIntosh apples but very low correlation was found for Delicious and Golden Delicious.

In general, nondestructive technology that detects internal properties may correlate well with firmness measurement in fruit when their internal properties change during ripening.

8. Example of experimental work

The technique used by Shmulevich et al. [80] and Galili et al. [81] was chosen to demonstrate a non-destructive measurement technique on apples, pears, tomatoes, mangoes, avocados and melons. Similar methods used by other researchers perform comparably, as was found by Galili and DeBaerdemaeker [82]. The data presented below shows the potential of non-destructive measurement. There are some difficulties due to the large variation of the data and the need to present the non-destructive tests by various acoustic factors. Results from the non-

destructive tests are also compared to destructive measurements. Possibilities for future developments using this technique will be discussed.

8.1 Piezoelectric-film based measurement system - Firmalon

An upgraded version of the piezoelectric-film based measurement system - Firmalon - (reported by Shmulevich et al., [83]) was constructed by Eshet Eilon Ltd., Kibbutz Eilon. A schematic view of the system is shown in Fig. 1. The system includes a force transducer to detect the fruits' mass, an instrumented fruit-bed with three equally-spaced piezoelectric sensors, and three electro-mechanical impulse hammers. The piezoelectric sensors are composed of a polyvinylidene fluoride film bonded to a soft polyethylene-foam padding, to enable free vibrations of the fruit. The impulse devices, consisting of a push-type solenoid and a pendulum, are located opposite the piezoelectric-film sensors. The piezoelectric sensors and the force transducer are coupled through an amplifier and an A/D board to a PC, which serves for data acquisition and signal analysis. The signal produced by the sensors is sampled at a rate of 5,000 samples/sec per sensor for 30 ms.

A data acquisition computer program (Test-Point®) was used to control the test operations, to select the resonant frequencies and to calculate the acoustic parameters of the fruit. The tested fruit is placed in the fruit-bed with its stem-calyx axis in the vertical position (when symmetrical fruits are used) and tapped sequentially by the three excitation devices. An average of the two closest first resonant frequencies (out of the measurement of the three sensors) is calculated and used for firmness evaluation.

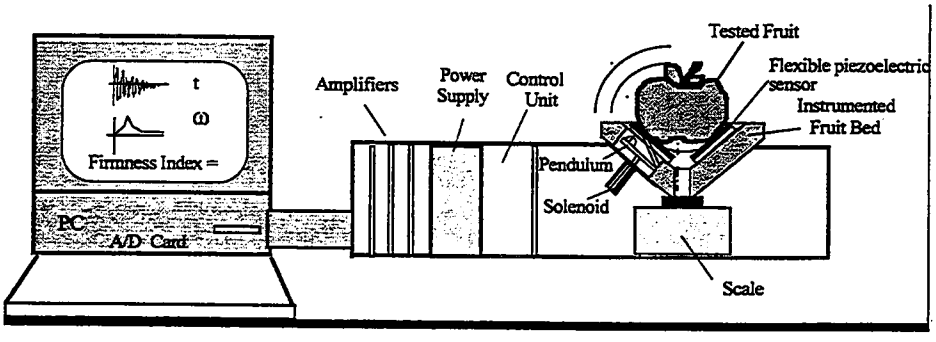

Figure 1: Piezoelectric-film based firmness measurement system - Firmalon

8.2 The acoustic parameters of a fruit

8.2.1 Natural frequencies and firmness index

In the work reported here, the natural frequency of the fruit was measured by a piezoelectric film that senses the vibrations of the fruit. The spectral analysis of the signal follows the same procedures as those for general vibration testing of structures. However, for automated, on-line firmness testing of fruit, the analysis methods used should ensure that the first mode of vibrations is detected even in the case of non-uniform and irregularly shaped fruit. An automated search algorithm was used to identify the first frequency of fruit response to impulse excitation. The conventional expression of Eq. 1 was employed for the firmness calculation, even though the fruits were not always spherical.

$$FI = f^2 m^{2/3} \qquad (1)$$

where: f is the first spheroidal resonant frequency of vibrating fruit and m is the fruit's mass. In the following examples, the firmness index of fruits will be expressed in the FI units (10^4 $kg^{2/3}$ s^{-2}).

8.2.2 Damping ratio

Damping in fruit may be associated with fruit maturity, degree of ripeness and composition of the fruit tissue. A simple and fast algorithm was developed for the calculation of the damping ratio for a specific resonant peak (see Galili et al., [81]):

$$\zeta = \frac{\left|1-\omega'^2\right|}{2\left[\left(\frac{H_m}{H}\right)^2 - \omega'^2\right]^{1/2}} \qquad (2)$$

where: H_m is the peak amplitude of the model, H is the signal amplitude at a frequency ω,ω_n is the resonant frequency and ω' is the frequency ratio ω/ω_n. The advantage of the suggested algorithm is its capability for fast calculation of the damping ratio for each discrete point in the frequency spectrum. In addition, since the first resonant frequency is of interest, only left-hand discrete values close to this frequency, which are less affected by the presence of higher (right-hand) resonant frequencies, are used. The expression described above was used for damping evaluation in sensitive fruit such as avocados, mangoes and melons.

8.2.3 *The centeroid of the frequency response*

An additional frequency-related parameter, denoted as f_c - the centeroid of the frequency response - was derived (see Galili et al. [81]). Since the digitized signal is equally spaced, a simple algorithm could be written as:

$$f_c = \frac{\sum_{i=1}^{n}(f_i H_i)}{\sum_{i=1}^{n} H_i} \qquad (3)$$

Here, f_i and H_i are local values of frequency and amplitude of the signal, respectively, and n is the total number of data points. The value of f_c does not depend on a specific resonant frequency, but on the entire spectrum of the frequency response; a feature that may be important when testing asymmetric fruits that have several closely spaced resonant peaks. The acoustic parameter, f_c, can be used to distinguish between fruit that exhibits different acoustic signatures; for example, damaged vs. undamaged fruit.

8.2.4 *Evaluation of acoustic signals*

Typical acoustic signals of a 'Jonagold' apple and a 'Flandria' tomato, acquired by piezoelectric-film sensors, are shown in Fig. 2 (Galili et al. [82]). Both fruits exhibited similar acoustic response with one dominant peak amplitude at the three locations (289 Hz and 674 Hz, respectively). The input signal, produced by electromechanical impulse hammer, varies for different fruit, as can be seen in Figs. 2a and 2d. In this technique, the input excitation energy is constant while the measurements detect the fruit's response on the opposite side of the fruit.

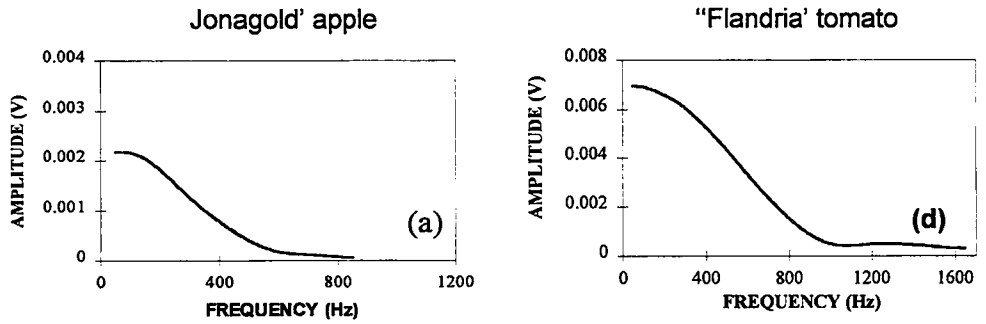

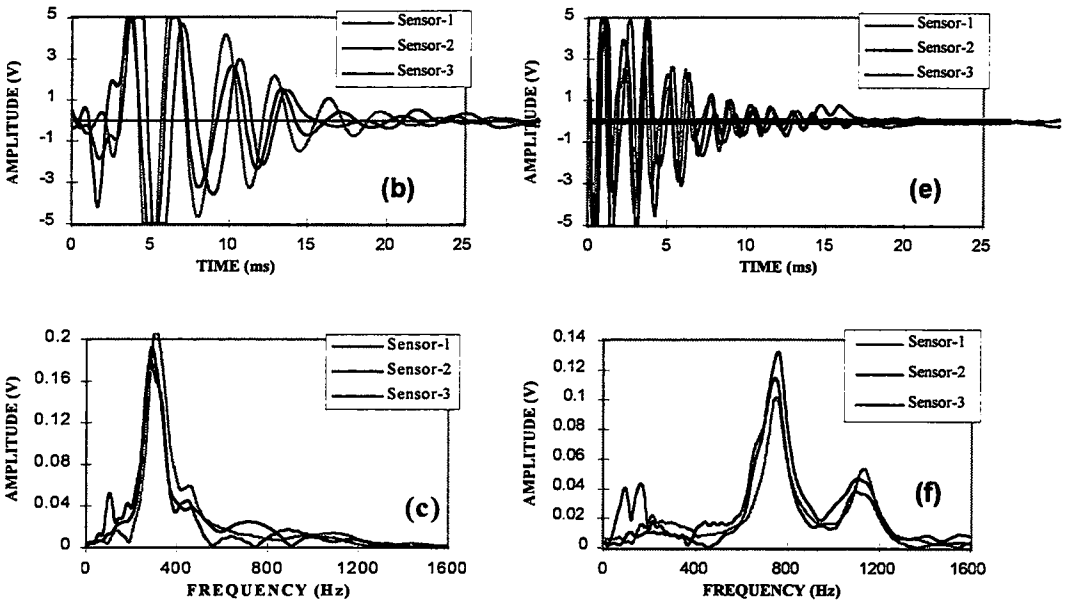

Figure 2: Typical acoustic signals of a 'Jonagold' apple (a, b, c) and a 'Flandria' tomato (d, e, f). Figures a and d are the input signals, b and e are the time domain signals and c and f are the frequency domain signals

Typical results of a melon's response in the time and frequency domains are presented in Fig. 3. In the frequency domain, the signals were shifted upward by 0.1 normalized units in order to show their behavior more clearly. It can be concluded that the three sensors measure the same frequency response, independent of sensor location. For Galia melons, at least five natural resonant frequencies were detected in the frequency spectrum.

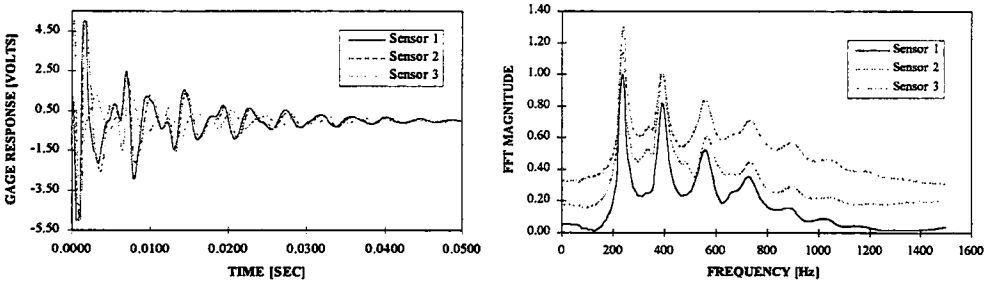

Figure 3: Typical signal for a melon, in the time and frequency domains

8.3 Acoustic and destructive tests of Israeli apples

500 apples of three varieties: Red Delicious, Golden Delicious and Granny Smith, were tested with the cooperation of the Israel Fruit Growers Association Cold Storage Research Laboratory in Kiryat Shmona. The apples were taken from orchards and stored in a controlled room, 20^0 C and 50% RH, for approximately one month. During storage, acoustic properties of all the apples were measured by the Firmalon device. In addition, on six different days, groups of 80 apples were tested destructively by the Magness-Taylor (MT) device. The acoustic test results for the last group of 80 apples were analyzed to determine whether the acoustic method follows the ripening of fruit during storage. The MT tests were the average of two tests taken from opposite sides of each apple. The accumulated data of all tests was used for comparison between the destructive MT tests and the Firmness Index (FI) tests.

A summary of the firmness index measurements for 80 Golden Delicious apples and their average values versus time is presented in Fig. 4.

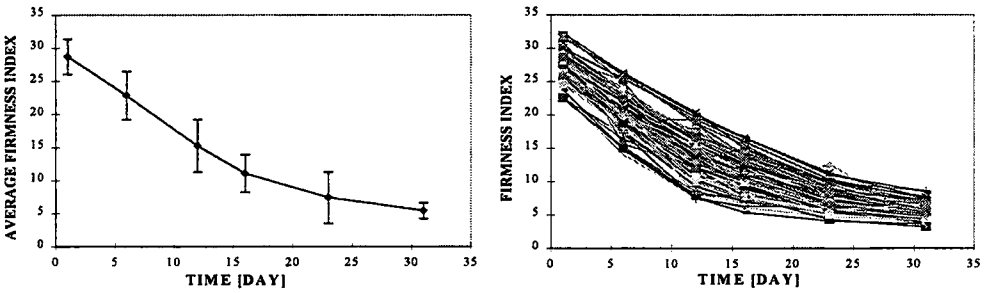

Figure 4: Firmness Index and average firmness index vs. time for 80 golden delicious apples

As expected for biological material, results from different fruits show a wide range variation. A fitted linear curve was applied to the data, as shown in Fig. 5a. The required shifting of each experimental point to the average curve was then found and an average shifting factor was calculated for each fruit. A new presentation of the Firmness Index versus the new "biological age" (after shifting each experimental point according to the average shifting time factor) was performed for all the experimental data. Figure 5b shows the FI versus "biological age" for 80 Golden Delicious apples after the time shifting process. The results demonstrate that the data spread in Fig. 4 is now fitted to a polynomial curve with a high correlation of R^2=0.93. Similar results were observed for the other two apple varieties. The method described provides a ripening master curve for monitoring fruits in storage. When the FI value is known upon storage, this curve can predict the time required to reach a certain quality index of fruit during storage.

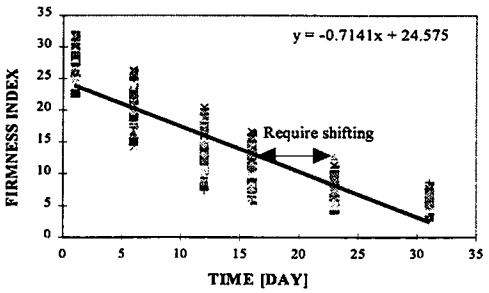

Figure 5a: Demonstration of the time shifting factor

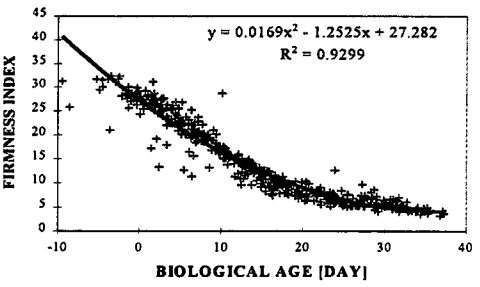

Figure 5b: Firmness Index vs. «biological age» for 80 golden delicious apples; after the time shifting process

The prediction equation needs to be verified for a wider range of apples from the same variety (for example, apples from different orchards, different management and post-harvesting techniques, different seasons, etc.).

A comparison between the MT and FI test results in Golden Delicious apples is presented in Fig. 6a. No correlation was found between the MT and FI for this storage condition. In addition, a low correlation was found between the two MT measurements taken from opposite sides of the same apple (not shown in the figure). Figure 6b shows the average FI, the average MT and the standard deviation for each day of measurement versus storage time. Figure 6b demonstrates why there is no correlation between MT and FI; the MT of the different fruits does not change much during the thirty days of shelf-life, while the FI values decrease with time. It was concluded that FI is much more sensitive to the ripening process of apples during shelf-life, as compared to the MT. Similar findings were reported by Galili et al. [84].

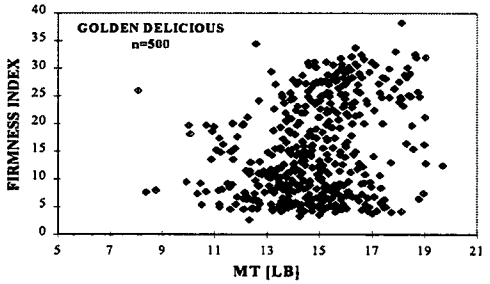

Figure 6a: Firmness Index vs. MT for 500 golden delicious apples

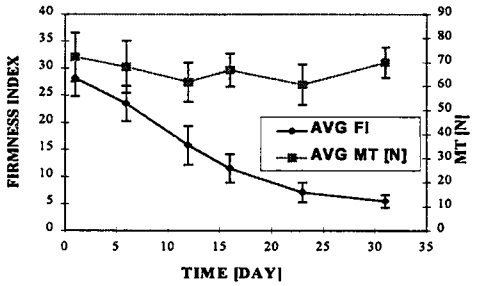

Figure 6b: Average Firmness Index and average MT vs. time

8.4 Acoustic and destructive tests of Washington apples

A full scale study of apple firmness was initiated at commercial facilities, Stemilt Growers, Inc., in Wenatchee, Washington State. The test program included seven apple varieties: Fuji, Braeburn, Gala, Granny Smith, Jonagold, Red Delicious, Golden Delicious, and D'Anjou pear variety. The fruits were stored in a commercial controlled atmosphere (CA) and tested every month for acoustically (Firmalon) and destructively (MT). Two trays, including twenty fruits of each variety, were tested nondestructively by the Firmalon and stored again in the CA rooms. Two more trays of each variety were removed from the CA storage and tested by the Firmalon and then the destructive MT test. The main findings of this study will be given for D'Anjou pears and Golden Delicious apples.

Figure 7 demonstrates firmness index versus time and "biological age" for 40 D'Anjou pears. The FI decreased dramatically from approximately 25 to 5 (FI units) over a period of 100 days. Thereafter, the FI remained almost constant. After shifting the time to biological age, with the procedure described above, a polynomial fitting curve of the second order fits the experimental data for the 40 D'Anjou pears with a correlation of R^2=0.958.

An example of firmness index versus time and "biological age" for 40 golden delicious (group 1) apples is given in Fig. 8. The figure shows that the 40 fruits decreased in firmness, on average, from approximately 30 to 23 (FI units). The inclination of the decrease is almost parallel. After shifting the time to "biological age", with the procedure described above, a linear fitting curve fits the experimental data of the 40 golden delicious apples with a correlation of R^2=0.928.

The FI prediction equation vs. "biological age", that was developed for the golden delicious apples (group 1), was applied to another 40 golden delicious apples (group 2). A correlation of R^2=0.764 was achieved between the measured data and the prediction curve.

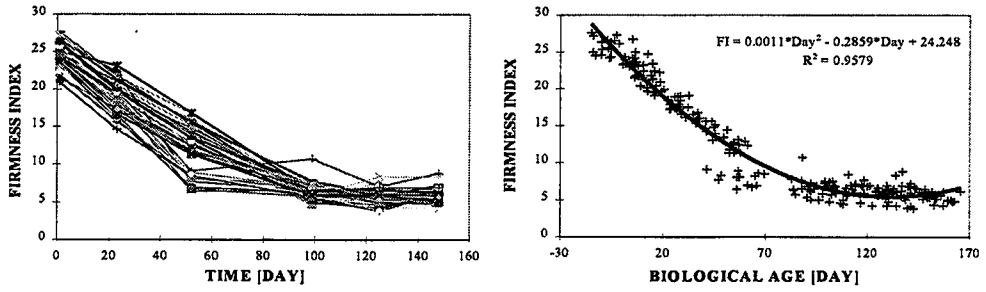

Figure 7: Firmness Index vs. time and «biological age» for 40 D'Anjou pears

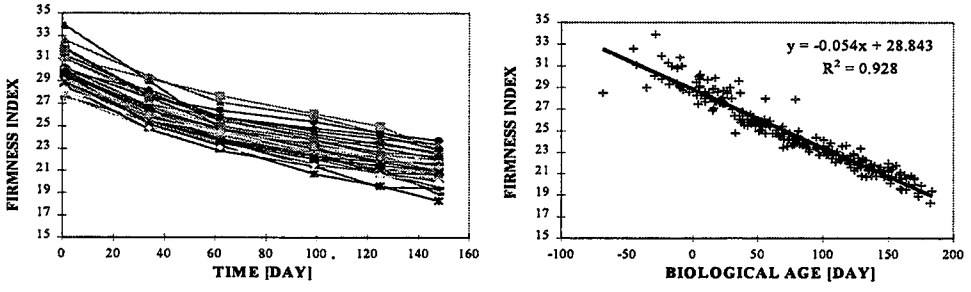

Figure 8: Firmness Index vs. time and «biological age» for 40 golden delicious apples

Similar results were obtained for the other apple varieties. For practical use, after developing the master curves and verifying the findings, growers can better design and control fruit production. The growers can develop time prediction tables for each fruit variety and its specific treatment from harvesting to marketing. According to this concept, by providing the Firmness Index measured value and a target minimum Firmness Index at storage, the grower will be able to predict the duration of storage.

8.4.1 Changes of firmness index and penetration force with time

A comparison between average measurements of non-destructive and destructive tests for apples and pears over time are given in Fig. 9. As in Fig. 6b, both cases demonstrated that the MT tests did not detect the ripening stage of the fruit over time while the FI did detect the ripening stage. The results for pears were even more convincing.

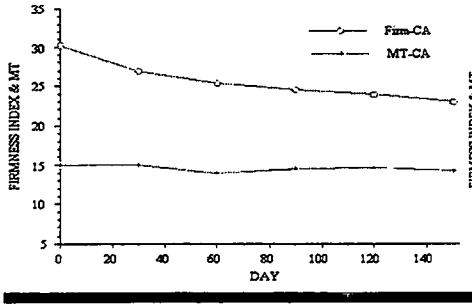

Figure 9a: Average Firmness Index and MT vs. time for golden delicious apples

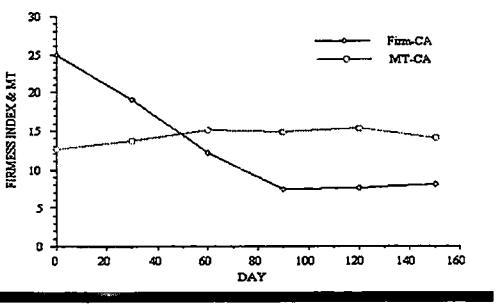

Figure 9b: Average Firmness Index and MT vs. time for D'Anjou pears

8.4.2 Correlation between FI and MT

One of the main purpose of the study was to look for a nondestructive method that may replace the destructive MT test. As shown in the figures, the storage conditions affected the acoustic FI, and did not affect the values of the penetration force very much. The different behavior of MT and FI during storage makes this task difficult. The correlation obtained between the two was quite low, and more work should be performed on this subject. Fairly good correlation was obtained between the destructive and nondestructive measurements on the first day of testing, before the long-term CA storage.

MT versus FI test results for all varieties except Red Delicious, before storage, are presented in Fig. 10a. Quite surprisingly, all the different fruit varieties fall on a linear curve (R^2 = 0.857), where the highest values of MT and FI belong to the Braeburn apples, and the lowest values to the D'Anjou pears.

The MT versus FI ratio for Red Delicious apples was different than that of the other fruits (Fig. 10b). As shown in the figure, the Reds seemed to be more firm than predicted by the acoustic tests. One possible cause for this phenomenon is the specific shape of the Washington Red Delicious apples, which are characterized by several lobes. This structure results in more complex vibration mode shapes which should be analyzed more carefully by a refined sorting algorithm.

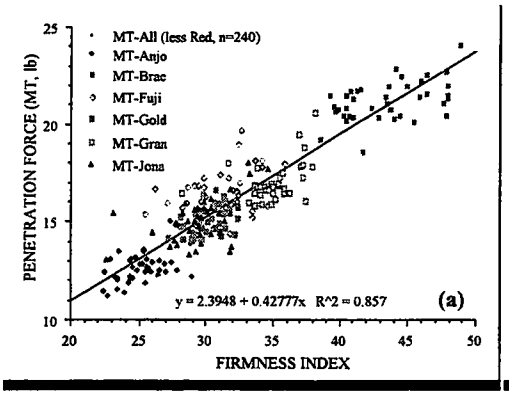

Figure 10a: Firmness Index vs. MT for several fruits except red delicious

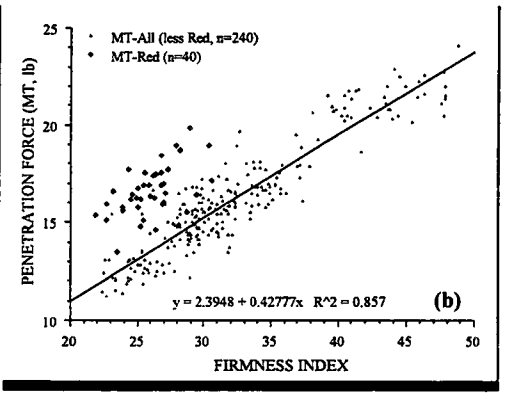

Figure 10b: Firmness Index vs. MT for several fruits (including red delicious)

Figure 10a was intended to meet industrial expectation: to define a one-to-one ratio (of the same numerical values) between the acoustic test and the MT. Again, these type of curves should be verified experimentally for different growing areas, harvest seasons and storage conditions.

8.5 Acoustic and destructive tests for mango fruits

Following the 1994/96 mango seasons, a modified version of the fruit bed and the operating program was constructed and tested at a fruit processing company in the Jordan Valley, Israel - Tzemach Avocado. A Firmalon device with one impulse hammer and one piezoelectric transducer was used to evaluate the mango's ripening process. A simulation of the fruit's shipping, for export, was conducted on 96 Tommy variety mangoes.The mangoes were placed in cold storage (12^0 C, 90 % RH) for 5 days and then 10 days at 20^0 C, 55 % RH. At the end of the storage period, the mangoes were tested destructively. Five penetration tests were conducted on each fruit, using an Instron loading machine and a conical probe of 600 and 6 mm in diameter. The rate of loading was 50 mm/min.

Figure 11 demonstrates the ripening of the 96 mango fruits and the FI vs. storage time. As was expected, during the first period of cold storage, the FI decreased slowly as compared to the second storage period at room temperature. The FI decreased by and average of 1.22 FI units per day for the export simulation.

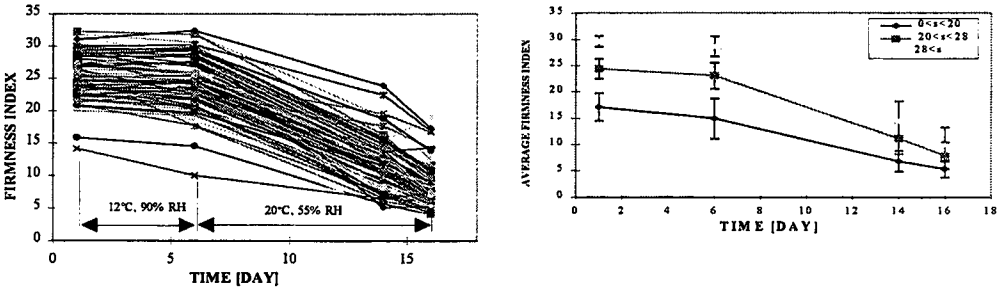

Figure 11: Firmness Index vs. time for 96 Tommy mangoes; during two storage periods and after sorting according to three Firmness Index groups

Figure 11 (on the right) shows mangoes that have been divided into three groups, according to the average of their FI measurements on the first day of testing. It was found that the mangoes remained in the same group throughout the experiments.

The average maximum penetration force (from five tests on each fruit) was correlated with the acoustic measurements and was found to be R^2=0.7705. Comparable studies were conducted on Kent and Keitt mango varieties. Results of these studies were similar to the Tommy variety.

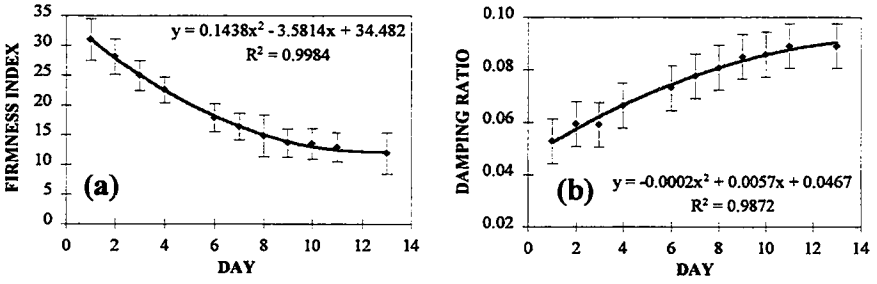

Figure 12: Average FI and damping ratio during the ripening process for 23 Kent mangoes

Figure 12 demonstrates the average ripening process detected for 23 mangoes of the Kent variety. The results demonstrate the decrease of FI over time while the damping ratio increases with time. Similar results were detected for other mango varieties and for avocados. In general, the quantitative measurements produced by the Firmalon device enable the best post-harvesting treatment (to determine the fruits' longest shelf life) to be chosen.

8.6 *Acoustic and destructive tests for melons*

A group of 96 Galia variety autumn melons, grown in the Harava Valley, was taken from Agrexco, at Lod Airport, before the shipment was exported. The fruits were brought to the laboratory for firmness testing by the Firmalon device, and tested in parallel by destructive tests. The fruits were stored at 12^0 C, 60 % RH for three days and then at 20^0 C with 50 % RH, to simulate the conditions of melons being exported.

The fruits were tested by the Firmalon device during an eleven day period. The weight and the acoustic parameters were measured at three points on the fruits' perimeter zone (120° apart). A special fruit bed was constructed to fit the size of the melons. Dimensions of the fruits (height and diameter) were also measured. Destructive tests were performed on a subgroup of twenty-four fruits, on days five, seven, nine and eleven of the test program. First, the whole fruit was compressed to 5 mm deflection at two points on the perimeter zone, at a constant rate of 50 mm/min. More details on this experiment can be found in Shmulevich and Galili [85]. As can be seen in Fig. 13, the FI signal decreased monotonically with time, from an average of about 6.0 to 3.0 FI units, over the course of ten days. The melons' «biological age» was calculated for further prediction of the fruits' behavior over time. A comparison between the FI measurement and the average maximum load to deflect the melon to 5 mm resulted in a correlation of R^2=0.62.

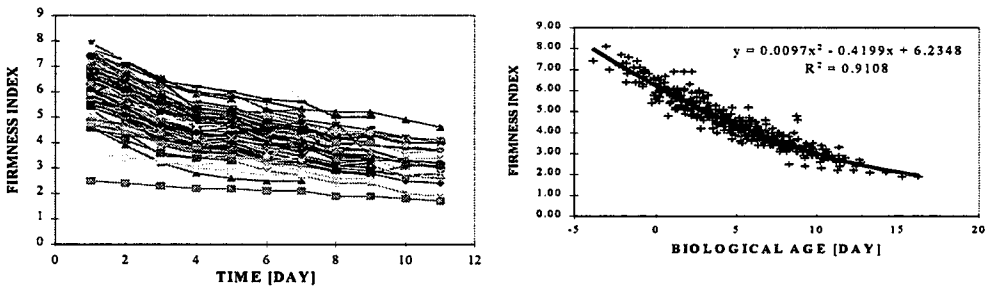

Figure 13: Firmness Index vs. time and FI vs. "biological age" for 96 Galia melons

Additional tests were performed in Agrexco terminal at Lod Airport, on spring and autumn Galia melons and other melons that were shipped from Israel to Europe. The analysis of these tests show similar results. Based on the research conducted, it is concluded that the Firmalon device is capable of detecting the ripening of melons.

8.7 Future developments with the acoustic technique

The achievements in detecting the ripening process of fruits by the non-destructive, acoustic methods described here have encouraged the development of two other applications based on the same measuring principle. One application is a fruit ripening sensor which detects the ripening process of several representative fruits in CA storage or during the artificial ripening process. The second application under investigation is a device to detect the changes in fruit maturity while the fruit is still in the field. These two applications are part of the «speaking plant» concept which uses new sensors to provide information on the current fruit conditions.

8.8 Conclusions of the experimental work

Technology known as the Firmalon was used to detect fruit and vegetable quality. The device is based on determining the acoustic response of fruit using flexible piezoelectric film. Tests conducted on apples, pears, tomatoes, avocados, mangoes and melons showed that this device can detect the ripening stage of fruit. Fairly good correlation was found between the firmness index and other destructive tests. Because of its simplicity, reliability and speed, this technology can be adapted commercially to measure fruit quality.

Acknowledgments

The author would like to thank Professor N. Galili from the Faculty of Agricultural Engineering, Technion-Israel Institute of Technology for his contribution to this work.

References

[1] Mohsenin, N.N. 1986. *Physical Properties of Plant and Animal Materials,* Gordon and Breach Science Publishers, Inc., New York.

[2] Chen, P. and Z. Sun. 1991. *A Review of Non-Destructive Methods for Quality Evaluation and Sorting of Agricultural Products.* JAER 49:85-98.

[3] Sarig, Y. 1991. Review: Impact Loading Associated with Agricultural Products. *Int. J. Impact Engng. Vol. 11, No. 3, pp. 251-275.*

[4] Pitts, M., J. Abbott, H. Arevalo, P. Armstrong, G, Brown, J. Brusewitz, M. Delwiche, S.J. Falconer, N. Galili, S. Gan-Mor, C.G. Haugh, R.B. Jordan, D. Massey, J. Mehlschau, R.A. Mills, A. Mizrach, D. Nahir, K. Peleg, R. Rohrbach, D. Rosenfeld, Y. Sarig, P.N. Schaare, Z. Schmilovitch, I. Shmulevich, B. Stevenson,

M. Stone, R. Stroshine and F. Younce. 1993. Nondestructive Sensing of Fruit and Vegetable Firmness. In Proc. US-Israel BARD Workshop, Spokane, WA, June 15-19, ASAE Publication 05-94, St. Joseph, MI. *Edited by Brown, G.K. and Y. Sarig. pp. 31-43.*

[5] Proc. Int. Workshop funded by the US-Israel Binational Agricultural Research and Development Fund (BARD), Spokane, WA, June 15-19, 1993. *ASAE Publication 05-94, St. Joseph, MI. Edited by Brown, G.K. and Y. Sarig.*

[6] Proc. Sensors for Nondestructive Testing International Conference. Orlando, FL. *Northeast Regional Agricultural Engineering Service Cooperative Extension.* Ithaca, NY, Feb. 18-21, 1997.

[7] Proc. *3rd International Symposium of Sensors in Horticulture.* Tiberias, Israel, Aug. 1997. Acta Horticulturae, in preparation.

[8] Bellon, V., J.L. Vigneau, and M. Crochon. 1993. *Non Destructive Sensing of Peach Firmness.* In Proc. IV Int. Symposium on Fruit, Nut, and Vegetable Production Engineering-Volume II, Valencia-Zaragoza, Spain, March 22-26. Published by Ministerio de Agricultura, Pescay Alimentación, Instituto Nacional de Investigación y Tecnología *Agraria y Alimentaria. pp. 291-297.*

[9] Fekete, A. 1993. *Non-Destructive Method of Fruit Elasticity Determination.* In Proc. IV Int. Symposium on Fruit, Nut, and Vegetable Production Engineering-Volume II, Valencia-Zaragoza, Spain, March 22-26. Published by Ministerio de Agricultura, Pescay Alimentación, Instituto Nacional de Investigación y Tecnología Agraria y Alimentaria. pp. 309-315.

[10] Mizrach, A., D. Nahir, and B. Ronen. 1992. *Mechanical thumb sensor for fruit and vegetable sorting.* Trans. of the ASAE 335(1):247-250.

[11] Hung, Y-C. and S.E. Prussia. 1995. *Firmness Measurement using a Non-Destructive Laser-Puff Detector.* In Proc. FPAC IV Conference, Nov 3-5. Chicago, IL. Published by ASAE, MI, USA.

[12] Finney E.E., Jr., and D.R. Massie. 1975. *Instrumentation for Testing Response of Fruits to Mechanical Impact.* Trans. of the ASAE 18(6):1184-1187.

[13] De Baerdemaeker, J., L. Lemaitre and R. Meire. 1982. *Quality detection by frequency spectrum analysis of the fruit impact force.* Trans. of the ASAE 25(1):175-178.

[14] Rohrbach R.P., J.E. Franke and D.H. Willits. 1982. *A Firmness Sorting Criterion for Blueberries.* Trans. of the ASAE 25(2):261-265.

[15] Franke J.E. and R.P. Rohrbach. 1981. *A Nonlinear Impact Model for a Sphere with a Flat Plate.* Trans. of the ASAE 24(6):1683-1686.

[16] Delwiche M.J. 1987. *Theory of Fruit Firmness Sorting by Impact Forces.* Trans. of the ASAE 30(4):1160-1166, 1171.

[17] Delwiche M.J., T. McDonald and S.V. Bowers. 1987. *Determination of Peach Firmness by Analysis of Impact Forces.* Trans. of the ASAE 30(1):249-254.

[18] Nahir D., Z. Schmilovitch and B. Ronen. 1986. *Tomato Grading by Impact Force Response.* ASAE paper No. 86-3028.

[19] Lichtensteiger M.J., R.G. Holmes, M.Y. Hamdy and J.L. Blaisdell. 1988a. *Impact Parameters of Spherical Viscoelastic Objects and Tomatoes.* Trans. of the ASAE 31(2):595-602.

[20] Lichtensteiger M.J., R.G. Holmes, M.Y. Hamdy and J.L. Blaisdell. 1988b. *Evaluation of Kelvin Model Coefficients for Viscoelastic Spheres.* Trans. of the ASAE 31(1):288-292.

[21] Delwiche M.J., S. Tang and J.J. Mehlschau. 1989. *An Impact Force Response Fruit Impact Sorter.* Trans. of the ASAE 32(1):321-326.

[22] Delwiche M.J. and Y. Sarig. 1991. *A Probe Impact Sensor for Fruit Texture Measurement.* Trans. of the ASAE. 34(1):187-192.

[23] Luan J.M. and R.P. Rohrbach. 1989. *Viscoelastic Impact Measurement using a Dot-Matrix Transducer.* ASAE paper No. 89-1601.

[24] Luan, J.M. 1990. *On the Direct Confirmation of Hertz Contact Pressure Distribution during Viscoelastic Impact.* Dissertation, North Carolina State University, Raleigh, NC.

[25] Thai, C.N. 1995. *A Soft Transducer for Firmness Measurement of Fruits and Vegetables.* In Proc. FPAC IV Conference, Nov 3-5. Chicago, IL. Published by ASAE, MI, USA.

[26] Schaare and McGlone. 1997. Design and Performance of a Fruit Firmness Grader. In Proc. Sensors for Nondestructive Testing International Conference. *Feb. 18-21, Orlando, FL. Northeast Regional Agricultural Engineering Service Cooperative Extension. Ithaca, NY. pp. 27-36.*

[27] Finney E.E., Jr. 1967. *Dynamic Elastic Properties of some Fruits during Growth and Development.* JAER 12(4):249-256.

[28] Finney E.E., I. Ben-Gera and D.R. Massie. 1968. *An Objective Evaluation of Changes in Firmness of Ripening Bananas using a Sonic Technique.* J. of Food Sci. 32:642-646.

[29] Finney E.E., Jr., and K.H. Norris. 1968. *Instrumentation for Investigating Dynamic Mechanical Properties of Fruits and Vegetables.* Trans. of the ASAE 11(1):94-97.

[30] Abbott J.A., G.S. Bachman, N.F. Childers, J.V. Fitzgerald and F.J. Matusik. 1968a. Sonic Techniques for Measuring Texture of Fruits and Vegetables. Food Technology 22:635-646.

[31] Abbott J.A., N.F. Childers, G.S. Bachman, J.V. Fitzgerald and F.J. Matusik. 1968b. *Acoustic Vibration for Detecting Textural Quality of Apples.* Amer. Soc. for Hort. Sci. 93:725-737.

[32] Finney E.E., Jr. 1970. *Mechanical Resonance within Red Delicious Apples and its Relation to Fruit Texture.* Trans. of the ASAE 13(1):177-180.

[33] Finney E.E., Jr. 1971. *Random Vibration Techniques for Non-Destructive Evaluation of Peach Firmness.* JAER 16(1):81-87.

[34] Stephenson K.Q., R.K. Byler and M.A. Wittman. 1973. *Vibrational Response Properties as Sorting Criteria for Tomatoes.* Trans. of the ASAE 16(2):258-260, 265.

[35] Peleg K. and S. Hinga. 1989. *Firmness Indexes of Viscoelastic Bodies by Vibration Testing.* J. of Rheology 33(4):639-657.

[36] Peleg K., U. Ben-Hanan and S. Hinga. 1990. *Classification of Avocado by Firmness and Maturity.* J. of Texture Studies 21:123-139.

[37] Peleg, K. 1993. *Comparison of Non-Destructive and Destructive Measurement of Apple Firmness.* J. Agric. Engng Res. 55:227-238.

[38] Peleg, K. 1994. *Scale Translation of Firmness Tests in Fruits.* Journal of Texture Studies. 25:163-177.

[39] Peleg, K. *Optimal Scale Translations in Noisy Measurement System.* NDTRE International. Vol. 28 No. 5 267-279.

[40] Abbott, J.A. and D.R. Massie. 1995. *Nondestructive Dynamic Force/Deformation Measurement of Kiwifruit Firmess* (Actinidia Deliciosa). Trans. of the ASAE. Vol. 38(6):1809-1812.

[41] Cooke J.R. and R.H. Rand. 1973. *A Mathematical Study of Resonance in Intact Fruits and Vegetables using a Three Media Elastic Sphere Model.* JAER 18:141-157.

[42] Yong Y.C. and Bilanski W.K. 1979. *Modes of Vibration of Spheroids at the First and Second Resonant Frequencies.* Trans. of the ASAE 22(6):1463-1466.

[43] Van Woensel, A. Wouters and J. De Baerdemaeker. 1987. *Relation between Mechanical Properties of Apple Fruit and Sensory Quality.* J. of Food Proc. Eng. 9:173-189.

[44] Van Woensel, E. Verdonck and J. De Baerdemaeker. 1988. *Measuring the Mechanical Properties of Apple Tissue using Modal Analysis.* J. of Food Proc. Eng. 10:151-163.

[45] Rosenfeld D., I. Shmulevich and G. Rosenhouse. 1991. *Three Dimensional Simulation of Acoustic Response of Fruit for Firmness Sorting.* ASAE paper No. 91-6046, American Society of Agricultural Engineers, St. Joseph, MI, USA.

[46] Rosenfeld D., I. Shmulevich and G. Rosenhouse. 1993. *Three Dimensional Simulation of the Dynamic Response of Fruit.* ASAE paper No. 93-6022, American Society of Agricultural Engineers, St. Joseph, MI, USA.

[47] Chen, H. and J. De Baerdemaeker. 1993. *Modal Analysis of the Dynamic Behavior of Pineapples and its Relation to Fruit Firmness.* Trans. of the ASAE. Vol. 36(5):1439-1444.

[48] Chen, H. and J. De Baerdemaeker. 1993. *Finite-Element-Based Modal Analysis of Fruit Firmness.* Trans. of the ASAE. Vol. 36(6):1827-1833.

[49] Chen, H. , J. De Baerdemaeker, and V. Bellon. 1996. *Finite Element Study of the Melon for Nondestructive Sensing of Firmness.* Trans. of the ASAE 39(3):1057-1065.

[50] Kimmel, E., K. Peleg, and S. Hinga. 1992. *Vibration Modes of Spheroidal Fruits.* J. Agric. Engng. Res. 52, 201-213.

[51] Affeldt, H.A. and J.A. Abbott. 1989. *Apple Firmness and Sensory Quality using Contact Acoustic Transmission.* Proc. 7th Int. Cong. on Agr. Eng., Dublin, Ireland, Vol. 3:2037-2045.

[52] Pitts, M.J. R.P. Cavalieri, S. Drake. 1991. *Evaluation of the PFT Apple Firmness Sensor. ASAE Paper No. 91-3017.* American Society of Agricultural Engineers, St. Joseph, MI, USA.

[53] Van Woensel and J. De Baerdemaeker. 1983. *Mechanical Properties of Apple during Storage.* Lebensm.-Wiss. u. -Technol. 16:367-372.

[54] Garrett R.E. and R.B. Furry. 1972. *Velocity of Sonic Pulses in Apples.* Trans. of the ASAE 15(4):770-774.

[55] Clark, R.L. 1975. *An Investigation of the Acoustical Properties of Watermelon as related to Maturity.* ASAE Paper No. 75-6004, American Society of Agricultural Engineers, St. Joseph, MI. 49805.

[56] Robinson, B.E. 1976. *An Evaluation of Acoustical Decay Time as a Measure of Watermelon Maturity.* M.Sc. Thesis. University of Georgia. Athens, Georgia.

[57] Yamamoto H., M. Iwamoto and S. Haginuma. 1980. *Acoustic Impulse Response Method for Measuring Natural Frequency of Intact Fruits and Preliminary Applications to Internal Quality Evaluation of Apples and Watermelons.* J. of Texture Studies 11:117-136.

[58] Yamamoto, H., M. Iwamoto and S. Haginuma. 1981. *Non-Destructive Acoustic Impulse Response Method for Measuring Internal Quality of Apples and Watermelons.* J. Japan. Soc.Hort. Sci. 50(2):247-261.

[59] Armstrong P., H.R. Zapp and G.K. Brown. 1990. *Impulsive Excitation of Acoustic Vibrations in Apples for Firmness Determination.* Trans. of the ASAE 33(4):1353-1359.

[60] Armstrong, P.R. , G.K. Brown and J. A. Abbott. 1992. *Progress on an Acoustic Technique for Estimating Apple Firmness.* ASAE paper No. 92-6050.

[61] Chen, P., Z. Sun and L. Huarng. 1992. *Factors Affecting Acoustic Response of Apples.* Trans. of the ASAE, 35(6):1915-1920.

[62] Chen, H., J. De Baerdemaeker and F. Vervaeke. 1992. *Acoustic Impulse Response of Apples for Monitoring Texture Change after Harvest.* Proceedings of the International Conference on Agricultural Engineering. Beijing, China, October, 9p.

[63] Sugiyama, J. T. Katsurai, J. Hong, H. Koyama and K. Mikuriya. 1997. *Portable Melon Firmness Tester using Acoustic Impulse Transmission.* In Proc. Sensors for Nondestructive Testing International Conference. Feb. 18-21, Orlando, FL. Northeast Regional Agricultural Engineering Service Cooperative Extension. Ithaca, NY. pp. 3-12.

[64] Farabee, L.M. and M.L. Stone. 1991. *Determination of Watermelon Maturity with Sonic Impulse Testing.* ASAE Paper No. 91-3013. American Society of Agricultural Engineers, St. Joseph, MI.

[65] Armstrong, P.R., M. Stone and G.H. Brusewitz. 1997. *Nondestructive Acoustic and Compression Measurements of Watermelon for Internal Damage Detection.* In Proc. Sensors for Nondestructive Testing International Conference. Feb. 18-21, Orlando, FL. Northeast Regional Agricultural Engineering Service Cooperative Extension. Ithaca, NY. pp. 172-182.

[66] Stone, M.L., P.R. Armstrong, X. Zhang, G.H. Brusewitz , D. D. Chen. 1996. *Watermelon Maturity Determination in the Field Using Acoustic Impulse Impedance Techniques.* Trans. of the ASAE 39(6):2325-22330.

[67] Sarker, N. and R.R. Wolfe. 1983. *Potential of Ultrasonic Measurements in Food Quality Evaluation.* Trans. of the ASAE 26(2):624-629.

[68] Arad, S., E. Benzioni, S. Lerman and S. Mendinger. 1985. *Failure in Melons.* Final report No. BGUN-ARI-15-85. The Institute for Applied Research. Ben-Gurion University of the Negev.

[69] Upchurch, B.L., E.S. Furgason and G.E. Miles. 1985. *Spectral Analysis of Acoustical Signal for Damage Detection.* ASAE paper No. 85-6014, American Society of Agricultural Engineers, St. Joseph, MI, USA.

[70] Upchurch B.L., G.E. Miles, R.L. Stroshine, E.S. Furgason, F.H. Emerson. 1987. *Ultrasonic Measurements for Detecting Apple Bruises.* Trans. of the ASAE 30(3):803-809.

[71] Watts K.C. and L.T. Russell. 1985. A Review of Techniques for Detecting Hollow Heart In Potatoes. *Canadian Agricultural Engineering. Vol. 27(2):85-90.*

[72] Mizrach A., N. Galili and G. Rosenhouse. 1989. *Determination of Fruit and Vegetable Properties by Ultrasonic Excitation.* Trans. of the ASAE 32(6):2053-2058.

[73] Mizrach, A., N. Galili, G. Rosenhouse and D.C.Teitel. 1991. *Acoustical, Mechanical and Quality Parameters of Winter Grown Melon Tissue.* Trans. of the ASAE 34(5):2135-2138.

[74] Mizrach, A. N. Galili, S. Gan-Mor, U. Flitsanov and I. Prigozin. 1996. *Models for Analyzing Ultrasonic Signal to Assess Avocado Properties.* Agricultural Engineering Research, 65:261-267.

[75] Stroshine, R.L., S.I. Cho, W.K. Wai, G.W. Krutz and I.C. Baianu. 1991. *Magnetic Resonance Sensing of Fruit Firmness and Ripeness.* ASAE Paper 91-6565. St. Joseph, MI:ASAE.

[76] Cho, S. I., and C.H. Chung. 1997. *Nondestructive Fruit Ripeness Sensing using NMR and Neural Networks.* In Proc. Sensors for Nondestructive Testing International Conference. Feb. 18-21, Orlando, FL. Northeast Regional Agricultural Engineering Service Cooperative Extension. Ithaca, NY. pp. 294-301.

[77] Abbott, J.A., W.R. Forbus, Jr. and D.R. Massie. 1993. *Temperature Damage Measurement by Fluorescence or Delayed Light Emission from Chlorophyll.* In Proc. US-Israel BARD Workshop, Spokane, WA, June 15-19, ASAE Publication 05-94, St. Joseph, MI. Edited by Brown, G.K. and Y. Sarig. pp. 44-49.

[78] Beaudry, R.M., N. Mir, J. Song, P. Armstrong, W. Deng, E. Timm. 1997. *Chlorophyll Fluorescence: A Nondestructive Tool for Quality Measurements of Stored Apple Fruit.* In Proc. Sensors for Nondestructive Testing International Conference. Feb. 18-21, Orlando, FL. Northeast Regional Agricultural Engineering Service Cooperative Extension. Ithaca, NY. pp. 56-66.

[79] DeEll, J.R., R.K. Prange, D.P. Murr. 1997. *Chlorophyll Fluorescence as an Indicator of Apple Fruit Firmness.* In Proc. Sensors for Nondestructive Testing International Conference. Feb. 18-21, Orlando, FL. Northeast Regional Agricultural Engineering Service Cooperative Extension. Ithaca, NY. pp. 67-73.

[80] Shmulevich, I., N. Galili and D. Rosenfeld. 1996. *Detection of fruit firmness by frequency analysis.* Trans. of the ASAE, Vol. 39(3):1047-1055.

[81] Galili, N., I. Shmulevich, and N. Benichou. 1998. *Acoustic Testing of Avocado for Fruit Ripeness Evaluation.* Trans. of the ASAE. In press.

[82] Galili, N. and J. De Baerdemaeker. 1996. *Performance of Acoustic Test Methods for Quality Evaluation of Agricultural Products.* In Proc. ISMA21-Int. Conference on Noise and Vibration Engineering, Leuven, Belgium, Sept. 18-20. Published by Katholieke Universiteit Leuven - Dept. of Werktuigkunde, Heverlee, Belgium. Vol. 3:1959-1972.

[83] Shmulevich, I., N. Galili and N. Benichou. 1995. *Nondestructive Acoustic Method for Measuring the Firmness and Shelf-Life of Mango Fruit.* Proc. FPAC IV Conference, Chicago, IL. Nov. 3-5. pp. 275-287.

[84] Galili, N., J. De Baerdemaeker and E. Versteken. 1996. *Performance Evaluation of Different Firmness Test Methods in Fruits.* PH '96 Int. Postharvest Science Conference, Taupo, New Zealand, Aug. 4-9.

[85] Shmulevich, I and N. Galili. 1998. *Acoustic Parameters and Firmness of 'GALIA' Melons.* Presented at XIIIth Int. Congress on Agricultural Engineering, Rabat, Morocco. Feb. 2-6.

Organisé par

Cemagref

The Workshop SENSORAL 98 was aimed at sensor measurement of agricultural product quality. It dealt with three main objectives: dissemination of the research results of two European projects, scientific and technical presentations of sensors and fast measurement systems by international researchers, enhancement of industry/ research exchanges through industrial presentations of joint research projects transferred to the industry.

For fruits and vegetables, the most important themes were: artificial vision, NIR spectrometry, aroma sensors and artificial intelligence simulating human classification. Animal product quality assessment through acoustic, NMR and electric impedance measurement was presented. Concerning process control, tracers or emerging techniques such as Magnetic Resonance Imaging were mainly dealt with.

Le colloque SENSORAL 98 était axé selon trois objectifs : être le support de dissémination des résultats de la recherche de deux projets européens, permettre aux chercheurs de la communauté internationale de présenter leurs avancées sur les systèmes capteurs et mesures rapides de produits agricoles, favoriser les échanges industrie/recherche par une présentation industrielle de projets de recherche conjoints ayant abouti à des transferts.

Pour le contrôle des produits végétaux, les thèmes forts qui émergent de ce Colloque sont la vision artificielle, la spectrométrie proche infra-rouge, les capteurs d'arômes, les méthodes d'intelligence artificielle pour simuler la classification humaine. L'appréciation des produits carnés est présentée au travers de l'acoustique, la RMN et l'impédance électrique. Le contrôle des procédés est abordé en proposant des marqueurs et également des techniques en émergence telles que l'Imagerie à Résonance Magnétique.

Avec le soutien

MINISTERE DE L'AGRICULTURE ET DE LA PÊCHE

REGION LANGUEDOC ROUSSILLON

ISBN 2-85362-499-4

Prix : 195 F TTC

9 782853 624992

ACTES DE COLLOQUE

Montpellier
24-27 février 1998

Cemagref France

volume 2

Sensoral 98

International workshop on Sensing Quality of Agricultural Products

Colloque international sur les capteurs de la qualité des produits agro-alimentaires

Edited by Véronique Bel

Cemagref EDITIONS

SENSORAL 98

International workshop on Sensing Quality of Agricultural Products

Colloque international sur "les capteurs de la qualité des produits agro-alimentaires"

Montpellier
24-27 février 1998

Volume 2

Edited by :
Véronique Bellon-Maurel

Actes du colloque **Sensoral 98 : International workshop on Sensing Quality of Agricultural Products.** 24-27 février 1998. **Volume 2**
Coordination de l'édition : Véronique BELLON-MAUREL. Secrétariat : Michèle EGEA. Mise en page : Sophie MORIN, Caroline REACH. Suivi de l'édition : Camille CEDRA
Impression et façonnage : Ateliers Cemagref-Dicova. Vente par correspondance : Publi-Trans, BP 22, 91167 Longjumeau Cedex 9, Tél. 01.69.10.85.85. Diffusion aux libraires : Tec et Doc Lavoisier, 14 rue de Provigny - 94236 Cachan Cedex.
ISBN 2-85362-499-4, dépôt légal 4ème trimestre 1998. Prix de vente : 195 F TTC

Part 5

Aroma sensors

Can an electronic nose replace sensorial analysis?

Est-ce que le nez électronique peut remplacer l'analyse sensorielle ?

Corrado Di Natale, Antonella Macagnano, Roberto Paolesse*, Enrico Tarizzo,

Alessandro Mantini and Arnaldo D'Amico

Department of Electronic Engineering and *Department of Chemical Science and Technology
University of Rome «Tor Vergata», via di Tor Vergata; 00133 Roma; Italy
e-mail: dinatale@eln.uniroma2.it

Abstract: *Electronic noses are designed and utilised for a variety of different applications. Undoubtedly, among these, food analysis has gained the major attention. Among the various aspects of food analysis that concerning with the utilisation of the natural olfaction and taste (sensorial analysis) is very appealing for electronic nose applications. In this context panels of well trained tasters and smellers are daily utilised to certify the goodness of foods and their fitting with the human taste. Sensorial analysis represents a practical field where performances of natural and artificial olfaction and taste can be compared and where an electronic nose can be utilised as an essential support of the human capabilities.*

In this paper some key issues concerning the applications of electronic noses to food analysis will be examined and examples of applications, related to the electronic nose developed at the University of Rome Tor Vergata will be illustrated and discussed.

Keywords: *Electronic nose, sensorial analysis, pattern recognition.*

Résumé : Les nez électroniques sont conçus et utilisés pour une large variété d'applications. Incontestablement, les analyses de produits alimentaires par les nez électroniques attirent notre attention. Parmi les différents aspects de l'analyse des produits alimentaires, ceux qui concernent l'utilisation de l'olfaction naturelle et du goût (analyse sensorielle) sont très attractifs pour les technologies de nez électroniques. Dans ce cadre, les panels de dégustateurs bien entraînés sont utilisés tous les jours pour certifier la qualité des produits alimentaires et leur acceptation par le goût humain. L'analyse sensorielle représente un champ pratique où les performances de l'olfaction naturelle et artificielle et du goût peuvent être comparées, où les nez électroniques peuvent être utilisés comme un support essentiel pour les capacités humaines. Dans ce papier, certaines applications de nez électronique à l'analyse des produits agro-alimentaires seront présentées et des exemples plus particulièrement développés à l'Université de Rome (Tor Vergata) seront illustrés et discutés.

1. Introduction

The advent of artificial sensorial systems (electronic noses) has open a variety of practical applications and new possibilities in many fields where the presence of odours is the relevant phenomenon. Many areas will be in the near future interested by these new instruments mainly due to their promising, even if still not fully understood, potentialities in terms of sensitivities, resolution, stability and it is foreseen a huge growth of new markets. Among these areas those applications concerning foods and beverages are extremely important.

An important role in food analysis is played by sensorial analysis. This discipline makes use of the natural senses as probes to test some features of a food. At this regard it is interesting to remark that between the natural senses, those responsible of the chemical interface between a living organism and the surrounding environment are, to some extent, characterised by particular features. Indeed the five basic senses can be divided in two groups: those detecting physical quantities and those detecting chemical quantities. The first group (hear, sight and tact) are sufficiently well know in terms of physical principles and, as a consequence, a wealth of successful studies to construct artificial counterparts have been done in the past years. On the other side the chemical interfaces of the living being are not so well know: in fact many aspects of the working principle of olfaction and taste are not clear from a physiological point of view.

It has to be remarked also a psychological difference between this two groups of senses. Indeed the information from the physical ones are adequately treated until to be fully verbally expressed and firmly memorised, while the chemical information, coming from the nose and the tongue, are surrounded by a vagueness which is reflected in the general poor description and memorisation capacity in reporting olfactory and tasting experience. For these intrinsic difficulties toward the understanding of the nature of these senses for many years only sporadic research on the possibility of fabricating artificial olfactory systems were performed [1, 2]. At the end of the eighties a very promising way was open by the paper [3] in which it was argued that an array of solid state chemical sensors could behave as an artificial olfactory system.
Many groups have dedicated their efforts to the manufacture of electronic noses, which are now coming to be a well assessed analytical instruments whose utilisation is showing benefits in many applications in different fields [4]. Among the fields which are expected to receive more benefits from this new class of instruments food analysis and control for a better quality of the life, is among the most important, in term of expected market.
This paper is mainly focused on the results obtained, in food analysis, by the *electronic nose project* of the Sensors and Microsystems group active at the University of Rome «Tor Vergata, between the Departments of Electronic Engineering and the Department of Chemical Science and Technology.

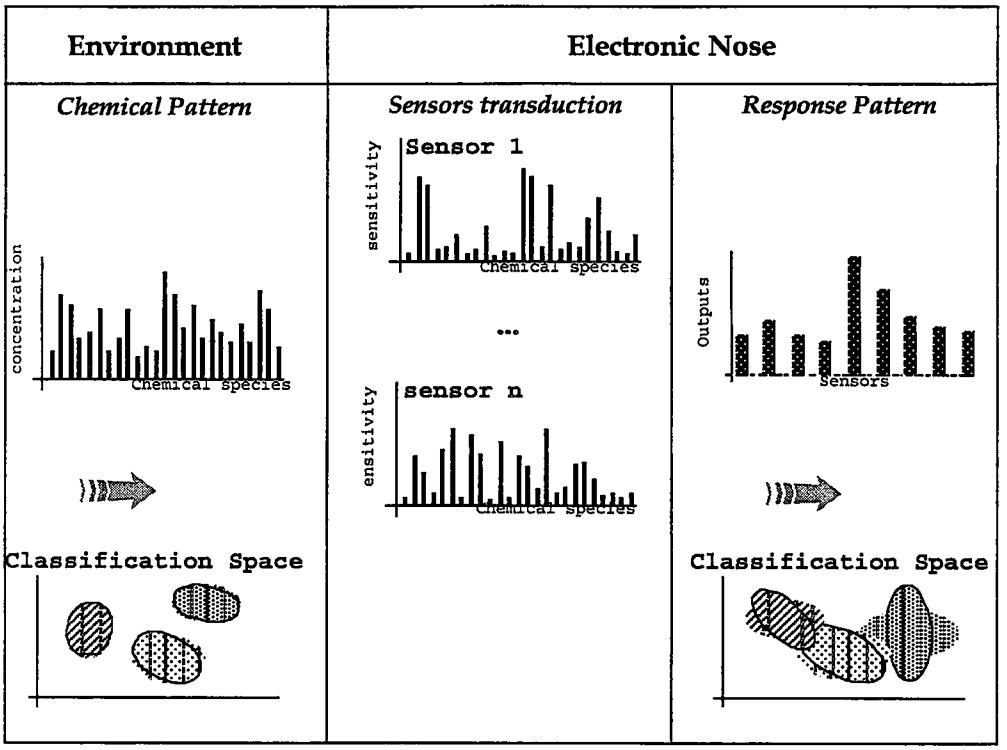

Figure 1: In figure the basic principles of electronic nose are shown. Real patterns occurring in the environment are transduced by the sensor array into a response pattern. In this process there is a drastic scaling of dimensions from the very high number of chemical species present in the environment down to the few units of sensor elements. The electronic nose works properly if the sensors selectivities ensure that in the transduction process those features necessary for correct classifications are preserved

2. Electronic nose principles

Electronic noses are instrumental apparatus based on the utilisation of an array of non-selective chemical sensors, where each sensor is characterised by its own degree of selectivity. This last feature is the key property on which the working principle of electronic noses is based. The main feature of an electronic nose is its ability in distinguishing among samples according to some classification scheme. Typical examples can be found in food analysis where sometimes very intuitive classes are adopted according to straightforward categories such as freshness or edibility.

The basic principle is illustrated in figure 1. The chemical patterns occurring in a certain environment are *«translated»* by the sensors into a response pattern. With respect to the chemical pattern, the response pattern is characterised by having less dimensions; basically it is a combination of all the components which form the chemical pattern. The rule of combination, generally non-linear, is given by the selectivities and the sensitivities of each single sensor. In each application optimal performances are achieved when the pattern translation process preserves those features allowing the discrimination among those classes which are relevant to the particular case. This procedure based on a reduction of dimensions in the patterns has, as a consequence, a reduction of the information content.

Data analysis is an important issue in electronic noses. Its usual role is to allow a correlation between sensor outputs pattern and the properties of the environment which are the object of the measurement strategy. Data analysis has been the main concern of many research papers since the first development of the field. They have been dealing with the application of several techniques, borrowed from other application fields. Chemometrics and neural networks are the disciplines from which the most utilised techniques are derived.

3. Issues in sensorial analysis

Food analysis is a discipline aiming at giving detailed measurements of the chemical composition of foods in order to determine their quality. From the electronic nose point of view the most important feature of food analysis deals with the determination of concentration of single species, although, in many cases, the target of the measurement is a qualitative description of the examined product in respect to some classification scheme.

An example can be done considering mineral water labels, where, at least according to the Italian legislation, a detailed list of the concentrations of many chemical species is reported. At the end of this information a consequent verbal classification of the water is reported as a synthesis of the analytical details. The benefit that an electronic nose can bring in this example is that it is an instrument able to provide directly this classification skipping the long, costly and sometimes not accurate analytical procedure.

Another aspect of food analysis that could be strongly improved introducing electronic nose analysis is the determination of the organoleptic properties through the so-called sensorial analysis. In this frame all the aspects concerning the taste, the odour, and all those hedonistic parameters characterising the interaction between man and food, are evaluated by panels of trained people. It can be easily understood that enormous problems of standardisation, of correct training, of stability and reproducibility of the evaluation, affect the measurements which furtherly are scarcely comparable with those coming from different panels. A key role in this methodology is the translation of the olfactive stimuli in a numeric value

utilised to represent the output of the sensorial analysis, and, as discussed in the introduction, the expression of olfactive experiences is extremely difficult to achieve and it is also largely dependent on the psychological state of the panellists.

Nevertheless the importance of the panels is growing along with the necessity of improving the reliability of their results as also the legislation, in various countries, is investing sensorial analysis of legal value. For instance again the Italian legislation for the denomination of olive oils introduced a classification of the products based on sensorial analysis of panels.

Electronic noses can offer, a useful instrument for calibration and standardisation of the panels in order to improve the reliability of the analysis. To this regard, in the final section of this paper, an example of integration of electronic nose and panel of tasters analysis will be shown.

Another aspect which positively characterises electronic noses is the fact that they do not require any particular sample preparation. This means that the analysis can be done not only in the laboratory but everywhere it is necessary. The capillary diffusion of analytical instruments is another important issue for food analysis in order to ensure an high quality of products.

4. The «Rome Tor Vergata» electronic nose project

Since two years at the Tor Vergata University in Rome extensive researches on the exploitation of porphyrins and related compounds for chemical sensors employed in electronic noses are carried out.

The instrument is based on eight quartz microbalances sensors coated with various tetrapyrrolics macrocycles (metallo-porphyrins). The aptness of these compounds to be utilised as coating of quartz microbalances and their utilization for food analysis was described elsewhere [5, 6]. The main feature of these sensors is the dependence of the sensing properties (in terms of selectivity and sensitivity) on the nature of both the central metal and peripheral substituents of the macrocycles. With small variations in the synthetic process it is possible to get sensors with different behaviour. This flexibility makes this compounds of a great interest for electronic nose applications.

The sensors whose utilisation is described in this paper are coated by the following eight compounds:

1 Ru-*meso*TetraPhenylPorphyrin
2 Rh-*meso*TetraPhenylPorphyrin
3 Mn-*meso*TetraPhenylPorphyrin
4 Co-*meso*TetraPhenylPorphyrin
5 Sn-*meso*TetraPhenylPorphyrin
6 Co-*meso*TetrapNO_2-PhenylPorphyrin
7 Co-*meso*Tetra-pOCH_3-PhenylPorphyrin
8 Mn-*meso*OctaMethylCorrole

Metallo-porphyrins can be deposited onto the quartz microbalance surface in many ways, well reproducible and stable films have been obtained adopting either *self assembled monolayers* [7] or *Langmuir Blodgett* techniques [8].

Sensors operate in a test chamber having a volume of 200 ml. Each sensor is part of an oscillator circuit. In order to maximise the electric dynamic range of the quartz oscillations, the Pierce circuital solution has been adopted. Frequency measurement has been accomplished utilising the frequency counter of a *Tektronix 2252* digital oscilloscope the measurements were supervised by a PC that also collected the data.

An extensive set of tools for data analysis has been made available. A number of chemometrics based methods (Principal Component Analysis and Cluster Analysis) and Neural Networks (Feed Forward back Propagation, Self Organizing Maps, Adaptive Resonance Theory) have been utilised to analyse electronic nose data for the extraction of the useful information.

The electronic nose has been tested in real environments without a particular conditioning strategy of the ambient conditions. All measurements herewith reported, have been performed at room temperature with relative humidity of 40% and under atmospheric pressure.

The aptitude of the electronic nose to be utilized for the analysis of foods has been tested measuring the sensor sensitivities towards several substances which are of interest in food analysis. These compounds are representative of various classes of species such as: organic acids, alcohol's, amines, sulphides, carbonyls.

Organic acids, and carbonyl compounds, with furans and pyranes are product of sugars fragmentation while aldheydes and sulphur compounds are products of aminoacids degradation. For example, in relation to fish freshness, long-chain carbonyls (e.g. myristaldehyde) and alcohol's (such as 1-octanol) could be correlated with the odour of fresh fish. Conversely the amount of short-chain alcohol's (among the others methanol, ethanol, 1-butanol), carbonyls (e.g. acetone, 2-butanone, propionic acid and diacetyl), sulphides (e.g. dimethylsulphide) and nitrogen compounds (e.g. amines) increases with the time and are responsible for the characteristic smell of bad fish. As another example, in relation to quality of tomatoes, the measurement of volatile acidity (e.g. D- and L-lactic acid and acetic acid), diacetyl, acetylmethylcarbinol and ethanol represents the products of demolition of sugars by micro-organisms degradation .

5. Examples of applications

Measurements were carried-out for two different foods: tomato paste and milks. In the following experimental details for each of them will be given.

5.1 Tomato paste and milk experiment

Tomato pastes were produced with tomatoes coming from two different kinds of cultivation: biological and conventional. For each of these, tomatoes were divided in four ranks, according to their quality, labelled from 0 (perfect) to 3 (bad). All tomatoes were divided in eight classes, for each class three samples were considered. Tomato pastes were then analysed by an electronic nose and by a panel of tasters and data were then analysed and compared.

The second experiment was aimed at measuring the presence and the intensity of the burned aroma in a number of commercial brands of Ultra High Temperature (UHT) milks. UHT milk is obtained through a high temperature treatment of fresh milk in order to stabilise the product and, as a consequence, to allow long conservation times. As a drawback of the procedure a burned aroma results.

5.2 Electronic nose measurements

Both the experiments were carried-out following the same methodology. Samples were closed into bottles from where headspaces were continuously transferred into the measurement chamber by a peristaltic pump. The speed of the pump was chosen in order to maintain equilibrium in the headspace of the sample. Dried ambient air was used as carrier, and measurements were performed at room temperature. In order to test the reproducibility of the measures each sample was measured three times.

5.3 Human panel measurements

Two experiments were aimed at evaluating different features: in case of tomato paste the aim was to evaluate the overall quality of the product while in case of UHT milk only one particular feature was searched. For this reason different methodologies were adopted by the panel in each experiment. The analysis has been carried out according to a methodology developed at the National Institute for Nutrition, Rome (Italy).

In both the experiment the panel was composed by seven people. In the case of tomato paste analysis, the panel was trained to recognise and to quantify several characteristics of the tomato. Nine parameters were considered. They include the colour, the presence of some compounds and the overall quality of tomatoes. Each parameter was then numerically expressed in a scale from 0 to 9.

The parameters are listed in table 1. It is important to note that parameters related to colour and the presence of compounds are objective in principle, while the third group of parameters takes into consideration quantities which are strongly related

to the personal perception of each panellist and therefore are subject to larger deviations. Nonetheless, these last quantities are those determining the acceptance of a food, so they are of paramount importance in defining the overall quality.

In case of the milk experiment the panel was trained to recognise and to quantify the presence of the burned aroma, and its intensity was numerically expressed in a scale from 1 to 9.

Results and discussion

Electronic nose and sensorial analysis data have been roughly analysed by using the Principal Component Analysis (PCA) while a more refined analysis was performed with the Self Organizing Map (SOM) according to a methodology outlined in ref. [9].

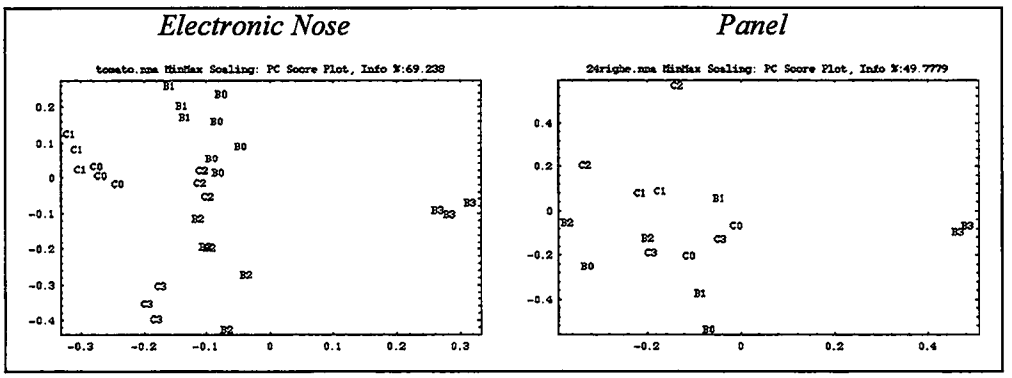

Figure 2: Score plot of PCA of electronic nose (3a) and sensorial analysis (3b) results of tomato paste experiments. Experimental data are labelled with the name of their class, as defined in the text. Generally both the analysis show the same conclusions concerning the great difference between class B3 and the rest of the samples. Furtherly electronic nose seems to have a better resolution in putting in evidence the existence of similarities between the other classes (e.g. C0-C1) that does not appear in fig. 3b

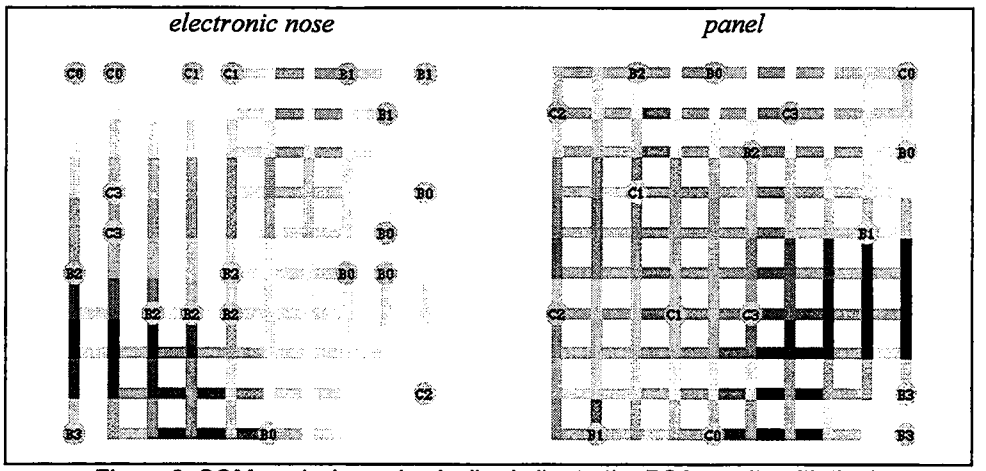

Figure 3: SOM analysis are basically similar to the PCA results with the important improvement that in this case is evident the capability of the electronic nose (4a) to correctly classify the tomato pastes classes. The classification is not achieved by the sensorial analysis data (4b)

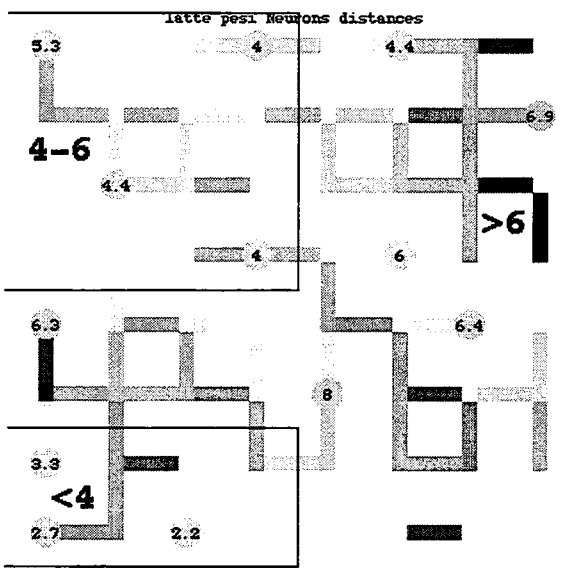

Figure 4: SOM analysis of the UHT milk data. Experimental data, corresponding to different brands, are displayed with the burned aroma indicator evaluated by the panel. According to this value it is possible divide the SOM grid in three regions each corresponding to a different level quality of the product. It is worth to remark the good reproducibility of the measures, indeed although each milk brand has been measured three times only one neurone per kind of milk has been necessary to represent the brand onto the SOM grid

Figure 2 shows the PCA score plot for both the experimental approaches; as can be seen, the score plots have a certain similarity, class 3B is clearly distinct, while the other classes are quite messed together, although the electronic nose data show a certain tendency to be better grouped in the pre-defined classes. A more accurate representation of the data can be achieved using SOM. Figure 3 shows the data of both analysis as they are projected onto SOM grids. It is necessary to remember that the SOM provides a representation of the data which is, in some sense, a sort of non-linear principal component analysis. It has to be noted that the SOM grid is a discrete space and that the distances between neurones, in the original sensor space, are not the same, but two neurones which are adjacent onto the grid are also adjacent in the original space (topology preservation property). From figure 3 it is possible to see that electronic nose analysis is more accurate in the separation of those classes which are not clearly separated by sensorial analysis.

In figure 4, SOM analysis results for UHT milks experiment are shown. In this test, 13 different brands of UHT milks, commercially available in Italy, were taken into consideration. Each of them has been analysed with the electronic nose while the panel searched for the presence and the intensity of specific sensation of burned milk aroma. In figure 4, the different milks are shown, and for each milk the average value of burned milk aroma, as indicated by each panellist, is reported. According to the sensorial measured burned milk aroma intensity, the electronic nose data can be grouped on the SOM grid into three well defined regions with different qualities: high (burned aroma intensity less than 4) medium (between 4 and 6) and poor (more than six). In this experiment, the electronic nose data were only correlated to the presence of the burned aroma, nevertheless an examination of the distances between neutrons (represented in figure 4 by lines in different grey level) reveals the existence of clusters whose nature has not been investigated in this paper.

The agreement between the sensorial analysis and the electronic nose is in this case more surprising, because sensorial analysis was aimed at evaluating only one feature of the aroma, while the electronic nose has given a classification which takes into consideration the whole aroma composition. This result can be explained either as a fortuitous event or as a hint that sensorial analysis results, also when it is aimed at looking for one precise feature, is influenced by the context, namely by the whole aroma.

Conclusion

Food analysis is a very complex discipline. Due to its strict interaction with the quality of life it is extremely important to improve the performances of the methods in the fields. EN seems to be a new instrument that can offer the unique advantage of providing fast and low expensive qualitative analysis of many kinds of foods. Due

to the peculiar character of solid-state sensors, EN can be utilised in real environment without paying particular attention to sample preparation.

Human senses play a significant role in food analysis for a series of fundamental analysis. In this paper an electronic nose has been proven to provide a classification of foods very close to that obtained by a panel of tasters. This is of great encouragement of pursuing researches in electronic noses in order to get instruments of a great social utility.

Acknowledgements

Authors would like to acknowledge the fruitful co-operation with Prof. Quaglia and Dr. Sinesio at the National Institute for Nutrition, Rome.

References

R. Moncrieff; *J. Appl. Physiol.*, 161 (1961) 742.

A. Dravicks, J. Trotter; *J. Sci. Instrum.* 42 (1965) 624.

K. Persaud, J. Dodds; *Nature*, 299 (1982) 352.

E. Kress-Rogers (ed.), 1996. *Handbook of biosensors and electronic nose*, CRC Press, Boca Raton (USA).

J. Brunink, C. Di Natale, F. Bungaro, F. Davide, A. D'Amico, R. Paolesse, T. Boschi, M. Faccio, G. Ferri; *Analytica Chimica Acta*, 325 (1996) 53-64.

C. Di Natale, A. Macagnano, F. Davide, A. D'Amico, R. Paolesse, T. Boschi, M. Faccio, G. Ferri; *Sensors and Actuators B,* 44 (1997) 521-526.

R. Paolesse, C. Di Natale, A. Macagnano, F. Davide, T. Boschi, A. D'Amico; *Sensors and Actuators B* in press.

C. Di Natale, R. Paolesse, A. Macagnano, V.I. Troitsky, T.S. Berzina, A. D'Amico; submitted to *Analytical Chemistry.*

C. Di Natale, A. Macagnano, A. D'Amico, F. Davide; *Measurement Science and Technology*, 8 (1997) 1236-1246.

Flavour sensors arrays become virtual electronic olfactometers: How to get reliable data from unstable sensors ?

Les capteurs d'odeurs deviennent virtuels : comment obtenir des données fiables à partir de capteurs instables ?

Mielle Patrick, Marquis Florence

INRA Laboratoire de Recherches sur les Arômes,
17 rue Sully, F - 21034 DIJON Cedex
e-mail : Patrick.Mielle @ dijon.inra.fr

Abstract: *The quality control, especially for foodstuffs, must include control of the aroma quality of the final products. The new technology of so-called «Electronic Noses» encounters many problems to come out from research laboratories to plants. The main problem is to limit the sensors drift as much as possible in order to maintain a correct search in the library patterns of the products database. A possible improvement can be done by using the same sensors, but in another way. To cancel the drift exhibited by sensors, we were seeking for stable parameters to build the database products. This paper deals with the history and mainly with the future of the «Electronic Noses» technology through a story of dimensions. This one starts from the first system including one unique sensor to the fifth dimension of parameters, including the introduction to Virtual Arrays. Up to now it was difficult to obtain a good precision in classifying samples which are relatively close in terms of flavour or which contain parasitic compounds of weak flavour impact but present at relatively high concentrations. This may be achieved by combining these new parameters.*

Keywords: *Electronic nose, flavour sensors, gas sensors, flavour analysis, quality control.*

Résumé : Le contrôle de qualité, en particulier des produits alimentaires, doit inclure l'appréciation de la qualité des arômes des produits finaux. Une nouvelle technologie appelée «Nez électronique» fait face à de nombreux problèmes lorsqu'elle doit passer du laboratoire à l'industrie. Le problème principal est de limiter la dérive des capteurs afin de faciliter la recherche de profils d'arômes dans une librairie. Une amélioration peut être apportée en utilisant les capteurs de manière différente. Pour éliminer la dérive, nous avons recherché des paramètres stables pour construire la banque de données. Cet article présente l'historique et peut-être le futur des nez électroniques à travers un problème de dimension : à partir d'un système à capteur unique jusqu'à un système à 5 dimensions incluant une matrice virtuelle. Jusqu'à présent, il était assez difficile de classer des produits proches en termes aromatiques ou comprenant des composés parasites de faible impact aromatique mais à fortes concentrations. Ceci peut être mené à bien en utilisant ces nouveaux paramètres.

1. Introduction

Now the consumers demand products of quality. A new trend in the food industry is to relate the overall quality of food to aroma quality. Aromas, flavours and odours are estimated or measured by using reference methods : sensory analysis (human evaluation) or instrumental analysis (separative techniques). Use of Flavour Sensors for global analysis is a promising alternative. This paper deals with their history and their future through a story of dimensions.

1.1 The consumers demand

Taste is becoming a fashion trend. Since the «glorious» decades which followed *World War II*, and during which increase of the production of foodstuffs was the sole purpose, the consumer has again become a centre of interest for the Food Industry, mainly in Europe. The strawberry is getting gradually more savoury. The main actors of the Food Industry are quite aware of that trend ; after «low calorie» food, the biofoods, taste and terroir are taken more and more into consideration.

This tendency was supported by the consumer's distrust concerning the origin of meat. Currently he demands to know what he is eating. However, terroir, tipicity and tastes of the old times, like children's memories of happy days spent with Grandma, are not sufficient. Tangible evidence of the presence of the typical aromas which remind us the that taste did exist formerly, is needed.

Quality control, especially for foodstuffs must include a control step of the aroma quality of the final products. That step is also compulsory to establish the certificate of quality. From there, everything becomes more complicated...

1.2 The development of new methods

The traditional methods used for the characterisation of the food aromas are very accurate, but costly and time-consuming. The new technology of the so-called «Electronic Noses» encounters many problems to come out from research laboratories to plants [i]. The main problem is to minimize the sensors drift as much as possible in order to maintain a correct search in the library. It is possible to point out the limitations when studying in details the functioning of such systems, mainly at the sensor level. It is an established fact that progresses in sensor manufacturing will be very slow [ii]. Besides, there is a great need of the industry for global analysis of target foods which can hardly be satisfied by the available sensors. As a consequence a possible improvement can be done by using the same sensors, but in another way.

1.3 The basic principle of an electronic olfactometer

Whatever kind of sensors you use, they all exhibit drifts in time. Parasitic compounds, such as ethanol, carbon dioxide and moisture in particular [iii], drastically restrict the use of such systems. It is also interesting to improve the separation of the clusters when classifying the samples using PCA. So, we are seeking for stable parameters to build the database products.

For this search, we must come back to the functioning of systems. A sample is characterised using sensors. Before this, target or reference products were measured by using the same technique, and profiles were introduced to build the product database. Then, a classification is done by comparison between the sample and the library patterns. So, the problem is to limit the sensors drift as much as possible in order to maintain a correct search in the library.

Gas sensors can only handle volatile compounds. The generation of volatile compounds from a sample is quite simple to understand, by using an hedonic comparison. Tasting the aromas of a wine or an old brandy is obtained by gently turning liquid aliquots in a tasting glass warmed in your hand. The released aromas are appreciated by sniffing. This is the principle of the static head-space used in the systems, the only difference being the replacement of the tasking glass by laboratory vessels, that of your hand by an oven or a water bath, and that of your nose by sensors ! The shape of the vessel, the respective volumes of liquid and gaseous phases, stirring and equilibration acts on the concentration of volatile and therefore influence tasting. The Partition Coefficient (or Partial Vapour Pressure in the case of a mixture) represents the ratio of the molar concentration in the vapour phase to that of the original products. It is related to : temperature, equilibration time, nature of the substrate, pressure... When all the parameters are kept constant, it is related to the nature and volatility of the compound.

Now, we will present a brief history of dimensions and their use.

2. A summarised history of dimensions

In the beginning was the human being. A human nose was provided as a standard equipment with any item. This human (whatever female or male), was directly derived from the mammalian family and was classically living in a three-dimensional world.

In the 70's, a Japanese researcher discovered and commercialised a gas sensor (TGS sensor) [iv]. He was the outcome of a Japanese government project for the development of a domestic gas leakage sensor. Then, generations of researchers

went on enlarging a range of diverse gas sensors for application fields very far from the original purpose. So the «Electronic Nose» was borne.

A first system was commercialized for the measurement of odours -and particularly flavours-, using discrete samples. The *Alabaster-UV* included only one gas sensor (TGS 800 serie). It was composed of a stainless steel measurement chamber, UV lamp based ozonolyse cleaning system, and an embedded active charcoal filter for the purification of the carrier air. Its main advantage was to exist. The samples were in the chamber during the experiment, enabling the equilibrium of the static head-space.

Entering the first dimension

Direct collection of data was not possible, and only the maximum response of the sensor was recorded as a one point bar graph. So, **nevertheless** this system gave a 2-dimension plot (time of the equilibration and intensity), only one dimension (intensity) was usable (*Figure 1*).

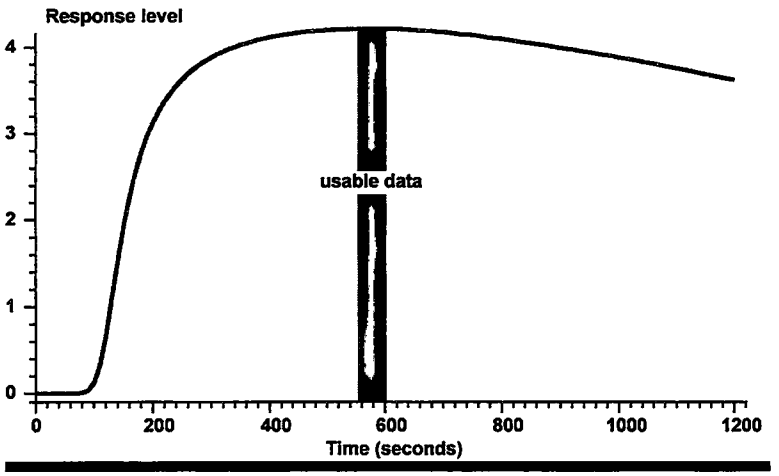

Figure 1: Typical plot of a monosensor system, and usable data

3. The second generation

The second generation of systems involved different kinds or sensors, included in homogeneous or heterogeneous arrays. The main advantage of using arrays is to get a better database. Semiconducting gas sensors exhibit a poor selectivity [v]. *Figure 2* shows the response of three types of *TGS* sensors for four chemicals. It can be noticed that all sensors respond to each stimulus, but with different ratios (the maximum selectivity being near 10 : 1).

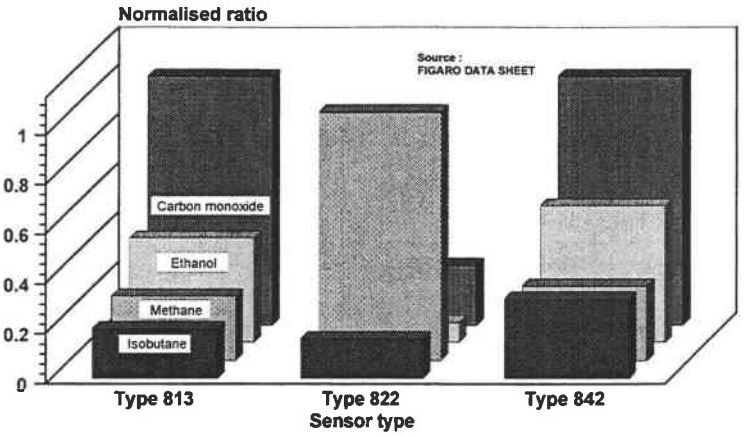

Figure 2: Relative selectivity of sensors in an array

So, to get a pattern -or 'fingerprint'-, they must be used in arrays, containing from 4 to 32 sensors having a partially different selectivity [vi]. Besides the better selectivity of such arrays, they lead in addition of redundant information, very useful in case of a sensor failure. Some sensors, such as conducting polymers or radiofrequencies sensors, have a better selectivity but they must also be used in arrays, to detect a wide range of chemicals, encountered in food products. Currently, all arrays are made of discrete sensors, except for conducting polymers which are highly integrated (near 30 sensors) on a substrate of few square millimetres [vii].

Entering the second dimension

An additional dimension is provided by the depth of the array (number of useful sensors). Those systems need an effluent transfer after the head-space equilibrium. In this case, a dimension is lost (time of equilibration), but another is created (the response time of the measurement cell -which must not be confused with the response time of the sensors-). In classical systems, data acquisition is relatively slow (one to few seconds for each point). The data processing software used to build the database products only takes in account the maximum response of each sensor -or a mean of responses inside a user-definite window- and use this as a one bar per sensor bar graph. So, nevertheless these systems gave a 3-dimension plot (response time of the measurement cell, intensity and number of sensors), only two dimensions (intensity & number of sensors) was usable (*Figure 3*).

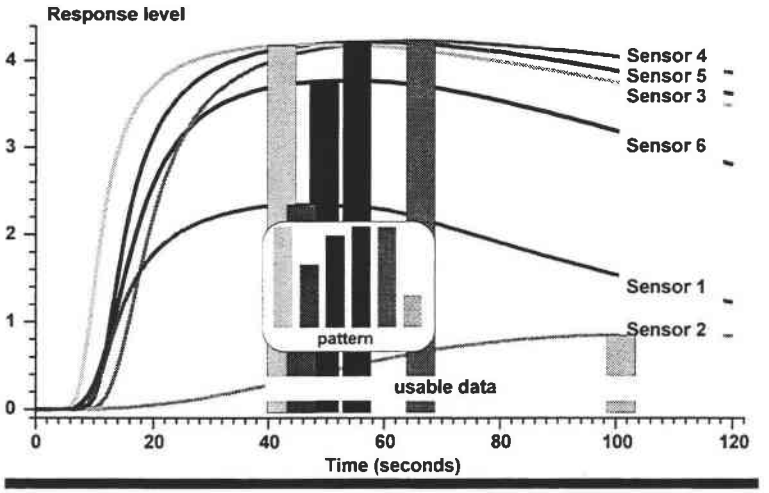

Figure 3: Typical plot of a multisensor system, and usable data (pattern)

By using a faster data collection (in the range of 1/10th second per point), it is possible to get more relevant information about the response. Data processing software can then use the dimension 'time', with is particularly rich, mainly in the kinetic phase.

Entering the third dimension

Then the system gave a real 3-dimension plot (response time of the measurement cell, intensity & number of sensors). In order to minimize the size of the product database, another team of INRA [viii].proposed to modelize the response for each sensor by using a Gompertz model $fg(x) = a.e^{-\frac{b}{c}.e^{-c.x}}$ or a Weibull model $f(t) = a.1\text{-}e^{-b.t\,c}$

This furnished 3 parameters **a**, **b** and **c** for each curve instead of keeping each point collected, thus reducing the size of the database. It is also possible compact the database by selecting only representative points on the graph.

Our team proposed a 15 selected points representation which is very close to the initial graph (1,000 points per curve), without needing a curve fitting, which is difficult to get in some cases (*i.e.* no plateau, artefacts on the signal, decrease of the signal). The discrete time scale is drawn as the Z-axis on the bargraph shown in Figure 4.

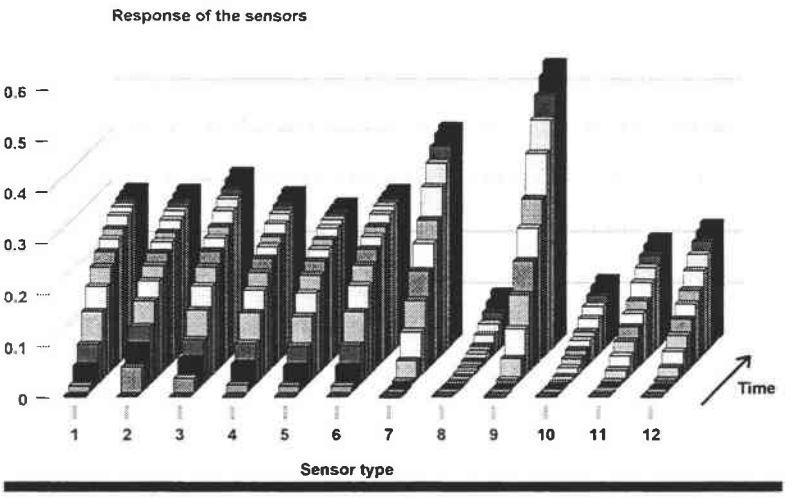

Figure 4: Typical plot of a multisensor system, using all selected data

4. Adding a dimension

At this time, the reliability of the database was greatly improved. But it is difficult to obtain a good precision in classifying samples relatively close in terms of flavour. Furthermore, the effect of parasitic compounds (ethanol, carbon dioxide, water vapour...) is relatively important, provoking distortion in the patterns and errors in pattern recognition when these compounds have a weak flavour impact. So, an additional parameter is of a great interest. But this parameter remains to be found...

We presented a paper [ix]. dealing with the control of the temperature of the sensing element when using semiconducting gas sensors. The interest of managing this temperature is of many orders : The drifts exhibited by sensors are partially due to the variations of the temperature of the sensing element consequently to cooling effect of the effluent flow, the catalytic effects of reactive compounds and a short term instability due to effluent, ambient temperature, or turbulence around the sensitive element. To reduce this part, we quantified the effects of dynamic thermal exchanges at the surface of the sensitive element and then canceled them by regulating the temperature. Then, we developed the programmation of the temperature allowing fast and easy changes in the set point. An electronic board was developed for this purpose (*Smart Flavour Sensors)* [x]. The interest of temperature programming was demonstrated for integrated sensors for better sensitivity (see *Figure 5*) and selectivity and reduction of sensitivity to moisture [xi]. Programming the sensor during an experiment enabled to get the missing parameter...

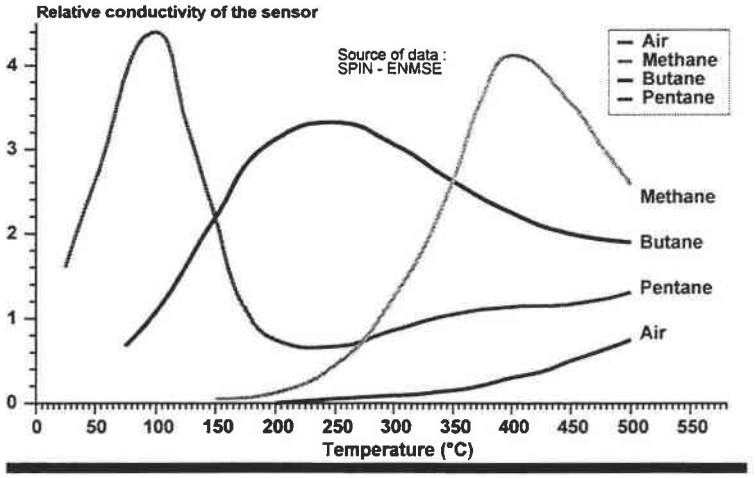

Figure 5 : The influence of a shift of the temperature of the sensing element on the response

Entering the fourth dimension

We got some problems to plot a 4-dimension graph ! So, we decided to ignore the previous third dimension (number of sensors) for plotting only. The plot in *Figure 6* shows 3 dimensions (response time of the measurement cell, intensity related to temperature). In this example, the head-space is static, but it can be dynamic, the response time of temperature programming being rapid.

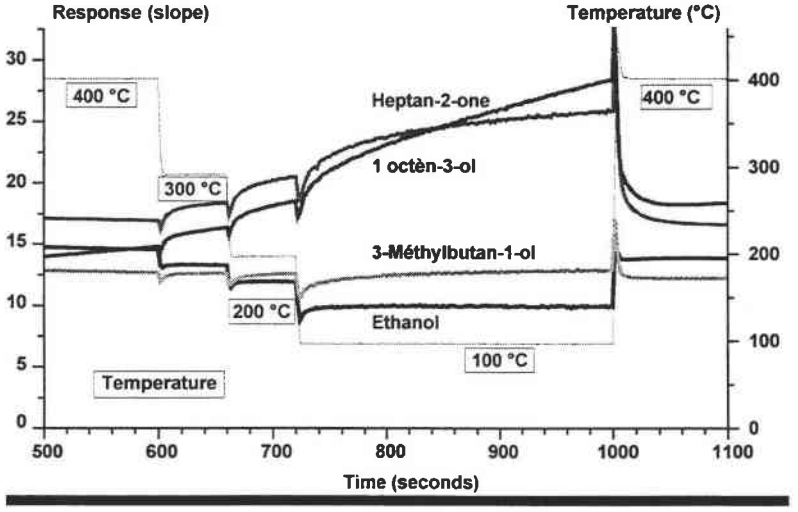

Figure 6: Influence of the programmed temperature of the sensing element on the response

5. Introducing virtual arrays

The control of the temperature is of a great interest because one can get many virtual sensors when setting the temperature to a value corresponding to the largest range of differences between samples. *Figure 7* gives an example of an emulated Virtual 'four sensors' Array. The patterns are very different for four different flavour compounds, enabling to classify these pure compounds with no error. The responses for each temperature step are normalised with respect to the response at 400 °C.

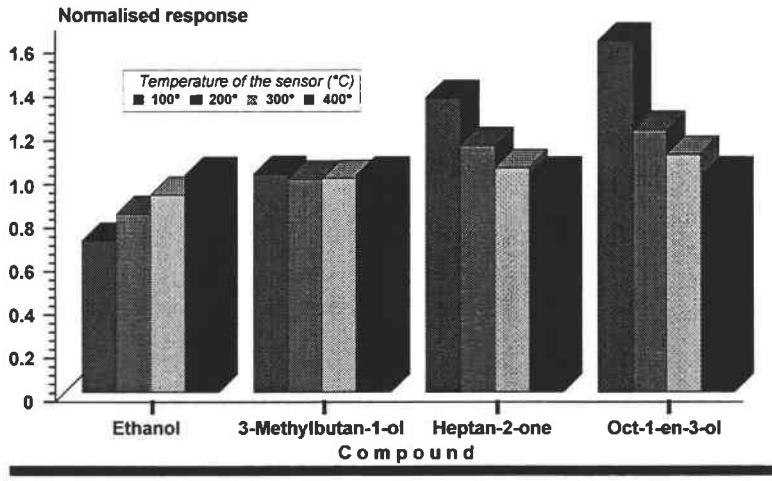

Figure 7: Thermally generated pattern for a 'Virtual Array' of one UNIQUE sensor

Emulation of an array by using only a unique sensor is not a goal by itself. -It is more efficient to enrich the pattern by using a true array, and to complement it with the emulation-. A classical array of 8 discrete sensors can become a Virtual Array of 32 sensors with no modification of the measurement cell. Furthermore, the thermal pattern obtained is only slightly subject to drifts in time.

5.1 Interest of a one sensor virtual array

One application of a one sensor Virtual Array is the monitoring of cooking with a domestic oven. A big company has already marketed an 'intelligent' oven, at the top of its products range. It uses one semiconducting gas sensor, combined with other physical sensors, to compute the end of cooking, before burning the meal... Other companies look in the same way, but for mid-range products. It is difficult -and expensive- to include a sensor array, even an integrated one, into these products. But we think it is possible to use only one sensor to emulate an array, thus

matching the manufacturing cost to the market. This can be achieved by modulating the working temperature of the sensitive element. The interest of temperature programming by means of fuzzy logic has been described for integrated sensors to get more sensitivity and selectivity and to reduce the sensitivity to moisture [xii].
We are developing a new release of electronic boards in this way.

6. Is-it reasonnable to add more dimensions ?

As previously seen, it is very useful to get more information obtained for each sample. This can reduce the level of error of the pattern recognition, so as the problems of drifts or the influence of parasitic compounds. We are presently adding two more dimensions to the pattern of each product.

Looking for the fifth dimension

As previously mentioned, one dimension was lost (the time of equilibration) each time another one was created (the response time of the measurement cell). So, it is of a great interest to recover the lost dimension - the equilibration kinetics of the head-space - which gives an interesting information about the compounds present in a product or a mixture. As shown on the plot (*Figure 8*) that the equilibrium of a static head-space for some pure chemicals (1 µl injected) is quite different, and related to the volatility, expressed as Kovatz indexes on an apolar GC column.

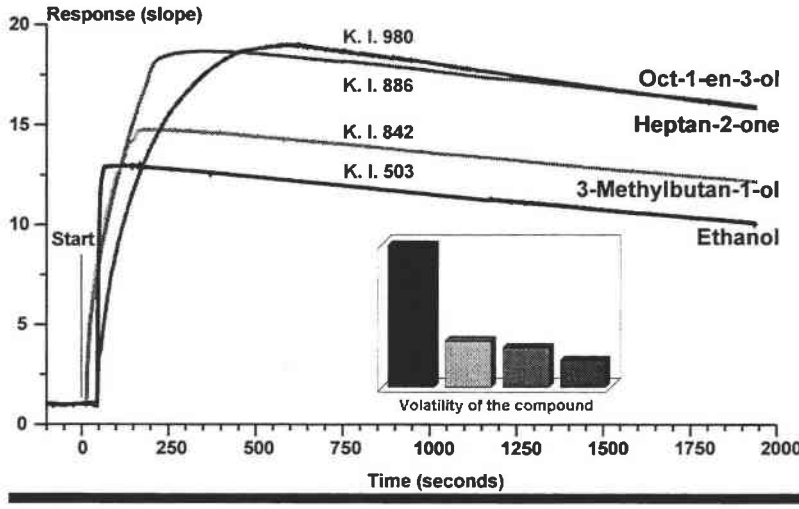

Figure 8: Influence of the compound on the equilibration kinetic (pure compound)

To recover the equilibration kinetics of the head-space, more explanations about the functioning of our prototype must be given. We demonstrated few years ago [xiii] that the response of sensors was correlated to the nature and volatility of the compounds. *Figure 9* shows an example of typical dynamic response for another set of aroma compounds flushed by vapour pulses onto the sensor [xiv].

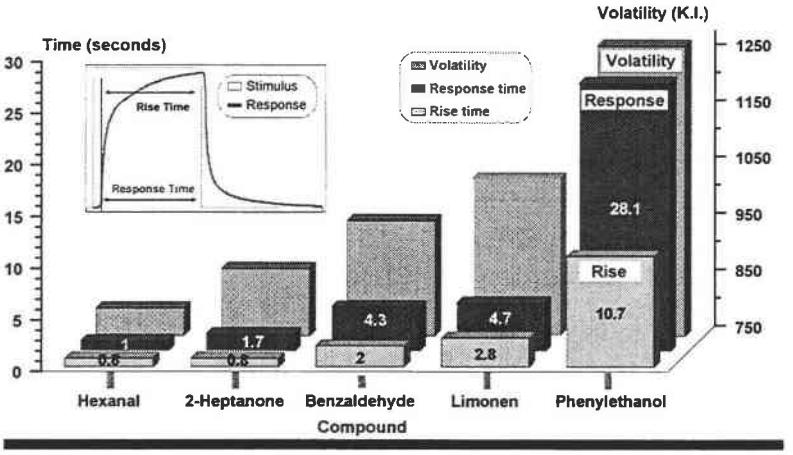

Figure 9: Response time of a semiconducting sensor as a function a the volatility of the compounds

The response time is defined as the delay between the start of the stimulus and the start of the sensor response. The rise time is defined as the delay needed to reach ninety percent of the final value of the response. The volatility of compounds is expressed as Kovatz Indexes, so it is decreasing when the indexes are increasing.

To exploit these parameters, we developed a new method enabling multi sampling of the head-space during its equilibration. The chemicals were at a concentration of 1000 ppm in pure water. The sample was introduced at time zero and the effluent was transferred to the measurement cell for 150 seconds, then substituted with pure air. This was done three times during each experiment. During the last sampling period, the equilibrium was close to be reached. The graph shown in *Figure 10* demonstrates that the envelope of the kinetics of equilibration can be retrieved during each sampling period. For the last period, the rise time corresponds to the rise time of the sensor itself.

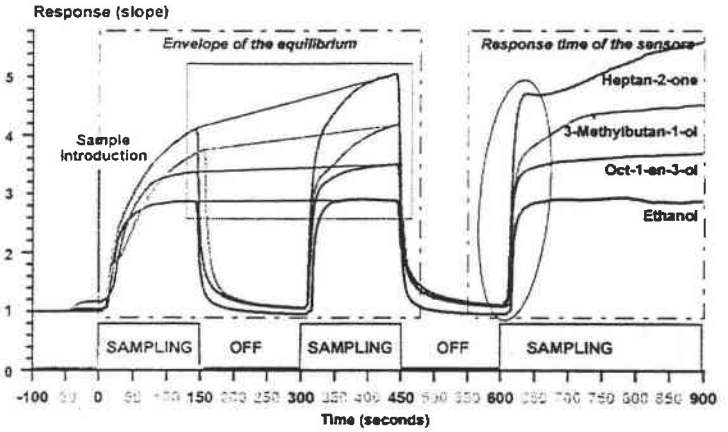

Figure 10: Recovering both the envelope of the equilibrium and the response time of the sensors from the kinetic response

So, we have replaced the measurement of the response time of the cell by two separate parameters of interest. This can be achieved only after a drastic reduction of dead volumes of the system.

The equilibration kinetics is only related to thermodynamics, so this parameter is not subjected to the sensors drift : the only important point is the control of the sample temperature. The response time of the sensors is not dependant of the sensor drift, except in the case of a poisoning occurrence.

Discussion

We have demonstrated that stable parameters can be found even when using classical sensors showing many drifts in the time. Most of these parameters can be used with other technologies of gas sensors. So, current system can be greatly improved avoiding time-consuming studies on the development of new sensors. Further work is looking for two more stable parameters which could improve the selectivity of semiconducting sensors.

In the beginning was the human being. Systems called the «Electronic Noses» have been greatly promoted in the last years and even during last months. The systems are dealing with virtual dimensions, when the human is classically living in a three-dimensional world. But the consumer, in every application field of such systems, is ever the last and the only deciding person (may be with a slight restriction for pet food).

Finally Man remains still superior to all systems...

Biography

The author was working for seven years at the French National Agency for Atomic Energy (CEA) as an electronician for safety. Then he turned in 1980 to a more ecological work and joined the newly created Flavour Research Laboratory at the French National Institute for Agronomical Research (INRA).

He developed in 1982 the first Flash Injection Purging and Trapping System and has designed in 1985 one of the first PC based High Resolution Data Acquisition System use for Gas Chromatography. For 15 years he was developing instrumental systems (mainly GC and GC/Sniff) for analysis of aromas and flavours. He is an expert in electronics applied to the analysis of flavours and volatiles. His domain of excellence covers GC, MS and NMR. He is working since 1993 on semiconducting gas sensors, to be used in food quality control. His main objective is to develop a system for fast and on-line analysis of food products.

He participates to an Interdepartmental program which aims is to build an "Electronic Nose" prototype. New programs will start in 1998 (European Community, technological programs and a Departmental Technological Step) for the development for global method for rapid characterisation of flavours.

Acknowledgments

The authors wishes to thank R. "Bob" Almanza for developing custom data acquisition software Pifomètre and A. Latrasse for kind advice.

The development of a new system by INRA is financially supported by a French Departmental and European Community project.

Parts of this document appeared in Seminar in Food Analysis [xv].

References

[1] Mielle P. (1996). «Electronic Noses» : towards the objective instrumental characterisation of food aroma. Trends in Food Science & Technology, *Flavour Perception Special Issue Vol.7, issue 12, 432-438.*

[2] B. Pâtissier et al., (1996). *Characterisation of micromachined gas sensors,* Proceedings of International Meeting on Chemical Sensors, 20 July 1996, Gaithersburg, USA. NIST ed., Gaithersburg, MD 20899, USA.

[3] VanGeloven P. et al., (1991). *The influence of relative humidity on the response of tin oxide gas sensors to carbon monoxide,* Sensors and Actuators B4, 185.

[4] Taguchi N. (1971). *Method for making a gas-sensing element.* United States Patent, 3, 625-756. December 7.

[5] Figaro Gas Sensor data book, *FIGARO engineering inc.,* Osaka, Japan.

[6] Aishma T. (1991). Aroma discrimination by pattern recognition analysis of responses from semiconductor gas sensor array. *J. Agric. Food Chem. 39, 752-756.*

[7] P.I. Neaves and J.V. Hatfield (1995). A new generation of Integrated Electronic Noses, *Sensors & Actuators B 26-27, 223-231.*

[8] Vernat-Rossi V. et al., (1996). Discrimination de produits agro-alimentaires par capteurs de gaz à semi-conducteurs fonctionnant avec l'air de l'atmosphère ambiante du laboratoire. Différentes approches de traitement du signal. *Analysis 24, 309-315.*

[9] Mielle P. (1995). *Flavour Sensors become smart...,* Proceedings of 2nd International Symposium Olfaction & Electronic Noses, 2-3 Oct. 1995. Toulouse, France, Alpha-MOS ed., Toulouse.

[10] Mielle P. (1996). Managing dynamical thermal exchanges in commercial semi-conducting gas sensors, Proceedings of Transducers'95-Eurosensors IX, 25-29 June 1995 Stockholm, Sweden, *in Sensors & Actuators B 34, 533-538.*

[11] Lalauze R. et al (1992). High sensitivity materials for gas detection, *Sensors & Actuators B 7, 237-245.*

[12] Jondas S. et al (1996). Temperature control of semiconductor metal oxide gas sensors by means of fuzzy logic, *Sensors & Actuators B 34 , 1-5.*

[13] Mielle P. (1994). *How to make an Intelligent Electronic Nose with silly gas sensors...* Proceedings of First International Symposium Olfaction & Electronic Noses, 26-27 Sept. 1994. Toulouse, France, Alpha-MOS ed..

[14] Hivert B. et al, (1995) A fast and reproducible method for gas sensors screening to flavour compounds, Proceedings of Eurosensors VIII, 25-28 Sept. 1994 Toulouse, France, *Sensors & Actuators B 26-27, 242-245.*

[15] Mielle P., Marquis F., (1998). *Enhancement of the products database reliability by using new dimensions.* Poceedings of 4rd International Symposium Olfaction & Electronic Noses, 6-7 Oct. 1997. Nice, France, in Seminars in Food Analysis, Thomson Science publisher, in print.

Contribution of the gas sensors for the characterisation of products

Contribution des capteurs d'odeurs à la caractérisation des produits alimentaires

C. Nicolas
Nestlé France, Laboratoire d'Evaluation Sensorielle, 7, bd Pierre Carle, BP 900 Noisiel - 77446 Marne-la-Vallée, Cecilia.Nicolas@fr.nestle.com

P. Carel
Centre de Recherche et Développement Friskies Amiens, BP 47 80800 Aubigny/Corbie

J. Hossenlopp
CEMAGREF, Equipe Qualité Alimentaire, QACF, 24 Avenue des Landais, BP 50085 - 63172 AUBIERE Cedex, joseph.hossenlopp@cemagref.fr

G. Trystram
INRA - ENSIA, Département de Génie Alimentaire Industriel, 1, av des Olympiades - 91744 Massy, Gilles.Trystram@massy.inra.fr

D.N. Rutledge
INA P-G, Laboratoire de Chimie Analytique, 16, rue Claude Bernard - 75231 Paris Cedex 05, rutledge@inapg.inra.fr

Abstract: *The purpose of this study was to see whether the odour sensors could be a good tool to predict sensory data, compared to more traditional instrumental techniques like Gas Chromatography (GC) or texture measurements. Twelve moist petfood were characterised with different analytical methods (Sensory Analysis, GC coupled with a Mass Spectrometer (MS), texture and odour sensor measurements). This presentation will first describe the use of Variance Analysis to detect and extract relevant information from the huge quantity of data generated by a sensor array. Then the links between the different instrumental measurements and the sensory data will be analysed by Multiple Factor Analysis (qualitative data) and by Partial Least Squares regression (quantitative results). The results show that the odour sensor can contribute to the characterisation of this particular set of manufactured products. When the odour sensor responses are combined with other rapid techniques such as texture measurements, the characterisation can be even richer.*

Keywords: *Petfood, sensory analysis, GC-MS, odour sensors, analysis of variance, multiple factor analysis, partial least squares.*

Résumé : L'objectif de cette étude est de déterminer si les capteurs d'odeur peuvent être un bon outil pour prédire les données sensorielles, en comparaison à des techniques instrumentales traditionnelles telles que la chromatographie gaz (GC) ou les mesures de texture. Cette présentation décrit tout d'abord l'analyse de variance utilisée pour détecter et extraire l'information pertinente d'une grande masse de données générées par la matrice capteur. Puis les liens entre les différentes méthodes analytiques et l'analyse sensorielle sont étudiés par Analyse Multifactorielle (qualitatif) ou Régression aux moindres carrés partiels (quantitatif). On montre que le capteur d'odeurs peut contribuer à la caractérisation des produits. Lorsque ses réponses sont combinées à celles d'autres techniques rapides comme la mesure de texture, la caractérisation est encore plus riche.

1. Introduction

In the food industry the analysis of food flavour is done with classical tools such as GC/MS or Sensory Analysis. Most of the time, these traditional methods are expensive and time consuming. Odour sensor arrays are now being investigated as an alternative technique to evaluate the odour quality of food products [1, 2]. Odour sensors have a characteristic electrical resistance which varies rapidly with the adsorption of volatile molecules. Electrical signals generated by an odour sensor array can be analysed using appropriate statistical methods in order to give a representation of different products. At the moment, artificial odour sensing systems arouse much interest in a number of industries as they seem to be a very promising rapid technique for aroma control.

Sensor arrays generate a huge quantity of data that must be reduced in order to extract the information relevant for a particular application. Of the different applications to be found in the bibliography, some are based on a response vector constituted only of the maximum values for all the sensors in the array [1, 3, 4]. Another approach takes into account the entire curves by decomposing the curves into a certain number of discontinuous values [5]. The drawback of this method is that to analyse the matrix generated in this way by a Factor Analysis method or by a Neural Network, it is necessary to get a large number of samples to have a reasonably balanced samples/variables ratio. Another approach consists in modelling the curves with a particular function, and then extracting the model parameters [6, 7]. Here an alternative method is presented, that can be applied to analyse the entire raw curves and to extract the relevant information in them by performing an Analysis of Variance at each point of the signals. This method is applied to the raw signals without proceeding to a modelisation step which may be time consuming and source of errors. This approach has been previously used in a similar way to analyse NMR relaxation curves [8].

After having extracted the relevant information from the sensor responses, this new data set will introduce and the extent to which it can be correlated to the sensory data will be studied. First of all, qualitative links will be established by Multiple Factor Analysis, MFA [9]. Then quantitative links will be established to predict sensory characteristics, using Partial Least Squares regression, PLS [10].

2. Material and methods

2.1 The products

The twelve products studied are two types of moist products for cats: chunks in gravy (*P2, P3, P4, P5, P8, P12*) and terrines (*P1, P6, P7, P9, P10, P11*). They are packaged in 400g cans, from the same batch, and have similar humidity (average 81.9%) and water activity (average 97.4%. at 20°C).

2.2 Sensory data

Sensory attributes were scored on a seven point intensity scale (from 1 - very weak, to 7 - very strong). There was a common questionnaire for the two types of products which included 28 attributes (16 odour attributes, 7 visual attributes and 5 texture attributes). Judges calibrated their evaluations by consensus after two round tables before the beginning of the test. Four complementary training sessions were then organised in boxes. These strengthened the calibration within the group and led to a repeatable and homogeneous panel. The six terrines and the six chunks in gravy products were then evaluated by 14 judges during four sessions in boxes. Three products were presented at each sessions in a random order. Each product was evaluated twice. The tests took place at room temperature, products were evaluated outside the cans. All attributes discriminated the products in a significant way (analysis of variance : $p<0.05$).

2.3 Chemical measurements

Measurements were done on the twelve products using GC/MS, in order to determine a certain number of peaks representing the volatile molecules of the vapour phase above the products. Measurements were done on the entire 400g contained in a can. A dynamic purge and trap headspace extraction with nitrogen was used (Teckmar LSC 2000 system). Then, a GC (5890 serie II, Apolar Column Chrompack) was used and Mass 5971 detection in scan mode was performed. Two repetitions were done for each product. Prior to these measurements, the stability of the instrument retention times was checked. Then 116 molecules were globally identified thanks to a spectral and retention index library constructed in collaboration with the Lausanne R & D Center. These molecules (m1 to m116) cover a vast range of different chemical families, such as alcohols (ex : ethanol, 1-butanol), aldehydes (ex : hexanal, heptanal), ketones (ex : 1-hydroxy-2-propanone), as well as hydrocarbons (ex : ethane), esters (ex : ethylacetate), bases (ex : pyrazine, pyrrole), sulphur compounds (ex : 2-methyl thiophene), furans (ex : furfural) and nitriles (ex : propane nitrile). For each molecule identified, an average between the areas of the two replicates was calculated. This way, a matrix was generated with the twelve products and the surfaces of the peaks of the 116 molecules. The correlation matrix between these 116 molecules was calculated. From this correlation matrix, 39 representative molecules were selected from the original 116, the threshold for the correlations between molecules being set at 0.7.

2.4 Physical measurements

Two texture parameters were measured with a Stevens LRFA 1000 instrument : firmness (*fer*) and breaking point (*ptr*).

2.5 Odour sensor responses

The twelve products were analysed with 32 polymer odour sensors of the Aroma Scan instrument manufactured by the University of Manchester [11, 12]. Four replicates were done for each of the twelve products, on 200g from four different cans. These 200g were put into a plastic bag, the plastic bag was inflated with pure 99.999% nitrogen (with a controlled humidity of 50%). The sample bags were left for five minutes at room temperature (20°C, constant) for headspace generation. The measurement took place using the following cycle : during one minute the pure nitrogen at 50% humidity was passed through the sensor chamber. The sensors' base resistances were calculated with this reference nitrogen. The headspace from the sample bag was then pumped for 100 seconds (150ml/min). The sensors were then washed with the headspace of a solution of water and 2% butanol for one minute. Finally the reference nitrogen was passed through the sensors again in order to reset them to their base resistances.

2.6 Detecting relevant information in odour sensor responses using Analysis of Variance

For each measurement, each of the 32 sensors generates a curve with an ascending phase and a second phase during which the slope decreases greatly (101 points in total for each sensor : one point per second for 101 seconds), Figure 1 :

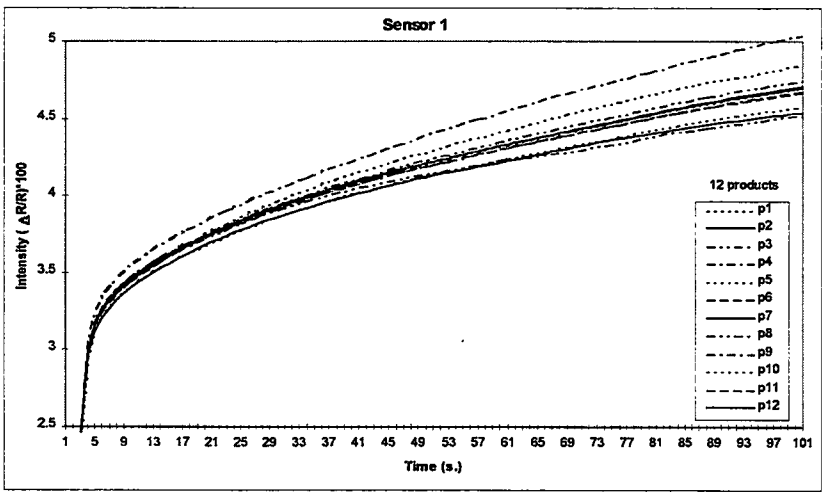

Figure 1: Average responses from sensor 1 to the volatile compounds of the twelve products

At a fixed time t=x , the signal $I_{t=x}$ generated by a particular sensor can be defined as:

$$I_{t=x} = 100*(R_{t=x} - R_{t=0}) / R_{t=} \qquad R_t = \text{resistance of the sensor at time t}$$

A matrix was created in which each sample was defined by the 32 sets of 101 points generated by each sensor, giving 3232 variables for each sample. Products are divided into twelve groups with four samples in each (four replicates of each product).

The Analysis of Variance was applied to determine the overall influence of the product on the sensor responses and to determine which regions of the curves are most sensitive to the product effect. Calculations were performed using a program developed in the Laboratory of Analytical Chemistry of INA P-G, and validated using MATLAB routines. This Analysis of Variance was done for each column of the matrix, i.e. for each of the 3232 variables. The Analysis of Variance measures the variability at each point in the curve which is due to the predefined grouping of the samples, and the variability which is not explained by the groups.

2.7 Multiple factor analysis to compare the different representation spaces1

Multiple Factor Analysis (MFA) is a technique adapted to matrices where products are described by different groups of variables. Its main interest is that it does a Factor Analysis where the influence of the different groups of variables is equilibrated [9].

The program firstly does a separate PCA on each group of variables (this PCA gives a few main components for each group called Partial Factors). Then it does a global balanced PCA on all the variables, based on the correlations between the Partial Factors of the different groups and thus on the correlations between the starting variables. In the final representation, on the main components, results are read by taking into account the contribution of each variable in the calculation of the component and also the representation index. The balanced weights of the different groups represented on each component should also be taken into account.

The purpose of the analysis is to study the links that exist between the different representation spaces taken two by two. Here we will focus on the one hand on the links between the GC data and the sensory data and on the other hand on the links between the odour sensor data and the sensory data.

1 Performed on the program ADDAD (B. Escoffier and J. Pagès, 1988)

2.8 Partial least squares regression to establish quantitative links between the different data sets2

Links observed between the different data sets (discussed below) were quantified by Partial Least Squares regression (PLS). PLS can establish links between sensory, chemical, physical data sets, in order to build predictive models [10]. In this analysis, the regression on the variables from the Y matrix is done on latent variables extracted from the explanatory X matrix (1st, 2nd, ... extracted factors). The algorithm is quite similar to that of Principal Component Regression. The only difference is that PLS constructs the factors (latent variables) that synthesise the variations within the X matrix by taking into account not only the correlations within X variables but also the covariances between X and Y variables. The Y matrix guides the construction of the explanatory factors from the X matrix.

PLS can give a representation of the products in a two dimensional space. This representation can be a little different from a PCA or a MFA plot, insofar as it takes into account the information contained in the Y matrix. But generally it gives almost the same information. The final results are the *B coefficients* which represent the coefficients by which X values have to be multiplied to obtain Y values (these coefficients are calculated successively for models that include one factor, two factors, three factors, etc.). In order to validate these successive models, *cross validations* were performed. B coefficients resulting from the model whose cross-validation shows the lowest error (and a reasonably good % of Y variance explained) are kept. In this study, variables from the Y matrix are all predicted using separate PLS regressions (PLS 1).

3. Results and discussion

3.1 Odour sensor responses : reliability of the data and relevant information extracted

The Analysis of Variance shows that the Group Variance increases almost constantly, for all sensors, from the beginning of the curve to the end of the curve (Figure 2). Furthermore, the variance between the twelve groups is significantly higher than the Residual Variance (Figure 3). Thus, in our study, the average values from the end of the curves appeared to be most relevant to discriminate the products. For the subsequent analyses, each sample was defined by 32 values corresponding to the average values from the end of the 32 sensor curves (averages calculated for ten points corresponding to ten acquisitions starting at time 85s.).

---

2 Performed on the program Unscrambler (H. Martens, available from Computer-Aided Modelling, P.O. Box 2893, N-7001 Trondheim, Norway)

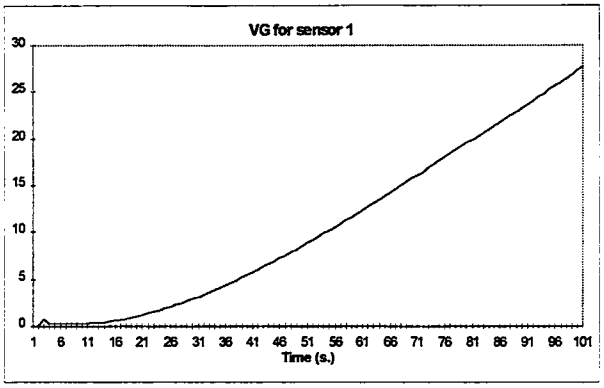

Figure 2: Evolution of the Group Variance between the twelve groups of moist cat food products

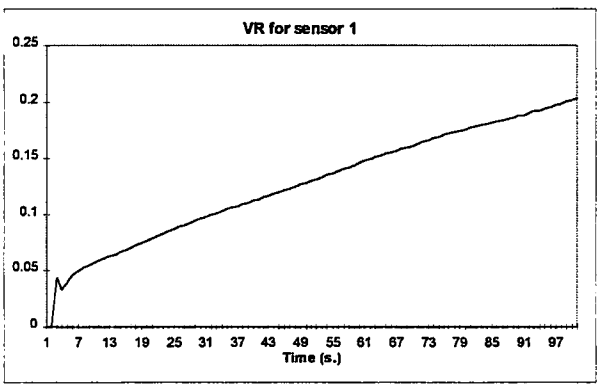

Figure 3: Evolution of the Residual Variance within the twelve groups of moist cat food products

The response vector for each sample, containing 32 values, was then normalised : $N_{t=x} = 100^* (I_{t=x})/(\Sigma_{1 \text{ à } 32} |I_{t=x}|)$, so that all the response vectors of the different samples were within the same constant radius hypersphere to minimise the influence of small variations in the quantity of product. Furthermore, no significant differences in Aw between the twelve products was detected. Aw values were not correlated with the sensor measurements (correlations ~ 0.2).

The repeatability of the measurements performed on the odour sensors was checked sensor by sensor. Four cans were analysed for each product. On the first two cans, two analyses were performed on the two halves of each can. The two analyses on the same can always gave statistically identical results, whereas there were significant differences between two cans of the same product for certain

sensors («can effect»). Therefore, it was decided to perform one measurement on two more cans. As the variability between two cans can be important it seemed preferable to analyse a larger number of cans for one particular product (in order to have more representative results for each product). Nevertheless, variability between the four replications on one product (due to manufacturing variations or to inaccuracies in sensor measurements) remained small enough not to mask differences among the twelve products displayed by the odour sensors. An average of the four replicates for each product and for each sensor was calculated.

3.2 *Qualitative links between the different data sets*

It is interesting to bring together sensory and GC data (Figures 4a and 4b).

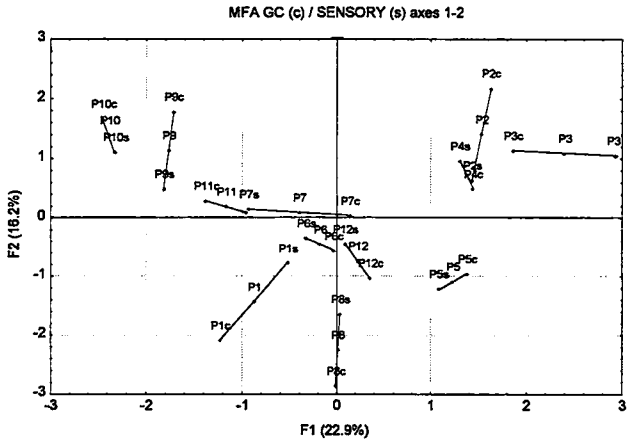

Figure 4a: MFA on GC and sensory data. Projection of the partial and global images of the products (1 : GC, 2 : sensory)

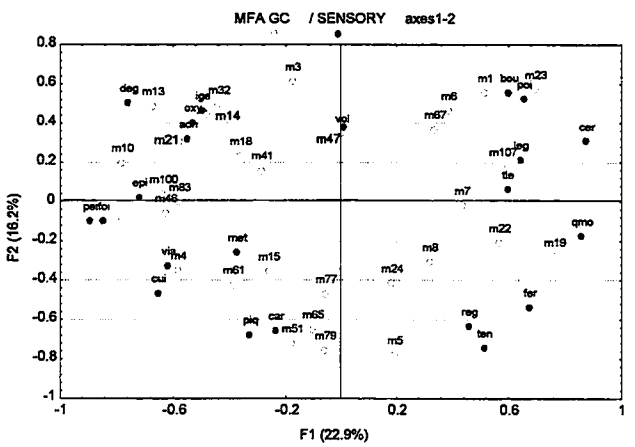

Figure 4b: MFA on GC and sensory data. Projection of the variables from GC and sensory data

This allows us to establish some hypotheses to explain a sensory attribute by the presence of some particular molecules. For example, many molecules can be associated with sensory characteristics like cereal-*cer* (m19, m23, m107), fish-*poi* (m1, m23, m6), vegetable-*leg* (m107), degraded-*deg* (m13, m14), persistent-*per* (m83, m100), spicey-*epi* (m83, m100), cooked-*cui* (m4, m61) or caramel-*car* (m79).

Odour sensor data and sensory data can also be brought together. Partial images of the products related to each data set are quite close. This shows the existence of common Partial Factors between the two data sets even if they are less obvious than for GC and sensory data. For example it can be seen that some odour sensors are correlated with certain sensory attributes such as degraded *(deg),* spicey *(epi),* overall odour intensity *(ige),* persistent *(per)* (Figures 5a and 5b). However odour sensors give a less rich information on product characteristics than GC data (for example sensory attributes like cereal *(cer)* or vegetable *(leg)* are located in a dimension which is not correlated with the odour sensors). This is due to the fact that sensors are all very mutually correlated.

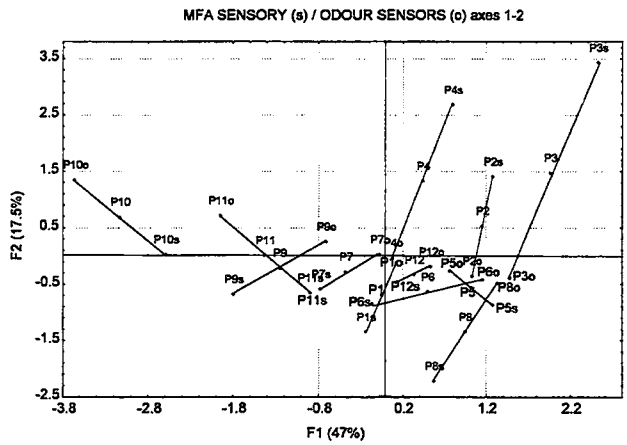

Figure 5a: MFA on sensory and odour sensor data. Projection of the partial and global images of the products (1 : sensory, 2 : odour sensors)

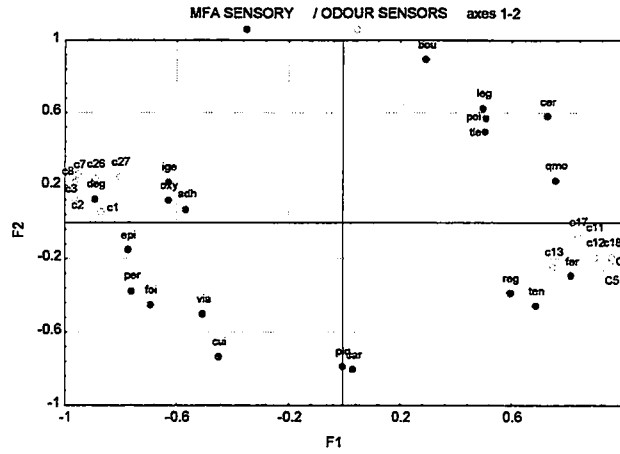

Figure 5b: MFA on sensory and odour sensor data. Projection of the variables from sensory and odour sensor data

3.3 Quantitative prediction of sensory attributes by GC, texture and odour sensor data

Furthermore, by Partial Least Squares regression, some quantitative links and some predictive models could be established (cross-validations were performed in order to avoid over-fitting). Particularly, some sensory attributes were predicted through the response of some odour sensors (mostly general intensity, degraded, spicey, fish, liver, persistent) with a quite small residual error (Table 1) :

Sensory variables predicted by the odour sensors	% of Yvariance explained by the model	Sum of the residual squares for the cross-validation
general intensity	36.0	1.368
degraded	70.9	0.365
spicey	89.2	0.674
fish	59.9	0.800
liver	23.0	1.020
persistent	35.0	0.800
quantity of pieces	31.3	0.700

Table 1: Results of PLS1 regressions between odour sensor data and different sensory attributes

When associated with texture measurements, the odour sensors can give even better predictions of some sensory attributes, as we introduce new dimensions in the predictive data set. Table 2 shows sensory attributes whose prediction is slightly improved when texture measurements are associated with odour sensor responses. Predictions for the attributes spicey, fish and quantity of pieces stay about the same. This improvement can be explained by the fact that texture characteristics can certainly determine the way odours are released. Moreover, liver pieces for example are very hard, whereas degraded and persistent odours are often associated with smooth textures. Obviously some sensory attributes related to texture can also be predicted to a certain extent.

Sensory variables predicted by the odour sensor and texture data	% of Yvariance explained by the model	Sum of the residual squares for the cross-validation
general intensity	98.2	0.784
degraded	92.6	0.426
liver	61.2	0.932
meat	37.8	1.297
cereals	45.3	0.869
persistent	36.1	0.892
firmness	61.8	1.319
regularity	81.8	0.741

Table 2: Results of PLS1 regressions between odour sensor and texture data, and different sensory attributes

Even if GC data still give a better prediction for more sensory attributes (Table 3), this is quite satisfactory and promising as odour sensors have the advantage of being rapid.

Sensory variables predicted by the GC data	% of Yvariance explained by the model	Sum of the residual squares for the cross-validation
general intensity	100.0	1.625
oxydised	100.0	1.412
degraded	80.2	2.386
cooked	71.7	0.865
spicey	83.7	1.313
metallic	82.7	1.038
fish	89.9	0.814
liver	95.4	0.449
vegetables	86.4	0.598
cereal	99.2	1.683
persistent	96.9	1.047
quantity of pieces	94.0	0.726

Table 3: Results of PLS1 regressions between GC data and different sensory attributes

Conclusion

First of all, it can be underlined, that the use of the Analysis of Variance to extract relevant information from sensor responses is a quite interesting technique as it is rapid and it can be applied to the entire raw signals.

Furthermore, it is clear from these results that odour sensors are a promising tool for the prediction of sensory data, compared to a more traditional instrumental techniques such as GC. In the future, it could be even more interesting if less correlated sensors could be used, so that the information from each individual sensor is less redundant and the complete array is more discriminant. Odour sensor measurements can also be associated with other rapid instrumental measurements.

It is also apparent that none of the predictor data sets is completely exhaustive in describing products and predicting their sensory attributes. This implies that there are other dimensions that are not taken into account with the analytical methods

used here, such as molecules that are not detected by either the odour sensors or the GC and which are important to a sensory point of view. However this work appears to be very interesting as all these descriptive data can help to estimate the palatability of the products.

References

[1] Gardner JW, Bartlett PN. *Sensors and Sensory Systems for Electronic Noses* (Gardner JW, Bartlett PN, eds), Kluwer Academic Publishers, 1992, vol 212.

[2] Gardner JW, Bartlett PN. A brief history of electronic noses. In *Sensors and Actuators B*, 18-19, 211-220, 1994.

[3] Gardner JW. Detection of vapours and odours from a multisensor array using pattern recognition techniques Part 1. Principal Component Analysis and Cluster Analysis. In *Sensors and actuators B*, 4, 109-115, 1991.

[4] Gardner JW, Bartlett PN. Intelligent CemSADs for Artificial Odor-Sensing of Coffees and lager Beers. In *Olfaction and taste XI* (Kurihara K, Suzuki N & Ogawa H eds), Springer-Verlag, Tokyo, 690-693, 1994.

[5] Mielle P. «Electronic noses»: Towards the objective instrumental characterisation of food aroma. In *Trends in Food Science and Technology*, 7, 432-438, 1996.

[6] Vernat-Rossi V, Vernat G, Berdague JL. Discrimination de produits agro-alimentaires par senseurs de gaz à semi-conducteurs fonctionnant en atmosphère ambiante de laboratoire. Différentes approches de traitement du signal. In *Analusis*, 24, 309-315, 1996.

[7] Eklov T, Martensson P, Lundström I. Enhanced selectivity of MOSFET gas sensors by systematically analysis of transient parameters. In *Analytica Chimica Acta*, 18343, 1-9, 1997.

[8] Rutledge DN. Chimiométrie et résonance magnétique nucléaire «Domaine Temps». In *Analusis*, 25, 1, 9-14, 1997.

[9] Escoffier B., Pages J. *Analyses factorielles simples et multiples.* Dunod, Paris, 1988.

[10] Martens M., Martens H. Partial Least Squares Regression. In *Statistical procedures in food research*, PIGGOTT J.R. (ed.), Elsevier Applied Science, 293-359, 1986.

[11] Persaud KC, Khaffaf SM, Pisanelli AM. Measurement of sensory quality using electronic sensing systems. In *Measurement and Control*, 17-20, 1996.

[12] Persaud KC, Qutob AA, Travers P, Pisanelli AM, Szyszko S. Odor Evaluation of Foods Using Conducting Polymer Arrays and Neural Net Pattern Recognition. In *Olfaction and taste XI* (Kurihara K, Suzuki N & Ogawa H eds), Springer-Verlag, Tokyo, 708-709, 1994.

Methodology for SnO2-gas sensor selection using stepwise multivariate analysis

Une méthodologie pour sélectionner les capteurs gaz SnO2 en utilisant une analyse multivariée pas à pas

ROUSSEL Sylvie, GRENIER Pierre, BELLON-MAUREL Véronique

Laboratoire Génie Instrumental pour la Qualité Agro-alimentaire,
CEMAGREF, 361, rue JF Breton, BP 5095, Montpellier, CEDEX 01

Abstract: *Electronic noses are very often said to have a great potential in food industry. However, metrology is not yet developed and several problems remains, such as signal processing, definition of optimal experimental conditions, and choice of useful sensors. Indeed, the number of sensors that can be used at the same time is fixed, whereas the number of potential sensors is larger and still growing. Thus, before each new application, one of the main problems is choosing the most suitable gas sensors. SnO_2-sensors have a large sensitivity, and a low selectivity. Their commercial specifications are evasive, e.g. «control roasting conditions» or «combustible detection». Furthermore, SnO_2-sensors are initially built, not for food applications but for chemical purposes and thus, their characteristics do not correspond to food product volatiles ; it is impossible to select the sensors with this available knowledge.*

An experimental methodology is proposed to help users to choose the most discriminant SnO2-sensors for each application, relatively to their sensitivity and redundancy. If the discriminant volatiles are known, the selection is based on either real or model samples representative of few classes.

We apply this methodology to the discrimination of satisfactory wine and vinegary-off-flavour-wine. However, in this first step, model solutions are prepared without ethanol to avoid sensor saturation. Thirty two model solutions are prepared to cover a large range of tainted wines. The frontier between the «good» and «bad» wine is determined by two volatile concentration thresholds: 700ppm of acid acetic and 200ppm of ethyl acetate.

Thirteen SnO2 sensors are studied, in three times, because the measurement cell contains five sensors only. During the whole experiment, one sensor presenting an average repeatability is kept as a reference. From each adsorption and desorption curves, ten features are extracted, e.g. adsorption maximum, maxima and minima of primary and secondary derivatives.

Two stepwise multivariate statistical analysis are performed on these measurements in order to choose the most discriminant sensors. Stepwise discriminant function analysis (DFA) with Wilks Lambda and Fisher Test

criteria, and stepwise k-nearest neighbour method (kNN) are applied to all the data set, selecting the sensors corresponding to the selected features.

The Fisher test method showed that the best classification is performed with two features, extracted from two different sensor curves. The five best sensors were selected using the first nine features chosen by the stepwise DFA, among the 150 features. The stepwise kNN selected only one sensor, using one feature. The selected features are extracted either from the signal and from the primary and secondary derivatives.

The validation of this sensor array selection is made by showing that any other discrimination is less powerful, whatever the sensor association.

This methodology, which is consolidated by a statistical approach, could be applied by every artificial nose user to select the most suitable sensors in an objective way.

Résumé : Les capteurs d'arômes ont un fort potentiel pour le contrôle de la qualité de produits agro-alimentaires. Cependant, aucune métrologie n'a encore été développée pour ce type de système multi-capteur et de nombreux problèmes subsistent, tels que l'extraction de l'information des signaux, la détermination de conditions expérimentales optimales ou le choix des capteurs les plus adaptés pour chaque application. Les capteurs semi-conducteurs en oxyde métallique sont sensibles à un grand nombre de molécules volatiles, mettant en évidence une très faible spécificité. De plus, leurs spécifications commerciales sont très évasives et ne correspondent pas aux arômes alimentaires ; il est donc impossible de les choisir grâce aux informations disponibles.

Dans cet article, une méthodologie expérimentale est proposée afin d'aider les utilisateurs de capteurs d'arômes à sélectionner les meilleurs éléments sensibles en fonction de leur sensibilité et de leur redondance. Ce choix peut être basé sur la mesure de solutions modèles si les molécules volatiles discriminantes sont connues.

Cette méthodologie est appliquée à la discrimination de vins sains et de vins piqués. Cependant, afin de s'affranchir de l'éthanol qui masque le signal des autres arômes, 32 solutions modèles exemptes d'alcool sont préparées, contenant différentes proportions en acide acétique et en acétate d'éthyle, molécules volatiles responsables du défaut de piqué. Si la concentration en acide acétique est supérieure à 700ppm et celle en acétate d'éthyle à 200ppm, alors la solution représente un vin piqué.

13 capteurs en oxyde métallique semi-conducteur sont étudiés, en 3 fois, car la cellule de mesure ne contient que 5 capteurs ; un capteur, présentant un répétabilité moyenne, est conservé durant toutes les expérimentations. 10

descripteurs sont extraits des courbes d'adsorption et de désorption, tels que des extrema des courbes, des pentes et des dérivées secondes.

2 méthodes statistiques multivariées pas à pas sont appliquées à cet ensemble de 150 descripteurs extraits : l'Analyse Factorielle Discriminante (AFD) pas à pas basée sur le Lambda de Wilks ou sur le Test de Fisher et la méthode des k-Plus Proches Voisins pas à pas (kPPV).

L'AFD basée sur le test de Fisher détermine que la meilleure classification est obtenue en utilisant seulement 2 descripteurs extraits de courbes de 2 capteurs différents. les 5 meilleurs capteurs sont choisis en sélectionnant les 9 premiers descripteurs grâce à l'AFD basée sur le Lambda de Wilks. Les kPPV sélectionnent un seul descripteur. Quelle que soit la méthode, les premiers descripteurs choisis sont les mêmes et sont aussi bien extraits du signal que de ses dérivées.

Cette méthode de sélection est validée par des tests de classification basés sur différentes associations de capteurs ; les meilleurs résultats sont délivrés par les 2 capteurs sélectionnés grâce AFD pas à pas basée sur le test de Fisher.

Cette méthodologie d'analyse statistique multivariée peut donc être employée par tous les utilisateurs de capteurs d'arômes afin de sélectionner objectivement les capteurs les plus appropriés à leur application.

1. Introduction

Dealing with gas sensors and electronic noses, many aspects have been investigated in order to improve selectivity and classification efficiency: pre-processing computations [1], pattern recognition techniques [2], drift assessment and counteraction [3&4] or sensor selectivity enhancement [5].

The gas sensors, such as metal oxide, polymers or quartz micro balance, respond broadly to a range of gases rather than to a specific volatile ; thus, they show overlapping sensitivity, with different selectivity levels. Therefore, it is of the highest interest to choose the most suitable sensors, able to provide the best classification results.

Though some electronic nose devices are able to enclose 24 (AlphaMOS, F) or 32 sensors (AROMASCAN, UK), it is impossible to gather all the commercialised gas sensors at each head-space analysis. Moreover, it is meaningless to carry out measurements with numerous sensors, since most of them are highly redundant and add noise to the multi-sensor array output. Therefore, sensor selection, adapted to each application, is crucial. SnO2-gas sensor manufacturers provide selectivity characteristics, such as « solvent vapour detection » or « cooking control », which are not precise enough and meaningless for quality assessment of food products.

Usually, in electronic nose studies, the choice of sensors adapted to a specific application, is not investigated thoroughly. Very few data collections exposing precise sensor characteristics are available. Concerning some basis volatiles, such as methanol, ethanol, hexane, benzene..., some sensor properties are detailed, but flavour discrimination is much more complex.

Gradually, some authors are taking into account sensor selection, determining the ones most related to the studied aromas. For example, four TGS metal oxide semiconductor gas sensors have been examined, using cluster analysis in order to compare the sensor output correlation [6]. Four Quartz Microbalance sensors have been studied using a self-organising map, which enables to evaluate the influence of each sensor and the sensor correlation on the whole domain of data (when measuring aroma mixtures) [7]. Furthermore, sensor output selection has been performed on a 32-element sensor array of conducting polymers, using Procrutes rotation in order to choose the sensors that better describe the variability on the flavour data set [8].

In this paper, we propose to select the most suitable sensors for each specific application, by performing feature subset selection methods. These approaches are currently used to choose variables coming from infrared spectra [9] or features extracted from images [10]. Among all these methods, two stepwise algorithms

have been chosen, performing ascendant and descendant selection, i.e. choosing and removing one by one feature at each iteration. This methodology is applied to the discrimination of wine model solutions showing vinegar off-flavour.

2. Materials

2.1 Experimental device

The measurement device is a metal oxide gas sensor array (LCA1000, Midivaleur, F) containing 5 FIGARO SnO2 sensors and modified to host a thermo-hygrometer and to acquire the sensor voltage on a 12 bit A/D converter. The metal oxide sensors are heated to a constant temperature, holding the sensor heater voltage to 5V.

The optimal experimental conditions have been determined during previous experiments, using experimental design method [11]. The head-space is generated in a 100ml heated vial, thermostatically controlled at 35°C, containing 10ml of liquid sample. 50ml of head space is injected with a syringe (« static » way of injection) in the 500ml measurement cell, thermostatically controlled at 60°C. After each measurement, the cell is cleaned by atmospheric air, thermostatically controlled, filtered on active charcoal and dehydrated, at 500ml/min flow-rate . (C.f. Figure 1).

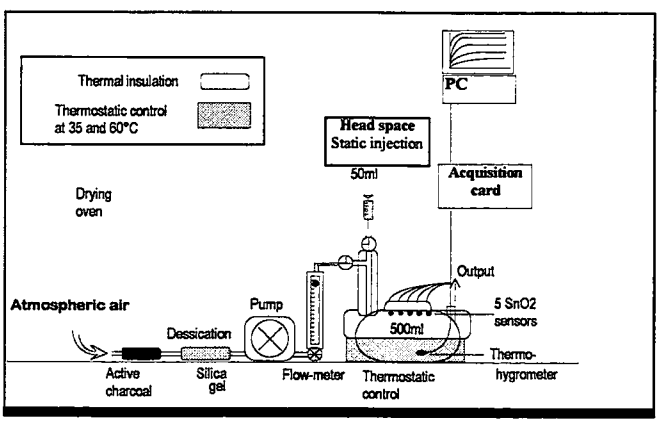

Figure 1: Experimental device, controlling temperature and hygrometry of measurement cell, carrier gas and sample vial

2.2 Model solutions

The sensor selection methodology is applied to the discrimination of satisfactory wines and unsatisfactory vinegar flavour wines. This taint has been chosen because it is the most widespread wine off-flavour ; furthermore, the tainting

molecules are identified and more concentrated (hundreds of ppm) than the ones responsible of other off-flavours. However, the 12% of alcohol in wine saturate the sensors and mask the aromas. Accordingly, model solutions are prepared without ethanol. Since volatiles are generally hydrophobic, they must be dissolved in a solvent : triacetin has been chosen, mainly because of its low volatility.

Since supervised pattern recognition techniques are performed on the data set, the data cannot be repetitions of the same sample measurements, but the sample set must be representative of each class. Therefore, 16 samples are prepared for each class, separated by two volatile thresholds: acetic acid at 700ppm and ethyl acetate at 150ppm (C.f. Table 1). Each day, samples are drawn from the original solutions. Head space is generated during sixteen minutes with a magnetic stirring. These conditions have proved to be the most repeatable and the best agreement between volatile concentration and the duration of gas sample generation.

Satisfactory wines *(Sample number)*					**Vinegar tainted wines** *(Sample number)*				
	Ethyl Acetate (mg/l)					**Ethyl Acetate (mg/l)**			
Acetic Acid (mg/l)	**50**	**66.6**	**83.2**	**100**	**Acetic Acid (mg/l)**	**200**	**233.3**	**266.6**	**300**
200	*1*	*2*	*3*	*4*	**700**	*17*	*18*	*19*	*20*
300	*5*	*6*	*7*	*8*	**800**	*21*	*22*	*23*	*24*
400	*9*	*10*	*11*	*12*	**900**	*25*	*26*	*27*	*28*
500	*13*	*14*	*15*	*16*	**1000**	*29*	*30*	*31*	*32*

Table 1: Description of the 32 samples, belonging to both classes of satisfactory and vinegar tainted wine

3. Methods

3.1 Sensors

Thirteen SnO2-sensors are examined, five by five, keeping one sensor in the measurement cell, in order to check the reproducibility of the experiments. TGS 822, chosen for its average repeatability, is used as this reference. Finally, fifteen sensor outputs will be analysed, considering the three measurements of the sensor TGS 822 independently. The 13 metal oxide sensors are FIGARO TGS: 825; 800; 824; 842; 822; 812; 815; 882; 880; 830; 831; 813; 4C23-3. Random sample measurements are carried out during one day for each subset of 5 sensors.

3.2 Experimental data

The whole signal is analysed, from the adsorption beginning to the desorption end, using extracted features. The most suitable features have been determined during

a previous study, according to their repeatability, discriminant distance and redundancy **Erreur! Signet non défini.**.

From these features, ten have been selected for this data processing: five different levels on the dynamic part of the adsorption curve, the adsorption maximum, i.e. the steady-state signal, the adsorption slope maximum, the desorption slope minimum, the adsorption deceleration maximum and the desorption acceleration maximum.

Two sequential algorithms of feature selection are performed, in order to select the best subset of *m* features from a *n*-feature set: the stepwise discriminant analysis and stepwise *k*-nearest neighbours.

3.3 Stepwise discriminant function analysis

The discriminant function analysis aims to find the data representation space, maximising the ratio of the between-group variance divided by the total variance. This intends to maximise the between-group variance and minimise the within-group variance, in order to discriminate groups.

The stepwise discriminant function analysis aims to select the most discriminant features among a set of variables characterising the samples. In stepwise discriminant analysis, a model of discrimination is built step-by-step. At each step, all variables are evaluated to determine which one contributes most to the discrimination between groups (forward stepwise analysis). Then, all the variables included in the model are reviewed (except the latest one), in order to check if the removal of one of them improves the model (backward stepwise analysis). The process starts again, until discrimination efficiency does not improve anymore.

Two discrimination indexes are used to assess model efficiency :

- the Wilks Lambda, aiming to minimise the ratio of the within-group variance divided by the total variance;

- the Fisher Test, assessing the homogeneity of class means calculated using the subset of selected features. When the risk percentage of the null hypothesis reaches zero, the most suitable subset is determined.

3.4 Stepwise k-nearest neighbours

The *k*-nearest neighbour method is a non-parametric supervised pattern recognition technique. An unclassified sample is assigned to the class represented by a majority of its *k-nearest neighbours* in the training set. The neighbourhood is computed by the Euclidean distance between the unknown vector and the training vectors. The number of neighbours *k* is fixed relatively to the number of samples,

usually computed as $k = \sqrt{\text{total sample number}}$, rounded to the closest odd number to avoid any majority ambiguity [13]. As this data set contains 32 samples, this classification method can be performed without reducing computations, with algorithms such as condensation or hierarchic computation.

The Stepwise *k*-nearest neighbour method consists in including (or removing, as forward and backward stepwise analysis are mixed, like in stepwise discriminant function analysis) step by step one feature which induces the best classification results. When correct classification percentage cannot be improved, the feature subset selection stops.

4. Results

These methods are performed on the whole data set, which means on 150 features extracted from the fifteen sensor outputs. The sensors corresponding to the first selected features are then chosen as the most suitable ones.

4.1 Stepwise discriminant function analysis

The stepwise discriminant function analysis performed on 150 features selects 32 features, relatively to the Wilks Lambda. The nine first ones correspond to 5 sensors (C.f. Table 2).

Sensor	features selected
TGS *815*	desorption slope minimum, adsorption deceleration maximum
TGS *882*	1^{rst} level, adsorption deceleration maximum
TGS *830*	adsorption maximum
TGS *822*	4th level, desorption slope minimum
TGS *813*	adsorption slope maximum, adsorption deceleration maximum

Table 2: Features selected and corresponding sensors

The sensors are not selected using the same type of feature, proving the usefulness of extracting various features from the adsorption and desorption curve, instead of using only the steady-state signal.

The TGS 822 has been selected in one of the 3 measurements (first series). If this output is removed, this sensor is also chosen, from the third measurement series. If these features are removed again, the TGS 822 is then selected from the second series, proving the reproducibility of the experiments.
If the same algorithm is applied, regarding to the Fisher index F, the subset of only 2 features provides the best classification results : the adsorption deceleration maximum of the sensor TGS 815 and the 2nd level of the sensor TGS 882.

4.2 Stepwise k-nearest neighbours

The advised number of neighbours is 5, the closest figure from $\sqrt{32}$. But, classification results were studied, using *k* from 3 to 13.
The stepwise *k*-nearest neighbours performed on 150 features selects only one feature, whatever the neighbour number : the 2nd level of the TGS 815. This means that the optimal classification is obtained using only one feature with *k*-nearest neighbours analysis. Oddly enough, this method selects the same first sensor as the stepwise discriminant function analysis, but by choosing an other feature.
If all the features extracted from this sensor are removed from the data set, the TGS 830 is then selected by the algorithm, using its 3rd level. If k is chosen strictly superior to 5, the TGS 813 is selected. But, all these further selections do not take into account the output redundancy with the TGS 815 features.

5. Discussion

At last, these three methodologies provide coherent but different results. The sensors are chosen in the same order, but the optimal number of sensors depends on the algorithm. The Stepwise *k*-nearest neighbours selects only one sensor (TGS 815) ; the stepwise discriminant function analysis based on the Fisher test selects two sensors (TGS 815, 882) ; the same method based on the Wilks Lambda arranges the sensors in descending discrimination efficiency order, selecting all the sensors except the TGS 824.

In order to determine the most suitable method, these sensor selections must be validated. The discriminant function analysis with leave-one-out cross validation provides 100% of correct classification using features extracted from only one sensor (TGS 815) or two sensors (TGS 815, 882). The same results are shown by performing the *k*-nearest neighbours with leave-one-out cross validation. In short, this selection validation, using supervised methods, means that the best classification is reached using only one sensor, the TGS 815.
Unsupervised classification methods can also be applied to the data set, like a principal component analysis (PCA), followed by a clustering analysis (CA). The following figures (n°1 to 8) show the spreading of the samples in the first factorial plane of a centred PCA performed on various data sets. A cluster analysis is performed on the two first principal components, using Euclidean distance and k-means (i.e. samples that are linked together are replaced in further calculations by their gravity centre).

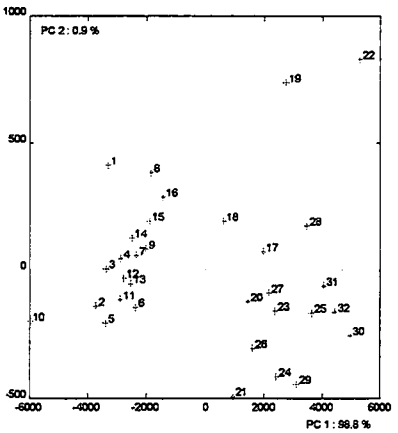

Figure 1: Centred PCA performed on 10 features extracted from the TGS 815

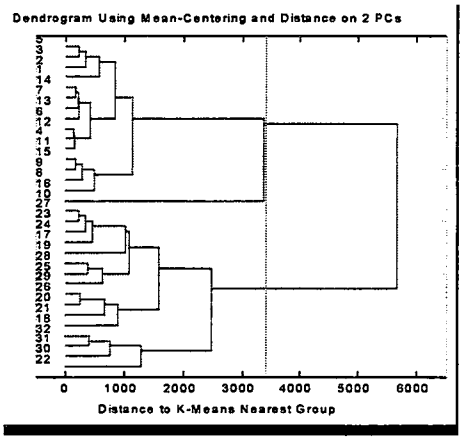

Figure 2: Clustering analysis performed on the two first principal components

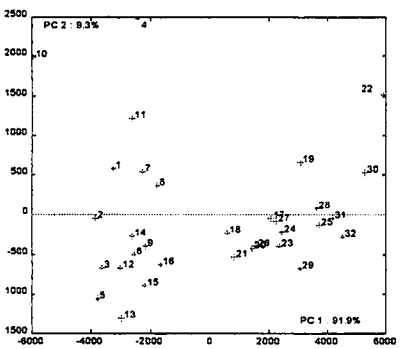

Figure 3: Centred PCA performed on 20 features extracted from the TGS 815 and 882

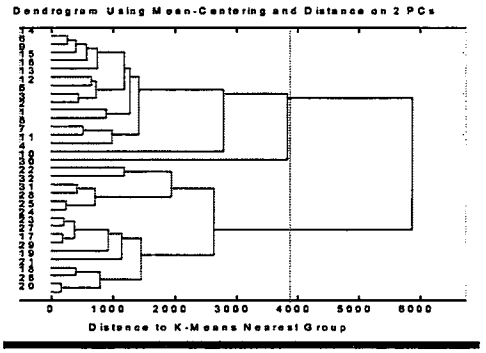

Figure 4: Clustering analysis performed on the two first principal components

Samples 1 to 16 correspond to the satisfactory wines and samples 17 to 32 correspond to the vinegar off-flavour wines (C.f. Table1).

These hierarchic classifications show that the best discrimination efficiency are provided by one (Figures 1 & 2) or two sensors (Figures 3 & 4). If the number of sensors increases (more than 4 sensors), the sample n°3 is no longer classified in the correct class (figure 5 to 8), but is rejected from both classes.

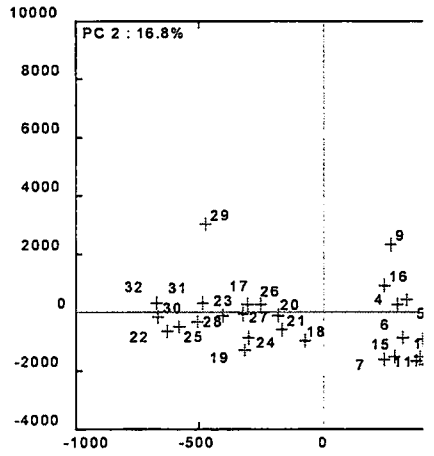

Figure 5: Centred PCA performed on 50 features extracted from the TGS 815, 882, 830, 822 and 813

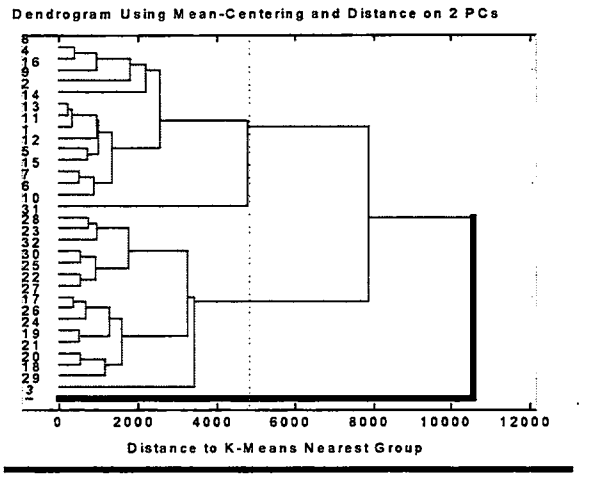

Figure 6: Clustering analysis performed on the two first principal components. The same results are shown, using up to 4 components, gathering 95.3% of total variance

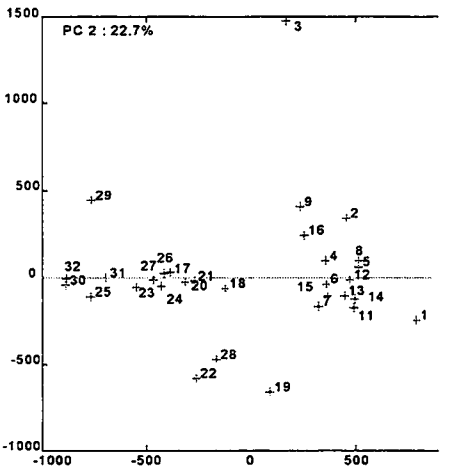

Figure 7: Centred PCA performed on all the data set (150 features)

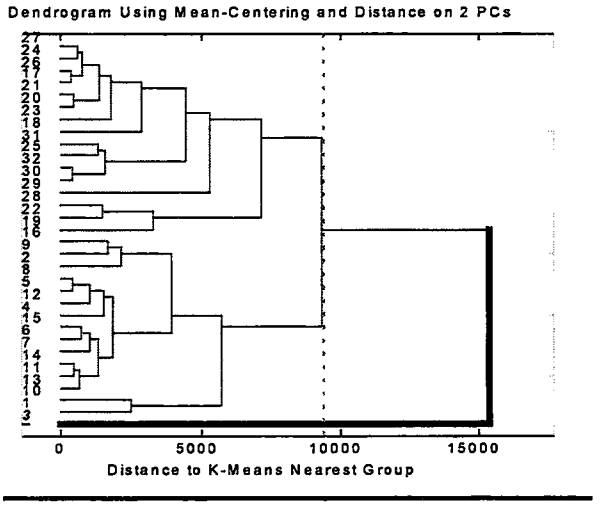

Figure 8: Clustering analysis performed on the two first principal components. The same results are shown, using up to 7 components gathering 95.7% of variance

If this non-supervised classification is performed on features extracted from one of the first selected sensors, 100 % of correct classification is only obtained with the TGS 815 ; the other sensors lead to 15% of wrong classifications, at least (for instance, C.f. Figure 9). This tends to prove that the actual most suitable sensors are chosen by these stepwise methods.

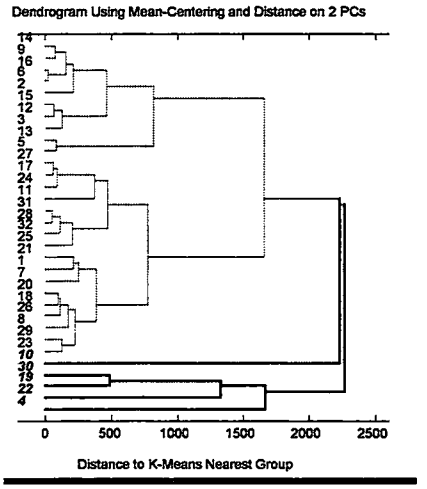

Figure 9: Cluster analysis performed on 10 features extracted from the TGS 882 (2^{nd} sensor selected)

Conclusion

Two stepwise feature selection methods have been performed, using different selection indexes, in order to choose the most discriminating gas sensors among a SnO_2-sensor array. The measurements have been carried out on model solutions representing satisfactory wines and vinegar off-flavour wines.

The stepwise discriminant function analysis based on the Fisher test method selected two features, extracted from two different sensors. The five best sensors were selected using the first nine features chosen by the stepwise DFA, with Wilks Lambda index. The stepwise *k*-nearest neighbours selected only one sensor, using one feature. The selected features are extracted either from the signal and from the primary and secondary derivatives.

The selection validation, using either supervised methods (DFA or kNN) or unsupervised method (PCA followed by Clustering analysis), proved that the best classification is provided by only one sensor, the first one selected by the three methods. In conclusion, the stepwise *k*-nearest neighbours and the stepwise discriminant function analysis based on the Fisher test gave the most discriminating subset of sensors, using different classification indexes and stop criteria. 100% of

correct classification is obtained using only the first and the two first selected sensors.

In this example, only one sensor was elected, which is a specific case due to model solutions. However, the whole methodology is totally usable for more complex mixtures. Both methods are able to determine the most suitable subset of sensors, adapted to each specific application, using few representative samples of each class.

References

[1] GARDNER, J.W., BARTLETT P.N., 1994. A brief history of electronic noses. In *Sensors & Actuators* B, 18-19, pp 211 -220.

[2] GARDNER J.W., HINES E.L., 1997. Pattern Analysis Techniques. (Handbook of Biosensors and Electronic Noses. Medecine, Food, and the Environment.). *CRC Press., Frankfurt, Germany. pp 933-651.*

[3] HOLMBERG M., WINQUIST F., LUNDSTRÖM I., DAVIDE F., DI NATALE C., D'AMICO A., 1996. A. Drift counteraction for an electronic nose. In *Sensors and actuators B,* 35-36, *pp 528-535.*

[4] DI NATALE C., DAVIDE F., D'AMICO A., 1995. A self-organizing system for pattern classification: time varying statistics and sensor drift effects. In *Sensors & Actuators* B, 26-27, pp 237-241.

[5] PIJOLAT C., SAUVAN M., DURAND J. 1997. Amélioration de la sélectivité de microcapteurs de gaz SnO2. Application à l'automatisation des procédés. *In Récents progrès en Génie des Procédés. pp 37-42.*

[6] WALMSLEY A., HASHWELL S., METCALFE E., 1991. Methodology for the selection of suitable sensors for incorporation into a gas sensor array. In *Analytica Chimica Acta,* 242, pp 31- 36.

[7] DI NATALE C., MACAGNANO A., D'AMICO A., DAVIDE F., 1997. Electronic-nose modelling and data analysis using a self-organizing map. *In Measurement Science & Technology, 8 (11), pp 1236-1243.*

[8] ROCHA S., DELGADILLO I., FERRER CORREIA A., BARROS A., WELLS P., 1998. Application of an Electronic Aroma Sensing System to Cork S Quality Control. In *J. Agric. Food Chem., 46 (1), pp 145-151.*

[9] JOUAN-RIMBAUD D., CENTNER V., VERDU-ANDRES J., WALCZACK B., DESPAGNE F., PASTI L., POPPI R., MASSART D.L. 1997. Comparaison de techniques de calibration multivariée appliquées à des données de spectroscopie proche infra-rouge. *In Chimiométrie 97. pp 15-18.*

[10] CHTIOUI Y. 1997. Reconnaissance automatique des semences par vision artificielle basée sur des approches statistiques et connexionnistes. Thèse en Sciences pour l'ingénieur. *Université* de *Nantes. IRESTE.199 p.*

[11] ROUSSEL S., FORSBERG G., GRENIER P., BELLON-MAUREL V. Optimisation of Electronic Nose Measurements. Part II: Influence of Experimental Parameters. *In J. Food Eng,, pp submitted in 1998.*

[12] ROUSSEL S., FORSBERG G., STEINMETZ V., GRENIER P., BELLONMAUREL V. Optimisation of Electronic Nose Measurements. Part I: Methodology of Output Feature Selection. In *J. Food Eng.,* pp submitted in 1998.

Utilization of the olfactory characteristics of fruit and vegetables as a potential method for determining their ripeness and readiness for harvest

La mesure de l'odeur des fruits et légumes : une méthode potentielle pour déterminer leur maturité et la date de la cueillette

Yoav Sarig

Department of Biological and Agricultural Engineering
University of California
Davis, CA, 95616, USA
e-Mail: ysarig@ucdavis.edu

Abstract: *Traditional quality evaluation of fruit and vegetables is associated, primarily, with appearance attributes, such as size, shape, surface colour and defects, or tactile characteristics, like firmness or hardness. Many methods and associated instrumentation based on these sensory characteristics have been developed in the past 30 years and are utilised commercially, to a certain extent, in the quality evaluation of many fruits and vegetables. However, a constant demand exists for improving quality evaluation and hence, there is still much room for improvement and additional technologies. It is known, that in many cases, fruit ripening is associated with an accumulation of aromatic volatiles during fruit ripening, whose measurements could provide good indicator of the fruit ripeness and can be related to internal composition during ripening. Many technologies already exist for sensing gases, utilising a variety of technologies, based primarily on semiconductor devices such as, thin and thick metal oxides, conducting polymers. Quartz Microbalances (QCM), Surface Acoustic Wave (SAW), FET and fibreoptics. In addition, quite an array of measuring and testing devices were developed and are available commercially for detecting and analysing gases and specifically, for sensing and evaluating odours. Most commercial instruments are aimed at detecting a single gas or vapour that has exceeded some threshold value. In olfaction, however, we use our sense of smell in a more sophisticated way for classifying and grading odours. Hence, a desire exists to develop an « artificial nose » that would mimic the abilities of the mammalian olfactory system for sensing and classifying volatiles. The complex chemical environment which tipyfies the human olfactory system, led to the multisensors approach, which is based on the principle that by utilising a number of non-specific sensors having suitable selectivity properties (each different from the others), it is possible to infer some information about the nature of the chemical environment under analysis. When coupled with pattern recognition and artificial network techniques, such a system shows some analogies with the olfaction structure of the mammalians. Several artificial, or electronic noses have been developed in the past 10 years, but while several proposed «artificial noses» are already employed commercially, there is not a universal nose at present that can solve all odour-sensing problems, or effectively respond selectively and sensitively to specific gases at an appropriate temperature. Many of the more advanced techniques need further development to be adapted to commercial scale which allows reproducibility in sensor production. Other*

adapted to commercial scale which allows reproducibility in sensor production. Other problems, such as eliminating drift because of aging, decreasing cost of production and better versatility, need to be addressed before commercialisation can be realised.

Keywords: *Smell, artificial nose, olfactory response, sensor.*

Résumé : Les systèmes d'évaluation de la qualité des fruits et légumes sont associés régulièrement à des paramètres liés à l'apparence comme la taille, la forme, la couleur de la surface et des défauts ou à des paramètres tactiles comme la fermeté. De nombreuses méthodes et leurs instrumentations associées basées sur ces caractéristiques sensorielles ont été développées dans les 30 dernières années et sont utilisées commercialement dans une certaine mesure pour évaluer la qualité de nombreux fruits et légumes. Cependant, une demande constante existe pour améliorer les systèmes d'évaluation de la qualité et de fait, nous pourrions développer de nouvelles technologies pour répondre à des attributs de qualité tels que la maturité. Il est connu de source sûre que la maturation des fruits est associée à une accumulation de composés volatiles aromatiques et les mesures de ces composés pourraient être un bon indicateur de la maturation du fruit et pourraient être reliées à la composition interne durant cette maturation. De nombreuses technologies existent aujourd'hui pour mesurer les gaz, basées principalement sur des semi-conducteurs, des polymères conducteurs, des micro-balances à quartz, ou des ondes acoustiques de surface. De plus, une association de ces techniques de mesure a été développée et certains systèmes sont disponibles commercialement pour détecter et analyser les gaz et spécifiquement, pour mesurer les odeurs. La plupart des instruments commerciaux visent à détecter un simple gaz qui a dépassé une valeur limite. Cependant, dans l'olfaction, des mammifères utilisent leur odorat de manière plus sophistiquée pour classer les odeurs. Ainsi, des nez artificiels capables de simuler la faculté olfactive du système des mammifères pour classer les volatiles ont été développés. L'environnement chimique complexe qui caractérise le système d'olfaction humain a mené à une approche multi-capteur. Elle est basée sur le principe qu'en utilisant un nombre élevé de capteurs non spécifiques, il est possible de dégager une information sur la nature de l'environnement chimique. Couplés avec des systèmes de reconnaissance, de formes, un tel système a des analogies avec la structure olfactive des mammifères. De nombreux systèmes nez électronique ont été développés ces dernières années. Mais, alors que des nez électroniques sont déjà vendus dans le commerce, il n'y a pas de nez universel qui pourrait résoudre tous les problèmes de mesure d'odeur pour répondre de manière sélective et suffisamment sensible à certains gaz à n'importe quelle température. De nombreuses techniques aujourd'hui développées doivent encore faire leur preuve au niveau de la reproductibilité. D'autres problèmes tel que l'élimination de la dérive due au vieillissement ou la diminution du prix de production et une meilleure adaptabilité doivent encore être résolus avant la commercialisation du système vraiment fiable.

1. Introduction

Traditional quality evaluation of fruits and vegetables is associated, primarily, with appearance attributes, such as size, shape, surface color and defects, or tactile characteristics, like firmness or hardness. Many methods and associated instrumentation based on these sensory characteristics have been developed in the past 30 years and are utilized commercially, to a certain extent, in the quality evaluation of many fruits and vegetables [76, 16, 19]. Nevertheless, with the increased competition in both, domestic and international markets, there is a constant demand for improving quality evaluation, in order to minimize potential losses to the grower and packer, or fast spoilage at the consumer end. The determination of the optimal timing for harvest and the exact stage of ripeness, are both, among the most important factors in the overall quality evaluation of many fruits and vegetables. However, although quite a few methods are already available for this evaluation, there is still much room for improvement and additional technologies to address all quality attributes.

Very little attention has been given, so far, to the utilization of the human olfactory response to fresh produce, as an additional, complementing, consumer-oriented and nondestructive quality evaluation method [77, 11, 12, 59]. At the same time, it is well known, that in many cases, fruit ripening is associated with an accumulation of aromatic volatiles during fruit ripening for both, climacteric and nonclimacteric fruits [50]. More than 60 aromatic volatiles have been identified in muskmelons, for example, and significant changes in the composition and relative concentration of aroma compounds were noticed in fruits during the ripening process [39, 48]. As the fruit approaches the climacteric peak, volatile constituents responsible for the full ripe aroma and flavor of the fruit are produced at a rapid rate. Overripeness, on the other hand, may lead to the development of undesirable flavor, associated in part with the overproduction of certain volatiles. Yabumoto [92] reported on progressive changes of volatile compounds produced by ripening melons. Similarly, Miyazaki and Ookubo [58] reported that aromatic volatiles and ethylene were much better indicators of melon maturity than was visual appearance. Chachin and Iwata [18] investigated the relationship between production of some volatiles and quality and concluded that volatiles were a better quality index than, for example, the measurement of soluble solids, by a refractometer. Similarly, Benady *et al.* [11, 12] have compared the measurements of volatiles from muskmelons, utilizing a newly developed sniffer, with traditional analytical methods of ripeness measurements. They were able to demonstrate that the sniffer method was better than all other parameters, both destructive and nondestructive.

More evidence of the importance of volatiles for quality evaluation of certain fruit (peaches, for example), were provided recently by Molto *et al.* [59]. In their work they have shown that, in many cases, a clear relationship exists between aging of some fruits and the quantity of the emission of some volatile compounds (i.e.

Linalool, or Benzaldehyde). It is already well established that the mechanism of ripeness of many fruits and vegetables is associated with generation of ethylene [14]. In addition, the compounds of Gamma and delta decalactone were also found to increase significantly during the final stages of fruit (peach) ripeness [59]. Aroma was found to be more apparent in peaches than in any other fruit, and like in other species, it changes as the fruit ripens. Moreover, breakage of the fruit skin due to mechanical damage (wind, rough handling of the produce, etc.), fungi disease or insect activity, result in many cases in an increased emission of volatiles.

It seems, that there is already substantial evidence that significant changes in the accumulation and concentration of aromatic volatiles occur during ripening of many climacteric and nonclimacteric fruits and vegetables, and even at their postharvest stage. Hence, these changes in volatiles can be related to the changes in internal composition during ripening. At least for some species (i.e. peaches, nectarines, melons and feijoa fruit, to name only few), consumers also tend to base their decision to purchase these fresh products, not only on their appearance and tactile characteristics, but also on the aroma aspect of a specific product [86]. A firm melon, for example, with impeccable appearance, is not a guarantee of a ripe and palatable fruit, ready for marketing. Most consumers would tend to smell this fruit before making a final decision to buy it. With other fruits, such as the feijoa, or mango, with no visual, or tactile characteristics of its maturity, the distinct aroma of this fruit may serve as the only reliable, nondestructive index for its readiness for harvest [37].

Often, varietal differences between fruits and vegetables mean different flavors. Some of these flavor differences are highly prized by the consumer. There is a continuous investment in plant breeding and more recently genetic engineering, to produce new, better tasting fruit and vegetable varieties with desired flavors and extended shelf lives. Hence, the ability to quickly screen fruits and vegetables to confirm variety type is becoming increasingly desirable.

Recently, a presentation of state-of-the-art nondestructive quality evaluation techniques for fresh fruits and vegetables took place in Spokane, WA in June 1993, within the framework of a workshop sponsored by the United States-Israel Binational Agricultural Research and Development Fund (BARD). In this workshop, the need and possible utilization of an aroma analysis technique has been cited for possible detection of physiological disorders in apples, mango, citrus, onion and pepper; temperature damage in citrus and internal composition in peaches, strawberry, pepper and melon. While the potential has been identified, it was evident that no practical technique is available at present and hence, more work needs to be done before this technique can be implemented commercially [16, 84]. Measurements of human olfactory responses to food and agricultural products are part of a comprehensive sensory evaluation, which is the science of judging and evaluating the quality of food, or an agricultural product, by the use of the senses, i.e. taste, smell, sight, touch and hearing [42, 68]. However, while overall sensory testing has been developed into a precise, formal, structured methodology, the

olfactory response by itself, especially when applied to fresh agricultural produce, needs far more development work before a practical, broad implementation can be effected.

Smell, or odor responses, are already being used quite extensively in the food industry [42, 68, 69, 74, 89]. A comprehensive list already exists of volatiles found in food [44, 69] and for many food products the exact quantitative composition of the volatiles has been published. However, no such detailed information is yet available for fresh fruits and vegetables.

The main reason for not utilizing commercially the additional source of information from the olfactory response, for quality evaluation of fruits and vegetables is, that modern man has a relatively small olfactory apparatus. Not only this apparatus is inferior, by far, to that of many other mammals, (like dogs, for example), but the human also makes very little use of his sense of smell for the determination of the quality of fresh produce. Current procedures have become, almost completely, reliant on man's senses of sight, hearing and touch. Moreover, not only do we possess the most clumsy instruments for detecting, recording and analyzing odors, we can not define, or measure their properties in physical units, as we do, for example, with light and sound. The color of light is related to its wave length, as is the pitch of a sound. In contrast, there is no known spectrum for neatly defining odors, or explaining their existence, as there is with wave theories of light and sound. The function of the sense of smell, as a whole, is the least understood of our senses. Statements in the literature are often fragmentary and frequently based upon assumptions [55, 13, 91, 42, 20]. This is especially true in the application of the sense of smell for the cited problem of determining maturity of fruits and vegetables, developing an index for their readiness for harvest and obtaining information on their internal composition. Nevertheless, in spite of the difficulties associated with the specific application and hence, the unavailability at present of suitable instrumentation, the current demand for gas sensors is sky-rocketing and it is driven by a broad range of applications. Hence, it is conceivable that our cited application will also be addressed eventually.

2. Statement of the problem

Past research work [17] has already provided evidence that odors appear to affect our behavior, although we may not be conscious of their existence or their effects. Hence, with the process of quality evaluation of fresh produce, an olfactory response to them may also play a role in the overall process of their quality assessment and marketability.

With the increased awareness of quality of the produce, on one hand and the market competitiveness, on the other, there is an incentive to develop a nondestructive quality evaluation method, which would assist in the complex classification of fresh produce, in order to optimize its quality evaluation and

enhance its marketability. The olfactory response to produce, being nondestructive and directly related to the way the consumer perceives the produce for its readiness for consumption, is a good candidate for the attempt to develop such a method.

The purpose of this review is to describe the human mechanism of smelling, delineate previous attempts to develop both, laboratory devices and commercial gas sensors and describe current state-of-the-art technologies for odor sensing and especially, their applications in agriculture. A further purpose, to suggest future trends and possibilities for a technique, and relevant instrumentation for, quality evaluation of selected fruits and vegetables utilizing their olfactory characteristics. There is already a wide and diversified range of information on the subject, indicative of the growing interest in the utilization of olfactory characteristics [75]. Because of the broad scope of the subject, only a small selection of references was given, which does not purport to cover comprehensively the existing literature and does not do justice to the wealth of information already available. Nevertheless, it is hoped, that even this rather limited review will provide some insight into this intricate subject and give the incentive to pursue some practical implementation of the olfactory characteristics in the quality evaluation of fruits and vegetables.

3. The mechanism of human smelling

Although smelling is clearly not a leading sensory characteristic in humans, it is, however, a complex process and the human nose is one of the most intricate and sensitive sensors. Even at the limit of instrumental sensitivity e.g. where no signal appears, our «biological detector» may still perceive an odor. It can detect certain substances by smelling over solutions of concentration of 1 in 10^{12} , or even less [53, 69].

The human olfactory organ contains about 10 million receptors, which are chemoreceptors that are activated by molecules in solution. To be detected, odorous substances must be volatile (in the form of airborne particles, or molecules), so that they can be sniffed into the nostrils. They must also be at least partly soluble in water, so that they can pass through the nasal mucus to the olfactory cells. Finally, they must be soluble in lipids (fatty substances), so that they can pass through the lipid layer that forms the surface membrane of the olfactory organ [8, 13, 5].

The sensation of smell arises from the stimulation of olfactory sensory cells by the odorant molecules given off by the substance being smelled. Odors may be simple, consisting of a single kind of odorant molecule, or complex, consisting of a mixture of odorant molecules. Virtually, all natural odors are mixtures containing, perhaps, several tens of different types of odorant molecules. The subtle distinctions we routinely make, e.g. between different types of tea, are attributed to variations in the relative amounts of the components of the complex odor.

Most odorous molecules are small (30-300 Dalton), hydrophobic organic molecules, containing, typically, a single polar group. Although there are some notable exceptions, molecules with more than one polar group are generally involatile and thus unable to reach the olfactory epithelium. A majority of odorants contain oxygen, typically in the polar group of the molecule. Nitrogen and sulfur compounds are less frequent, although the nitrogen containing pyrazines and other heterocycles are an important class of odorants in roasted products, and sulfur occurs in many important natural odorants from animals.

When these molecules interact with the sensory chemoreceptors in the nose, they send specific nerve impulse-patterns to the brain. The brain then compares the incoming signal with other signal-patterns held in the memory store and, depending whether or not it can find a matching pattern, it assigns a meaning to the signal and decides on the most appropriate response [57].

The three important properties of odorants are the odor type, the threshold value and the form of the intensity curve. It is known that the shape, size and polar properties of the molecule determine its odor properties. However, the precise rules are poorly understood and the relationship between the molecular structure of the odorant and its odor - the olfactory code - is complex. Natural smells, in particular, like in the case of fruits and vegetables, are almost always complex mixtures of chemicals, containing, at least, tens and more often hundreds of constituents. Differences in the relative amounts of these constituents affect the odor and flavor. In some instances the odor of a natural material is dominated by a single odorant and the other components exert a secondary, more subtle, effect.

The complex mixtures of chemicals found in fruit and vegetable present us with the difficult issue of classification. The difficulties in the classifications of odor type are the result of the subjective perception which use common names to signify the odor (e.g. fruity, flowery, musk, etc.). Even a single, highly pure odorant may require several terms to describe its odor. Furthermore, the classification is imprecise (fuzzy) because it must be based on subjective associations and because an individual's sense of smell is not invariant with time or physical health. A second difficulty arises from the large number of physiochemical properties describing the molecules. This large number of variables in any analytical model means that the number of odorants studied in any structure-odor experiments will be prohibitively large [17, 22].

Nursten [69] suggested a very rudimentary system for classifying food produces, in which he differentiated between food whose aroma resided largely in one compound (e.g., banana, grapefruit, lemon, pear, almonds, cucumber, potato); those whose aroma was due to a mixture of small number of compounds (e.g., apple, raspberries, tomato, onion); those whose aroma could only be reproduced reasonably faithfully by the use of quite a large number of compounds (e.g., apricot and peach, pineapple, walnut) and those whose aroma could not be reasonably

reproduced, even by a complex mixture of specific compounds from among the volatiles identified (e.g., strawberry).

The underlying rules of the relationship existing between molecular properties and smell sensation, the olfactory code, is yet poorly understood. Humans tend to specify odors in terms of associations rather than by the attributes of the odor, leading to ambiguous descriptions [73]. The development of a comprehensive odor classification system is further complicated by the fact that some chemicals with very similar structures may have very different odor qualities. Conversely, similar odor perceptions can be caused by structurally very different molecules [63].

In an attempt to clarify the processes involved in the coding of olfactory sensation, Amoore *et al.* [4] suggested that there are seven primary odors , including *camphoraceous* (mothballs), *musky*, *floral* (roses), *peppermint*y, *putrid* (rotten eggs), *etherreal* (dry-cleaning fluid), and *pungent* (vinegar). These seven primary odors were established from the subjective sensations reported by panels of human odor testers. Hence, it is very likely that there are also other kinds of primary odor. However, regardless of what basic odors are postulated, the question remains as to how their stimulus qualities are coded.

Several theories of the olfaction response have been proposed, which attempted to tackle this problem, and one of the most widely accepted explanation of this process is the stereochemical theory [4]. According to this theory, there are distinct receptor cells for the various primary odors (mentioned above) and that molecules of odoriferous material produce their effects by fitting into the correct «receptor slots».

A major contender to this theory is the vibrational theory suggested by Wright [91], who considered that seven receptor sites are too few to give the number of combinations required for all the odors that we can smell. He proposed that there should be twenty to thirty kinds of receptors and in his vibrational theory suggested that the odoriferous nature of a molecule was imparted by its low-frequency vibration. Molecules of different substances have characteristic, if complex, vibrations, each molecule vibrating at several frequencies. Wright suggested that in each kind of receptor there are molecules that vibrate at the same frequency as one of the primary odors. When an odor molecules meets the right receptor molecules, the two resonate together at a slightly different frequencies and this is the start of a nerve impulse.

It is beyond the scope of this review paper to give a comprehensive description (which, by itself may not provide a tractable and well defined explanation) of all the theories involving the olfactory system. A rather detailed description of the mammalian olfactory system was given by Graziadei [36], covering many different facets, along with an extensive list of relevant references. In addition, McCartney [55] has tried to clarify some of the speculations involving various theories of the olfaction process, as Beets [9] and Schultens and Schild [79], who also have made

a significant contribution and provided a valuable bibliography. All those information (and numerous other useful references not listed here) should prove to be useful in obtaining a better understanding of the olfaction process and hence, assist in the eventual development of suitable instrumentation.

4. Sensing and measuring of gases

Quite an array of measuring and testing devices were developed and are available commercially for detecting and analyzing gases and specifically, for sensing and evaluating odors. In addition, many patents exist for different gas detection and measurement devices for the determination of hazardous gases thresholds and inspection of containers for the presence of substances, such as explosives and drugs. Some of the patents for apparatuses to discriminate odors, also include several aimed specifically for measuring concentrations of odors in fruits and food items as an indication of their specific quality, such as freshness and maturity [25, 41, 78, 2].

A distinction should be made between laboratory and field measurements. Laboratory analytical instruments are, inherently, more precise, but require relatively long times for data acquisition and processing, do not operate continuously, are difficult to correlate with perceived odor and, in general, are quite expensive. Field applications, on the other hand, are aimed, in general, at having a sensor, or a sensor array, which is small and portable, can be taken to the field and can perform analyses «on-the-spot» like the human nose. Such a sensor should contain, therefore, the data acquisition element to obtain the needed information, as well as be able to provide this information to the user, in order to solve an existing and specific analytical problem. However, a field instrument, in addition to the complex problem of maintaining suitable size and weight, is also faced with the limiting factors of, usually, low concentration of the volatile in the head space volume and interference from the exposure to ambient conditions.

Another distinction should also be made between subjective and objective sensory testing. Subjective tests involve human evaluation by objective panelists, while objective testing employs the use of lab instruments only, with no involvement of the human sense of smelling. Both tests, however, are important in sensory evaluation of food and food products [56, 61].

4.1 Human evaluation of odor

Various subjective human evaluation tests are practiced in sensory perception of a product, especially in the food industry. They have been developed into a precise, formal, structured methodology to establish the worth or acceptance of a commodity [55, 56]. For food stuff quality applications, as well as other agricultural oriented utilizations and environmental studies, the human judgment is the major

factor and all other measurements have to be, ultimately, related to its perception and discrimination. Also, the sensitivities of the various currently available sensing technologies are several orders of magnitude below the sensitivity of the human nose [73] and hence, their application is limited to problems where individual odor components are present in concentrations ranging from ppb-ppm levels. While this may not present a major limitation to a variety of areas where concentrations in the headspace of a given sample are generally high, they are inadequate for field applications, such as sensing *in situ* the aromas of fruits and vegetables.

In addition to direct human judgment, more advanced methods involve the use of dedicated instruments, which combine odor evaluation by a sensing element with an odor evaluation by a human panel. These instruments, which are called in general «olfactometers», provide a neutral reference odor of known concentration in the air and call on humans (the jury) to compare the intensity of a tested odor with the reference odor. Several such instruments are available commercially, designed in general for a particular application. A review of various olfactometers was given by McCartney [55].

'Tecnodor' is an example of such an instrument, manufactured in France by 'Technovir Int.' Inc. Using the 'Tecnodor', the intensity and profile of an odor are determined by means of a series of measurements. For each measurement, the apparatus generates a new concentration of the referencing odor (butanol), which is presented to the nose of a juror by an inhalation cone. The juror then compares the intensity of the ambient odor with that of the reference odor and indicates the relative value of the two intensities on a tactile screen of a computer. If required, the 'Tecnodor' can be coupled with a gas chromatograph - mass spectrometer (GC-MS). This allows identification of one or more gases causing the odor and makes it possible to establish links between perceived intensity and concentration.

Another olfactometer was developed by 'St. Croix Sensory', Inc., in the U.S.A., where odors are evaluated in accordance with ANSI (American National Standards Institute) and ASTM (American Society for Testing and Materials) standard practices. An odor panel consists of trained individuals (panelists) who follow a sniffing practice according to the ASTM Standard Practice for odor concentration determination (ASTM E679-91). The determination of odor is carried out by a set practice of Forced-Choice Ascending Concentration Series of Limits.

Both of the above mentioned instruments (and a few others, which will not be mentioned here), are aimed primarily at monitoring environmental odors, although the applications listed by the manufacturer include many other sectors, such as: agriculture, slaughterhouses, paper industries and even coffee roasting. The use of these instruments, combined with sensory panels, has some merit and they are still being used for certain applications. Nevertheless, a high degree of accuracy can not be attained with these instruments, and their performance is also affected by concurrent impressions from other senses. Moreover, their being subjective by nature and prone to drifting, render them unsuitable for performing an objective,

continuous, in-field, or automated measurement at a relatively low cost, as required, for example, in applications in quality evaluations of fruits and vegetables.

4.2 Analytical methods

Many analytical laboratory methods are available for the analysis of gases and they include the Gas Chromatography (GC) method; High-performance Liquid Chromatography (HPLC); High-Performance Thin Layer Chromatography (HPTLC); spectroscopic techniques such as: Mass Spectroscopy (MS), Nuclear Magnetic Resonance (NMR); Infra-red Spectroscopy (IRS); Fourier Transform Infra-Red Spectroscopy (FT-IR), continuous flow immunosensors and various combinations of these methods. All these methods provide a reliable qualitative analysis, which is often used for the assessment of aromas in food products [23]. However, because of the cost factor involved and the duration of tests, they are not done on a routine basis and their major use is in research. These methods are not only time-consuming but the results are often inadequate. For example, there are some key flavor constituents of beer that are below the detection limit of most gas chromatographs [56]. It is also interesting to note, that the human nose is more sensitive and more selective than any other GC- detector, and a sniffing person can describe the intensity and the quality of an odor, and is able to locate the components of a sensory value in a chromatogram.

A few dedicated, commercial aroma analyzers, are also available, based on gas chromatography techniques. The 'CharmAnalysis' system, e.g. developed in the Flavor Chemistry Laboratory at the New York State Agricultural Experiment Station of Cornell University, is based on analyzing aromas with a Gas Chromatography-Olfactory (GCO) system, by utilizing quantitative and descriptive GCO techniques to detect aromas in extracts of food and fragrance materials. 'CharmAnalysis' is equipped with high resolution gas and liquid chromatographs, a mass spectrometer and two high resolution gas chromatographs - olfactometers (GCO) to yield chromatograms in which the ordinates or y-axes are measures of odor potency, titer, or multiples of odor threshold. Peaks in these chromatograms can be integrated and associated with descriptive words.

4.3 Solid state gas sensors

While analytical laboratory instruments are of significant importance, they do not provide the means for interaction with the real world - the environment. Therefore, there is a clearly defined need for suitable sensors, which will provide the interface between the available (and future) microelectronics and microprocessors and the environment to be monitored. Gas sensor technology is based primarily on solid state gas sensors, of which three are currently in most widespread use: the solid electrolyte potentiometric sensors; the catalytic gas detector for combustible gases and the semiconducting oxide gas sensor. While several other types of gas sensors

or detectors are also produced, these three types of solid state device dominate the market and will continue to do so for many years to come [61].

To deal adequately with even the principal types of solid state gas sensors is far beyond the scope of this review paper, but the subject is well covered in the literature [61, 87], to name only few. Only selected areas, which are more commonly used, or which are important in new device development and relevant to the cited problem will be described briefly in the following sections.

4.3.1 Semiconducting gas sensors

4.3.1.1 Metal oxide sensors

Semiconductor sensors can sense gases by monitoring changes in the conductance during the interaction of a chemically sensitive material with molecules to be detected in the gas phase. At present, these devices are based mainly on the use of metal oxide semiconductors as the sensing material. The most generally used are semiconducting oxides and catalytic metals, such as tin oxides (SnO_2), tungsten oxide (WO_3) and zinc oxide (ZnO). A metal oxide sensing element is placed between two electrodes, and the sensing element is maintained at an elevated temperature, typically 350^{0}C. Electrical current is passed between the electrodes, through the metal oxide. Interactions between gaseous species and the metal oxide sensor surface give rise to a change in resistance measured across the sensor. These interactions are generally limited to the oxidation of gas molecules via electron transfer from the gas to the metal oxide. A decreased resistance across the sensor is indicative of the presence of a gas. Typically, a direct current is passed through the sensing element, and a voltage change across the sensor is measured. Alternatively, alternating current may be used, and it has been shown that by measuring resistance at different alternating current frequencies, a constant voltage may also be used, and changes in current monitored.

Metal oxide sensors are generally less selective than many other sensor technologies. Selectivity may be achieved, however, using several methods. Some sensors utilize an array of identical tin oxide sensors, each operated at different temperature. It was shown that different temperatures produce different sensor selectivities. That is, by changing the operating temperature of a sensor, the species to which the sensor responds, or the degree of response could be altered. A more common approach is doping the metal oxide with a small amount of rare earth metal. Using different metal dopants results in sensors which respond preferentially to particular classes of compounds.

Over the past few decades solid-state gas sensors based on SnO_2 have become the predominant solid-state devices for gas sensors alarms used on domestic, commercial and industrial premises [3, 8, 29, 82]. The tin oxide gas sensors have a number of advantages which make them attractive for a dedicated odor sensor,

both for laboratory use and field applications. First and foremost they are readily available because they are commercially produced. Secondly, they have high sensitivities to a range of organic vapors (although, sometimes, with doubtful repeatability). Thirdly, a variety of different types are available with broadly different sensitivities so that an array can be constructed. In addition, they are characterized by a relatively fast response, typically less than 10 seconds. This last characteristic, although not fast enough for an on-line fruit sorting, makes them, nevertheless, amenable to other *in situ* measuring techniques for gas emission monitoring and enables real-time control. The disadvantages of these devices include their size and the fact that they operate at elevated temperatures, so that their power consumption is high.

The basic technology and fabrication of these devices has been described in detail in the literature [87, 8].

Metal oxide gas sensors may be subdivided into thick film and thin film devices. In general terms, thick film devices are easier to produce, as they rely on depositing a paste of material between two electrodes, often using standard lithographic techniques. However, these devices have some distinct disadvantages, such as poor selectivity, poor unit-to-unit consistency of performance, dependence on ambient temperatures and relative humidities, long stabilizing times after energization and large power consumption [8, 45]. Nevertheless, because of the ease in their production, many of the commercially available metal oxide sensors are based upon thick film technology (e.g., 'Figaro' sensors).

Several disadvantages of today's thick-film SnO2 sensors might be substantially overcome by using modern thin-film technologies [45, 87]. The construction of thin film devices generally relies upon the use of vapor deposition technologies to achieve a very thin film of metal oxide between two electrodes. In principle, such devices should combine the advantages of the 'Figaro' sensors, but be suitable for fabrication as small integrated arrays. They offer significantly higher sensitivities and are made with a lower power consumption per device. However, they are generally more expensive, more difficult to produce and tend to suffer from instability.

4.3.1.2 Conducting polymer sensors

Some of the limitations in the use of both, thick and thin film devices, can be overcome by the use of sensors using conducting polymer and biological lipid coatings. With these materials there is a much wider choice of operating conditions, they can be operated close to room temperature (20-60^{o}C) and more importantly, functional groups that interact with different classes of odorant molecules can be built into the active material, thus providing for high sensitivities of, typically 0.1-100 ppm [8, 34, 40].

Many polymers, under the right conditions, are electrically conductive, for example, polypyrrole, polyaniline and polythiopene. These polymers may be deposited between two electrodes and used as gas sensors. A change in the conductive properties of the polymer results from exposing the sensor to a gas species. This change may be monitored by passing a current between the two electrodes and observing the change in the voltage across the conductive polymer.

Organic materials tend to be easier to process than oxides and may, in principle, be much more easily modified than inorganic materials to react with specific gaseous species. Moreover, with different methods of sensor production, a better control is achieved of sensor selectivities. Selectivity of a given sensor is theoretically controlled by using different chemical functional groups on the top layer of polymer. Of particular importance is the improved reproducibility, which is key to the cited application of sensing and classifying aromas in fruits and vegetables.

The disadvantages of organic materials in gas sensing are that they are usually very poor conductors, and conductivity measurement can therefore be difficult. They are also usually thermally unstable, so that it is often impossible to use them at temperatures at which gas-solid interactions proceed quickly and reversibly. In addition, regardless of their means of production, conducting polymers age with time to some degree. Calibration algorithms must therefore be used in order to compensate for drift which occurs over long period of time.

A variety of approaches has been employed commercially in the production of conducting polymer sensors. These approaches result in fundamentally different sensors, hence rendering them suitable for a variety of applications [15, 72, 40, 73, 80].

4.3.1.3 Quartz crystal microbalances

Quartz crystal oscillators (QCM) are piezoelectric devices which are used in electronic circuitry for a variety of purposes, such as timing clocks, because they can provide a highly accurate timing signal based upon their frequency of oscillation. The term «quartz crystal microbalance» is derived from the fact that if a mass is adsorbed or placed onto the quartz crystal surface, the frequency of oscillation changes in proportion to the amount of mass. By measuring the change in the frequency of oscillation, the amount of mass can be determined.

These devices have been used as gas sensors by coating a crystal with a material which is selective towards the gaseous species of interest. For example, a QCM could be coated with a non-polar material such as dimethylpolysiloxane, which preferentially absorbs non-polar species, such as n-alkanes. If the coated QCM was exposed to a gaseous sample, changes in oscillation frequency could be attributed to non-polar species being absorbed by the coated QCM. By coating QCM with different materials, selectivity of response can be attained.

The ability to control a QCM's selectivity by applying different coatings is an extremely important feature, and makes this sensor type extremely versatile. Virtually, any kind of selective coating may be used. However, the coating of QCM may also be, ironically, their greatest drawback, because of the inadequate reproducibility involved in the process and since for a sensor technology to be commercially viable, sensors must be reproducible. Several different methods have been employed to physically apply coatings to QCMs, but all these techniques, however, have, as yet, not proven very reproducible on a commercial scale.

In spite of the latter deficiency these devices have been used in many different applications and examples of their uses are numerous [10, 7, 28, 35, 49, 64, 65, 66, 70].

4.3.1.4 Surface acoustic wave

Surface acoustic wave sensors (SAW) are similar to quartz crystal microbalances (QCM) sensors in many respects. Both technologies use coated oscillators from which a frequency change is measured upon exposure to an analyte, due to absorbed mass by the coating. QCMs can be considered bulk acoustic wave devices (BAWs), because the entire crystal oscillates. Surface acoustic wave devices generate Rayleigh waves down the surface of a quartz or silicon substrate onto which a thin coating has been applied. A change in mass absorbed by the coating generates a corresponding change in frequency. The coatings used for QCMs and SAWs are often similar materials, and it is the selection of coating by which specificity in response is obtained [68, 90].

SAW devices generally operate at much higher frequencies than do QCMs, most commonly in the 250 Mhz range (as compared with 10 Mhz used with QCMs), though sensors with operating frequencies approaching 1 Ghz have also been reported.

These gas sensors are distinguished by high reliability, by immunity to extreme temperatures, contamination or aggressive media, by a small response time and by their output, which is a frequency signal and unaffected by many forms of electrical interference [6]. The response of SAWs to hydrogen or methane in the air, for example, is less than one second, without using a catalyst. The SAW sensor arrays also have the potential to be used in a portable-type instrument. First, SAW devices respond with high sensitivity to changes of surface mass and, as a result, can be used for a wide range of potential analyses. Secondly, the amount of vapor sorbed by the sensor coating on the device is typically a linear function of the vapor concentration over the useful concentration range (i.e. less than a few hundred parts per million by volume). Thirdly, efficient operation is possible at ambient temperatures. Indeed, vapor sorption decreases exponentially with increasing temperature, so higher sensitivity is obtained at lower temperatures. Finally, since the response to a given vapor will depend strongly on the functional groups

incorporated into the structure of the polymer, judicious selection of polymers can lead to significant differences in the response patterns for different vapors [68]. Of particular interest is the application of the SAW technique to films deposited on suitable piezo-electric materials, mainly on vacuum-sublimed and Langmuir-Blodget (LB) films [15, 60].

In theory, because of their distinct advantages and better performance, SAWs devices hold promise of sensitivity increases over other gas sensor technologies. However, there exist two obstacles which must be overcome before the devices becomes viable within a dedicated sensor platform. The devices operate at high frequencies, and often small frequency changes need to be monitored. The associated electronics can be complex, and it is imperative that noise be eliminated from the system. Secondly, as with QCMs, only perhaps more importantly, the coating technology needs to be adapted to a commercial scale, which will allow reproducibility in sensor production.

Both, SAW's and QMB devices have similar performance limitations, which include the lack of specificity, sensitivity to moisture and response reproducibility. These disadvantages are not totally unexpected, since the physiochemical sorption of any environmental gas or vapor will increase the mass of the coating on the detector and produce a sensor response. Thus, specificity, remains an elusive performance feature for these devices.

4.3.1.5 Field-effect-transistor-based (FET) gas sensors

Field-effect devices sensitive to ions and gas molecules have been around for about 20 years. Such devices are of interest in the development of sensor arrays, since they are based on a well developed technology.

A field-effect structure is in principle a «metal» insulator semiconductor structure where the gate, the «metal», can be any conducting layer or medium (e.g. metal, semiconductor, electrolyte, or polymer) The conducting layer can furthermore be allowed to have a rather small conductivity and still work well as a gate material for a field effect device. The possibility of finding a suitable gate materials for a given sensing situation is therefore quite large [51, 52].

Recently, gas sensors based on field-effect transistors (FET) concepts, have become of increasing interest because of a possible application in Microsystems and because they can be used to make a large array of gas sensors on a single chip. This, in principle, should make it possible to produce a two-dimensional response map, that is an «image» of the mixture of gases.

The FET is basically a semiconductor device, which acts as an amplifier with the same function as a junction transistor, although with a different construction. Different approaches for FET configuration have been tested, with specific

advantages and disadvantages. The MOSFET - Metal-Oxide-Semiconductor FET, is quite a common configuration, which has many advantages, such as high sensitivity, mechanical sturdiness, small size and low cost. However, these sensors, up to now, are not in wide spread commercial use as gas transducers, because sometimes, the reproducibility of the sensor electrical characteristics and its sensitivity, are not sufficient for use in a real measuring system, particularly, for multiple-component gas mixtures. [51, 52].

Another approach is the SGFET - fabrication of a Suspended Gate on metal-oxide-semiconductor (MOS) devices. With this technology, an air gap between the gate and the insulator is formed and a chemically reactive layer is deposited right underneath the gate metalization. When subjected to the passage of volatiles, the chemisorption or physiosorption of the gaseous species causes a shift of the threshold voltage of the FET, due to the change of the semiconductor work function difference.

Another configuration is the ISFET - Ion - Sensitive FET, which is basically a potentiometric transducer, which has some advantages, such as an improved signal-to-noise ratio and fast response. Their major disadvantages are their relatively high drift and hysteresis.

Intensive investigations of ISFET's during the last few years, led, e.g., to the fabrication of sufficiently small, rugged, convenient to use and stable pH sensors, that are now commercially available. However, further development is required for practical application of these sensors in medicine, agriculture, environmental studies, etc.

4.3.2 Fibre optic sensors

This category of sensors encompasses a wide range of technologies, as there are many applications of small scale optical devices within the gas sensing arena. One of the technologies with relevance to the applications of aroma sensing is the use of bundled fibre optics, through which fluorescence measurements from photodeposited polymer sensing elements are made. On one end of a fibre optic bundle, small regions of polymer/fluorescent dye mixture are photodeposited. As many as thirty regions may be deposited on the tip of a fibre optic bundle. A flash of light at an excitation wavelength is applied to the other end of the fibre optic, and fluorescence intensity at selected wavelengths from the polymer/dye mix is subsequently measured back through the fibre optic. Different polymer/dye combinations interact with gases differently, such that upon exposure to a given sample, the different regions or sensors, provide unique information. A fluorescence emission spectrum from each of the regions can actually be measured, such that a tremendous amount of data becomes available.

In addition to fluorescence luminescence, attention has been also given in recent years to phosphorescence luminescence, which is slightly different from the former,

by exhibiting luminescence that continues even after incident radiation stops. These kind of sensors have several inherent advantages over fluorescence sensors, including longer excited-state lifetimes and emission wave lengths more compatible with existing monitoring technology.

These sensors have not yet been commercialized for use in dedicated sensing instruments [2]. However, due to the vast amount of information which they provide, they may hold promise for future applications. Other optical technologies, such as infrared (IR), and some of those used for biosensor applications, may also be applicable to the aroma sensing instrument platform.

5. The «artificial nose»

The artificial, or electronic nose, is, as its name implies, a simulation of the human olfactory system. It aims to do exactly the same as the human nose, but with considerably fewer sensors and with a simulated brain. Thus, it differs from the standard area of gas sensing, where the objective is to detect a single gas or vapor that has exceeded some threshold value. In olfaction we use our sense of smell not only to detect noxious vapors, but also in a more sophisticated way for classifying and grading odors.

Although an analogy is made with the human sense of smell, the electronic nose should not be thought of as an electronic equivalent. By careful choice of the sensors used it may be possible for an electronic nose to be tuned to respond to similar aroma molecules as a human, but the mechanism involved is fundamentally different. It is important to note, however, that while the electronic nose responds to the same chemicals that are responsible for the sensation of smell in humans, they can also respond to other chemicals which are odorless to humans.

While the mechanism of smelling may be different, the requirements from an electronic sensing emulator are similar to those met by the human sense of smell. Hence, the sensing instrument envisioned should be able to address the following classes of sensory requirements: (i) Detectability - may be absolute (is there anything which can be detected?), or differential (is there a detectable difference between two samples?); (ii) Intensity - how large is the difference? how much of a particular attribute is present?; (iii) Quality - what is the nature, character or description of the attributes present?.

For our particular application it is also vital to know how the sensory data from the artificial nose relate to the human sense of smell and the general human judgment of product acceptability.

The human nose is indeed a valuable tool in many areas of industry, but the response of subjects to different odors and odor concentrations is highly subjective [53, 67]. Differences of two or more orders of magnitude between subjects is not

uncommon. Hence, an instrument that could perform simple odor discrimination and provide measurement of odor intensity devoid of subjective influences could be most useful.

The attempt to mimic the abilities of the human olfactory system is an ambitious goal, not only because of the chemical complexity of the stimuli with which such a device would be confronted, but also because of the paucity of detailed knowledge available about the biochemistry and neural processing within the human olfactory system [31]. Nevertheless, the desire to produce useful devices, coupled with the desire to improve our understanding of the functioning of the human olfactory system, have prompted many researchers to try and develop artificial analogues.

The volatiles emanating from fresh fruits and vegetables, as those from food products, present a special complex chemical environment problem, which can be described in terms of chemical patterns of a number of chemical species, each at a certain concentration level. A chemical sensor exposed to this complex environment produces an output which, in some sense, represents the synthesis of the whole pattern. The synthesis process depends on the selectivity property of the sensor, which is related to the sensitivities of the sensor to each of the species composing the pattern.

The complex chemical environment which typifies the human olfactory system, led to the multisensors approach, which is based on the principle that by utilizing a number of non-specific sensors having suitable selectivity properties (each different from the others), it is possible to infer some information about the nature of the chemical environment under analysis. Such a system shows some analogies with the olfaction structure of humans, being able to discriminate between very large number of gases, odors and mixtures, by utilizing only a small number of chemical sensors. For this reason, multisensor applications in chemical sensing are now commonly referred to as electronic, or artificial noses.

The earliest work on the development of an instrument aimed, specifically at detecting odors, probably dates back to Moncrieff [32]. This was really a mechanical nose and the first electronic noses were reported by Wilkens and Hatman [32]. However, the concept of an electronic nose as an intelligent chemical array sensor system for odor classification did not really emerge until nearly 20 years later from publications by Persaud and Dodd at Warwick University in the UK [30]. A brief history of the development of electrical noses was given by Gardner and Bartlet [32] and an overview of electronic noses and their applications by Elliott-Martin *et al.* [26].

In principle, a large variety of sensors can be utilized for electronic nose applications. However, in general, the definition of an electronic nose restricts the term to those types of intelligent chemical array sensor systems, or chemical sensoric array devices (ChemSADs), that are specifically used to sense odorant molecules in ways analogous to those of the human nose.

Recent advances in sensor technology have led to the development of many chemical sensor arrays, utilizing, in general the various existing technologies for gas sensing. Especially noteworthy is the development of microsensors based on conducting polymers - molecular chains that can carry electric currents, SAWs. and QCMs. Fabrication techniques developed in the microelectronics industry have proven extremely useful in the production of new electrode systems and configurations. Advances in electrochemical instrumentation allow very small currents to be monitored while potential waveforms may be conceived and produced at will. These advances, coupled with the rapid progress made in the application of new materials, now make feasible the design and construction of sensing systems at the molecular level [31, 40].

Nevertheless, as in natural olfaction, a key role is played by proper data analysis which makes it possible to find out a correlation between the sensor outputs and the target of analysis, when such a correlation exists. The target of electronic nose function is, not only to sense the environment, but to process the data input and find out a classification scheme for the environment under analysis. The classification scheme always describes a global feature of the environment, disregarding its analytical attributes (as an a example, freshness, or firmness are global attributes of foods).

The existing gas-sensing materials, such as metal oxides, organic polymers and piezoelectric crystals, while being of great importance, have relatively poor selectivity, thus presenting us with a major problem of classification. But, even the more advanced conducting-polymer technology provides responses which are, almost always, nonspecific.

This rather complex problem has given impetus to utilize pattern recognition methodology, which involves the mimicking or modeling of human intelligence, in concert with an array of differently constituted sensors. This approach has already been implemented in many studies where various types of gas transducers were employed in combination with some pattern recognition algorithm. Thus, Kaneyaso *et al.* [45], for example, have compared the output from an array of six thick-film metal oxides sensors with the patterns of electrical activity in the rabbit olfactory bulb, as observed by Moulton [62]. In their study they used seven individual odors and analyzed the results using a *correlation technique.* Abe *et al.* [1] have also investigated the use of 'Figaro' gas sensors in automated odor sensing. In their studies they used eight different sensors and 30 different individual odors. In this work the odors were assigned to four classes - ethereal, ethereal-minty, ethereal-pungent and pungent. Using *cluster analysis* these workers were then able to establish a correlation between the pattern of responses from the eight sensors and the odor. A variety of pattern recognition techniques were then applied to the data. The best predictive results were obtained from the *potential function* method [31]. Likewise, Pelosi and Persaud [72] have looked at the responses of five sensors, each based on a different conducting organic polymer, to 28 odorants. Following

ternary classification of the sensor responses they could discriminate 14 of the odors.

A more recent development in this area is the application of Artificial Neural Networks (ANN) techniques to the processing of data from a sensor array [27, 30, 65, 33, 85, 46, 47]. Also referred to as connectionist architectures, parallel distributed processing, and neuromorphic systems, an artificial neural network (ANN) is an information-processing paradigm inspired by the way the densely interconnected, parallel structure of the mammalian brain processes information. ANN are collections of mathematical models that emulate some of the observed properties of biological nervous systems and draw on the analogies of adaptive biological learning. The key element of the ANN paradigm is the novel structure of the information processing system. It is composed of a large number of highly interconnected processing elements that are analogous to neurons and are tied together with weighted connections that are analogous to synapses.

Part of the attraction of ANN lies in its description of a parallel distributed processing system from neuroscience. ANN techniques offer potential advantages, such as fault tolerance, adaptability and high data-processing rates, over classical pattern recognition methods, owing to their inherent parallelism.

The incorporation of ANN in odor sensing have already been demonstrated in various applications: monitoring food and beverage odors [30], automated flavor and perfume control [65], discriminating the smoke from different brands of cigarettes [81], identifying different types of alcohol [30], identifying odors from household chemicals [46], quantifying individual components in gas mixtures [85] and discrimination of coffees. It has also been demonstrated that the ANN technique can be applied successfully to the processing of data from a quartz resonator conducting polymers and SnO_2 sensor arrays [31, 34]. This array has also been incorporated in a single stand-alone portable instrument, combining the odor-sensing array (based on a 'Figaro' gas sensor) and an artificial neural emulator (ANE), to yield a microprocessor-based instrument which can intelligently classify the signals from an array of odor-sensitive sensors [36]. After sampling the odor for about 60s, the unit can classify the odor in much less than a second and display the results on a two-line LCD dot matrix display.

Matching various sensor array systems with pattern recognition and ANN techniques in an integrated sensing system, has already spawned several electronic noses which are commercially available, or close to it. A detailed description of the various commercial odor monitors and electronic noses was given by Gardner and Bartlet [32].

Four noted commercial instruments, which have been in use for quite some time and therefore are worth mentioning in particular are: the 'AromaScan' (Alphatech International), the 'NOSE' (Neotronics Olfactory Sensing Equipment; Neotronics), the 'Bloodhound' (University of Leeds Innovations Ltd.) and 'Fox 2000 Intelligent

Nose' (Alpha MOS, France). Each of these uses for sensing, primarily, an array of conducting polymer-coated microelectronics for the data acquisition system, combined with an ANN machine for data processing and classification. Other interchangeable sensing technologies have also been cited.

The digital aroma technology of the 'AromaScan' was first developed at the University of Manchester, Institute of Science and Technology (UMIST). In 1980, research began into biological olfaction systems and gas detection, with a specific objective to develop a multi-element aroma sensor that emulates the human nose. By 1990, a prototype instrument has been developed, which eventually evolved into the current 'AromaScan' instrument. The system is using a thermally stabilized array of 32 conducting polymer elements and a pattern recognition - artificial network methodology for data analysis and classification. Their proprietary software allows the user to subtract, or to overlay, the sensor response of one sample from that of another sample. This feature helps to visualize the variance of the sensor response between samples. This technique has been applied successfully in measuring the response of, e.g. grapefruit and orange essence oil samples and in sensing differences in the aroma of tomato pastes at different stages of lactic acid spoilage.

The 'Neotronics' Olfactory Sensing Equipment (NOSE^R) utilizes an array of patented conducting polymer sensors which, due to their design, have rapid response times and stable outputs. The reaction of the tested vapor with the conducting polymer causes a change in conductivity and this change is dependent on a complex interaction between the components of the vapor and the polymer, as each sensor responds to a number of components in a unique manner. The use of an expanding range of polymers makes comparative analysis of complex vapor structures realizable. A twelve sensor array is located in a sealed compartment and the sensor head is automatically lowered out of its sealed compartment into the vapor above the sample. Measurements from the sensors are taken at this point, and the sensor head is raised automatically after each analysis. The outputs from each sensor are combined and compared to a previously measured pattern of the particular aroma. The «fingerprint patterns» obtained from the instrument can be analyzed and displayed in different formats and the currently available software package provides for using various statistical methods, including the latest in artificial networks techniques.

Of special relevance to applications involving fruits and vegetables are the reported results of a study involving the 'NOSE' on the discrimination between varieties of tomatoes, based on their, presumably, different olfactory characteristics and tomatoes of the same variety, which varied in age (postharvest time). Results of this study clearly indicated the ability of the 'NOSE' to discriminate between four different varieties of tomato and successfully evaluate tomato fruit age. However, these results were not obtained with intact fruit, but rather, with liquefied samples of the tomatoes. Similar results were reported by the Scottish Crop Research Institute (SCRI), where researchers have used the 'NOSE' as part of their raspberry

breeding program for successful discriminations of four varieties of raspberry, based on the difference of their aroma.

The «Bloodhound « sensory system is a spin-off from a 10 years of research conducted at the University of Leeds in the UK. At present, a prototype of the system - BH 114 is available from «Bloodhound Sensors» Ltd. It consists of an array of 14 conducting polymers, utilizing various statistical methods for its output analysis, including pattern recognition and artificial networks.

The 'Fox 2000', manufactured by 'Alpha MOS' in France, and developed in collaboration with the University of Warwick, UK, consists of an array of 20 conducting polymer chemoresistors and the 'Intelligent Nose' of an array of six metal oxide sensors, each capable of running at one or two temperatures. Both instruments require a separate computer to calibrate and run the odor-sensing arrays.

All these instruments use chemoresistive sensors in a monotype nose. That is, they rely on a single class of sensing material and of transduction principles, such as conducting polymers or semiconducting oxides chemoresistors. However, the real world is multifaceted in nature and in order to meet the emerging needs of the industry and the complicated conditions of the agricultural environment, the need exists for a multitype electronic instrument, or hybrid nose, consisting of an array of sensors. Such a system could extend the olfactory range of the artificial nose and improve its discrimination power. An experimental design of such an array has been reported recently by Dyer and Gardner [24], who claim to have developed a high-precision intelligent interface for a hybrid electronic nose. According to their report, their multitype nose can both, measure the signals from an array of chemoresistive and piezoelectric odor sensors, which have a stable circuit that can detect changes in frequency of a few hertz in many megahertz over a long periods of time and implement numerical pre-processing algorithms, which render this device suitable for membership in the next generation of electronic noses.

Numerous other research centers have also tried in recent years to meet the challenge of developing an «artificial nose», for both laboratory and field applications. Over 25 different research centers, universities and commercial companies were cited in various reports on work aimed at developing an «electronic», or «artificial» nose for a multitude of applications. These represent a manifestation of the growing interest in the subject and hence, increase the probability of an efficient system being developed, even for the specific application of nondestructive quality evaluation of fruit and vegetables. Only the major developments will be described here, but with the realization that much broader work has been, or still is being done, worldwide.

A group of researchers at the Tor Vergata University in Rome have done extensive research work in the past 2 years for the development of an electronic nose [21]. The device consists of 8 chemical sensors prepared by coating cut quartz crystals,

having a fundamental frequency of 5 Mhz. Coatings have been obtained by depositing a specified quantity of a diluted solution on compounds which are known to act as catalysts in oxidation reactions. After the evaporation of the solvent, 50 μg of coating was deposited on the quartz. Each sensor is part of an oscillator circuit, the frequency response measurements of which were obtained by utilizing the frequency counter of a digital oscilloscope. Data analysis and extraction of the relevant information from the data were accomplished by a set of tools including a number of chemometrics-based methods (Principal Component Analysis and Cluster analysis) and Neural Networks (Feed Forward Back Propagation trained networks, Self Organizing Maps, Adaptive Resonance Theory based networks).

The aptitude of this electronic nose to be utilized for the analysis of foods has been tested by measuring the sensor sensitivities with regard to several substances which are of interest in food analysis. These compounds are representative of various classes of species such as: organic acids, alcohols, amines, sulfides, carbonyls. For example, in relation to quality of tomatoes, a measurement was made of volatile acidity (e.g. D- and L- Lactic acid and acetic acid), acethylmethynolcarbinol and ethanol, which represent the products of sugars degradation of micro-organisms.

A joint research group from the University of Southampton and the University of Warwick in the UK, are involved in a research aimed at designing an instrument that mimics the human sense of smell [30]. This aim differs from a previous related area of gas sensing, where the objective was to detect a single gas or vapor that has exceeded some threshold value. Like in the human olfaction system, the objective of this development was to be able also to classify and grade odors. Since direct mimicking of the human sensory receptors seemed an exceedingly complex approach to the problem, the scientists selected an alternative and simpler solution, which has been exploited in their work, based on the use of a range of materials which show a considerable variation in electronic behavior on exposure to a range of different vapors. Like similar designs, their system uses an array of sensors which are made from electrically conducting organic polymers, the conductivity of which changes on exposure to different odors. As each sensor in the array is composed of a different conducting polymer, each will behave slightly differently towards a particular odor. This creates a pattern of responses which will be unique for a particular odor and hence, could be used to characterize it. The output signals from the «electronic nose» show a variation in the conductivity of each sensor site with time and when combined, represent a «fingerprint» of a particular smell or mixture of odors. For their data processing the researchers suggested two approaches: displaying the results obtained in the form of a radar plot in which the response of each sensor is plotted using polar co-ordinates, or interpreting the results by using pattern recognition software.

The scientists involved in this development suggested that the present technology already offers the possibility of both, quantitative measurement and considerable miniaturization leading to very high sensitivity. One application which is currently

under evaluation (and can be of relevance to our cited application for measuring the responses from fresh fruits and vegetables) is the detection of ketosis in dairy cattle, a problem which is thought to be an early indication of the potentially serious disease mastitis.

Another group in the UK is operating at the University of Glasgow, at the Department of Electronics and Electrical Engineering. They reported recently on their current interest in developing an 'Electronic Nose» using conducting polymers as transducers, which will have some of the capabilities of the human olfactory system. By an analogy to the human system, which is believed to utilize only a small number of chemical sensors to discriminate among a very large number of gases, odors and mixtures, the present project intends to use a similar approach. The model nose uses a finite array of sensors (typically 3 to 64 sensors); the sensors are independent, but each sensor is sensitive to a very wide range of odors. Odors are identified by an adaptive pattern recognition analysis of the signals induced by the sensor array. The system module which handles the signal processing is a sophisticated parallel-processing system, which is used for the dual purpose of modeling the human olfactory system, as well as for providing engineering solutions to other problems in olfaction. The main applications concern on-line quality control of food, drinks and perfumed goods, the detection of toxic and dangerous vapors and medical diagnostics. At present, the group of researchers are constructing a second-generation electronic nose which has enhanced sensitivity and pattern recognition features. It is being applied to problems in agriculture and veterinary science.

The Pacific Northwest National Laboratory (PNNL) in Oregon, has been working for several years on an artificial nose project, with the objective of demonstrating the potential information processing capabilities of the neural network paradigm in chemical vapor identification. They have been involved in the development of a prototype system that is composed of nine tin-oxide vapor sensors ('Figaro'), a humidity sensor and a temperature sensor, coupled with an ANN. During operation a chemical vapor is blown across the array, the sensor signals are digitized and fed into the computer, and the ANN (implemented in software) then identifies the chemical. The identification time is limited only by the response time of the chemical sensors, which is in the order of seconds [46, 47]. Although each sensor is tuned to a specific chemical vapor, each responds to a wide variety of chemicals. Collectively, these sensors respond with unique signatures (patterns) to chemical vapors. Coupling the sensor array with a neural network has the advantage that most of the intense computation takes place during the training process. Once the neural network is trained for a particular task, operation consists of propagating the data through the neural network. During operation, the system can rapidly identify the composition of a vapor, provided that the vapor is composed of chemicals used during the training process. The prototype nose has been used to identify common household chemicals by their odor, but other potential applications included also, the monitoring of food and beverage odors, automated flavor control, analyzing fuel mixtures and quantifying individual components in gas mixtures..

However, while initial reports of their work were very promising, no continuation is taking place at present.

The Biomedical Instrumentation Lab at North Carolina State University (NCSU) is also currently attempting to develop an artificial nose system. Their artificial nose consists of a gas chamber with an array of gas sensors and additional hardware to support the gas flow through the chamber. The system utilizes 16 gas sensors of 'Figaro' type, but is also able to accommodate gas sensors of the 'Capteur' type. The nose system is able to test odors in two ways. First, a continuous flow of odor can be sampled. That way, fresh odorant is supplied to the sensors during the measurement. Second, a volume of odorant can be introduced into the chamber for a stagnant measurement. 'LabView' software of 'National Instruments' is used to control the measurement cycle and collect sensor outputs.

Another, rather recent development, is the Electronic Nose ('ENOSE'), which is a device under development at the Jet Propulsion Laboratory (JPL) of the California Institute of Technology (Caltech). This work, which was also inspired by the human olfactory system, originated as a result of research advances made by Prof. Lewis of Caltech, working in collaboration with Prof. Freund of Lehigh University [54]. In this collaborative effort, JPL is responsible for the instrument design and construction, including: sensor assembly, electronics and the neural net pattern recognition engine, as well as providing space flight validation. Caltech researchers, building upon earlier efforts by British and Japanese research groups, have been able to develop a way of monitoring changes in gaseous environment by using polymeric films impregnated with an electrically conducting material. The properties of the polymeric films can be varied broadly in a controlled way, but only the electrical conductivity changes are used to generate the electronic signals which are related to the sensed chemicals and enable detection of specific gaseous. The Electronic Nose ('ENOSE') consists of an array of different polymeric thin film sensors that have been shown to respond to a number of organic and inorganic compounds in the ppm (parts per million) range. It is based on the multisensing principle, in which the distributed response of an array is used to identify the constituents of a gaseous environment. Individual sensor films are not specific to any one gas; it is through the use of an array of different sensor films that gases and gas mixtures can be uniquely identified by the pattern of measured electrical response. Currently under development is an experimental instrument to monitor the air quality on the Space Shuttle. For this application, which aims at sensing twelve compounds that have been detected on the Space Shuttle, the instrument under development will consist of an array of up to 32 polymers which are deposited on four small ceramic substrates. Each deposited polymer will create a sensing film of about 2 mm on the side and a few microns thick. The sensor substrates will be in a sealed enclosure less than 15cc in volume with provisions for letting sample air in and out. The polymer sensor response to gases will be detected electronically by measuring changes in electrical conductivity. The data will then be analyzed by a neural net pattern recognition software engine, which

deconvolutes the data to identify the sensed compounds and their concentrations. For this experiment, where there will be no on-board data processing and merely data storage. JPL researchers are looking at coming generations which will reduce the instrument to a credit-card size. In addition to the current development intended for the Space Station, the researchers list a multitude of additional possible applications, including: industrial processes, detection of environmental toxins and pollutants, for medicine and body functions, for the use in food processing and for measuring the military environment and its toxicology.

The European Space Agency (ESA), which is an international organization involved in space applications systems, reported recently on the development of an artificial nose, which is based on a multi-element polymer array for the sensing of volatile chemicals. New conducting polymer materials together with advanced microelectronics and computational techniques have enabled the development of a new range of chemical sensors capable of mimicking some aspects of the biological system. Chemical sensing is achieved by the use of around 32 sensory inputs (mounted on a chip-sized package) from which a pattern of relative responses to chemical stimuli is used as the basis for detecting selected gases. The patterns generated are used as descriptors of simple or complex chemical stimuli and in this way a library of gas and odor «signatures» can be built up. Specitivity is achieved by using neural networks to process the signals obtained from the individual sensor elements, which have different ranges of selectivity for any given class of chemicals. Response time is rapid (of the order of hundreds of milliseconds) at ambient temperatures, making the system capable of real-time monitoring of volatiles. A neural network algorithm based on backpropagation learning, allows the system to recognize a user-defined set of volatiles. Feedback compensation has been used, for offsetting sensor drift due to characterisable variables such as temperature and humidity. This sensor is already being used in several industrial and experimental applications and, according to the developers, has proven its accuracy and effectiveness and hence, offers a versatile new alternative to existing, more expensive techniques. The possible applications cited for this system are in environmental monitoring, quality control of food, beverages and odorous products and process control. Further miniaturization of the system is currently in progress through the production of a special chip-set for the signal processing tasks.

Another development of an artificial nose associated with the space technology is that, which was developed at RST Rostock Raumfahrt und Umweltschutz GmbH of the Daimler-Benz Aerospace industry. Their technology - the SAM-QMB6 is a spin-off from their activities in space research and is aimed for the monitoring, control and evaluation of complex gas mixtures. It consists of a multiple sensor array - quartz crystal micro balance sensors, which provide high selectivity and high sensitivity to individual molecules and generate different responses to the volatiles which describe the unique signature, or 'fingerprint', of the gas-mixture or odor. The sensors are coated with different gas-sensitivity materials and respond differently to the gases and vapors to be analyzed. A total of six sensors is built into a

temperature-controlled measuring chamber in connection with a special oscillatory circuitry for each sensor element. The adsorption of volatiles on the gas sensitive coating of a sensor element results in a frequency change of the oscillator which can be used as sensor signal for further evaluation. The evaluation of the 'fingerprint' is subsequently analyzed with modern pattern recognition methods, e.g. statistical software and an artificial network. This software compares signal patterns from actual measurements with patterns memorized in the system library of the identification and classification patterns of individual odors and gas mixtures. While the available instrumentation is laboratory-oriented, the company is currently developing a portable system with a temperature range of 30-150^{0}C, based on a modular concept, which would enable the usage of different sensor technologies, such as quartz micro balance sensors (QMB), surface acoustic wave (SAW) sensors, metal oxide sensors (MOS) and semiconducting polymers.

A recent development has been published by 'Instrument Specialists', Inc. which is a manufacturer's representative firm aiming at providing various sensing and measuring technologies, based on state-of-the-art developments. Their design of the artificial nose consists of 6 small semiconducting odor sensors, which can be upgraded with several more arrays to 6, 12, or 18 sensors. These include the Metal Oxides Sensors (MOS), Surface Acoustic Wave (SAW), as well as conducting polymers which make up the complete available range. The company claims to be able to mimic the human nose by using these multiple sensors and list a variety of applications in agriculture (such as measurements of freshness /storage of fruits and vegetables), food industry (drinks and beverage flavors; meat and fish quality, food and raw materials quality), cosmetics and chemistry (evaluating odors from oxidized oils, measuring odors of polymers and the penetrability of aroma through packaging.

Quite a different approach has been taken recently by a group of scientists at Tufts University in Massachusetts. They claim that most previous developments, utilizing SAWs, QMBs and metal oxides and conducting polymers techniques, were able to 'observe' only one parameter, so expanding the number of molecules they can detect means significantly increasing the number of sensors. To get around this problem, they have used optical fibers as sensors, because they can provide many kinds of complex information simultaneously, including changes in intensity, fluorescence lifetime, wavelength and spectral shape. Although, admittedly, fibre optic arrays have been used before, the scientists at Tufts university claim that they have no report of their utilization in a «broad-band chemical sensing tool of this nature».

Their current design consists of a bundle 19 individual polymer-coated optical fibers, where each fibre sensor acts like an individual sensory receptor cell in a vertebrate's olfactory system. This array is exposed to various chemical vapors, precisely pumped by an automatic delivery system, simulating a «sniffing» action. A xenon arc lamp with a standard bandpass filter sends light at 535 nm through the fiber. When exposed to the vapors, the polymers fluoresce at 610 nm, and the

signal from each fiber travels through the bundle to a CCD camera. The system collects and compares the sequence of images, or response profiles, and stores the data in its «neural network», so when the «nose» comes in contact with the vapor again, the network recognizes the pattern and can remember the chemical. The research team used video images of the sensor's responses as the input signals to «train» a neural network to recognize the test vapors. They claim that their system can identify vapors at different concentrations with 'great accuracy'.

Preliminary results reported for this device suggests that it is highly effective in identifying components of mixtures, as well as characterizing analytes (test compounds) on the basis of their chemical characteristics, such as functional groups and relative molecular weight. While no specific application in agriculture has been cited for this device, a broad range of possible uses is described by the researchers, including detecting contaminants in food, water and air and even diagnosing diseases by «sniffing out» various chemical compounds in the blood. Moreover, it was stated that the device would even surpass the human ability of smell, by detecting dangerous odorless gases like carbon monoxide. Nevertheless, according to the researchers, no commercial venture will be attempted by them, before the performance of their device will have progressed to the point it can be considered as a real emulation of the human nose. This is not expected for another 10 years.

A development of a Gas Sensor Microsystem was reported by the Karlsruhe Research Center in Germany, working in collaboration with universities in Karlsruhe, Heidelberg, Freiburg, Tubbingen and Darmstadt in Germany. The characteristic feature of the gas sensor chip developed at this center is the unique way of fabricating the metal oxides sensor elements. At present, the gas sensor chip is equipped with 40 sensor elements, each one consisting of two parallel platinum electrode stripes, which measure the conductivity of the metal oxides between them. It was found that, in many cases, the sensitivity of the sensing array was quite sufficient to detect gases in concentration of only 1 ppm. Using tin oxide and tungsten oxide allowed detection below 1 ppm, a high degree of selectivity and a response time of one second. However, the developers themselves state, that this development has only just began, and the gas sensor chip has, by no means, reached its upper limit yet. Nevertheless, the report from the research center expresses confidence, that chips developed in the future will be able to discriminate even more gases or odors, respond even faster and will yield a low-cost (less than DM 100 for a complete integrated system - gas sensor chip + electronics, based on an annual output > 100,000 items.

In addition to the aforementioned developments, more work was cited as being carried out at various research centers, universities and commercial companies. Part of the available information R & D at research centers, as cited in different sources include:

(i) an aroma sensing system developed at the University of Wollongong Australia, which is based on conducting polymers (polypyrrole and polyaniline), combined with an ANN ; (ii) a system based on metal oxide and an ANN, developed at the Hongkong University of Science and Technology; (iii) an odor sensing system, developed at the University of Derby, UK, for which the technology is based on an array of 12 metal oxide sensors combined with an ANN; (iv) odor sensing technology (a «robot that can smell») developed at the Griffith University in Brisbane, Australia (with no details on the technology developed, but a claim, that «this kind of sensor has never before been created»); (v) a multi-component gas mixture measurement system, developed at the University of Greenwich, UK, which is using an array of gas sensors and a pattern recognition data analysis and classification system. No details were given on the type and number of sensors; (vi) a new type of a sensor for an electronic nose, developed at the University of Antwerp, The Netherlands, based on conducting polymers - large molecules with alternating single and double bonds. The developers state the advantages of their sensor as being easy to synthesize, having high responses towards 8 organic vapors, having no chemical side-reaction with water and good stability; (vii) application of an electronic nose to remote sensing problems has been reported by the Department of Agricultural Engineering at Texas A & M University at College Station, Texas. The researchers used the tin oxide method for their sensing technology, combined with a neural network machine for data analysis and classification; (viii) an electronic odor sensing system has been developed by at the Polytechnic Institute of Toulouse, France. The instrument - 'Odorimtre LCA', is based on tin oxide/paladium technology, coupled with a pattern recognition system; (ix) a prototype of a gas sensing instrument is being developed at the Physics Department of Concordia University in Canada. The sensor is based on SAW technology and a pattern recognition system.

In addition to the scientific work carried out at research centers and universities (with the ultimate goal of developing a commercial useable sensing instrument), development work is also being carried out by various companies, worldwide. Thus, e.g. an electronic nose was reported to have been developed by the 'Nordic Sensor Technologies AB' in Sweden for different gas sensing applications, such as: quality control, process control, environmental analysis and medical diagnosis. It is claimed, that the instrument is able to identify, classify and also quantify odors and gaseous emissions. The instrument is based on a unique array of MOSFET-gas sensors, the result of extensive research work at Linkoping University in Sweden, and selected for their selectivity and large sensitivity. Another development of an electronic nose is the 'MOSES' (Modular Sensor System), developed by 'Lenhartz Electronic' in Germany, in close cooperation with the Center for Interface Analytics and Sensors at University of Tubingen in Germany, based on an array of 2x8 tin oxides and quartz balances (BAW), combined with a pattern recognition package. Other companies include the 'Arraytech' Ltd. in the UK, developing a sensor based on the QCM method; 'GEC' in the UK, also developing an aroma sensor based on the same method and 'LG Electronics' in Denmark, using the MOS method for their sensor.

This list is, by no means comprehensive and only serves to illustrate the great interest in developing gas sensors, worldwide.

6. Current applications in agriculture and the food industry

The complexity of the agricultural environment, insufficient interest by the industry to develop tailor-made solutions for agricultural applications and the stage of development of the relevant technology, are among the factors responsible for not having, so far, suitable technology for the problem cited (and other related issues in the food industry). Most researchers involved in the study of the olfactory characteristics of fresh produce have considered the following aspects:

- determination of the composition of aromas from several fruits with distinct volatiles, by means of conventional gas chromatography (GC);

- finding relationships among the GC readings with some accepted quality attributes;

- testing commercial gas detection transducers for their suitability to detect fruit volatiles both, in the laboratory and, if possible, in the field.

Nevertheless, the realization in recent years, of the potential for the utilization of olfactory characteristics for nondestructive, consumer-oriented, quality evaluation of fruits and vegetables, has provided the incentive for several researchers, to investigate this potential, with the eventual objective of developing dedicated instrumentation.

Trenkle et al., [88] obtained a patent (assigned to 'International Flavors & Fragrances' in New York), for a method and apparatus for simultaneously analyzing aroma emitted from the interior and exterior of living fruit. However, the essence of this patent is the mechanism for trapping the volatiles emitted from the outside and the interior part of the fruit. No details were given on the sensing and discriminating method.

A Japanese company, 'New Cosmos Electrical Company', which was a subsidiary of a company specializing in gas detecting instruments, developed a hand-held device (about 700g) for the determination of stage of ripeness in melons, by measuring the total emission of volatiles from the fruit. The device - «Sakata Fruits Tester» was based on a semiconductor gas sensor and relevant microelectronics and, according to the manufacturer, was able to detect between unripe, ripe and over ripe melons with 99% accuracy. Sarig and Beaumelle [77] carried out an exploratory research utilizing the same device testing its efficacy on melons, feijoa and orange fruit. Their research concentrated on postharvest studies, in which other ripeness indices (color, firmness, SS, respiration and ethylene production)

were compared to the output of the instrument. They found consistent relation between the instrument output and the age of the fruit, and observed a trend between the instrument readout and fruit firmness. In another experiment, they connected the instrument to a digital oscilloscope and a computer and were able to get a reproducible signal for a given fruit after 10s, giving an evaluation rate of 1 fruit/min. Additional time is needed to purge accumulated gases from the previous measurement, but their conclusion was that it is conceivable to expect in the future (after additional development work) the achievement of 1 fruit/s.

Benady *et al.* [12] developed a fruit ripeness sensor, based on electronic sensing of aromatic and nonaromatic volatiles. Their sensor utilized a commercially available semiconductor gas detector ('Figaro' gas sensor TGS 822), which is positioned within a small cap that is placed on the fruit surface. Natural gases emitted by the ripening fruit accumulate in the cup and cause a change in the conductivity of the sensor, which is measured by a computer-based data acquisition system. The changes in the electrical resistance were shown to be directly related to total concentration of aromatic volatiles as measured by gas chromatography and verified by GC/Mass Spectrometry (Benady *et al.* [11]. Ethylene is only one of the volatiles measured by the sensor. Measurements on muskmelons indicated that, while ethylene production decreased as the melons went from half-ripe to full-ripe and then to over-ripe, the total emission rate of aromatic volatiles continued to increase. In laboratory tests using the semiconductor sensor, classification into ripe or unripe categories was successful 90.2% of the time (2-way classification), while a success rate of 83% was achieved for sorting into three ripeness classes (unripe, half-ripe and ripe fruit). Fruits were sampled for one second, followed by an approximately equal delay time for desorption before evaluation of the next sample. The sensor was also tested under ambient conditions in the field on melon fruit growing on the vine, with temperatures ranging from 18 to 41^{0}C, and relative humidities ranging from 37 to 85%. Classification accuracies of fruit under these conditions were 88% and 78.3% for 2-way and 3-way classification, respectively [12]. The conclusions from their research was that the comparison of their sniffer performance with traditional analytical methods of ripeness determination demonstrated that it was better than all other parameters, both destructive and nondestructive and hence presents a highly feasible technique for nondestructive sampling of fruit ripeness. The researchers indicated that with a planned future prototype, they expect to be able to measure volatiles from an individual fruit in a fraction of a second, while separating ripe and over-ripe fruit and classification into four ripeness stages.

In a recent work in Spain, an aroma sensor was developed for assessing peach quality [59]. Two commercially available transducers were originally considered for incorporation in a dedicated instrument. The gas detector was based on infrared technology Polytron IR Ex from DGER and semiconductor gas transducers. The infrared transducer was not able to detect low concentrations of the emission of G and D Decalactones, which were found to correlate well along the ripening process of peaches, and hence, this apparatus was discarded. The semiconductors, on the

other hand, were able to detect even low concentrations of decalactones and have a better response time than the infrared system and, therefore, were incorporated in the dedicated sensor. The results with two versions of the sensor have indicated that it was possible to classify the peaches in two categories, comparing the sensor output with peach quality parameters (color, firmness, estimated maturity). This classification was obtained with a 75-85% success rate. The sensors were able to detect skin breakage produced by physical or microbiological causes and showed a good correlation with firmness measurements using a penetrometer. However, no correlation was found with sugar levels measured in ^{0}brix. While the researchers suggested that the proposed method has good possibilities for a nondestructive fruit quality evaluation, they have, nevertheless, cited the relatively long response time as the current major drawback.

Some reports were also obtained from industry ('Neotronics Scientific Inc. in Georgia, USA), describing the utilization of an «Electronic Nose», based on a plug-in sensor modules of a range of sensor types - conducting polymers, metal oxides, resonant type, for the discrimination of tomato and raspberry varieties and the determination of tomato freshness, based on the difference in their olfactory response.

A joint research group of Purdue University, IN in the US and the Institute of Agricultural Engineering in Israel, have completed recently 3 years of research, funded by the US-Israel Bi-National Fund for Research and Development in Agriculture (BARD). In this research, the issue of electronic sensing of fruit ripeness based on volatile gas emissions was studied. The researchers reported on two prototype systems which were designed, constructed, modified and tested, for the determination of fruit ripeness. The first was based on a single head sensing unit for use as a single or paired unit placed on an individual fruit surface for application in the field, laboratory, or industry. The second electronic sniffer utilized a matrix of gas sensors, each selected for different sensitivity to a range of volatile compounds. The second sniffer was designed for sampling fresh-cut or whole packs of fruits, such as packaged strawberries and blueberries. The researchers claim to have used successfully the aroma sensing for classifying ripeness in different cultivars of muskmelons, apples, blueberries, strawberries and tomatoes.

Utilization of an electronic nose for specific applications in agriculture is currently also being studied at CEMAGREF in Montpellier, France.

A quite unique application has been reported by NCR Co. in Ohio, based on a recently obtained patent for an olfactory sensor identification system for rapidly identifying fruits and vegetables by their aroma. The object (fruit) to be identified is placed in close proximity to the testing chamber. The air pressure within the testing chamber is then lowered below ambient, thereby causing ambient air to flow past the object being identified and into the testing chamber. As air flows past the object being identified, the aroma of the object becomes mixed with the air and is carried into the testing chamber. Once within the testing chamber, the aroma/air mixture is

exposed to an array of gas sensors. The gas sensors detect the levels of various gases comprising the aroma/air mixture and produce a sensor pattern capable of being identified using pattern recognition techniques. The company plans to use this system to automatically ring up prices of fruits and vegetables at the supermarket, or green grocer check-out - identifying them by their smell.

Conclusion

The control of food quality and the ability to determine ripeness of fruit and/or its freshness, are of prime interest for both the consumer and the food industry. A non-destructive approach is desirable, which correlates information available outside the product with its stage of ripeness [86]. Various nondestructive techniques are already available (such as, sonic, ultrasonic, tactile, UV, IR, NIR), but their use is limited to certain produce items only, and most of them are not suitable for use in the form of a portable field instrument. The characterization of typical odors of specific compounds in the gas phase ('headspace') of food, or fresh fruits and vegetables, also represents another possible nondestructive approach.

The human olfactory system is inferior, as compared with that of other mammals, or with other human sensing characteristics. Nevertheless, it has been (and still is) utilized extensively for a wide range of applications, from comparing the effectiveness of deodorants, distinguishing authentic perfumes from artificial aromas, grading the quality of fish and authentication of wines, to its utilization in the diversified food industry. While the human nose is, remarkably, able to discriminate between a whole range of odorants, it is subjective, qualitative by nature and would be impractical for an on-line applications. Recent developments, both in microelectronics and in data processing, utilizing advanced sensing and pattern recognition and artificial network techniques, may eventually replace the human nose in many applications. Two different concepts may be applied in the analysis of odors: the detection of specific compounds with highly selective sensors, or the characterization of different odors by patterns generated with sensor arrays, using sensor elements with partly overlapping selectivities. Examples for the latter method have already been published in the literature and include the characterization of tea, coffee, grain freshness and tobaccos [33, 34, 72, 73, 81, 82].

An alternative concept is based on the knowledge of volatile compounds. For their detection, a sensor, or a sensor array, can be designed. This approach has been utilized in the study of meat and fish freshness [80].

While several proposed «artificial noses» are already employed commercially, there is not a universal nose at present that can solve all odor-sensing problems, or effectively respond selectively and sensitively to specific gases at an appropriate temperature. Many of the more advanced techniques need further development to improve their sensitivity, selectivity and time of response and be adapted to

commercial scale which allows reproducibility in sensor production. Other problems, such as eliminating drift because of aging, decreasing cost of production and better versatility, need to be addressed before commercialization can be realized.

Especially for the problem cited, we need to develop application-specific electronic nose (ASEN) technology appropriate to the specific need. This means developing dedicated sensor structures, appropriate sensor materials and appropriate pattern-recognition (PARC) methods. Moreover, for agricultural applications it is highly desirable to have a portable, field instrument, hence adding to the complexity of the design. Thus, the application cannot be divorced from the instrumentation. Based on the conclusion drawn by Gardner and Bartlet [32], it is not surprising that no applications have been cited, so far, for utilizing the olfaction characteristics of fruits and vegetables *in situ*. With the need for more nondestructive quality evaluation techniques on one hand, and the continuing progress in the development of the technology on the other, an appropriate technique should therefore be developed also for the cited problem. More work is needed before such an application could be realized, especially for the difficult case of a needed, portable, field apparatus for *in situ* sensing of volatiles emanating from fruits and vegetables. These difficulties are augmented by the broad range of factors that may effect the nature and concentration of the volatiles, such as growing conditions, fertigation schemes, climatic and soil conditions, which in addition may vary, yearly, from place to place. Several research centers, worldwide are working at present on the general subject of odor sensing and they are bound to yield some practical results in the near future. Nevertheless, with all the gamut of the available results of past and present work, no commercial instrument, or even current research could be cited, related directly to the specific application of the olfactory characteristics of fruit and vegetable as a quality attribute. Hence, the need exists for a dedicated future research, working in concert with plant physiologists, plant breeders, postharvest physiologists and biochemists, to ensure a meaningful application of the sensing attribute to the cited problem and in accordance to the way the consumer perceives quality characteristics.

Finally, although the stated problem relates to a specific application for nondestructive quality evaluation of fruits and vegetables, the instrument envisioned for the future could lend itself also to a multitude of other applications. These may include gaseous sensing in fields such as, food processing, medicine/body functions both, in humans and animals, environmental toxins and pollutants, detection of plant diseases and insects effects, toxicology, space and military environment. These additional important applications should provide another incentive for the development of the system desired.

References

[1] Abe, H., Yoshimura, T., Kanaya, S., Takahashi, Y. and Sasaki, S. 1988. Extended studies of the automated odor-sensing system based on plural semiconductor gas sensors with computerized pattern recognition techniques. *Anal. Chim. Acta, 215:155-168.*

[2] Adolfsson, M., Brogardth, T., Goransson, S. and Ovren, C. 1985. *Fiber optical measuring device, employing a sensor material with a non-linear intensity response characteristic for measuring physical quantities.* US Patent No. 4498004.

[3] Adrian, P. 1991. *New developments in chemical/gas sensing.* Part I: Tin oxides. Sensors 8(13).

[4] Amoore, J.E., Johnson, J.W. and Rubin, M. 1964. The stereochemical theory of odor. *Scientific American 210:42-49.*

[5] Anholt, R.R.H. 1992. *Molecular aspects of olfaction.* In: Serby and Chober (Eds.) Science of Olfaction. Springer-Verlag Publ. New York, N.Y.

[6] Arn, D., Amati, D., Blom, N., Ehrat, M. and Widmer, H.M. 1996. *Surface acoustic wave gas sensors: developments in the chemical industry.* Sensors and Actuators B, 8:27-31.

[7] Bartera, R.E. 1975. *Multiple crystal oscillator measuring apparatus.* US Patent No. 3879992.

[8] Bartlet, P.N. and Gardner, J.W. 1992. *Odour sensors for an electronic nose.* In: Sensors and Sensory Systems for an Electronic Nose. (Gardner and Bartlett, Eds.), Kluwer Academic Publ. Dordrecht, UK.

[9] Beets, M.G.J. 1970. *The molecular parameters of olfactory response.* Pharmacol. Rev. 22:1-34.

[10] Beltzer, M. 1973. *Coated piezoelectric analyzers.* US Patent No. 3744296.

[11] Benady, M., Simon, J.E., Charles, D.J. and Miles, G.E. 1992. *Determining melon ripeness by analyzing headspace gas emissions.* ASAE Paper No. 92-6055, St. Joseph, MI.

[12] Benady, M., Simon, J.E., Charles, D.J. and Miles, G.E. 1995. *Fruit ripeness determination by electronic sensing of aromatic volatiles.* Trans. Amer. Soc. Agric. Engrs. 38(1):251-257.

[13] Bennett, T.L. 1978. *The sensory world. Brooks/Cole Publ.* Monterey, CA.

[14] Bliss, M.L. and Pratt, H.K. 1979. *Effect of ethylene, maturity and attachment to the parent plant on production of volatile compounds by muskmelons.* J. Am. Soc. Hort. Sci. 104(2):273-277.

[15] Bott, B. and Thorpe, S.C. 1991. *Metal phthalocyanine gas sensors. In: Techniques and Mechanisms in Gas Sensing* (Mosley, Norris and De Williams, Eds.) Adam Hilger Publ. Bristol, UK.

[16] Brown, G.K and Sarig, Y. (Eds.). 1993. *Nondestructive technologies for quality evaluation of fruits and vegetables.* Proc. Int. Workshop funded by the United States-Israel Binational Agricultural Research and Development Fund (BARD), Spokane, WA 15-19 June, 1993. ASAE Publ. 05-94.

[17] Burton, R. *The Language of Smell.* Routletdge & Keagan Publ. London, UK.

[18] Chachin, K. and Iwata, T. 1988. Physiological and compositional changes in 'Prince Melon' fruit during development and ripening. *Bull. Univ. Osaka Pref. Series B 40:27-35.*

[19] Chen, P. 1996. Quality evaluation technology for agricultural products. *Proc. Int. Conf. on Agric. Machinery. Nov 12-15, 1996, Seoul, South Korea. Vol I:171-204.*

[20] Coleman, J.R (Edit). 1990. Development of sensory systems in mammals. *John Wiley & Sons Publ.*

[21] Di Natale, C., Macagnano, A., Davide, F., D'Amico, A., Boschi, T., Faccio, M. nd Ferri, G. 1996. *An electronic nose for food analysis.* Proc. of the Eurosensors X Conference, Lueven, Belgium.

[22] Dodd, G.H., Bartlett, P.N. and Gardner, J.W. 1992. *Odours - the stimulus for an electronic nose.* In: Sensors and Sensory Systems for an Electronic Nose (Gardner, J.W. and Bartlett, P.N Eds.). Kluwer Academic Publ. the Netherlands.

[23] Durr, P. 1983. *Measuring sensory quality: assessing aroma by gas chromatography.* In: Sensory Quality in Food and Beverages: Definition, Measurement & Control. Ellis Horwood Ltd, Publ. Chichester, UK.

[24] Dyer, D.C. and Gardner, J.W. 1997. High-precision intelligent interface for a hybrid electronic nose. *Sensors & Actuators A, 62:724-728.*

[25] Ehara, K., Koizumi, T. and Wakabayashi, Y. 1988. *Method for measuring concentrations of odors and a device therefor.* US Patent No. 4770027.

[26] Elliot-Martin, R.J., Bartlett, P.N., Gardner, J.W. and Mottram, T.T. 1995. *An overview of electronic noses and their applications.* Sensors and their Applications VII, Inst. of Physics, Dublin, September, 1995.

[27] Erdi, P. and Barna, G. 1991. *Neurodynamic approach to odor processing.* Proc. 1991 Int. Joint Conf. on Neural Networks (IJCNN'91), 2:653-656.

[28] Frechette, M.W. and Fasching, J.L. 1978. *Piezoelectric probe for detection and measurement of gaseous pollutants.* US Patent No. 4111036.

[29] Fukui, K., Shigemori, T. and Ehara, K. 1991. *Smell sensing element and smell sensing device.* US Patent No. 5047214.

[30] Gardner, J.W. 1990. *Electronic nose development at Warwick.* Electronic Engineering, 62(764):15.

[31] Gardner, J.W. and Bartlett, P.N. 1991. *Pattern recognition in gas sensing.* in: Techniques and mechanisms in gas sensing. (Mosley, P.T., Norris, J. and Williams, D.E, Eds.) The Adam Hilger Series on Sensors, IOP Publ. UK.

[32] Gardner, J.W. and Bartlett, P.N. 1994. A brief history of electronic nose. *Sensors and Actuators B, 18-19: 211-220.*

[33] Gardner, J.W., Hines, E.L. and Wilkinson, M. 1990. *Applications of artificial neural networks in an electronic nose.* Meas. Sci. Technol. 1(5):446-451.

[34] Gardner, J.W., Pearce, T.C., Friel, S., Bartlett, P.N. and Blair, N. 1994. A multisensor system for the flavor monitoring using an array of conducting polymers and predictive classifiers. *Sensors and Actuators. B, Chemical; 18(1-3):240-243.*

[35] Gardner, J.W., Shurmer, H.V. and Tan, T.T. 1992. Application of an electronic nose to the discrimination of coffees. *Sensors and Actuators B, 6:71-75.*

[36] Graziadei, P.P. 1990. *Olfactory development.* In: Development of Sensory Systems in (Coleman, Edt.). John Wiley & Sons Publ. N.Y.

[37] Harman, J.E. 1987. Feijoa fruit: growth and chemical composition during development. *New Zealalnd J. of Exp. Agric. 15:209-215.*

[38] Hines, E.L. and Gardner, J.W. 1994. An artificial neural emulator for an odor sensor array. *Sensors and Actuators B, 18-19:661-664.*

[39] Horvat, R.J. and Senter, S.D. 1987. Identification of additional volatile compounds from cantalope. *J. Food Sci. 52(4):1097-1098.*

[40] Imisides, M., John, D. and Wallace, G.G. 1996. Microsensors based on conducting polymers. *Chemtech 26(5):19-25.*

[41] Iwanaga, S., Sato, N., Ikegami, A., Isogai, T., Noro, T. and Arima, H. 1984. *Gas detection device and method for detecting gas.* US Patent No. 4457161.

[42] Jellinek, Gisela. 1985. *Sensory evaluation of food.* Theory and Practice. Ellis Horwood Ltd. Publ. Chichester, UK.

[43] Jenkins, A. 1976. *Inspection apparatus.* US Patent No. 3942357.

[44] Jennings, W.G. 1969. *Chemistry of flavor.* Lebensm. Wiss. Technolo. 2:75.

[45] Kaneyasu, M., Ikegami, A., Arima, H. and Iwanaga, S. 1987. *Smell identification using thick film hybrid gas sensor.* IEEE Trans. Components, Hybrids, Manuf. Technol. **CHMT-10** 267-273.

[46] Keller, P.E., Kangas, L.J., Liden, L.H., Hashem, S. and Kouzes, R.T. 1995. *Electronic noses and their applications.* A paper presented at Neural Network Applications Studies Workshop in the IEEE Northcon/Technical Applications Conference (TAC '95). Portland, Oregon.

[47] Keller, P.E., Kouzes, R.T., Kangas, L.J. and Hashem, S. 1995. *Transmission of olfactory information for telemedicine.* A paper presented at the Medicine Meets Virtual Reality III, 19-22 January, 1995. San-Diego, CA.

[48] Kemp, T.R., Stoltz, L.P. and Knavel, D.E. 1972. Volatile components of muskmelon fruit. *J. Agric Food Chem. 20(2):196-198.*

[49] King, W.H. 1964. Piezoelectric sorption detector. *Anal. Chem, 36(9):1735-1739.*

[50] Kitamura, T., Umemoto, T., Iwata, T. and Akazawa, T. 1976. Studies on the storage of melons III. Varietal differences in the fluctuation of the amount of volatile constituents produced during ripening. *J. Japanese Soc. Hort. Sci. 44(4):417-421.*

[51] Lundsrom, I., Holmberg, M., Sundgren, H. and Winquist, F. 1994. Gas sensitive field effect devices in odor identification. Actes du Symposium: *Olfaction and Electronic Nose. September 1994, Toulouse, France, pp 5-13.*

[52] Lundstrom, I., Hedborg, E., Spetz, A., Sundgren, H. and Winquist, F. 1992. *Electronic noses based on field effect structures.* In: Sensors and Sensory Systems for an Electronic Nose (Gardner and Bartlett, Eds.), Kluwer Academic Publ., Dordrecht, The Netherlands.

[53] Macleod, P. 1994. Odour detection and recognition by human olfaction. A paper presented at a symposium on «Olfaction and Electronic Nose», *Toulouse, France September 1994. pp 1-2.*

[54] May, M. 1996. A scent circuit. *American Scientist 84(1):24-25.*

[55] McCartney, W. 1968. *Olfaction and odors.* Springer-Verlag Berlin. Heidelberg. New York.

[56] Meilgaard, D., Civille, G.V. and Carr, B.T. 1991. Sensory evaluation techniques. *Boca Raton CRC Press.*

[57] Meredith, M. 1992. *Neural circuit computation: complex patterns in the olfactory bulb. Brain Res., 29:111-117.*

[58] Miyazaki, T. and Ookubo, M. 1989. Effects of maturity and postharvest techniques on keeping quality of melons. *J. Japanese Soc. Hort. Sci. 58:361-368.*

[59] Molto, E., Selfa, E., Ferriz, J. and Conesa, E. 1996. *An aroma sensor for assessing peach quality.* Paper No. 96F-004, presented at the AgEng 96, Madrid, Spain.

[60] Moritzumi, T. 1988. Langmuir-Blodget films as chemical sensors. *Thin Solid Films. 160:413-429.*

[61] Moseley, P.T. and Tofield, B.C (Eds.) 1987. *Solid State Gas Sensors.* Adam Hilger Publ. Bristol, UK.

[62] Moulton, D.G. 1963. *Olfactory and taste.* Oxford: Pergamon Publ.

[63] Mozel, M.M. 1971. *Spatial and temporal patterning.* In: Beidler (Ed.) Handbook of Sensory Physiology. Springer-Verlag Publ. New York, N.Y.

[64] Nakamoto, T. and Moriizumi, T. 1988. Odor sensor using quartz-resonator array and neural-network pattern recognition. *Proc. IEEE Ultrasound. Symp., Chicago, IL pp. 613-616.*

[65] Nakamoto, T., Fekuda, A. and Moriizumi, T. 1993. Perfume and flavor identification by odor sensing system using quartz-resonator sensor array and neural-network pattern recognition. *Sensors and Actuators B, 10:85-90.*

[66] Nanto, H., Kawai, T., Sokooshi, H. and Usuda, T. 1993. Aroma identification using quartz-resonator in conjunction with pattern recognition. *Sensors and Actuators. B, 13-14:718-720.*

[67] Neaves, P.I. and Hatfield, J.V. 1995. A new generation of integrated electronic noses. *Sensors and Actuators B 26-27: 223-231.*

[68] Nieuwenhuisen, M.S. and Venema, A. 1989. Surface acoustic wave chemical sensors. *Sensors Mater., 1:261-300.*

[69] Nursten, H.E. 1977. *The important volatile flavor components of foods.* In: Sensory Properties of Foods (Birch *et al.*, Eds) . Applied Science Publ., Essex, UK.

[70] Okahata, Y. and Shimizu, O. 1987. Olfactory reception on a multilayer coated piezoelectric crystal in a gas phase. *Langmuir, 3:1771-1772.*

[71] Omahony, M. 1986. *Sensory evaluation of food.* New York Marcel Deckker, Inc.

[72] Pelosi, P. and Persaud, K. 1988. Sensors and sensory systems for advanced robots (NATO ASI SERIES Vol F42) *Ed. Pario, P. (Springer-Verlag, Berlin) pp 361-381.*

[73] Persaud, K.C., Khaffaf, S.M., Payne, J.S., Pisanelli, A.M., Lee, D.-H. and Byun, H.-G. 1996. Sensor array techniques for mimicking the mammalian olfactory system. *Sensors and Actuators, B 36(1-3):267-274.*

[74] Rothe, M. 1978. *Ein fuhrung in die Aromaforschung.* In: Handbuch der Aroma-forschung. Academie-Verlag, D.D.r-1000 Berlin.

[75] Roussel, Sylvie. 1996. *Synthese bibliographique sur les capteurs d'aromes.* mimeo, CEMAGREF, Montpellier, France.

[76] Sarig, Y. 1989. *Quality oriented nondestructive techniques for fruit and vegetable.* Proc. Int. Conf. on Agr. Engr. September, 1989, Beijing, China.

[77] Sarig, Y. and Beaumelle, D. 1993. *Preliminary experiments with an electronic sensor for measuring aromatic volatiles in fruits.* Unpublished mimeo, Institute of Agricultural Engineering, Bet Dagan Israel.

[78] Sato, T. and Hirono, J. 1996. *Method and apparatus for discriminating chemical/physical quantity based on the transient response.* US Patent No. 5541851.

[79] Schultens, H.A. and Schild, D. 1992. *Biophysical properties of olfactory receptor neurons.* In: Sensors and Sensory Systems for an Electronic Nose (Gardner, J.W. and Bartlett, P.N Eds.). Kluwer Academic Publ. the Netherlands.

[80] Schweizer-Berberich, P.M., Vaihinger, S. and Gopel, W. 1994. Characterization of food freshness with sensor arrays. *Sensors and Actuators B, 18-19:282-290.*

[81] Shurmer, H.V. 1990. The fifth sense: on the scent of the electronic nose. *IEE Review:95-98.*

[82] Shurmer, H.V. and Gardner, J.W. 1996. Odor discrimination with an electronic nose. *Sensors and Actuators, B 8:1-11.*

[83] Slater, J.M., Paynter, J. and Watt, E.J. 1993. Multi-layer conducting polymer gas sensor arrays for olfactory sensing. *Analyst: 118(4):379-384.*

[84] Stroshine, R. L., Dull, G.G., Abbot, J., Bellon, V., Beumelle, D., Benadi, M., Cavalieri, R., Chen, P., Forbus, W.R., Galili, N., Mizrach, A., Nelson, S., Sarig, Y., Slaughter, D., Simon, J.E. and Zion, B. 1993. Nondestructive sensing of internal composition. In: Nondestructive technologies for quality evaluation of fruits and vegetables. Proc. Int. Workshop of BARD. *ASAE Publ. 05-94.*

[85] Sundgren, H., Winquist, I., Lukkari, I. and Lundstrom, I. 1991. Artificial neural networks and gas sensor arrays: quantification of individual components in gas mixtures. *Meas. Sci. Technol., 2:464-469.*

[86] Taniguchi, Y., Yonehara, Y., Masuda, K., Hirakawa, Y. and Uemura, M. 1992. New approach for non-destructive sensing of fruit taste. Tech. Digest, 4th Int. Meet. *Chemical Sensors, Tokyo, Japan Sept. 13-17, 1992, pp 514-517.*

[87] Tofield, B.C. 1987. *State of the art and future prospects for solid state gas sensors.* In: Solid State Gas Sensors (Mosely, P.T. and Tofield, B.C. Eds.). Adam Hilger, Bristol.

[88] Trenkle, R.W., Mookherjee, B.D., Zampino, M.J., Wilson, R.A. and Patel, S.M. 1993. *Method and apparatus for simultaneously analyzing aroma emitted from the interior and exterior of living fruit.* US Patent No. 5269169.

[89] Williams, A.A. and Atkin, R.K. (Eds.). 1983. *Sensory Quality in Food and Beverages.* Definition, Measurements & Control. Ellis Horwood Ltd. Publ. Chichester, UK.

[90] Wohltjen, H. 1984. Mechanism of operation and design considerations for surface acoustic wave device vapor sensor. *Sensors and Actuators, 5:307-325.*

[91] Wright, R.H. 1982. The Sense of Smell. *CRC Press, Inc.*

[92] Yabumoto, K., Yamaguchi, M. and Jennings, W.G. 1978. Production of volatile compounds by muskmelon, *cucumis melo. Food Chemistry 3(1):7-16.*

Part 6

Measurements in animal based products

Ultrasonic muscle sample classification

Classification d'échantillons de muscles par ultrasons

S. Abou El Karam, P. Berge And J. Culioli
INRA, Station de Recherches sur la Viande, 63122 Saint Genès-Champanelle France.

Abstract: *Ultrasonic bovine muscle samples classification was achieved from ultrasonic data.*
On samples extracted from three muscles (Semimembranosus, Semitendinosus and Biceps Femoris), chemical composition and ultrasonic measurements were performed. The chemical parameters determined were: dry matter, lipids and collagen. The acoustic parameters measured for these samples were speed, attenuation and backscattering intensity, and were performed at different temperatures (5, 10, 20 and 30°C). The sample classifications according to two biological factors (castration and muscle type) were carried out from ultrasonic and chemical data. The classification results obtained from ultrasonic data (80% of TWC: Total of Well Classified) are better than those obtained by chemical dosages (over 70% of TWC). Certain ultrasonic parameters combinations resulted in 100% successful classifications.
Ultrasounds provide better classifications because they are not only sensitive to chemical information but also to physical properties. Furthermore, by varying the experimental conditions (temperatures, fibre muscle orientations) ultrasounds can provide new information about the samples studied.
Most of classification results were then related to samples chemical composition (dry matter, collagen and lipid contents). The classification results obtained are encouraging, and they show the potential of this ultrasonic technique to classify meat samples.

Keywords: *Speed, attenuation, backscattering, muscle tissue, tissue composition.*

Résumé : La classification de muscles de bœuf est réalisée à partir de données ultrasoniques.
Sur des échantillons extraits de 3 muscles (Semimembranosus, Semitendinosus et Biceps Femoris), la composition chimique est analysée et des mesures ultrasoniques sont menées. Les paramètres chimiques sont : matière sèche, lipide et collagène. Les paramètres acoustiques mesurés pour ces muscles, la vitesse l'atténuation et l'intensité rétrodiffusée, ont été mesurées à différentes températures (5, 10, 20 et 30°C). Les échantillons sont classés en fonction de 2 critères biologiques (la castration et du type de muscle) à partir des données chimiques et ultrasoniques. Les résultats de classification sont meilleurs pour les données ultrasoniques (80% de bon classement) que pour les données chimiques (plus de 70% de bon classement). La combinaison de certains paramètres donne une bonne classification de 100%.
Les ultrasons donnent une meilleure classification car ils ne sont pas seulement sensibles informations chimiques mais également aux informations physiques. De plus, en faisant varier les conditions expérimentales, les ultrasons apportent une information nouvelle sur les échantillons étudiés.
La plupart des résultats de classification sont reliés à la composition chimique. Les résultats de classification obtenus avec la technique ultrasonique montrent l'intérêt de cette méthode pour classer des échantillons de viande.

1. Introduction

Ultrasound is an effective technique to analyse physico-chemical properties of biological tissues. Such analysis is rapid, non destructive and non invasive. The ultrasonic equipment can be made portable, robust, and relatively inexpensive and suitable for industrial applications. Ultrasound has already been used to assess the fatness of live animals or that of carcasses; subcutaneous fat thickness and *Longissimus* muscle section area were measured for sheep, beef and pork grading [5, 8, 13]. To characterise correctly meat it is necessary to get information on chemical composition, constituent distribution and structure. The ultrasonic properties reflect aspects of some physical and chemical characteristics of the medium, and they can be helpful for meat characterisation. For this purpose, there are some useful analytical techniques based on the measurement of wave propagation velocity, ultrasonic backscattering intensity, or spectral analysis of an echographic signal [9, 11, 12, 14].

The aim of this study was to use acoustic parameters, such as the velocity of wave propagation, attenuation and backscattering intensity, in order to achieve classifications of various bovine muscles according to biological factors, such as castration and muscle type. These classifications were compared to those obtained with chemical data (dry matter, collagen and lipid contents). The chemical composition was also used to explain the results obtained with the acoustic parameters.

This study took into account meat anisotropy. The high variance explained is encouraging. Some groups were 100% successfully classified. Furthermore, we showed the effect and emphasised the importance of temperature variations.

2. Material and methods

Meat samples (7 x 5 x 4 cm) were taken from *Semitendinosus* (ST), *Semimembranosus* (SM) and *Biceps femoris* (BF) muscles from eight 16-month-old Montbéliard bovines. The samples were vacuum-packed and placed in a temperature controlled water tank that composed the ultrasonic bench. Ultrasonic transducers (5 MHz) were used to scan the samples. The motors, the emitter-receiver generator connected to transducers, the signal acquisition and treatment were computer controlled.

Meat anisotropy was taken into account analysing the samples with their fibres both orthogonal and parallel to the direction of the wave propagation. The experiment was performed at 5, 10, 20 and 30°C.

The ultrasonic beam scanned a 20 x 20 mm region of interest (ROI) in two orthogonal directions (x and y) with a 1 mm step, and 20 planes of 20 lines were obtained, corresponding to 400 equidistant points.

Velocity (m/s), attenuation ($dB.MHz^{-1}.cm^{-1}$) and backscattering intensity (homogeneous to the squared amplitude) were measured for each of the 400 sounding points of the ROI.

The Bergman and Loxley (1963) method was used to determine the collagen (hydroxyproline) content in samples; the Arneth method (1972) for intramuscular lipid content. After oven drying at 105°C for 24 hours, the content in dry matter was measured.

Variance and discriminant analyses were achieved using the SAS software (6.11 Version). Two factors were tested: castration and muscle type.

3. Results and discussion

3.1 Global results

Some global results previously presented in [15] are recalled below. The classifications of meat samples according to biological factors (castration, muscle type and animal age) are global and take into account animals aged 4, 8, 12 and 16 months.

	Castration factor	Muscle factor	Age factor
Ultrasonic parameters	78 %	78 %	88 %
Chemical parameters	64 %	73 %	58 %

Table 1: Comparison of total correctly classified samples using ultrasonic or chemical data

Table 1 gives a comparison of the classifications obtained with ultrasonic and chemical data. As we can see, the ultrasonic data gave higher scores than chemical data for castration, muscle and age factors. This result could be expected since chemical assays provide information on sample composition only, whereas ultrasonic measurements also give information on its physical properties, *i.e.* spatial distribution of the constituents, tissue structure or its mechanical properties.

Globally, the classification results obtained are interesting but not fully satisfactory, particularly in regard to chemical data. This is probably due to the low variation and a large overlap of the sample composition values. The age classes are not clearly distinguished probably because the range of animal ages was small, particularly for the classes 4, 8 and 12 months. These results should be improved by focusing on a particular age class.

3.2 16-month age class results

In the following, only the results of 16-month-old animals will be presented. The meat from these animals is more comparable to that commercially available. Furthermore, this restriction allows a more detailed study of this sample population.

3.2.1 Chemical composition

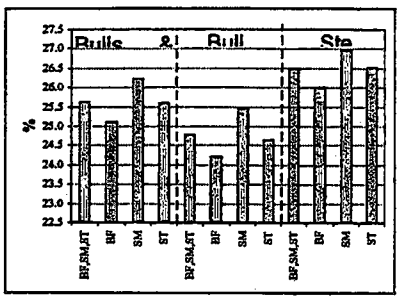

Figure A: Dry matter

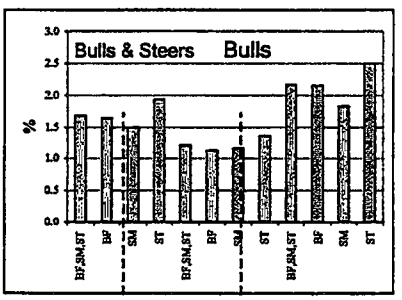

Figure B: Lipid content

Figures A, B and C present the values of chemical composition and show averaged values for bulls and steers, separately and together for each of the three parameters (dry matter (DM), lipids and hydroxyproline (HyPro)). Bulls and steers clearly differed in dry matter and lipid contents but not in collagen content which varied between muscles. One should note that the variations in amount of dry matter content are related those of lipids.

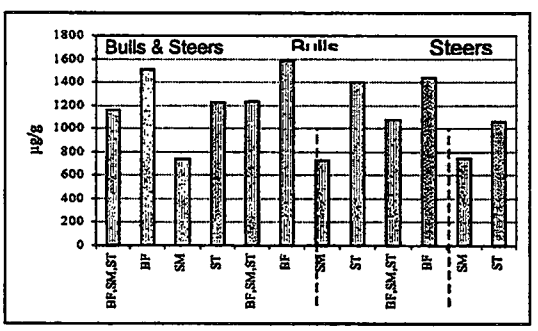

Figure C: Hydroxyproline content

3.2.2 *Analysis of variance*

Statistical tests were performed on these chemical data, and the results are given in the following table:

Castration	F ratio	Steer	Bull	rsd
DM (%)	30.13 ***	26.5 A	24.8 B	0.76
Lipids (%)	20.2 ***	2.2 A	1.2 B	0.52
HyPro. (µg/g)	3.68	1082	1239	201

*Table 2: Anova for castration factor. (***: P<0.0001)*

Muscle	F ratio	SM	ST	BF	rsd
DM (%)	4.19 *	26.2 A	25.6 BA	25.1 B	0.76
Lipids (%)	1.48	1.5 A	1.9 A	1.6 A	0.52
HyPro. (µg/g)	29.96 ***	741 C	1230 B	1510 A	201

Table 3: Anova for muscle factor. (: P<0.05, ***: P<0.0001)*

As shown in Tables 2 and 3, castration directly influenced dry matter and lipid contents and muscle significantly influenced collagen content (hydroxyproline).

Table 2 shows that the dry matter and lipid contents are highly significantly influenced by the castration. From these two measurements we can expect a good classification of bulls and steers. On the contrary, no significant difference is provided by collagen for this factor.

In Table 3, regarding muscle, only collagen gave a high F ratio (P<0.0001). The HyPro content in each muscle was significantly different from that in the two other muscles. The F ratio was much lower but still significant with DM; lipid content was not significantly different between the three muscles. Thus, collagen measurement is expected to provide a good classification according to muscle type.

3.2.3 *Classification results*

In order to understand how classification by discriminant analysis could be influenced, different combinations of chemical (Figure 5) and ultrasonic (Figure 6) parameters were tested.

3.2.3.1 Classification with chemical data

Figure 5 shows the total percentage of well classified samples according to muscle and castration. The classifications were performed using different combinations of chemical parameters. Some combinations did not improve the classifications: for example [DM] or [DM & Col.] gave the same result (88%) for castration.

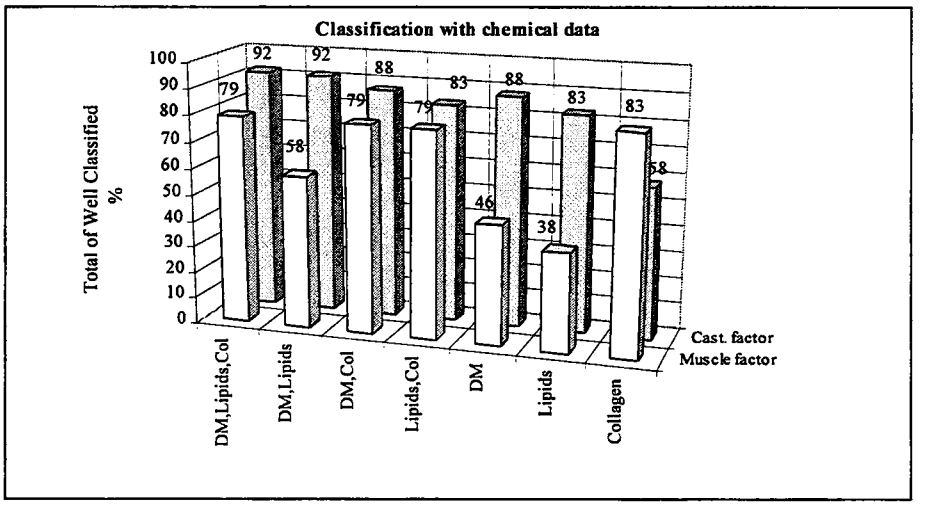

Figure 5: Total of Well Classified samples according to muscle and castration factors with different chemical parameters DM (Dry Matter), Lipids, Collagen (Col.) and their combination

On the chemical parameter basis, it was not possible to discriminate completely the samples according to castration or muscle. Using the three variables, only 92% of samples for castration and 79% for muscle were correctly classified. Dry matter and lipid contents were well suited to classify samples according to castration with 88% and 83% respectively. Collagen seems to be more suitable for muscle classification with 83% correctly classified samples (Figure 5).

3.2.3.2 Classifications with ultrasonic data

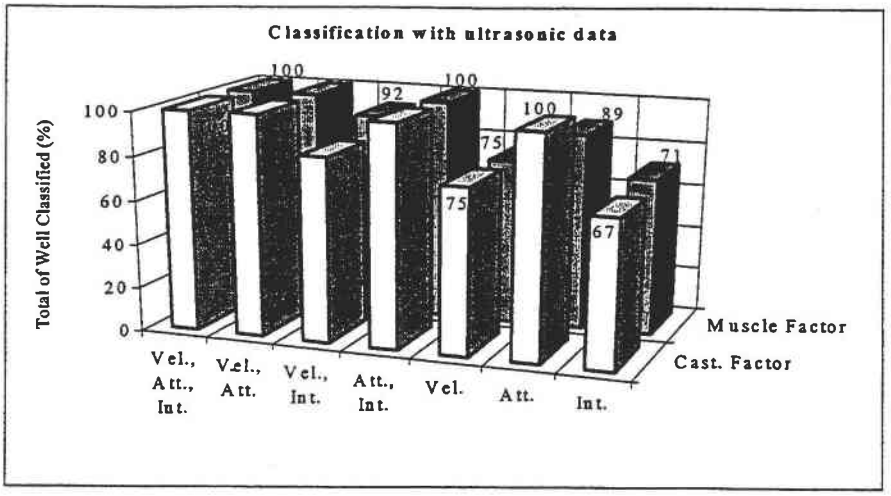

Figure 6: Total of Well Classified samples with different combinations of ultrasonic parameters according to muscle and castration factors. With: Vel.: Velocity, Att.: Attenuation, Int.: Intensity

Figure 6 shows the total percentage of well classified samples according to age and castration obtained with different combinations of ultrasonic data. As we can see, some of them gave the perfect (100%) classification ([Vel., Att., Int.]; [Vel., Att.]; [Att., Int.]).

Overall, the percentages of well classified samples were higher using ultrasonic variables individually than using the chemical assays either individually or combined. This is due to the number of parameters used in this experiment: there were more values taken for ultrasonic parameters compared to the three chemical ones. Indeed, new partially correlated acoustical values can be generated by varying the temperature, and, by choosing relevant temperatures, new independent values can then be produced. Moreover, taking into account muscle fibre orientation (anisotropy), further values are obtained. In this way, eight values were determined for each ultrasonic parameter.

In order to simplify the discussion, only the individual variables Velocity, Attenuation, backscattering Intensity and their combination [Vel., Att., Int.] will be considered. Figure 6 presents results that are more detailed in Figures 7 to 14 which show the sample classification distribution. These figures show how samples were classified according to the two biological factors, and to explain the ultrasonic classifications in terms of chemical composition.

Velocity, Attenuation and Intensity combined:

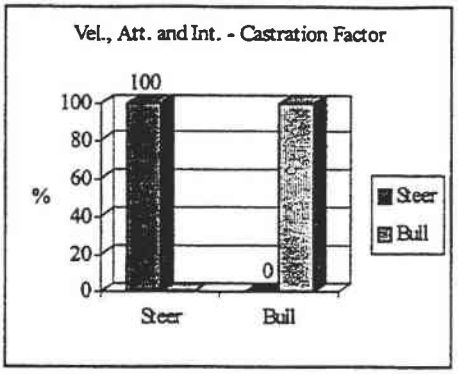

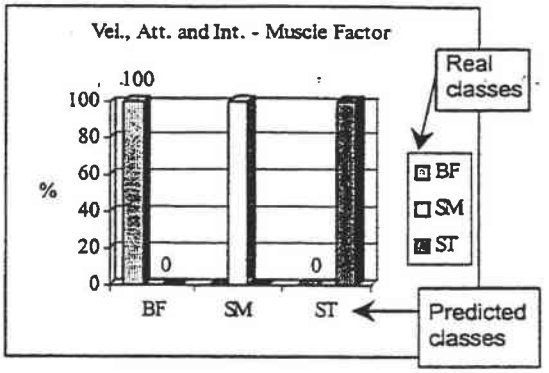

Figure 7: Total of Well classified: 100%

Figure 8: TWC: 100%

A combination of the three parameters gave a perfect classification, *i.e.* the score of 100% is obtained for both factors (Figures 7 and 8). Chemical data gave 92% and 79% respectively for castration and muscle factors, of total well classified samples (Figure 5).

The three ultrasonic parameters correctly classified the samples and we now consider each of them individually.

Velocity:

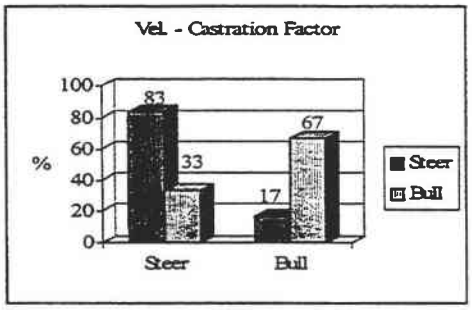

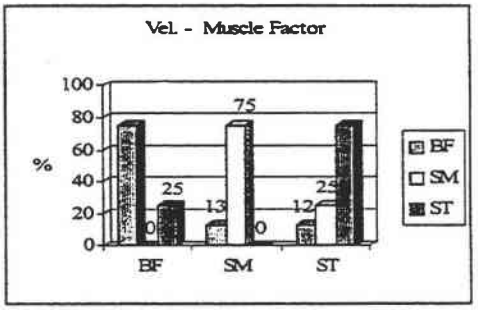

Figure 9: TWC: 75%

Figure 10: TWC: 75%

With velocity, as it could be expected using only one parameter (Figures 9 and 10), the number of correct classifications is lower than previously, and reached 75% for both factors. Steers were much better classified (83%) than bulls (67%). This could be due to the composition in collagen: the only significant difference existing between steer and bull samples was for the ST muscle; thus, the confusion of bull with steer samples is probably due to BF and SM muscles.

Attenuation:

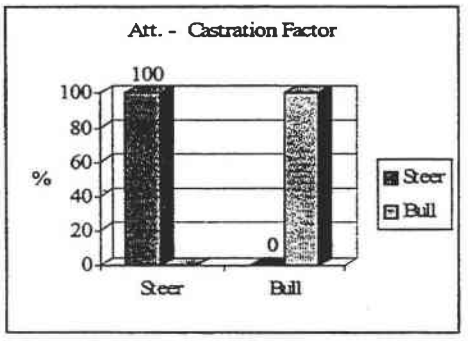

Figure 11: TWC: 100%

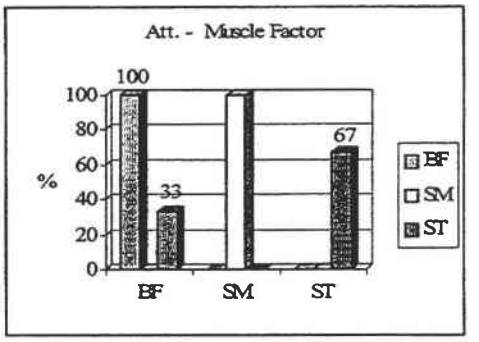

Figure 12: TWC: 89%

As shown in Figures 11 and 12, attenuation gave better classifications than velocity: all the samples were correctly classified for castration and 89% for muscle. BF and SM muscle samples were classified at 100%; whereas ST muscle only at 67%. 33% of ST samples were classified as BF samples. This was due to the small difference in collagen content between some ST and BF samples.

The classification with attenuation only (see Figure 11) was 100% for both bulls and steers. This result can only be explained by DM and lipid components. The main difference between bulls and steers was found in their dry matter content and, to a lesser extent, in lipids (Table 2).

Since bulls and steers differed in dry matter and lipid, and muscles were differentiated by collagen, the attenuation was expected to be correlated with these chemical measures. But correlation coefficients (results non presented here) between attenuation and dry matter or lipids were surprisingly very low ($r \leq 0.2$). This lack of correlation can be explained by the small variation in sample composition. Another reason could be related to the variability in composition that exists within each sample. Since, due to experimental conditions, chemical determination and ultrasonic measurements were performed on different muscle subsamples, these chemical data must be considered as a trend of sample composition, rather than as their precise composition.

Intensity:

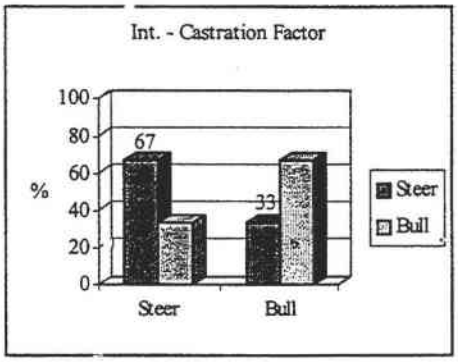

Figure 13: TWC: 67%

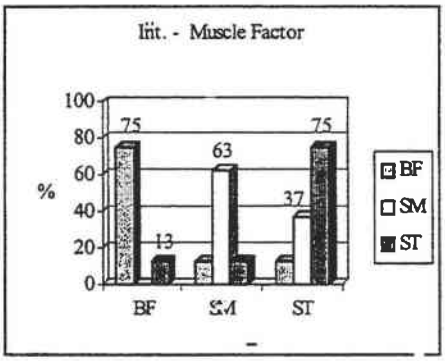

Figure 14: TWC: 71%

Backscattering Intensity parameter gave the lowest scores: 67% and 71% correct classifications respectively for castration and muscle (Figures 13 and 14). No clear relationship could be established between intensity classifications and chemical composition. This parameter is probably not directly related to the sample chemical composition, but to its structure and mechanical properties.

Conclusion

We showed that the ultrasonic method used can provide a good classification of meat samples from different biological origins, despite the low correlation between chemical and ultrasonic variables and the small range of variation in chemical composition.

Almost all classifications were explained by variations in chemical composition.
The better score obtained with ultrasound, compared to chemical data, is due to the fact that ultrasonic waves are not only sensitive to chemical composition but also to physical properties. Moreover, the number of ultrasonic parameters used was greater than the number of chemical ones.

The physical properties of a medium depend on its temperature, and ultrasound can provide new information at each new temperature. Thus, for a single sample and by varying experimental conditions (different temperature and muscle fibre orientation), several acoustical values can be determined. This can be very useful for sample characterisation.

Acknowledgements

The authors thank Lénaïck Jehannin and Ch. Suchorski for their helpful assistance, J.F. Martin and Christine Viallon for their help in the statistical treatment, R.

Fournier and C. Damergi for the chemical analyses. This work has been supported by the European Union (AIR project CT96-1107).

References

[1] S. Abou El Karam, B. Buquet, P. Berge, J. Culioli, 1997. Ultrasonic characterization of bovine muscles. *In Proceedings of the 43rd ICOMST, pp. 310-311,*

[2] W. Arneth, 1972. Uber die refraktometrische schellfettbestimmung nach rudisher in fleisch und fleischwaren. *Fleischwirtsch, vol.52, pp.1455-1458.*

[3] Bergman, R. Loxley. Two improved and simplified methods for the spectrophotometric determination of hydroxyproline. *Anal. Chem., vol.35, pp.1961-1965, 1963.*

[4] J.R. Brethour, 1990. Relationship of ultrasound speckel to marbling score in cattle. *J. Anim. Sci., vol. 68, pp. 2603-2613.*

[5] J.W. Edwards, R.C. Cannell, R.P. Garrett, J.W. Savell, H.R. Cross and M.T. Longnecker, 1989. Using ultrasound, linear measurements and live fat thickness estimates to determine the carcass composition of market lambs. *J. Anim. Sci.*, vol. 67, pp. 3322.

[6] X. Fernandez, G. Monin, J. Culioli, I. Legrand and Y. Quilichini, 1996. Effect of duration of feed withdrawal and transportation time on muscle characteristics and quality in Friesian Holstein calves. *J. Anim. Sci., vol. 74, pp. 1576-1583.*

[7] D. Julian Mc Clements, 1997. Ultrasonic characterization of foods and drinks: principles, methods and applications. *Critical Reviews in Food Science and Nutrition, vol. 37, pp. 1-46.*

[8] D.G. McLaren, D.F. Novakofski, L.L. Parett, S.D. Singh, K.R. Neumann, F.K. Mc Keith, 1991. A study of operator effects on ultrasonic measures of fat depth and longissimus muscle area in Cattle, sheep and pig. *J. Anim. Sci., vol. 69, pp. 54-66.*

[9] C.A. Miles, A.V. Fisher, G.A.J. Fursey, S.J. Page, 1987. Estimating beef carcass composition using the speed of ultrasound. *Meat Science, vol. 21, pp. 175-188.*

[10] C.A. Miles, G.A.J. Fursey, S.J. Page and A.V. Fisher, 1990. Progress towards using the speed of ultrasound for beef leanness classification. *Meat Science, vol. 28, pp. 119-130.*

[11] B. Park, A.D. Whittaker, R.K. Miller, D.S. Hale. Ultrasonic spectral analysis for beef sensory attributes. *J. Food Science*, vol. 59, pp. 697-701 & 724, 1994.

[12] B. Park, Y.R. Chen, 1997. Ultrasonic shear wave characterization in beef longissimus muscle. *Transactions of the ASAE, vol. 40, pp. 229-235.*

[13] C.A. Terry, J.W. Savell, H.A. Recio and H.R. Cross, 1989. Using ultrasound technology to predict pork carcass composition. *J. Anim. Sci., vol. 67, pp. 1279.*

[14] A.D. Whittaker, B. Park, B.R. Thane, R.K. Miller, J.W. Savell, 1992. Principles of ultrasound and measurement of intramuscular fat. *J. Anim. Sci., vol. 70, pp. 942-952.*

[15] S. Abou El Karam, P. Berge, J. Culioli. Application of Ultrasonic Data to Classify Bovine Muscles. *Proceedings IEEE 97*, Toronto 1997.

Use of ultrasound reflection for fresh hams classification

Utilisation de la réflexion des ultrasons pour classer la viande de jambon

Myriam CHANET

Cemagref, Division Qualité de l'agriculture et de l'alimentation
24 avenue des Landais, BP 50085, 63172 Aubière cedex 1, France
e-mail : myriam.chanet@cemagref.fr

Abstract: *One of the criteria of classification of fresh hams is the thickness of subcutaneous fat. At Fleury-Michon's company, this classification is achieved by an operator who estimates the fatness of the ham on the cut. We propose to replace this visual appraisal by ultrasonic measurements.*

Keywords: *Ultrasound, fresh ham, classification*

Résumé : Un des critères de classification des jambons frais est l'épaisseur de gras sous cutanée. Chez Fleury-Michon, cette classification est effectuée par un opérateur qui estime la quantité d'un gras d'un jambon sur la tranche. Nous proposons de remplacer cette appréciation visuelle par des mesures ultrasoniques.

1. Introduction

The sorting of hams at delivery is an important stage for the meat product processing companies. The fat thickness is one of the checked parameters in addition to pH, temperature or even the colour of the meat. It is often appraised visually [1].

Devices already exist for the measurement of fat thickness, but they are often invasive [2]. We propose to develop a non invasive and fast system which would be based on ultrasound wave propagation.

1.1 Sorting of hams at delivery

The hams processed in the Pouzauges factory of the Fleury-Michon company are sorted, at the time of acceptance, in terms of four criteria: weight, pH, state of surface (appearance) and thickness of subcutaneous fat. As a function of these criteria, the hams will supply various production lines.

As far as the fat thickness is concerned, three classes are kept: strictly inferior to 12 mm corresponding to the class 1, from 12 to 20 mm corresponding to the class 2, and strictly superior to 20 mm corresponding to the class 3. The price paid to the supplier depends among other things on this grading.

1.2 Currently used means

Since September 1990, the Pouzauges factory has been equipped with a partly automatized sorting line. The hams are displayed flat on their lateral side (rind side) on a roller conveyor by a worker who appreciates at this time the state of surface. A second worker sets the pH probe on a ham, the measurement being acquired by the computer. Simultaneously, he visually estimates the fat thickness of the next ham, before entering on keyboard the corresponding grading and the appearance mark (in function more particularly of the state of surface) previously announced by the first operator. Then, the weighing is automatically carried out by a weighing section of the conveyor connected to the computer.

The computer orders an automatic sorting system which distributes the hams into compartments as a function of the above parameters. The whole works at a rate of 1000 to 1200 hams/hour.

In case of contentious matter with a supplier, the fat thickness is measured with a ruler on the cut at the vertical of the thighbone, the ham being laid on its middle side, like the ham on figure 1.

1.3 Expressed need

We notice in what precedes that the appearance of surface and the fat thickness of the ham are visually assessed by two operators, one of them carrying out nearly simultaneously three different tasks: positioning the pH probe, estimating the thickness and entering data with the keyboard.

Our aim is to achieve a grading according to the fat thickness which would be objective, that is to say independent from the operator. Thus we would suppress, or at least considerably reduce, the number of grading errors, which may result in contentious matters or in downgradings, due to a difference of appreciation between the sorting line operator and the one who controls the supplying of hams on processing lines.

The uncertainty of the measurement must be inferior to the one attributed to visual evaluation, that is to say $\pm$ 1 mm.

1.4 Principle of the proposed measurement

The principle of the proposed measurement consists in using one or several subcutaneous fat thickness measurements by ultrasound reflection, that is to say by measurement of the time delay between the emission of an ultrasound signal and the reception of the echo returned by the interface between adipose tissue and muscle tissue, the ultrasound wave propagation velocity in adipose tissues being known (this speed depends on the tissues temperature). This echo results from the difference between the respective acoustical impedances of the tissues: one part of the energy of the incident wave is reflected and one part of this energy is transmitted.

1.5 Objective of the experiments

The experiments which are further described had as aims:

- to study the correlation between the ultrasound measurements and the visual appraisal currently in operation;
- to test the accuracy of this measurement;
- to compare this measurement with the ruler measurement previously signalled.

They should allow to answer, among others, the following questions:

- must it be used, in order to get the grading, one, two, even three sites of measures on each ham?

- Is it necessary to measure the temperature of the ham or can one use an average temperature and so an average propagation velocity?

- since the ultrasounds are not propagated in the air at the used frequency, is the use of water as a coupling element between ham and transducer necessary and efficient?

2. Development of the experiments

2.1 Notations

The notations used in this paper are given in table 1.

Class 1	Corresponds to a subcutaneous fat thickness strictly inferior to 12 mm
Class 2	Corresponds to a subcutaneous fat thickness included between 12 mm and 20 mm
Class 3	Corresponds to a subcutaneous fat thickness strictly superior to 20 mm
R	Measurement of subcutaneous fat thickness with a ruler
ClassR	Class assigned by the ruler measurement
ClassO	Class assigned by the operator
ClassP	Class assigned by the ponderation equation of ultrasound measurements

Table 1: Notations

2.2 Products

The three sets of experiments have concerned samples of 100 hams for the first, 200 hams for the second, and at last 80 hams for the third one, therefore a total number of 380 hams. These samples should include a sufficient number of hams whose fat thickness should be near the two extreme values met in the usual supply of the company.

2.3 Measurements

2.3.1 Visual grading

The 300 hams of the two first samples have been treated on the sorting line according to the usual protocol, and the whole of corresponding data, collected by the operator, has been supplied for data analysis. We finally used only the class assigned by the operator, noted ClassO.

The 80 hams of the last sample have been treated according to the usual protocol, but the class assigned by the operator has been immediately compared to that

assigned by ultrasound measurements, so as to find out the causes of the differences of grading stated during the two first sets of experiments.

2.3.2 *Measurement of temperature*

The measurement of the temperature of subcutaneous fat has also been achieved on each ham from the two first samples.

2.3.3 *Measurement with ruler*

On each ham, the measurement of fat thickness with the ruler, as it is practiced in case of commercial contentions, has been performed. From this measurement, noted R, we determine a "ruler" class (class 1: $R < 12$ mm, class 2: $12 \leq R \leq 20$ mm, class 3: $R > 20$ mm), noted ClassR.

2.3.4 *Ultrasound measurements*

The ultrasound measurements have been achieved in three sites, as shown on figure 1, slightly recessed from the cut: the site of the measurement with the ruler (site 2) and the two ends of the superficial layer of fat (sites 1 and 3). The reason is that the grading achieved by man results from a global visual evaluation of fat thickness at the cut. The ham lays on its medial side during the measurements.

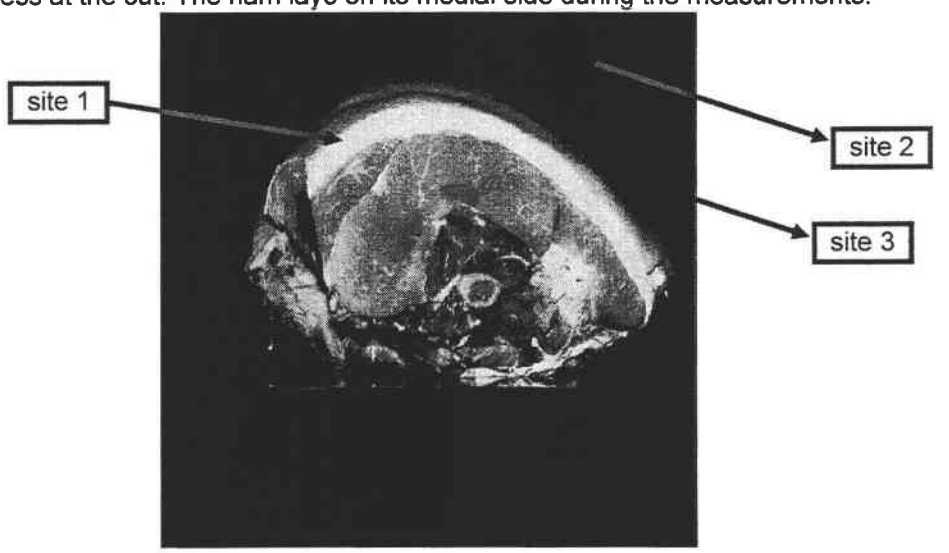

Figure 1: Sites of ultrasound measurements (photo Cemagref Rennes)

The calculation of thickness at the three sites of measurements has been done from the time taken by the signal to go from the transducer to the interface lean-fat

and to come back to the transducer, and from the ultrasound velocity in adipose tissue at the average measured temperature.

3. Results and discussion

3.1 Visual grading

Among the 380 hams, the visual grading gave 137 hams of class 1, 212 hams of class 2 and 31 hams of class 3.

3.2 Measurement of temperature

The data concerning the temperature allow to judge the necessity or not to introduce in the calculation of thickness a correction due to the variation of ultrasound velocity as a function of temperature.
The surveyed temperatures were varying from 2,6 °C to 5,2 °C. The study of the curve representing the velocity of ultrasound waves in adipose tissues as a function of temperature [3] has therefore led to use a constant mean value of the velocity of propagation: 1650 m/s.

3.3 Measurement with ruler

Among the 380 hams, ClassO and ClassR are different in 114 cases, distributed in the following way:

- for 86 hams ClassO is superior to ClassR: hams "over-graded" by the operator,
- for 28 hams ClassO is inferior to ClassR: hams "under-graded" by the operator.

The measurements with the ruler of the 28 "under-graded" hams are included between 12 and 14 mm (11 hams at 12 mm, 10 at 13 mm and 7 at 14 mm). These hams have been classed in class 2 by the measurement with the ruler and in class 1 by the operator. This can be summarised by the table 2.

R (in mm)	Number of concerned hams		ClassO	ClassR
12	11 (a)		1	2
13	10 (a)		1	2
14	7		1	2
	Total	28		

Table 2: "Under-graded" hams

These differences may be explained either by a nearly uniform fat thickness on the whole cut, or by thicknesses at sites 1 and 3 very inferior to that of site 2, which involves a grading in class 1 by the operator.

The 86 "over-graded" hams are distributed according to table 3.

R (in mm)	Number of concerned hams	ClassO	ClassR
7	1	2	1
8	3	2	1
9	4	2	1
9	1	3	1
10	33	2	1
11	20 (a)	2	1
12	3	3	2
13	4	3	2
14	5	3	2
15	3	3	2
17	2	3	2
18	5	3	2
20	2 (a)	3	2
	Total 86		

Table 3: "Over-graded" hams

These differences can probably be explained by a rather important fat thickness at sites 1 and 3 compared to site 2.

It must also be stated that the incertitude is ± 1 mm, so a ham whose measurement with the ruler is included between 11 and 13 mm, or 19 and 21 mm, can be over-graded or under-graded by the operator. It is the case of the 43 hams stated (a) in tables 2 and 3. This would bring the number of hams for which ClassO is equal to ClassR to 309 instead of 266.

Considering these two tables, we may ask whether the definition of grades only based on the measurement with the ruler is sufficient.

3.4 Ultrasound measurements

The measurements carried out at site 2 are directly compared to measurements carried out with ruler, so as to detect a possible systematic deviation between the two measurements, which could be due to a bias of one or the other method.

There is no systematic deviation between the measurement at site 2 and R. But a single measurement at site 2 is not sufficient to determine the grade of hams: ClassO is matched in 210 cases over 380, which can be explained at the same way that for the comparison between ClassO and ClassR. ClassR is matched in 236 cases over 380, which can be explained:

- either by the presence of two layers of subcutaneous fat at site 2: in this case, because of the characteristics of the transducer and the generator which are used (lack of power), it is likely that the echo returned by the interface between these two layers has been used for the measurement, the echo coming from the interface between fat and muscle being not detectable;

- or by the crushing of the cut or, in the case of two overlapping layers, by the withdrawal of the internal layer, hence a value of R less high than that of measurement at site 2.

We have therefore investigated the correlations between visual appraisal and the various possible combinations of ultrasound measurements, so as to seek the best compromise between reliability of results and convenience of measurements (linked especially to the number of sites and their position). A ponderation equation taking into account the three ultrasound measurements has allowed to define a class, noted ClassP, defined the same way as ClassR.

We have chosen to consider, first, the data of the 266 hams for which ClassO and ClassR are identical, so as not introduce a bias in the comparisons with the ultrasound measurements. The ponderation equation provides then the same grading as the visual appraisal in 199 cases over 266, that is to say 75%.
The 67 cases where ClassO is different from ClassP are given in table 4.

Number of concerned hams		ClassO	ClassP
12		1	2
49		2	1
6 (b)		3	2
Total	67		

Table 4: Unmatched cases

First we state that there are only deviations of one class. For 41 of these 67 cases, the thickness determined with the ponderation equation is equal to 12 mm ± 1 mm. Taking this tolerance in account, the percentage of correct grading is brought to 90% (instead of 75%). For the 6 cases referenced (b), the fat thickness was probably too big to be determine with the used apparatus.

When we consider the 380 hams, the equation of ponderation matches with the visual grading in 230 cases over 380 and the ruler-grading in 277 cases over 380. All the cases can be summarised in table 5.

	ClassP compared to ClassO			ClassP compared to ClassR		
	ClassP = ClassO	ClassP ≠ ClassO		ClassP = ClassR	ClassP ≠ ClassR	
		± 1 mm	other cases		± 1 mm	other cases
ClassO ≠ ClassR (114 hams)	31 (27%)	29 (26%)	54 (47%)	78 (69%)	23 (20%)	13 (11%)
ClassO = ClassR (266 hams)	199 (75%)	41 (15%)	26 (10%)	199 (75%)	41 (15%)	26 (10%)
Total	230 (61%)	70 (18%)	80 (21%)	277 (73%)	64 (17%)	39 (10%)
(380 hams)	300 (79%)		80 (21%)	341 (90%)		39 (10%)

Table 5: Summary

Conclusion

Taking in account the incertitude of ± 1 mm, the rate of matching of the grading achieved with ultrasound measurements with the visual grading is 79% (ClassP = ClassO of table 5) and with ruler grading 90% (ClassP = ClassR of table 5).

The 80 hams of the last sample have been classified using an ultrasonic device better adapted to the measurement than the one of the two first tests. If we only consider these 80 hams, the rate of success is 95% instead of 81%.

We can therefore plan to substitute the ultrasound measurements to visual appraisal. However various problems, due to the principle of measurement, can arise:

- the amplitude of the echo is too weak to be visible, because the thickness of fat is too high;

- several echoes are present resulting from two layers of fat or from a small thickness of fat which allows to get two echoes (or both reasons);

- it is not possible to distinguish the echo from the emission signal, because the thickness of fat is very weak;

- the parasitic echo due to the use of apparatus at a temperature of 5 °C must not be mistaken with the first echo of the interface.

The automatization and the industrialisation of the device need therefore the achievement of investigations and development for:

- the determination of the optimal characteristics of the transducer and of the generator allowing to solve the above mentioned problems;

- and the automatic determination of the position of the echo due to the interface fat-lean in the ultrasound signal.

It will be necessary to take into account a few constraints of implementation:

- need to make three measurements by ham,
- need to achieve a coupling with water,
- achievement of measurements in a duration consistent with the hourly rate (1 000 to 1 200 hams/hour).

This step of industrialisation needs therefore that the skills and the means of development of an equipment manufacturer will be added to those of the initial partners.

Acknowledgements

The author wishes to thank the Fleury-Michon company and more particularly Mr Jeanot for his time and help brought in the achievement of these works.

References

M. Gontan-Ingold, 1994. Une électrode intégrée dans le tri des jambons. *In Process n°1099, p.51.*

D. Sicot, 1991, Mesures du gras, à l'heure de la haute technologie. *In Filières Viande et Pêche, p.79.*

C.A. Miles, 1986. *The ultrasonic properties of meat*, In On-line measurement of meat characteristics, INRA, Theix.

Application of electrical conductimetry to the control of a meat emulsification process

Application de la conductrimétrie électrique pour le suivi d'une opération d'émulsification de viande

Corinne CURT

Cemagref - Division Qualité de l'Agriculture et de l'Alimentation
Equipe Qualité Alimentaire
24, avenue des Landais - BP 50085 - 63172 AUBIERE Cedex 1
e-mail : corinne.curt@cemagref.fr

Abstract: *Meat emulsions are studied during their manufacture (chopping) by use of electrical conductimetry. Study consists of: 1) determination of temperature coefficients on emulsion, according to two linear models necessary to express conductivity at a reference temperature; 2) test of repeatability which depends of homogeneity degree of emulsion (when emulsion is considered as homogeneous, precision found is about 3%); 3) determination of optimal duration: quality of final product (texture, colour, sensory properties, losses during cooking) depends mainly on chopping duration. Continuous measurements of electrical conductivity are realised at pilot scale.*

Keywords: *Electrical conductivity, meat emulsion, process control.*

Résumé : Les procédés d'émulsification de viande sont étudiés lors du cutterage en utilisant la conductimétrie électrique. L'étude consiste à : 1. Déterminer les coefficients liant conductivité et température en fonction de 2 modèles linéaires utiles, ceci pour exprimer la conductivité à une température de référence ; 2. Tester la répétabilité de la mesure qui dépend de l'homogénéité de l'émulsion (quand l'émulsion est considérée homogène, la précision est d'environ de 3%) ; 3. Déterminer la durée optimale : la qualité du produit fini (texture, couleur, propriété sensorielle, perte lors de la cuisson) dépend principalement de la durée du cutterage. Des mesures continues de conductivité électrique sont réalisées à l'échelle pilote.

1. Background and objectives

There is a need for real-time sensors that are able to manage the main characteristics of food product: composition, flavour or colour for example. Various physical techniques such as electrical conductimetry have been investigated to evaluate their ability to do rapid quality control. Food industry uses specific applications of conductimetry for product characterisation (composition, detection of contamination, evaluation of texture) and for process control (ripening, emulsification, fermentation, heat and cold treatments...) [1].

The study aims at controlling an emulsification operation: emulsions are an important part of industrial food production : natural such as milk or processed, like frankfurter, processed cheese, ice cream, mayonnaise... They are characterised by various properties : type (oil in water - water in oil), pH, viscosity, droplet diameter, stability... Stability parameter is a major characteristic of emulsions because it influences quality of the final product and its evaluation may guarantee a product of optimum and constant quality for consumer. Our study deals with a particular emulsification operation: the chopping phase which is a main stage during the manufacture of meat emulsions such as frankfurter-type sausages.

1.1 Meat emulsions

During chopping, different raw materials are structured into an homogeneous mixture which is called meat emulsion. It consists of a fairly coarse dispersion of a solid in a liquid:

- continuous phase is water, which also contains various water-soluble components as salt,

- dispersed phase is fat,

- meat proteins, especially salt-soluble proteins, are considered as emulsifying agents.

As emulsion is a mixture of two immiscible products, its structure is thermodynamically unstable and the dispersion must be made with a given amount of shear force during the chopping operation.

Quality of final product after thermal processing (fat and water losses during cooking, sensory properties, texture and colour) depends mainly on the determination of the optimal duration of this chopping operation. For example, Girard et Dantchev (1983) [2] described yield evolution *vs.* chopping duration (figure 1). Yield (%) is expressed by "weight of product after cooking/weight of

product before cooking" and it is often considered as a reference method for stability evaluation [3, 4]; losses (%) are defined by 100 - yield (%).

Three zones are distinguished on the curve by these authors:

- under-chopping: emulsion is not yet created, fat is not sufficiently dispersed,
- optimal zone,
- over-chopping: temperature is high and this leads on one hand, to a protein denaturation that cannot act anymore as emulsifiers and on the other hand, to a fat melting.

So, chopping operation must be stopped during optimal zone, where stability is maximal.

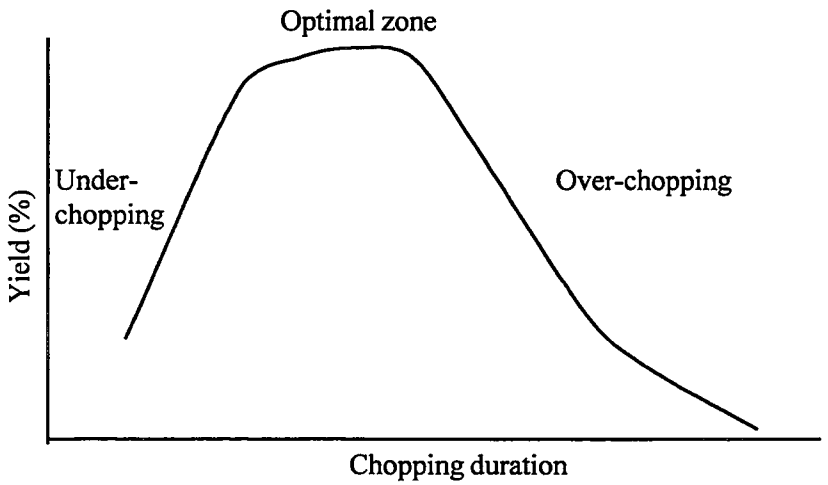

Figure 1: Yield evolution vs. chopping duration

In industrial practice, a method based on temperature evolution during chopping has been proposed to evaluate optimal duration [5], but quality product mainly relies on chopping operator know-how.

A review [6] shows that it is possible to characterise "emulsion stability", in food products, through different methods and particularly electrical conductimetry.

1.2 Principle of electrical conductimetry

The principle of electrical conductimetry lies on ability of products to conduct electrical current. It consists in measuring conductance or conductivity, which is linked to the structure and composition of the product: modifications of structure or composition induce modifications of electrical signal (figure 2). In practice, two to

four electrodes, which formed the measuring cell, are immersed into a product to measure its conductivity. Alternative current of sufficiently high frequency (4 kHz here) is used to avoid polarisation phenomenon.

Cell constant, electrode shape, electrode material and frequency must be suited to product type: food products have biological nature and are likely to be modified when an electrical current is applied (for example, if too high a voltage is applied, meat undergoes a contraction).

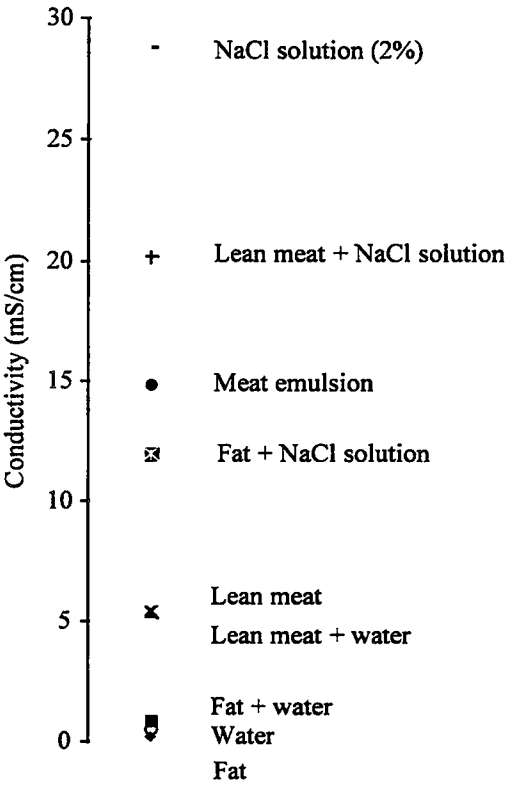

Figure 2: Range of conductivities for the different components of meat emulsion (after [7])

Electrical conductivity depends on several parameters [8]: pH, temperature, viscosity, concentration of the solution... Variation of an electrical measurement is linked on a global variation of chemical state, so it is necessary to bind it to a unique phenomenon: some parameters must be held constant or corrected.

2. Preliminary studies

2.1 Determination of temperature coefficients

2.1.1 Background

In our study, while temperature increases during the chopping phase due to the energy created by the rotating knives, conductivity must be expressed at a reference temperature. The relative variation of conductivity against temperature is within the range 0,015-0,07 $°C^{-1}$, depending on the type of solution: for water or salt solutions, it is about 0,02-0.03 $°C^{-1}$ [8], for milk, 0,020-0,025 $°C^{-1}$ [9], for sugar solution, 0,02 $°C^{-1}$ [10] and for muscle, influence of temperature on resistivity is around -0,02 $°C^{-1}$ [11]. Moreover, the temperature coefficient is usually itself a function of temperature.

2.1.2 Materials and methods

Composition of the mixture corresponds to that of frankfurter-type sausages: 40% lean meat, 30% water, 30% fatty tissue; common salt concentration is 2%. Samples are prepared in a laboratory equipment (DITO-SAMA, K55 ; volume: 5,5 L).

Emulsion conductivity is measured using an electrode (WTW, LTA/S) with a cell constant of 1 cm^{-1}, connected to a conductivity meter (WTW, LF 530).

The ten different times of chopping range from 115 s to 370 s. This range of time allows to work on the three different states of emulsion structure. Temperature and conductivity are jointly recorded for each processing time, on 10 samples of 100 mL.
Temperature coefficient is determined by regression analysis according to two models:

(1) $C = aT + C_0$ and
(2) $C = C_0 (1 + b (T - T_0))$ with C: conductivity at T °C, C_0: conductivity at T_0 =18 °C.

2.1.3 Results and discussion

Correlation coefficients between conductivity and temperature are higher than 97.66%: the two models are appropriate within the range of temperature studied, *i.e.* 12-30 °C.

Analysis of variance shows that there is no significant difference between the coefficient evaluated during an increase of temperature and that determined during a decrease (figure 3), it is therefore possible to carry out experiments for determining influence of temperature on conductivity using any of these two thermal treatments.

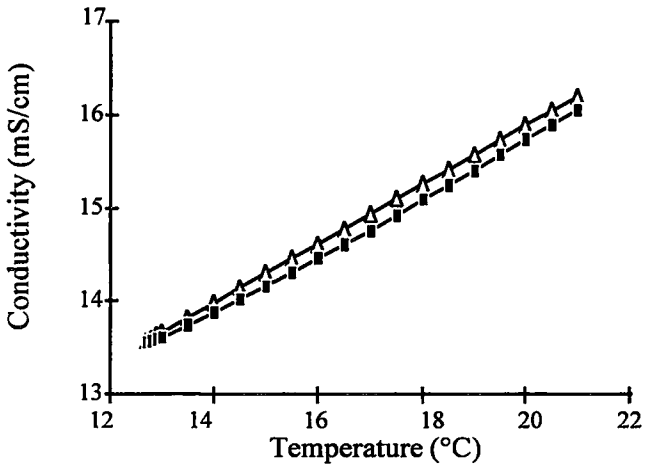

Figure 3: Evolution of conductivity vs. temperature when sample is cooled then warmed (after [7])

Mean values of temperature coefficients at the different processing times are compared by the analysis of variance:

- model 1: it can be considered that there is no significant differences between temperature coefficients for the various durations, i.e. a = 0,306 mS/cm °C, except for duration of 115 s. In the case of this shorter duration, emulsion presents high heterogeneity due to pieces of fatty tissue (characterised by a resistant behaviour) inside the homogeneous mixture of proteins and salt solution (characterised by a conducting behaviour) (figure 4). Hence, the measurement takes into account more or less pieces of fatty tissue and this leads to variation of conductivity value.

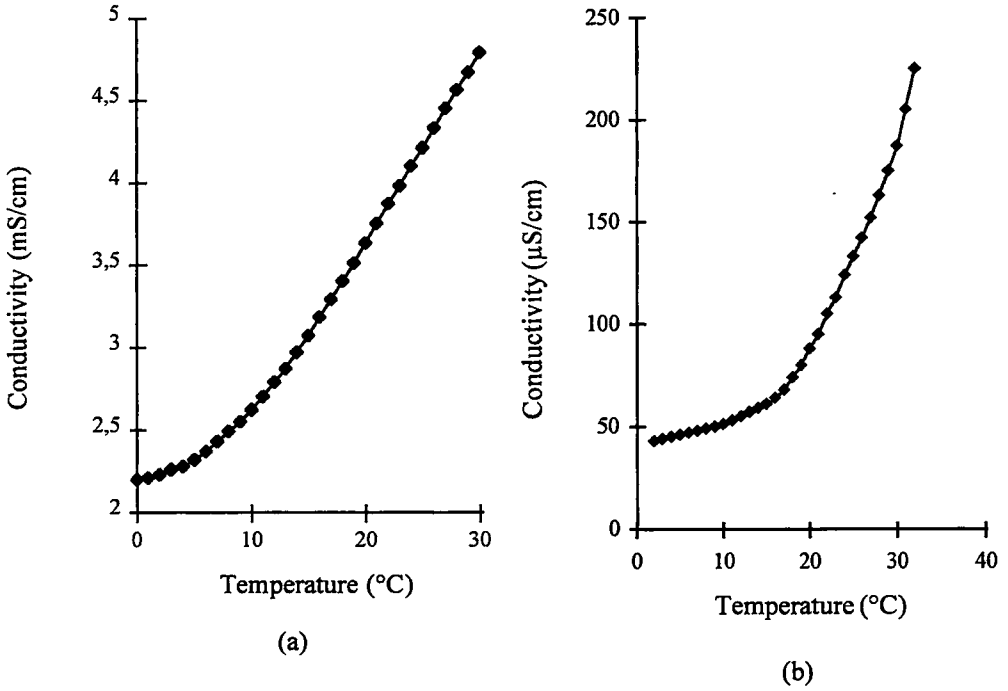

Figure 4: Conductivity vs. temperature for (a) lean meat (conductivity in mS/cm) and (b) fatty tissue (conductivity in µS/cm)

- model 2: the coefficient b is considered to be the same at 115 s, 130 s, 145 s: 0.0230 °C-1; 180 s, 215 s, 250 s: 0.0208 °C-1; 280 s, 310 s, 370 s: 0.0217 °C-1. According to the standard error, the second model is the most reliable.

2.2 Test of repeatability

2.2.1 Methods

Emulsion is made as the same way as for "determination of temperature coefficients".

Thirteen times of chopping are tested within the range 115 s-370 s. Temperature and conductivity are jointly recorded for each processing time, on fifteen samples of 100 mL of emulsion: evaluation of repeatability is done with values at 18 °C.

Repeatability is determined according to the ISO 5725 Standard (AFNOR, 1987), for each processing time.

Repeatability is estimated by: $r = 2{,}8x\sqrt{S_r^2}$

$$\text{where : } S_r^2 = \frac{\sum s_i^2}{p}$$

$$S_{ij} = \sqrt{\frac{1}{n-1}\left[\sum_{k=1}^{n} y_{ijk}^2 - \frac{1}{n}\left(\sum_{k=1}^{n} y_{ijk}\right)^2\right]}$$

with :
- n : number of repetitions (n = 5),
- y_{ijk} : conductivity value at 18 °C,
- i : time index,
- j : sample index,
- p : number of samples (p = 15).

2.2.2 Results and discussion

The precision depends on processing time (figure 5)

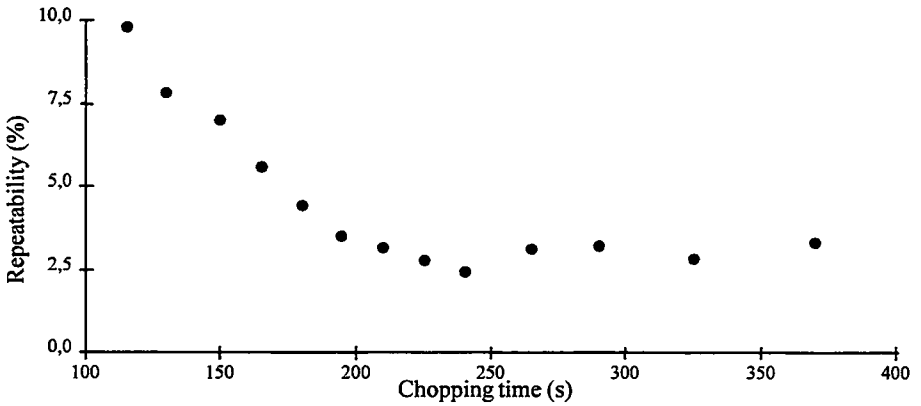

Figure 5: Repeatability vs. chopping duration

The repeatability found is about 3% for chopping times in the range 195 s-370 s, where emulsion can be considered as homogeneous according to structure. On the other hand, composition is not completely controlled, due to the presence of lipids in the lean meat and that of proteins in the fatty tissue. The composition influences the conductivity because the various components of the emulsion get conductivities, at the same temperature, very different one from another (figure 2) and consequently, repeatability values.

For the lowest chopping durations, repeatability is linked to the duration: the longer the duration, the best repeatability is. That must be due to the degree of homogeneity of emulsion which increases with duration.

3. Determination of optimal duration

These experiments are intended to determine if it is possible to show up a structure modification of the product during chopping, and so to determine an optimal duration.

3.1 Materials and methods

Emulsion is made as the same as for "determination of temperature coefficients".
The thirteen tested times of chopping range from 115 s to 370 s.
Two different series of experiments have been made:

Series 1 (ten samples)

Temperature and conductivity are jointly recorded for each processing time. Conductivity at 18 °C is used to build the graph.

For determination of yield (reference method), a sample of emulsion (P1 = $30 \pm 0{,}05$ g) is cooked during 30 min in a water-bath at 70 °C. After cooking, liquids which exsude are eliminated and «solid emulsion» is weighted (P3). Yield is expressed as $\frac{P3}{P1} x100$.

Series 2 (ten samples)

Temperature and conductivity are jointly recorded.

A slope break (slope becomes negative) is supposed to be linked to structure modification of emulsion. To determine whether conductivity is a reliable method to control chopping operation, time corresponding to this slope break is determined and the value obtained in the case of yield method is compared with the value obtained in the case of conductivity method.

3.2 Results and discussion

Conductivity values are 11 to 18 mS/cm, for both series.

3.2.1 Relation between yield and conductivity (series 1)

Determination of optimal duration with conductivity method is possible (mean: 263 s, standard deviation: 37 s).

For half of the samples, optimal durations determined by conductivity and those determined by reference method are very close (table 1).

Optimal duration determined with conductivity (s)	301	252	239	297	250
Optimal duration determined with reference method (s)	300	270	240	270	240

Table 1: Optimal durations determined by two ways

For other half of samples, yield curves have not the expected behaviour (figure 1): in addition of very low values, yield values decrease when duration increase. All these atypical curves are obtained with meat coming from a same ham. We can suppose -we didn't measure it- that this meat has a PSE (Pale Soft Exsudative) character that generate important losses during cooking. Moreover, yield determination is time-consuming: several minutes are necessary to do this measurement and emulsion might be perturbed within the time necessary for determination. To avoid emulsion perturbations, we have chosen to study only temperature and conductivity, in a second series of experiments.

3.2.2 Evolution of conductivity during chopping (series 2)

It is possible to distinguish different phases on the graph "conductivity *vs.* chopping duration" (figure 6):

- increase of conductivity,
- fairly steady trend,
- conductivity decreases more or less markedly.

It is possible to determine an optimal duration, for the ten samples, within the range 224-289 s (mean: 256 s and standard deviation: 17 s).

Figure 6: Conductivity vs. chopping duration

If one compare the optimal durations determined by conductivity on one hand, on series 1 and on the other hand, on series 2, the results are more dispersed in case 1. This might be related to the possible destabilisation of emulsion within the time necessary for yield measurement.

This study was conducted on a pilot plant (with collaboration of ADIV - Association pour le Développement de l'Institut de la Viande) with an industrial cell (Endress+Hauser) which allows continuous measurement (figure 7). Complementary research is needed to confirm this behaviour.

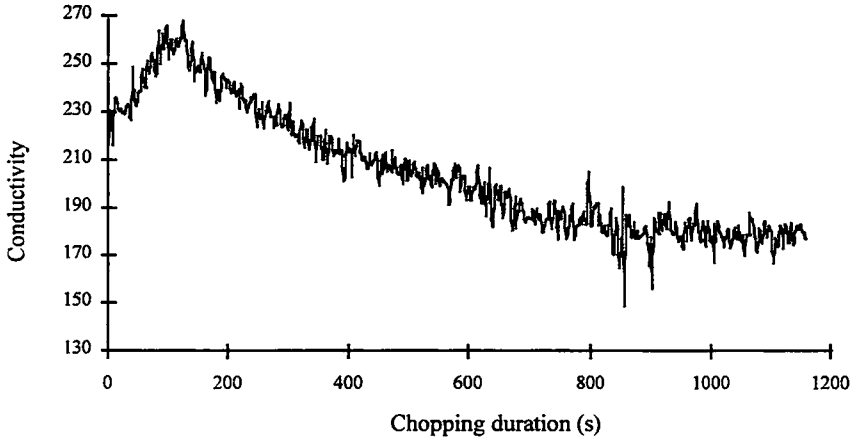

Figure 7: Continuous measurement of conductivity

Conclusion

We have demonstrate the possibility to conduct the chopping operation on laboratory stage and pilot stage through electrical conductivity measurement. Preliminary studies concerning correction of electrical values (temperature coefficients and precision of measurement) have been used in the next experimental step: determination of optimal duration. These experiments have shown that it is possible to show up a structure modification of the product during chopping and so to determine an optimal duration

Complementary research is now necessary for design of a measuring cell and to test on industrial size so electrical conductivity might be used as a chopping control method to support operator in decision.

References

[1] C. Curt. Caractérisation de produits et de procédés alimentaires par conductimétrie électrique. *In Sciences des Aliments, vol 17, pp. 435-456, 1997.*

[2] J. P. Girard, S. Dantchev. Effect of cutting duration on some technological properties of the sausage meat of emulsion-type sausages. *In Meat Industry, n°2, pp. 51-55, 1983.*

[3] S. Bruno, A. NGuyen, J.L. Martin., B. Jacquet. Gestion de production en charcuterie cuite : *I Mise au point d'un test prédictif. In Viandes et Produits Carnés, vol 11, n° 2, pp. 61-67, 1990.*

[4] N. Cariou, P. Joannic. Qualités liantes des viandes destinées à la transformation en produits de charcuterie. *In La Bretagne Agro-Alimentaire, pp. 2-10, janvier-février 1989.*

[5] J.E. Reichert. Einfache Methode zur Bestimmung der optimalen Kutterbedingungenbei der Herstellung von Brühwurstbräten. *In Die Fleischerei, n° 10, pp. 681-685, 1982.*

[6] C. Curt. Revue : méthodes d'évaluation de la stabilité des émulsions - Principe, applications, avantages et inconvénients. *In Sciences des Aliments, vol 14, n° 6, pp. 699-724, 1994.*

[7] C. Curt. Evolution de la conductivité en fonction de la température pour des mêlées de pâtes fines de charcuterie - Détermination du coefficient thermique. *In Viandes et Produits Carnés, vol 16, n° 2, p. 49-54, 1995.*

[8] P. Benoit, E. Deransart. Les mesures physico-chimiques dans l'industrie, P. Benoit, E. Deransart (ed.), *Technique et Documentation : Entreprise Moderne d'Edition, Paris, 1976.*

[9] G. Roeder. *In Milchwissenschaft Forschung, n°12, p. 236, 1931.*

[10] J. C. Obert. Les capteurs en sucrerie. Les capteurs et les industries agro alimentaires - l'intégration des capteurs dans les machines et systèmes en vue de leur automatisation, *APRIA, pp. 127-146, 1980.*

[11] P. Salé. Appareil de détection de viandes décongelées par mesure de conductance électrique. *In Supplément au Bulletin de l'Institut International du Froid, n° 2, pp. 265-274, 1972.*

[12] AFNOR. Fidélité des méthodes d'essai - Détermination de la répétabilité et de la reproductibilité d'une méthode d'essai normalisée par essais interlaboratoires, *NF ISO 5725, 1987.*

NMR relaxometry as a rapid technique to evaluate the consistency and the oxydizability of adipose tissues

La relaxométrie RMN, une technique rapide pour évaluer la consistance et la tendance à l'oxydation des tissus adipeux

A. Davenel, P. Marchal
Cemagref
17 avenue de Cucillé
35044 Rennes Cedex, France

A. Riaublanc, G. Gandemer
INRA
BP 71627,
44316 Nantes Cedex, France

Abstract: *Low consistency of pig adipose tissues leads to meat products insufficiently dried, very oxydable and with lack of cohesion in cutting. Consistency of adipose tissues is related to the physical state lipids which depends on their triacylglycerol composition. One of the simplest and quickest method to characterise physical state of lipids is to measure their solid fat content (SFC) by Nuclear magnetic resonance relaxometry. In this study, the solid fat content at 20°C (SFC20) and the solid fat content at -5°C (SFC-5) of a large collection of adipose tissues were related to their triacylglycerols composition. The SFC20 variability was closely related to that of the proportions of disaturated triacylglycerols and more specially to palmitoyl-stearoyl-oleoyl-glycerol (R^2 = 0.92). SFC-5 brought a further information on the oxydizability of adipose tissues related to the proportion of triacylglycerols OOL and SOL.*

Keywords: *NMR relaxometry, adipose tissues, solid fat index, triacylglycerols, fat quality.*

Résumé : Une faible consistance des tissus adipeux de porc peut mener à des produits insuffisamment séchés, très oxydables et qui perdent leur cohésion lors du tranchage. La consistance des tissus adipeux est reliée à l'état physique des lipides qui dépend de la composition en triacylglycerol. Une des méthodes les plus simples et les plus rapides pour caractériser l'état physique des lipides est de mesurer la teneur en matière grasse solide par résonance magnétique nucléaire. Dans cette étude, la teneur en matière grasse solide à 20°C (SFC-20) et la teneur en matière grasse solide à -5°C (SFC-5) d'un ensemble de tissus adipeux sont mises en relation avec la composition en triacylglycerol. La variabilité en SFC20 est reliée de manière très forte aux proportions de triacylglycerol déssaturé et plus spécialement, aux palmitoyl-stearoyl-oleoyl-glycerol (R^2=0.92). SFC-5 a donné des informations supplémentaires sur l'oxydabilité des tissus adipeux reliés à la proportion de triacylglycerol OOL et SOL..

1. Introduction

Lack of consistency of adipose tissues is one of the main problems the manufacturers of dried meat products have to face. The meat products containing these adipose tissues show large defects such as insufficient drying, oily aspect, rapid rancidity and the lack of cohesion between meat and lard in cutting. That why the producers need a simple method for selecting adipose tissues at the industrial scale. They presently select adipose tissues with an indirect method based on carcass lean content (<57%) and on the backfat thickness (>15 mm). This method is based on observations which established that adipose tissues with the lowest thickness lack of consistency because they have the highest proportion of polyunsaturated fatty acids and the lowest one of saturated fatty acids[1, 2]. Although this method limits the risk to get pig carcasses with soft fat [3], it would be inefficient to control adipose tissue quality because many soft tissues escape to the selection.

Consistency of adipose tissues is related to the physical state of lipids which depends on both fatty acid and triacylglycerol compositions. One of the simplest method to characterise physical state of lipids is to measure their solid fat content (SFC) by H- Nuclear magnetic resonance relaxometry. It could be an efficient method for on line grading of adipose tissues because it is very fast. However very few data have been published on the solid fat content of pig adipose tissues [4]. The aim of this study was to determine the relationships between solid fat content measured at different temperatures and the lipid composition of a collection of adipose tissues to find new rapid and efficient indicators of the consistency and the oxydizability of adipose tissues.

2. Material and methods

2.1 Animals and sample preparation

Samples were taken from 65 pigs in four slaughterhouses. Samples of sub-cutaneous adipose tissue including the two layers were taken at the cut between ham and loin along the vertebra column. Pig females and castrated males were selected to cover a broad range of carcass lean content measured using a Fat-O-Meter.

Sample including the two layers was minced after meat and skin were removed. A 2g sample was placed in an oven at 103°C during 3 hours for melting lipids. A sample of minced adipose tissue and an aliquot of melted lipids (about 0.5 g) from each animal were transferred into 10 mm diameter NMR tubes. An aliquot (10 mg) of melted lipids was dissolved in one ml of chloroform. All samples were stored at -20°C until chemical analyses and NMR measurements.

2.2 Solid fat content by NMR

Frozen biopsies as they stood and extracted lipids were stabilised at -5°C and 20 °C during ten minutes before NMR measurement in 5 seconds with Bruker Minispec 20 MHz spectrometer according to the well-known method using the recording of the free induction decay signal measured just after rotating the magnetisation of the sample by a radiofrequency pulse in the plan perpendicular to the permanent field (figure 1).

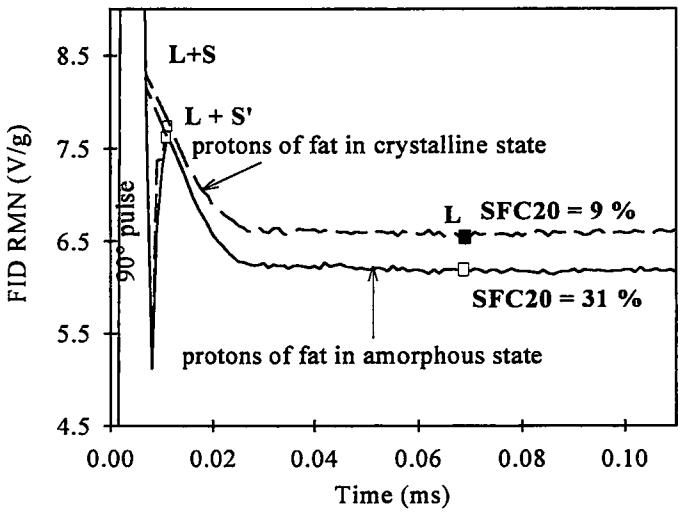

Fig.1. Free induction decay signals of two samples

The solid fat content was calculated with the following formula using a calibration factor of 1.37 to take into account the lag time of 11µs.

$$SFC = 100\frac{f[(L+S')-L]}{f[(L+S')-L]+L}$$

2.3 Chemical analysis

Triacylglycerol composition: An aliquot of melted lipid was dissolved in a mixture of chloroform/ methanol (1/1; v/v) to obtain a 5 mg/ml solution. Molecular species of triacylglycerols were separated in 45 minutes by reverse phase HPLC using a linear gradient of chloroform in acetonitrile. Molecular species were detected with a

light scattering detector. It was assumed that the molecular species of triacylglycerol have a similar response and results were expressed as a percent of total molecular species present.

Fatty acid composition : Fatty acids were analysed by gas liquid chromatography after methylation of 10 µg of lipids by a mixture BF_3/methanol. The gas chromatograph was equipped with an on-column injector and a flame ionisation detector. The results were expressed as percent of the total methyl esters present. Iodine value was calculated from fatty acid composition and expressed as mg of iodine per 100 g of fatty acids.

3. Results

The average SFC20 at 20°C which expresses the consistency at ambient temperature was 23.5% and the variability of SFC20 was important because the gap between the extreme values was 22 SFC points. Lipids from adipose tissue contained mainly four fatty acids which accounted for 95% of total fatty acids: two saturated fatty acids, palmitic acid (P) and stearic acid (S), one monounsaturated acid, oleic acid (O), and one diunsaturated acid, linoleic acid (L). Twenty triacylglycerols molecular species were identified. Seven species accounted for 90% of triacylglycerols and three of them for at least 75% : POO (38.4%), PSO (25.5%) and POL (12.9%). Trisaturated triacylglycerols account for a very small proportion of the triacylglycerols in pig adipose tissue.

	Average	Standard Deviation	Minimum	Maximum
Solid fat content (%)				
- at -5°C	67.5	4.3	53.5	71.2
- at 5°C	32.8	5.3	18.9	36.5
-at 20°C	23.5	4.8	9.5	31.5
Main fatty acids (%)				
Palmitic (P)	23.1	1.4	19.5	26.8
Stearic (S)	14.5	1.7	10.8	17.9
Oleic (O)	41.9	1.9	36.9	45.3
Linoleic (L)	11.4	2.2	6.8	17.8
Iodine value (mg iodine/100 g fatty acids)	63.8	4.4	54.5	76
Main triacylglycerols (%)				
OOL				
POL	2.3	1.2	0.6	6
OOO	11.2	3.3	4.6	20.7
POO	3.7	1.0	1.7	6.3
PSL	38.4	4.2	27.4	47.8
PPO	3.1	0.9	1.9	5.6
PSO	4.5	0.9	2.3	7.2
	25.5	5.4	13.6	35.4

Table 1: Solid fat content, fatty acid and triacylglycerol compositions of the adipose tissues

The SFC20 could be accurately predicted from the proportions of three triacylglycerols (PSO, PPO and PSL) which explained 95% of SFC20 variability. The relationship between SFC20 and these species species containing two saturated fatty acids, was:

$$SFC20 = 0.635\ PSO + 0.789\ PPO + 0.665\ PSL - 0.853\ (R^2 = 0.95,\ \sigma = 0.96)$$

The variability of PSO proportion explained alone 92 % of the SFC20 variability (figure 2). The relationship between these parameters was:

$$SFC20 = 0.73\ PSO\ (R^2 = 0.92,\ \sigma = 1.24)$$

The presence of two saturated fatty acids in a same triacylglycerol molecular species give them a high melting point. We can deduce that the solid phase of lipids contains a large majority of triacylglycerols with two saturated fatty acids because trisaturated triacylglycerols account for a very small proportion of the triacylglycerol in pig adipose tissue.

SFC20 gives a good estimate of the consistency of adipose tissue. The average of solid fat content at 5°C(SFC5) was 32.8% and that at -5°C (SFC-5) was 67.5%. SFC5 and SFC20 were highly correlated (R^2 = 0.91). For practical use of the determination of the consistency of adipose tissue SFC20 could be substituted by SFC5 immediately measured on sample taken on backfat of refrigerated carcasses and SFC20 deduced in using the following expression:

$$SFC20 = 0.68\ SFC5$$

The information on consistency at 20°C could be eventually completed by the measurement of the solid fat content at -5°C. Two useful mathematical relations between SFC-5, lipid composition and SFC20 have been calculated:

1) $SFC\text{-}5 = 63.1 - 1.87\ SOL - 2.18\ OOL + 0.46\ SFC20$ (R^2=0.94 σ = 1.2)

2) $SFC\text{-}5 = 63.6 + 0.263\ PSO - 2.88\ OOL + 0.81\ PPO$ (R^2=0.93 σ = 1.3)

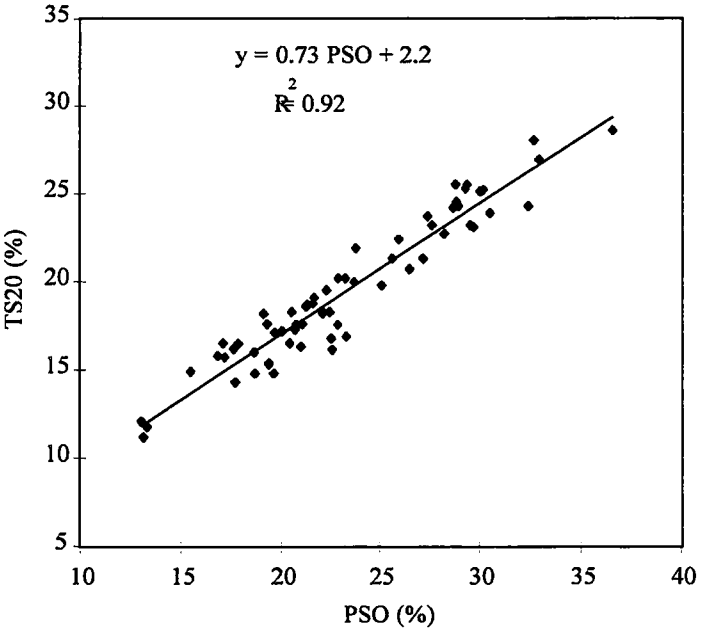

Figure 2: Relationship between solid fat content (SFC20) and Palmitoyl-Stearoyl-Oleoyl-glycerol (PSO) proportion in adipose tissues

These relations show that SFC-5 is also positively correlated to SFC20 as planned (R^2 =0.79) but less than SFC5. SFC-5 brings a further information on the oxydizability of adipose tissues related to the proportion of triacylglycerols OOL and SOL which have lower melting point than OOO and SOO.

Conclusion

According to the limit values of parameters such as iodine value, linoleic and stearic acid proportions widely used to define soft and hard tissues, we can postulated that soft tissue should have a SFC20 lower than 15% and hard one should have a SFC20 higher than 18 %. However complementary studies are required to define more precisely the limit values of SFC20 to get adipose tissues adapted to the production of dry-cured meat and to know if SFC20 is a sufficient indicator of the oxydizability of adipose tissues or if SFC-5 must be also measured.

The NMR measurement of SFC20 could be an interesting method for selecting adipose tissues in slaughterhouses because it is fast to perform. We have shown that resulted on biopsies of adipose tissues as they stood instead of melted lipids were similar (R^2 =0.97). These results suggest that the method could be automated for selecting adipose tissues at the industrial scale. The high correlation between SFC20 and SFC-5 suggests that, for practical use of the determination of the consistency of adipose tissue SFC20 could be substituted by SFC5 immediately measured on sample taken on backfat of refrigerated carcasses. Further works are necessary to find representative localisation of the consistency of fat tissues in each carcass.

References

[1] C.H. Lea, P.A.T Swoboda, D.P. Gatherum, 1970. A chemical study of soft fat in cross-bred pigs. In *J. Agric. Sci. Camb, 74, 279-289.*

[2] J.D. Wood, M.B. Enser, H.J.H. MacFie, W.C. Smith, J.P. Chadwick, M. Ellis, R. Laird, 1978. Fatty acid composition of backfat in large white pigs selected for low backfat thickness. In Meat Science, 2, 289-300.

[3] V.Rampon, G. Gandemer, P. Le Jossec, J. Boulard, 1994. Qualité des tissus adipeux chez le porc. Situation en Bretagne. In *J. Rech. Porcines en France*, 26, 157-162.

[4] M. Le Meste, G. Cornily, D. Simatos, 1984. Le comportement thermique des lipides musculaires et de dépôt chez le porc. In *Rev. Fr. Corps Gras, 31, 3, 107-115.*

Measurement of acoustic impedance to estimate the fish sol density[1]

Mesure de l'impédance acoustique pour l'estimation de la densité des soles

Y. Mevel

Laser Photoniques Industriels,
Ecole Centrale Paris, Grande Voie des vignes,
92295 Chatenay Malabry, France,
tél. (33) 01 41 13 15 57,
e-mail: mevel@lpi.ecp.fr

M. Mastail, R. Baron

IFREMER, Département Valorisation des Produits, Laboratoire Génie Alimentaire,
rue de l'Ile d'Yeu,
BP 1135, 44311 Nantes Cedex 03, France,
tél (33) 01 40 37 40 90,
e-mail: rbaron@nantes.ifremer.fr

Abstract: *In spirit of crab like meat stick, we develop a new fish texturation process, using a cooling extrusion to used common species, which permit a wide range of textured product. Inevitable heterogeneity of raw material induce perturbation in the process. A model is use to control and stabilise around a given reference trajectory. Acoustic transducers permit the estimation of specific weight, and give a predictive image of the future product.*
We describe the on-line measurement of acoustic impedance, combined with velocity to obtained the density.

Keywords : *Extrusion, gelation, specific weight, density, specific impedance acoustique, velocity.*

Résumé : Nous avons développé un nouveau procédé de texturation du poisson utilisant une extrusion refroidie afin de créer des produits proches des bâtons de surimi au crabe. L'hétérogénéité inévitable des matières premières entraîne des perturbations du procédé. Un modèle est utilisé pour contrôler et stabiliser le procédé autour d'une trajectoire donnée. Des transducteurs acoustiques permettent d'estimer le poids spécifique et donnent une prédiction du produit futur. Nous décrivons la mesure en ligne de l'impédance acoustique combinée à la vitesse pour obtenir la densité.

1 This work is covered by a patent (Fr 9706298) entitle: "Mesure de la masse volumique d'un produit pâteux ou liquide"

1. Introduction

Natural resource management is a major concern for our future. It includes improving the valorisation of fish products. Surimi• production techniques may be considered in this perspective.They are mainly based on fish protein gelation properties. According to several authors [1], two distinct steps : the destructuration of the myofibrillar structure and the restructuration yielding new interactions between proteins in the presence of salt.

The constraints resulting from the specificity of species needed for the production of surimi on the one hand, and the difficulty to have access to these species on the other hand, gave incentive at IFREMER to look for another texturing process. The objective of such a process is to use common species, mainly small pelagics (mackerel, sardine), to valorise by-products resulting from the filleting of noble species (salmon, cod , halibut), and to allow a direct texturation of fish pulp.

Fish protein gelation can be decomposed in two distinct steps : the destructuration of the myofibrillar structure in the presence of salt and the restructuration yielding new interactions between proteins.

The fish extrusion-gelation process consists of two steps. The first one concerns the extrusion at low temperature (destructuration phase) performed by a twin-screw co-rotating extruder (Clextral BC 45) and the second step is carried out in a cooking tunnel. A scheme of a twin-screw extruder is presented in figure n°1

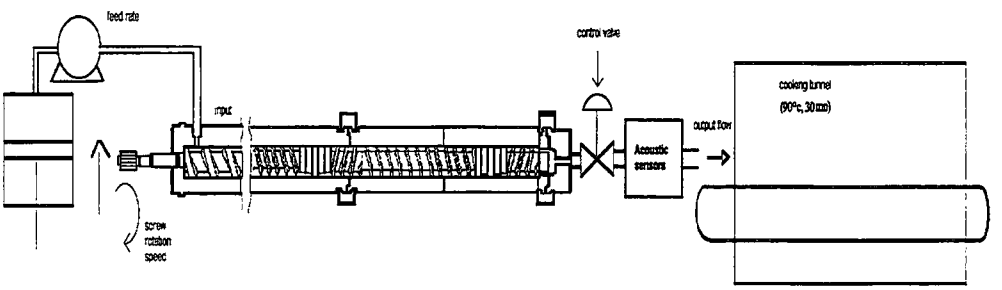

Figure 1: Twin-screw extruder followed by the acoustic transducers and the cooking tunnel

In this context, extrusion is very promising. Its main advantages, compared to surimi production machines, are compactness, modularity, continuity and low water consumption. Its flexibility allows the use of a large diversity of raw materials, and the extruded final product can have a wide range of textures Nevertheless, up to

now, from a biochemical point of view, the texturation principles are not completely understood and, as far as dynamical aspects are concerned, the extrusion is still considered as a process which is hard to modelize. Additional difficulties can be identified: the fluctuations of the characteristics of fish and unmodelled perturbations such as those affecting the feed rate. They may be attenuated by the control design.

2. Process control

The control aspects of a new fish extrusion process was studied [2]. The product quality is defined in terms of the output flow rate and the size of the bubbles and the quality control problem is addressed. The trajectory planning is solved, using the differential flatness property of the model and a feedback law that tracks the corresponding trajectories is designed.

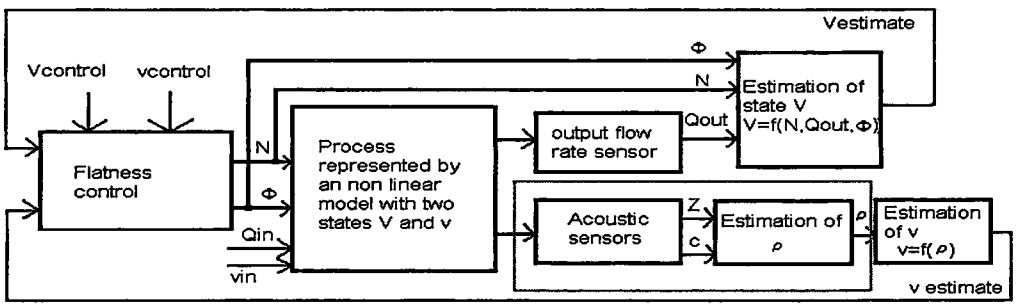

V : Volume of the accumulated fish mince
v : average volume of one bubble capted in the network structure
Vcontrol : Volume setpoint of the accumulated fish mince
vcontrol : average volume setpoint of one bubble capted in the network structure
ρ : specific weight
Qin : input flow rate
vin : input v
Qout : output flow rate
N : screw rotation speed
ϕ : die restriction (=f(valve position))
Z : electric impedance (=f(Za))
Za : acoustic impedance (Za = ρ*c)
c : celerity

So, a work has been done within a collaboration between the laboratory Genie Alimentaire of IFREMER and Centrale Recherche of ECP to study ultrasonic techniques in this application.

Low-intensity ultrasound is a non-destructive technique that provides information about physicochemical properties, such as composition, structure, physical state and flow rate. The three parameters that are measured most frequently in ultrasonic experiments are the ultrasonic velocity, attenuation coefficient and acoustic impedance.

In this presentation, we describe the on-line measurement of acoustic impedance to estimate the fish sol density at the end of low temperature extrusion.

3. Acoustic in viscous-elastic medium

The longitudinal waves propagate in all medium according to the following equation :

$$\nabla^2 p = \frac{1}{c^2} \cdot \frac{\partial^2 p}{\partial t^2}$$

They generate pressures. The pressure can be described as below :

$$p = P_0 \exp. j(k\,x-\omega t)$$

where P_0 , x, ω, k are the amplitude of the pressure at x=0, the co-ordinate measured in the direction of the wave travel, the pulsation, and the wave number.

The propagation velocity depends of the media where they are travelling :

$$c_1=((\lambda+2\mu)/\rho)^{0,5}$$

where ρ is the density, λ and μ are the Lamb's constants of the material.

The specific acoustic impedance Z equals the product of the density and the velocity. We chose to use a piezoelectric disc to measure the specific acoustic impedance, the density can then be computed : $\rho=Z/c_1$.

4. Piezoelectric ceramic

4.1 Equivalent circuit of the piezoelectric disc

The piezoelectric disc is a electromechanical converter which can be described by the following equivalent circuit :

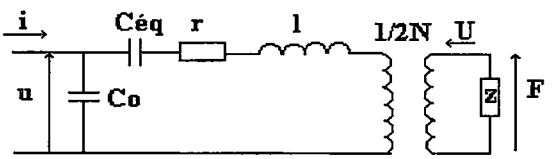

Figure 2: Equivalent circuit of the piezoelectric disc

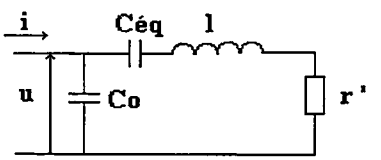

Figure 3: Simplified circuit

From this equivalent circuit the admittance y can be calculate,

$$y = \frac{r'}{r'^2 + \left(l \cdot \omega - \frac{1}{C\acute{e}\, q \cdot \omega} \right)^2} + j \left[Co \cdot \omega - \left(\frac{l \cdot \omega - \frac{1}{C\acute{e}\, q \cdot \omega}}{r'^2 + \left(l \cdot \omega - \frac{1}{C\acute{e}\, q \cdot \omega} \right)^2} \right) \right]$$

and these admittance at the resonance (at the resonance frequency the imaginary part of the admittance becomes nil).:

$$y = \frac{1}{r + \frac{Z}{(2N)^2}} + j \cdot Co \cdot \omega$$

Where N, Co and r are the converter yield, the static capacitor. and the internal resistance of the piezoelectric disc.

4.2 Characteristics of the piezoelectric disc

PZ 27 and P1.88 ceramics are used to make the part of our measurements. Theirs mains characteristics are following:

The diameter is 25 mm and the height is 2 mm.

Electrical Properties			
Relative dielectric const. at 1 kHz	1800	Diel. dissipation factor at 1 kHz	0,017
Electricomechnical Properties		Frequency constants Hz.m	
coupling factors kp	0,59	Np	2010
coupling factors kt	0,47	Nt	1950
coupling factors k31	0,33	N1	1400
coupling factors k33	0,69	N3	1500
density	7,7	Mechnical Quality factor	80

The ceramic is charged by the unknown medium.

4.3 Ceramic disc charged by a tube

The ceramic disc has a diameter of 25 mm. Its resonance frequency is 950 kHz. Therefore the acoustic beam is very narrow.

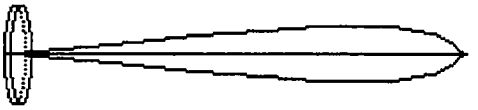

Figure 4: Acoustic beam

ES Saidi [7] shows that we can assume the ceramic is loaded by a tube of medium. The diameter of the tube equals the ceramic diameter.
This tube is equivalent at a line.

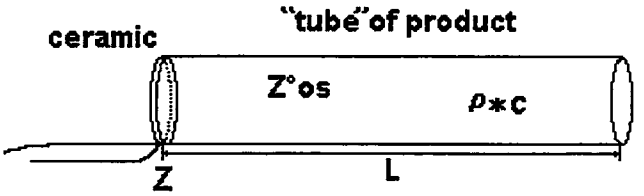

Figure 5: Load of the ceramic disc

The method of calculus of the electric lines can be applied: Z= Z * os th[(b+jq) L].
The extruded fish flesh attenuates much ultrasonic waves therefore Z equals Z*os
For the standard products L is chosen very high to obtain Z equals Z*os.

5. Impedance measurement

5.1 Apparatus

Two apparatus are employed to make the impedance measurement. The first one is described on the diagram below:

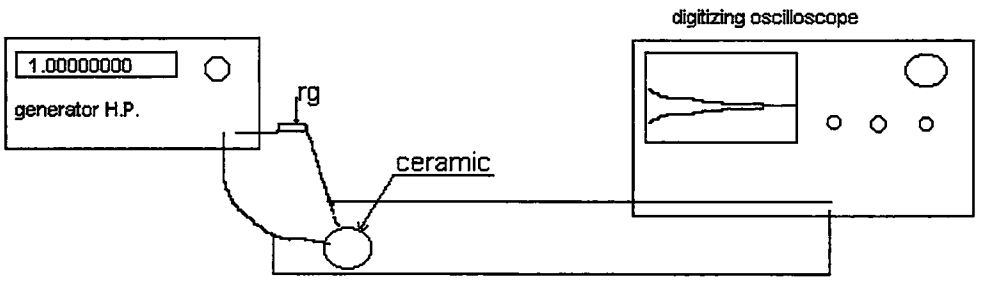

Figure 6: Impedance measurement apparatus

The H.P. generator is connect to ceramic through a resistance r_g. The oscilloscope is connected at the ceramic disc. 60 cycles burst are used to measure the peak to peak voltage. Several points are measured around of the resonance frequency, at the 3 dB points and at antiresonance frequency.

The second apparatus is a Hoki impedancemeter. It performs the on line measurements.

6. Velocity measurement

The velocity measurement are made with PANAMETRIC transducer.

7. Density calculus

We obtain r (the internal resistance of the piezoelectric disc) by measuring the impedance of the ceramic in the air (r = r'. in the air).

The impedance of the extruded fish flesh or of the standard products r' are record.
Z', the total corrected impedance equals the impedance reduce of r.
Zcort is the equivalent impedance at the primary of the converter.

$$Z = \frac{Zcort}{4 \cdot N \cdot S}$$

N and S are the converter yield, and the ceramic surface.
The specific acoustic impedance Z equals the product of the density and the velocity: $Z=\rho.c_1$.
There fore, the density equals the yield of the impedance on the velocity:$\rho = Z/c_1$
After discussing the modelling assumptions, the sensor calibration is considered.
We obtain r (the internal resistance of the piezoelectric disc) by measuring the impedance of the ceramic in the air (r = r' in the air).

Sensor calibration in laboratory condition with standard product are being tested. We measure the impedance of the disc loaded by standard products (with known characteristics : ρ) as to establish the proportionality ratio N' between Z and their measured values r', $Z=(r' -r)\cdot(2N')^2$.
The velocity of each standard product is measured to calculate the density $\rho=Z/c_1$.

8. Results

8.1 Standard products results

All calculus made, we obtain the following results :

- for the alcohol ρ=773 kg/m^3 instead of 809.5 kg/m^3 (error = 4,4%),
- for the glycerol ρ=1180 kg/m^3 instead of 1259 kg/m^3 (error = 6,3%),

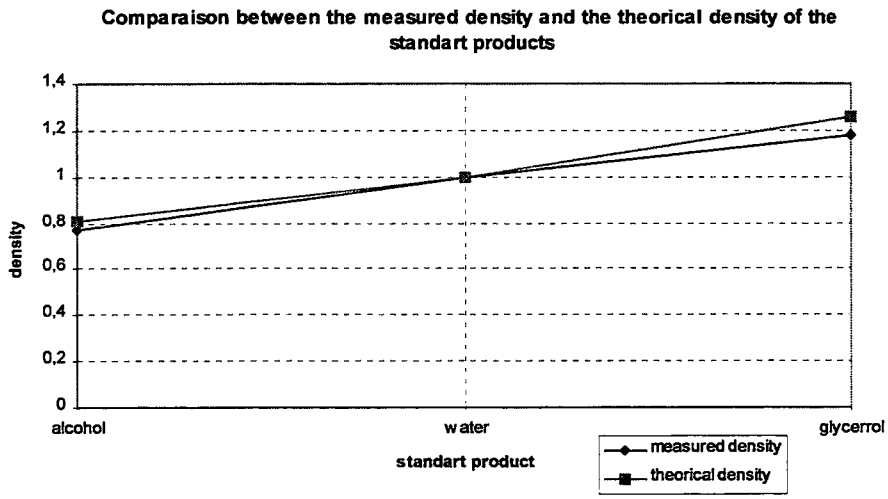

We assume than relative error is less ten percent.

8.2 On-line measurements results

density measured by weighing	1,08	1,03	0,98
impedance (Ohm)	16,2	15,19	14,6
ratio	0,067	0,068	0,067

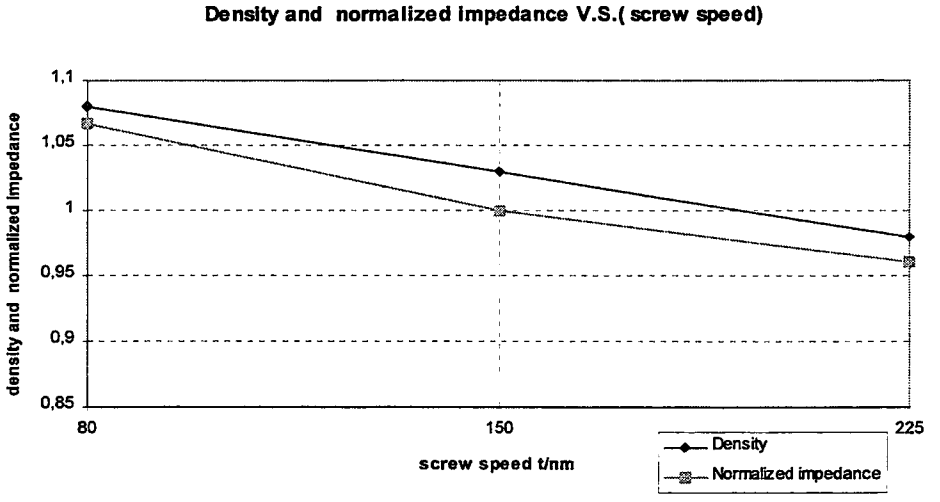

On-line extrusion measurements present good correlation with analytical method (see the chart and the figure above).

Conclusion

The impedance measurement combined with the velocity measurement permit to obtain the density.
We discuss about the industrial application and extension of those results.
The density points the ratio on air bubbles to a pastry or to dairy products like light cream cheese.
The density shows the proportions variations in a biphasic products.
If we use the impedance measurement alone, this device permits to follow a gelation, a solidification or in the other hand a liquefaction.
The impedance measurement is useable in high attenuating medium. It's a low cost system
These process can be followed with velocity measurements but it use two transducers. The chart below explains the advantages of each method.

References

[1] R. Baron, M. Mastail, J.L. Vallet and Lukomska. Texturation de la pulpe de poisson par extrusion à froid. *Sciences des aliments, 16(1),1996, pp 71-78.*

[2] R. Baron, J. Lévine and M. Mastail. *Modelling and Control of a Fish Extrusion process.* In Proc. 1st.int.symp on Mathematical Modelling and Simulation in Agriculture and Bio-industries, Bruxelles, 1995.

[3] R. Baron. 1995. *Modélisation et commande d'un procédé d'extrusion de pulpe de poisson.* PhD.thesis. Université Paris Sud.

[4] R. Baron, J. Lévine and M. Mastail. Control of a fish extrusion process using flatness. Symposium or Control, Optimisation and Supervision- *CESA 96, Lille, 1996, p.200-205*

[5] Y. Mével, 1993. *Contrôle de la fluidisation du sédiment marin par une mesure d'impédance acoustique ramenée*, 3ème journées d'acoustique physique sous-marine et ultrasonore du Havre.

[6] Y. MEVEL, 1994. *Contrôle de la fluidisation du sédiment sableux sous l'action de la houle par des méthodes acoustiques.* Mémoire d'ingénieur du C.N.A.M., Paris.

[7] A.ES SAIDI. *Caractérisation acoustique de matériaux isotropes par impédancemétrie électrique.* Thèse de doctorat de l'université des sciences et technologie de Lille, le 12/12/ 1994.

• Surimi is a japanese term for mechancally deboned fish flesh that has been washed with water and mixed with cryoptrotectants for a good frozen shelf life

Beef tenderness prediction by near infrared reflectance spectroscopy

Prédiction de la tendreté du boeuf par spectrométrie proche infrarouge

Bosoon Park and Yud-Ren Chen
Instrumentation and Sensing Laboratory
Beltsville Agricultural Research Center
Agricultural Research Service, USDA
Beltsville, Maryland 20705-2350
Phone: (301)504-8450; Fax: (301)504-9466
e-mail: ychen@asrr.arsusda.gov

Abstract: *Tenderness is the most important factor affecting consumer perception of eating quality of meat. In this paper, the development of the principal component regression (PCR) models to relate near-infrared (NIR) reflectance spectra of raw meat to Warner-Bratzler (WB) shear force measurement of cooked meat was presented. NIR reflectance spectra with wavelengths from 1100 to 2498 nm were collected on 119 longissimus dorsi meat cuts. The 1st principal component (or factor) from the absorption spectra log(1/R) showed that the most significant variance from the spectra of tough and tender meats were due to the absorptions of fat at 1212, 1722, and 2306 nm and water at 1910 nm. The distinctive fat absorption peaks at 1212, 1722, 1760, and 2306 nm were found in the 2nd factor of the second derivative spectra of meat. Also, the local minima in the 2nd principal component of the second derivative spectra showed the importance of water absorption at 1153 nm and protein absorption at 1240, 1385, and 1690 nm. When the absorption spectra between 1100 nm and 2498 nm were used, the coefficient of determination (r^2) of the PCR model to predict WB shear force tenderness was 0.692. The r^2 was 0.612 when the spectra between 1100 nm and 1350 nm were analyzed. When the second derivatives of the spectral data were used, the r^2 of the PCR model to predict WB shear force of the meat was 0.633 for the full spectral range of 1100 to 2498 nm and 0.616 for the spectral range of 1100 to 1350 nm.*

Résumé : La tendreté de la viande est un des facteurs de qualité les plus importants pour le consommateur. Dans cet article, des modèles de Régression en Composantes Principales (PCR) sont développés pour relier les spectres de réflectance NIR à la force de cisaillement de Warner-Bratzler (WB) obtenue sur viande cuite. Les spectres NIR en réflectance de 119 morceaux de longissimus dorsi sont enregistrés dans la gamme 1100-2400 nm. Le premier composant principal (ou facteur) du spectre d'adsorption montre une variance significative entre viandes dures et tendres aux longueurs d'onde 1212, 1722, 2306 nm (matière grasse) et 1910 nm (eau). L'absorption spécifique des pics de MG à 1212, 1722, 1760 et 2306 nm est déterminée dans le 2ème facteur de la dérivée seconde du spectre. Les minima locaux du deuxième composant principal de la dérivée seconde du spectre d'absorption montrent l'importance de l'eau à 1153 nm et des protéines à 1240, 1385 et 1690 nm. Dans la gamme 1100-2498 nm, le coefficient de corrélation au carré pour la prédiction de la force de cisaillement par le modèle PCR est 0,692. Le R2 était 0,612 en utilisant la gamme 1100-1350 nm. Lorsqu'on utilise les dérivées secondes, les coefficients de corrélation au carré sont respectivement 0,633 pour la gamme complète (1100-2498 nm) et 0,616 pour la gamme 1100-1350.

1. Introduction

Among the many quality factors of meat such as texture, flavor, juiciness, appearance, and aroma, the texture or tenderness in particular is considered the most important in determining the meat eating quality [1,2,3]. Inconsistency in meat tenderness has been identified as one of the major problems facing the beef industry [1,4,5]. Because consumers consider tenderness to be the major determinant of eating quality of meat, it is important to develop methodologies to objectively predict meat tenderness to supplement or replace the current USDA quality grading system. Even though tenderness is considered to be the major determinant of meat quality, no rapid method exists for the grader or retailer to use to determine tenderness of meat. The current tenderness measurement by taste panels is a subjective method, and is a time-consuming process, because it requires long sample preparation time. The Warner-Bratzler (WB) shear device is widely used in the United States for measuring tenderness of cooked meat. Although it is an objective method, it also time consuming and destructive. Thus, an objective, nondestructive and rapid technique for assessing beef tenderness needs to be developed.

Near-infrared (NIR) spectroscopy has become an important tool to measure chemical composition and moisture content of meat and meat products. Ben-Gera and Norris [6] investigated NIR transmittance for measuring fat and moisture contents in emulsions of meat products. Later NIR spectroscopy was used to measure moisture and biochemical properties such as fat and protein in emulsified lamb, pork, and beef [7,8,9]. These studies, however, were carried out on ground or emulsified meats. NIR spectroscopy also has been applied for the measurement of chemical composition and textural attributes of raw and cooked meat. The composition (moisture, fat, and protein) has been measured for raw poultry [10,11]. Recently, Marks and Chen [12] evaluated cooked ground poultry patties using NIR spectroscopy. NIR spectroscopy also was applied to predict total pigment values by measuring optical density of raw fresh meat [13]. NIR reflectance and interactance measurements were used to classify wholesome and unwholesome carcasses based on myoglobin measurement, which affects pigment content of poultry meat [14,15,16,17]. Changes in NIR spectra of beef muscles during conditioning and aging of beef were investigated and the feasibility of NIR spectroscopy in the prediction and assessment of meat sensory attributes was reported [18]. Although NIR spectroscopy has been demonstrated to be a promising method for assessing meat quality of individual carcasses, none of the research resulted in systems which are accurate, reliable, practical, low cost, and rapid that can be readily adopted by the meat industry for measuring tenderness. NIR technology has the potential to be used for assessing the tenderness of meat. Thus, research is needed to develop measurement techniques using the NIR spectra for the accurate prediction of meat tenderness. The objective of this study is to develop a technique to use near-infrared (NIR) spectroscopy of raw meat to predict its tenderness

rapidly and nondestructively. More specifically, the objectives are 1) to measure NIR reflectance on raw meat and 2) to develop models to relate NIR reflectance spectra of raw meat to WB shear force measurement of cooked meat, using the principal component regression (PCR) technique.

2. Materials and methods

2.1 Materials

The meat samples of longissimus dorsi (LD) muscle from 119 beef carcasses were used for establishing NIR spectra measurement. About 24 mm thickness steaks were excised from the LD muscles of the thirteenth rib from the right side of each carcass. The samples were vacuum-packed in polyethylene bags and frozen and stored at -40 °C in the U.S. Meat Animal Research Center, Clay Center, Nebraska, then transported to the Instrumentation and Sensing Laboratory, Beltsville, Maryland. The samples were completely thawed for 24 h at 2 °C before NIR spectra were collected. From each steak two cylindrical shaped samples of about 38 mm diameter were excised using a stainless steel punch force corer which allowed the meat sample to fit in a quartz window-clad cylindrical cell. In the sampling procedure, excessive fat and connective tissue were avoided to minimize sampling errors. Each sample was cut to make three or four (the number depended on the size of ribeye muscle) circular slices of 8 mm thickness from the cylindrical pieces of meat. A total of 405 disks cut meat samples were used to collect NIR reflectance spectral data.

2.2 NIR reflectance measurement

A scanning monochromator1 (model 6500, NIRSystems, Silver Spring, MD) was used to collect reflectance (R) readings over a wavelength range of 1100 - 2498 nm in 2 nm increments, yielding 700 values per spectrum. Two pairs of lead sulfide detectors collected the reflectance spectra. The absorbance spectrum, recorded as log(1/R) for each meat sample, was gathered on a spectrophotometer equipped with a rotating drawer. Reflected energy readings were referenced to corresponding readings from a ceramic disk. A reference scan was collected and stored to computer memory before each sample was scanned. The spectra from three or four circular slices of each sample were averaged to produce one spectrum per sample for the development of chemometric models to predict meat tenderness. The spectrum of a meat sample was the average of 32 successive scans (i.e. grating oscillations), altogether taking approximately 20 seconds per slice.

1 Mention of any company or trade name does not imply endorsement of the products by the U.S. Department of Agriculture. It is for purpose of description only.

2.3 Shear force analyses

Steaks were cooked on an electric grill to an internal temperature of 70°C. Copper-constantan thermocouples were placed in the geometric center of each steak and temperature was monitored. These samples were cooled overnight at 4 °C. Six 13-mm diameter cores were taken from each steak parallel to the muscle fibers. The shear force for each steak was measured by Warner-Bratzler (WB) shear tester [19]. The averages of the maximum force readings were used in the reference data analysis. These shear force values were used as the reference to develop prediction models for meat tenderness by NIR measurement.

2.4 Principal component analysis

Principal component analysis (PCA) or spectral decomposition produces a reduced representation of the training data based on the maximum variations between the spectra. This produces a small set of defined numbers that can be used for discrimination, since it provides an accurate description of the entire training set. Effectively, PCA finds a set of mathematical spectra (or factors) which contain the maximum variations common to all spectra in a data set. This sets up a new space where each spectrum in the original group of data can be modeled by a linear combination of these factors [20]. The linear combination coefficients or scores, which determine how much of each factor is needed to reconstruct the original spectrum, can be calculated from this set of factors and the original data. Each spectrum will have its own unique set of scores; therefore a spectrum can be represented by its PCA scores in the factor space instead of intensities in the wavelength space.

2.5 Principal component regression model

$$A = S\,V + E_A \tag{1}$$

The mean spectrum was first calculated from all of the calibration spectra and then subtracted from every calibration spectrum. Mean centering would enhance the subtle differences between the spectra. Since eigenvector methods calculate the principal components based on changes in the absorption data, the ability of the calculation to detect the differences between the calibration spectra would improve the model. When the PCA algorithm has processed the training data, it is reduced to two main matrices; the eigenvectors and the scores.

The matrix expression of the PCR model for the spectral data can be obtained by equation (1)

$$A = S\,V + E_A \tag{1}$$

where A=spectral absorption matrix (n by w), S=score values matrix (n by m), V= eigenvector matrix (m by w), E_A=residual spectra matrix (n by w), n=number of spectra, w=number of wavelengths, m=number of principal component eigenvectors.

As the scores in the S matrix are calculated from each spectrum and a spectrum is represented by a collection of absorption at a series of wavelengths, it is possible to regress concentrations against the score matrix as equation (2).

$$Y = C\,S' + E_Y \tag{2}$$

where Y=constituent concentrations matrix (p by n), C=regression coefficients matrix (p by m), E_Y=error matrix (p by n), p=number of constituents for calibration. As with least square regression, the coefficients matrix can be solved by the regression equation (3). Prime indicates the transpose of the matrix.

$$C = Y\,S\left(S'\,S\right)^{-1} \tag{3}$$

From equation (1), the score matrix of the spectra can be obtained by equation (4) after eliminating the noise error matrix.

$$S = A\,V^{-1} = A\,V' \tag{4}$$

For the equation (4), the transpose matrix of V can substitute its inverse matrix because V matrix of eigenvector is an orthonormal matrix. By combining the concentration equation (2) with the score equation (4), the PCR regression equation can be obtained as equation (5).

$$Y = C\;\;V\,A' + E_Y \tag{5}$$

As described above, the PCR is a two-step process, the PCA eigenvectors and scores, which represent the largest common variations among all the spectra in the calibration data, are calculated first and then the scores are regressed against the constituent concentrations using a regression method. A PCR model should be built by performing a selection on the scores to determine which factors should be used to build a model for each constituent.

3. Results and discussion

The meat samples were excised from the longissimus muscle of 119 beef animals, with tenderness ranging from 2.01 kg_f to 11.7 kg_f (measured in WB shear force). The mean WB shear force of the samples and its standard deviation were 5.46 kg_f and 2.21kg_f, respectively. For the shear force prediction, the coefficients of

determination (r^2) of the best PCR models were determined by applying the cross-validation procedure.

3.1 NIR reflectance characteristics of longissimus muscle

Figure 1 shows that the tough meat (shear force, 11.7 kg_f) had a higher absorption than the tender meat (shear force, 3.8 kg_f) at most wavelengths, particularly for the wavelengths between 1100 and 1350 nm. This is similar to the result of a previous report by Hildrum et al. [18].

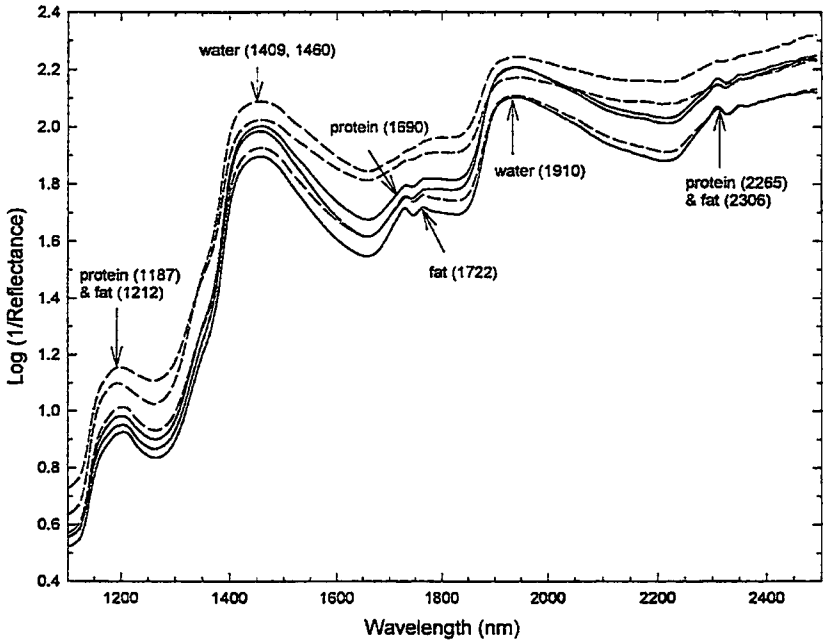

Figure 1: Near-infrared reflectance spectra of longissimus muscles for tenderness measurement. The shear force values of the samples were 3.8 kg_f (tender; solid line) and 11.7 kg_f (very tough; dash line)

Obvious absorption differences existed between tough and tender meats at protein absorption bands at 1187, 1690, and 2265 nm; fat absorption bands at 1212, 1722, and 2306 nm; and water absorption bands at 1409, 1460, and 1910 nm, respectively. Significant variations in spectra among samples from the same steak were also found. This showed that a gradient in tenderness exists within the longissimus muscle and proved that a tenderness gradient exists within a steak obtained from the longissimus muscle [21,22,23]. In our model development, because the tenderness of each steak was represented by a WB shear force value for the steak, the spectra of disk samples sliced from each steak were averaged and used for the calibration and validation to minimize variation within the samples.

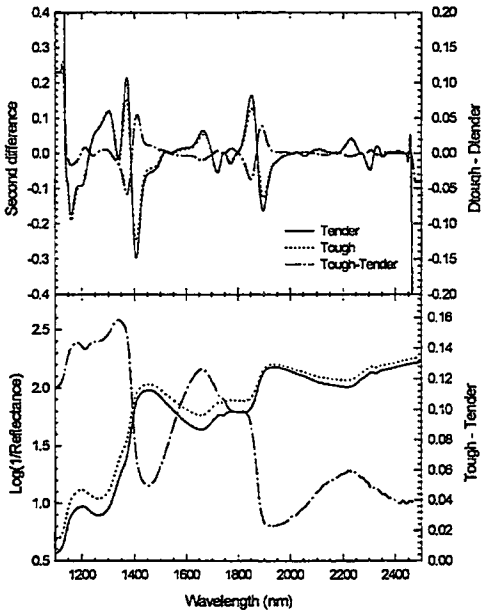

Figure 2: Absorption of near-infrared spectra and their second derivatives of tender and tough meat samples. The shear force values of each categories were tender (3.8 kg_f - 4.3 kg_f) and tough (10.1 kg_f - 11.7 kg_f)

Figure 2 shows the comparison of the absorbance between tender (3.8 - 4.3 kg_f) and tough (10.1 - 11.7 kg_f) meats and their second derivatives. As shown in the Figure 2 (bottom), the absorptions of tough meats were obviously higher than tender meats at all wavelengths. The peaks of the difference curve were mostly at the protein and fat bands. The smallest differences between tender and tough meats were found at the water bands. Thus, the tenderness of meats would be affected by the concentration of protein and fat constituents. At water bands (1450 and 1910 nm), the difference of absorption between tough and tender meats was minimal. Since the effects of the second derivatives of NIR spectra are resolution of overlapping peaks and removal of baseline variations [24], the second derivatives of spectra of tender and tough meat were compared as shown in the Figure 2 (top).

The wavelength bands, which occurred at the transition from maximum to minimum or the vice versa of the second derivatives of the spectra, were 1380 and 1870 nm.

3.2 Principal component analysis for meat tenderness

Principal component analysis (PCA) was used to reduce the contribution of noise in the modeling procedure and the absorption and second derivative spectra were used to correlate with WB shear force values of the meat. Figure 3 shows the first three principal components extracted from the calibration data set of the absorption spectra. For the 1st principal component (or the first factor) from the absorption spectra, the most significant variance from the spectra of tough and tender meats was due to absorptions of fat at 1212, 1722 and 2306 nm; protein at 1187 nm; and water at 1910 nm. In the 2nd factor, the peaks of absorption were also found at 1458 nm for protein and 1460 and 1910 nm for water. As shown in the 3rd factor of Figure 3, the high absorption bands of fat were found clearly at the wavelengths of 1212, 1722, 1760, and 2306 nm. Also, high absorption peaks were observed at 1910 and 2345 nm of water and protein, respectively.

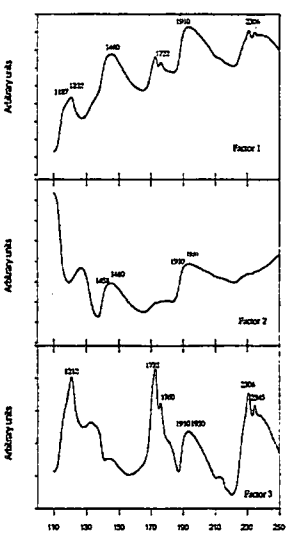

Figure 3: First three principal components extracted from the calibration data set of the NIR spectra

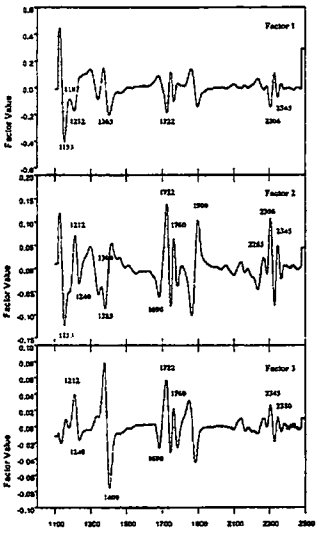

Figure 4: First three principal components extracted from the calibration data set of the second derivative NIR spectra

Figure 4 illustrates the absorption wavelength bands of the second derivative spectra of the longissimus dorsi meat cuts. It shows that the major contribution to the variance among the tough and tender meats was from fat absorptions. For the 1st principal component, the peaks occurred at the fat absorptions at 1212, 1722, and 2306 nm, and the protein absorptions at 1187, 1365, and 2345 nm. The distinctive fat absorption peaks at 1212, 1722, 1760, and 2306 nm occurred in the 2nd factor. The water absorption at 1900 nm, the fat or protein absorption at 2265 nm, and the protein absorption at 2345 nm were also presented in the 2nd factor of the second derivative spectra of the meat. The valleys in the 2nd factor of the second derivative spectra indicated the importance of water absorption at 1153 nm and protein absorption at 1240, 1385, and 1690 nm even if these peaks were not significant compared to the wavelength bands of fat absorption. For the 3rd factor. the absorption bands for fat and protein were significant at 1212, 1722, 1760, and 2380 for fat and 1240, 1690, and 2345 nm for protein, respectively.

3.3 PCR model for meat tenderness prediction

Based on the absorption spectra, log(1/R) and their second derivatives, principal component regression (PCR) models for predicting tenderness (WB shear force) were developed. Ranges of wavelengths were selected for the models. When the absorption spectra between 1100 nm and 2498 nm were used, the coefficient of

determination (r^2) of the PCR model to predict WB shear force tenderness was 0.692. When the spectra between 1100 nm and 1350 nm were analyzed, the r^2 was 0.612. The r^2 was 0.535 when 4 wavelength bands of 1567 to 1617 nm, 1663 to 1713 nm, 1829 to 1879 nm, and 2115 to 2165 nm (selected from the multivariate data analysis) were used (Figure 5). When the second derivatives of the spectra were used for developing the PCR models for predicting the WB shear force of the meats, the r^2 was slightly better than the model with absorption spectra between 1100 and 1350 nm wavelength bands. When the full spectral range of 1100 to 2498 nm was used, the r^2 of the PCR model to predict WB shear force of the meat was 0.633. The r^2 was 0.616 when the second derivatives of the spectra of wavelengths between 1100 and 1350 nm were selected (Figure 6).

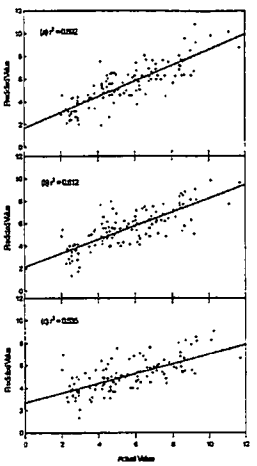

Figure 5: Beef longissimus muscle tenderness prediction by NIR spectroscopy using PCR model for the wavelength of (a) 1100- 2498 nm; (b) 1100 - 1350 nm; (c) selected 4 wavelengths with 1567 - 1617 nm, 1663 - 1713 nm, 1829 - 1879 nm, and 2115 - 2165 nm

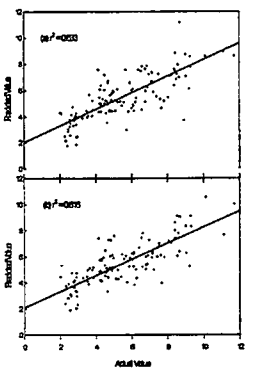

Figure 6: Beef longissimus muscle tenderness prediction by NIR spectroscopy using PCR model for the second derivative of wavelengths with (a) 1100 - 2498 nm; (b) 1100 - 1350 nm

Summary and conclusions

An objective, nondestructive and rapid technique for assessing beef tenderness needs to be developed. The principal component regression (PCR) technique was utilized to determine cooked meat tenderness using NIR reflectance measurement on raw meat. The tough meat (shear force, 11.7 kg_f) had an overall higher absorption than the tender meat (shear force, 3.8 kg_f) at most wavelengths,

particularly for the wavelengths between 1100 and 1350 nm. There existed obvious absorption differences between tough and tender meats at protein absorption bands at 1187, 1690, and 2265 nm; fat absorption bands at 1212, 1722, and 2306 nm; and water absorption bands at 1409, 1460, and 1910 nm.

For the 1st principal component from the absorption spectra, it can be seen that the most significant variance from the spectra of tough and lean meats was due to the fat absorptions at 1212, 1722, and 2306 nm and water absorption at 1930 nm. For the 2nd principal component of the second derivative spectra of the meat, the distinctive absorption peaks due to fat absorption at 1212, 1722, 1760, and 2306 nm; water at 1,900 nm; fat or protein at 2265 nm; and protein at 2345 nm were also presented. In this factor, significant absorption was found for water at 1153 nm and protein at 1240, 1385, and 1690 nm.

Based on the absorption spectra, log(1/R), the coefficient of determination (r^2) of principal component regression (PCR) model to predict Warner-Bratzler (WB) shear force tenderness was 0.692 when the absorption spectra between 1100 nm and 2498 nm were used. In case of the second derivatives of the spectra, the r^2 was 0.633 when the full spectral range of 1100 to 2498 nm was used. In this study, the biochemical constituent composition of fat and protein were identified as absorbers of NIR spectra. Other factors that affect meat tenderness such as collagen, connective tissue amount should be studied for better understanding how those parameters would be correlated with the absorption of NIR spectra.

References

[1] J.B. Morgan, J.W. Savell, D.S. Hale, R.K. Miller, D.B. Griffin, H.R. Cross, and S.D. Shackelford. 1991. National beef tenderness survey. *J. Anim. Sci. 69:3274-3283.*

[2] M. Koohmaraie, T. L. Wheeler, and S. D. Shackelford. 1994. Beef Tenderness: regulation and prediction. In Beef Vanguard 94. *International Congress Buenos Aires, Argentina. 18 pages.*

[3] M.F. Miller, K.L. Huffman, S.Y. Gilbert, L.L. Mammon, and C.B. Ramsey. 1995. Retail consumer acceptance of beef tenderized with calcium chloride. *J. Anim. Sci. 73(8): 2308-2314.*

[4] J.B. Morgan, J.B. 1992. *The Final Report of the National Beef Quality.* Audit-1991. Colorado State University.

[5] J.W. Savell and S.D. Shackelford. 1992. Proc. *Recip. Meat Conf. 45:43.*

[6] I. Ben-Gura, and K.H. Norris. 1968. *Direct spectrophotometric determination of fat and moisture in meat products.* J. Food Sci. 33:64.

[7] W.G. Kruggel, R.A. Field, M.L. Riley, H.D. Radloff, and K.M. Horton. 1981. *Near-infrared reflectance determination of fat, protein, and moisture in fresh meat.* J. Asso. Off. Anal.Chem. 64:692.

[8] M. Iwamoto, K.H. Norris, and S. Kimura. 1981. *Rapid prediction of chemical compositions for wheat, soybean, pork, and fresh potatoes by near-infrared spectrophotometric analysis.* Nippon Shokuhin Kogyo Gakkaishi 28:85.

[9] E. Lanza. 1983. *Determination of moisture, protein, fat, and calories in raw pork and beef by near infrared spectroscopy.* J. Food Sci. 48:471.

[10] J.A. Renden, S.S. Oates, and R.B. Reed. 1986. Determination of body fat and moisture in dwarf hens with near-infrared reflectance spectroscopy. *Poultry Sci. 65: 1539-41.*

[11] E.V. Valdes and J.D. Summers. 1986. Determination of crude protein and fat in carcass and breast muscle samples of poultry by near-infrared reflectance spectroscopy. *Poultry Sci. 65:485-490.*

[12] B.P. Marks, and H. Chen. 1996. *Endpoint evaluation of the previous thermal treatment of cooked meat via near-infrared spectroscopy.* ASAE Paper No. 966064. ASAE, St. Joseph. MI.

[13] M. Mitsumoto, S. Maeda, and T. Mitsuhashi. 1991. Near-infrared spectroscopy determination of physical and chemical characteristics in beef cuts. *J. Food Sci. 56(6):1493-96.*

[14] Y.R. Chen and D.R. Massie. 1993. Visible/near-infrared reflectance and interactance spectroscopy for detection of abnormal poultry carcasses. *Trans. of the ASAE 36(3): 863-869.*

[15] Y.R. Chen, B. Park, and R.W. Huffman. 1994. *Instrument inspection of poultry carcasses.* ASAE Paper No. 946026. ASAE, St. Joseph, MI.

[16] Y.R. Chen, R.W. Huffman, and B. Park. 1996. Changes in the visible/near-infrared spectra of chicken carcasses in storage. *J. Food Process Engineering 19: 121-134.*

[17] Y.R. Chen, B. Park, M. Nguyen, and R.W. Huffman. 1996. Instrumental system for on-line inspection of poultry carcasses. *SPIE 2786: 121- 129.*

[18] K.I. Hildrum, B.N. Nilson, M. Mielnik, and T. Naes. 1994. Prediction of sensory characteristics of beef by near-infrared spectroscopy. *Meat Sci. 38: 67-80.*

[19] H.W. Ockerman, C.J. Pierson, and R.R. Hodges. 1981. Design and evaluation of a modified shear head for the Warner-Bratzler shear to evaluate tenderness of cooked ground beef patties. *J. Food Sci. 46: 1948-1949.*

[20] Y.R. Chen, M. Nguyen, and B. Park. 1997. *Improving performance of neural network classifiers by input data pretreatment with principal component analysis.* ASAE Paper No. 973050, ASAE, St. Joseph, MI.

[21] R.L. Alsmeyer, J.W. Thornton, and R.L. Hiner. 1965. *Some dorsal-lateral location tenderness differences in the longissimus dorsi muscle of beef and pork.* J. Anim. Sci. 24:526.

[22] N. Sharrah, M.S. Kunze, and R.M. Pangborn. 1965. *Beef tenderness; Comparison of sensory methods with the Warner-Bratzler and L.E.E.-Kramer shear presses.* Food Technol. 19:238.

[23] G.C. Smith, Z.L. Carpenter, and G.T. King. 1969. *Considerations for beef tenderness evaluation* J. Food Sci. 34:612.

[24] W.R. Hruschka. 1987. *Data Analysis: Wavelength selection methods.* In: Near-Infrared Technology in the Agricultural and Food Industries. (in. Eds. P.C. Williams and K.H. Norris), Am. Assoc. Cereal Chem. St. Paul, MN: 35-55.

Part 7

NIR spectrometry

Spectrometer techniques for process analysers

Techniques spectrométriques pour l'analyse de procédés

Markku Känsäkoski, Pentti Niemelä, Mauri Aikio, Jouko Malinen and Jouni Tornberg

VTT Electronics, P.O. Box 1100, FIN-90571 Oulu, Finland
e-mail: markku.kansakoski@vtt.fi

Abstract: *The use of optical spectroscopic methods for quantitative composition measurements in process control is increasing rapidly and the use of imaging spectroscopy for visual inspection and piece sorting is growing even faster. A number of different optical configurations are in use today and many more are being developed to accomplish the wavelength selectivity needed in spectroscopic methods. The development of compact and rugged spectrometers has been one of the major tasks of the optical measurements research team at VTT Electronics. Some of the techniques developed will be presented in this paper.*

Keywords: *Spectrometer, on-line measurement, process analyser.*

Résumé : L'utilisation de méthodes de spectroscopie optique pour mesurer la composition des produits en contrôle de procédés s'accroît rapidement. L'utilisation de vision multispectrale pour l'inspection visuelle et le tri de pièces connaît également un fort développement. Différentes configurations optiques sont mises en oeuvre et bien d'autres sont en cours de développement pour sélectionner les longueurs d'onde en spectroscopie. Le développement de spectromètre compact et robuste a été l'une des activités majeures de l'équipe de recherche sur les mesures optiques à VTT Electronics. Certaines de ces techniques sont présentées dans cet article.

1. Introduction

Several optical configurations are in use or being developed to achieve the wavelength selectivity needed in spectroscopic measurement methods (Table 1) [1]. A large number of possible configurations makes it rather difficult to determine the best instrument for each application. This is difficult enough with laboratory applications and even more difficult with on-line applications. The selection procedure involves specifying such factors as wavelength range, wavelength resolution, dynamic range and measurement time. In addition to these, on-line applications have some special requirements, e.g. ruggedness, stray light rejection and sample presentation. Most existing near infrared (NIR) analysers employ either a rotating filter wheel or mechanically scanned diffraction grating. These types of analysers are not very well suited for measuring fast moving process streams. Many of these instruments have been developed to be versatile and can thus be regarded as mainly research grade instruments. Due to the versatility demand and the use of moving parts these devices are likely to be rather expensive and their construction large and fairly complicated. The approach for process applications has often involved mounting the laboratory instrument in a special housing, which will further increase the cost.

	Fixed wavelengths	Full spectrum measurement
Scanning:	Filter wheel LEDs and lasers (also parallel) Acousto-optical filter	Tilting filter Variable wavelength filter Oscillating grating Acousto-optical tuneable filter LED array and monochromator Tuneable lasers Fabry-Pérot interferometer
Scanning parallel:		Moving mirror interferometer Hadamard transform spectrometer
Parallel:	Multichannel detector	Spectrograph and detector array Spatial interferometer

Table 1: Techniques for wavelength separation in spectroscopic instruments

The rapidly extending recognition and acceptance of NIR (and other spectroscopic methods) as a real problem solver and the increasing number of proven applications are creating a new kind of market: a market for specific spectroscopic analysers and sensors featuring fixed operational parameters (wavelength or

wavelength range, resolution and sample presentation) for each specific application. The solutions offered by research grade instruments are too cumbersome and expensive for on-line purposes.

The Optoelectronics Research Area of VTT Electronics is using optoelectronic hybrid integration to develop compact and low cost, while still high-performance techniques that can be used as OEM modules for spectroscopic analysers and sensors. This paper describes three hybrid techniques that are based on a multiple detector and either a detector or light emitting diode (LED) arrays, providing parallel or nearly parallel measurement at each wavelength without any moving optical or mechanical parts. This kind of constructions inherently offer high resistance to environmental stresses.

2. NIR and MIR instruments for process applications

Three optoelectronic techniques developed especially for process and field instruments will be described in the following paragraphs. The first configuration is an integrated module based on an array of LEDs and a fixed grating monochromator. This construction enables electrical wavelength scanning and overcomes the main problems affecting the use of LEDs in analytical instruments, i.e. wavelength and response instability and unit to unit wavelength variations. Together with a large area detector, this technique is especially suitable for near-infrared transmission instruments using short-wave NIR. The module operating between 832 and 1048 nm with a resolution of 12 nm measures one spectrum in milliseconds; the dimensions of the solid glass construction are 5 x 5 x 7 cm.

VTT has designed a novel spectrograph for use with linear and matrix detectors in post-dispersive applications, in which the wavelength separation takes place on the detector side of the analyser. The spectrograph module employs a dispersing prism-grating prism (PGP) element. The element is composed of a volume transmission holographic grating, which is glued between two prisms. The basic idea of the PGP element with two identical prisms is that the central wavelength of the specified wavelength range passes through the element without any radial or angular deviations. All the optical components are positioned on the optical axis and the spectrum is formed perpendicular to the optical axis with a good linearity, while the location of the spectrum is insensitive to slight tilting errors in the mounting of the PGP components. Thanks to these features the spectrograph is compact, easy to assemble and adjust, thus fairly inexpensive to manufacture. Equipped with a 2-dimensional detector matrix, e.g. charge coupled device (CCD), it forms a compact imaging spectrometer.

The integrated multichannel detector technique offers several advantages over the conventional filter wheel construction in applications requiring only a few wavelengths. It enables an exactly simultaneous measurement at each wavelength and provides a rugged construction without any moving parts. Two to four

wavelength channels can be integrated into a TO-8 window package. The technique has been implemented in several processes and in truly hand-held NIR analysers.

2.1 LED-array spectrometer

Light emitting diodes are promising radiation sources for spectroscopic analysers: they are superior to incandescent lamps thanks to their longer lifetime, high brightness, low power consumption and possibility for electrical modulation. VTT Electronics has recently developed a LED array spectrometer design optimised for high-performance hand-held analysers and process analyser applications.

The design employs a powerful temperature-stabilised 32-element NIR LED array source comprising various types of surface-emitting LEDs. The grating monochromator optics are optimised for low stray light and high optical throughput. The assembly procedure includes methods for adjusting and permanently fixing the wavelength scale to target specifications. In this case, the range from 832 to 1048 nm was selected. A fibre optic bundle serves as an exit slit and delivers the exit beam to a sample illumination unit. This solution allows direct illumination of the sample in various transmittance, reflectance and transflectance measurement applications. Optical detection is normally arranged with a single large-area low-noise silicon pin diode detector. Control electronics can be integrated with the unit, depending on application requirements. Figure 1 illustrates the operating principle of the LED array spectrometer in transmission measurement mode.

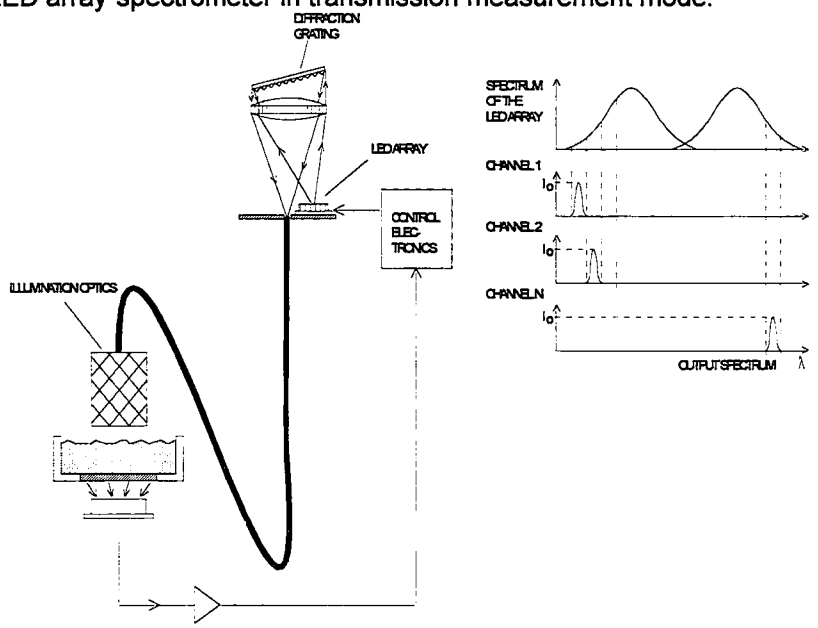

Figure 1: The operating principle of the LED array spectrometer

High optical output is an essential requirement for the LED spectrometer to achieve a good signal-to-noise ratio (SNR) in the transmission measurements on high-absorbance samples. The optical output was measured for each wavelength channel separately. The corresponding LED was turned on by supplying a dc current of 50 mA. The output beam was measured at the exit end of the fibre bundle using an optical radiometer fitted with a calibrated 1 cm^2 silicon sensor. Figure 2 presents a comparison of the optical output of the developed prototype unit with the corresponding data of the previous design [2]. The improvement in the measured output is remarkable, about two decades in the short-wave and long-wave ends of the scale and by a factor of 2 ... 5 for the central bands. The measured output ranges from 6 to 76 μW. The loss in the 0.5 m long fibre bundle is included in these power figures ($T_{fibre} \approx 50$ %). Figure 3 illustrates a typical wavelength scale of a LED spectrometer unit, ranging from 832 to 1048 nm.

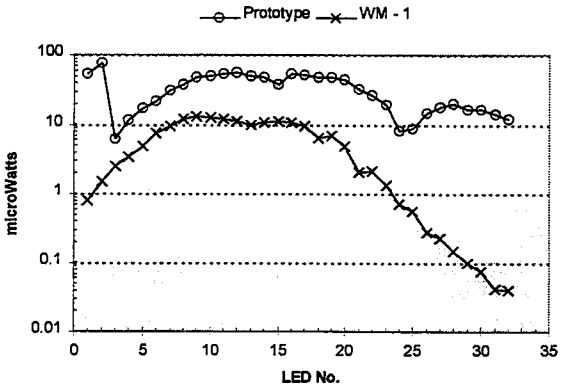

Figure 2: LED spectrometer output power data, prototype of new design compared with an older design (WM-1)

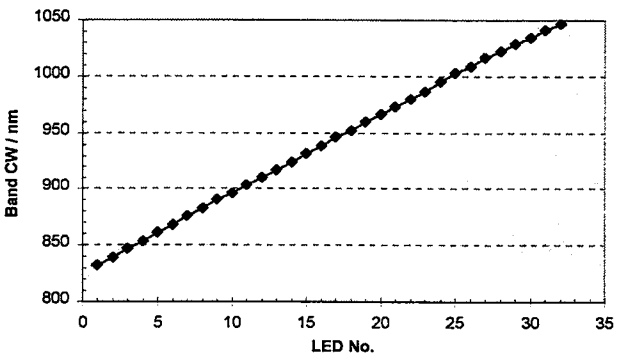

Figure 3: The wavelength scale of the LED spectrometer unit

The developed LED array based spectrometer unit provides 32 electrically scanned wavelengths ranging from 832 to 1048 nm for use in spectroscopic composition analysers. Extensive testing was arranged to thoroughly examine the performance of the developed unit, covering performance in normal operating conditions, characteristics vs. temperature, unit-to-unit variation and preliminary environmental testing. Table 2 summarises the main characteristics.

The combination of technical performance, small size, rugged construction and the potential for low manufacturing costs make the unit developed by VTT a promising alternative for developing competitive high-performance analysers for various NIR applications. The most potential applications of the LED spectrometer are expected to be hand-held composition meters as well as spectroscopic sensors for process automation. The applications with a LED array spectrometer using a short-wave NIR wavelength range are especially suitable for measuring the content of moisture, oil or fat, protein and sugar on optically thick samples (grain, meat, fruit, etc.).

❑ typical optical output from 6 to 76 μW per band, up to 2 decades of improvement compared to the previous design
❑ capability of at least 7 decades of dynamic range in transmission measurements (i.e., SNR in excess of 1000 with 4A sample)
❑ stable output due to integrated temperature stabilisation of the LED array
❑ band CW unit-to-unit tracking much better than with interference filters
❑ minimum drift in band CW vs. operating temperature
❑ optical stray light approximately 0.1 % for majority of bands

Table 2: The main figures of performance for the developed LED spectrometer unit

The developed spectrometer technology is not limited to the current short-wave NIR design. A module for mid-infrared (MIR) wavelengths has also been developed [3]. The wavelength scale can be modified to meet various application requirements. The main limitations for potential applications are the availability of LEDs for the light source and monochromator design. At present, commercial high-efficiency LEDs cover wavelengths from blue 400 nm to at least 2500 nm in the near-infrared region. Figure 4 illustrates the wide variety of different wavelengths of commercially available LEDs. Modifying the spectrometer design to cover new wavelength regions could, in addition to increasing the number of applications for spectroscopic analysis, extend the scope of applications to colorimetry, as well.

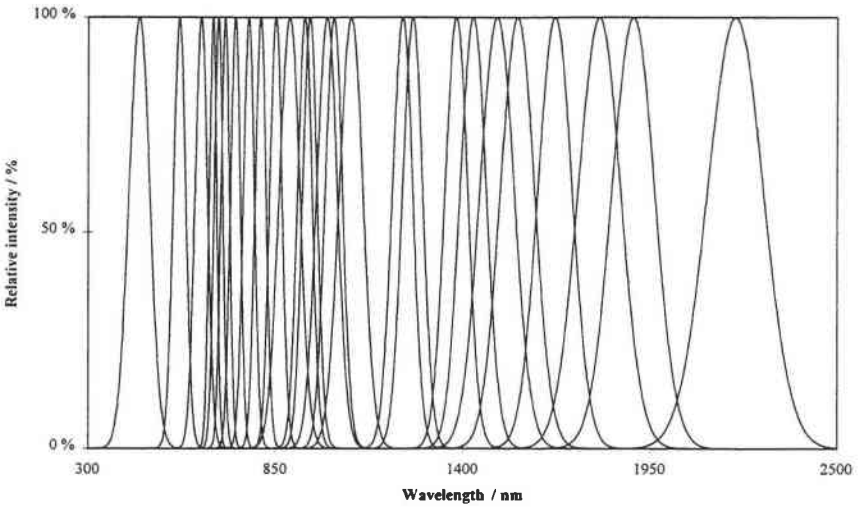

Figure 4: Commercial LEDs cover visible and NIR wavelengths

2.2 Imaging spectrometer

The compact spectrometer module employs the well-known construction of a spectrograph with an array or a matrix detector. The construction, which is very simple to assemble and adjust, features a PGP component using on-axis optics only offering minimised aberrations. Equipped with a matrix detector (e.g., CCD), it forms a compact imaging spectrometer, which provides significant advantages compared with a colour line scan camera: a high spectral resolution and additional information beyond the visible region. One dimension of the array detector constitutes a line image through the entrance slit, while the other dimension is used to measure the spectrum of each line image element (Figure 5). If the target is a moving object (e.g., web or process stream) a full spectral image can be formed. Imaging spectroscopy is a new versatile and powerful method for efficient simultaneous measurement of spatial and spectral maps of various objects.

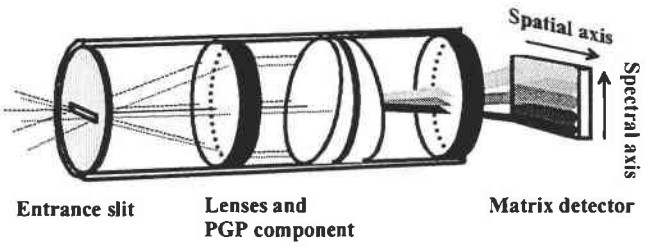

Figure 5: Schematic of an imaging PGP spectrograph construction using a matrix detector

This imaging spectrometer module provides a unique, simple and cost-effective means of adding spectral resolution to an existing B/W (black and white) vision system, allowing use with already installed systems (for example shape or dimensional inspection originally) and new installations alike. The module fits directly onto a standard B/W CCD camera via the C-mount and converts it to a spectral line imaging camera, in which each frame includes one spatial line image at multiple wavelengths. This offers a low-cost solution for adding colour information to machine vision systems. The principle of this concept is presented in Figure 6.

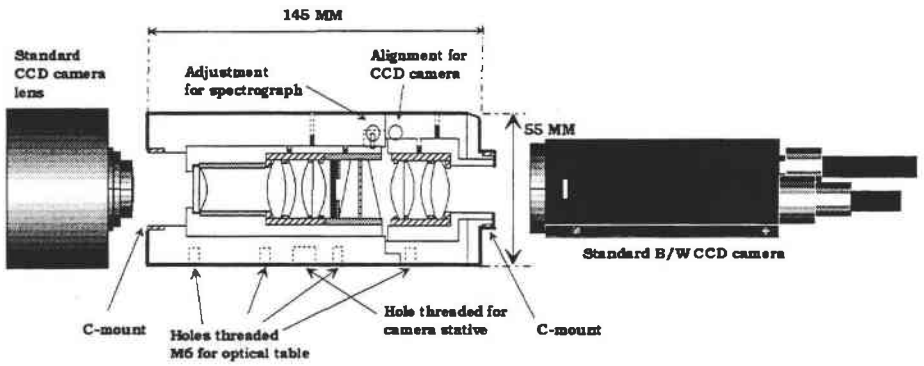

Figure 6: The simplest version of imaging PGP spectrograph: The spectrograph optics can easily be assembled between a standard CCD camera lens and a B/W CCD camera with a C mount

The PGP technique can be employed in the wavelength region ranging from 340 nm over the visible region to the NIR up to 2400 nm. The silicon detector technology, covering wavelengths from UV to 1100 nm, is the most advanced and mature matrix detector technology using either diode or CCD matrixes. The spectral resolution is typically 5 nm over a spectral range of 300 nm.

Since imaging PGP spectrographs have been constructed for some time for airborne applications, in addition to on-line process control and quality inspection purposes, they are now commercially available [4,5,6]. An imaging spectrograph instrument for ultraviolet - near-infrared microspectroscopy has also been developed for laboratory use, consisting of two PGP spectrographs for VIS and NIR and an UV spectrograph based on reflective concave grating [7].

Also a multichannel PGP spectrograph for fibre optic remote spectroscopy has been developed [8,9]. By replacing the entrance slit with an array of fibres, a fibre-optic multiplexer system with up to 30 channels can be built without any moving parts. The design is presented in Figure 7.

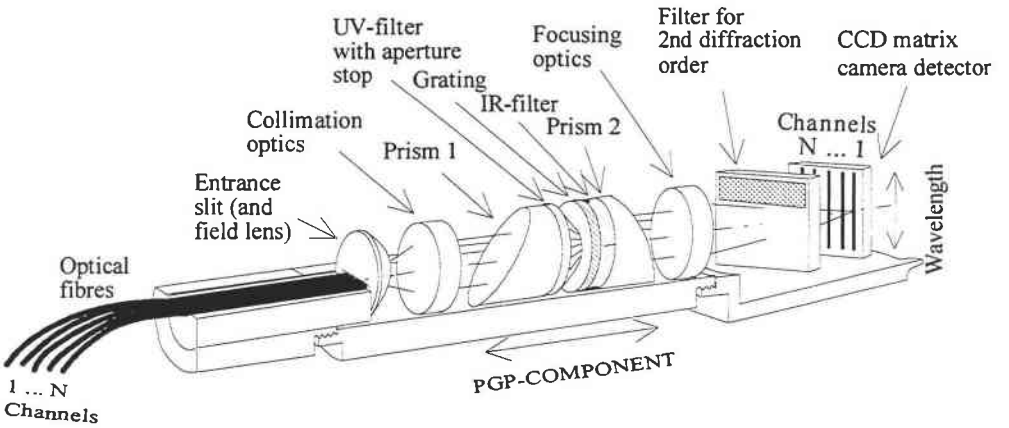

Figure 7: A multipoint spectrograph, comprising a CCD matrix camera and a specially designed imaging PGP spectrograph connected with N optical fibres

Detector technologies (Ge, InGaAs, PbS and PtSi) covering the upper NIR region are becoming more feasible for industrial applications, especially those requiring only a limited spectral region, which can be covered by arrays of a few or a few dozens of elements. Commercial InGaAs matrix detectors and cameras are now available for wavelengths ranging from 850 to 1700 nm in different formats, 128x128 pixels, 320x240 pixels and 256x256 pixels. As a result of the rapidly developing detector technology VTT Electronics has developed a new version of imaging spectrometer for NIR wavelengths (850-1750 nm).

2.3 Integrated multichannel detector

In applications requiring only few measuring channels, the integrated detector technique developed by VTT Electronics can be used instead of the traditional filter-wheel construction. The integrated detector has 2 to 4 parallel channels, each of them comprising a specific interference filter. The channel components are mounted on a metal frame, each channel in a chamber of its own for preventing optical crosstalk. The metal frame is mounted on a Peltier cooler for stabilising the temperature below the ambient; a bead thermistor is used for temperature measurements. All these components are mounted in a hermetically sealed window package (Figure 8).

The technique developed at VTT Electronics offers obvious advantages for process applications as well as for hand-held devices. It provides a small and rugged instrument construction without having to use any moving parts in the case, while electronic chopping techniques can be used. The interference filters, which are often made of soft and even hygroscopic materials, are well-protected against ambient stresses in the hermetic package. The parallel channels provide an exactly

simultaneous measurement at each wavelength, thus minimising the noise caused by rapid variations in fast moving process streams.

Our multichannel detector construction can be used over a wide spectral range from UV to IR by selecting the detector type and the window material according to the specific need. Up to now we have used mainly PbS and PbSe detectors in the 1-5 μm spectral region. The temperature of these photoconductive detectors has to be stabilised carefully, because of their high temperature coefficient 2-5 %/°C. In our construction, the change of the ratio of the channel signals caused by variations of the ambient temperature is typically ca. 100 ppm/°C.

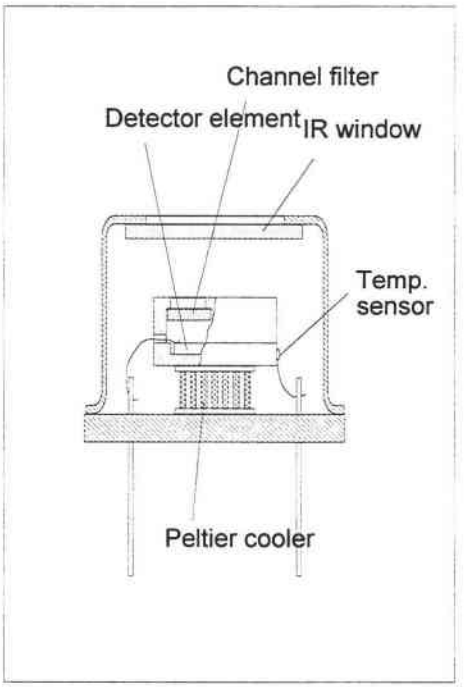

Figure 8: Schematic of an integrated two-channel detector

VTT Electronics has developed several process analysers based on multichannel detector techniques. One of the applications was developed for measuring the on-line water content of lubricating oils in circulating oil systems [1]. The measuring wavelength band was selected at 2.95 μm, where the broad water absorption band has its maximum, and the compensating wavelength band at the adjacent wavelength region, where water has a negligible absorption. The length of 0.5 mm was selected for the transmission path of the flow-through cell to give a fairly linear response over the 5000 ppm measurement range with a detection limit of 50 ppm. The two-channel system compensates for the turbidity caused by solid particles

and air bubbles as well as emulsified water, thus making it possible to measure true water absorption.

The potential of this technique has not yet been fully utilised and new industrial analysers for demanding applications are under development. One of the newest applications is a four-channel hand-held analyser, which is showing promising results in measuring the maturity of vegetables (Figure. 9). The standard error of calibration (SEC) is as low as 1.0 %, which is adequate for pea maturity measurements.

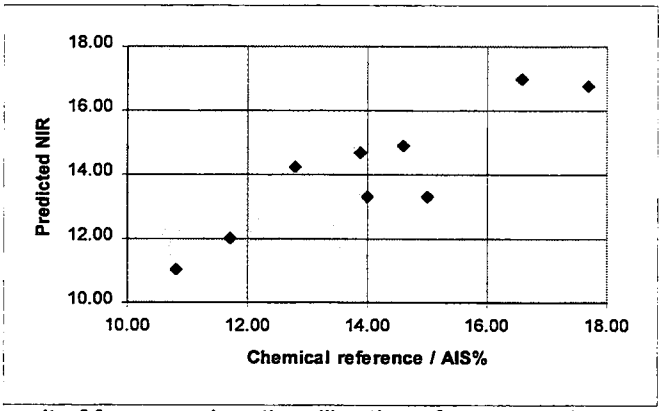

Figure 9: Result of four wavelength calibration of pea maturity measured with a multichannel detector prototype

Conclusion

The hybrid integrated optoelectronic techniques presented in this paper provide new ways of implementing smaller, more compact, rugged, while still less expensive spectroscopic analysers, guiding the way from spectroscopic instruments to spectroscopic sensors.

Both the LED array technique and the integrated multichannel detector technique offer obvious advantages for spectroscopic analysers in process applications and portable instruments alike. The LED array technique is especially suitable for NIR instruments in the 800-1060 nm region, while new and powerful LEDs are offering new opportunities for using NIR wavelengths up to 2500 nm and, furthermore, for colorimetric applications alike. These provide a compact light source without any moving parts, allowing electrical scanning of the wavelength, with a resolution better than the bandwidth of the LEDs, and in which the stability problems of the LED emission spectrum can be overcome. In the upper NIR region, the multichannel detector technique makes the rotating filter wheel redundant. This technique has been successfully used in developing high-performance hand-held instruments, and process analysers requiring exactly simultaneous measurement at each wavelength.

The third technique described in this paper, the imaging spectrometer, is a new and potential tool for industrial measurements providing enhanced possibilities and advantages over conventional instruments. It has already been applied to adding spectral resolution to existing B/W (black and white) vision systems, in on-line process control and quality inspection applications and for airborne use. The NIR (850-1700 nm) imaging spectrometer developed recently is a powerful tool for measuring the chemical composition (e.g., moisture, fat, protein) of process streams. It is capable of measuring not only the true composition but also the distribution of this composition in real time, providing a full coverage of the whole process stream.

The hybrid integrated optoelectronic techniques presented in this paper provide a new means of developing specific process analysers and hand-held instruments to supplement the present supply of versatile research spectrometers and laboratory analysers. We expect that after the first successful demonstrations there will be a rapidly increasing market for small, rugged, easy-to-use and low-cost analysers for a variety of applications in e.g. food industry and agriculture, pulp and paper industry, petrochemical industry and environmental monitoring.

References

[1] T. Hyvärinen and P. Niemelä, 1991. *Rugged multiwavelength NIR and IR analyzers for industrial process measurements, SPIE, Vol. 1266, pp. 99-104.*

[2] M. Känsäkoski, 1991. 32-kanavainen NIR-analysaattori, MSc Thesis, The University of Oulu, p. 43.

[3] J. Malinen, T. Hannula, N.V. Zotova, S.A. Karadandashov, I.I. Markov, B.A, Matveev, N.M Stus, G.N. Talalakin, 1993. *Nondispersive and multichannel analyzers based on mid-IR LEDs and arrays, SPIE, Vol. 2069, pp.95-100.*

[4] E. Herrala, J. Okkonen, T. Hyvärinen, M. Aikio and J. Lammasniemi, 1994. *Imaging spectrometer for process industry applications, SPIE, Vol. 2248, pp. 33-40.*

[5] O. Hagman, 1996. *On reflections of Wood, Wood quality features modelling by means of multivariate image projections to latent structures in multispectra images,* Doctoral Thesis, Luleå Univ. of Tech.

[6] B. Braam, J. Okkonen, M. Aikio, K. Mäkisara, J. Bolton, 1993. *Design and first test results of the Finnish Airborne Imaging Spectrometer for Different Applications (AISA), SPIE, Vol. 1937.*

[7] T. Johansson and A. Pettersson, 1997. *Imaging spectrometer for ultraviolet - near-infrared microspectroscopy, Rev.Sci.Instrum. 68 (5), pp. 1962-1971.*

[8] T. Vaarala, M. Aikio, H. Keränen, 1997. *An advanced prism-grating-prism imaging spectrograph in on-line industrial measurement, SPIE, Vol. 3101-38.*

[9] M. Aikio, T. Vaarala, H. Keränen, 1997. *Intelligent prism-grating-prism spectrograph for multipoint fibre optic remote spectroscopy, OSA, Technical Digest Series, 16, pp. 552-555,*

Influence of the optical configuration on model prediction performance for non-destructive measurement of fruit quality by means of NIR spectroscopy

Influence de la configuration optique sur la performance du modèle de prédiction pour la mesure non destructive de la qualité des fruits par spectroscopie NIR

Jeroen Lammertyn, Bart Nicolaï, Veerle De Smedt, Josse De Baerdemaeker

Flanders Centre for Postharvest Technology
Willem De Croylaan 42
B-3001 Heverlee
e-mail: jeroen.lammertyn@agr.kuleuven.ac.be

Abstract: *In this paper some issues related to the nondestructive measurement of apple quality attributes by means of NIR reflectance spectroscopy are addressed. In a first experiment the penetration of NIR radiation in apple tissue is investigated. It is shown that the intensity of the light source is high enough to penetrate through the skin of the apple and the gather information about the apple parenchym. In a second experiment a comparison is made between two optical configurations which can be used to perform the measurements: the bifurcated and the 0°/45° optical configuration. To this end, a relation has been established between the reflectance spectra (880-1650nm) and the quality parameter of the apple, the soluble solid content. Depending on the data preprocessing correlation coefficients between 79% and 91% were obtained. It was found that the results obtained with the bifurcated fiber were only marginally better than those obtained with the 0°/45° configuration.*

Keywords: *Quality, PLS, light penetration, sugar, optical configuration, apple.*

Résumé : Dans cet article sont discutés les problèmes de mesure non destructive de la qualité des pommes par NIR. Dans une première expérience, la pénétration d'une radiation NIR dans une pomme est étudiée : l'intensité de la source est suffisante pour pénétrer sous la peau et recueillir des informations dans le parenchyme. Dans une deuxième expérience, une comparaison est faite entre 2 configurations optiques : la fibre bifurquée et la configuration 0°/45°. Une relation a été établie entre le spectre de réflectance à 880-1650 nm et les paramètres de qualité des pommes tels que le taux de sucre. Des coefficients de corrélation de 79 à 91 % sont obtenus. Les résultats obtenus avec des fibres optiques bifurquées ne sont que faiblement supérieurs à la configuration 0°/45°.

1. Introduction

In recent years research has been focused on the development of non-destructive measurement techniques for quality attributes of apples such as pH, sugar content and firmness. The advantages of these techniques include fast execution, limited sample preprocessing, easy use in process control and grading systems. NIR-spectroscopy has been suggested recently as a non-destructive technique to measure quality parameters of various fruits and vegetables. NIR methods have already been used to detect bruises on apples (e.g., Upchurch et al., 1994; Pen et al., 1985). Kawano (1992) studied the sugar content in peaches with an optical fiber in interactance mode. Slaughter (1995) determined that visible and NIR-spectroscopy could be used to measure non-destructively the internal quality of peaches and nectarines as characterised by their SSC, sugar content, sorbitol content and chlorofyll content. Bellon-Maurel (1992) used the wavelength region between 800-1050 nm to built a model for sugar measurement. In a recent study, Moons et al. (1997) established a relation between NIR-spectra and apple fruit quality parameters such as acidity, pH and sugar content.

For internal quality measurements, it is important that the NIR radiation penetrates the apple tissue sufficiently. In literature only a few studies on this topic are mentioned. Chen en Nattuvetty (1980) measured the penetration depth by separating the source and the detector fiber by a black knife. On average the detector signal was fading away with a knife depth of 2.5cm. But the results were found to be strongly dependent on the wavelength, the intensity of the light source and the configuration of the spectrophotometer. Hother et al. (1995) followed the changes in reflectance properties of unpeeled apple disks with varying thickness. They found that , depending on the variety and the wavelength, the penetration depth varied between 0 and 7 mm. For Jonagold the maximum depth equaled 5.5 mm. However, the authors only considered a wavelength range between 480 and 800 nm. It should be observed that, even if the radiation sufficiently penetrates the apple tissue, it is required to separate the reflected radiation due to internal scattering from that due to specular reflection. Several optical configurations have been used in the literature, including bifurcated light guides and 0°/45° configurations. It is not clear how the configuration affects the quality of the calibration models.

The objective of this paper were (i) to evaluate the penetration of NIR radiation through apple skin, and (ii) to compare two optical configurations for measuring internal apple quality attributes by means of NIR reflectance measurements.

2. Materials and methods

Apples

The Elstar apples used for both experiments (70 apples) were purchased at a local auction and stored for 2 days in a climate room at 20°C and 70% relative humidity to equilibrate. For the calibration models 60 Elstar apples were used. From each apple four spectra (880-1650nm) with the bifurcated and with the 0°/45°-configuration (see further) were taken at exact the same position. The soluble solid content, which is strongly correlated with the sugar content, is measured at the same positions with a refractometer (PR-101 Palette Series, ATAGO CO., Ltd., Japan).

Reflectance measurements

For each apple 4 reflection spectra (880-1650 nm, wavelength increment 0.5 nm) were taken at four equidistant positions along the equator, with a spectrofotometer (Optical Spectrum Analyser (OSA) 6602, Rees Instruments Ltd., Godalming, UK). The light source consists of a 12V/100W tungsten halogenlamp (Phillips 7724.M/28) that can be used both in the visible and near infrared region. Two different optical configurations can be used. With the bifurcated optical configuration (type MIO-6134) the light is guided to the sample by source fibres, and from the sample with the detector fibres. In the head of the bifurcated cable the source- and detector fibers are situated randomly (see figure 1). The fiber has an active surface of 4 mm^2 and is held directly to the skin of the fruit which has the advantage of a higher light intensity. It can only be used in the wavelength range from 380 to 1650nm. The 0°/45° optical configuration (see figure 2) consists of a black box (type 6151) in which the source and the detector fibres are positioned under an angle of 45°. The incident beam falls perpendicularly onto the sample, to avoid specular reflection, and is detected under an angle of 45°. Since the illuminated surface is larger the intensity will be lower than with the bifurcated cable. In both cases the reflected light is divided into individual wavelengths by the diffracting gratings of the monochromator. Grating A (type 6632) is used for the wavelength range from 300 to 1080 nm and grating B (type 6633) for the range 1080-1650 nm. A silicon detector (type 6632) is used for the visible and the beginning of the near infrared range (300-1100 nm) and a PbS detector (type 6633) is used in the NIR range (1000-2000 nm). The signals are processed with software, model 6857 v1.30. The configuration is calibrated with a He/Ne laser and a spectrum from a $BaSO_4$-disc served as reference.

An average spectrum for each apple was calculated and the data were preprocessed by reducing the number of points of measurement and taking the second derivative using the method of Savitzky-Golay (Savitzky and Golay, 1964).

The second derivative or multiplicative scatter correction (MSC) is used to correct for additive and multiplicative effects in the spectra (Martens and Naes, 1987). The result was used together with the quality parameters in the statistical analysis. The technique used for the analysis of the spectral data is partial least squares (PLS). The calculations were executed with The Unscrambler, a statistical software package for multivariate calibration.

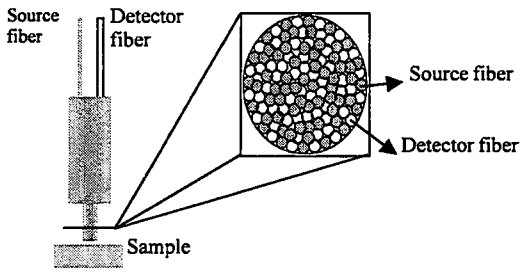

Figure 1: The bifurcated optical configuration

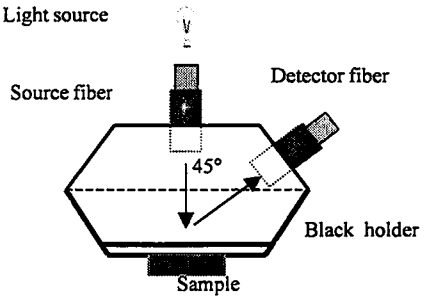

Figure 2: The 0°/45° optical configuration

Light penetration experiment

To obtain information about the light penetration properties an experiment based on earlier work of Lillesaeter (1982) was performed. Lillesaeter (1982) divides the information in a reflectance spectrum of a leaf into two components: information coming from the leaf and information coming from the background, being the ground. In this study the leaf surface is replaced by the skin of the apple and the background corresponds to the tissue under the skin

The total reflected radiation (R_R) consists of two components: the inherent skin component, R, which is the radiation reflected by the skin with a perfectly black background, and a background component, R', being the radiation reflected by a non black background, changed by transmission through the skin. With I the intensity of the incident light beam and τ the transmission of the skin the following formula can be derived:

$$R_R = R + R' = rI + r'\tau^2 I \qquad (1)$$

with r and r' respectively the reflectance of the skin and the background. The apparent reflectance of the skin is defined as:

$$r_s = \frac{R_R}{I} = r + r'\tau^2 \qquad (2)$$

Two measurements with a different background (D en L) are sufficient to solve the equations in the skin parameters τ^2 and r.

$$r_{sD} = r + r'_D \tau^2 \quad (3)$$

$$r_{sL} = r + r'_L \tau^2 \quad (4)$$

$$\tau^2 = \frac{r_{sD} - r_{sL}}{r'_D - r'_L} \quad (5)$$

$$r = r_{sD} - r'_D \tau^2 \quad (6)$$

All the measurements for this test were executed with the spectrophotometer as described above using the 0°/45° optical configuration. For this test a piece of the red and the green side of the apple were used. The skin is carefully isolated from the fruit flesh. This undamaged skin is used for the measurements with the different backgrounds.

3. Results and discussion

3.1 Light penetration experiment

Figure 3 shows the spectra of the different backgrounds. Remark that the black background is not perfectly absorbing and that the white background is not completely reflecting the incident radiation. The green background has a low reflection at 692nm, which is the typical absorption wavelength for chlorofyll. Both papers do also show water absorption bands at 1495nm. The wood has in addition a high absorption at 1180nm an other typical water absorption band.

Figure 4 shows the inherent reflectance, r, of a green and a red piece of apple skin as a function of the wavelength. For different combinations of two backgrounds (black and white, black and green, green and wood, ...) the system of two equations was solved to obtain the skin parameters, r en τ^2. The r values calculated on different measurements fall close to each other for one colour of the skin. On average the red skin gives higher inherent reflectance values than the green one and the chlorofyll absorption (692nm) is higher for the green skin, because the red side of the apple has seen more sunlight and is in a further ripening stage. The ripening is reflected in a decreasing content of chlorofyll.

The transmission, τ^2, is plotted as a function of the wavelength in figure 5 for green and red apple skin. The thin curves indicate the calculated values for τ^2. The two thick curves are the mean transmission curves. For the green apple skin, the mean transmission curve is strongly influenced in the colour range (400-700nm). This is a measurement error since by definition the value of τ^2 can never exceed 1 (or

100%). The mean τ^2 values for the two skin colours are almost equal. At first sight the two means seems to be quite different but taking only the NIR-range (800-2000nm) into account, τ^2 for the green skin is only a vertical translation compared to the red skin, which indicates that there is no large difference in transition properties of the red and the green skin. This additive effect is caused by light scattering (Williams et al., 1987) and can be corrected by MSC-correction techniques or by calculating a second derivative spectrum.

Figure 6 shows the reflectance spectra for the red apple skin with white and black background. Since the reflectance of a black background is very small, the inherent reflectance of the red apple skin has to be equal to the reflectance spectrum of the skin with the black background. This is shown by figure 6. This figure also illustrates that background information can be found in a NIR-spectrum, since the spectrum is dependent of the background. But also the fact that τ^2 differs from zero proves that light is penetrating through the skin. The area between the curve of the average inherent reflectance of the red skin and the reflectance spectrum of that skin with a certain background is an indicator for the amount of information coming from the background. Intuitively can be said that the amount of information from the background exceeds the amount of information from the skin, since the transmission coefficient is larger than the inherent skin reflectance. This experiment is also performed with a piece of apple tissue as background, which leads to the same conclusions. It can be concluded that a NIR-spectrum can contain information about the underlying fruit flesh.

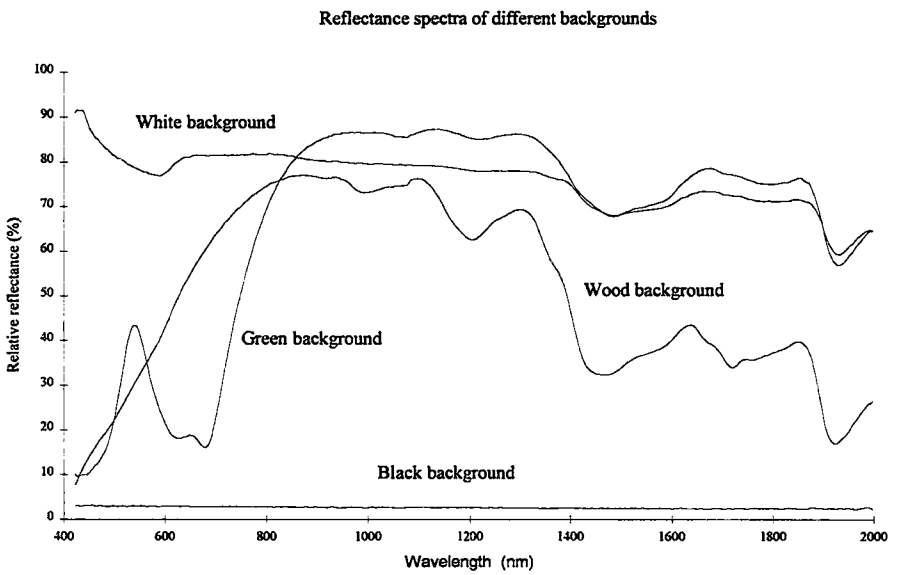

Figure 3: Reflectance spectra of the different backgrounds

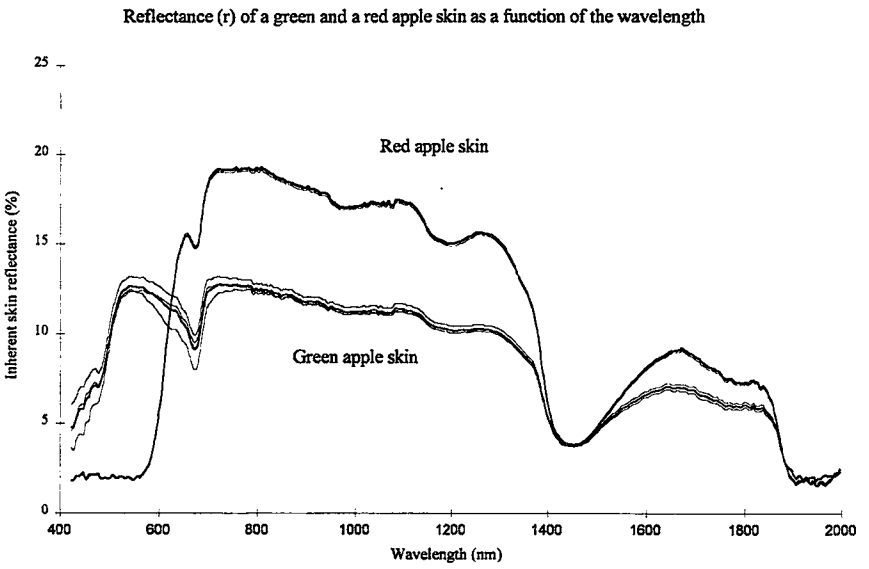

Figure 4: The inherent reflectance of a green and red apple skin

Figure 5: The transmission spectrum of a green and red apple skin

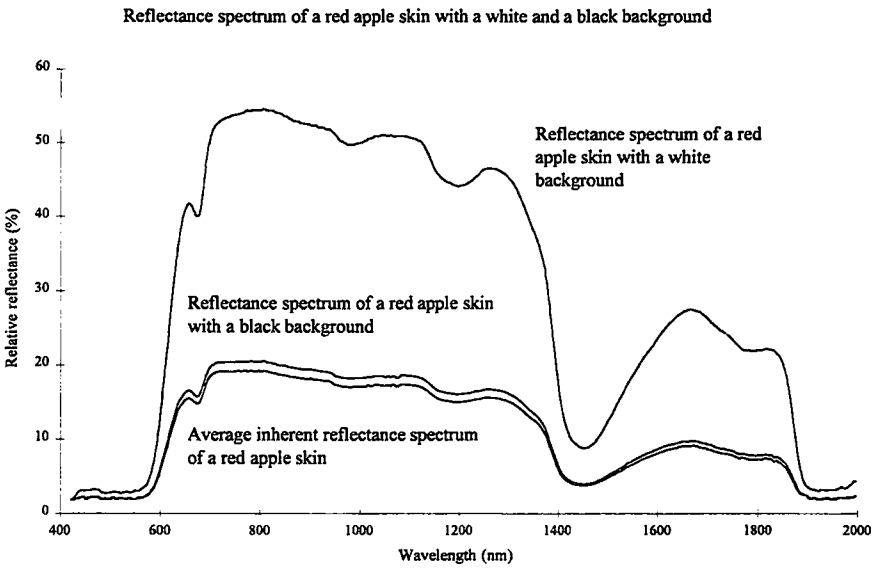

Figure 6: The influence of the background on the reflectance spectrum of a red apple skin

3.2 Comparison of the optical configuration

In table 1 and table 2 a serie of regression models is displayed for the prediction of the soluble solid content of Elstar apples for both the bifurcated and the 0°/45° configuration. Choosing the best model is difficult, since it depends on a number of parameters: the root mean squared error of prediction and calibration (RMSEP and RMSEC), the difference in explained y-variance between the calibration and the validation set, the difference between RMSEP and RMSEC, the correlation coefficient between the predicted and the measured values, the number of latent variables, ... Full cross validation is used to validate the models.

Table 1 gives a survey of different models based on spectra taken with the bifurcated optical fiber.
The model with MSC treatment has a low RMSEP value (0.55) and a small difference between RMSEC and RMSEP. A large difference indicates that the calibration set does not represent the validation set. The correlation coefficient between measured and predicted values equals 0.91 (See figure 7).

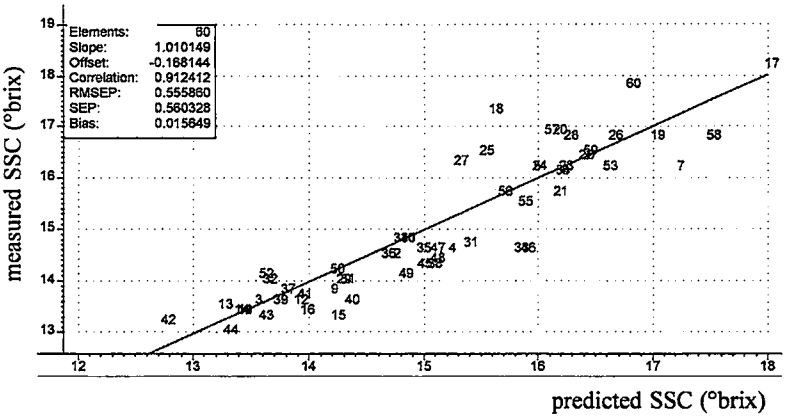

Figure 7: The predicted versus the measured SSC-values for model 1, measured with the bifurcated optical fiber

Table 2 shows the models calculated for the 0°/45° configuration. The same pretreatments are used to compare the two optical configurations. Three remarks are to be made.

First, model 6 with MSC-treatment gives a good RMSEP, a low number of latent variables and a small difference in explained y-variance between calibration and validation set. The models based on the second derivative of the spectra require more latent variables which corresponds with a higher explained y-variance for the calibration set.

A second remark concerns the curvature of the plot of the residual y-variance as a function of the model complexity. For the 0°/45° configuration this plot is characterised by a sharp peak as the

Model	Pretreatment			Lat. Var.	RMSEC	RMSEP	Correlation
1	•10		!	5	0.45	0.55	0.91
2	•10	5		7	0.37	0.73	0.85
3	•10	10		7	0.43	0.59	0.90
4	•10	15		6	0.43	0.57	0.91
5	•10	20		7	0.47	0.62	0.88

•x indicates the size (x) of the reduction of the original spectrum, x denotes the half of the interval (x) used for the calculation of the second derivative using the method of Savitzky-Golay en ! indicates the MSC treatment.

Table 1: Survey of the prediction performance of the different calibration SSC-models for the bifurcated optical fiber

Model	Pretreatment			Lat. Var.	RMSEC	RMSEP	Correlation
6	•10		!	5	0.61	0.72	0.83
7	•10	5		7	0.39	0.84	0.79
8	•10	10		7	0.52	0.70	0.86
9	•10	15		6	0.53	0.65	0.87
10	•10	20		5	0.56	0.66	0.87

•x indicates the size (x) of the reduction of the original spectrum, x denotes the half of the interval (x) used for the calculation of the second derivative using the method of Savitzky-Golay en ! indicates the MSC treatment.

Table 2: Survey of the prediction performance of the different SSC-models for the 0°/45° optical configuration

minimum, which makes it easy to choose the optimal number of latent variables. For the bifurcated fiber this plot has an exponential curvature. The choice of the number of variables is not so easy.

As a final remark it is important to mention that leaving out some samples can influence the prediction performance of the model.

Conclusion

In the first experiment it was proven that a NIR-spectrum, measured with a 0°/45° configuration, can contain information about the state of the fruit flesh. The background influences the spectrum of the skin and the transmission coefficient differs from zero. The proportion of the inherent reflectance to the transmission coefficient is an indicator for the amount of information coming from the background compared to that coming from the skin.

A general overview of table 1 and table 2 leads to the conclusion that the bifurcated optical fiber gives only slightly better prediction results than the 0°/45° configuration. First, the RMSEP values are, on average, less in table 1 than in table 2. In addition, for a comparable number of components, the explained y-variance and the validation correlation are higher for the bifurcated cable. The low cost, the possibility to measure contactless and the only slightly worse results compared to the bifurcated cable, make the 0°/45° configuration the best choice for commercial applications.

Acknowledgements

The authors wish to thank the EU (FAIR project CT95-0302) and the Flemish Minister of Science and Technology for financial support.

References

Bellon-Maurel, V. *Application de la spectroscopie proche infrarouge au contrôle en ligne de la qualité des fruits et légumes.* Thèse de doctorat, l'Institut National Polytechnique de Toulouse, 1992.

Chen, P. & V. R. Nattuvetty. Light transmittance through a region of an intact fruit. *In Transactions of the ASAE 23, no. 3: pp. 519-522, 1980.*

Hother, K., B. Herold & M. Geyer. Grenzen der Erkennung von Qualitätsfehlern im Apfelgewebe bei Messung der spektralen Reflexion. *In Gartenbauwissenschaft 60, no. 4: pp. 162-166, 1995.*

Kawano, S., H. Watanabe & M. Iwamoto. Determination of sugar content in intact peaches by near infrared spectroscopy with fiber optics in interactance mode. *In Journal of Japanese Society of Horticultural Sciences 61, no. 2: pp. 445-451, 1992.*

Lillesaeter, O. Spectral reflectance of partly transmitting leaves: laboratory measurements and mathematical modeling. *In Remote Sensing of Environment 12: pp. 247-254, 1982.*

Martens, H. & T. Naes. *Multivariate calibration by data compression.* In: Near-infrared technology in the agricultural and food industries. Williams & Norris (Eds.) St. Paul, Minnesota, USA: American Association of Cereal Chemists, Inc., 1987.

Moons, E., A. Dubois, P. Dardenne and M. Sindic. *Non-destructive visible and NIR spectroscopy for the determination of internal quality in apple.* In Proceedings from the Sensors for Non-destructive Testing International Conference, Orlando, Florida, February, 1997.

Pen, C. L., W. K. Bilanski & D. R. Fuzzen. Classification analysis of good and bruised peeled apple tissue using optical reflectance. *In Transactions of the ASAE 28, no. 1: pp. 326-330, 1985.*

Savitzky, A. & M. J. E. Golay. Smoothing and differentiation of data by simplified least squares procedures. *In Analytical Chemistry 36: pp. 1627-1639, 1964.*

Upchurch, B. L., J. A. Throop & D. J. Aneshansley. Influence of time, bruise-type, and severity on near-infrared reflectance from apple surfaces for automatic bruise detection. *In Transactions of the ASAE 37, no. 5: pp. 1571-1575, 1994.*

Williams, P. C. & K. H. Norris. *Qualitative applications of near-infrared reflectance spectroscopy.* In Near-infrared technology in the agricultural and food industries. Williams & Norris (Eds.)St. Paul, Minnesota, USA: American Association of Cereal Chemists, Inc., 1987.

Spectral amplification in NIR spectroscopy and sorting of whole apples*

Amplification spectrale en spectrométrie laser NIR et tri des pommes

Marc MEURENS and Emmanuelle MOONS

UNIVERSITY OF LOUVAIN, Laboratory of NIR Spectrometry
Place Croix du Sud 2(8), 1348 Louvain-la-Neuve, Belgium
e-mail: meurens@bnut.ucl.ac.be

Abstract: *The spectral amplification methods aim at the increase of the signal to noise ratio in spectroscopy. A first way to perform this increase in NIR spectroscopy has previously been described with the DESIR technique of sample preparation for the analysis of aqueous liquids. With an intense light source such as a laser and a sensitive CCD detector, it is also possible to achieve a spectral amplification in NIR spectroscopy of solid sample such as apples for example. A comparison of spectra taken by a CCD spectrometer on apples illuminated by a 700-mW Titanium:Sapphire continuous wave laser and a 150-W tungsten halogen lamp is presented here to demonstrate the advantage of transmission measurements with strong sources and sensitive detectors in apple sorting according to the internal quality.*

Keywords: *NIR laser spectroscopy, transmission, reflection, optical pathlength, apple sorting.*

Résumé : «L'amplification spectrale» a pour objectif d'accroître le rapport signal/bruit en spectroscopie. Une première méthode a été décrite dans la technique DESIR, technique de préparation des échantillons liquides. Avec une source puissante comme un laser et un détecteur CCD, il est également possible de réaliser l'amplification spectrale d'échantillons solides tels que les pommes par exemple. Une comparaison entre le spectre enregistré par une caméra CCD d'une pomme illuminée par un laser continu Ti:Saphir de 700 mW et une lampe tungstène halogène de 150 W est présentée pour montrer l'avantage de la mesure en transmission lorsqu'on utilise des sources puissantes et des détecteurs sensibles pour le tri des pommes en fonction de la qualité.

* *Research funded by the Belgian Federal Ministery of Agriculture*

1. Introduction

Near infrared (NIR) light transmission is an established nondestructive technique for evaluating the internal quality of many horticultural products. Although an apple for example transmits less than 0.1 percent of the light falling on it, the characteristics of this transmitted light have been related to the fruit interior quality. Already in 1958, Birth and Norris (1) described an instrument for measuring NIR transmittance spectra of whole fruits such as intact apples to evaluate maturity and internal defects due to physiological disorders. A measuring wavelength related to the desired characteristic and a reference wavelength must be carefully selected to successfully evaluate the fruit interior quality. This instrument has been termed horticultural spectrophotometer or 'hortispect'. The arrangement of components making up the 'hortispect' was a 100-watt ribbon filament lamp, standard microscope lenses, an integrating sphere and a multiplier type phototube.

The difference ΔOD (700 - 740 nm) between the optical densities (OD) at 700 and 740 nanometers has been reported as a good index of chlorophyll content and maturity level (2), whereas the difference ΔOD (760 - 810 nm) between the optical densities at 760 and 810 nanometers has been reported as a good index for water core (3).

According to Lovasz et al. (4), parameters that can determine maturity (refractive index, firmness) and some other parameters (dry matter, alcohol insoluble solids) are predictable with acceptable accuracy from NIR transmission spectra of apples. According to Kawano et al. (5), the NIR transmittance spectroscopy is also accurate enough to determine the maturity level of oranges. However these authors have used dispersive scanning NIR spectrometers (Tecator Infratec 1255, Pacific Scientific Model 6250) which are too slow for a convenient apple sorting in fruit conditioning stations.

Today it is interesting to test new fast spectrometers based on diode array detectors and laser sources which could fit better to the requirement of on line fruit sorting. So we have tested a coupled charge device (CCD) spectrometer with two different strong sources : a 150-W halogen tungsten lamp and a 700-mW titanium:sapphire (TiSa) laser.

2. Material and methods

Fifteen Jonagold apples at the same maturity level and without (external and internal) defects were used as samples in the spectroscopic measurements.

The white lamp was a 150-W Osram tungsten halogen lamp lighting up the 350 - 2500 nanometers (nm) spectral range. The OD (log 1/T) spectra of the light

transmitted through the apples were taken directly from 500 to 850 nm within 1 second on each apple by the CCD spectrometer.

The NIR laser source was a tunable continuous wave Spectra-Physics 3900S titanium: sapphire laser pumped by a 7-W Spectra-Physics Stabilite 2017 argon ion laser so that a monochromatic light is delivered at a power of 0.7 W in the 700 - 1000 nm spectral range. The spectra of the NIR laser light transmitted through the apples were taken step by step at intervals of 5 nm manually selected by a micrometric screw from 730 to 830 nm.

In both cases the NIR transmitted light has been measured by a CCD Ocean Optics S2000 spectrometer connected by a fiber optic cable to the apple skin at the opposite side from the light source (Fig.1).

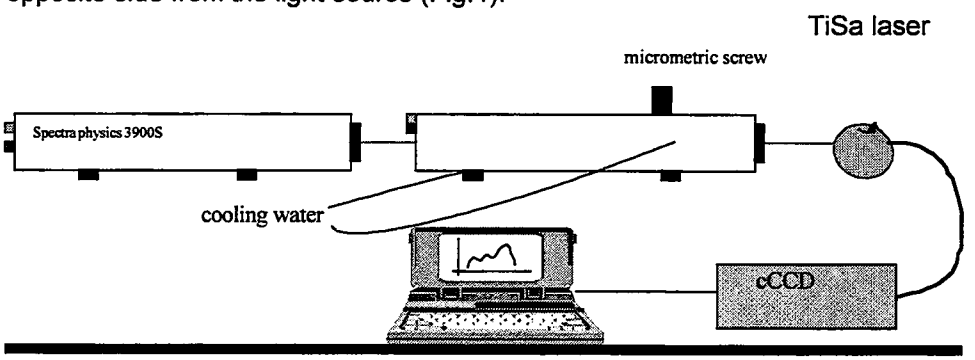

Figure 1: Schematic drawing of the titanium:sapphire laser spectrometer

3. Results and discussion

The spectral data acquired in transmission mode with the two different light sources have been treated in multiple linear regression (MLR) versus the physico-chemical reference data that are the refractive index (Brix), the acidity and the firmness in order to see what is the correlation with maturity parameters. In using spectral data at two to four different wavelengths, a better correlation is obtained with the TiSa laser (R^2 = 0.8) than with the white lamp (R^2 = 0.5) for the Brix. An equivalent correlation (R^2 > 0.8) has been obtained with both light sources for the acidity and the firmness.

Transmission spectra taken with the two different sources and the same apples were recorded in a graph (Fig. 2).

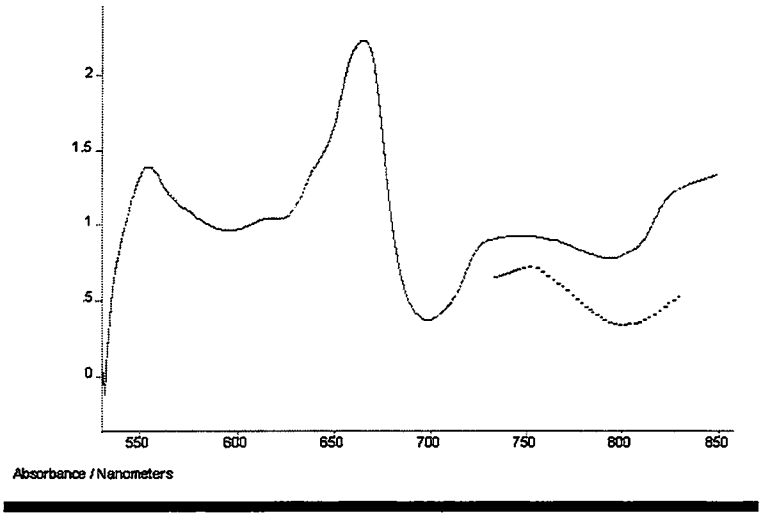

Figure 2: Spectra of whole apple with white lamp between 500 and 850 nm and with laser between 730 and 830 nm

We can observe that the transmission spectra present a larger OD variation than the corresponding reflection spectra in the same wavelength range (500 - 850 nm) but also that between 730 and 830 nm the TiSa laser produces a larger OD variation than the white lamp. So we can say that there is a spectral amplification in transmission.compared with reflection and that this spectral amplification is stronger at least on the studied wavelength range with the laser than with the white ligth source.

An explanation of this spectral amplification can be found in studies of light absorption and scattering in biological tissues (6). When light travels through biological tissue it is attenuated due to the effects of both scatter and absorption, and hence the effects of both of these phenomena must be taken into account when considering spectroscopic measurements.

In a non scattering medium, there is a relationship between the light attenuation, the concentration of absorber and the optical pathlength. This relationship is given by the Beer-Lambert law equation : $A = log (I_o/I) = \alpha . c . d$

where $A =$ *absorbance, light attenuation or optical density (OD),*
$I_o =$ *light intensity incident on the medium,*
$I =$ *light intensity transmitted through the medium,*
$\alpha =$ *specific extinction coefficient in mmolar^{-1}. cm^{-1},*
$c =$ *concentration of the absorber in mmolar,*
$d =$ *thickness of the crossed medium in cm.*

When a scattering medium is considered, the Beer-Lambert equation must be modified to include an additive term *G*, due to scattering losses and a multiplicative factor *B*, to account for the increased optical pathlength due to scattering. The photons travel a mean distance which is greater than the simple thickness *d* of the crossed medium. This true optical distance has been defined as the differential pathlength :

$$\beta = B \, . \, d$$

where *B* is the multiplier or the differential pathlength factor. The modified Beer-Lambert law which incorporating these two additions is expressed as :

$$A = a \, . \, c \, . \, d \, . \, B + G.$$

The explanation of the more pronounced spectral variation indicated by a larger difference of light attenuation ΔOD (750 - 800 nm) between two selected wavelengths in transmission measurement through whole apples than in refection measurement on the apple skin, overall with a laser source more than with a white source, can be found in the assumption that a longer mean distance is travelled by the photons inside the apple flesh than inside the apple skin overall when the incident beam has the very high spatial and spectral density of the TiSa laser beam.

Another comparative study (7) of diffuse transmission and reflection leads to a very near conclusion about the importance of the optical pathlength in NIR spectroscopy. In that other study we speak of light pathlength shortening, here we prefer to speak of optical pathlength extension and of spectral amplification.

We can say also that effect of spectral amplification observed in transmission measurement with a very intense ligtht source looks like the effect that we obtain in the dry extract (DESIR) technique (8) of sample prepation for the NIR analysis of aqueous liquids. Moreover a similar effect of spectral amplification is presented by a poster of Meurens in this same Sensoral 98 conference.

Conclusion

The obtained results show that below 1100 nm the NIR light transmission measurement through whole apples by a CCD spectrometer give better OD differences than the light reflection measurement on the fruit skin by diode array or scanning NIR spectrometers.
The results show also that the light transmission measurement through whole apples give better OD differences inside a limited wavelength range (730-830 nm) with a laser than with a white lamp. These differences of results between the measurement modes and the light sources could be explained by longer optical pathlengths in transmission measurement with laser source.

If the observation of a spectral amplification is confirmed by more complete experiments on a larger part of the NIR spectrum, an interesting improvement of the NIR instruments will be possible for better performances of whole apple sorting by NIR spectroscopy.

References

[1] G.S. BIRTH and K.H. NORRIS (1958). The difference meter for measuring interior quality of foods and pigments in biological tissues. U.S. Dept. Agr. Tech. Bul. 1341, 20 pp.

[2] J. N. YEATMAN and K.H. NORRIS (1965). Evaluating internal quality of apples with new automatic fruit sorter. Food Technol, 15 : 75 - 78.

[3] K. L. OLSEN, H. A. SCHOMER and G. S. BIRTH (1962) Detection and evaluation of water core in apples by liht transmittance. Wash. State Hort. Assoc. Proc. 58 : 195 - 197.

[4] T. LOVASZ, P. MERESZ and A. SALGO (1994). Application of near infrared transmission spectroscopy for the determination of some quality parameters of apples. J. Near Infrared Spectrosc. 2,213-221.

[5] S. KAWANO, T. SATO and M. IWAMOTO (1995). Determination of sugars in satsuma oranges using NIR transmittance. Proceedings of the 6th International NIR Spectroscopy Conference, Montreal, Canada.

[6] C.Y.E. ELWELL (1995). A practical users guide to near infrared spectroscopy. Hamamatsu Photonics KK and University College of London, UK.

[7] M. MEURENS and G. ALFARO (1990). Comparison of diffuse transmission and reflection in NIR spectroscopy. Proceedings of the European Workshop of FTIR Spectroscopy. Universitaire Instelling van Antwerpen (UIA), Antwerp, Belgium.
[8] M. MEURENS (1990). A sample preparation device for the analysis of liquids by NIR spectroscopy. World Patent PCT WO 90.

Real-time NIR sensor to sort fruit and vegetables according to their sugar content

Un système proche infrarouge temps-réel pour le tri en ligne des fruits en fonction de leur taux de sucre

J.M. Roger, V. Bellon-Maurel, L. Dusserre-Bresson, P. Fayolle, G. Ranou

CEMAGREF GIQUAL - Sensor and Information Engineering for Food Quality and Agriculture
BP 5095 34033 MONTPELLIER Cedex 1, France
e-mail : jean-michel.roger@cemagref.fr

Abstract: *Researchers have been showing that Near Infrared Spectroscopy (NIR) can be used to measure sugar in the fruits for about 10 years. However, the lack of robustness of the prediction model remains an obstacle for the development of on-line sensors.*
CEMAGREF research aims to develop robust methods for spectral analysis by taking into account some external variables responsible of prediction model drifts.
In the early 1998, more than 200 fruits have been sorted using these methods on the SHIVA machine (European Esprit project), showing a Standard Ecart of Prediction (SEP) less than 1 °Brix, and a repeatability of 85%.

Keywords: *NIR sensors, sugar measurement, fruit and vegetable sorting.*

Résumé : Les recherches de ces dix dernières années ont montré que le proche infrarouge (NIR) peut être utilisé pour mesurer le taux de sucre des fruits. Toutefois, le manque de robustesse du modèle de prédiction est un obstacle au développement de capteurs en ligne. Le but de la recherche au Cemagref est de développer des méthodes d'analyse spectrale robustes en tenant compte de certaines variables externes, responsables des dérives du modèle de prédiction. Début 1998, plus de 200 fruits ont été triés en utilisant ces méthodes sur la machine SHIVA (Projet Européen ESPRIT), montrant un écart standard de prédiction inférieur à 1 °Brix et une répétabilité de 85%.

1. Introduction

Near-Infrared has been shown for years to be an adequate technique to non-destructively measure the sugar content in various fruits: peaches [1], pealed melon [2], apples [3]...

However, although near-infrared spectroscopy is more and more found in on-line systems [4], most of the systems dealing with fruits are not usable in an industrial environment. The reasons are their lack of reproducibility and the difficulty to calibrate them.

Our aim was to bridge the gap between the laboratory experiments and real applications in fruit quality control by near infrared. In 1992, we have built a multiplexed system to measure sugar content in fruits [5]. However, robustness still had to be improved in regard to the wavelength drift of the spectrometer (λ ; in nm). This lack of robustness causes some real problems on line because the spectrometer is exposed to mechanical vibrations and temperature variations that cause offset drift. With the device we used, this offset can reach 4 pixels, that is to say 1,2 nm.

After a preliminary discussion about robustness, the method we adopted is exposed. Some results are then presented as a conclusion.

2. Discussion about robustness

2.1 Quantification of the problem

The notion of robustness is rarely quantitatively defined. Here, the robustness relative to a variable V is evaluated by the calculation of the first derivative of the prediction error with respect to V. The prediction error is S_p-S_r, where S_p is the predicted sugar content value and S_r the reference one. Then, the robustness index is :

$$I_v = \frac{\delta S_p}{\delta V}$$

The lower this value, and the more robust the model.
The model established in laboratory is based on a classical Partial Least Squares (PLS) learning process. A 0,6 °Brix SEP was obtained. Some experiments have shown the following robustness index value :

$$I_\lambda = 3°Brix/nm$$

From these value, and with a specification of 1°Brix for the error of prediction, it is easy to calculate the maximal variation for λ :

$$\Delta\lambda_{max} = 0{,}33 \text{ nm.}$$

In on-line conditions, keeping the calibration of the spectrometer within 1 pixel variation is not ensured, especially with low cost devices. This entirely justifies the need of improving the robustness of the prediction model.

2.2 Preliminary remarks on the robustness improvement

Whatever the variable V, which is the source of error, two main methods are available to improve the robustness of the PLS prediction model :

The first one takes into account the value of V (provided by any means or estimated on-line). The prediction model is adjusted with regard to this value, by to ways :

- the spectral data are corrected to place the model in the same conditions than during the learning process,

- the prediction model is corrected, or takes into account the value of V.

The second one consists of integrating the variations of V into the learning set. Two methods can be employed :

- building a learning set covering the entire variation domain of V,
- pre-processing the spectrum to make the model less dependent on V.

If it is possible to modify the model in relation with the value of V, the first method should be preferred, because it may induce less noise on the model than the second one. Then, this kind of method has preferably been investigated. However, it is limited by some severe constraints :

- the results directly depend on the precision of the evaluation of V,
- much more computation may be needed in real time.

3. Method

Two kind of wavelength drift can occur: a static one, when the process starts, or a dynamic one, appearing during the process. Their effects are not identical. Since a reference measurement is taken before starting, the static offset affects the spectra with a pure translation (because I and I_0 are shifted with the same value). On the other hand, a dynamic offset entails a combination of a translation and a deformation. Because it is less simple, only this latter case has been treated.

3.1 Problem analysis

At first sight, the sensitivity of the PLS model with regard to the wavelength drift appears virtually obvious. However, the value attached to a specific wavelength is

strongly correlated to its neighbours. Then, a wavelength offset should not be so critical. Moreover, it is easy to see that the sensitivity is not dependent on the smoothing of the spectrum (which however increases the correlation between wavelengths).

Then the understanding of this problem requires a finer analysis of the PLS functioning. The PLS deals with an iterative reduction of the variance of the original and residual spectra. At each step the sugar contents of the apples can be determined. The computed sugar contents, for each step of the algorithm, is shown in Fig 1.

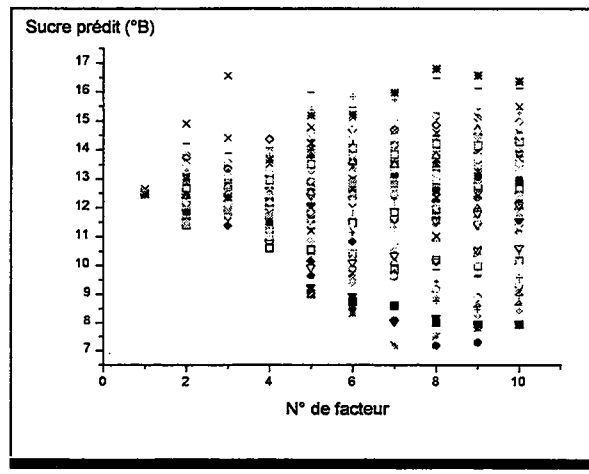

Figure 1: Evolution of the predicted concentration during the iterative process of variance reduction

It is clear that the first factors give an average evaluation of the sugar contents, and the other ones are responsible of the separation between the samples. In other words, the precision of the prediction is only due to the further factors of the model, the last ones also generating noise. Then it becomes clear that an offset, which especially affects the last residual spectra, directly affects the differentiation phase.

3.2 Taking λ drift into account

Since it is very simple to correct the spectral data in regard to a known offset drift (translation of the spectrum before dividing by I_0), the methods based on the integration of λ variations into the learning phase have been cancelled.

The wavelength offset is a slow phenomenon. Then, the identification of λ is based on the measurement repetition, as illustrated in the following scheme (Fig.2)

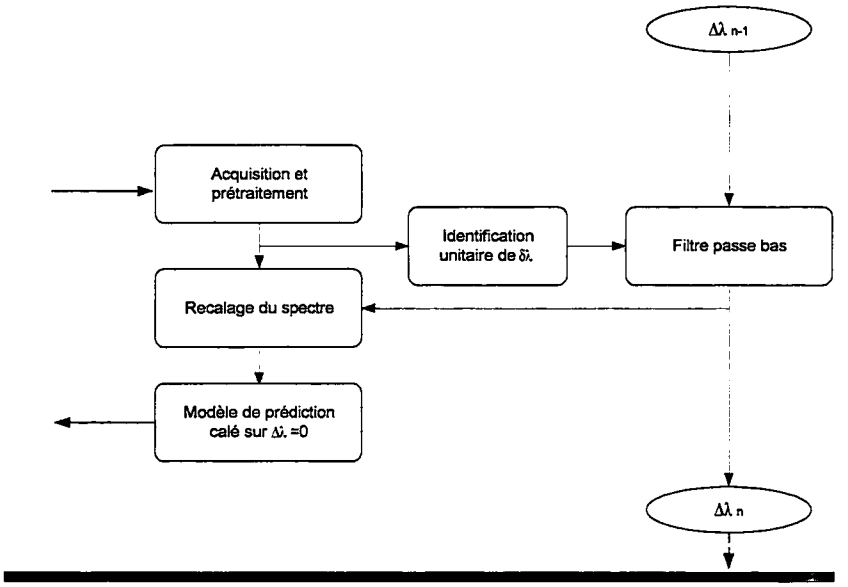

Figure 2: Principle of slow λ drift identification

Two kinds of principles have been tested for the identification of λ drift :

- analytical (geometry based) ones,
- black box (learning based) ones.

The analytical methods only will be presented.

These methods are simply based on the recognition of a characteristic element of the spectrum, which is bound to a specific wavelength. Different characteristics have been explored. For each of them, a criterion C_λ is computed as the standard deviation of prediction of λ on a set of examples taken without any offset. If this criterion is satisfied, the ability of the criterion is tested for the prediction of I, which essentially relies on its invariance with regard to the offset (at least locally).

First of all, two simple geometrical points on the absorbance spectrum have been tested : the maximum and the main inflexion point, as represented in Fig.3 :

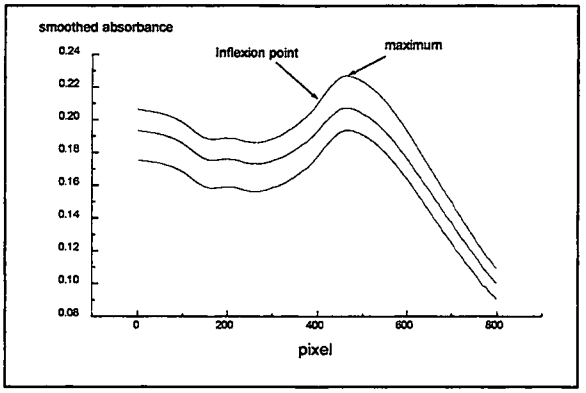

Figure 3: Two simple geometrical characteristics on the absorbance spectrum

For these two points, the standard deviation of the abscissa is about 3 pixels, that is to say 1 nm. The following histogram (Fig.4) presents the dispersion of the abscissa of the maximum. It shows that the distribution is not symmetric, that could lead to some systematic error in the slow identification process.

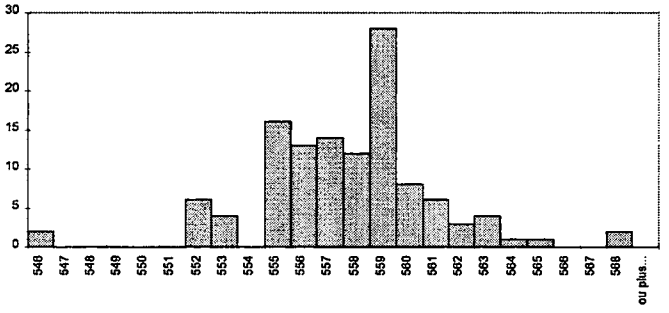

Figure 4: Distribution of the maximum abscissa of the absorbance spectrum

The distribution of the inflexion point abscissa approximately follows the same shape. The dispersion has been judged too important for continuing in this way.

A second geometrical approach is based on the spectra intersection. It has been seen that after a particular pre processing, all the spectra cross more or less at a common point (G). The Figure 5 illustrates this phenomenon :

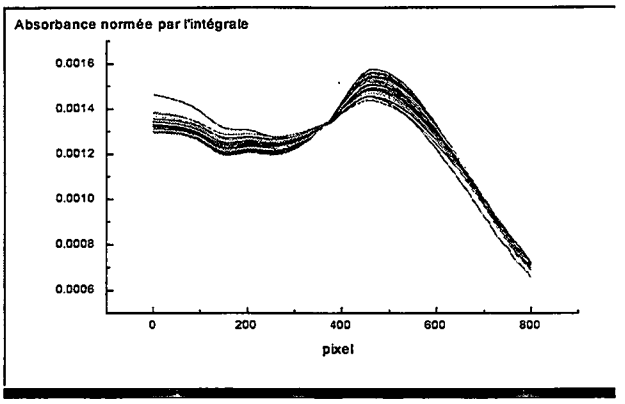

Figure 5: Illustration of the point G

The repartition of the abscissa of G (XG) is represented on the following histogram (Fig. 6). The standard deviation is 1,5 pixel, that is to say C_λ=0,5 nm.

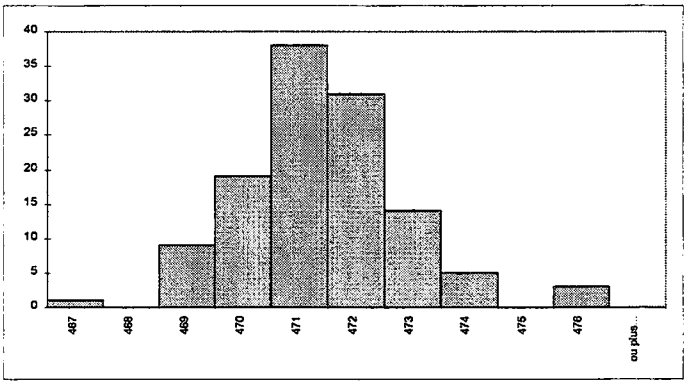

Figure 6: Distribution of X_G

Given this encouraging results on G point stability, more tests have been conducted in order to determine its independence with regard to the wavelength offset.
Because the G point is obtained by geometrical computation, it is obvious that its position is affected by the wavelength offset. Commonly, the absorbance spectrum is obtained by division of I (which is translated by the offset) by I_0, which is not translated. Then, the slope of I nearby the theoretical abscissa of G (P_G) could be an important factor for sensitivity. Some tests have been conducted in this way. The Figure 7 shows the dependency of G position drift (Δ_G) with regard to P_G :

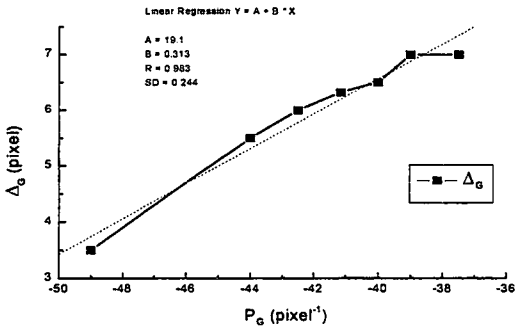

Figure 7: Relationship between X_G drift and the slope of I nearby X_G

Then, G point appears as a good characteristic of the wavelength offset, on condition that the slope of the spectrum nearby X_G is taken into account. This way for identifying λ has not been more investigated, but is very promising, especially because the computation charge is very light.

4. Results and conclusion

The research described in this paper has been tested on the SHIVA prototype (European ESPRIT project), demonstrated on February 1998.

A method based on the spectrum shape analysis has been developed to correct the wavelength drifts. Intensive tests have confirmed the efficiency of this offset detection method. Thanks to this correction, in on-line conditions, a SEP of 0,7 °Brix has been reached, that is to say more or less the same value than the laboratory one (0,6 °Brix).

Repeatability tests, consisting of sorting again the fruits preliminary sorted in a given class, have given a 85% ratio. This result is very satisfactory, especially with regard to the variability of sugar contents inside the same fruit (up to 1°Brix).

Further work has to be achieved on the other variables causing a lack of robustness, like fruit temperature or incoming signal variation (due to dust on the fibre optic).

Acknowledgement

This work has been sponsored by the ESPRIT Program of European Community (EP 9230).
We acknowledge Jean Claude Jacques for his knid technical assistance during this work

References

[1] Kawano S., Watanabe H., Iwamoto M (1989) *Measurement of Sugar content in intact peaches* by NIRS. in Proc. of the second international Near Infrared Spectroscopy Conference. *Iwamoto and Kawano Eds, National Food research Institute, Tsukuba, japan, pp.343-352.*

[2] Dull G.G., Birth G.S. Leffler, Smitle DA. (1989) *J. Food Science 54, 393-398.*

[3] Lavosz T., Salgo A. (1992) *Investigation of the apple quality by near infrared technique* (1992) in Near Infrared Spectroscopy- bridging the gap between data analysis and NIR applications, Editors KI Hildrum, T. Isaksson, T. Naes and A. Tarnberg, Matforsk , Norvegian *Food Research Institute. p. 365-370.*

[4] Benson I., B. (1995) *The characteristics and scopes of continuous on line near infrared measurement*, Spectroscopy Europe, 7 (6) 18-24.

[5] Bellon V, Vigneau J.L., Leclercq M (1992) *Feasibility and performances of a new, multiplexed, fast and low-cost fiber optic NIR spectrometer for the on-line measurement of sugars* in fruits. Applied Spectroscopy (47), 7, 1079-1083.

Part 8

Classification and multisensor fusion

SHIVA (European project): A robotic system for fruit sorting

SHIVA (Projet européen) : Un système robotisé de tri des fruits

Antoine Bourely

PELLENC SA, 84122 Pertuis, France

Abstract: *The Esprit Project 9230, SHIVA, has brought together during 3.5 years five partners of Research and Industry, around two key objectives for the fruit industry : to ensure quality control of each individual fruit, especially for taste related criteria (maturity, sweetness), and to pack each fruit automatically and without damage.*

The SHIVA partners have developed industry compatible sensors derived from laboratory sensors, and robotic principles for soft fruit handling ; they have adapted classical packing line elements, and developed new CIM components for packing house supervision. They have integrated these components into a Pilot Line, and demonstrated its operation in semi-industrial conditions on apples and peaches, with speeds around 1000 fruits/hour. As a result, several combinations of these elements will lead to commercial products in the near future, especially for high quality grading units and for automatic sample inspecting machines.

Résumé : Pendant 3 ½ ans, le projet ESPRIT EP 9230, SHIVA a rassemblé 5 partenaires de la recherche et de l'industrie autour de 2 objectifs clefs pour l'industrie des fruits : assurer un contrôle de qualité de chaque fruit individuel, en particulier pour les critères reliés au goût (maturité, teneur en sucre) et empaqueter chaque fruit automatiquement et sans dommage. Les partenaires SHIVA ont développé des capteurs compatibles avec des contraintes de l'industrie à partir de systèmes de laboratoire et ont validé des principes robotiques pour la manipulation des fruits fragiles. Ils ont adapté les éléments de conditionnement classique en ligne et ont développé de nouveaux composants CIM pour la supervision de la station de conditionnement. Ces composants ont été intégrés dans une ligne pilote qui a été testée en conditions semi-industrielles sur des pommes et des pêches à une vitesse approximative de 1000 fruits par heure. Plusieurs combinaisons de ces éléments conduiront à des produits commerciaux dans un futur proche, en particulier pour des unités permettant de trier des fruits de haute qualité et pour des machines automatiques d'inspection de lots de fruits.

1. The partners

PELLENC SA is the project co-ordinator
manufacturing company specialised in automated agricultural machinery
Contact persons : Antoine BOURELY, Alain CONSTANS
Address : BP 47, 84122 PERTUIS Cédex, France
tel : +33/4.90.09.47.15 ; fax : 33/4.90.09.64.09; e-mail : pellenc@aix.pacwan.net

FOMESA : manufacturing company specialised in fruit packing machinery
Contact persons : Jorge PUIG, Francisco NAVARRON
Address : Jesus Morante Borras, 24, 46012, VALENCIA, Spain
tel : +34/963.16.54.00; fax : 34/963.67.79.66; e-mail : fomesa@ibm.net

CEMAGREF : French Institute for Agricultural and Environmental Engineering Research, with labs specialised in sensor development for food products
Contact persons : Véronique BELLON-MAUREL, Vincent STEINMETZ
Address : BP 5095, 34033 MONTPELLIER Cédex 01, France
tel : +33/4.67.04.63.19 ; fax : 33/4.67.04.63.06
e-mail : veronique.bellon@cemagref.fr

IVIA : research centre for agriculture specialised in fruit and vegetables
Contact persons : Enrique MOLTO, Florentino JUSTE
Address : Carretera de Moncada-Naquera, km 4,5, 46113, MONCADA, VALENCIA, Spain
tel : +34/961.39.10.00; fax : +34/961.39.02.40; e-mail : emolto@ivia.es

EICAS : software company specialised in plant automation software.
Contact person : Giovanni PEROTTO
Address : Via Vela 27, 10128 TORINO, Italy
tel : +39/11.562.3798; fax : +39/11.436.0679; e-mail : gperotto@eicas.it

2. Objectives

2.1 Approach and methodology

The original idea of the SHIVA project was elaborated as early as 1991. It was to make a revolution in the way fruits were sorted :

- go away from quick sorting on apparent quality (size and colour),
- get into detailed individual sorting based on internal quality (taste and maturity) ;
- reduce fruit falls during sorting to reduce damage.

The weapon for this was the integration of several recent advances :

- the power and flexibility of robotic technology ;
- the rapid advances in solid state sensor technology at affordable cost ;
- the rapid progress in computer management of production.

A huge gap was noticed between the many features measured on biological products in the lab and the very few features measured on a standard packing line. As long as laboratory methods were destructive (penetrometer, refractometer), the gap could not be bridged. With the advent of non destructive methods, the gap could be bridged : we just had to demonstrate that sensors (firmness, NIR, aroma) could be brought in contact to the fruit in a practical way. Robotics offered this potential.

Additionally, robotics enabled to image all the surface of a fruit, reaching a theoretically perfect detection (for colour and defects), and even to orient the fruit in any final configuration (however, this capability is more related to visible than to true quality). Thus, even with «classical», non contact sensors, like vision, robotics could greatly improve the type of processing.

From the beginning, it was obvious that the drawback for this was a much slower sorting cycle : several seconds per fruit, instead of several fruits per second. The bet was to achieve industry and consumer acceptance of the additional cost, based on a guaranteed quality.

Like all revolutions, it had to be universal : all spherical fruits and vegetables had to be considered, even if we had to eliminate many of them on the way for practical reasons. At least, these reasons had to be explained.

2.2 List of project objectives

Based on the above rationale, we have decided of the partnership, and we have split the project in the several objectives. We state them below with a brief summary of the corresponding achievements :

2.2.1 Develop new sensor systems for on-line sorting and quality evaluation

- 4 species of fruits have been selected, two of them completely tested : peaches and apples ;
- 4 sensor technologies have been tested and integrated :
  - aroma, sugar content, firmness, machine vision
- sensor fusion has been tested on 3 species, one of them integrated on line

2.2.2 Develop fruit handling robot cells with integrated vision /sensor systems

- Each piece of fruit has been individually handled by two robot units :
  - an inspecting / orienting unit, and a handling / packing unit;

- Quality sensors have been integrated into the handling process (inspecting unit).

2.2.3 Design new types of packing houses

- New, more flexible packing house elements have been designed and tested :
  - unstackers, cleaners, stackers

- Classical elements have been implemented and optimised to connect the robotic packing unit to a classical pre-sorting line.

2.2.4 Design a CIME system optimized for selecting highly variable products

- A Line Manager software for line supervision has been integrated into the robotic line;

- A Plant Manager software has been developed for a more generic packing line.

2.2.5 Build a pilot plant to integrate and test technical developments

- A pilot line integrating two robotic devices, the handling of 12 commercial boxes, all sensors except the aroma sensor, all connection elements to a pre-sizing line, and the Line Manager software has been built.

- Two generations of the Pilot Line have been built : one in 1996, the other one in 1997;

- The latter Pilot Line has been intensively tested first on peaches (July 1997), and then on Apples (December 97).

- A complete sorting cycle in 4 seconds was achieved.

3. State of the art

The classical automated packing houses are based on parallel lines massively conveying fruits or vegetables, which are on-line inspected and on-line sorted to be packed. Each fruit is individually carried in a cradle, and then dropped on a transverse line after sorting. Two main sorting criteria are measured electronically : weight, and more recently, colour. A typical plant uses a 6 to 12 line system and processes 2500 to 4000 fruits per minute, i.e. 30 to 40 tons/hour, with 30 to 100 workers for control and packing tasks. The number of output lines varies between 5 and 40, leading to important plant surface areas.

These workers are mainly concentrated at the outlet of the main lines, on the most delicate and complex tasks : fine inspection of the product and optimised orientation in the output box or tray. Their tedious work creates fatigue and translates into wrong assessments along the day.

Contact sensors, such as firmness or fibre optic sensors, can not be applied on such architectures. Prototype machines performing firmness measurements at speeds of 1 fruit/second per line have been demonstrated [1], but they did not find a wide commercial acceptance.

Due to the high processing speed, damage to the fruit can become a serious issue, especially at the dropping site. For this reason, several packing houses very sensitive to quality have abandoned the classical mass packing lines to come back to manual labour, despite of the high cost. Recent machines [4] were especially designed to minimise these chances of damage, by hanging the fruits instead of carrying them.

4. Project results

4.1 A very significant market identified

Starting by the examination of many fruit and vegetable species, we quickly narrowed down to four main species : oranges, apples, peaches, and tomatoes.

Pears and melons were considered, because quality issues are essential for them, but then eliminated for handling reasons (shape constraints). It is interesting to note that these same fruits are handled with very little automation in standard packing lines, for the same reasons. The level of technology to efficiently handle pear shapes is still beyond reach.

Within the fruits of round shape and average size, two groups appeared :
- apples and peaches with a high potential for quality improvement ;

- citrus and tomatoes, with a lower, more specialised potential.

Citrus have a lower potential essentially because of their thick peel, preventing a physical inspection from the outside, and also because lots are very homogeneous : partial sampling is then an adequate method for quality evaluation. Specific problems, like detecting puffy mandarins, have been solved through the application of some SHIVA concepts.

Tomatoes also have a thick peel, and since they have very little sugar, they were not concerned by one main feature of SHIVA, NIR inspection. However, acidity is a big issue for them, and they might come back into a similar project if someone invents a non destructive acidity sensor (the existing technique, NMR, is far too expensive).

Fortunately, apples and peaches are very appropriate species, with a high potential added value for quality, and all experiments have been concentrated on them. Their market accounts for 11,400,000 Tons/ year, i.e. 40 % of all fruits produced in Europe in terms of weight.

4.2 The pilot line : a comprehensive demonstrator

Most major technical results are presented in the 1997 Pilot Line. The line is multi-product. It can handle apples, peaches, or other spherical fruits. This line has been working in typical packing house environment, with dust, temperature and humidity variations, etc... and has validated the applicability of the results.

A short description of the Line operation will help to understand the following discussion.

Figure 1 shows a top view of the Line. Fruits are carefully deposited to form a single even layer, then they are placed one by one on a grommit conveyor to form a line (see Entry Section).

Figure 2 shows a simplified side view of the Inspection Cycle, divided into three sequential steps.

The first step in the sorting is the dynamic weighing of the fruit, that also measures firmness, through impact analysis (Figure 3). Fruits are dropped from the conveyor under the control of the inspection computer, only when they are needed.

Then, the fruit is transferred by a suction cup to the visual inspection site : by image analysis, its characteristics are very accurately determined : diameter, colour, and aspect defects (bruises, spots). The fruit is visualised on 100 % of its area in 4 successive views (Figure 4) : 3 views in the first suction cup, then it is passed to a second suction cup, and the lower portion is visualised.

Staying in the second suction cup, the fruit is carried on to the third step, the sugar content measurement. An optical fibre comes into contact with the fruit (Figure 5). It provides strong infra-red lighting under the fruit skin, in order to determine sugar content. Several measurements must be carried out sequentially around the fruit. The analysis uses a real time spectrometer adapted to industrial operation.

Combining the data from all the different sensors, the fruit is automatically classified into a maximum of 12 quality classes. The fruit is then ready for the last step, the packing in alveolar trays, carried out by a three axis spherical robot arm (Packing Section, Figure 1). The working space of the arm enables it to reach 12 trays, each with a capacity of 20 to 30 fruits.

As soon as a tray is full, it is automatically replaced by an empty one (Empty Box Unit and Full Box Unit in Figure 1).

4.3 Most sensors found to be applicable on line

NIR spectroscopy (see also [2]) :

It is the typical laboratory method that had a hard time coming down to the factory floor. Usual architectures at the beginning of the project were still based on off-line sensors with moving parts. The prototype we started from has the right structure for applicability : a multispectral sensor and no moving parts.

Despite some implementation problems typical of a prototype, the sensor worked well enough to determine the conditions for applicability :

- close contact to the fruit skin is a key condition for valid measurements ;
- at least two measurements at opposite points on the fruit are necessary ;
- invalid measurements are detected ;
- reference taking and periodic cleaning are compulsory and can be easily automated ;

After applying these conditions, we obtain a method of reasonable precision, although far from the precision of refractometry : the standard error of measurements is very close to 1° Brix. We can thus classify fruits into 3 classes of sugar content, and there is simply no substitute available, even manually. Note that this technology is intimately bound to robotic technology, because it is the only practical way to apply several measurements in contact to the fruit.

Vision

Together with NIR, this is the most important achievement in the project. It is not obvious, since colour vision already exists on current packing lines, routinely determining diameter and colour. However, although some commercial systems claim to find defects on fruits, they concentrate on very obvious and coarse defects. The results of the SHIVA vision system are clearly better :

- the level of detection achieved in the project is much finer (e.g. it takes into account russetting on apples) ;

- Stem/Calyx detection has been demonstrated on peaches AND apples;

- it is based on imaging 100 % of the surface of the fruit, giving a much better guarantee of quality.

Note that most of these results can be applied without robotic handling, except the last point.

Of course, it is a continuing effort, since it was not possible to solve all the problems on all fruit varieties within the project. The success achieved on the examples we handled shows the generic potential of the vision system, including :

- the lighting configuration giving light uniformity with no shine (figure 2) ;
- the high quality colour camera ;
- the right choice of technologies, mainly based on low cost PC solutions ;
- the flexibility and power of the colour based algorithms developed.

Firmness

Several methods have been investigated in the detail, and two of them have been implemented on the robot : one brings the sensor to the fruit (1996), the other one makes the fruit fall on the sensor (1997). The second one is the more effective method, mainly for its easy integration into a line (see Figure 3). Here, we did not take directly advantage of the robotic structure, but simply of the relatively longer time available with respect to usual packing lines. The impulse response analysis has given, as known in the literature, good results. The application is restricted to peaches, where it is useful, but the sensor is always used, because it performs two more useful tasks :

- cycle synchronisation, because it detects fruit arrival ;
- fruit weighing after stabilisation.

This weight detection capability is worth noting, when one compares the setting used in SHIVA with the complicated weight sensing systems on usual packing

lines : they are long devices (more than one meter), and they require that each fruit be carried in a specific cradle. (The cradle is designed so that the fruit be completely supported by the weight sensor when above it.)

Aromas

This was a very ambitious idea, that many people did not think realistic at Project Start. Even in the lab, the technology could not be considered to be ripe. Therefore, it might have been too early to include it into SHIVA.

Interesting results were obtained on peaches with very simple sensors, and relatively short sensing times (less than 500 ms). However, we preferred to give up the integration into a Pilot Line, because recovery time was high, leading to complicated settings with more than one sensor. Moreover, the type of information provided (ripeness, rotten fruit), could be easier and more precisely provided by other sensors in the Project (vision, firmness).

Data fusion (see also [3])

The fusion of information from different sensors has been found useful in significant cases, giving more precision and repeatability, both to sugar content and to firmness prediction. Even if results can depend from varieties (Golden Delicious apples change colour when ripening, opposite to other varieties), the result is important.

4.4 A compromise found between robotic and packing line technologies

An appropriate arm structure

The efficiency of the spherical robot structure chosen was demonstrated in industrial operation. With several millions cycles, a cycle time of 2.1 sec, and a reach of more than one meter in all directions, the arm is a reliable tool. Its weight has been decreased by more than half since project start, thanks to carbon fibre technology, and its electric power was more than doubled.

Two complementary technologies

At first, robotics was thought as an alternative technology to the classical packing line architecture. Fruit sorting should have been organised in « flexible cells », getting rid of the very concept of a packing « line ». However, transportation issues quickly brought back conveyors into the picture, and it was found more logical to organise the packing house around them. We then shifted to the current structure

of the Pilot Line, i.e. mixing two technologies with complementary advantages, which gave us the best basis for customer acceptance :
- a classical line for the bulk of the fruits, providing speed of operation for pregrading ;

- robotic cells for high quality grading, installed at specific line outputs.

Robotic packing into trays

A sophisticated 12 tray handling system was developed, based on classical line components of high reliability. It was successfully tested together with the robot arm, although the available space was very limited. It is the basis of an industrial sub-system to be developed, even if the cost is not negligible and can be further reduced.

2D, rather than 3D orienting

The complete control of the final fruit orientation was part of the 1996 pilot line design. But it was found to be unreasonably complicated and slow. On the other hand, it was a low priority for the end user. The final inspector structure enables 2D re-orienting (thanks to the 2 suction cups), which is good enough in most cases, and the machine is much simpler.

Good cycle times, with more improvements to come

We have demonstrated : 3.8 seconds / fruit for handling alone, 5.5 sec / fruit for the total inspection cycle. The first figure is the more important one, since the difference is mainly due to a change in the NIR cycle and some non masked time in vision. These details will be solved on the industrial version. Moreover, the handling cycle itself can be accelerated, although less than expected (2.5 s), because of the dimensions of the vision chamber.

Upgrading classical packing components

We have performed a technological upgrade of « classical » packing line elements (unstackers, cleaners, stackers) to raise their level of flexibility and automation, and bring it in line with the new developments. The improvements were absolutely necessary in the SHIVA concept, but can also be exploited separately.

4.5 The appropriate level of computer management determined

Hardware optimisation

The number of computers, initially 10, has been progressively reduced to 6. The best compromise found at reearch stage (one computer per partner) is different

from the best compromise at production stage (one computer per module that can be sold separately). This means that further simplifications will come, but the good news is that they will no longer change the basic architecture that has been validated.

Dialogue and User Interface (UI)

The main choice for integration was to base the dialogue on heterogeneous networks, namely an Ethernet network with TCP /IP protocol. A subsequent step has been the integration towards a single UI at Line Manager level. The remaining computers (without a UI) are equivalent to simple programmable controllers.

Pragmatic software choices

The low level, real time operation of the components has been made quasi independent from the supervision and UI level. This ensures compatibility with existing packing lines, that do not always have a supervision level.

User Interface and classification criteria were made «practical»

All technological complexity has been masked from the final user. Although some more work (and user feedback) is still necessary to ensure applicability, we can already say that parameters related to sensors, sensor fusion, robot control, or image processing are hidden from the final user. Only fruit related issues appear in the classification tables, with clear parameter units, and operation statistics are simple to use.

A user friendly classifier

With many new quality parameters, the direct application of classical classifiers would lead to unreasonable numbers of quality classes : for instance, 5 sizes x 8 colours x 3 defect levels x 2 firmness levels x 3 sugar levels = 720 classes ! The classification table developed maintains a reasonable number, i.e. 12 classes as a maximum, and all parameters can be adjusted by the user.

The software developed, at Line Manager and Plant Manager levels, is flexible enough to be applied either in SHIVA products, or in other types of packing houses.

5. Exploitation plan

As a result of the project, several products have been rapidly defined. Feedback from future users will form an essential part of the final product definition. This section highlights the two main products, and gives some indications of the other ones.

5.1 SHIVA product n°1 : inspection and packing line

Definition

The product consists in the global concept developed during the project, and includes all the elements of the Pilot Line. The application will be the only one in the market able to guarantee a specific quality, both external and internal, for each fruit.

Implementation

The objective is to place the inspection and the packing at the end of a conventional sizing and packing system, either mechanical or electronic, to sort and pack some determined presorted fruit classes.

Keypoint is quality

Given the production capacity of such an inspection and packing line and its costs, the best justification of its commercial success is on the created added value of the fruit sorted.

Curently, grading according to bruises is manually done, and grading according to taste related parameters (sugar, firmness) can only be done by sampling. Sampling is not appropriate when fruits exhibit a high individual variability.

Securing a certain internal quality of the fruit would give the user a clear competitive advantage. In overproduction cases, quality control might be the only way to sell the fruits.

The Product includes

- a feeding section with singulation of fruits ;
- a firmness and weight detection unit ;
- an NIR unit for sugar content measurement ;
- a machine vision unit, for defects and colour ;
- a robot arm and supporting structure ;
- a commercial box handling system.

Throughput

The work speed, if we consider an average of 2.5 to 3.5 seconds per fruit, i.e. 1000 to 1440 fruits/hour, will be 200 to 290 kg/hour.

Price

Around EURO 84,000.

Market

Apple and peach packings, who wish to offer a guaranteed quality at a higher price. We have estimated for the European market the potential sales around 30 modules a year.

Sensitivity analysis

The Return on Investment (ROI) time has been calculated to be between 1.7 and 3.5 years, which are durations usually accepted in the sector. This calculation has been done for high quality peaches, with the following assumptions :

- a sale price of a high quality peach around EURO 1 per kg ;
- a 20 to 25% price increase for quality guaranteed fruit can be justified ;
- a yearly campaign between 1000 and 1800 hours.

An important saving would be obtained by not including in the line the Commercial Box Handling System, nor the robot arm, saving 45 % of the investment. We would then obtain acceptable ROI with just 700 hours/season.

5.2 SHIVA product n°2 : automatic sample inspector

Definition

The function of this inspection is to evaluate a sample (0.5 to 1 %) of each batch delivered to the packing house, to have a first report of the main characteristics of each particular batch, diameters, colours, superficial and internal qualities.

Implementation

As a separate device placed at the entrance of conventional packing houses.

Keypoint is information

The user, i.e. the packing house manager, will have entrance details of the fruit related with its quality and thus will be able to better manage his business. He will also have the following advantages :

- to pay his suppliers according to the quality received;

- to improve his production by knowing beforehand the kind of products that he will have;
- to be sure of what he is offering to the customers;
- to be able to target specific customers with the knowledge of the products he has.

The Product includes

- a size range control unit, counting too big or too small fruits ;
- a feeding section with singulation of fruits ;
- a firmness and weight detection unit ;
- an NIR unit for sugar content measurement ;
- a machine vision unit, for defects and colour ;
- a bulk refilling system for field boxes.

Throughput

With an average of 3 seconds per fruit, and if we sample 0.5 % of a fruit lot, a single module would be able to service packing houses with an input production around 40 Tons/hour. On smaller packing houses, bigger samples will be evaluated.

Price

Around EURO 50,000. Neither the arm of the robot nor the commercial box feeding system are necessary, because the fruit is again placed in bulk into the field boxes after its analysis. Comparable, less sophisticated systems are currently sold for EURO 35,000.

Market

Many small and medium packing houses, not equipped with a pre-sizing line. For bigger packing houses, already equipped with sampling units, the system will be sold later as an upgrade of their existing system. With only one module sold on the average per packing house, we can hope to reach an average market of 17 units/year in Europe.

Sensitivity analysis

With a price around EURO 50,000, the price increase of EURO 15,000 over a conventional sampler is fully justified :

- compared with the existing samplers, the system would save labour, as just one person would attend it, instead of 3 to 5 presently. If we save 2 workers during 100 days/year, the saving amounts to EURO 10,000 to 15,000 per year. Thus, just based on this saving, the pay-back period is close to one year ;

- if we suppose a small price increase (say 2 %) based on a better assessment of quality (although not as good as with 100 % inspection), we end up with even bigger benefits.

5.3 Other subsystems

Many individual subsystems can be marketed, either separately or in any combination :

- an on-line firmness sensor, with a capacity between 3000 and 5000 fruits / hour ;

- a high quality colour and defect detection system with a capability to view 100 % of the fruit area, with a capacity of 1500 to 2500 fruits / hour ;

- an on-line sugar sensor, with a capacity between 3000 and 5000 fruits / hour;

- a robot based packing unit, with a capacity of 1500 to 2500 fruits / hour ;

- a packing line supervision software, for all packing houses interested in managing a lot of quality parameters.

Conclusion

If we now summarise the above points and compare them to the original concept as described, we can say that we have covered roughly :

- 40 % of the original market ;
- 80 % of the original sensor technologies (only aromas left aside);
- 65 % of the original handling principles ;
- 60 % of the planned throughput, to be improved.

Since the original concept was intentionally very broad, it is obvious that we could not expect a 100 % fulfilment of any of the above topics. Moreover, we have come up with many new ideas for partial exploitation.

As planned, one to two years of industrial development is now necessary to reach commercially acceptable results. This will be made in parallel to several presentations that will give us user feedback :

- scientific presentation : Sensoral, Montpellier, Feb. 98,
- commercial presntations : Euroagro, Valencia, april 98, and Feria de Lerida, Sept 98.

References

[1] : PICUS Matt, PELEG Kalman (Technion Israel Institute of Technology, HAIFA 32000) : *«Adaptive Simulation of Human Assessment of Fruit Quality»* Sensoral 98 Conference, Feb. 98, Montpellier, France.

[2] : Roger J.M., Fayolle P., Steinmetz V., Dusserre-Bresson L., Bellon-Maurel V. : *«An On-Line NIR System to Sort Fruits According to Sugar Content»* Sensoral 98. Montpellier, France. Feb. 98.

[3] : Steinmetz V., Bellon-Maurel V., Sevila F. 1998. *«A methodology for sensor fusion design: application to fruit quality assessment».* Sensoral 98. Montpellier, France. Feb. 98.

[4] : Brochure of the *«Calistar»* product, Caustier and Aweta companies, at SITEVI, Nov. 97, Montpellier. Caustier France, 110, Av. Georges Caustier, 66000 Perpignan, France.

[5] : E. Moltó, J.Blasco, V.Steinmetz, A. Bourély, F.Navarrón, G.Perotto. 1997. SHIVA: «A robotics solution for automatic handling, inspection and packing of fruit and vegetables». *Bio-Robotics'97 International Workshop on robotics and automated machinery for bio-productions. Gandia, Valencia, Spain. Sept 97. pp. 65-70.*

A measurement method for ordered category scales

Une méthode de mesure pour les échelles de catégories ordonnées

Michel Maurin

INRETS-LEN, case 24, 69 675 Bron cedex, France
e-mail : maurin@inrets.fr

Abstract: *successive intervals apply measurement precautions to responses on ordered category scales.*

Keywords*: Measurement theory, psychophysics, category scale, successive intervals.*

Résumé : Les intervalles successifs, une méthode qui permet d'appliquer les préceptes de la théorie du Mesurage aux réponses données sur des échelles de catégories ordonnées.

1. Introduction

Many times subjective responses in surveys are recorded following a very simple way with ordered category scales. This is a classical method, quite in the field of Psychophysics as exposed in [14, 25], for instance when studying road noise surveys and related annoyance of people [12]. Many times also there is a (more or less) strong numbers appeal (and/or tropism) and numerical processing intents ; then a not at all trite involved question is how to deal with categorical data with respect to meaningfulness and technical number's properties.

This is what is to-day a measurement question, and fortunately, as many psychophysical protocols, ordered categories have been recovered and renewed as an application of measurement theory, more specially in a pioneering paper of Suppes and Zinnes [24], developping a previous one of Adams and Messick [1], (in relation with thurstonian transforms).

Here we recall some of the main findings of successive intervals, and its related association between phychophysics and measurement theory.

2. Ordered category scales

Ordered category scales is a common way to collect responses of people (Appendix 1 page 569) ; the (a priori) categories proposed for answers may be defined by semantic descriptors (not at all, little, medium, ...) or no. Because an important need of numerical processing, many times in order to get a numerical relationship between quantified responses and physical stimulations values, ordered categories are usually scored by their rank and crude arithmetical and statistical processing are used, such as arithmetic means, Pearson correlation coefficients and so on ..., in a sort of «a bit hair raising» calculations as said by Luce and Galanter [14].

3. The measurement theory

The matter of measurement theory is to provide relevant numerical images for each element e_i of a global set E of observed (or recorded) phenomena ; the image $\Phi(e_i)$ is a particular numerical value assigned to e_i. Of course there is no meaning to assign values anyhow or following arbitrary rules, and the specific content of theory is to take some wise cares. In many times observations fulfill experimental ralations (conditions, laws, axioms $R_{(h)}$, Appendix 2 page 573), then the main purpose is to provide numerical assignments under conditions that every qualitative relation is correctly recovered by numerical images. This means one is looking for a suitable correspondance Φ between the set of e_i and a set of $\Phi(e_i)$ (homomorphism of

structures yielding a numerical representation of data). Once theorems have been developped $R_{(h)}$ conditions become testable in order to conclude about the formal existence of representation.

As Gaston Bachelard declared in a sort of preview (in fourties) «notre but est d'établir une correspondance entre les pensées expérimentales et les pensées algébriques» [3], or following one of his usual and forceful aphorism «il faut réfléchir pour mesurer et non pas mesurer pour réfléchir» [2] [our purpose is to get a correspondance between experimental thoughts and algebraical ones / one has to think about in order to measure and not the reverse].

Psychophysics has become an important field of applications and developments of measurement theory ; here we consider the successive intervals as method applying this theory to ordered category scales.

4. The successive intervals

4.1

As mentioned by Suppes and Zinnes about Adams and Messick paper (1958), successive intervals results are «measurement-orthodox».

Here we suppose observed people are exposed to stimulations S_i i = 1... I and give their responses on categories C_j j = 1...J ; then raw data are absolute frequencies n_{ij} in a two-way contingency table, say the number of reponses for people exposed to S_i and choosing C_j, or resulting conditional observed frequencies ϖ_{ij} =

$$\frac{n_{ij}}{\sum_1 n_{il}}$$ j =1...J for every i = 1...I.

4.2

One considers a simulation implies a discriminal random process S_i which here is described by the density function $f_i(x) = \frac{1}{\sigma_i} f(\frac{x-\mu_i}{\sigma_i})$ with mean $\mu_i + m_f \sigma_i$ and variance $\sigma_f^2 \sigma_i^2$, m_f and σ_f^2 the respective mean and variance of a given f density, F its related cumulative function, μ_i and σ_i parameters attached to S_i. The model says also that every category C_j is represented by an interval $[t_{j-1}, t_j]$ on the same continuum than x and μ_i, with $t_0 = -\infty$, $t_{J+1} = \infty$, and that for every boundary t_j

common to C_j and C_{j+1} it corresponds a random variable T_j with a Dirac distribution δt_j. If ϖ_{ij} is the probability of C_j response when exposed to S_i , say $P\{C_j \mid S_i\}$, then the probability of conditional event $\{C_1 \cup ... \cup C_j \mid S_i\}$ is given by $Prob(S_i - T_j < 0) = \sum_{l=1..j} \varpi_{il} = F(\frac{t-\mu_i}{\sigma_i}) = \int_{-\infty}^{t_j} f(\frac{x-\mu_i}{\sigma_i}) \frac{dx}{s_i}$ [25].

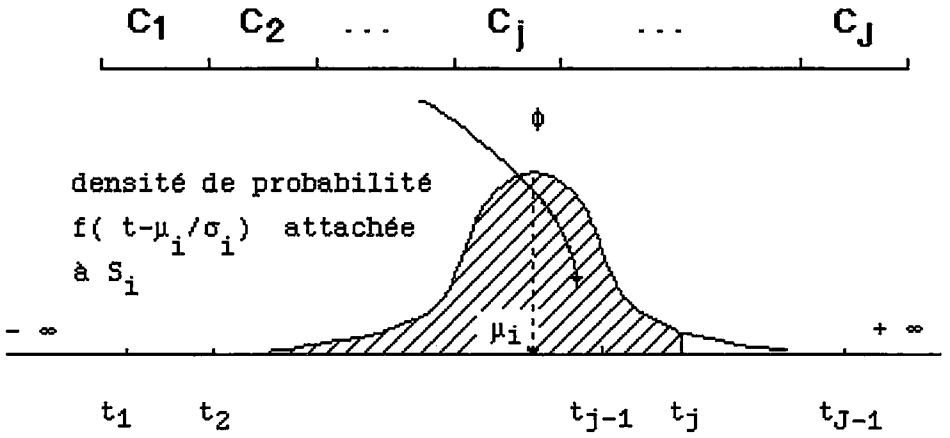

4.3

If π_{ij} are cumulated observed frequencies $\sum_{l=1..j} \varpi_{il}$, the $z_{ij} = F^{-1}(\pi_{ij})$ are given by $\frac{t-\mu_i}{\sigma_i}$. The Adams and Messick conditions says that experimentally observed z_{ij} fit linear relations

$z_{nj} = a_{nm} z_{mj} + b_{nm}$ for every indices m, n = 1,...,I et j = 1,...,J-1 with no mention to unknown parameters μ_i, σ_i and t_j, (a_{nm} are positive, of course such linear relations are testable).

The measurement theorem states that whenever $z_{ij} = F^{-1}(\pi_{ij})$ checks such linear relations there exist simultaneously three scales of measurement (the representation), one ratio scale for standard deviation σ_i, one interval scale for stimuli μ_i and one for boundaries t_j (each of them with the same change of unit, the uniqueness, Appendix 2), in accordance with Thurstone and usual psychophysical postulates. This is a result quite included in measurement theory in early times ([24], 1963) and more or less forgotten since this time [16] .

4.4

What may be recalled, in order to show differences between classical resolutions of successive intervals and Adams and Messick result is related to probabilistic distributions of random variables S_i and T_j. For thurstonian practices there are normal laws with respective means and standard deviations, and this involves too many unknown and cumbersome methods of identification [25], Appendix 1 ; but following Adams and Messick S_i laws are normal or no (on Re), and T_j laws are Dirac, then one gets conjointly a generalisation (for S_i laws) and a simplification (for T_j laws) which render possible more convenient conditions as exhibited by Adams and Messick.

4.5

The scaling step : once μ_i, t_j and σ_i do exist it may be useful to calculate them, this is a scaling step which is very simple with a mere least square adjusment.

Indeed $z_{ij} = F^{-1}(\pi_{ij}) = \frac{t_j - \mu_i}{\sigma_i}$ may be rewritten $z_{ij} = a_i t_j + b_i$, $a_i = \frac{1}{s_i}$, $b_i = \frac{-\mu_i}{\sigma_i}$,

and when the scales of measurement do exist the scaling may be to minimize $Q = \sum_{i,j}^{I,J-1} (z_{ij} - a_i t_j - b_i)^2$ under additional conditions such as $\sum_{j=1}^{J-1} t_j = 0$ and $\sum_{j=1}^{J-1} t_j^2 = C$ because the two free parameters of an interval scale. We are led to a simple matrix question ; let I_K identity matrix, e_K unit vector in R^K and z the z_{ij} table, when the z table is complete, the set of a_i values is the latent vector of matrix $M = z \{I_{J-1} - \frac{1}{J-1} e_{J-1} e_{J-1}'\} z'$ corresponding to the biggest latent root [15]. When z table is incomplete solutions are given by an iterative convergent processing [17].

4.6

Example : in a french road noise annoyance survey one recorded annoyance on a 4 categories scale and corresponding noise levels (L_i split in nine 3 dB range physical intervals). The survey yields raw data n_{ij} then conditional distribution frequencies ω_{ij}, and π_{ij} and z_{ij} with the cumulative distribution function F of Gumbel law (say extreme law) [19].

Usual crude presentation gives % of responses by levels of exposures (below left), while measurement processing yields relevant values for simulations L_i and

category boundaries t_j (below right). For instance one may observe a sort of S shape for the relationship, and that categories have not at all the same range.

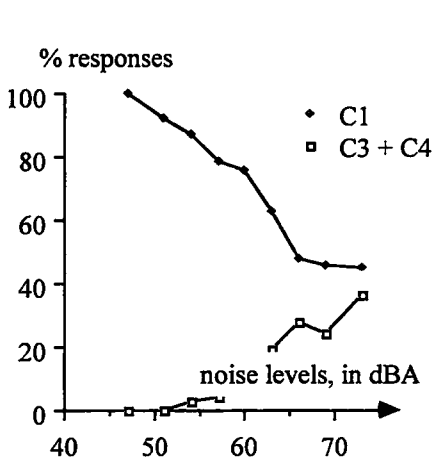

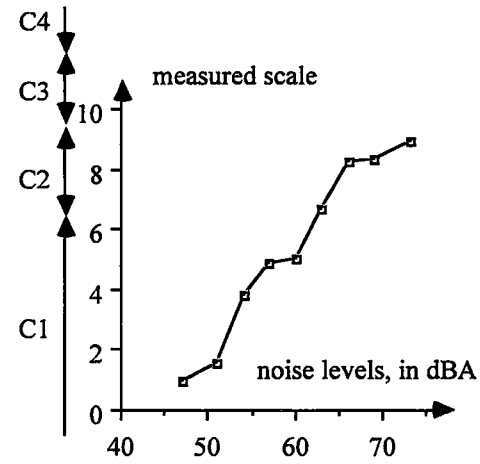

legend : C_1 not annoyed -> C_4 very *ordinate : L_i and t_j reported values*

Other applications (and different shapes of numerical relationships) are shown in [18] for instance.

Conclusion

When one deals with ordered category scales in records or surveys, successive intervals is a fine method around which the measurement theory and psychophysics meet each other ; it renders possible to get numerical measurement for the boundaries of categories and for the physical stimulations on a same interval scale, following the cares of measurement démarche.

Then it leads also to a numerical correspondence between physical and subjective continuum because the two respective set of values for physical stimulations S_i i = 1...I.

Références (text, appendices)

[1] Adams E., Messick S., 1958, An axiomatic formulation and generalisation of successive intervals scaling, *Psychometrika, 23 n°4, 355-368.*

[2] Bachelard G., 1934, *Le nouvel esprit scientifique,* PUF.

[3] Bachelard G., 1948, *Le rationalisme appliqué,* PUF.

[4] Cliff N., 1973, Scaling, *Annual review of Psychology, 473-506.*

[5] Coombs C.H., Dawes R.M., Tversky A., 1970, *Mathematical psychology,* Englewood cliff, New-Jersey, Prentice-Hall.

[6] Falmagne J.C., 1974, Foundations of fechnerian psychophysics, in Krantz, Atkinson, Luce, Suppes, *Contemporary develop. in math. psych., vol II, San Francisco, Freeman, 127-159.*

[7] Falmagne J.C., 1976, Random conjoint measurement and loudness summation, *Psychological review, 83 n°1, 65-79.*

[8] Falmagne J.C., 1985, Elements of Psychophysical theory, *Clarendon Press - Oxford.*

[9] Galanter E., Messick S., 1961, The relation between category and magnitude scales of loudness, *Psychological review, 68 n°6, 363-372.*

[10] Hamerle A., Tutz G., 1980, goodness of fit tests for probabilistic measurement models , J. of Math. *Psychology, 21, 153-167.*

[11] Krantz D.H., Luce R.D., Suppes P., Tversky A., 1971, *Foundations of measurement, vol 1, 2 and 3, AC. Press.*

[12] Langdon F.J., 1975, The problem of measuring the effects of traffic noise, in Alexandre, Barde, Lamure, Langdon, Road traffic noise, *Applied Science, 27-69.*

[13] Luce R.D, Edwards W., 1958, The derivation of subjective scales from just noticeable differences, *Psychological review, 65 n°4, 227-237.*

[14] Luce R.D., Galanter E., 1963, Discrimination, Psychological scaling, in Luce, Bush, Galanter, *Handbook of math. psychology, vol 1, J. Wiley, 191-243 and 245-307.*

[15] Maurin M., 1983, An another least-square solution for the successive intervals following Adams and Messick, *3rth european meeting of the Psychometric society, Jouy-en-Josas.*

[16] Maurin M., 1986, L'association du mesurage additif conjoint et des intervalles successifs, *Mathématiques et Sciences Humaines, n° 96, 5-29.*

[17] Maurin M., 1987, *Le traitement des échelles de catégories, rapport INRETS n° 37.*

[18] Maurin M., Versace R., Peris JL., 1988, *Noise annoyance measurement, category scales and context effect, vol 3, 235-240,* 5th Int. C. on noise as a public health problem, Stockholm.

[19] Maurin M., Lambert J., 1990, Exposure of the French population to transport noise, *Noise Control Engineering Journal, vol 35 n° 1, 5-18.*

[20] Pfanzagl J., 1973, *Theory of measurement*, Physica Verlag, Wurzburg, Wien.

[21] Roberts F.J., 1979, *Measurement theory*, Reading Massachussetts, Add. Wesley P. Co.

[22] Stevens S.S., 1966, A metric for the social concensus, *Science, 151, 530-541.*

[23] Stevens S.S., 1971, Issues in psychophysics, *Psychological review, 78 n°5, 426-450.*

[24] Suppes P., Zinnes J.L., 1963, Basic measurement theory, in Luce, Bush, Galanter, *Handbook of math. psychology, vol 1, J. Wiley, 1-76.*

[25] Torgerson W.S., 1958, *Theory and methods of scaling,* J. Wiley.

- Appendix 1 -
A general framework for psychophysical laws

Introduction

The subject of psychophysics as founded by Fechner is to "quantify" the sensations experienced when exposed to different intensities of a physical stimulus, and to set a "psychophysical law" or relationship between the measured stimulus and the numerically evaluated sensation (Fechner was coming from physics). There are a number of ways in which a sensation can be measured [14, 25] that can be roughly schematized as in figure A.

1. A first set of direct relationships

1.1

The Fechner law : Fechner (1860) followed a semi-direct way on «adding» together what is called just noticeable differences «jnd» with reference to a confusion-discrimination scale. Let the jnd Δu allowing perceived difference between sensations respectively equal to u_F and $u_F + \Delta u$, corresponding to physical intensities x and $x + \Delta x$; a previous Weber law says $\frac{\Delta x}{x} = K$ and because Fechner law is «$\Delta u_F = C$» with no dependency in Δ_F, Fechner concluded that $\frac{\Delta u_F}{\Delta x} = \frac{C}{Kx}$, or $\frac{du_F}{dx} = \frac{C}{Kx}$ in a differential option then leading to a famous logarithmic correspondence $u_F = C' \text{ Log } x + C''$, say the sensation is a logarithm of physical excitation. Fechner imposed his point of view for a long time without any discussion while there is matter to do so. When revisited Weber law allows to-day more correct formulation and analytical solutions, still implying logarithm [8, 13] (but in a less absolute way).

1.2

The Stevens law : Stevens ($\approx$ 1937) evaluated the sensation directly on making use of the usual proportional properties of real positive numbers and proposed the power law $u_S = \gamma x^{\alpha}$ (magnitude estimation method and scale). This may be applied to many «prothetic» stimuli, with exponents varying between 0,3 (loudness) or 3,5

(electric shock) [21, 22] ; truly there is no reason to oppose the two démarches (but confusion happened somewhat).

1.3

Psychometric functions : Let $P(x_i, x_k)$ the probability with which x_i stimuli is judged higher than x_k (Urban psychometric functions, 1907) ; this leads to the method of constant or standard stimuli when $x_k = x_0$ fixed, and Sandford, Titchener simplified the method on rating the stimuli into adjacent ordered categories, the limits of which intervening as fictitious stimuli. This is the single stimulus method, yielding a partition scale ; soon a discrepancy has been observed between Stevens and single stimulus results (the Stevens partition paradox).

2. Indirect thurstonian methods

2.1

In 1927 (between Fechner and Stevens) Thurstone proposed an another approach in order to quantify sensations on a confusion-discrimination scale. The procedure is based on the randomness of subjective evaluations involved by discriminal processes due to stimuli ; the numerical values are (here normal) random variables whose means are numerical evaluations respectively corresponding to each stimulus.

This is the «law of comparative judgment», and because this global view introduces too many parameters Thurstone proposed different processing options as cases I, II ... or later conditions A, B, ... [25].

2.2

Towards 1935 this thurstonian procedure is applied to partition scales, every category C_j is represented by an interval $[t_{j-1}, t_j]$ on the numerical continuum for sensation evaluation whose category boundaries t_{j-1} , t_j correspond to new another discriminal processes ; this provides the «law of categorical judgements».

Here again the equations contain more unknown parameters than relations, it is therefore necessary again to consider additional options in order to resolve the sensations' scaling, as for instance conditions A, B, ... [25].

3. As a closure, the final formal network

In 1961 Galanter and Messick employed their version of thurstonian transform to loudness data (on a category scale), and surprisingly they discovered «happily ... the processed category scale is a logarithmic function of the magnitude scale, ...

the form of the (non linear) relation is no longer a mystery» [9], and then explained and resolved the partition paradox.

In the same time Ekman law set a new link between Fechner and Stevens evaluations [4, 22], say a logarithmic relation as $u_F = C''' \text{ Log } u_S + C''''$, enhanced again by Falmagne [6].

We should note here how :

a) once the paradox is solved we get a complete framework of coherent relations between the different psychophysical measuring procedures, including category partition scales and successive intervals method's relevancy ;

b) technically speaking the logarithmic relation may be associated with the fact that the confusion-discrimination scale is an interval scale and magnitude estimation one a ratio scale. This is consistent with the more or less implicit assumptions made by Fechner and Thurstone.

4. Additional comments

In later papers Stevens [23] was aware of «nomothetic» results, meanwhile he did not mention this global framework.

Nowadays emphasis is preferably put on a «fechnerian representation» included in probabilistic consistency models, checking the formulation $P(x_i, x_k) = F[u(x_k) - u(x_i)]$, with an utility function u and a cumulative distribution function F [6, 8, 21] ; this recovers Urban Sandford Titchener and Thurstone views with respect to confusion and discrimination processes and scale, and may entail some framewok shortcuts.

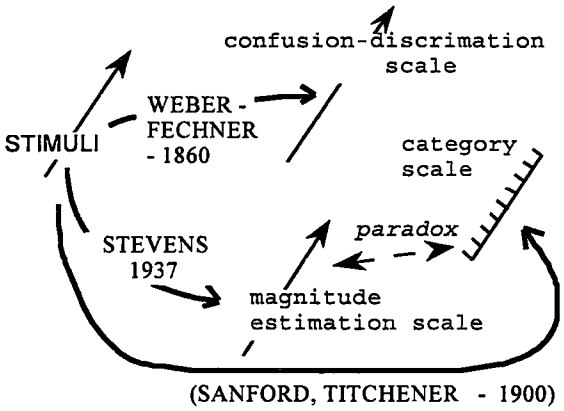

1 - WEBER-FECHNER and STEVENS laws, single stimulus method, partition paradox

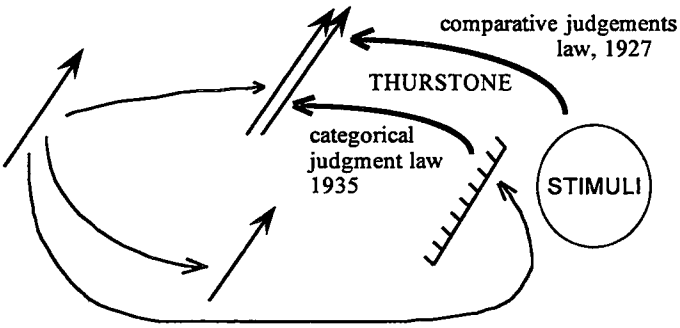

2 - thurstonian technics

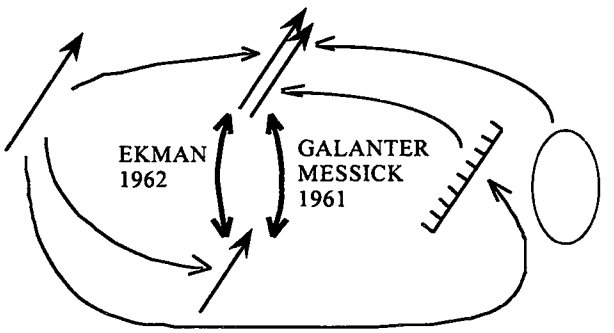

3 - EKMAN and GALANTER-MESSIC laws, paradox solution

Figure 1: An overall Psychophysical framework

- Appendix 2 -
Some words about the measurement theory
[11, 20, 21]

1.

The need of getting a numerical assignments for «objects» of our environment is very ancient, for instance the geometry or better geo-metry is said to be due to the recovering of fields after every yearly Nilus flood, one of the first Bible's title is devoted to Numbers and counting (and then promoted mathematical developments).

The success of classical physics (from $XVII^{e}$) is partly due to the possibility of attaching a function for every physical variable, and the power of differential Calculus (with properties able to recover some anthropomorphic intuitions as continuity, regularity ...). With surprising quantum physics and essential discontinuity in sub-atomic nature (XX^{e}), an another class of mathematical tools have been proposed for the same purpose, say the hermitian operators with their latent roots discrete spectrum.

2.

The measurement theory appears to be a new one again methodology in order to provide a suitable and meaningfull numerical assignment for observations, from sixties. Of course this is useless for previous successful démarches but important for qualitative observations and phenomena as in economics or human sciences, and its major technical support is set theory.

2.1

One considers the global set E of observations e_i of an experiment among which there are some observed relations, as order relations, preferences (binary relations), more complex n-ary relations, internal operating rules (as 3-ary relations, setting two masses on a same pan of a two-pan balance and equilibrium with a third,...), ... ; all of this constitutes an algebraic structured set called empirical relational system $E = \{E, R_{(1)}, R_{(2)}, ..., R_{(k)}\}$ with mention to set E and relations $R_{(h)}$.

The main (and rather natural) idea is to get numerical images only if one may show there exists an ad hoc mathematical structured set V with analogous relations $S_{(h)}$ called a numerical relational system $V = \{V, S_{(i)}, S_{(2)}, ..., S_{(k)}\}$ and an application ϕ between both, such that related images $v_i = \phi(e_i)$ check relations $S_{(h)}$ so as e_i do

check $R_{(h)}$ (they are homomorphic structures). For instance V is the set of real numbers Re or an euclidean real vectorial space :
$R_{(h)}(e_{i1}, e_{i2}, \ldots, e_{ih}) <=> S_{(h)}(\phi(e_{i1}), \phi(e_{i2}), \ldots, \phi(e_{ih}))$.

The triple {E, V, ϕ} is the scale of measurement for e_i and E.

Then one gets numerical assignments with respect to qualitative informations observer has discover about data, but without any a priori postulated scaling, and this constitute the cares and precautions in order to avoid more or less arbitrary assignments. It is the first step of measurement, the Representation step, whose conclusion is the formal existence of numerical values with respect of experimental (and then testable) properties, quite based upon mathematical demonstrations (and some algebra).

Relations $R_{(h)}$ are also called qualitative laws, deterministic conditions or again axioms.

2.2

There may be no unicity for ϕ and consequently many possible scales. Many times, under some natural conditions of regularity, these solutions are g 0 ϕ with a class of internal transforms g into V. The class of admissible g is a sub-group G of V-automorphisms, and the nature of G provides keen informations about the scale ; this is the Uniqueness step.

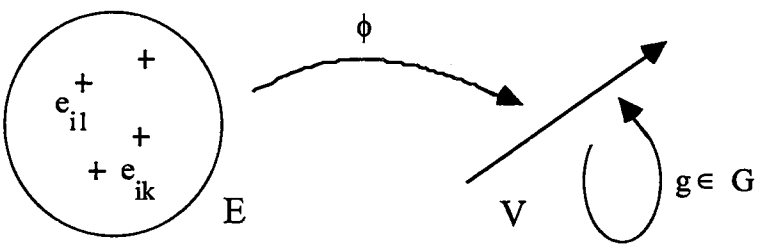

When V = Re the most common situations are :

admissible g	scale type	exemples
g = identity	absolute	counting
g(x) = c x , c positive	ratio	mass, length
g(x) = c x + b , c positive	interval	temperature C°
g increasing	ordinal	hardness
g bijective	nominal, qualitative	labeling

2.3

This renders possible the Meaningfulness step related to numerical statements. Indeed once we get numerical values one may be tempted to use them in new formal numerical statements and to deal with them rather than with original observations, say $\Psi[\phi(e_{i1}), \phi(e_{i2}), ..., \phi(e_{ih})]$. However when we are considering a such statement it may be a nonsense or no, for instance player with jersey n° 23 in a basket-ball team is probably not 23 times better than player with jersey n° 1 !, and so on .... The meaningfulness step of the theory is devoted to investigate the relevance of the content of every statement, a clear response is to say that Y is meaningfull or no according to $\Psi[g\ 0\ \phi(e_{i1}), g\ 0\ \phi(e_{i2}), ..., g\ 0\ \phi(e_{ih})]$ is always true or false for every g of previous G coming from uniqueness (an invariant under the action of G sub-group).

This part has been sensed for the special use of ordinary statistical statements, in a general way geometric means for ratio scales, arithmetic for interval scales, quantiles for ordinal scales, mode and entropy for nominal scales [22].

3.

When one looks for numerical values one may have a scaling step [5] ; there are also other parts of discussion in relation with derived or fundamental scales (according to there is a previous fundamental scale or no in the conditions for the Representation).

An another important extension is related to the probabilistic measurement [7, 10], with respect to the general idea that because observations are randomly noised (as every thing) a strict and determinstc fulfillment of algebraic axioms is not possible ; then there is a need to introduce random in measurement presentation in order to deal with noised data.

Real time quality evaluation of biscuit during baking using sensor fusion

Fusion multi-sensorielle pour l'évaluation temps réel de la qualité des biscuits pendant la cuisson

N. Perrot, G.Trystram
ENSIA - INRA,
1, ave des Olympiades,
91305 MASSY, France

F. Chevrie, N. Schoesetters, F. Guely
ICT, EPAP, Telemécanique,
BP 204,
92002 NANTERRE, France

Abstract: *For the control of food processes, several ways are encountered. The role of the operators is not easy to take into account and not many industrial applications are proposed. The potential of new tools from artificial intelligence seems to be great. Progresses are recognised, for example with neural computing. The use of Fuzzy logic is not so extended. Some results concern the implementation of fuzzy controler and the comparison with PID control. But the power of fuzzy controler is much better for helping the operator for piloting the plant. We propose some applications and reflexions concerning: the design and validation of fuzzy sensor, the data treatment using fuzzy classifier and the development of an expert system based upon a fuzzy rules base. The applications presented here concern the baking of biscuit.*

Keywords: *Baking, biscuits, color, fuzzy sets, sensor fusion.*

Résumé : Pour contrôler les procédés agro-alimentaires, plusieurs voies sont possibles. Il n'est pas aisé de prendre en compte le rôle de l'opérateur et peu d'applications industrielles sont proposées. Le potentiel de nouveaux outils tirés de l'intelligence artificielle semble important. Les progrès sont reconnus par exemple en programmation de systèmes neuronaux. L'utilisation de logique floue n'est pas très développée. Certains résultats concernent l'implémentation de contrôleurs flous et la comparaison avec un contrôle par PID. Mais le contrôleur flou est mieux adapté pour assister l'opérateur dans la gestion de l'usine. Nous proposons des applications et des réflexions sur : la conception et la validation d'un capteur flou, le traitement de données utilisant un classificateur flou, le développement d'un système expert fondé sur une base de règles floues. Les applications présentées concernent la cuisson des biscuits.

1. Introduction

In the food industries, processes are often complicated because of non linearity, interactions and the gap of knowledge concerning their control, lack of sensors for example. Classical automatic control seems to be difficult, and many open loop are encountered in which the role of the human operator become more and more important. Product properties which contribute to qualities, and process productivity depend mainly on the accuracy of his reaction.

In order to decide on modifications to actuators, the human operator uses on line measurements performed by sensors. But it is not the only source of information. A large part is obtained from subjective evaluation. For example, in the case of baking of cereal products, color, shape and decor are important properties for the product. Often there are no sensors available to measure such information in real time, on line. The only way is the human evaluation.

It is well known that it is difficult to establish a link between human evaluation and sensor measurements. Nevertheless the search of a relationship between human evaluation and sensors output is an interesting way for progress in control applications. Because the food quality is a complex information, the use of sensor fusion seems to be a way for the integration of several information. Sensor fusion is an intersting approach which consists on the definition of process indicators able to be processed on line, oin real time, from more than one measurement using smart data treatments, like classification, modelling etc... Classification methods are one of the tools able to perform such fusion tasks, especially because the human evaluation is often more a classification than continuous evaluation. Because they are numerous studies of classification techniques for such problems, the purpose of this study is to apply classification methods combined with sensors measurements in order to perform the same job as a human operator for the subjective evaluation of the color of biscuits after the baking oven.

Color is an important property of biscuit which is in fact a complex three dimensional information. Two approaches of classification could be compared. A classical Bayes approach is developed, which was never applied for baking, results are not described at lenght here. And a fuzzy based classification approach is developed and validated. Applications concern an industrial oven for several kind of biscuits. Two others applications are presented for building tools for decision support sytem.

2. Materials and methods

2.1 Products and ovens

For the purpose of this work, industrial ovens are used. They are direct fired multi burner oven, heated with natural gas. It consists of four combustion chambers in the roof and base, equipped with 30 burners each. Temperature both for roof and base are independently controlled in each section.

Biscuits are crackers. Several kind of biscuits are considered here and different monitoring are performed on each product in order to obtain a sufficient data base. Two results are considered for two kind of biscuits as biscuit 1 and biscuit 2.

2.2 Measurements

Subjective evaluation of color

Operator have an important task which consist on the evaluation of product qualities, specifically color. A comparison with a reference allows him to sort the biscuit in five classes. This classification allows the human operator to monitore the oven. Operators could be considered as a reproducible measurement system. This work takes into account existing classes.

Sensors color

The sensor used in this work is the Colorex from Infrared Engineenring. The principle is quite simple. A light (D65) is generated, filtered (3 filters) and the reflected light from the top of the biscuit is analysed before conversion into an electrical signal. 3 data outputs are available (L, a, and b for example), which permit to represent the color in the three dimensionnal space which charaterizes the color (14). The sensor is located at 25 mm from the top of the biscuit, without contact with it. The measurement is inhibited between each biscuit, when the sensor is used in real time, on line. Calibration is realized from sampling and comparison with a laboratory spectrocolorimeter. A very good correlation was obtained, the error between the two measurement apparatus is less than 1%.

2.3 Methods

Fuzzy classification

In today's literature we can find different fuzzy classification technics. Some of them are an adaptation of hard classification techniques (9, 7, 4). For more details

see (2). Other classifications are more specifically based on the concept of fuzzy logic. Thus, for example, (6, 8) as well as (12), use fuzzy if then rules to perform classification. The rules are generated automatically from numerical data. The pattern space is partitionned in fuzzy subspaces and each fuzzy subspace is associated to a class. Therefore the choice of a fuzzy partition is both very important and difficult. Moreover if the shape of the classes is complex, the size of the training set must be important.

To cope with this problem, some authors partition the pattern space into an arbitrary shape. Thus (13) use a neural network inspired from the structure of fuzzy if then rules to partitionned the space on an arbitrary shape.

Other approaches are proposed based upon fuzzy tools. The most used method is the k-nearest neigbourh (7). The principle is to search the k neigbouhr as near as possioble with the sample we want to sort.

A recent work (1) presents the same results but with classical fuzzy if then rules. Thus they introduce an interesting concept appropriate to the color perception. Indeed they use a fuzzy sensor to evaluate human color perception from three numerical variables: R, V, B. This sensor is based on the concept of fuzzy subset in multidimensional spaces. This notion is well adapted to our problem. Indeed we do not need the use of fuzzy inferences because we are upstream of the decision.

This method's domain appears to be close to our problem. Therefore, we'll use this method to link the colors of biscuits to the linguistic notions manipulated by the operators (fig. 1).

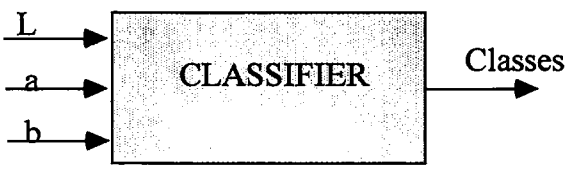

Figure 1: Principle of the classifier

The fuzzy multicomponent membership function concept (1) generalizes the classical notion of fuzzy membership function. This one is developped in fuzzy set theory (15). A fuzzy subset E of X, is defined by a fuzzy membership function that associates to each element x of X, its membership degree to A in the range [0,1], denoted as A(x). The fuzzy membership function is an extension of the characteristic function associated to the classical sets.

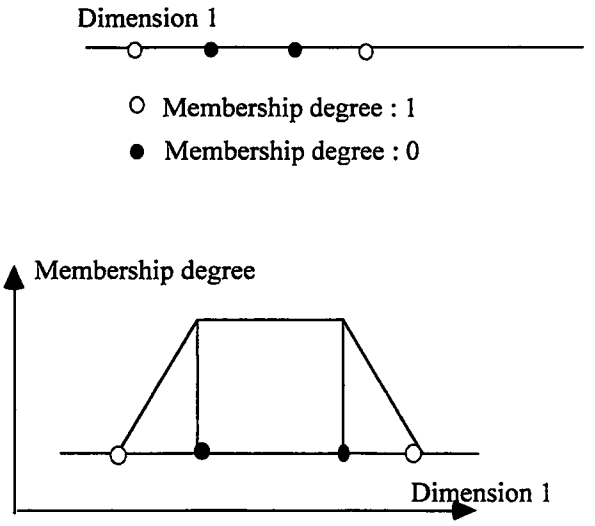

Figure 2: Principle of the fuzzy membership function in one dimension

More generally, the typical points of a fuzzy membership function can be represented first on the X axis; second by adding the vertical axis of the membership degrees (fig. 2).

We can imagine a generalization of this notion if we define the linguistic term on more than one variable (for example the linguistic notion: "color" should be defined on three variables: R (red), G (green), B (blue)). The corresponding linear relationships between the points of a classical fuzzy membership function is obtained by triangulation (method of meshing by Delaunay (5). Fig. 3 shows an example of a fuzzy multicomponent membership function.

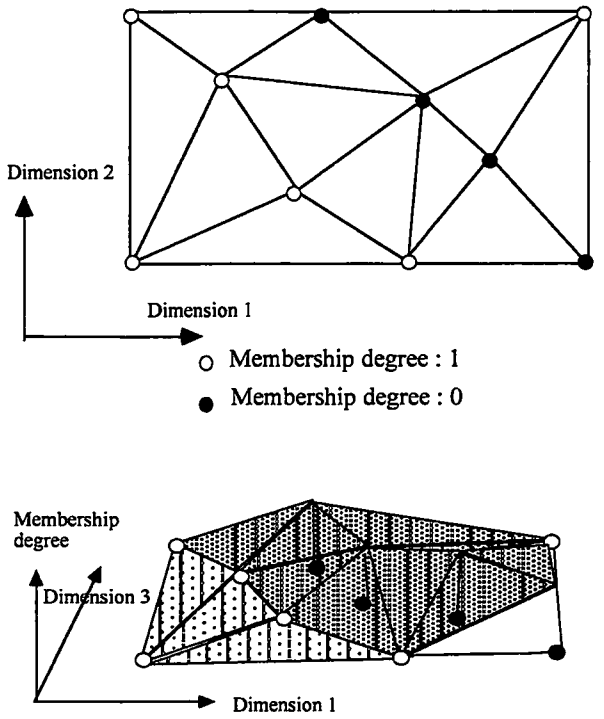

Figure 3: Principle of the fuzzy membership function in two dimensions

The adjustment of the fuzzy multicomponent membership function is realized during a training stage. The triangulation is achieved on the base of the points labeled by the operators. The training stage is performed with about 5 points per class. Other points' description is then defined based on the training set.

This classification method has been put on a PC and adapted to our experiment (3). The program is composed of two parts: part 1 for triangulation; part 2 for the extraction of membership degrees of the point of the different classes.

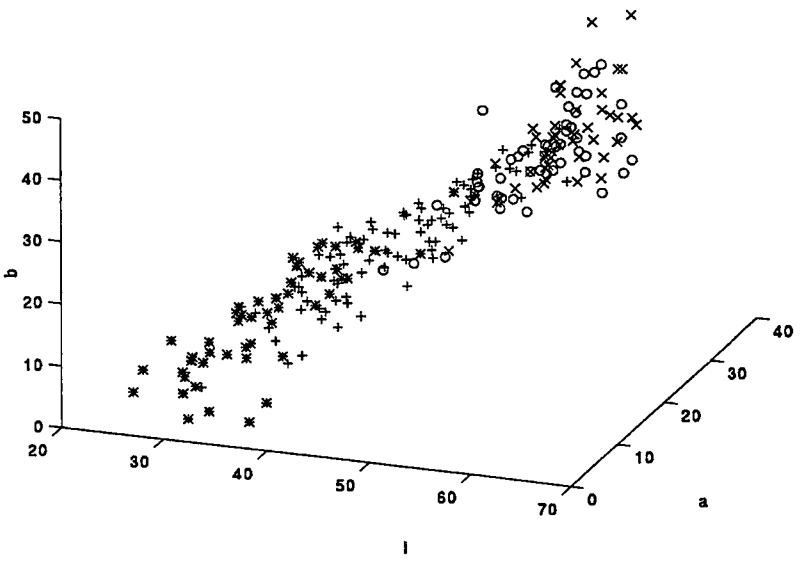

Figure 4: Presentation of classes of color biscuits in the L,a,b, space

Experimental method

Samples of cookies are taken out from the oven on different ovens of an industrial site (10). Color measures (L, a, b) are done on this samples. Two type of cookies are considered. For each of these type four classes are dealt with. Each sample is labeled by an operator. For each sample, 4 color measurements are taken.

Validation on testing points

In order to take into account less noisy measures, we consider one learning sample as the means of the four real color measurements performed on each sample. For each class the learning sample must be representative of the class. The learning sample is composed of about 5 points, which belong to a certain class without any ambiguities.

The testing points are noisy. Fig. 4 represents all points for each class and for all the learning and test samples of cookies of type 1 in the pattern space (L, a, b). This figure shows the complexity of the shape of the classes. Furthermore, we must consider, first, that the three parameters L, a, b are essential to the characterization of each class. Second there is no simple relation between L, a, b. Last we can indicate that these points could not be classified by an hyperplan.

Real time validation

In this experiment, the goal is to validate the predictive character of the classifier. The cookies are of type 2. The experimentation is conducted from the moment the oven is turned on. At this time the cookies are often over cooked. Then the operator's work is to bring back the cookies to a satisfactory class of color. To do this, he continuously controls the color of the cookies and simultaneously acts up on his oven. During this stage we set apart each two minutes samples of cookies that have been previously labeled by the operators. Color measurements L, a, b are taken from these samples. The protocol of the experiment is: 6 samples of cookies are analysed at each time. The mean of the 6 results of classification for each class is calculated. On this mean the barycenter of the classifications is take into account.

Points	L(%)	a(%)	b(%)	Operator classification	Bayesian classification	Fuzzy classification (%)
TYPE1						
P1	64.1	7.8	31.9	C1	C1	**C1=94** et C2=4
P2	69.3	5.8	31.5	C2	C2	C1=5 et **C2=94**
P3	74.6	1.20	25.10	C3	C3	C3=26 et C4=67
P4	73.7	1.9	26	C3	C3	**C3=98** et C4=0
P5	75.7	2	26.6	C4	C4	C3=22 et C4=77
TYPE2						
P6	30.6	3.3	7.9	C1	C1	**C1=97**
P7	31.9	4.3	9.8	C1	C1	**C1=96**
P8	53.1	15.9	35.5	C2	C2	**C2=50** et C3=38
P9	45.8	12.7	22	C2	C2	**C2=88**
P10	47.1	12.1	28.1	C2	C2	**C2=93**
P11	61	21.4	40	C3	C4	**C3=72** et C4=21
P12	49.9	16.9	21.6	C3	C3	**C2=75**
P13	58.1	21.2	33.7	C3	C4	C2=29 et **C3=65**
P14	52.7	21.7	34	C4	C3	C2=26 et **C3=73**
P15	54.4	26.3	36.9	C4	C3	**C3=46** et C4=41

Table 1: comparative classification of test points by operators, fuzzy classifier and Bayesian classifier. The fuzzy membership degree: 0 % are not indicated in this table

3. Discussion

In this part chapter our purpose is to discuss, first the results obtained with the classifier on test points; second the results obtained during the real time experiment.

3.1 Results on test points

Fig. 5 shows the results on test points for two types of cookies (type1 and type2). The same results are presented in details in table 1. As opposed to the Bayesian classifier, the fuzzy classifier's result is a fuzzy membership degree to the different classes. For example the test point 1 is labeled by the operator as class 1 and by the fuzzy classifier as class 1 with a degree of 0.94, and as class 2 with a degree of 0.04.

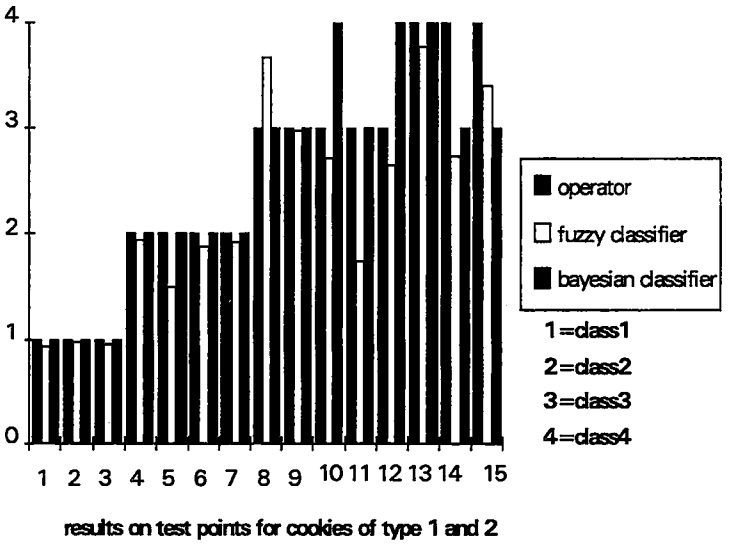

Figure 5: Comparisons of prediction for classification, operator and fuzzy classifier

Results appear to be good. Indeed 11 points over 15 are well classified. Besides the results are coherent even in case there is a classification mistake. Indeed first the error is non hazardous (for example classify in C1 rather than C4) but between two consecutive classes. Second the mistake seems coherent compared to the position of the point in the pattern space. For example point 7 (fig. 5) is closest to class 4 than to class 3 in this space. This is coherent with the results of the fuzzy classifier (26% C3 and 67% C4). This can be explained by an operator's classification mistake. It is possible if we consider that the operator's evaluation is subjective.

To complete this study we test the response of the fuzzy classifier at the intersection of two different classes. Indeed it is important to check the graduality of our classifier. To do that 10 points uniformly spaced between the

two centers of gravity of each class were generated and tested. The results reveals a good graduality between two consecutive classes.

3.2 Real time experiment

Fig.6 shows first the recording and comparison between operator and fuzy classifier and second the comparison of the results given by the Bayesian classifier, the fuzy classifier. The results given by the two classifiers are comparable. Nevertheless the fuzzy classifier is nearer to the gradual evaluation of the color of cookies by the operators than the Bayesian classifier.

The results point out a global coherence betvveen the two classifiers: Bayesian and fuzzy. Those results are good (73% of good classification).

Figure 6: Recording of prediction using the fuzzy and bayesian classifiers, comparisons with operator classification

Criterion	Bayesian classifier	Fuzzy classifier
Nature of the informations	probabilistic	gradual and deterministic Possibility to do predictive control
Number of learning points	about 60	about 5
Sensibility of the classifier to the learning points	no	yes
Limitations on the size of the pattern vector	no	classifier limited to 3 entry variables
Assumptions	statistical law for the distribution of the points (Gaussian in our experiment) Classes équiprobables	no
Implementation	easy	difficult

Table 2: Characteristics of the two classifers

For the comparison of the two classifiers differences could be emphasized (table2). The learning protocol is different for the two classifiers. The fuzzy classifier needs few learning points (20), but is sensitive to a good classification of these points. On the contrary the Bayesian classifier needs a rather big number of learning points (60), but is less sensitive to badly classified points. Otherwise it must be mentionned that in order to use the Bayesian classifier the points must follows a known probability distribution. In contrast no assumption is made in the case of the

fuzzy classifier. finally some practical ideas could be taken into account such as the limitation of the fuzzy classifier to 3 inputs and a more complex implementation for this classifier.

References

[1] BENOIT E., FOULLOY L., 1993. Un exemple de capteur symbolique flou en reconnaissance des couleurs. *RGE N°3, pp 22-27.*

[2] BEZDEK J. C., PAL S. K.; 1992.- Fuzzy models for pattern recognition. *IEEE Press.*

[3] CHEVRIE F., 1994. *Intégration de la logique floue dans les automates Télémécanique-Schneider Electric.* Mémoire du Conservatoire National des Arts et Métiers.

[4] CHUNG FL., LEE T., 1994.- Fuzzy competitive learning. *Neural network, vol 7, n°3, pp 539-551.*

GEORGE P., HERMELINE F., 1989. Maillage de Delaunay d'un polyedre convexe en dimension d. Extension à un polyedre quelconque. *Rapport de recherche INRIA, N°969.*

[6] ISHIBUSHI H., NOSAKI K., YAMAMOTO N., 1993. Selecting fuzzy rules by genetic algorithm for classifications problems. *2nd IEEE conf. on fuzzy systems, San Francisco, pp 1119-1124.*

[7] KELLER J., GRAY M., GIVENS J., 1985. A fuzzy k-nearest neighbor algorithm. *IEEE Trans. Man, Cybern., vol 15, n°4, pp 580-585.*

[8] NOSAKI K., ISHIBUSCHI H., TANAKA H., 1994.- Trainable fuzzy classification systems based on fuzzy if-then rules. *Proceedings 3ème IEEE conf. on fuzzy systems, vol 1, pp 498-502.*

[9] PAL S., MAJUMDER D., 1977.- Fuzzy sets and decisionmaking approaches in vowel and speaker recognition. *IEEE Trans. syst. Man and Cybern., pp 625-629.*

[10] PERROT N., 1994. Applications de la logique floue à la conduite des fours de cuisson en biscuiterie. *DEA ENSIA Génie des procédés, 1994.*

[11] SAVOYE-BARBOTTEAU I., 1993. Etude et modélisation d'un four tunel de biscuiterie à chauffage indirect au gaz naturel. *Thèse spécialité Génie des Procédés, ENSIA Massy.*

[12] SUN CT., JANG JS., 1993. A neuro fuzzy classifier and its applications. *2nd IEEE int. conf. on fuzzy systems. San Francisco. pp 94-98.*

[13] TAKAGI H., HAYASHI I., 1991. *NN-driven fuzzy reasonning. International journal of Approximate Reasonning.*

[14] TRYSTRAM G., ALLACHE M., COURTOIS F., 1993. *Real time measurements for baking of biscuits, EFFOST congress, September, 1993, Porto.*

[15] ZADEH A., 1965.- Fuzzy sets. *Information and control, N°8, pp 338-353.*

Adaptive simulation of human assessment of fruit quality

Simulation adaptative de l'appréciation humaine de la qualité des fruits

Matt Picus and Kalman Peleg

Agricultural Engineering. Department
Technion Israel Institute of Technology, Haifa 32000 Israel
e-mail: kalmanp@tx.technion.ac.il
FAX: 972 4 8221529
Phone: 972 4 8293626

Abstract: *Automated assessment of fruit quality is a classification task of partitioning a p-dimensional space of characterizing fruit features into regions, where each region carries a grade label. Each of the p dimensions represents a particular feature of the classified fruit. The features encapsulate significant attributes of the fruit that allow it to be distinguished from fruits in other grades. The probability of classifier errors in automated grading of fruits is much greater than in traditional well-defined and highly-separated, static classification tasks such as in industrial production lines for quality control. Presently, operators of conventional sizers and color sorters adjust the estimating standard boundaries manually based on observations of obvious misclassification trends in the packed fruit. However, the next-generation sorting machines will utilize many features to reach the grade decision. A human operator will be unable to control the multitude of parameters under control. Any mode of estimating the between-class discriminant functions requires estimation of the a-priori class probabilities ("priors") and the class-conditional probability densities. The time-varying nature of the priors and the probability densities may result in unsatisfactory classifier performance. To solve these problems an adaptive grading approach by "Prototype Populations" is proposed. The produce stream is considered as a "signal" (in statistical terms) to be classified into a discrete number of prototype streams or populations by a global "population classifier". Then for each unique prototype population a separate, optimal "grade classifier" can be designed for sorting individual fruits. The global "population classifier" utilizes a finite-length stack of features continuously updated from the most recently sorted produce. The statistical attributes of the features sample in the stack are analyzed to determine which produce population is currently passing through the system. When the population classifier determines that the stack contents have originated from a different prototype population, it changes the active "grade classifier" to the most appropriate one for the current fruit population. An example of simulated adaptive versus conventional grading is*

presented on datasets from sorting of dates. The example demonstrates that adaptive grading by prototype populations yields lower misclassification rates in comparison to conventional sorting.

Résumé : L'appréciation automatique de la qualité des fruits est une tâche de classement équivalant à partitionner l'espace de dimension p des paramètres caractéristiques du fruit en régions, chacune d'elle correspondant à une classe de qualité. Les paramètres contiennent des attributs des fruits qui permettent de les distinguer de fruits d'autres classes. La probabilité d'erreur dans l'agréage automatique des fruits est beaucoup plus élevée que dans les tâches de classification bien définies, statiques et bien séparées, comme on en trouve en contrôle de production industriel. Actuellement les opérateurs des lignes de tri en fonction de la couleur ajustent les limites standards manuellement en fonction de l'observation d'erreurs grossières de classification. Cependant, la génération future de classifieurs utilisera plusieurs paramètres pour classer. Un opérateur humain sera incapable de contrôler tous ces paramètres. Chaque manière d'estimer des fonctions discriminantes inter classe exige d'estimer les probabilité des classes a priori et les densités de probabilités conditionnelles. La nature changeante des probabilités a priori peut se traduire en une mauvaise performance. Pour faire face, une approche adaptative fondée sur une population prototype est proposée. Le flux de produit est considéré comme un signal (en termes statistiques) à classer en un nombre discret de flux ou de populations «prototypes» par un classifieur global. Puis pour chaque population prototype unique, un classifieur optimal est conçu pour trier chaque fruit. Le classifieur global utilise une pile finie de paramètres continuellement renouvelée à partir du dernier produit trié. Les attributs statistiques d'un exemple de la pile sont analysés pour savoir quel type de population est en train de passer dans le système. Quand le classifieur détermine que le contenu de la pile a été généré par une population prototype différente, il change de classifieur pour activer le plus adapté à la population de fruits. Un exemple d'approche adaptative comparée à l'approche classique est présenté (tri de dattes). Il montre que cette technique se traduit par moins d'erreurs que le tri conventionnel.

1. Introduction

Grading agricultural produce has so far eluded full automation. Automated grading of fruit and vegetables differs from traditional classification tasks in four major areas:

a) The criteria for classification are set with respect to a "reference standard," which may be either a "reference sensor" which measures some objective physical properties of the fruit, or a subjective panel of human experts. Sometimes, the precision and repeatability of grade determination by the human expert sorters ("reference sensors") may be worse than those of the "estimator sensors". Nevertheless, the goal of an automatic classifier that uses "estimator sensors", is to imitate the human judgment and minimize classification errors with respect to the human expert "reference sensor", in spite of the "noisy" grade judgment.

b)The on-line inspection system utilizes an "estimated standard" from a set of features derived from one or more "estimating sensors". The estimated standard at best correlates highly to the reference one, and at worst can differ greatly from it.

c) The class membership feature vectors do not cluster naturally in the feature space. The boundary between classes is usually fixed by marketing or packaging concerns, and often this boundary will pass through an area of the feature space densely filled with feature points.

d) The a-priori class probabilities and the class conditional distributions of the measured features change with time, growth conditions and locations, seasonal variations, storage time, etc. The classifier must reliably grade hundreds of thousands of items per day under time-varying conditions.

Using "estimator sensors" to divide a feature space into arbitrary categories will lead to classification errors. The errors will be concentrated at the category borders. The density of the feature space at the category borders will determine the misclassification rates. These errors can be minimized using the Bayes rule for fixing the class discriminant boundaries, but the errors will be finite and measurable. Any estimate of Baysian discriminant functions requires estimation of the a-priori class probabilities ("priors") and the class-conditional probability densities. The time-varying nature of the priors and the probability densities together with the finite sensor errors have, up to now, yielded in unsatisfactory classifier performance in automated agricultural produce sorting.

We propose to view the produce stream as a "signal" (in statistical terms) to be classified into a finite number of prototype streams or populations. Then for each unique prototype population a separate, optimal "grade classifier" can be designed for sorting individual fruits, (Peleg and Ben-Hanan (1993). A global "population

classifier" decides to which prototype population the current stream of produce belongs, and switches to the appropriate grade classifier. The population classifier utilizes a finite-length stack of features continuously updated from the most recently sorted produce. The statistical features of the stack are analyzed to determine which population is currently passing through the system. When the population classifier determines that the stack contents have originated from a different prototype population, it changes the active grade classifier to the most appropriate one for the current population.

The adaptive classification by prototype population scheme may use some or all of the features used by the grade classifiers, as well as "metafeatures." Examples of metafeatures of a data set are the mean vector of the current stack values, the class-dependent covariance matrices calculated from the stack, or the sample of the cumulative distribution function (CDF) represented by the data in the stack. Use of the CDF in theory and practice will be described, as it is the most appropriate of the metafeatures. The metafeatures may be treated as any other feature in the prototype population classification task. This attempt to use the metafeatures in classification tasks assumes that a finite number of prototype populations exist in the data with different meta-features.

The classification scheme is based on the human compensation for changing sorting conditions. Experienced sorters will recognize obvious global changes in the current produce stream and will change the sorting criteria accordingly.

2. Adaptive sorting algorithm

The adaptive sorting algorithm can be modelled by a discrete process $X=\{x_1,x_2, \ldots x_N\}$ where $x = \Re^p$ is sampled. and the feature vector x (with p elements) is calculated for each item in the sample $X=\{x_1,x_2, \ldots x_n\}$. We shall not describe here the actual feature extraction, but will assume that previous work has been done to insure that among the p features there exist $\not\in \leq p$ optimal features for discriminating between the ω_i grades (i=1..C). With these assumptions, the sampling process can be modeled as:

$$X = \{x_1,x_2,\ldots x_n\} \subseteq X \text{ where } x = \Re^p \text{ is a single item of } X \qquad (1)$$

2.1 Non-adaptive classification

All classification schemes rely on a "reference sensor" to label a training set X with grade labels ω. The reference sensor will most oftern be a human expert or panel of experts in agricultrual applications as no hard and fast rules for the grade labesl exist. The reference sensor may use the featrue space $\Re^p$ but more commonly will

use a totaly different set of features. Traditional non-adaptive classification schemes use any supervised classification techniques to design a grade classifier $\omega=g(x)$ for the n vectors in X, Each of these vectors is derived from the readings of the "Estimating Sensors" of the automatic sorting machine,.

In the on-line process, this grade classifier is used to classify the items $x \in X$. The design of the grade classifier is dependent on the training set used. Any variations in the actual data X that are not presented in the training set X, if they are even noticed while the classifier is being used, require an adjustment of the classifier to compensate for the new data. While solutions to this problem in one- or two-dimensions exist (see for example Gutman et.al. (1994)), modern sorting machines with multiple sensors overwhelm the capacity of the human operator to compensate for changes in the produce stream.

2.2 Adaptive classification

In the adaptive sorting process, the dataset is partitioned into K a-priori known, sequential populations X_k , k=1,2,...K, each of length n_k :

$$Xk=\{xm+1,xm+2, \ldots xm+n_k\},\ k=1,2,\ldots K,\ m=\sum_{j=1}^{j=k-1} n_j \quad \mathbf{X}=\bigcup_k \mathbf{X}_k\ , \tag{2}$$

For each source population, a grade classifier $\omega=g_k(x)$ is designed, as described above :

$$\omega=g_k(x)\ \forall\ x \in X_k \tag{3}$$

The parameters for each classifier are stored. A population classifier k = G(X) is also designed. Usually, the feature vectors themselves will not suffice to discriminate between prototype populations, and some function of the feature set f (X) must be calculated. The population classifier then becomes:

$$\begin{gathered} k = G(f(X))\ k=1,2, \ldots K \text{ where} \\ f(X) \text{ is a function of the set or subset of features in X} \end{gathered} \tag{4}$$

We estimate the sample's single-dimensional-feature cumulative probability distribution function and compare it to the prototype population's feature cumulative distribution. Other approaches to the function f (X) have been evaluated, but were less successful..

In the on-line operation of the sorter, the past q data are stored in a First In First Out (FIFO) stack. The stack can be modeled as:

$$\begin{gathered} X = \{x_m, x_{m+1}, \ldots x_{m+q-1}\} \text{ where q is the length of the stack and} \\ m = 1,2,\ldots N-q \text{ is the index of the items to be sorted.} \end{gathered} \tag{5}$$

After a certain number of new items have been classified, the features of the stack are calculated and the population classifier is used to determine the current population. The appropriate grade classifier $g_k(x)$ is then used for subsequent grade classification. We demonstrate the advantage of this technique by comparing the actual grade label ω_r to a vector of labels obtained by applying the three types of classifier functions discussed:

$$\omega = [\omega_a, \omega_p, \omega_t, \omega_1, \omega_2, \ldots \omega_K]^T \text{ where} \quad (6)$$

$\omega_a = g_k(x) \mid x \in X_k$ (the adaptive classifier with an erring population classifier),

$\omega_p = g_k(x) \mid x \in X_k$ (the adaptive classifier using a non-erring population classifier),

$\omega_t = g(x) \mid x \in X$ (the non-adaptive classifier trained on a sample from all populations), and

$\omega_k = g_k(x) \mid x \in X$, k=1,2..K (the K non-adaptive classifiers trained on single populations then used on all the data)

The "non-erring" adaptive classifier uses the inspected item's known population label, and thus flawlessly identifies the proper population. It can be used only in laboratory conditions.

The sorting simulations of dates described in the following sections show a clear reduction in misclassification rate for ω_a compared to the other strategies.

The adaptive classification scheme must also recognize new prototype populations. To this end, the initial classifier design utilizes a statistical hypothesis test to check the current prototype population. When the population classifier returns a "not-recognized" label for the data sample X

$$k = G(X),\ k \notin \{1,2,..K\} \quad (7)$$

the machine will know that currently in the stack there is an unknown population. Either the stack is in transition between two populations, or indeed the process has encountered a distinctly new population. The Kolmogorov-Smirnov two-sample test, described in Press (1992), is one example of a non-parametric statistical test particularly suited to the task, and is described below.

Note that while the prototype populations may be distinguishable, they may not require unique grade classifiers. Reduction in the number of prototype populations and subsequent simplification of the population classifier may improve the system's robustness and reduce overall misclassification rates. This can be accomplished by comparing the grade classifier's performance on the "wrong" populations:

$$\omega_p = g_k(x): x \in X_j,\ j \neq k \quad (8)$$

where the symbols are as in (6), and using the misclassification rates as an indication of the "distance" between the populations. Those populations where the misclassification rates are not significantly different can be combined.

3. Population classifier design

The requirements of the population classifier are:

- It must accept as inputs the current contents of the stack $X = \{x_m, x_{m+1}, \ldots x_{m+q-1}\}$ where q is the length of the stack and m+q-1 is the current item x being processed;

- It must return as outputs the current stack population $k = G(X)$ and a confidence measure α, $0 \leq \alpha \leq 1$;

- It must be sensitive to a new population even before the stack completely empties of the previous population;

- In order to allow the dynamic adjustment of the stack length, the population classifier's confidence measure α must be insensitive to, or at least compensate for, changes in the stack length.

3.1 Stack parameters

The population classifier can err in two cases. As a new population enters the stack, an optimal population classifier would immediately recognize the data as belonging to a new population and change the grade classifier accordingly. However there is some latency in the identification of a new population. The machine continues to classify the grade by the old grade classifier, until it notices that something has changed. Subsequently, the stack continues to fill with the second population. The population classifier may classify the mix as a third population, and sort the items according to its decision. As the first population empties out of the stack, the population classifier should settle on the correct identification of the new population.

Optimization of the stack length q was also studied. A shorter stack length will lead to less "lag" in the decision to change the grade classifier, resulting in fewer items belonging to the new population classified by the grade classifier of the previous population. However, too short a stack will not enable the population classifier to confidently identify the actual prototype population. Rather than using a fixed length q for all populations, q can be allowed to vary dynamically, according to the current confidence level of the population classifier decision.

3.2 Using CDFs to identify prototype populations

The Cumulative Distribution Function (CDF) incorporates within it the class-dependent probability distributions and the a-priori probability of that class in the data. It therefore reflects the parameters needed to calculate the a-posterior probabilities. If a classifier can be designed that accurately estimates the a-posterior class-dependent probabilities, it will approach the optimal Bayes classifier (Duda and Hart, 1973). Any changes in the data that mandate a change in the Bayes classifier must be expressed in the a-posterior probabilities, and will change the CDF. Therefore the CDF is a good starting point for a population classifier statistic.

The sample-estimate of the CDF (created by sampling the random variable and for each value calculating the proportion of data with that value or less) is also much less noisy than its derivative, the probability density function (PDF) most often estimated with histogram techniques. It must be a monotonically increasing function, and its steps are in increments of 1/N where N is the number of data points in the sample. The PDF estimate, however, is dependent on the difference between consecutively ordered values of the sample. It usually requires some signal-processing type of smoothing to provide useful results.

The CDF is visually less satisfying, since it is not obvious from the S-shaped curve whether the distribution is unimodal, skewed, or contains outliers. But a wide variety of theoretical non-parametric techniques for analyzing differences between CDFs are known in the literature (Fukunaga 1990, Conover 1980).

Peleg and Ben-Hanan (1993) trained a neural network to identify the population's CDF. They tested a two-population data set collected on apples, with limited success. The neural network was built in such a fashion that it could return not only the distance metric but a measure of the confidence in its decision, as described in the previous paragraph. In the present study the Kolmogorov-Smirnov goodness-of-fit test was found to be more useful, and will be described in detail below.

3.3 Population classification by the kolmogorov smirnov statistic

The Kolmogorov-Smirnov two-sided statistic T, as described in Press (1992) was proposed by Kolmogorov and tabulated by Smirnov. It is defined as the maximum difference between two cumulative distribution functions:

$$T = max\left|S_1(x) - S_2(x)\right| \text{ where } S_n(x) \text{ is the sample cumulative distribution function for a sample drawn from a random variable } X_n \text{ with a distribution of } P_n(x). \quad (9)$$

Under the hypothesis H_0 that $P_1(x)=P_2(x)$, the distribution of T can be tabulated as a function of the number of samples in X_1 and X_2 . An analytical expression to calculate the significance of the T value was proposed by Stephens (1963). The probability that the distributions characterized by two CDFs are NOT different is:

$$\text{Probability(H0: P1(x)=P2(x) | T)} = f_{KS}\left(T \bullet \left[\sqrt{N_e} + 0.12 + 0.11/\sqrt{N_e}\right]\right) \quad (10)$$

where Ne is the effective number of points: $N_e = \frac{N_1 * N_2}{N_1 + N_2}$, N_m=number of points in sample X_m and $f_{KS}(\lambda) = 2\sum_{j=1}^{\infty}(-1)^{j-1}e^{-2j^2\lambda^2}$, $0 \le f_{KS}(\lambda) \le 1$

The hypothesis test can act as a population classifier k = G(X) :

G(X) = n: (Tn < Tm $\forall$ m $\neq$n), where

$T_n = \max\left|S_n(x) - S_{STACK}(x)\right|$, where (11)

$S_n(x)$ is the sample cumulative distribution function from the population n in the training set, and S_{STACK} is the current stack's CDF.

In addition $\alpha = f_{KS}(T_n * N_s)$ where $N_s = \frac{N_{STACK} * N_n}{N_{STACK} + N_n}$ gives the probability that the CDFs are, indeed, equal. Thus the KS test can answer the first two requirements for the population classifier as stated above.

Sensitivity to a new population entering the stack

The KS test is not sensitive to the order of the data in the stack. At its core it reorders the data to find the CDF. It is not feasible to somehow emphasize the first few datum in the stack to improve the sensitivity of the classifier to a new population, as would be possible with a different family of classifiers. However the CDF itself is very sensitive to changes in the stack composition, and the entrance of a new population to the stack rapidly changes the measure α described above.

Ability to compensate for changing stack length

The measure N_s takes into account the stack length N_{STACK}. The classifier accuracy depends on both the size of the training set and the size of the stack, but its performance depends greatly on enough data present in the stack to estimate the CDF.

4. Simulation of the adaptive sorting algorithm

Adoption of the adaptive sorting algorithm makes new demands on sorting machine users and manufacturers. A user friendly proof of the advantages of the adaptive techniques is necessary to convince commercial interests. The possible reduction in classification errors must be clearly demonstrated in actual packing house conditions. A software tool was developed for this purpose that permit use of the adaptive algorithm while using a unified data input and presentation interface. Both synthetic data and actual data may be used with the program.

The simulation was built in Matlab (Mathworks 1994), using Graphical User Interface (GUI) capabilities to display the data and significant results while allowing the user to easily change the simulation environment. As the simulation runs, it displays a series of sorting matrices. These compare the actual grade labels ω_r as determined by a reference sensor to those determined by classifiers as described in Equation (6) above.

After processing the entire test data, the program displays information about the performance of the strategies, including the number of items processed and the number of errors made by the population classifier used in the adaptive technique, as well as the overall misclassification rate expressed as a "Weighted Grade Contamination Index" C_ω, described in Peleg (1985):

$$C_\omega = 1 - P_\omega = 1 - \sum_i P_{gi} W_i \qquad (12)$$

P_ω is the opposite of C_ω and is termed "Weighted Grade Purity Index", while P_{gi} is the pure product fraction of grade i, resulting from the sorting operation.

$W_i = K_i P_i / \sum_i K_i P_i$ is a weighting function composed of the relative costs or penalties Ki for misclassifying grade i while the a-priori grade probablities Pi are determined by the proportion of grade i in the sorted produce stream. ..

In practice, larger penalties K_i are associated with the higher priced grades but in the context of this project we assumed equal penalties for all grades, $K_i = 1$.

After processing the entire test data, the program displays information the performance of the strategies, including the number of items processed and the number of errors made by the population classifier used in the adaptive technique.

5. Adaptive sorting of dates

The sorting experiments with artificial datasets were useful for studying the structure and operation of the adaptive sorting scheme by prototype populations. They were furthermore very useful for exploring sensitivities to the system's parameter changes. For the sake of brevity we report herein only experiments with real data, e.g. from a commercial sorting operation of dates.

We demonstrate a basic premise of the project, i.e. that global feature spaces of commercial produce grading systems can be beneficially subdivided into prototype populations. Furthermore, we wanted to confirm and demonstrate that these prototype populations are sufficiently dissimilar, whereby a population classifier can be designed to distinguish between them and by using separate grade classifiers for each, the overall misclassification rate can be significantly reduced.

Dates are currently sorted by hand, a labor intensive operation that is error-prone and expensive. The fruit is spread across a conveyor belt, and the human sorter must separate the fractions by moving each item to the proper partition. Most of the sorting criteria are visual: color, size, shape, blemishes, folds and blistering in the skin, shininess, and uniformity. However the sorter also feels the date for softness, and while moving it can change the classification.

The date data was collected from the Ardom Regional Packing House, in the Southern Arava region of Israel, near Eilat. This packing house recently installed, (with the supervision of one of the researchers), a newly developed date sorting machine. Using a set of 25 features obtained by machine vision and a hierarchical classifier, it can sort about 20 dates per second.

The manufacturers of the machine agreed to modify the software so that the machine saves the features of the last 24 dates sorted once every five minutes. The packing house tracks the source of the date lots through the packing process to properly compensate the growers, thus an a-priori population label is available and was stored as well as the time the sorting took place and the output of the sorting machine.

For commercial reasons, the manufacturer requested that the actual physical meaning of the features and the exact structure of the grade classifier remain in confidence. This was not a problem since the adaptive sorting simulation program was designed to work with any type of grade classifier and accept various feature structures, as may be used by various commercial sorting machines, which employ conventional non-adaptive sorting algorithms.

5.1 Data preparation

The raw data were supplied as a number of ASCII files. Since the processing platform of choice is Matlab, a number of conversions were necessary to input the data. The data were parsed into a matrix form, with each row representing a data vector. Unreasonable data were rejected. All data where the output grade label reflected the inability of the machine to reach a decision were rejected. All clear outlier data on any feature was rejected.

The result was a data set of ~20,000 vectors. The first element represents the time the date passed through the machine, the second was the shipment ID (every incoming shipment of dates receives a unique label which is used to track its progress through the packing house and to compensate the grower) The third was the machine that sorted the date (there are 2 machines working in parallel) and elements 4-28 are features.

A unique demi-population label was constructed from the following:
- Time and date sorted;
- Shipment ID;
- Machine sorted on (1 or 2).

5.2 Feature selection and date grade classifier design

The general structure of the hierarchical classifier used by the machine is depicted in Figure 1. In classification phase 1, a first subset of the 25 features set is used to compute a primary score termed F1 (an integer 1-5). In the second classification phase a linear discriminant classifier uses a second subset of the 25 features to compute a secondary score F2 (an integer 1-4). In the third phase the scores F1 and F2 are combined in various ways to yield quality grades. The combinations of the F1 and F2 values and the number of quality grades is fixed by the destination market supply and demand situations and time of the year.

Score F1 was one dimensional while F2 was composed of 24 features. Although the values of F1 and F2 were supplied in the dataset the features composition of F2 was not disclosed by the manufacturer. Consequently, we adopted the values of F1 and F2 as measurements by a reference sensor and the grades labels of the machine as reference labels. As the estimating sensor succeeded in estimating F1 very accurately, (less than 1% misclassification) it was decided that there would be no further improvement by adaptively estimating the F1 score. Consequently, the goal of the sorting simulation was limited to adaptively executing phase 2 - estimating F2.

In the machine, the third phase is performed by the sorting line operator. Using a touch screen for input, the operator chooses combinations of F1 and F2 to form

particular quality grade. The actual mapping of F1 and F2 to a grade label depends on the destination of the finished product and the market forces. This process is beyond the realm of the adaptive sorting algorithm.

Through consultation with the machine manufacturer, and after considerable experimentation we constructed estimating feature subsets to approximate F1 and F2 and a hierarchical grade classifier similar to the one used in the machine (see Figure a).

Subsequent to dividing the dates into subgroups by F1, linear discriminant classifiers as described in the SAS package (SAS 1985) were used to determine the estimate of F2:

$$\hat{F}2 = g_{F1}(x) = \min(D_{W(i)c}(x)) \text{ where} \qquad (13)$$

$D_{W(i)c}(x) = (x - \overline{\boldsymbol{X}}_{\omega(i)c})^T S_{W(i)c}^{-1} (x - \overline{\boldsymbol{X}}_{\omega(i)c}) + \log|S_{W(i)c}| - 2\log P(\boldsymbol{X}_{\omega(i)c})$,

$\boldsymbol{X}_{\omega(i)c}$ is the data in the training set for the grade class w_i with F1 = c,

$\overline{\boldsymbol{X}}_{\omega(i)c}$ is the mean vector of $\boldsymbol{X}_{\omega(i)c}$, $S_{W(i)c}$ is the covariance matrix, and

$P(\boldsymbol{X}_{\omega(i)c})$ is the prior probability of $\boldsymbol{X}_{\omega(i)c}$ in the part of the population with F1 = c.

This classifier is based on multivariate normal (Gaussian) distributions. However the data is decidedly non-normal. Each feature was examined for skew (the degree of asymmetry around the mean). As some of the features were highly skewed a sequence of Tukey ladder functions (...x^{-2}, x^{-1}, $x^{-1/2}$, $x^{-1/4}$, log(x), $x^{1/4}$, $x^{1/2}$, x, x^2, ...) (Tukey 1977) was applied to each feature until the skew was less than 1. While the grade classifier construction has been described at some length here, the adaptive sorting algorithm is external to the particular grade classifier and assumes the machine manufacturer or the packing house staff can provide a suitable grade classifier. The specific case in-hand demonstrates the adaptive classifier's ability to incorporate even a complicated grade classifier.

A blind stepwise process (patterned after the STEPWISE procedure in SAS (SAS 1985) of feature selection was used to chose the features to be used for estimating F2. An upper limit of 9 features yielded acceptable performance. Using a global training set, this classifier provided an overall misclassification rate of 35%, versus the reference labels given by the machine.

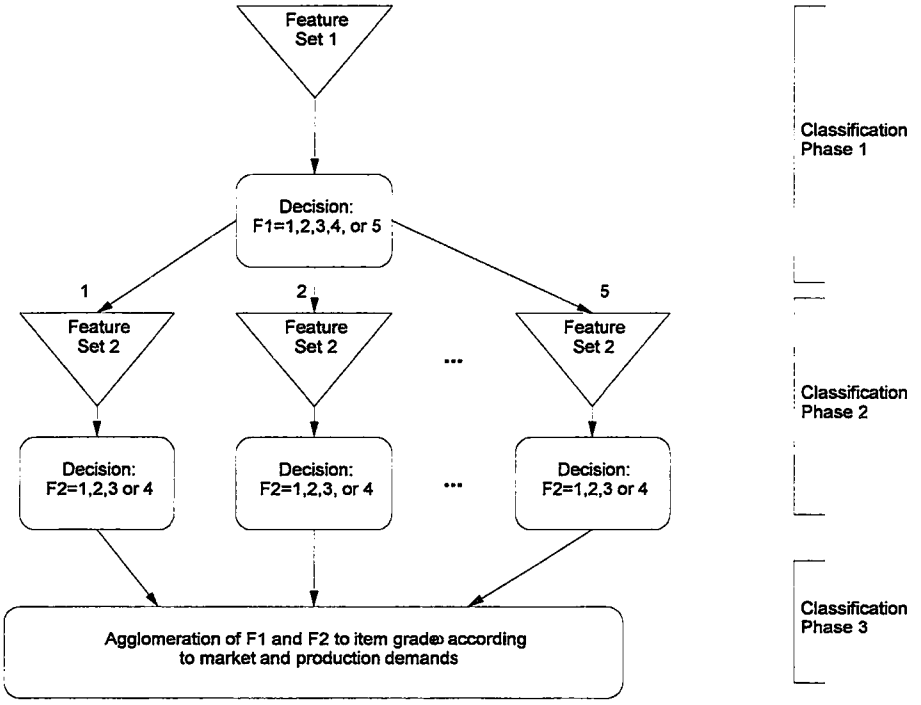

Figure 1: Schematic description of hierarchical classification system

5.3 Partitioning the data into prototype populations

The first step in partitioning the data into prototype populations involves choosing an optimal feature for characterizing prototype populations by CDFs and the K-S statistic. Some consideration was given to using a two- or higher-dimensional form of the K-S statistic. These have been developed by Smallwood (1996) , Feltz and Goldin (1991), and others. However, one of the prime advantages of the K-S statistic is its non-parametric character: the test does not depend on the underlying distribution of the data. In the tests developed for higher dimensions, this characteristic is not preserved. In addition, the "curse of dimensionality" (as described in Scott 1992) requires more data to adequately describe the two dimensional distribution than the one-dimensional distribution.

The fact that the population classifier utilizes only one feature may not be a severe handicap. In most cases, the actual classification task relies on a main feature, with nuances supplied by the others. Many of the acquired features are highly dependent. Any change in the makeup of the produce stream that has repercussions for sorting, will manifest itself in all the dependent features, including the one chosen for population classification.

Even with one dimensional CDFs, optimal partitioning of the data into prototype populations is a difficult task. A necessary precondition for a feasible partition is that the prototype populations must be "Identifiable", i.e. the differences between the resulting CDFs must be sufficiently large. One measure of the identifiability of the prototype populations is the K-S statistic α, another is the misclassification rate in the resultant classifier. Obviously, there may be many identifiable partitions which will invariably provide a "payoff" in terms of increasing the weighted grade purity index P_ω versus non-adaptive sorting, wherein the entire dataset comprises just one prototype population.

Among the various identifiable partitions, the optimal partition should provide the maximal "payoff": $\max(P_\omega)$. However, the partition with the minimal population misclassification rate is not necessarily the one which provides the maximal payoff $\max(P_\omega)$. A full exploration of these fine details, for finding optimal prototype populations will be included in a future paper.

In the context of this work, a semi-optimal partition of the date dataset was determined by choosing an optimal feature for generating CDFs and reducing the number of a-priori prototype populations, as follows:

The maximum distance in the training-set sample CDFs between all possible binary combinations of a-priori known date populations was determined. Then an agglomerative process (based on the CLUSTER process of SAS (1985)) of combining populations based on this distance measure was carried out. This resulted in a dendogram depicted in Figure 2, which shows the estimated confidence that the populations are different. Each feature's dendogram was examined, and the feature with the maximum separation of the a-priori populations was chosen.

The dendogram also provided a rationale for combining populations. The original 20 populations were reduced to 16 by combining those with a low (<0.6) probability of coming from different populations.

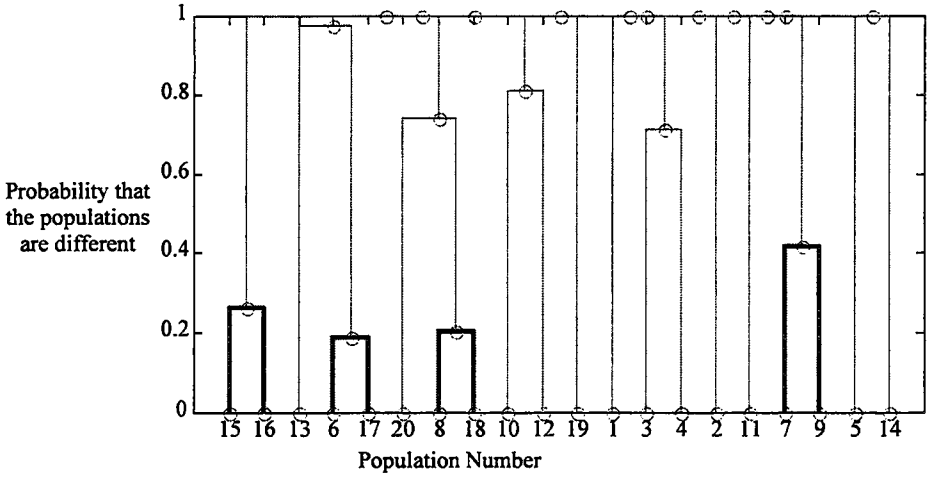

Figure 2: Dendogram of the probability of differences between the a-priori populations

6. Population classifier performance

The performance of the population classifier was tested by dividing the data into a training and test set. The test set data was formed into an indexed sequence of data, and the data fed into a FIFO stack for classification. The length of the stack was varied. The results are depicted in figure 3. It may be seen that the population classifier exhibits the expected behavior. For a given training set size an optimum stack length is obvious.

The misclassification rate has a minimum as a function of the stack size, since on the one hand increasing the stack length improves the accuracy of the classification, but it also increases the number of classifications made while the stack is in transition between two populations.

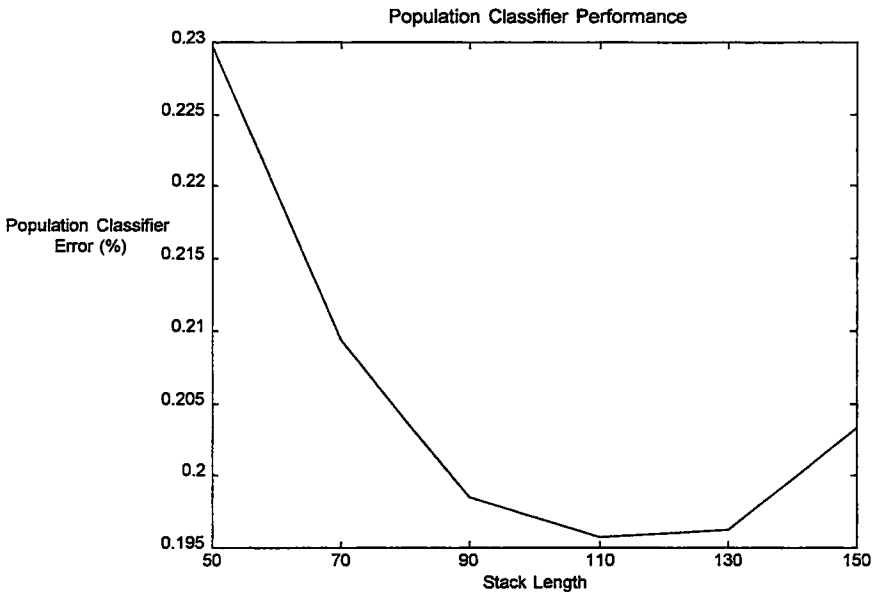

Figure 3: Population classifier performance as a function of stack size

7. Adaptive vs. Non-adaptive classifier performance

The size of the training set used for the various classifiers was altered while all other parameters were held constant. The size of the stack used in the population classifier and the size of the data set were varied independently while all other parameters were held constant.

The test set data were classified and the estimated quality value compared to the known, reference value. Various sizes of training sets were run through the process. The classifier was also trained and tested on each a-priori population separately. Again, the incorrect decisions were counted as a percent of the data. Table 1 consolidates the misclassification rates of the grade classifier, by training and test set.

The misclassification rates clearly demonstrate the advantage of adaptive sorting. Using the same training set a clear reduction in misclassification can be obtained by "tailoring" the classifier to the particular feature space currently being sorted. The table also emphasizes the price of a mistake in the population classifier. Using the wrong grade classifier for any extended period will undo all the reduction in overall misclassification.

Table 2 presents the overall comparison of the different classification strategies. The best-case and worst-case non-adaptive classifiers are compared to the adaptive classification strategy with an erring and non-erring population classifier. In real-life situations, the non-adaptive classifier performance will always be significantly worsened, as the training set cannot anticipate all possible variations in the produce. The adaptive classifier avoids this problem through the identification of new populations. It can notify the packing house staff that something has changed and adjustments are necessary much before post-sorting quality control (if it exists).

Training set from Population	1	2	3	4	5	6	7	8	9	10	11	12	13	14	15	16	all
C_ω on test set from only the trained population	22.4	29.0	20.4	23.6	15.8	13.5	23.3	16.2	27.9	19.5	29.3	21.0	11.6	31.6	24.3	21.8	33.3
C_ω on test set from the entire data	39.2	45.8	43.2	43.6	39.5	49.9	64.9	39.8	36.1	51.9	47.3	43.8	48.2	51.6	46.7	58.4	

Table 1: Non-adaptive grade classifier performance - Misclassification rates for each of the hierarchical grade classifiers trained. Training set size is 30% of each population

Classifier	Misclassification Rate
Worst Case Non-Adaptive	64.9%
ω_t - Best Case Non-Adaptive	33.3%
ω_p - Adaptive w/ Non-erring Population Classifier	22.6%
ω_a - Adaptive w/Erring Pop. Class	26.2%

Table 2: Overall classifier performance comparison of C_ω, stack length at 100 and training set size at 30%

Conclusion

We have presented a detailed description of an adaptive simulation of human assesment of fruit quality. At the root of the simulation is the concept of prototype populations. This concept mimics the reaction of the experienced human sorter as the produce stream changes. The description was augmented by an example of sorting date fruits, and the effect of changing various parameters in the sorting process on the misclassification rate was explored. While the scope of the project was to develop the theory behind the adaptive sorting scheme, the actual simulation implementation takes into account the need to convince non-technical sorting line managers of the superiority of the adaptive approach. The simulation software can be used with almost any type of grade classifier. The adaptive algorithm itself can easily be incorporated into an existing sorting machine, with little

intervention in the current sorting software. The authors hope that this approach will ease the introduction of complicated, next-generation sorting machines to the relatively low-tech sorting world.

References

Conover W.J. 1980. *Practical Nonparametric.* Statistics 2ed John Wiley & Sons, NY.

R. Duda and P. Hart 1973. *Pattern Classification and Scene Analysis*, John Wiley & Sons, NY.

Gutman P., Peleg K. and Ben-Hanan U. 1994. "Classification by Varying Features with an Erring Sensor" *Automatica, 30(12) pp. 1943-1948.*

Mathworks Inc. 1994. *Matlab User Guide Ver.4.* The Mathworks Natick Mass.

Press W, Teukolsky S, Vettering W, Flannery B., 1992. Numerical Recipes in FORTRAN, *2nd Edition, Cambridge Univ. Press.*

Scott D.1992. *Multivariate Density Estimation*, John Wiley and Sons.

Smallwood R.H 1996. "A two-dimensional Kolmogorov-Smirnov test for Binned Data", *Phys. Med. Biol. , 41:125-135.*

Feltz C., Goldin G. 1991, *"Generalization of the Kolmogorov-Smirnov Goodness-of-Fit Test, Using Group Invariance",* DIMACS Technical Report 91-25, March 1991.

Stephens M.A. 1965. *Journal of the Royal Statistical Society*, ser.B. 32:115-122.

Tukey J.W. 1977. *Exploratory Data Analysis.* Addison-Wesley, Reading MA.

SAS Institute Inc. 1985. *SAS User's Guide:* Statistics, Version 5 Edition. SAS Institute Inc., Cary NC.

Peleg K. 1985. *Producd Handling Packaging and Distribution.*

Use of sensor fusion to detect green picked and chilled tomatoes

Utilisation de la fusion de capteurs pour détecter des tomates cueillies vertes ou gelées

Sarah Schotte, Research Engineer

Josse De Baerdemaeker, Professor
Departement of Agro-Engineering and -Economics, K.U.Leuven
Kardinaal Mercierlaan 92, B 3001 Heverlee - Belgium
e-mail: sarah.schotte@agr.kuleuven.ac.be

Abstract: *Quality of vegetables and fruits is determined by a number of characteritsics. Therefore it is interesting if this quality can be defined by a combination of parameters such as color, mechanical- and electrical impedance, refractometry and spectroscopy. Earlier work has shown that tomatoes with a low quality, caused by chilling, can be distinguished by using sensor fusion. Also it is possible that tomatoes with the same color have a totally different history and therefore a different quality.*

The aim of this work was to study the advantages of using a combination of measurement techniques to study the quality of tomatoes.

Green, orange and red picked tomatoes were stored at 2°C and 95% relative humidity (RH) and at 12°C and 95% RH. This way both the effect of color at picking time and storage temperature could be investigated. The fruits were stored for at least two weeks and every 2 or 3 days the firmness, the electrical impedance, the color, the NIR reflectance spectra and the °Brix were measured.

After the test period the data were analyzed, using discriminant analyses. The purpose was to find a (combination) of parameters which makes it possible to discriminate between tomatoes with the same color but with a different color at picking time and/or a different storage temperature.

It could be seen that on basis of a combination of electrical and mechanical impedance data, green picked tomatoes, stored at 12°C until they reach a red color, could be distinguished from mature red picked tomatoes of the same color with a misclassification error of 0%. The possibility of separating green from red picked fruits at a moment that this difference is not visible anymore, is of particular importance because red picked tomatoes have a much better aroma and taste.

After storage at different temperature, fruits with the same color could be classified according to this storage temperature with a classification error of 12.5%, 18.95% and 22.65% for respectively green, orange and red picked fruits. The better dicrimination for the

green picked fruits is due to the effect of chilling injury in this way that immature fruits are more susceptible to chilling injury.

Keywords: *Quality, tomato, sensor fusion.*

Résumé : La qualité des fruits et légumes est déterminée par un certain nombre de caractéristiques ainsi la qualité peut être définie par une combinaison de paramètres telle que la couleur, l'impédance mécanique et électrique, la réfractométrie, et la spectroscopie. Les travaux préliminaires ont montré que des tomates de mauvaise qualité (du fait du gel) peuvent être détectées par fusion multi-capteurs. Ainsi certaines tomates de même couleur ont une histoire totalement différente et ainsi une qualité différente.

L'objectif de ce travail est d'étudier les avantages de la combinaison de techniques de mesures pour apprécier la qualité des tomates. Des tomates cueillies vertes, oranges et rouges sont stockées à 2°C et 95 % HR (Humidité relative) et à 12°C et 95 % HR. De cette manière on étudie les effets de la couleur lors de la récolte mais également de la température de stockage. Les fruits sont stockés au moins deux semaines et tous les 2 ou 3 jours, la fermeté, l'impédance électrique, la couleur, le spectre de réflectance proche infrarouge et le ° brix sont mesurés. Après la période de tests, les données sont analysées par analyse discriminante. Le but est de trouver une combinaison de paramètres qui permette de discriminer des tomates de même couleur mais cueillies à des couleurs différentes et/ou conservées à des températures différentes. On a montré que, par combinaison des données d'impédance électrique et mécanique, des tomates cueillies vertes et stockées à 12°C jusqu'à atteindre la couleur rouge pouvaient être distinguées de tomates mûres cueillies rouges avec un taux d'erreur de 0 %. Cette possibilité de séparer des fruits cueillis verts ou rouges à un moment où cette différence n'est plus visible est particulièrement importante car les tomates cueillies rouges ont un meilleur arôme et un meilleur goût. Après stockage à différentes températures, des fruits de même couleur peuvent être classés en fonction de cette température de stockage avec des erreurs de 12,5 %, 18,95 %, et 22,65 % respectivement pour des fruits cueillis verts, oranges et rouges. La meilleure discrimination (fruits cueillis verts) est due à l'effet du gel car les fruits immatures sont plus susceptibles d'être endommagés par le gel.

1. Introduction

Quality of vegetables and fruits is determined by several characteritsics. Therefore it is interesting to describe the «condition» of fruits as completely as possible by using more quality parameters such as color, mechanical- and electrical impedance, refractometry and spectroscopy (NIR). Earlier work revealed that defects in fruits, caused by stressfactors as chilling, can not be detected by a single method but can be detected with combined measurements (4). Also it is known that tomatoes with the same color can have a completely different history and therefore a different quality.

Thorne and Alvarez (1) have shown that development of color and softening of tomatoes are not necessarily correlated and that the temperature regime during storage can be used to color the tomatoes without causing a great firmness loss. Cheng et al. (2) found that tomatoes do not show a color change if stored under 6°C. Also Rosenfeld (3) concluded that firmness can not be predicted by color. Moreover, green picked tomatoes, even after developing a red color, can be tasteless as a consequence of abnormal ripening. This was concluded in a test with a consumerpanel (4).

Fruit firmness is the second most important attribute in judging quality of tomatoes. Firmness is a measure for the ripening (softening) of the fruitf lesh. Pectin, the cementing factor of the cellwall, is present in the middellamella and is been solubilised during the ripeningprocess. This results in a decrease of the cohesion of the cells and consequently in a texture change. To determine firmness the acoustic impulse response technique can be used.

As a third measurement technique to investigate fruit quality, the electrical impedance is proposed. When fruits or vegetables ripen or deteriorate there is a severe change in the cellular structure, which can be measured in the electrical conductivity and the permitivity of the cells.

During ripening starch is divided into glucose and saccharose is converted into fructose and glucose. The amount of sugar can be determined in several ways. An easy and quick method is the use of refractometry, where the quantity of sugars is represented as °Brix.

NIR-spectroscopy is used as a routine technique for non destructive measurements of the quality of agricultural products. When light falls on a fruit different phenomena can happen such as absorption, reflection, transmission,... The outcoming or internally reflected light carries information about the internal composition of the fruit (5).

2. Objectives

The objective of this work was to investigate the advantages of sensor fusion. The queqtion is if it is necessary to use more than one quality parameter and which parameters are the most important.

Two factors were investigated: color at picking time and storage temperature. Tomatoes with the same color were divided into classes according to these factors.

3. Materials and method

In June 1997 3*200 tomatoes (var. Grace) of color green, orange and red were picked at the experimental station of St-Katelijne Waver, Belgium. The fruits were then stored at 12°C and 95% RH (Relative Humidity). Twice a week, during 4 weeks, 15 tomatoes were measured with the above mentioned techniques: mechanical- and electrical impedance, refractometry and NIR spectroscopy and color.

3.1 Firmness: acoustic impulse response technique

The acoustic impulse respons method is a non destructive technique to measure the firmness of fruits and vegetables. In this technique the tomato is placed with its stalk horizontal on a fruit holder and then exited by gently hitting it with a small hammer. The responding vibration is captured with a microphone. By means of a Fast Fourier Transformation the frequencyspectrum is generated. Out of this spectrum the first resonant frequency is selected. The resonance frequency (RF) was determined at 4 point of the fruit equator. Correcting the average frequency for the mass yields the firmness:

$$S = m^{2/3} * RF^2 \quad (1)$$

with
S: firmness (10^6 $Hz^{2}*g^{2/3}$)
m: mass (g)
RF: first resonance frequency (Hz)
In the following the firmness index of the fruits will be expressed in the units 10^4 $kg^{2/3}*s^{-2}$. Tomatoes have a firmness between 1(very soft) and 10 (extremely hard).

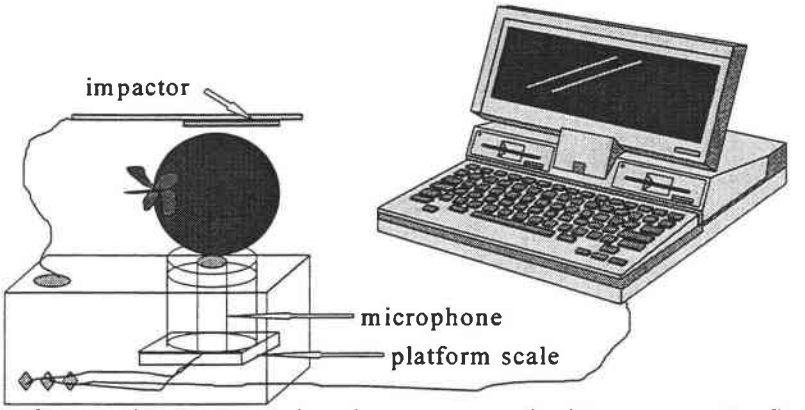

Figure1: Set up of the acoustic impuls respons method to measure the firmness

3.2 Color: colorchart

The color was measured at the blossom end with a color chart used in auctions (ranging from 1: very green to 12: very red).

3.3 Electrical impedance: two point technique

The fruit impedance was measured from 20 Hz up to 1 MHz, at 48 different frequencies, with a Hewlett Packard precision RLC meter model *hp* 4284A, using a two point set-up, with wet contacts (filter paper disks soaked in 150 mM NaCl) (4). At the contact place of the electrodes, the skin was removed. The pressure of the electrodes upon the fruitflesh is excerted by the fruit weight itself. The applied signal was 20 mV_{RMS} and the electrode area 0.78 cm^2.

Fruit tissue is a cellular biological material. Its impedance representation in the complex plane reveals semicircles having the center above the abscissa, as shown in figure 2.

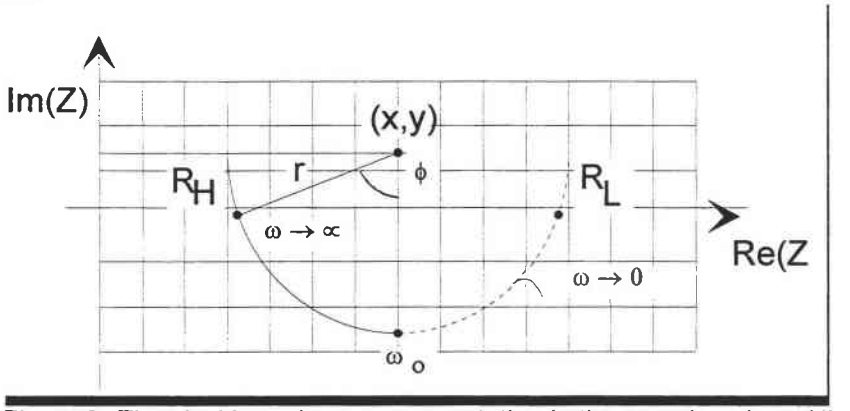

Figure 2: Electrical impedance representation in the complex plane (4)

This circle can be completely defined by four parameters: three geometrical ones and one containing the characteristic frequency information. The five chosen parameters to define the measured data are: R_L- low frequency resistance, R_H- high frequency resistance, Φ_o- constant phase angle (CPA), $f_0 = \frac{\omega_0}{2\pi}$ characteristic frequency (maximum reactance frequency), Co: the characteritsic capacitance. In this way the 48 points resulting from a frequency sweep were replaced by five parameters, which for the moment are meaningless and there is no clear link between them and physiological values. The parameter extraction was performed, based on a least squares fitting of the data. The characteristic frequency was determined by polynomial interpolation of the measured data around the point of maximum reactance on the fitted circle.

3.4 Optical spectra: NIR spectrometry

Every optical instrument consists of 5 basic components: light source, light conductor, sample holder, wavelength selection mechanism, a detector and a processor.

In this work a spectrometer (Optical spectrum analyzer (OSA) 6602, Rees Instruments Ltd., Godalming, UK) connected to a computer was used. The configuration was 0°/45°, meaning that - detector- and - source fibers make an angle of 45°C.

Because of the non homogeneous character of tomatoes, 4 measurements on the equator were made for each fruit.

3.5 Sugar content: refractometry

This method is one of the most simple techniques to measure sugar. It is based on the law of Descartes-Snellius for determining the refractive index. This index is a measure for the amount of dissolved material and is expressed as °Brix.

A digital refractometer was used (PR-101, Palette Series, ATAGO CO., Ltd., Japan). The calibration was done with destilled water (0 °Brix). For fruits and vegetables, the °Brix consists of the total amount of sugars, organic acids and pectins. Between 5 and 40°C there is a temperature compensation. About 0.1 ml juice was used for each measurement.

Both NIR and refractometry were used to have more information on the internal quality of the tomatoes.

4. Method of dataprocessing

The aim of the study was to use sensor fusion as a basis to distinguish:

a) green, orange and red picked tomatoes,
b) tomatoes stored at different temperatures on the moment that they have the same color.

The classification technique used was discriminant analysis.

4.1 Color at picking time

Red picked tomatoes (color 9) on the first day were compared to orange and green picked fruits after respectively 10 and 17 days storage at 12°C/95% RH. At those moments all of the fruits had the same red color and thus distinction could not be based on visual inspection.

All of the measured parameters, except for color, were used to separate between the three classes, e.g. red, orange and green picked fruits.

4.2 Storage temperature

Tomatoes with the same color at picking time were divided into two classes, according to their storage temperature (2 or 12°C). For every picking color all fruits with a color of 6, 8 or 10 for respectively green, orange and red picked tomatoes, were selected. This gives 3*2 classes of tomatoes that can not be separated just on visual percepeptance (color).

	color at picking time	color at time t	storage temperature (°C)	storage period (days)	(*)
a	green	9	12	10	A
	orange	9	12	17	A
	red	9	12	0	A
b	green	6	2		B
	green	6	12		B
	orange	8	2		C
	orange	8	12		C
	red	10	2		D
	red	10	12		D

(*) classes with the same letter were compared with discrimation analyses

Table 1: Set-up of the experiment

Discriminant analysis

Discriminant analysis supposes that each class has a multivariate normal distribution. Additional suggestions are that the a-priori probability of each class is the same and that the group specific density at x can be defined. The posterior possibility $p(t/x)$ is the probability that x belongs to class t and is calculated according to Baeys theorem:

$$p(t/x) = f_t(x)/f(x)$$

with

x: n-dimensional vector of the quantitative variables of the observations

t: class specific density estimated at x for class t and $f(x) = \sum_t f_t(x)$

$p(t/x)$: posterior probability that an observation x belongs to class t

An observation is classified in class u if $t = u$ has the largest value of $p(t/x)$.

The used program was written in SAS.

When the input is an ordinary SAS data set and there is no independent set available then the data set can be used for training as well as for validation. The resulting error has an optimistic value and is called the «apparent» errorrate. To get a more realistic estimate of the error rate a crossvalidation was used. Crossvalidation treats n-1 of the n observations as training data and uses the last observation for validation. This method gives an unbiased estimate of the error rate but with a relatively large variance.

Out of the classification error of the separate quality parameters, the best discriminating parameter between classes could be established.

5. Results

The results of the discriminant analysis are given in table 2 as a classification error, which is the percentage of misclassified tomatoes.

The classification error was determined by crossvalidation.

	dicriminating factor	best discriminating parameter	best combination of parameters	maximum classification error
a	color at picking time	S	S Co Fo	21.69
b				
green	storage temperature	phi	S phi Co	12.5
orange				18.95
red				22.65

Table 2: Maximum classification error (S: firmness, R_l: low frequency resistance, R_H: high frequency resistance, phi: constant phase angle, f_o: caracteristique frequency, c_o: characteritsic capacitance, Brix: ° sugar)

The results show that color at picking time can best be seen in a combination of the firmness (S), the characteritsic electrical capacitance (Co) and -frequency (Fo). The maximum classification error is 21.69%. However it can be said that separation of green and red picked tomatoes was 100% correct. This result is very important especially for consumers because earlier work has shown that green picked tomatoes develop less taste than red picked.
Further it can be concluded that the best discriminating parameter is the firmness.
Discrimination according to storage temperature gives a classification error of 12.5%, 18.95% and 22.65% for green, orange and red picked fruits. The better results for green picked tomatoes is due to the fact that these are more sensitive to chilling injury and therefore show an abnormal ripening process at 2°C, which is reflected in the quality parameters. The best discriminating parameter is the constant phase angle.

Conclusion

Fruit quality consists of several aspects, each of them to be measured with other techniques. This work has shown that sensor fusion can be used to separate green from red tomatoes with a very good result, based on measurement of firmness and electrical impedance. Also it could be seen that especially firmness and the characteritsic capacitance are of great importance in classification of tomatoes.

Acknowledgements

The research was done with the financial support of the Ministerie van Landbouw en Kleine en Middelgrote Ondernemingen (contract 5758A of 8/12/96).

References

[1] Thorne, S. en Alvarez, J.S.S, 1982. 'The effect of irregular storage temperatures on firmness and surface colour in tomatoes', *Journal of Science and Food Agriculture, 33, 671-676.*
[2] Cheng, T.-S. & Shewfelt, R.L. 1988. 'Effect of Chilling Exposure of tomatoes During Subsequent Ripening', *Journal of Food Science, 53 (4), 1160-1162.*
[3] Rosenfelt, D., Shmulivich, I. en Galili., N. 1994. *Measuring fimness trough mechanical acoustic excitation for quality control of tomatoes'*, Presented on The Food meeting, Florida, Orlando.
[4] Varlan, A.R., Sansen, W., Schotte, S. & De Baerdemaeker, J. 1996. *'Evaluation of tomato ripening process by combining four non destructive tests'*, ASAE Annual International Meeting, Phoenix, Arizona, July.
[5] Lamertyn, J. 1997. *'Niet destructieve meting van kwaliteitseigenschappen van appels met behulp van NIR spectroscopie'*, thesis, K.U.Leuven ,Belgium.

A methodology for sensor fusion design: application to fruit quality assessment

Une méthodologie pour la fusion de capteurs : application à l'appréciation de la qualité des fruits

V. Steinmetz, V. Bellon-Maurel
Cemagref. Division GIQUAL
361, rue JF Breton. BP 5095
34033 Montpellier Cedex 1 France
e-mail: vincent.steinmetz@cemagref.fr

F. Sévila
ENSAM. UFR Génie des Equipements - Génie Rural
2, place Viala
34060 Montpellier, France

Abstract: *The non destructive evaluation of food produce needs to use various sensors, which is more than a simple accumulation of independent sensors. Sensor fusion intends to have a collaborative approach of those sensors, in order to improve the quality assessment of the product and assure the consumer a high quality produce. Various applications of sensor fusion have already been made for fruit quality, but there is a lack of a general methodology for sensor fusion design. A methodology in eight steps is proposed. This methodology has been tested and validated on various commodities, and two examples are described (melon, peach). Those examples show the importance of sensor fusion as a multidisciplinary approach, and the difficulty in choosing the proper fusion technique. The proposed methodology turns out to be sufficiently general to be applicable to other food products.*

Keywords: *Quality assessment, sensor fusion, food produce.*

Résumé : L'évaluation non destructive des produits alimentaires demande d'utiliser plusieurs capteurs, ce qui est plus qu'une simple accumulation de capteurs indépendants. La fusion multi-sensorielle met en œuvre une approche collaborative de ces capteurs de manière à améliorer l'évaluation de la qualité du produit et à assurer aux consommateurs un produit de haute qualité. De nombreuses applications de fusion multi-sensorielle ont déjà été étudiées pour la qualité des fruits mais une méthodologie générale de fusion multi-sensorielle est encore attendue. Une méthodologie en 8 étapes est proposée. Cette méthodologie a été testée et validée sur différentes espèces et deux exemples sont décrits (melons, pêches). Ces exemples montrent l'aspect multi-disciplinaire de la fusion multi-sensorielle et les difficultés dans le choix d'une technique de fusion appropriée. La méthodologie proposée s'est révélée suffisamment générale pour être appliquée à d'autres produits alimentaires.

1. Introduction

The problem of assessing and maintaining the quality of fruits and vegetables limits the profitability and competitiveness of the fruits and vegetable producers and processors. Significant progress has been made towards developing sensors to measure both the external and internal quality parameters.
Fruit quality determination can be enhanced by employing modern sensing techniques. These techniques are different from classical sensing techniques in that the information is determined from signal patterns as opposed to a single signal value. Furthermore, information may be determined across multiple sensors as opposed to an isolated single sensor value. Multiple inputs entail the need for careful consideration of the signal processing step as an integral part of sensor system design. Sensor fusion is analogous to the cognitive process used by humans to integrate data continually from their senses to make inferences about the external world. So far it has been widely applied to military situations (battlefield surveillance, tactical situation assessment), or non-military purposes (robotics, automated manufacturing, remote sensing). The advent of sensor fusion approaches [6] enables rapid and economical on-line implementation for fruit quality assessment. The benefits of using multiple inputs are significant considering the economic premiums that are placed on consistent, superior quality in the marketplace.

In this paper, we intend to present the recent applications of real time and low-cost sensor fusion to fruit quality assessment, to present a general methodology that can be applied with this approach, and to present the applications of the methodology on various commodities.

2. State of the art

Fildes [4] describes the interest of sensor fusion techniques for the food processing industry, and presents the sensor fusion approach as a necessary method in order to avoid the simple addition of numerous and autonomous sensors. In the fruit sector, sensor fusion has been applied by using neural network on tomatoes quality assessment [13] by combining firmness, colour and acidity. Different techniques (Bayes, non-parametric by using the Parzen estimator, multi-layer neural network, Hopfield network) have been applied on melons [9]. Sensor fusion has also been applied more recently to peach firmness by combining two different kinds of firmness sensors [1], and to the detection of green picked and chilled tomatoes [12]. From a general point of view, there is a strong need for a methodology dedicated to the design of multisensor system for fast and non-destructive evaluation of fruit quality. This methodology is presented below.

3. Proposed methodology

The proposed methodology [17] consists in eight steps described in Figure 1 and detailed below.

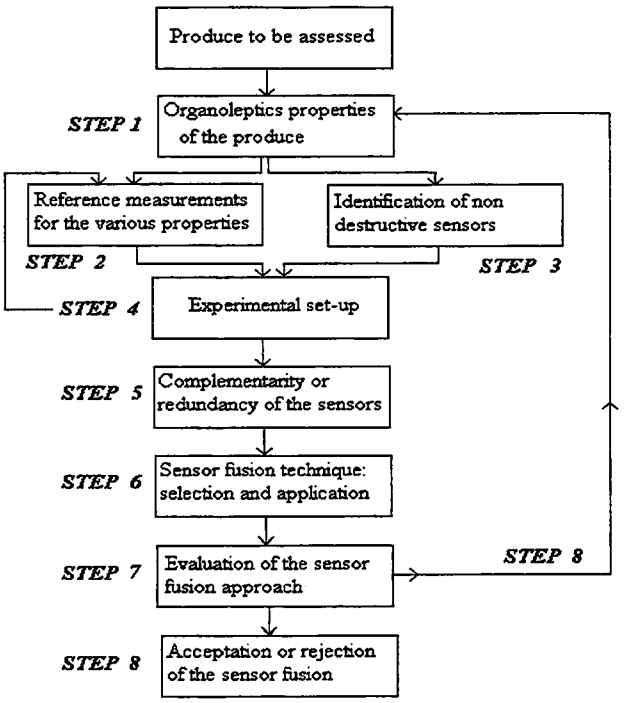

Figure 1: Description of the proposed methodology

3.1 Identifying the properties of the produce that are important for its organoleptics properties (step 1)

In this first step, it is important to take benefit of the knowledge from possible relations that may exist, event if this relation is not exactly known, between the different properties of the produce (for example, between the colour of the fruit and it sugar content). This step involves a strong co-operation of the sensor fusion «designer» with the technical specialists of the produce area, but also with the fundamental knowledge of the produce (Food Science). The result of this step is a list of physical or chemical properties related to the organoleptics property of the produce, and a list of possible relations between those properties.

3.2 Identifying the reference methods (qualitative or quantitative) that are currently used for assessing the quality of the produce (step 2)

These methods may be destructive measurements performed on the produce thanks to analytical tools when they are available, or expert judgements providing qualitative information. In the former case, the measurements can be used in order to build an automatic classification. In the latter case, we shall speak of supervised classification. The choice of the reference method will enable the validation of the information provided by the non-destructive sensors (step 3). A co-operation of the sensor fusion «designer» with the technical specialists of the produce area, with the sensory analysis area and with a specialist of the chemical and physical metrology on the produce should lead to the success of this step. The result of this step is a list of destructive sensors, or a human expertise, related to the properties selected in step 1.

3.3 Identifying the non destructive methods that can be used for measuring the selected properties of the produce (step 3)

This step is based on perception model that enables the development of non destructive methods for measuring physical or chemical properties (for example, the elasticity theory provides a model for sensors measuring firmness, light diffusion model within a fruit provide a theoretical base for non destructive sugar content measurement). The signal and features extracted from each sensor and leading to the measurement of the properties identified at step 1 must be determined at this point. This step must also take into account real time and costs constraints. It may occur that some property can be measured with some sensors, however in a too slow or a too costly way. Those sensors are thus not selected. For example, Resonance Magnetic Nuclear has been studied for internal defects detection in fruits [2], but they are still too expensive and their price restrain their on-line integration. Sensor selection is also performed based on:

- the complementarity or the redundancy of the sensors that will be used in the system,
- the nature of the problem to be solved.

The way for the success of this step goes through a good knowledge in metrology. The expected result of this step is a list of non-destructive sensors associated to the properties listed in step 1. It is clear that step number 2 does not necessarily occur before step number 3: they can be performed in parallel, as illustrated in Figure 1. However, the current uses of some reference methods in the studied produce area usually lead to the order as it is presented above.

3.4 Data acquisition on the produces with the selected non destructive sensors and reference methods (step 4)

An experimental design phase [11] may be used at this point if the influence of one or some properties on the produce. The experimental design phase is interesting for some produces that involve different ingredients, such as dough making [10], or when some parameters related to the measurements (frequency, acquisition time, temperature) have to be optimised. The experimental design phase is more difficult to perform with fruit quality assessment, when the quality is mainly the result of climatic conditions that cannot be controlled, except for greenhouse production. The choice of the reference method may depend on the analysis of the relation between a classification provided by experts, and measurements provided by destructive sensors. Therefore, there is a loop between step 4 and step 2.

3.5 Assessing the level of redundancy or complementarity in the non-destructive sensors (step 5)

Before performing sensor fusion, it is important to check whether or not the sensors provide the same information. When the sensors are supposed to measure different properties from a sample, the sensors are complementary. In the opposite case, some of the sensors may be redundant, and the failure of one can be tolerated. The description of the level of redundancy within the sensors may use the knowledge related to the selected sensors, but also to the *a priori* knowledge related to the produce (step 1). The current step must validate (or invalidate) the choices made at step 3, i.e. the level of complementarity of redundancy that was expected from the sensors. The result of this step is a measurement of the redundancy between the sensors. It enables the elimination of redundant sensors and consequently useless features, or on the contrary, the improvement of the robustness of the system with respect to sensor failures when some sensors are redundant.

3.6 Selecting and applying the proper sensor fusion method (step 6)

3.6.1 Biological models

Man usually disposes of different sensory organs currently listed in five different senses: taste, smell, vision, touch and hearing. Those senses are our link between the external world and our consciousness.

3.6.1.1 Interaction between senses

Interactions between our senses have already been studied. For example, Greer [5] shows that there is a strong interaction between smell and taste by performing

experiences on human with ethyl-butyrate and saccharin. More recent research contributes to the exploration of taste and smell interaction [20]. Similarly, Marks [8] studied the interaction between hearing and vision, and showed that both senses take part into information transmission for food products. Stillman [19] has also demonstrated the influence of colour on flavour identification (flavour is defined as the combination of the taste and the smell). Senses are generally presented as perception and transmission of information tools, each sense being specialised in a single kind of information. This approach turns out to be a narrow one, because the senses do interact. As a matter of act, different senses may take part in the transmission of the same information, and senses share numerous properties in their process. We will now intend to understand the mechanism of the sense interaction.

3.6.1.2 Interaction mechanisms

Various studies made on animals, such as cats, or monkeys and rats [3] have shown the importance of neurones: there are different kinds of neurones in the brain. Some neurones (or areas of neurones) are fired by a single sense, since others are fired by different senses. However, in general, the physiological mechanisms of sensory interactions in the human brain are far of being fully understood by researchers. The understanding of the fusion mechanisms of different senses in the human brain is in his early steps. If some neurones do have an active role in this fusion process thanks to networks, it is still a challenging task to simulate the human perception in general, particularly the sense interaction, even if the use of neural network is currently diffusing in the food processing and agriculture area.

As a conclusion, it can be said that the models of sensor fusion are partially inspired from biological models, i.e. neural networks. However, we will see that the sensor fusion techniques are not only an imitation of the human brain.

3.6.2 Sensor fusion techniques

Different sensor fusion techniques can be used as described in Hall [7]. These techniques can be separated in three different levels: high level, (Figure 2), an intermediate level (Figure 3), and a low level (Figure 4). It is important to note that the three levels use :

- features extraction, transforming the raw signal provided by the sensor into a reduced vector of features describing parsimoniously the original information, and

- identity declaration that affects a quality class to the measured produce based on the feature extraction process.

The high level fusion is performed by using the identity declaration provided by each sensor; the fusion of the identity declaration is then made by using heuristic techniques, Bayesian techniques, or Dempster-Shafer method.

The intermediary level fusion is performed by using the estracted features step from each sensor and the identity declaration based on this extracted features. the identity declaration process include techniques such as knowledge based approach (expert system, fuzzy logic), or training based approach (such as discriminant analysis, neural networks, Bayesian technique, k nearest neighbours, centre mobile algorithms).

The low-level fusion consists in combining before any processing the signals provided by different sensors. It implies that the sensors must be similar, and the consequently the signal commensurate. The combination of the signals is realised by using physical models, or based on relationship that may exist between the sensors. Low-level fusion may be used for example for fusing two images of the same object: one in the visible range, the other in the infrared range. Signals are commensurate. The combination of the signal may be a simple summation of the intensities of each pixel. Features extraction is then realised on the «virtual» image made of the sum of the two images. Identity declaration is then performed based on those two images.

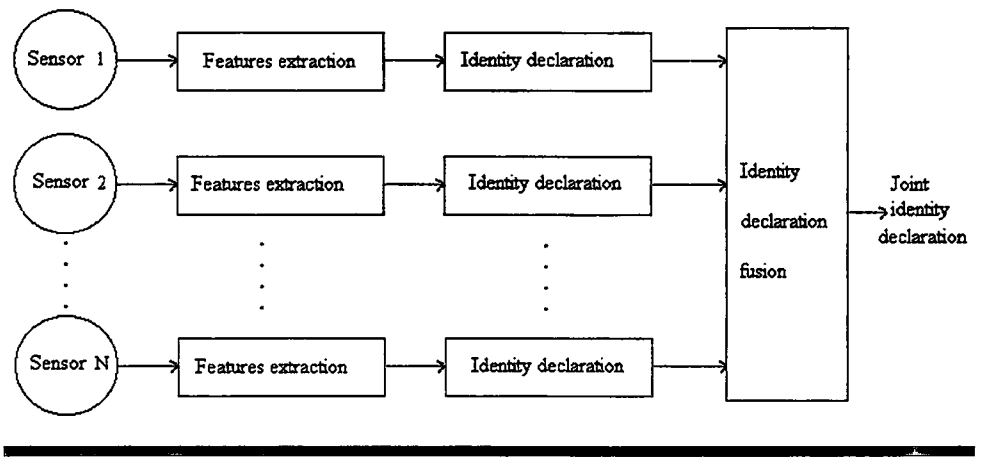

Figure 2: High level sensor fusion

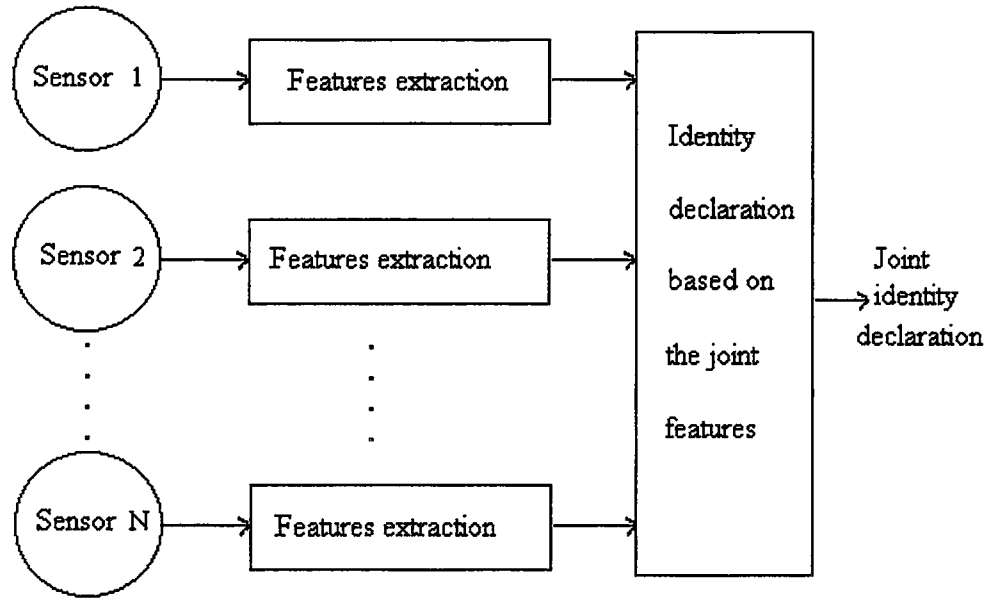

Figure 3: Intermediate level sensor fusion

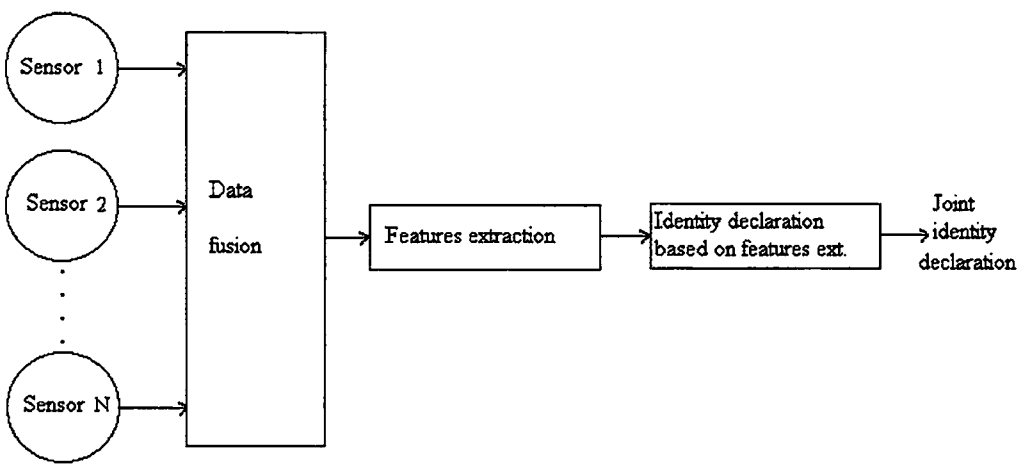

Figure 4: Low level sensor fusion

The different levels may be combined together. Let us consider four sensors that have to combined, two out of the four being similar (Figure 5). Using a low-level fusion technique may fuse those two similar sensors, and a feature extraction is performed based on the signal provided by those two sensors. The features

extracted can be combined with the features extracted from the third sensor in order to provide an identity declaration. This declaration can be then fused with the identity declaration from the fourth sensor. This simple example illustrates a combination of the three level of fusion, but shows a critical point in the sensor fusion design: how to choose the sensor fusion level, or, in other words, how to choose the sensor fusion technique. This will be discussed in the next sections.

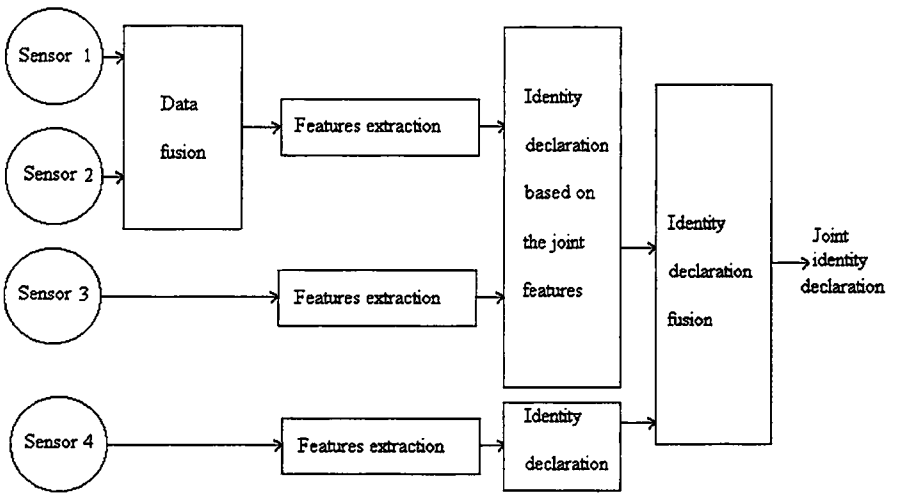

Figure 5: Scheme of combining different sensor fusion levels

3.6.3 Selecting sensor fusion level

In theory, the fusion process should be the most efficient by working at a low level. However, this level includes some practical limitations. First of all, it is rare that identical or commensurate sensors are used in a system. Secondly, this approach implies high memory capacity, and high-speed data processing that are currently not available. Intermediate and high level fusion techniques use a reduce information with respect to the raw signal provided by each sensors; eventually, this transformation includes already errors that will propagate into the fusion process. However, both techniques are well adapted to practical cases (sensors of different nature), and they use techniques that are well known and already largely used. The choice of the fusion level is of course related to the choice of the techniques.

3.6.4 Selecting sensor fusion technique

The application of the fusion approach shows successes with techniques ranging from expert system to probabilistic techniques. It does no exist a rule for selecting the proper fusion technique. Some authors [7] have proposed a method based on a

trial and error approach: it consists in trying different methods, then comparing them. Moreover, Hall [6] Hall D.L. 1992. *Mathematical techniques in multisensor data fusion.* Artech House. Boston. proposed a detailed frame that crosses fusion techniques and area of applications. However, this frame is mainly related to military applications. It is therefore a tricky task of providing advice for the fusion technique selection process for a given multisensor system. However, we do list below some criterions that have to be thoroughly considered for food products in general, fruits in particular:

- the nature of the sensors to be combined,
- the level of accuracy of the extracted features,
- the available knowledge that exists for the product,
- the extracted features space dimension.

Each technique includes advantages and problems, but it is clear that it does not exist a «unique and universal» fusion technique that can solves the problems of fruit (and food in general) quality assessment. This step involves specialist from the complex data processing area. The expected result is a selected fusion technique, and a model of fusion built based on this selection and on the data obtained through step 4.

3.7 Evaluating the sensor fusion system developed by comparing its performance to the reference methods (step 7)

Model evaluation is relevant for the comparison of single sensor system to a multisensor system. The result of this step is a list of indices [15] that enable to evaluate the performance of the multisensor system. Performance is defined here as the ability for the fusion model in performing a better prediction of the properties of the produce than the prediction made by a single sensor. This step intends to validate the fact that the multisensor approach is valuable with respect to a single sensor approach.

3.8 Loop to step 2 or 3 if the proposed sensor fusion method needs improvement (step 8)

If the conclusion of the step 7 is to reject the multisensor fusion approach, the different steps need to be evaluated in order to study the reason of this rejection, identification ot the encountered problems, and to draw conclusions that may be:

- choices to be corrected in the various steps of the methodology (using different sensors or different references, testing different fusion techniques),

- rejection of the sensor fusion approach.

4. Applications to fruit quality

The methodology has been applied on melons. Rather than to describe again all the applications that have already been widely reported in the mentioned papers, we intend below to report the results of the applications of the methodology on two selected fruits (melon and peach), and which experience do we gain from the application of this methodology.

4.1 Melons

- melons are mostly graded after harvesting based on their weight or size with mechanical systems, and based on colour. The latter characteristic is so far performed by human graders in charge of removing the non-mature or advanced-mature fruits based upon subjective visual determination (colour or changes in the physical exterior aspect such as the appearance of a slip near the stem). Some systems such as include invasive sensors for measuring sugar content.

- two different ways were used for defining the reference for those organoleptic properties:

- a classification in four quality classes performed by an human inspector, and destructive measurements using a refractometer and a manual penetrometer (Magness-Taylor);

- the selection of the non-destructive sensors lead to the use of an artificial vision system, and an electronic sniffer;

- about 180 fruits were used as experimental samples from the same cultivar («Galoubet»). After this experimental step, it was shown that the classification provided by the experts was poorly related to fruit maturity (measured with destructive measurements), and that the repeatability of the expert classification is poor (step 2 of the methodology). Therefore, an unsupervised classification of the fruit maturity was also provided based on destructive measurements (loop from step 4 to step 2);

- the non-destructive sensors were shown to be complementary, but by using a principal component analysis, it was shown that the electronic sniffer is partially related to sugar content;

- two intermediate level fusion techniques have been used: a multi-layer neural network and discriminant analysis;

- the evaluation of the sensor fusion techniques shows that the best results (although modest due to the poor repeatability of the expert) were obtained by

predicting the reference class defined by the expert by using the information from the vision system. The redundancy study showed that aromas are related to sugar content. This was confirmed by using a neural network for sugar content prediction of the melon by using the signal from an electronic sniffer.

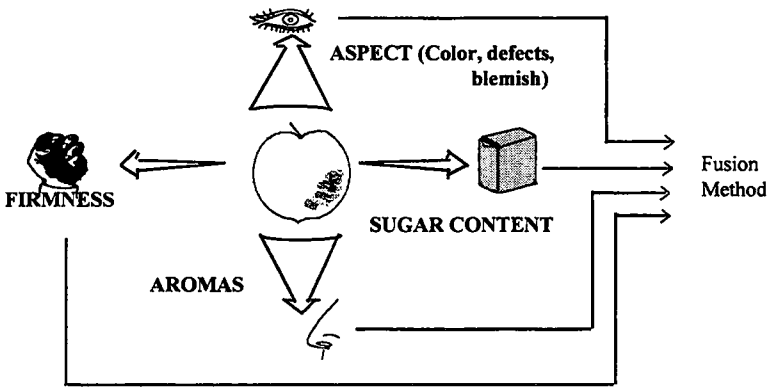

Figure 6: Scheme for fusion of various sensors applied to melon quality assessment

The application of the methodology enables to have a critical look at the reference used (in this case, the expert). It also shows the relationship between aromas and sugar content, which is a critical organoleptic parameter for melons, and the high importance of visual aspect for manual grading though mot related to maturity of the fruit.

4.2 Peaches

- peach organoleptic quality depends on the combination of different factors such as firmness, sugar content, visual appearance and aromas. In particular, sugar content is directly connected to maturity, and colour is often accepted as the second index of maturity. Firmness is important because the peach has to be firm enough to minimise damage during packing and shipping;

- the reference for those organoleptic properties were defined by using destructive measurements using a refractometer and a manual penetrometer (Magness-Taylor);

- the selection of the non-destructive sensors lead to the use of an artificial vision system, various firmness sensors (based on sound, impact and micro-deformation), and a near infrared spectrophotometer;

- two experimental sets were conducted: one in 1993, with 203 fruits from different cultivars («Pavie», «Early Red Haven», «Royal Glory») and that used only firmness

sensors (Figure 7); the other one was conducted in 1995 with 120 fruits from the same cultivar («Pavie») and by using the various selected non destructive sensors as illustrated in Figure 6;

- concerning the experiments run in 1993, two non-destructive firmness sensors were shown to be complementary: the one based on impact, and the other one based on micro-deformation. This was explained by the fact that they perform a local measurement of firmness since the sound based sensor performs a global firmness assessment;

- two fusion levels have been selected:

  - a high-level fusion that combines a Bayesian classifier associated with each sensor, and a majority voting process based on the classification of each sensor; this was possible because each sensor provided an assessment of the same property of the fruit (firmness);

  - an intermediate level, that uses a multi-layer neural network.

- by combining three different kind of firmness sensors based on different technologies (based on sound, impact, or micro-deformation), it was shown that the assessment of firmness can be improved. Combining the colour of the fruit and its firmness with the sugar content prediction provided by the spectrophotometer enables to improve the prediction of its sugar content. Similarly, the combination of the sugar content and colour firmness with the firmness prediction provided by the impact sensor enables to improve the prediction of firmness.

It was also shown that the choose of a reference sensor for firmness is a difficult task, but that some non destructive sensors were highly efficient for classifying very soft or very firm fruits. Armstrong [1] have recently confirmed this approach, i.e. combining different firmness sensors. The results in our application were slightly better with the intermediate level, confirming the fact that the closer to the information source, the better the classification should be.

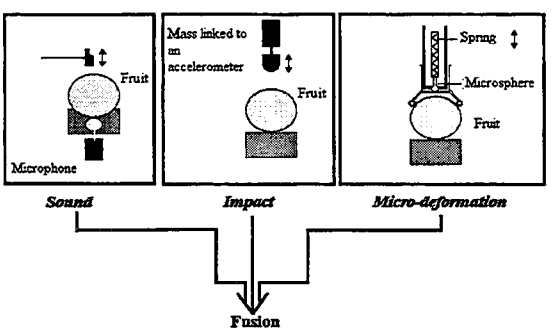

Figure 7: Scheme for fusion of firmness sensors applied to peach

4.3 Discussion

The different applications of the methodology show the importance of the multidisciplinary in the sensor fusion approach. It also shows that the sensor fusion approach may be more valid for some fruits than for others (the results for peaches are more interesting than the one for melons). The use of low cost and fast sensors enable to provide a satisfying quality assessment of the produce, but the lack of some sensors make it difficult the assessment of some organoleptics properties (as for acidity, or sugar content in fruits with thick skin). The different fusion methods shows that similar results are expected when working at different levels (high and intermediary; the low level was not used because none of the used sensors were similar in terms of technology and signal). However, working at the intermediary level seems to provide better results. Moreover, it must be strengthen that the fusion process to be developed for each fruit depends a lot of the cultivar of the fruit. The flexibility of the fusion process is a trade-off between the use of various sensors, enabling the measurements of various properties on different possible cultivars, and the way in which the various signals are combined, which depends on the fruit and cultivar.

Conclusion

In this paper, we have pointed out the need for a general methodology in the design of sensor fusion systems for food quality assessment. We propose a methodology that is applied to different horticultural produces. The application of this methodology shows that the sensor fusion approach is valuable for fruit quality assessment. However, the choice of the sensor fusion method is a difficult task. The proposed methodology is fully applicable to other food produces and products, and strengthens the need for a strong multidisciplinary co-operation in the sensor fusion design process. The application of the methodology is now currently visible on an industrial prototype developed in the frame of the European SHIVA ESPRIT project (EP 9230 - "Integrated System for Handling, Inspection and Packing of Fruits and Vegetables").

References

[1] Armstrong P.R., Stone M.L., Brusewitz G.H. 1997. Peach firmness determination using two different nondestructive vibrational sensing instruments. *Transactions of the ASAE. 40(3):699-703.*

[2] Chen H., Kauten R., McCarthy M.J. 1988. *Potential use of NMR for internal quality evaluation of fruits and vegetables.* ASAE International Winter Meeting. 13-16 December. Chicago, Ill. USA.

[3] Chudler E.H., Sugiyama K., Dong W.K. 1995. Multisensory convergence and integration in the neostratium and globus pallidus of the rat. *Brain Research. n 674 :33-45.*

[4] Fildes J.M., Cinar A. 1995. Sensor fusion and intelligent control for food processing. ASAE. *Food Processing Automation Conference IV. pp 67-72.*

[5] Greer C. 1991. Structural organization of the olfactory system. In « Smell and taste in health and disease ». Ed. Getchell T., Doty R., Bartoshuk L., Snow J. *pp 65-82. New York: Raven Press.*

[6] Hall D.L. 1992. *Mathematical techniques in multisensor data fusion.* Artech House. Boston.

[7] Hall D.L., Linn R.J. 1987. Algorithm selection for data fusion systems. Proceedings of the 1987 tri-service data fusion symposium. June 1987. John Hopkins University, Baltimore. *Naval Air Force Center, Warminster, Pennsylvania. pp. 100-110.*

[8] Marks L.E. 1991. *Metaphor and the unity of the senses.* Sensory Science Theory and Applications in Foods. Ed. Institute of Food Technologists.

[9] Ozer N., Engel B.A., Simon J.E. 1995. Fusion classification techniques for fruit quality. *Transactions of the ASAE. 38(6):1927-1934.*

[10] Reach C. 1996. *Instrumentation d'un pétrin de boulangerie en vue de la caractérisation de l'optimum de pétrissage.* Rapport de DAA - Option Agrotique. Ecole Nationale Supérieure Agronomique de Montpellier, France.

[11] Sado G., Sado M.-C. 1991. *Les plans d'expérience : de l'expérimentation à l'assurance qualité.* 2nde édition. AFNOR.

[12] Schotte S., De Baerdemaeker J. 1998. *Use of sensor fusion to detect green picked and chilled tomatoes.* SENSORAL 98. International Workshop on sensing quality of agricultural products. Montpellier, France, February 23-27 1998.

[13] Shmulevich, I., Rachmani D., Edan Y. 1994. *Quality grading tomatoes by mechanical properties using a neural network system.* Paper No. 94-G-064. Conférence AGENG'94. Milan, Italy.

[14] Steinmetz V., Crochon M., Talou T., Bourrounet B. 1995. Sensor fusion for fruit quality assessment: application to melon. *Proceedings of the International Conference ASAE 'Harvest and post-harvest technologies for fresh fruits and vegetables'. Mexico. pp. 488-496.*

[15] Steinmetz V., Crochon M., Bellon-Maurel V., Garcia Fernandez J. L., Barreiro Elorza P., Verstreken L. 1996[a]. Sensors for fruit firmness assessment: comparison and fusion. *Journal of Agricultural Engineering Research. 64(1):15-28.*

[16] Steinmetz V., Biavati E., Molto E., Pons R., Fornes I. 1996[b]. *Non destructive determination of quality in peaches with a multisensor approach.* International conference on Agricultural Engineering. AGENG, Madrid, Spain. Paper 96F-006.

[17] Steinmetz V. 1997[a]. *Real time multisensor fusion applied to qualitative decisions for food produces quality assessment.* PhD thesis (in French). ENGREF Paris. Biological and industrial process engineering.

[18] Steinmetz V., Biavati E., Moltó E., Pons R., Fornes I. 1997[b]. *Predicting the maturity of oranges with non-destructive sensors.* Actae Horticulturae n° 421.

[19] Stillman J.A. 1993. Color influences flavor identification in fruit-flavored beverages. *Journal of Food Science. Vol. 58.*

[20] Villanueva-Rodriguez S.J. 1997. *Contribution à l'étude des interactions entre entrées sensorielles :* effets de l'addition d'une stimulation buccale (gustative ou trigéminale) à une stimulation olfactive sur les paramètres inspiratoires et sur la perception de l'intensité et de la qualité de la sensation olfactive. PhD thesis (in French). ENSBANA Dijon, France.

[21] Wallace M.T., Stein B.E. 1997. Development of multisensory neurons and multisensory integration in cat superior colliculus. *Journal of Neuroscience. Vol. 17. pp. 2429-2444.*

Organisé par

Cemagref

The Workshop SENSORAL 98 was aimed at sensor measurement of agricultural product quality. It dealt with three main objectives: dissemination of the research results of two European projects, scientific and technical presentations of sensors and fast measurement systems by international researchers, enhancement of industry/research exchanges through industrial presentations of joint research projects transferred to the industry.

For fruits and vegetables, the most important themes were: artificial vision, NIR spectrometry, aroma sensors and artificial intelligence simulating human classification. Animal product quality assessment through acoustic, NMR and electric impedance measurement was presented. Concerning process control, tracers or emerging techniques such as Magnetic Resonance Imaging were mainly dealt with.

Le colloque SENSORAL 98 était axé selon trois objectifs : être le support de dissémination des résultats de la recherche de deux projets européens, permettre aux chercheurs de la communauté internationale de présenter leurs avancées sur les systèmes capteurs et mesures rapides de produits agricoles, favoriser les échanges industrie/recherche par une présentation industrielle de projets de recherche conjoints ayant abouti à des transferts.

Pour le contrôle des produits végétaux, les thèmes forts qui émergent de ce Colloque sont la vision artificielle, la spectrométrie proche infra-rouge, les capteurs d'arômes, les méthodes d'intelligence artificielle pour simuler la classification humaine. L'appréciation des produits carnés est présentée au travers de l'acoustique, la RMN et l'impédance électrique. Le contrôle des procédés est abordé en proposant des marqueurs et également des techniques en émergence telles que l'Imagerie à Résonance Magnétique.

Avec le soutien

MINISTÈRE DE L'AGRICULTURE ET DE LA PÊCHE

REGION LANGUEDOC ROUSSILLON

ISBN 2-85362-499-4

Prix : 195 F TTC

9 782853 624992